

Supporting information

Mn(III)-mediated C-P bond activation of diphosphines: Toward highly emissive phosphahelicenes cations scaffold and modulated circularly polarized luminescence

¹Bo Yang, ¹Suqiong Yan, ³Chengbo Li, ¹Hui Ma, ¹Fanda Feng, ¹Yuan Zhang, ^{1,2}Wei Huang*

¹State Key Laboratory of Coordination Chemistry, School of Chemistry and Chemical Engineering, Nanjing University, Nanjing, Jiangsu Province 210093, P. R. China

²Shenzhen Research Institute of Nanjing University, Shenzhen, Guangdong Province, 518057, P. R. China

³School of Materials and Energy, University of Electronic Science and Technology of China, Chengdu, 610000, P. R. China

Table of contents

Section A: Materials and experimental methods.....	2
Section B: Synthetic procedures of substrates and products.....	6
Section C: Chemical structure stability of compound [1b] ⁺ [Cl] ⁻	48
Section D: X-ray crystallographic data.....	51
Section E: Reaction mechanism study.....	76
Section F: Theoretical computation	79
Section H: CD, CPL spectra data, and LCs self-assembly	101
Section H: NMR spectra.....	109

Section A: Materials and experimental methods

Materials and Methods. All precursor reagents, solvents, and high-purity nuclear magnetic resonance (NMR) solvents were purchased from commercial sources (Aladdin, Adamas, and Sigma) and used as supplied unless otherwise indicated. Solvents were distilled from calcium hydride (toluene, DCM, chloroform, tetrahydrofuran). The dry solvents were stored in the activated 4 Å molecular sieve (4 Å MS) before being used. The 6,6' and 7,7'-substituted diphosphine substrates were synthesized via Monsanto Method (**Scheme S1**).¹⁻³ The 5,5'-substituted diphosphine substrates were synthesized from brominated BINAPO compounds via Suzuki-Miyaura coupling and reduction reaction.⁴ All oxygen or moisture-sensitive reactions were performed under an argon atmosphere using a standard Schlenk operation. The phosphoniums or phospho[5]helicenes were prepared from diphosphine substrates with anhydrous MnCl₂ in mixed solvents of CHCl₃/EtOH (v/v = 2:1) in O₂. The O₂ was sealed in the Schlenk tube at 1 bar for Mn(II)-mediated cyclization.

NMR: ¹H NMR, ¹³C NMR, and ³¹P NMR spectra were recorded using a Bruker Avance III 400 MHz spectrometer. The CDCl₃ or CD₃OD was used for the NMR test at room temperature. The phosphoric acid was used as the external standard for ³¹P NMR spectra. Only one isomer was listed for NMR spectra to avoid redundancy of data flow in SI.

HRMS: High-resolution mass spectrums for all compounds in methanol (LC) were recorded on Thermo Fisher-Q Exactive at room temperature.

X-ray Crystallography: Firstly, all crude compounds were purified by flash chromatography at room temperature (200-300 mesh), and then dried on a rotary evaporator with reduced pressure at 20-30 °C. Single crystals of enantiomeric and racemic [2a]⁺[X]⁻ and diphosphine ligands were grown in mixed dichloromethane/*n*-hexane/ethanol solutions after slow evaporation at room temperature. The crystalline [(6b)⁺]₂[MnCl₄]²⁻ could be obtained from the reaction solution in the Schlenk tube after slow cooling. Other crystals of compounds were obtained after anion exchange. SCXRD data were collected at 173 K using a Bruker diffractometer with an X-ray tube with Mo/Kα (λ = 0.77 Å) or Ga/Kα (λ = 0.83 Å) radiation. Program APEX3 was used for the data collection and reduction. The structures were solved with an intrinsic phasing of SHELXT and refined by full-matrix least-squares on *F*² using OLEX2 or SHELXTL version 6.10. softwares, which utilizes the SHELXL-2015 module. In the case of complexes [(*P*)-2b]⁺[BF₄]⁻, [(*M*)-2b]⁺[BF₄]⁻, and [(*Rac*)-3c]⁺[BF₄]⁻, it was found that the solvent molecules were highly disordered. Attempts to locate and refine the solvent peaks were unsuccessful. So, contributions to scattering due to these solvent molecules were removed using the SQUEEZE routine of PLATON. The structures were then refined again using the data. As a result, one level A type alert 'PLAT602_ALERT_2_A Solvent Accessible VOID(S) in Structure !' was reported. The detailed crystallographic data and experimental details of all complexes are shown in Tables S2-S6. Crystallographic data were deposited with the Cambridge Crystallographic Data Centre (CCDC) (2130476, 2130479, 2130454, 2130459, 2225461, 2225466-2225474, 2225477-2225478, and 2225482).

Anion exchange: Initial compounds ([A]⁺[Cl]⁻) were mixed with equivalent amounts of

Supporting information

halide scavengers (AgBF₄ or AgPF₆) in DCM/EtOH (5:1), and the mixture was shaken for 2 minutes via ultrasonic operation. The turbid mixture was filtrated by filter membrane (1 μm), and the filter liquor was stored at room temperature for 1-2 days. Finally, the microcrystals were collected after the volatilization of the solvents.

Microscope: Polarized optical microscopy (POM) and fluorescence microscope (λ_{ex} =365 nm) measurements were performed on a Caikang XP-550C instrument.

UV-vis and PL: Ultraviolet-visible absorption spectra were measured on a Shimadzu UV-2600 spectrophotometer by using a 10 mm optical-path quartz cell at room temperature. The photoluminescence (PL) spectra were measured on the HITACHI F-4600 and HORIBA-FL3 at room temperature. Absolute quantum yields were measured using the calibrated integrating sphere system at room temperature in DCM or solid state. The time-resolved PL measurements were taken on the HORIBA-FL3 instrument to measure the excited state lifetime. A diode laser with λ_{ex} =370 nm was used as the excitation source, and the time-correlated single-photon counting (TCSPC) method was used to collect photographs. Transient fluorescence decay curves were obtained via biexponential fitting.

CD and CPL: Circular dichroism (CD) spectra were measured on a JASCO J-810 spectrometer (Measurement limit: -2000 to +2000 mdeg). Circularly polarized luminescence (CPL) spectra were recorded on a JASCO CPL-300 spectrophotometer, the excitation wavelength was 360 nm for all samples. The g_{abs} value was determined by $g_{abs} = 2[\varepsilon_L - \varepsilon_R]/[\varepsilon_L + \varepsilon_R] = CD[mdeg]/(32980 \times lg^{Abs})$, where ε_L and ε_R are the ellipticities of the left- and right-handed circularly polarized absorptions. The g_{lum} value of CPL was determined by $g_{lum} = 2(I_L - I_R)/(I_L + I_R)$, where I_L and I_R are the intensities of the left- and right-handed circularly polarized emissions. The angle-dependent CPL was done to evaluate the linear dichroism (LD) artifact of microcrystalline powder and LCs films. The CD and CPL spectra are slightly changed when altering the rotation angle, confirming that the contributions of LD to the CD/CPL signals are negligible, while the signs of CD/CPL were unchanged for the front/back side films, confirming that true CD/CPL signals instead of birefringence artifact (Fig.s S44, S48, S49-S50).⁵

Electrochemical Tests. Cyclic voltammetry (CV) measurements were performed on a BioLogic-Science Instrument (Bio-Logic VSP-3e). CV experiment of BINAPs and DPEPhos were measured in anhydrous DCM solution (1×10^{-3} mol L⁻¹) with 0.1 mol L⁻¹ tetrabutylammonium hexafluorophosphate as the supporting electrolyte at a scan rate of 100 mV s⁻¹. Counter electrode: Pt wire, reference electrode: Ag/AgCl (0.1 mol L⁻¹ in dry acetonitrile), and working electrode: glassy carbon.

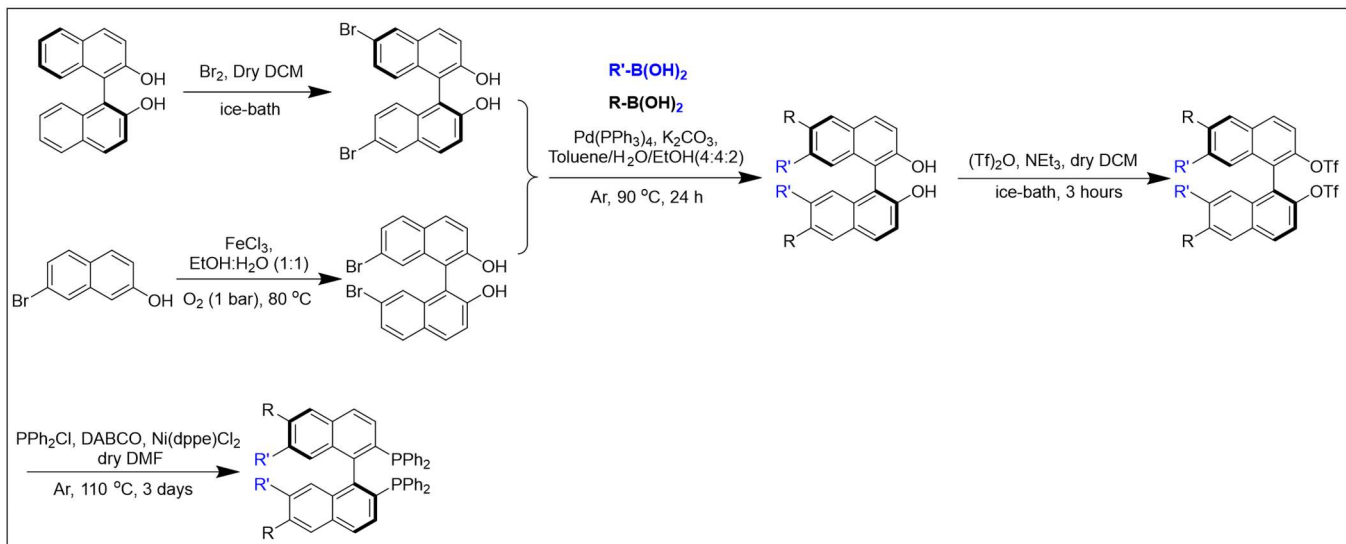
Preparation of ternary-chiral liquid crystals (LCs) system. The 5CB (4'-pentyl-[1,1'-biphenyl]-4-carbonitrile) was a commercial nematic (N) phase LCs molecule. The phase transition sequence was K → N (22.5 °C) → Iso (35.5 °C). 5CB shows achiral nematic (N) phase behavior at room temperature. In this work, the ternary component 5CB (host), instantaneous chiral phosphahelicenes/phosphonium (emitters, guest A, 2 wt%), and permanent chiral assister (inducer, 0.5-4 wt%, 4',4'''-(((1,1'-binaphthalene)-2,2'-diylbis(oxy))bis(hexane-6,1-diyl))bis(oxy))bis((1,1'-biphenyl)-4-carbonitrile)) were dissolved in DCM, and then the mixture was drop-cast on the clear glass plate (without treatment of orientation) and heated at 40 °C for a few minutes to remove the DCM. Another

Supporting information

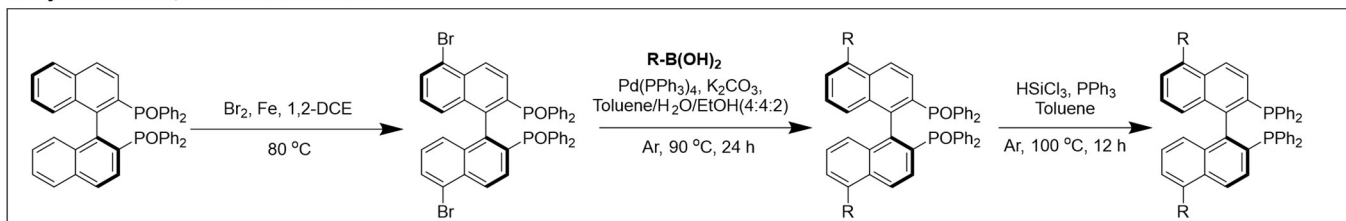
glass sheet was covered on the dry sample. The above-mentioned solid mixture would melt (isotropic liquid, Iso) when heated to a clear-point temperature ($T_c > 60$ °C), and the initial self-assembling state could be completely erased. Finally, the isotropic liquid was cooled to room temperature (25 °C) slowly, where a new chiral nematic (N*, cholesteric phase) mesophase was formed. The supramolecular helical structures and amplified optical activities of LCs films (about 10 μm) were checked via POM, XRD, and CD/CPL spectra.

Supporting information

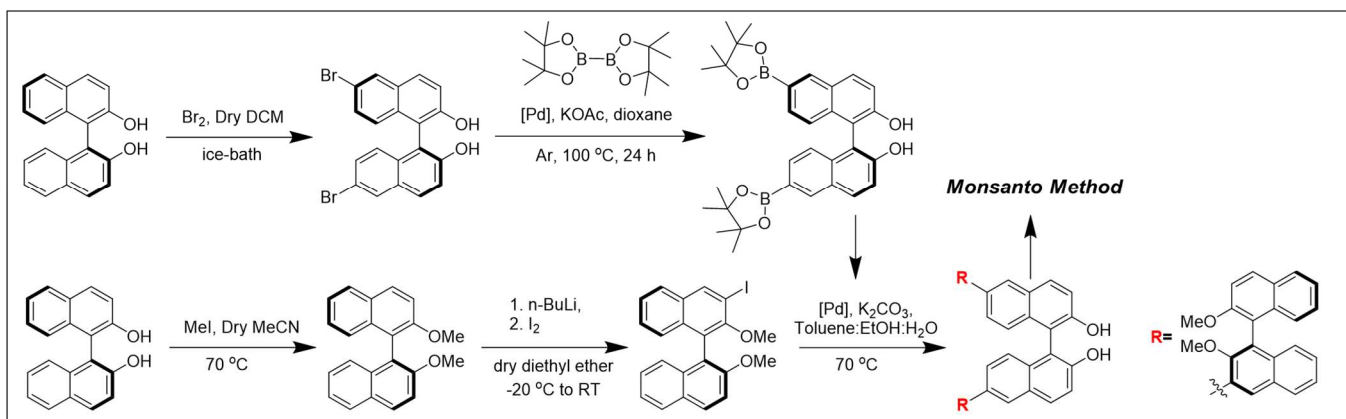
I. Monsanto Method



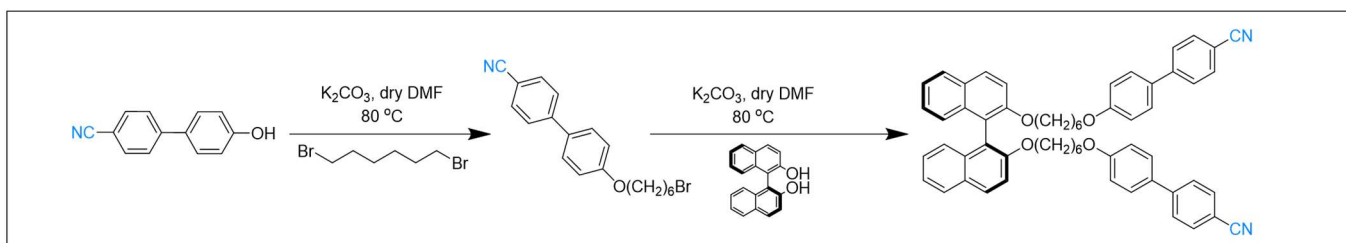
II. Synthesis of 5,5'-substituted BINAPs



III. Synthesis of 6,6'-substituted with permanent chiral arms

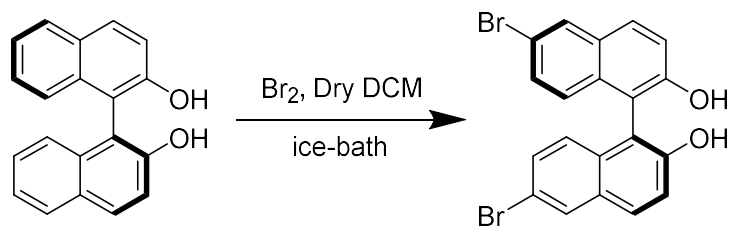


IV. Synthesis of 2,2'-substituted with permanent chiral guest

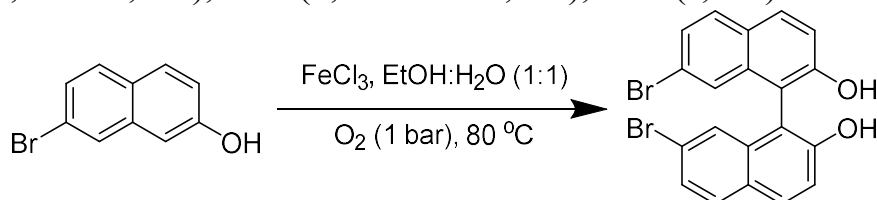


Scheme S1. Synthetic procedures of substrates.

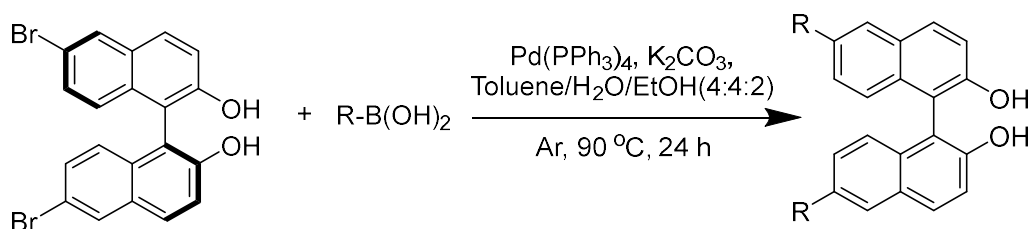
Section B: Synthetic procedures of substrates and products



1. General procedure for the synthesis of starting materials 6,6'-dibromo-[1,1'-binaphthalene]-2,2'-diol: In a 250 mL round-bottomed flask was placed (*S*)-BINOL (10 g, 35.0 mmol) and 150 mL of dry CH₂Cl₂. Bromine (5.6 mL, 105 mmol, 3 eq) was added dropwise at 0 °C. The mixture was stirred at room temperature for 48 h. The organic phase was extracted successively with 1 M aqueous sodium hydrogen sulfite solution, brine, and saturated sodium hydrogen carbonate solution, dried, and evaporated to obtain the bis-brominated product. The white solid (14.8 g, 95%) was obtained after recrystallization from *n*-hexane. ¹H NMR (400 MHz, CDCl₃) δ 8.05 (d, *J* = 1.9 Hz, 2H), 7.89 (d, *J* = 9.0 Hz, 2H), 7.38 (dd, *J* = 9.8, 7.9 Hz, 4H), 6.96 (d, *J* = 9.0 Hz, 2H), 5.04 (s, 2H).



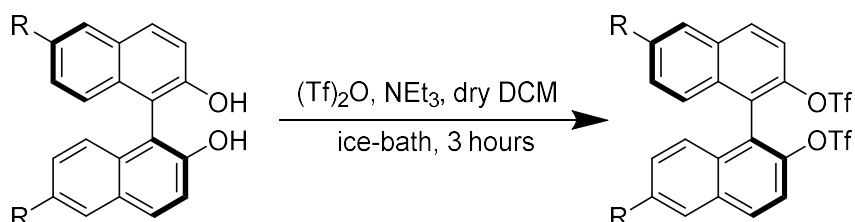
2. General procedure for the synthesis of 7,7'-dibromo-[1,1'-binaphthalene]-2,2'-diol: In a 250 mL round-bottomed flask was placed 7-bromonaphthalen-2-ol (10 g, 44.8 mmol), FeCl₃ (3.0 eq) and 100 mL of mixed solvent (EtOH/H₂O = 1:1). The mixture was refluxed at 90 °C in O₂ for 48 h. The mixture was extracted successively with water and CH₂Cl₂ solution, dried and evaporated. The organic solvent was removed by decompressing vaporization. The resulted residue was purified by column chromatography with PE:CH₂Cl₂ (1:3), and then the grey solid powder was obtained with 93 % yield. ¹H NMR (400 MHz, CDCl₃) δ 7.96 (d, *J* = 8.9 Hz, 2H), 7.77 (d, *J* = 8.7 Hz, 2H), 7.48 (dd, *J* = 8.7, 1.9 Hz, 2H), 7.39 (d, *J* = 8.9 Hz, 2H), 7.23 (d, *J* = 1.8 Hz, 2H), 5.08 (s, 2H).



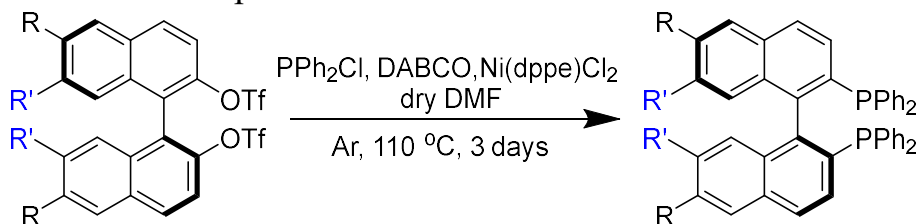
3. General procedure for the synthesis of substituted BINOLs: In a 250 mL round-bottomed flask were placed 6,6'-dibromo-[1,1'-binaphthalene]-2,2'-diol (1.0 g, 35.0 mmol), substituted benzoboric acid (3.0 eq), K₂CO₃ (6.0 eq), Pd(PPh₃)₄ (5 mol%), and 25 mL of mixed toluene/EtOH/H₂O (10/5/10) solvent. Other similar reactions of substrates were consistent with this general condition. In addition, the weaker base (NaHCO₃) was used for the preparation of the optically pure product to avoid racemization during coupling. The organic phase was extracted successively with brine and dichloromethane. The organic

Supporting information

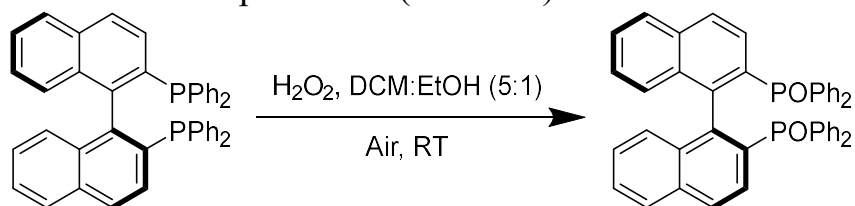
phase is dried with anhydrous MgSO_4 and filtered. The solvent is removed by decompressing vaporization. The organic phase is dried with anhydrous MgSO_4 and filtered. The solvent is removed by decompressing vaporization. The resulting residue was purified by column chromatography with $\text{PE}:\text{CH}_2\text{Cl}_2$ (1:3), and then the white solid powder was obtained with a good yield.



4. General procedure for the synthesis of substituted BINOLs-OTf: In a 100 mL round-bottomed flask was placed substituted BINOLs (1.0 g) and 20 mL of dry CH_2Cl_2 . NEt_3 in DCM (2.5 eq) was added dropwise at $0\text{ }^\circ\text{C}$ for 10 min. The $(\text{Tf})_2\text{O}$ in DCM (2.5 eq) was added dropwise at $0\text{ }^\circ\text{C}$ for about 15 min. The reaction was reacted at room temperature for 3 hours. The mixture was extracted successively with brine and CH_2Cl_2 solution. The organic layer was dried with MgSO_4 and filtered. The organic solvent was removed by decompressing vaporization. The resulting residue was purified by column chromatography with $\text{PE}:\text{CH}_2\text{Cl}_2$ (8:1), All substituted products get a high yield (>92%). The detailed NMR values are listed in the NMR spectra section.



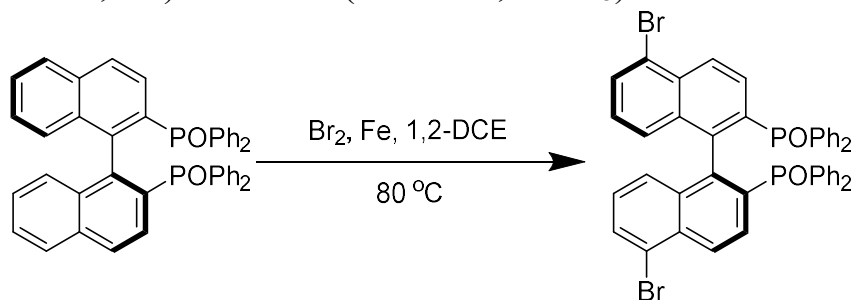
5. General synthesis of substituted BINAPs at 6,6' and 7,7'-positions: In a 25 mL Schlenk tube was placed substituted BINOLs-OTf (1.0 g), $\text{Ni}(\text{dppe})\text{Cl}_2$ (0.2 eq), Zn powder (3.0 eq), DABCO (3.0 eq), and 10 mL of dry DMF . The mixture was degassed and filled with Ar . The PPh_2Cl was added to the tube. The deaeration step was repeated and the Ar was filled. The mixture solution was reacted at $110\text{ }^\circ\text{C}$ under an Ar atmosphere for about 2-3 days. The mixture was extracted successively with brine and CH_2Cl_2 solution. The organic layer was washed with brine about 3-4 times to remove DMF , dried with MgSO_4 , and filtered. The organic solvent was removed by decompressing vaporization. The resulting residue was purified by column chromatography with $\text{PE}:\text{CH}_2\text{Cl}_2$ (8:1), and then the white powder was obtained with 30-54% yields. The stereochemistry of the enantiotopic substrate was preserved throughout the synthetic sequence, which was also proved by single crystal diffraction data with a low flack parameter (Table S2).



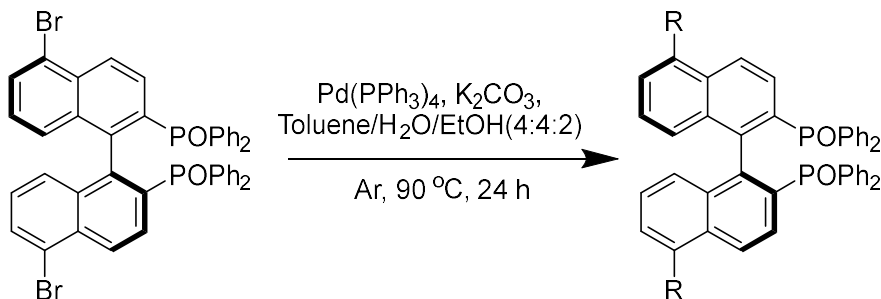
6. Synthesis of (S)-(5,5'-dibromo-[1,1'-binaphthalene]-2,2'-diyl)bis(diphenylphosphine

Supporting information

oxide): In a 100 mL round-bottomed flask was placed substituted (*S*)-BINAP (5.0 g, 8.0 mmol), 40 mL of dry CH₂Cl₂ and 10 mL EtOH. A hydrogen peroxide solution (30 vol%, 2.5 eq) was added dropwise at 0 °C. The reaction was reacted at room temperature for 2 hours until the starting material was completely consumed. The mixture was extracted successively with brine and CH₂Cl₂ solution. The organic layer was dried with MgSO₄ and filtered. The organic solvent was removed by decompressing vaporization. The white powder was obtained with 99 % yield. ¹H NMR (400 MHz, CDCl₃) δ 7.86–7.79 (m, 4H), 7.73–7.64 (m, 4H), 7.45–7.32 (m, 12H), 7.28–7.26 (m, 2H), 7.23 (ddd, *J* = 8.9, 5.2, 1.9 Hz, 6H), 6.78 (t, *J* = 4.5 Hz, 4H). ³¹P NMR (162 MHz, CDCl₃): δ 28.6.



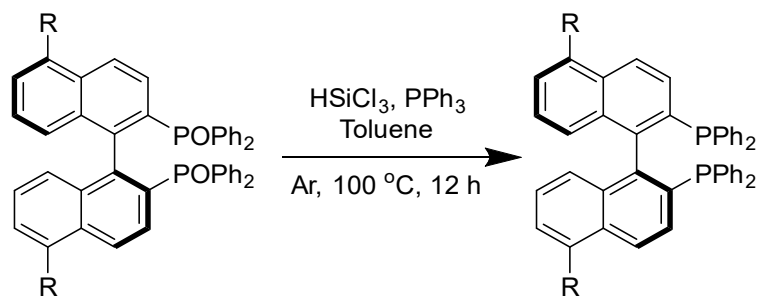
7. Synthesis of substituted (*S*)-BINAPO: In a 100 mL round-bottomed flask was placed substituted (*S*)-BINAPO (5.0 g, 7.65 mmol), Fe powder (1.5 eq, 11.5 mmol), 40 mL of dry 1,2-DCE solvent. The reaction was refluxed at 80 °C for 30 min. Br₂ solution (30 vol%, 2.5 eq) was added dropwise to refluxing mixture. The mixture was refluxed overnight until the starting material was completely consumed. The organic phase was extracted successively with 1 M aqueous sodium hydrogen sulfite solution, brine, and saturated sodium hydrogen carbonate solution, dried, and evaporated. The mixture was filtered to remove any iron. The organic phase was extracted successively with 1 M aqueous sodium hydrogen sulfite solution, brine, and saturated sodium hydrogen carbonate solution, dried, and evaporated. The resulting residue was purified by column chromatography with CH₂Cl₂:EA (6:1), and then a white powder was obtained with 74 % yield. ¹H NMR (400 MHz, CDCl₃) δ 8.30 (dd, *J* = 8.9, 1.7 Hz, 2H), 7.72–7.63 (m, 6H), 7.54 (dd, *J* = 11.4, 8.9 Hz, 2H), 7.42–7.36 (m, 8H), 7.32–7.26 (m, 6H), 7.25–7.22 (m, 2H), 6.71 (d, *J* = 8.5 Hz, 2H), 6.61 (dd, *J* = 8.5, 7.4 Hz, 2H). ³¹P NMR (162 MHz, CDCl₃) δ 28.1. Spectral properties were in agreement with those previously reported.



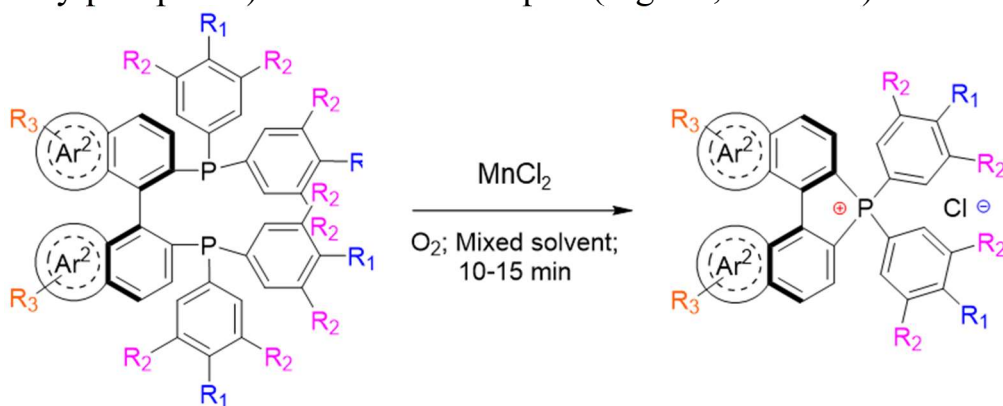
8. General synthesis of 5,5'-substituted (*S*)-BINAPO: In a 25 mL Schlenk tube was placed Dibromo-BINAPO (1.0 g, 1.23 mmol), substituted benzoboric acid (3.0 eq), K₂CO₃ (6.0 eq), Pd(PPh₃)₄ (5 mol%), and 25 mL of mixed toluene/EtOH/H₂O (10/5/10) solvent. The mixture solution was reacted at 90 °C under an Ar atmosphere for about 24 hours. The organic phase was extracted successively with dilute hydrochloric acid and dichloromethane. The organic

Supporting information

phase was dried with anhydrous MgSO_4 and filtered. The solvent was removed by decompressing vaporization. The resulting residue without purified and used next reducing reaction.



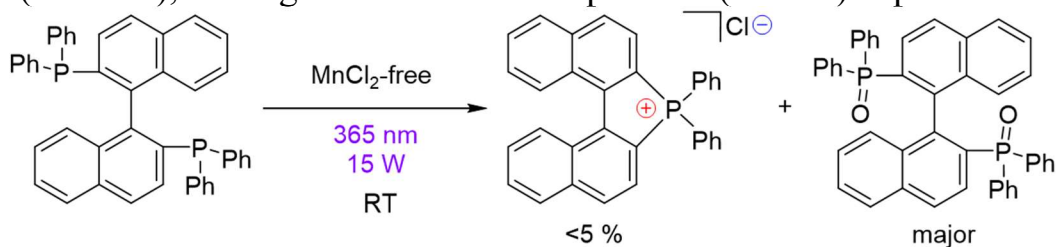
9. General synthesis of 5,5'-substituted (*S*)-BINAP: In a 25 mL Schlenk tube was placed unpurified 5,5'-substituted (*S*)-BINAPO (1.0 g, 35.0 mmol), PPh_3 (2.2 eq), HSiCl_3 (3.0 eq), and 15 mL of dry toluene. The mixture solution was reacted at 90 °C under an Ar atmosphere for about 12 hours. The organic phase was extracted successively with brine and dichloromethane. The organic phase was dried with anhydrous MgSO_4 and filtered. The solvent was removed by decompressing vaporization. The organic phase was dried with anhydrous MgSO_4 and filtered. The solvent was removed by decompressing vaporization. The resulting residue was purified by column chromatography with PE: CH_2Cl_2 (10:1), and then the white solid powder was obtained with 85 % yield (based on Dibromo-BINAPO). The stereochemistry was preserved throughout the synthetic sequence, which was also proved by single crystal diffraction structure (*S*)-(5,5'-di-*p*-tolyl-[1,1'-binaphthalene]-2,2'-diyl)bis(diphenylphosphane) and references report (Fig. S6, Table S2).



10. General synthesis of substituted achiral phosphoniums and phospha[5]helicenes: In a 25 mL Schlenk tube was placed diphosphine ligand substrate (0.2 mmol), MnCl_2 (3.0 eq), and 15 mL of dry mixed solvent ($v_{\text{CHCl}_3}:v_{\text{EtOH}}=2:1$). The mixture solution was reacted at room temperature or heating (30 °C/RT: 1b-3b, 50 °C: 4b-7b; 9b-17b, 80 °C: 20b-22b) under an O_2 atmosphere (1 bar) for 5-10 minutes until the starting material was completely consumed (the solution color transformed into a deep claybank after substrate completely consumed). The organic phase was extracted successively with saturated brine/deionized water and dichloromethane. The organic layer was washed 3 times with saturated brine/deionized water to remove residual Mn(II) ions. The organic phase is dried with anhydrous MgSO_4 and filtered. The solvent was removed by decompressing vaporization. The resulting residue was purified by column chromatography with CH_2Cl_2 :EtOH (10:1 to 5:1), and then the yellow/white solid powder was obtained. The structure and purity were

Supporting information

identified by nuclear magnetic resonance (^1H , ^{31}P , ^{13}C NMR), single-crystal X-ray diffraction (SCXRD), and high-resolution mass spectrum (HRMS) experiments.

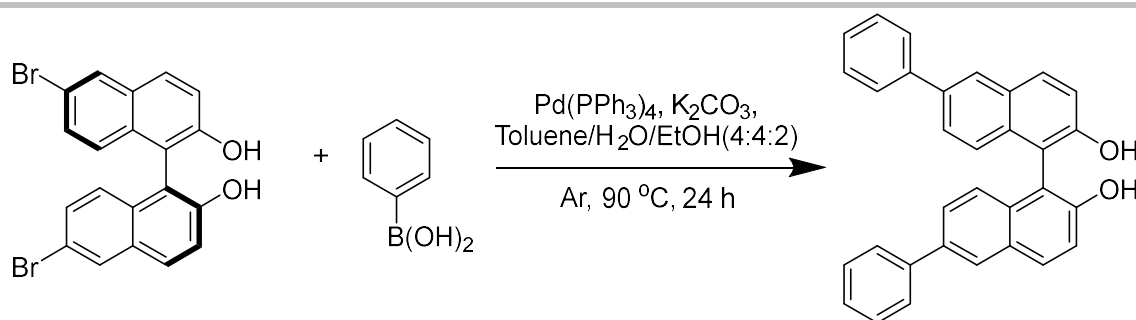


11. General operation for photo-induced cyclization of (*S*)-BINAP

In a 25 mL quartz glass tube was placed BINAP ligand substrate (31.2 mg, 0.05 mmol) and halogen additives (0/1.0/2.0 eq: pyridine hydrochloride or excess hydrochloric acid), and dry mixed solvent ($v_{\text{CHCl}_3}:v_{\text{EtOH}}=2:1$, 5 mL). The solution was stirred at room temperature under 365 nm radiation (15 W UV-lamp) in the air for 30 min.

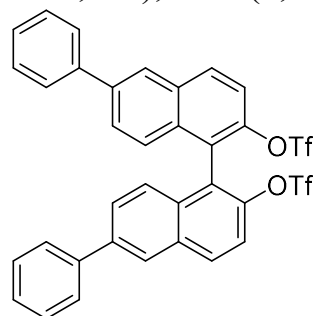
12. General preparation of enantiomeric $[2\text{b}]^+[\text{Cl}]^-$ at low temperature (-10 to -15 °C)

In a 25 mL Schlenk tube was placed diphosphine ligand substrate (0.2 mmol), MnCl_2 (1.0 eq), and 10 mL of dry mixed solvent ($v_{\text{CHCl}_3}:v_{\text{EtOH}}=2:1$) at -15 °C (ice-salt baths). The mixture solution was stirred at -15 °C for 15 min in O_2 . The excess MnCl_2 (2.0 eq) was added to aforesaid reaction solution. The mixture was stirred at 30 °C until the color changed to yellow (radical reaction was initiated, about 1 minute), and the Schlenk tube further was transferred to ice-salt baths and reacted at -15 °C for 30 min. The crude product was purified by column chromatography (the sandwich-type chromatographic column was filled with flowing cooling liquid) with cooling solvent $\text{CH}_2\text{Cl}_2:\text{EtOH}$ (5:1) at -10 °C. The DCM solvent was removed by decompressing vaporization in ice-salt baths condition (-15 °C). The product was stored in residual EtOH solvent at -15 °C in the ice-salt baths.



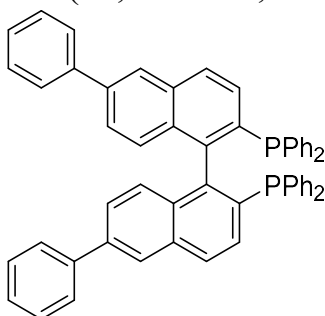
Synthesis of substituted (*Rac*)-6,6'-diphenyl-[1,1'-binaphthalene]-2,2'-diol (*Rac*)-9b1):

In a 50 mL Schlenk tube were placed 6,6'-dibromo-[1,1'-binaphthalene]-2,2'-diol (1.0 g, 2.25 mmol), benzoboric acid (3.0 eq), K₂CO₃ (6.0 eq), Pd(PPh₃)₄ (5 mol%), and a 20 mL of mixed toluene/EtOH/H₂O (8/4/8) solvent. The mixture solution was reacted at 90 °C under an Ar atmosphere for about 24 hours. The organic phase was extracted successively with dilute hydrochloric acid and dichloromethane. The organic phase was dried with anhydrous MgSO₄ and filtered. The solvent was removed by decompressing vaporization. The resulting residue was purified by column chromatography with PE:CH₂Cl₂ (1:3), and then the white solid powder was obtained with 87 % yield. ¹H NMR (400 MHz, CDCl₃) δ 8.10 (d, *J* = 1.8 Hz, 2H), 8.03 (d, *J* = 9.0 Hz, 2H), 7.69 – 7.65 (m, 4H), 7.58 (dd, *J* = 8.7, 1.9 Hz, 2H), 7.48 – 7.40 (m, 6H), 7.36 (dt, *J* = 9.2, 4.2 Hz, 2H), 7.26 (d, *J* = 8.7 Hz, 2H), 5.12 (s, 2H).



Synthesis of substituted (*Rac*)-9b2 (-OTf): Prepared by general method with 95 % yield.

¹H NMR (400 MHz, CDCl₃) δ 8.20 (dd, *J* = 5.4, 3.7 Hz, 4H), 7.69 (ddd, *J* = 13.5, 9.4, 5.2 Hz, 8H), 7.48 (t, *J* = 7.5 Hz, 4H), 7.38 (dd, *J* = 16.0, 8.1 Hz, 4H).

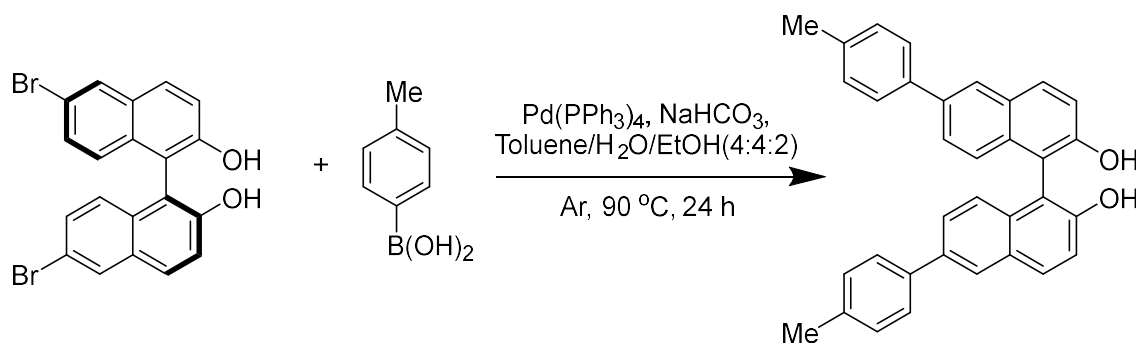


Synthesis of substituted (*Rac*)-9b3 (-PPh₂): Prepared by general method with 51 % yield.

¹H NMR (400 MHz, CDCl₃) δ 8.03 (d, *J* = 1.7 Hz, 2H), 7.95 (d, *J* = 8.5 Hz, 2H), 7.63–7.59 (m, 4H), 7.49 – 7.43 (m, 6H), 7.36 (ddd, *J* = 7.3, 3.9, 1.2 Hz, 2H), 7.21–7.06 (m, 22H), 6.89 (d, *J* = 8.8 Hz, 2H). ³¹P NMR (162 MHz, CDCl₃) δ -15.1. ¹³C NMR (101 MHz, CDCl₃) δ 141.0 (s), 139.1 (s), 134.4 (d, *J* = 21.8 Hz), 133.7 (s), 133.5 (s), 133.2 – 132.6 (br), 131.0 (s), 128.9 (s), 128.6 (d, *J* = 3.2 Hz), 128.2 (d, *J* = 3.2 Hz), 127.7 (s), 127.4 (d, *J* = 2.2 Hz), 127.4 (s), 125.6 (d, *J* = 16.6 Hz). HRMS found for [C₅₆H₄₀P₂]+H⁺: *m/z* = 775.2683, calcd

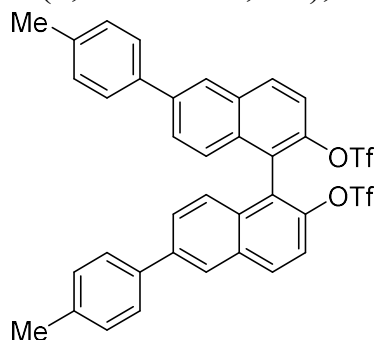
Supporting information

for [C₅₆H₄₀P₂]⁺H⁺: m/z = 775.2651.



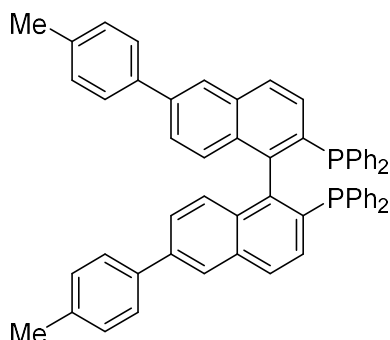
Synthesis of substituted (*Rac*)-6,6'-diphenyl-[1,1'-binaphthalene]-2,2'-diol ((*S*)-10b1):

In a 50 mL Schlenk tube were placed 6,6'-dibromo-[1,1'-binaphthalene]-2,2'-diol (1.0 g, 2.25 mmol), *p*-tolylboronic acid (3.0 eq), NaHCO₃ (6.0 eq), Pd(PPh₃)₄ (5 mol%), and 20 mL of mixed toluene/EtOH/H₂O (8/4/8) solvent. The mixture solution was reacted at 90 °C under an Ar atmosphere for about 24 hours. The organic phase was extracted successively with dilute hydrochloric acid and dichloromethane. The organic phase was dried with anhydrous MgSO₄ and filtered. The solvent was removed by decompressing vaporization. The resulted residue was purified by column chromatography with PE:CH₂Cl₂ (1:3), and then the white solid powder was obtained with 78 % yield. ¹H NMR (400 MHz, CDCl₃) δ 8.08 (d, *J* = 1.7 Hz, 2H), 8.04 (d, *J* = 8.9 Hz, 2H), 7.60–7.55 (m, 6H), 7.42 (d, *J* = 8.9 Hz, 2H), 7.27 (d, *J* = 6.6 Hz, 4H), 7.25 (d, *J* = 4.6 Hz, 2H), 5.10 (s, 2H), 2.41 (s, 6H).



Synthesis of substituted (*Rac*)-10b2 (-OTf): Prepared by general method with 97 % yield.

¹H NMR (400 MHz, CDCl₃) δ 8.20–8.16 (m, 4H), 7.67 (dd, *J* = 8.9, 1.8 Hz, 2H), 7.64 (d, *J* = 9.1 Hz, 2H), 7.60 (d, *J* = 8.2 Hz, 4H), 7.34 (d, *J* = 8.8 Hz, 2H), 7.29 (d, *J* = 7.9 Hz, 4H), 2.41 (s, 6H).

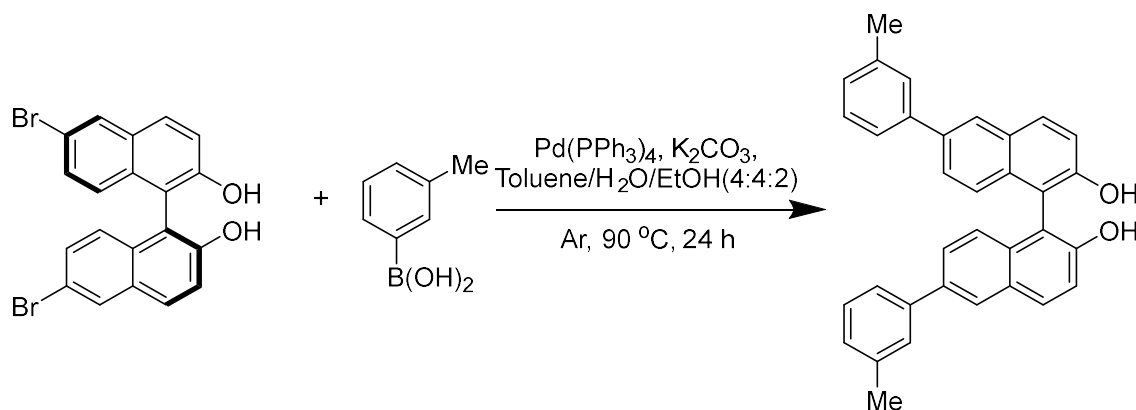


Synthesis of substituted (*Rac*)-10b3 (-PPh₂): Prepared by general method with 47 % yield.

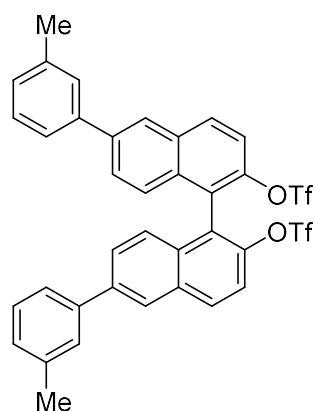
¹H NMR (400 MHz, CDCl₃) δ 8.01 (d, *J* = 1.7 Hz, 2H), 7.93 (d, *J* = 8.5 Hz, 2H), 7.51 (d, *J*

Supporting information

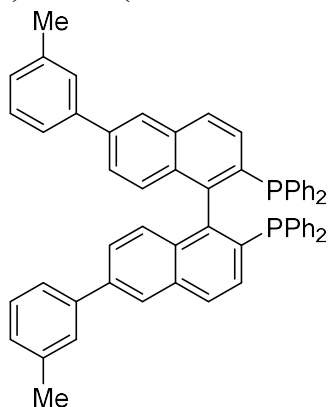
= 8.2 Hz, 4H), 7.49–7.44 (m, 2H), 7.27 (s, 4H), 7.20–7.06 (m, 23H), 6.88 (d, $J = 8.8$ Hz, 2H), 2.40 (s, 6H). ^{31}P NMR (162 MHz, CDCl_3) δ -15.1. ^{13}C NMR (101 MHz, CDCl_3) δ 139.0 (s), 138.1 (s), 137.3 (s), 134.4 (d, $J = 18.8$ Hz), 133.7 (s), 133.6 (d, $J = 5.6$ Hz), 133.2 – 132.7 (br), 132.5 (s), 130.9 (s), 129.7 (s), 129.6 (s), 128.2 (d, $J = 28.3$ Hz), 127.3 (d, $J = 3.7$ Hz), 127.2 (s), 125.3 (d, $J = 17.0$ Hz), 21.2 (s). HRMS found for $[\text{C}_{58}\text{H}_{44}\text{P}_2]^+\text{H}^+$: $m/z = 803.2996$, calcd for $[\text{C}_{58}\text{H}_{44}\text{P}_2]^+\text{H}^+$: $m/z = 803.2914$.



Synthesis of substituted 6,6'-di-m-tolyl-[1,1'-binaphthalene]-2,2'-diol (11b1): Prepared by general method with 74 % yield. ^1H NMR (400 MHz, CDCl_3) δ 8.10 (d, $J = 1.8$ Hz, 2H), 8.05 (d, $J = 8.9$ Hz, 2H), 7.59 (dd, $J = 8.7, 1.9$ Hz, 2H), 7.45 (dd, $J = 15.8, 9.1$ Hz, 6H), 7.35 (t, $J = 7.5$ Hz, 2H), 7.27 (s, 1H), 7.25 (s, 1H), 7.18 (d, $J = 7.5$ Hz, 2H), 5.12 (s, 2H), 2.44 (s, 6H).

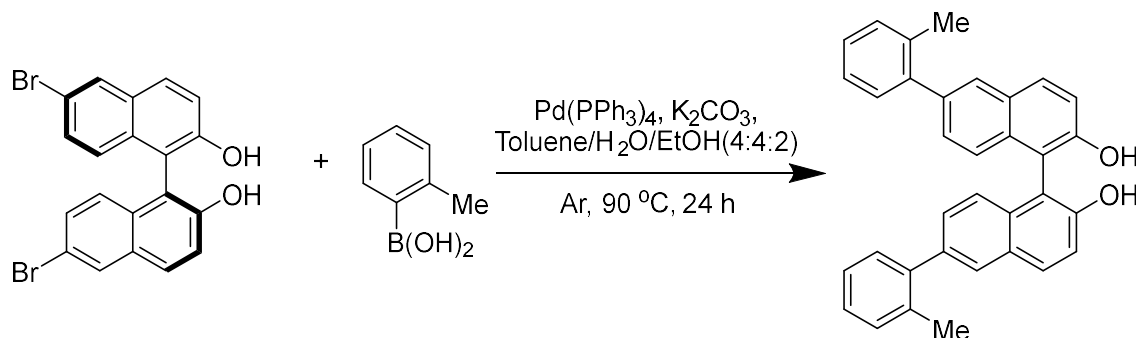


Synthesis of substituted (*Rac*)-11b2 (-OTf): Prepared by general method with 97 % yield. ^1H NMR (400 MHz, CDCl_3) δ 8.22–8.17 (m, 4H), 7.70–7.62 (m, 4H), 7.51 (d, $J = 9.8$ Hz, 4H), 7.37 (dd, $J = 14.8, 8.1$ Hz, 4H), 7.22 (d, $J = 7.4$ Hz, 2H), 2.45 (s, 6H).

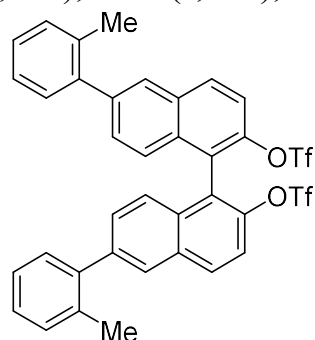


Supporting information

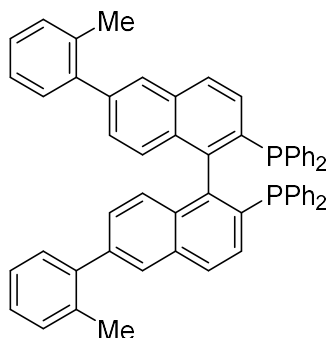
Synthesis of substituted (*Rac*)-11b3 (-PPh₂): Prepared by general method with 40 % yield. ¹H NMR (400 MHz, CDCl₃) δ 8.02 (d, *J* = 1.7 Hz, 2H), 7.95 (d, *J* = 8.5 Hz, 2H), 7.49 – 7.39 (m, 6H), 7.34 (dd, *J* = 8.0, 3.9 Hz, 2H), 7.20–7.07 (m, 24H), 6.89 (d, *J* = 8.7 Hz, 2H), 2.44 (s, 6H). ³¹P NMR (162 MHz, CDCl₃) δ -15.11. ¹³C NMR (101 MHz, CDCl₃) δ 140.96 (s), 139.18 (s), 138.41 – 138.27 (br), 134.75 – 134.07 (br), 133.54 (s), 133.25 – 132.54 (br), 130.92 (s), 128.75 (s), 128.16 (d, *J* = 28.2 Hz), 125.56 (d, *J* = 4.7 Hz), 124.49 (s), 21.63 (s). HRMS found for [C₅₈H₄₄P₂]+H⁺: *m/z* = 803.2996, calcd for [C₅₈H₄₄P₂]+H⁺: *m/z* = 803.2926.



Synthesis of substituted 6,6'-di-*o*-tolyl-[1,1'-binaphthalene]-2,2'-diol (12b1): Prepared by general method with 71% yield. ¹H NMR (400 MHz, CDCl₃) δ 7.99 (d, *J* = 8.9 Hz, 2H), 7.84 (d, *J* = 1.5 Hz, 2H), 7.42 (d, *J* = 8.9 Hz, 2H), 7.34 (dd, *J* = 8.6, 1.7 Hz, 2H), 7.29 (dd, *J* = 5.8, 3.6 Hz, 6H), 7.28–7.24 (m, 4H), 5.13 (s, 2H), 2.31 (s, 6H).



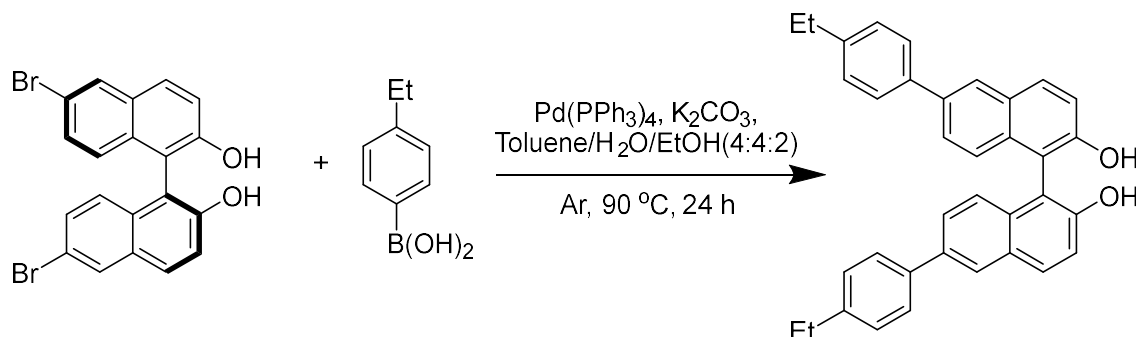
Synthesis of substituted (*Rac*)-12b2 (-OTf): Prepared by general method with 97% yield. ¹H NMR (400 MHz, CDCl₃) δ 8.15 (d, *J* = 9.1 Hz, 2H), 7.94 (d, *J* = 1.4 Hz, 2H), 7.66 (d, *J* = 9.1 Hz, 2H), 7.44 (dd, *J* = 8.7, 1.7 Hz, 2H), 7.33 (ddd, *J* = 11.5, 7.5, 5.2 Hz, 10H), 2.29 (s, 6H).



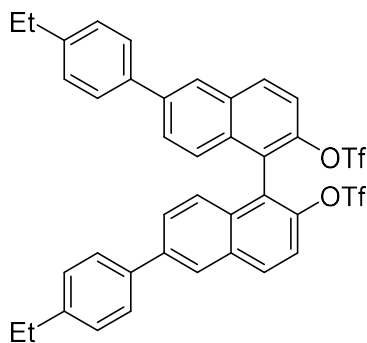
Synthesis of substituted (*Rac*)-12b3 (-PPh₂): Prepared by the general method with 42% yield. ¹H NMR (400 MHz, CDCl₃) δ 7.91 (d, *J* = 8.5 Hz, 2H), 7.76 (s, 2H), 7.51–7.47 (m, 2H), 7.28–7.24 (m, 10H), 7.19–7.12 (m, 20H), 6.91 (d, *J* = 1.0 Hz, 2H), 2.21 (s, 6H). ³¹P

Supporting information

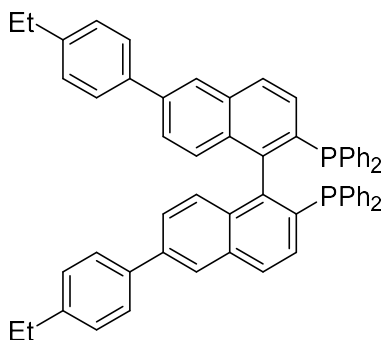
NMR (162 MHz, CDCl₃) δ -15.3. ¹³C NMR (101 MHz, CDCl₃) δ 141.7 (s), 140.1 (s), 135.6 (s), 134.9 – 133.4 (br), 133.0 (d, J = 21.5 Hz), 132.8 (d, J = 9.8 Hz), 130.9 (s), 130.3 (s), 129.9 (s), 128.6 (s), 128.4 – 127.9 (br), 127.8 – 127.1 (br), 125.8 (s), 20.6 (s). HRMS found for [C₅₈H₄₄P₂]⁺H⁺: m/z = 803.2996, calcd for [C₅₈H₄₄P₂]⁺H⁺: m/z = 803.2975.



Synthesis of substituted (*Rac*)-6,6'-bis(4-ethylphenyl)-[1,1'-binaphthalene]-2,2'-diol ((*Rac*)-13b1): Prepared by the general method with 81% yield. ¹H NMR (400 MHz, CDCl₃) δ 8.09 (d, J = 1.7 Hz, 2H), 8.04 (d, J = 9.0 Hz, 2H), 7.59 (ddd, J = 7.5, 4.4, 1.9 Hz, 6H), 7.43 (d, J = 8.9 Hz, 2H), 7.31 (s, 4H), 7.27 (s, 1H), 7.25 (s, 1H), 5.10 (s, 2H), 2.71 (q, J = 7.6 Hz, 4H), 1.28 (d, J = 7.6 Hz, 6H).



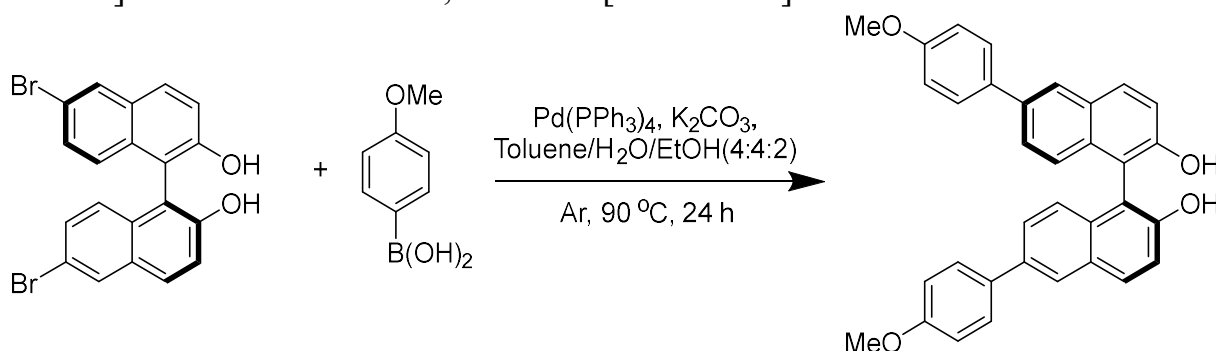
Synthesis of substituted (*Rac*)-13b2 (-OTf): Prepared by the general method with 92% yield. ¹H NMR (400 MHz, CDCl₃) δ 8.18 (dd, J = 5.4, 3.7 Hz, 4H), 7.66 (ddd, J = 11.8, 8.5, 2.2 Hz, 8H), 7.33 (dd, J = 10.5, 8.6 Hz, 6H), 2.72 (q, J = 7.6 Hz, 4H), 1.29 (t, J = 7.6 Hz, 6H).



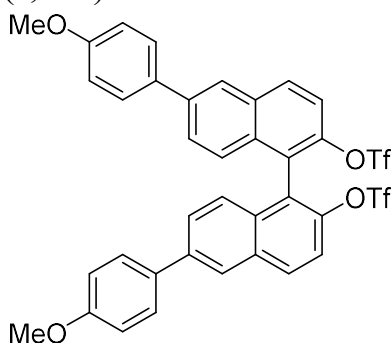
Synthesis of substituted (*Rac*)-13b3 (-PPh₂): Prepared by the general method with 42% yield. ¹H NMR (400 MHz, CDCl₃) δ 8.01 (d, J = 1.7 Hz, 2H), 7.93 (d, J = 8.5 Hz, 2H), 7.53 (d, J = 8.2 Hz, 4H), 7.50–7.46 (m, 2H), 7.27 (d, J = 8.1 Hz, 4H), 7.19–7.07 (m, 22H), 6.90 (d, J = 8.8 Hz, 2H), 2.68 (q, J = 7.6 Hz, 4H), 1.27 (t, J = 7.6 Hz, 6H). ³¹P NMR (162 MHz, CDCl₃) δ -15.1 (s). ¹³C NMR (101 MHz, CDCl₃) δ 144.9 (d, J = 41.8 Hz), 143.6 (s), 139.0

Supporting information

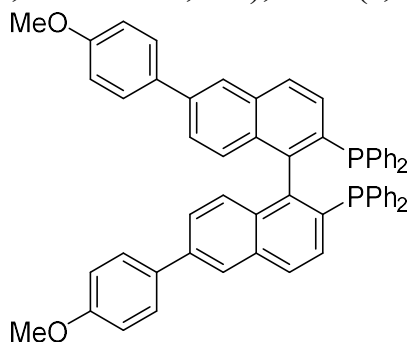
(s), 138.3 (s), 137.89 (d, $J = 11.9$ Hz), 137.3 (d, $J = 13.8$ Hz), 135.5 (d, $J = 6.0$ Hz), 134.8 – 134.0 (br), 133.56 (s), 133.3 – 132.6 (br), 132.5 (s), 130.9 (s), 128.2 (d, $J = 31.3$ Hz), 127.8 (d, $J = 26.1$ Hz), 127.3 (s), 125.4 (d, $J = 16.9$ Hz), 28.6 (s), 15.6 (s). HRMS found for $[C_{60}H_{48}P_2]^+H^+$: $m/z = 831.3309$, calcd for $[C_{58}H_{44}P_2]^+H^+$: $m/z = 831.3398$.



Synthesis of substituted (*S*)-6,6'-bis(4-methoxyphenyl)-[1,1'-binaphthalene]-2,2'-diol ((*S*)-14b1): In a 50 mL Schlenk tube were placed 6,6'-dibromo-[1,1'-binaphthalene]-2,2'-diol (1.0 g, 2.25 mmol), (4-methoxyphenyl)boronic acid (3.0 eq), NaHCO₃ (6.0 eq), Pd(PPh₃)₄ (5 mol%), and 20 mL of mixed toluene/EtOH/H₂O (8/4/8) solvent. The mixture solution was reacted at 90 °C under an Ar atmosphere for 24 hours. The organic phase was extracted successively with dilute hydrochloric acid and dichloromethane. The organic phase was dried with anhydrous MgSO₄ and filtered. The solvent was removed by decompressing vaporization. The resulted residue was purified by column chromatography with PE:CH₂Cl₂ (1:3), and then the white solid powder was obtained with 84% yield. ¹H NMR (400 MHz, CDCl₃) δ 8.03 (d, $J = 1.7$ Hz, 2H), 8.00 (d, $J = 8.9$ Hz, 2H), 7.62–7.57 (m, 4H), 7.54 (dd, $J = 8.7, 1.9$ Hz, 2H), 7.40 (d, $J = 8.9$ Hz, 2H), 7.24 (d, $J = 8.9$ Hz, 2H), 7.02–6.96 (m, 4H), 5.13 (s, 2H), 3.84 (s, 6H).

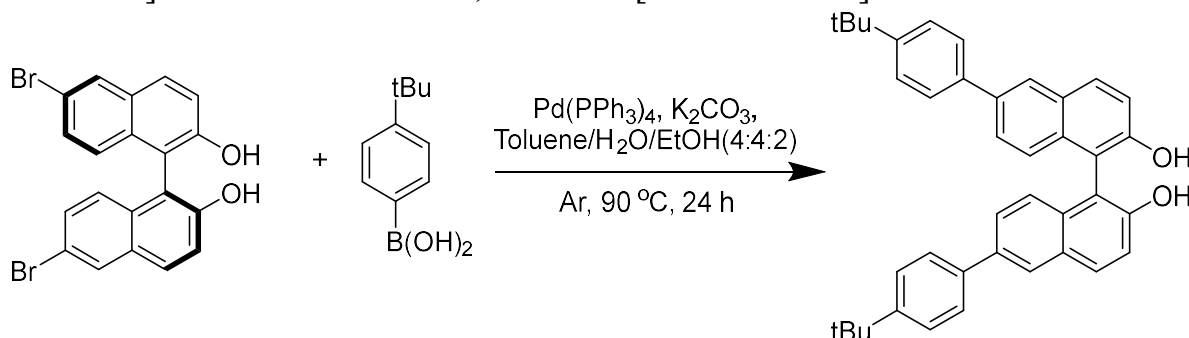


Synthesis of substituted (*Rac*)-14b2 (-OTf): Prepared by the general method with 91% yield. ¹H NMR (400 MHz, CDCl₃) δ 8.20 – 8.12 (m, 4H), 7.64 (dd, $J = 8.5, 5.9$ Hz, 8H), 7.33 (d, $J = 8.8$ Hz, 2H), 7.01 (d, $J = 8.7$ Hz, 4H), 3.86 (s, 6H).

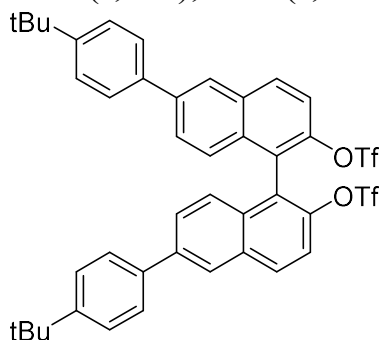


Supporting information

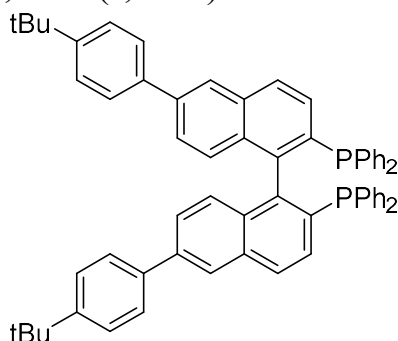
Synthesis of substituted (*Rac*)-14b3 (-PPh₂): Prepared by the general method with 45% yield. ¹H NMR (400 MHz, CDCl₃) δ 7.97 (d, *J* = 1.7 Hz, 2H), 7.93 (d, *J* = 8.5 Hz, 2H), 7.59–7.51 (m, 4H), 7.49–7.44 (m, 2H), 7.21–7.05 (m, 22H), 7.01–6.97 (m, 4H), 6.88 (d, *J* = 8.8 Hz, 2H), 3.85 (s, 6H). ³¹P NMR (162 MHz, CDCl₃) δ -15.2. ¹³C NMR (101 MHz, CDCl₃) δ 159.3 (s), 145.0 (d, *J* = 42.2 Hz), 138.7 (s), 135.4 (d, *J* = 8.1 Hz), 134.8 – 134.0 (br), 133.5 (d, *J* = 16.0 Hz), 133.2 – 132.6 (br), 133.2 – 132.7 (br), 132.6 – 132.0 (br), 130.9 (s), 128.2 (d, *J* = 19.2), 127.6 (s), 125.1 (d, *J* = 44.4 Hz), 114.3 (s), 55.4 (s). HRMS found for [C₅₈H₄₄P₂O₂]+H⁺: *m/z* = 835.2895, calcd for [C₅₈H₄₄P₂O₂]+H⁺: *m/z* = 835.2841.



Synthesis of substituted 6,6'-bis(4-(tert-butyl)phenyl)-[1,1'-binaphthalene]-2,2'-diol (15b1): Prepared by general method with 76% yield. ¹H NMR (400 MHz, CDCl₃) δ 8.09 (d, *J* = 1.7 Hz, 2H), 8.04 (d, *J* = 8.9 Hz, 2H), 7.64 – 7.57 (m, 6H), 7.49 (d, *J* = 8.4 Hz, 4H), 7.42 (d, *J* = 8.9 Hz, 2H), 7.25 (s, 2H), 5.11 (s, 2H), 1.37 (s, 18H).



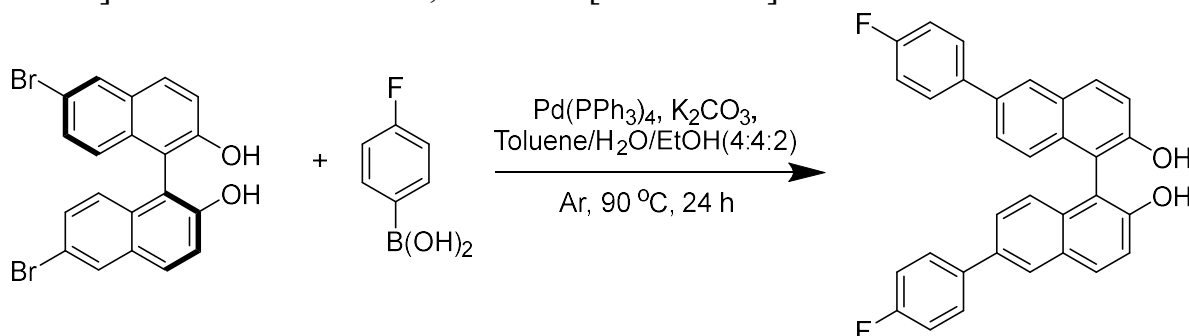
Synthesis of substituted (*Rac*)-15b2 (-OTf): Prepared by general method (3) with 97% yield. ¹H NMR (400 MHz, CDCl₃) δ 8.18 (dd, *J* = 5.3, 3.7 Hz, 4H), 7.70–7.63 (m, 8H), 7.51 (d, *J* = 8.5 Hz, 4H), 7.36 (s, 2H), 1.37 (s, 18H).



Synthesis of substituted (*Rac*)-15b3 (-PPh₂): Prepared by general method with 50% yield. ¹H NMR (400 MHz, CDCl₃) δ 8.02 (s, 2H), 7.94 (d, *J* = 8.5 Hz, 2H), 7.56 (d, *J* = 8.4 Hz, 4H), 7.50–7.45 (m, 6H), 7.21–7.07 (m, 22H), 6.90 (d, *J* = 8.7 Hz, 2H), 1.37 (s, 18H). ³¹P NMR (162 MHz, CDCl₃) δ -15.2. ¹³C NMR (101 MHz, CDCl₃) δ 150.5 (s), 145.0 (d, *J* =

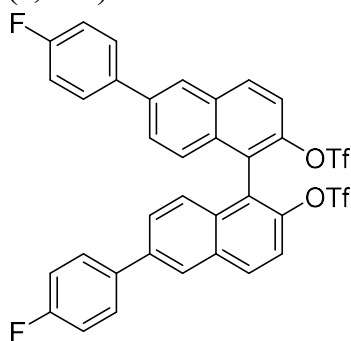
Supporting information

42.0 Hz), 138.9 (s), 138.1 (s), 137.4 (d, $J = 13.5$ Hz), 135.5 (s), 135.0 – 133.9 (br), 133.6 (s), 133.2 – 132.7 (br), 132.6 (d, $J = 5.3$ Hz), 130.9 (s), 128.4 (d, $J = 7.3$ Hz), 128.0 (d, $J = 35.2$ Hz), 127.0 (s), 125.8 (s), 125.4 (d, $J = 14.3$ Hz), 34.6 (s), 31.4 (s). HRMS found for $[\text{C}_{64}\text{H}_{56}\text{P}_2]^+\text{H}^+$: $m/z = 887.3935$, calcd for $[\text{C}_{64}\text{H}_{56}\text{P}_2]^+\text{H}^+$: $m/z = 887.3968$.



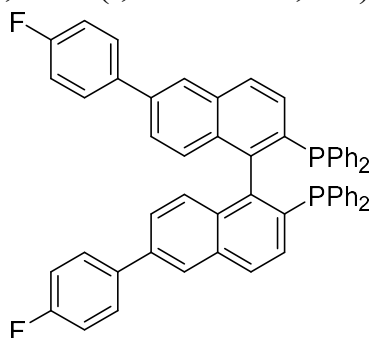
Synthesis of substituted 6,6'-bis(4-fluorophenyl)-[1,1'-binaphthalene]-2,2'-diol (16b1):

Prepared by general method with 83% yield. ^1H NMR (400 MHz, CDCl_3) δ 8.03 (t, $J = 5.5$ Hz, 4H), 7.64–7.59 (m, 4H), 7.52 (dd, $J = 8.7, 1.8$ Hz, 2H), 7.45–7.40 (m, 2H), 7.26–7.22 (m, 2H), 7.18–7.11 (m, 4H), 5.12 (s, 2H).



Synthesis of substituted (Rac)-16b2 (-OTf): Prepared by general method with 95% yield.

^1H NMR (400 MHz, CDCl_3) δ 8.20 (d, $J = 9.0$ Hz, 2H), 8.15 (d, $J = 1.7$ Hz, 2H), 7.69–7.61 (m, 8H), 7.35 (d, $J = 8.8$ Hz, 2H), 7.18 (t, $J = 8.7$ Hz, 4H).

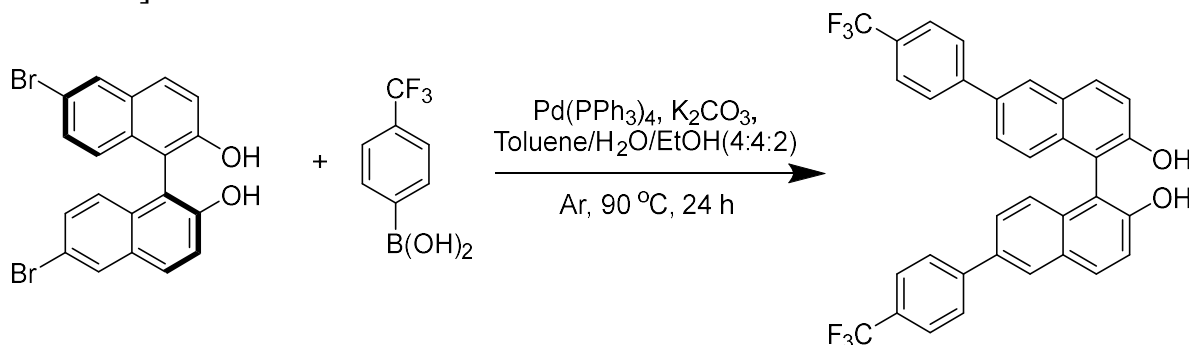


Synthesis of substituted (Rac)-16b3 (-PPh₂): Prepared by general method with 49% yield.

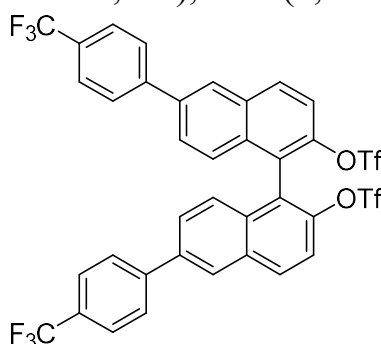
^1H NMR (400 MHz, CDCl_3) δ 7.95 (dd, $J = 12.3, 5.1$ Hz, 4H), 7.58–7.51 (m, 4H), 7.50–7.46 (m, 2H), 7.20–7.11 (m, 20H), 7.09–7.05 (m, 7H), 6.87 (dd, $J = 6.5, 3.8$ Hz, 2H). ^{31}P NMR (162 MHz, CDCl_3) δ -14.8. ^{13}C NMR (101 MHz, CDCl_3) δ 163.8 (s), 161.4 (s), 145.0 (d, $J = 3.5$ Hz), 144.7 (d, $J = 20.9$ Hz), 138.1 (s), 137.7 (s), 137.0 (d, $J = 3.3$ Hz), 136.0 (d, $J = 8.4$ Hz), 134.6 (d, $J = 4.9$ Hz), 134.4 (d, $J = 10.9$ Hz), 133.5 (s), 133.2 – 132.7 (br), 132.5 (s), 131.4 (d, $J = 8.1$ Hz), 131.2 (s), 128.9 (d, $J = 8.0$ Hz), 128.8 – 127.5 (br), 125.4 (d, $J = 22.7$ Hz). HRMS found for $[\text{C}_{56}\text{H}_{38}\text{P}_2\text{F}_2]^+\text{H}^+$: $m/z = 811.2495$, calcd for

Supporting information

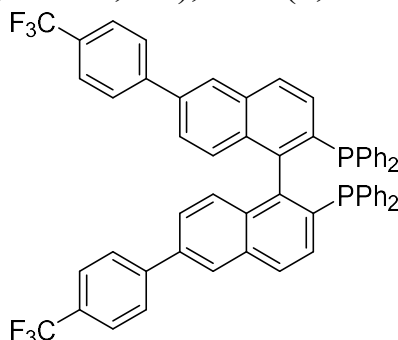
[C₅₆H₃₈P₂F₂]+H⁺: m/z = 811.2439.



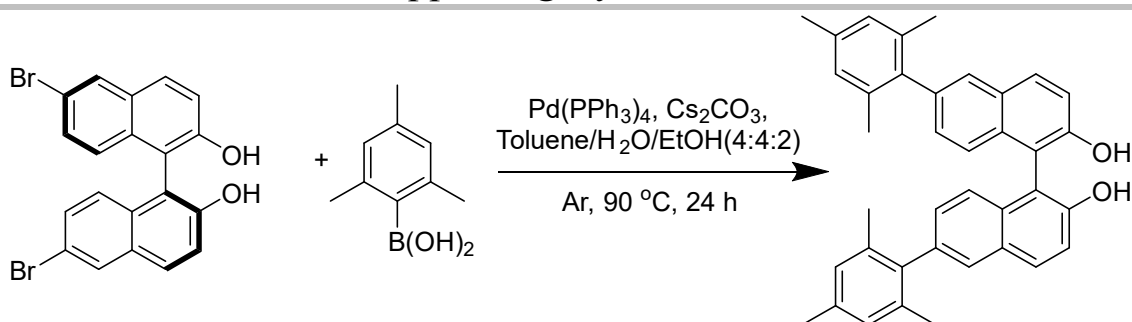
Synthesis of substituted 6,6'-bis(4-(trifluoromethyl)phenyl)-[1,1'-binaphthalene]-2,2'-diol (17b1): Prepared by general method with 85% yield. ¹H NMR (400 MHz, CDCl₃) δ 8.13 (d, *J* = 1.6 Hz, 2H), 8.08 (d, *J* = 9.0 Hz, 2H), 7.74 (dd, *J* = 22.6, 8.4 Hz, 9H), 7.58 (dd, *J* = 8.7, 1.8 Hz, 2H), 7.46 (d, *J* = 8.9 Hz, 2H), 7.28 (d, *J* = 8.7 Hz, 2H), 5.15 (s, 2H).



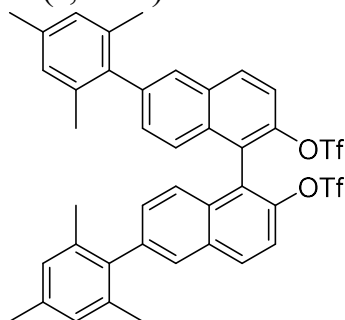
Synthesis of substituted (*Rac*)-17b2 (-OTf): Prepared by general method with 92% yield. ¹H NMR (400 MHz, CDCl₃) δ 8.24 (d, *J* = 9.1 Hz, 4H), 7.81 (d, *J* = 8.3 Hz, 4H), 7.75 (d, *J* = 8.4 Hz, 4H), 7.67 (dd, *J* = 8.2, 2.4 Hz, 4H), 7.39 (d, *J* = 8.8 Hz, 2H).



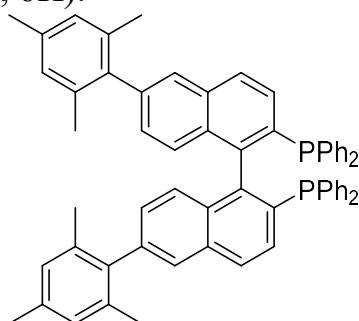
Synthesis of substituted (*Rac*)-17b3 (-PPh₂): Prepared by general method with 35% yield. ¹H NMR (400 MHz, CDCl₃) δ 8.05 (s, 2H), 7.98 (d, *J* = 8.5 Hz, 2H), 7.71 (d, *J* = 5.3 Hz, 8H), 7.51 (d, *J* = 8.6 Hz, 2H), 7.21–7.07 (m, 22H), 6.88 (d, *J* = 8.7 Hz, 2H). ³¹P NMR (162 MHz, CDCl₃) δ -14.8. ¹³C NMR (101 MHz, CDCl₃) δ 144.7 (s), 144.3 (d, *J* = 10.9 Hz), 137.6 (s), 137.5 (s), 136.97 (d, *J* = 13.2 Hz), 134.6 (d, *J* = 11.0 Hz), 134.4 (d, *J* = 5.8 Hz), 133.4 (s), 133.0 (d, *J* = 10.1 Hz), 132.9 (s), 131.2 (s), 129.7 (s), 129.3 (s), 128.6 (d, *J* = 3.8 Hz), 128.4–128.0 (br), 127.9 (s), 127.6 (s), 126.2 (s), 125.8 (d, *J* = 3.7 Hz), 125.0 (s), 122.9 (s), 77.2 (s). HRMS found for [C₅₈H₃₈P₂F₆]+H⁺: m/z = 911.2431, calcd for [C₅₈H₃₈P₂F₆]+H⁺: m/z = 911.2449.



Synthesis of substituted 6,6'-dimesityl-[1,1'-binaphthalene]-2,2'-diol (18b1): Prepared by general methods with 67% yield. $^1\text{H NMR}$ (400 MHz, CDCl_3) δ 7.96 (d, $J = 8.9$ Hz, 2H), 7.67 (d, $J = 1.4$ Hz, 2H), 7.42 (d, $J = 8.9$ Hz, 2H), 7.31 (d, $J = 8.6$ Hz, 2H), 7.19–7.14 (m, 2H), 6.96 (s, 4H), 2.34 (s, 6H), 2.04 (s, 12H).

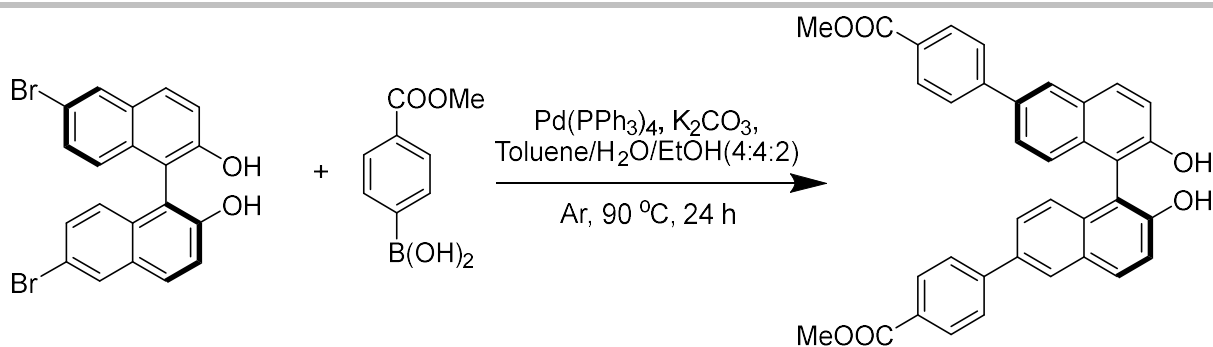


Synthesis of substituted (*Rac*)-18b2 (-OTf): Prepared by general method with 91% yield. $^1\text{H NMR}$ (400 MHz, CDCl_3) δ 8.11 (d, $J = 9.1$ Hz, 2H), 7.78 (d, $J = 1.3$ Hz, 2H), 7.64 (d, $J = 9.1$ Hz, 2H), 7.45 (d, $J = 8.6$ Hz, 2H), 7.29 (d, $J = 1.6$ Hz, 1H), 7.27 (s, 1H), 6.97 (s, 4H), 2.35 (s, 6H), 2.05 (s, 6H), 1.97 (s, 6H).

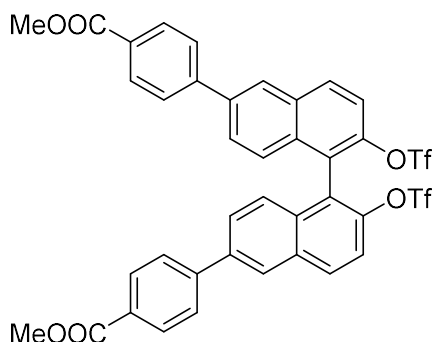


Synthesis of substituted (*Rac*)-18b3 (-PPh₂): Prepared by general method with 37% yield. $^1\text{H NMR}$ (400 MHz, CDCl_3) δ 7.88 (d, $J = 8.4$ Hz, 2H), 7.60 (d, $J = 1.4$ Hz, 2H), 7.49 (dd, $J = 8.5, 2.5$ Hz, 2H), 7.23–7.12 (m, 20H), 7.01 (d, $J = 8.6$ Hz, 2H), 6.93 (d, $J = 7.9$ Hz, 4H), 6.76 (dd, $J = 8.6, 1.7$ Hz, 2H), 2.33 (s, 6H), 1.99 (s, 6H), 1.91 (s, 6H). $^{31}\text{P NMR}$ (162 MHz, CDCl_3) δ -16.0. $^{13}\text{C NMR}$ (101 MHz, CDCl_3) δ 139.4 (s), 139.0 (d, $J = 77.2$ Hz), 138.7 (s), 136.7 (s), 136.3 (s), 136.1 (d, $J = 30.8$ Hz), 136.0 (s), 134.7 – 134.0 (br), 134.7 – 133.7 (br), 133.4 (s), 133.349 (s), 133.1 – 132.1 (br), 131.0 (s), 128.6 (s), 128.4 – 127.8 (br), 127.6 (d, $J = 23.4$ Hz), 21.0 (s), 20.9 (s). HRMS found for $[\text{C}_{62}\text{H}_{52}\text{P}_2]^+\text{H}^+$: $m/z = 859.3622$, calcd for $[\text{C}_{62}\text{H}_{52}\text{P}_2]^+\text{H}^+$: $m/z = 859.3684$.

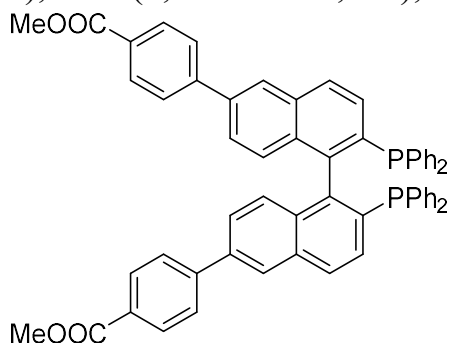
Supporting information



Synthesis of substituted dimethyl (*S*)-4,4'-(2,2'-dihydroxy-[1,1'-binaphthalene]-6,6'-diyl)dibenzoate (19b1**):** In a 50 mL Schlenk tube were placed 6,6'-dibromo-[1,1'-binaphthalene]-2,2'-diol (1.0 g, 2.25 mmol), (4-(methoxycarbonyl)phenyl)boronic acid (3.0 eq), NaHCO_3 (6.0 eq), $\text{Pd(PPh}_3)_4$ (5 mol%), and 20 mL of mixed toluene/EtOH/ H_2O (8/4/8) solvent. The mixture solution was reacted at 90 °C under an Ar atmosphere for about 24 hours. The organic phase was extracted successively with dilute hydrochloric acid and dichloromethane. The organic phase was dried with anhydrous MgSO_4 and filtered. The solvent was removed by decompressing vaporization. The resulted residue was purified by column chromatography with PE: CH_2Cl_2 (1:3), and then the white solid powder was obtained with 87% yield. $^1\text{H NMR}$ (400 MHz, CDCl_3) δ 8.10–8.01 (m, 8H), 7.70 (d, $J = 8.5$ Hz, 4H), 7.57 (dd, $J = 8.8, 1.9$ Hz, 2H), 7.44 (d, $J = 8.9$ Hz, 2H), 7.27 (s, 1H), 7.24 (s, 1H), 5.43 (s, 2H), 3.92 (s, 6H).



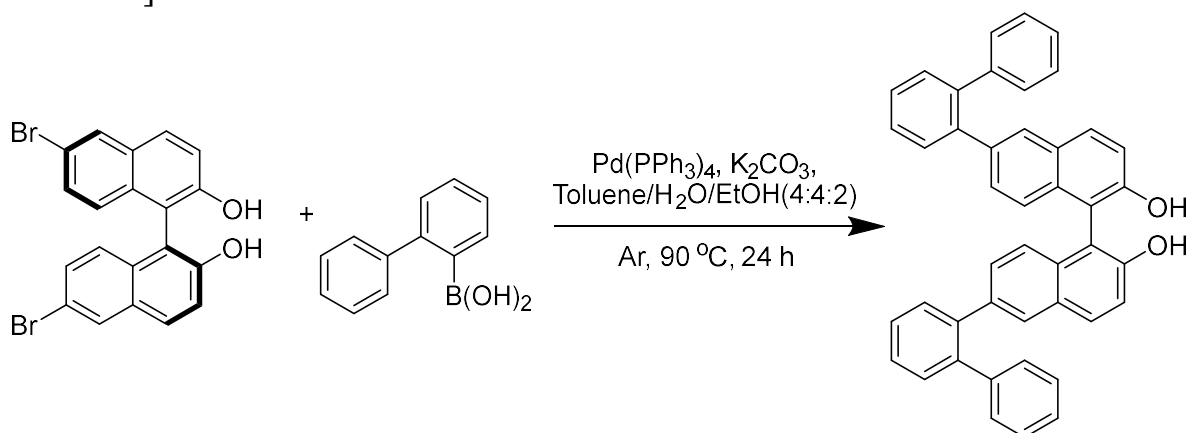
Synthesis of substituted (*Rac*)-19b2** (-OTf):** Prepared by general method with 87% yield. $^1\text{H NMR}$ (400 MHz, CDCl_3) δ 8.25 (dd, $J = 8.3, 5.4$ Hz, 4H), 8.19 – 8.13 (m, 4H), 7.81–7.75 (m, 4H), 7.73–7.66 (m, 4H), 7.38 (d, $J = 8.8$ Hz, 2H), 3.95 (s, 6H).



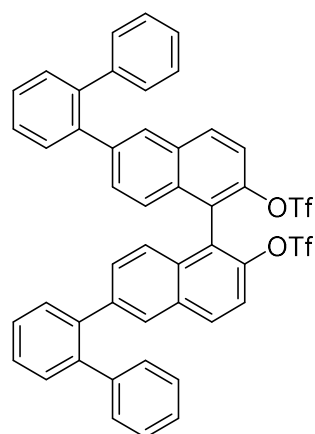
Synthesis of substituted (*Rac*)-19b3** (-PPh₂):** Prepared by general method with 34% yield. $^1\text{H NMR}$ (400 MHz, CDCl_3) δ 8.12 (d, $J = 8.5$ Hz, 4H), 8.07 (d, $J = 1.7$ Hz, 2H), 7.97 (d, $J = 8.4$ Hz, 2H), 7.67 (d, $J = 8.6$ Hz, 4H), 7.52–7.48 (m, 2H), 7.22–7.05 (m, 22H), 6.87 (d, $J = 8.8$ Hz, 2H), 3.95 (s, 6H). $^{31}\text{P NMR}$ (162 MHz, CDCl_3) δ -14.8. $^{13}\text{C NMR}$ (101 MHz,

Supporting information

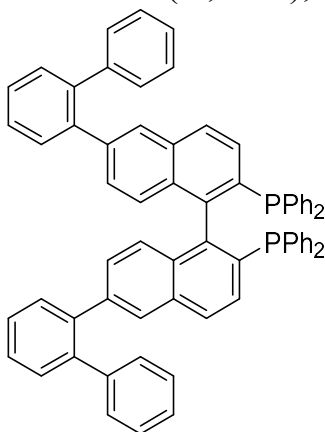
CDCl_3 δ 167.0 (s), 145.3 (s), 137.7 (s), 134.9 – 133.9 (br), 133.4 (s), 133.2 – 132.6 (br), 131.1 (s), 130.2 (s), 129.0 (s), 128.5 (d, $J = 6.4$ Hz), 128.4 – 127.6 (br), 127.2 (s), 126.1 (s), 125.1 (s), 52.2 (s). HRMS found for $[\text{C}_{60}\text{H}_{44}\text{P}_2\text{O}_4]^+\text{H}^+$: $m/z = 891.2793$, calcd for $[\text{C}_{60}\text{H}_{44}\text{P}_2\text{O}_4]^+\text{H}^+$: $m/z = 891.2805$.



Synthesis of substituted 6,6'-di([1,1'-biphenyl]-2-yl)-[1,1'-binaphthalene]-2,2'-diol (20b1): Prepared by general method with 72% yield. ^1H NMR (400 MHz, CDCl_3) δ 7.83 (d, $J = 8.9$ Hz, 2H), 7.74 (d, $J = 1.6$ Hz, 2H), 7.53–7.49 (m, 2H), 7.44 (dd, $J = 4.6, 2.4$ Hz, 6H), 7.31 (d, $J = 8.9$ Hz, 2H), 7.15 (m, 10H), 7.01 (dd, $J = 8.7, 1.8$ Hz, 2H), 6.93 (d, $J = 8.7$ Hz, 2H), 5.02 (s, 2H).



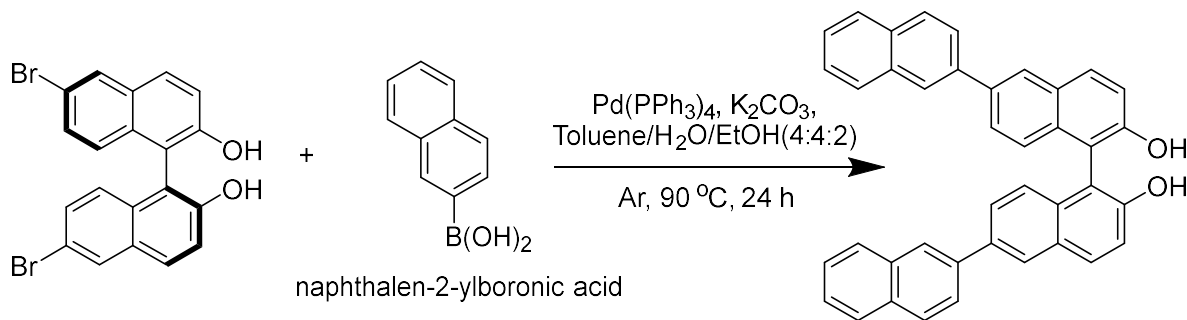
Synthesis of substituted (Rac)-20b2 (-OTf): Prepared by general method with 91% yield. ^1H NMR (400 MHz, CDCl_3) δ 7.98 (d, $J = 9.1$ Hz, 2H), 7.84 (d, $J = 1.2$ Hz, 2H), 7.54 (t, $J = 5.8$ Hz, 4H), 7.50–7.44 (m, 6H), 7.12–7.03 (m, 12H), 7.00 (d, $J = 8.8$ Hz, 2H).



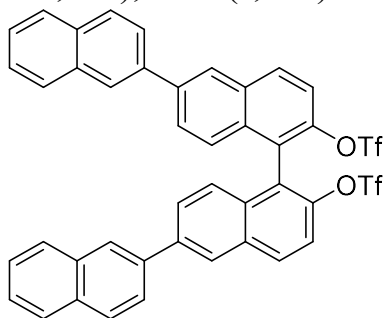
Synthesis of substituted (Rac)-20b3 (-PPh₂): Prepared by general method with 51% yield.

Supporting information

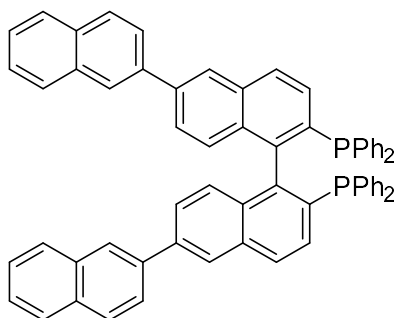
^1H NMR (400 MHz, CDCl_3) δ 7.76–7.71 (m, 4H), 7.46–7.42 (m, 8H), 7.36 (dd, $J = 8.5, 2.6$ Hz, 2H), 7.14–7.02 (m, 28H), 6.71 (d, $J = 1.0$ Hz, 4H). ^{31}P NMR (162 MHz, CDCl_3) δ -16.4. ^{13}C NMR (101 MHz, CDCl_3) δ 145.5 (d, $J = 43.2$ Hz), 141.3 (d, $J = 6.1$ Hz), 141.2 (s), 140. (d, $J = 4.6$ Hz), 140.61 (s), 140.4 (s), 140.1 (d, $J = 13.2$ Hz), 139.1 (s), 138.2 (d, $J = 14.1$ Hz), 137.8 (d, $J = 12.0$ Hz), 135.2 (d, $J = 8.0$ Hz), 134.0 (d, $J = 21.2$ Hz), 133.7 – 132.5 (br), 132.2 (s), 130.5 (d, $J = 12.2$ Hz), 129.1 – 127.2 (br), 127.0 (s), 125.6 (s), 125.1 (s). HRMS found for $[\text{C}_{68}\text{H}_{48}\text{P}_2]^+\text{H}^+$: $m/z = 927.3309$, calcd for $[\text{C}_{68}\text{H}_{48}\text{P}_2]^+\text{H}^+$: $m/z = 927.3357$.



Synthesis of [2,2':5',1'':6'',2'''-quaternaphthalene]-2'',6'-diol (21b1): Prepared by general method with 64% yield. ^1H NMR (400 MHz, CDCl_3) δ 8.25 (d, $J = 1.7$ Hz, 2H), 8.14–8.08 (m, 4H), 7.96–7.83 (m, 8H), 7.74 (dd, $J = 8.7, 1.9$ Hz, 2H), 7.49 (ddd, $J = 14.2, 7.9, 5.3$ Hz, 6H), 7.33 (d, $J = 8.7$ Hz, 2H), 5.17 (s, 2H).



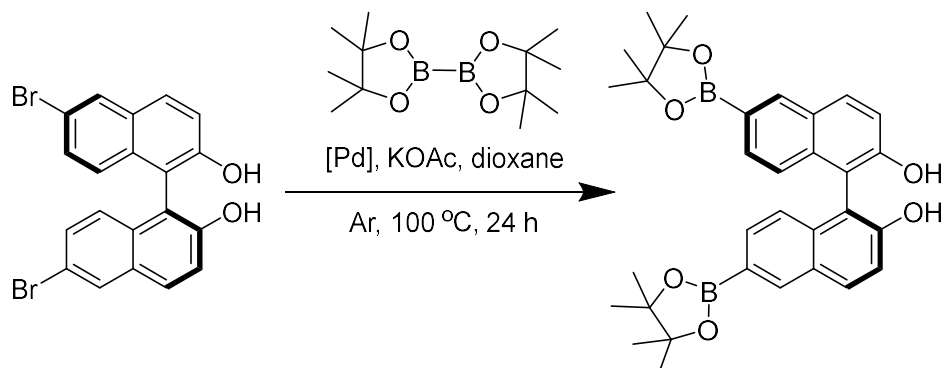
Synthesis of substituted (*Rac*)-21b2 (-OTf): Prepared by general method with 91% yield. ^1H NMR (400 MHz, CDCl_3) δ 8.34 (d, $J = 1.7$ Hz, 2H), 8.25 (d, $J = 9.1$ Hz, 2H), 8.17 (d, $J = 0.8$ Hz, 2H), 7.99–7.81 (m, 10H), 7.69 (d, $J = 9.1$ Hz, 2H), 7.55–7.49 (m, 4H), 7.43 (d, $J = 8.8$ Hz, 2H).



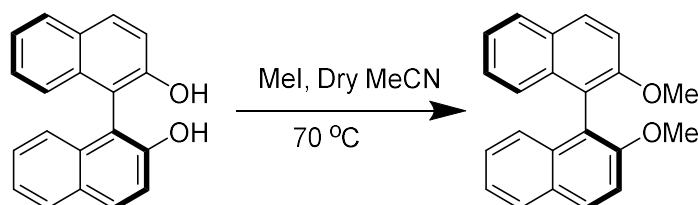
Synthesis of substituted (*Rac*)-21b3 (-PPh₂): Prepared by general method with 51% yield. ^1H NMR (400 MHz, CDCl_3) δ 8.17 (d, $J = 1.6$ Hz, 2H), 8.06 (s, 2H), 8.00 (d, $J = 8.5$ Hz, 2H), 7.90 (dt, $J = 8.7, 5.2$ Hz, 6H), 7.78 (dd, $J = 8.6, 1.7$ Hz, 2H), 7.50 (ddd, $J = 9.1, 4.8, 2.2$ Hz, 6H), 7.27 (d, $J = 1.9$ Hz, 1H), 7.25 (s, 1H), 7.23–7.10 (m, 20H), 6.95 (d, $J = 8.8$ Hz, 2H). ^{31}P NMR (162 MHz, CDCl_3) δ -15.0. ^{13}C NMR (101 MHz, CDCl_3) δ 145.0 (d, $J = 42.5$),

Supporting information

138.9 (s), 138.2 (s), 138.0 – 137.7 (br), 137.1 (s), 136.4 – 135.6 (br), 134.5 (d, $J = 19.0$), 133.7 (d, $J = 7.7$ Hz), 133.3 – 132.5 (br), 131.0 (s), 128.5 (d, $J = 2.2$ Hz), 128.4 – 127.8 (br), 127.7 (s), 126.4 (s), 126.1 (d, $J = 1.6$ Hz), 125.9 (s), 125.6 (d, $J = 3.4$ Hz), 125.6 (s). HRMS found for $[C_{64}H_{44}P_2]^+H^+$: $m/z = 875.2996$, calcd for $[C_{64}H_{44}P_2]^+H^+$: $m/z = 875.2943$.

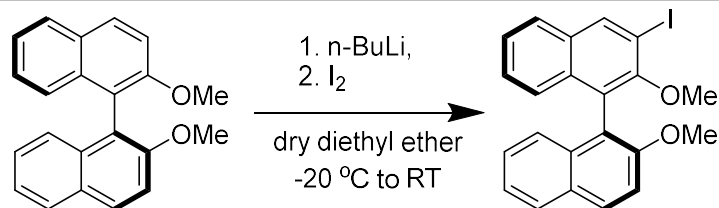


Synthesis of (S)-6,6'-bis(4,4,5,5-tetramethyl-1,3,2-dioxaborolan-2-yl)-[1,1'-binaphthalene]-2,2'-diol: In a 250 mL Schlenk bottle were placed (S)-6,6'-dibromo-1,1'-binaphthalene-2,2'-diol (5.0 g, 11.3 mmol), 4,4,4',4',5,5,5',5'-octamethyl-2,2'-bi(1,3,2-dioxaborolane) (3.0 eq), KOAc (6.0 eq), Pd(dppf)Cl₂ (5 mol%), and 20 mL of dry dioxane solvent. The mixture solution was reacted at 90 °C under an Ar atmosphere for about 24 hours. The organic phase was extracted successively with dilute hydrochloric acid and dichloromethane. The organic phase was dried with anhydrous MgSO₄ and filtered. The solvent was removed by decompressing vaporization. The resulted residue was purified by column chromatography with EA:CH₂Cl₂ (1:20), and then the white solid powder was obtained with 64% yield. ¹H NMR (400 MHz, CDCl₃) δ 8.42 (s, 2H), 8.02 (d, $J = 8.9$ Hz, 2H), 7.65 (dd, $J = 8.4, 1.0$ Hz, 2H), 7.37 (d, $J = 8.9$ Hz, 2H), 7.10 (d, $J = 8.4$ Hz, 2H), 5.10 (s, 2H), 1.36 (s, 24H).

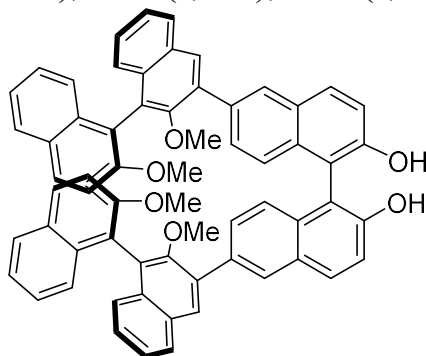


Synthesis of (S)-2,2'-dimethoxy-1,1'-binaphthalene: In a 250 mL Schlenk bottle were placed (S)-BINOL (5.0 g, 17.5 mmol), MeI (2.5 eq), K₂CO₃ (3.0 eq), and 20 mL of dry acetonitrile solvent. The mixture solution was reacted at 70 °C under an Ar atmosphere for about 4 hours. The organic phase was extracted successively with dilute hydrochloric acid and dichloromethane. The organic phase was dried with anhydrous MgSO₄ and filtered. The solvent was removed by decompressing vaporization. The resulted residue was purified by flash chromatography with PE:CH₂Cl₂ (5:1), and then the white solid powder was obtained with 98% yield. ¹H NMR (400 MHz, CDCl₃) δ 7.96 (d, $J = 9.0$ Hz, 2H), 7.85 (d, $J = 8.2$ Hz, 2H), 7.45 (d, $J = 9.0$ Hz, 2H), 7.30 (ddd, $J = 8.1, 6.7, 1.2$ Hz, 2H), 7.20 (ddd, $J = 8.1, 6.7, 1.3$ Hz, 2H), 7.10 (dd, $J = 8.5, 0.4$ Hz, 2H), 3.75 (s, 6H).

Supporting information

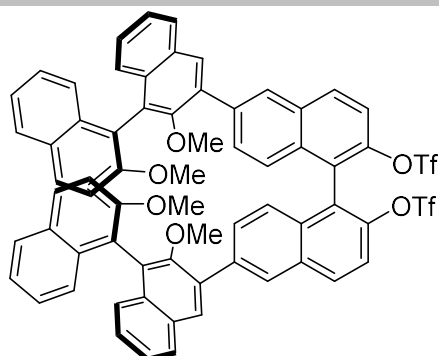


Synthesis of (S)-3-iodo-2,2'-dimethoxy-1,1'-binaphthalene: An oven-dried RB flask, equipped with a magnetic stir bar, was charged under Ar with Synthesis of (S)-2,2'-dimethoxy-1,1'-binaphthalene (5 g, 15.9 mmol) and dry diethyl ether (50 mL). After cooling the mixture at -20 °C (ice-salt baths), n-BuLi (2.5 M in hexanes, 15.9 mmol, 1.0 eq) was added dropwise over 5 min. After the addition was completed, the mixture was stirred for 30 min at -20 °C and then for a further 5 h at room temperature. The mixture was cooled again to -20 °C and iodine (15.9 mmol, 1.0 eq, in dilute dry THF solution) was added dropwise over 2-3 min, followed by stirring at RT for 20 h. The reaction was quenched at 0 °C by adding 3 mL MeOH, followed by dilution with 100 mL distilled water. The mixture was extracted with DCM, and the combined organic phase was washed with brine, dried over anhydrous MgSO₄, filtered, and concentrated under reduced pressure. The resulted residue was purified by flash chromatography (PE:CH₂Cl₂ = 5/1) afforded the corresponding product as a white solid with 54% yield. ¹H NMR (400 MHz, CDCl₃) δ 8.49 (s, 1H), 8.01 (d, J = 9.0 Hz, 1H), 7.87 (d, J = 8.1 Hz, 1H), 7.77 (d, J = 8.2 Hz, 1H), 7.45 (d, J = 9.1 Hz, 1H), 7.38 (ddd, J = 8.1, 6.8, 1.2 Hz, 1H), 7.33 (ddd, J = 8.1, 6.8, 1.2 Hz, 1H), 7.25–7.21 (m, 2H), 7.09 (dd, J = 11.9, 4.4 Hz, 2H), 3.80 (s, 3H), 3.40 (s, 3H).

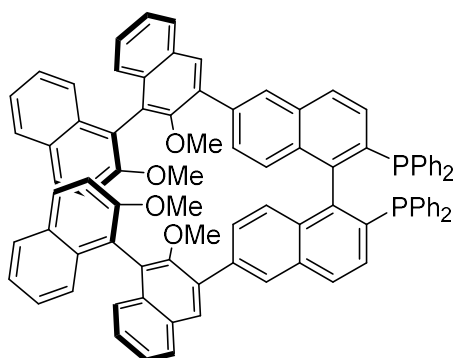


Synthesis of (S,S)-22b1: Prepared by general method with 74% yield. ¹H NMR (400 MHz, CDCl₃) δ 8.32 (d, J = 1.5 Hz, 2H), 8.06 (d, J = 9.0 Hz, 2H), 8.01 (dd, J = 11.6, 6.6 Hz, 4H), 7.89 (dd, J = 15.1, 8.1 Hz, 5H), 7.76 (dd, J = 8.7, 1.7 Hz, 2H), 7.47 (d, J = 9.1 Hz, 2H), 7.44–7.37 (m, 5H), 7.32 (dd, J = 8.4, 2.6 Hz, 4H), 7.24–7.22 (m, 4H), 7.14 (d, J = 8.4 Hz, 2H), 5.16 (s, 1H), 3.82 (s, 6H), 3.13 (s, 6H).

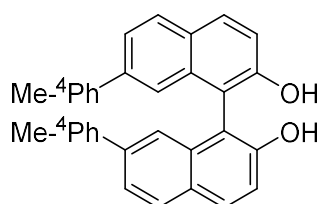
Supporting information



Synthesis of (S,S)-22b2: Prepared by general method with 91% yield. ^1H NMR (400 MHz, CDCl_3) δ 8.43 (d, $J = 1.5$ Hz, 2H), 8.21 (d, $J = 9.1$ Hz, 2H), 8.08 (s, 2H), 8.00 (d, $J = 9.0$ Hz, 2H), 7.93 (d, $J = 8.1$ Hz, 2H), 7.90–7.84 (m, 4H), 7.65 (d, $J = 9.1$ Hz, 2H), 7.47 (d, $J = 9.1$ Hz, 2H), 7.41 (dd, $J = 11.0, 5.0$ Hz, 4H), 7.32 (ddd, $J = 8.1, 6.5, 1.5$ Hz, 2H), 7.28–7.25 (m, 2H), 7.25–7.19 (m, 4H), 7.15 (d, $J = 8.5$ Hz, 2H), 3.81 (s, 6H), 3.09 (s, 6H).

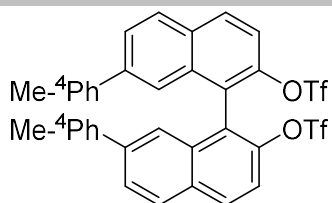


Synthesis of (S,S)-22b2: Prepared by general method with 31% yield. ^1H NMR (400 MHz, CDCl_3) δ 8.26 (d, $J = 1.2$ Hz, 2H), 7.94 (ddd, $J = 39.1, 12.8, 8.6$ Hz, 12H), 7.49–7.30 (m, 12H), 7.16 (dd, $J = 23.0, 12.9$ Hz, 24H), 7.00 (d, $J = 8.8$ Hz, 2H), 3.81 (d, $J = 3.8$ Hz, 6H), 3.06 (s, 6H). ^{31}P NMR (162 MHz, CDCl_3) δ -15.5. ^{13}C NMR (101 MHz, CDCl_3) δ 153.8 (s), 145.9 (s), 145.4 (s), 136.7 (s), 135.2 (s), 133.4 (s), 133.1 (s), 133.0 – 132.6 (br), 132.3 (d, $J = 6.0$ Hz), 132.0 – 131.2 (br), 130.6 (d, $J = 5.7$ Hz), 129.2 – 125.5 (br), 124.1 (d, $J = 15.3$ Hz), 123.7 – 123.1 (br), 122.0 (d, $J = 9.3$ Hz), 121.7 (s), 120.7 (s), 119.7 (s), 117.8 (s), 116.5 (s). HRMS found for $[\text{C}_{88}\text{H}_{64}\text{P}_2\text{O}_4]^+\text{H}^+$: $m/z = 1247.4358$, calcd for $[\text{C}_{58}\text{H}_{44}\text{P}_2]^+\text{H}^+$: $m/z = 1247.4329$.

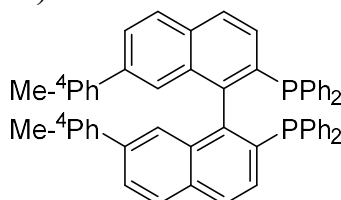


Synthesis of substituted (Rac)-1c1: Prepared by general method with 87% yield. ^1H NMR (400 MHz, CDCl_3) δ 7.99 (d, $J = 8.9$ Hz, 2H), 7.95 (d, $J = 8.4$ Hz, 2H), 7.61 (dd, $J = 8.4, 1.8$ Hz, 2H), 7.38 (d, $J = 8.9$ Hz, 2H), 7.36–7.34 (m, 2H), 7.31 (d, $J = 8.1$ Hz, 4H), 7.12 (d, $J = 7.9$ Hz, 4H), 5.12 (s, 2H), 2.31 (s, 6H).

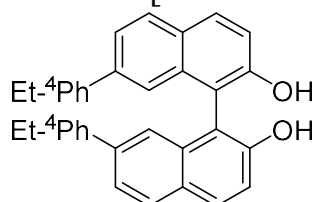
Supporting information



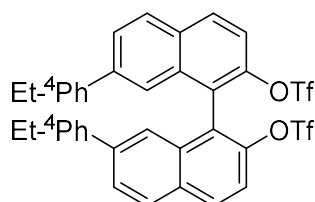
Synthesis of substituted (*Rac*)-1c2 (-OTf): Prepared by general method with 94% yield. ^1H NMR (400 MHz, CDCl_3) δ 8.14 (d, $J = 9.0$ Hz, 2H), 8.04 (d, $J = 8.5$ Hz, 2H), 7.79 (dd, $J = 8.5, 1.7$ Hz, 2H), 7.60 (d, $J = 9.0$ Hz, 2H), 7.43–7.37 (m, 2H), 7.26 (d, $J = 8.2$ Hz, 4H), 7.11 (d, $J = 7.9$ Hz, 4H), 2.29 (s, 6H).



Synthesis of substituted (*Rac*)-1c3 (-PPh₂): Prepared by general method with 57% yield. ^1H NMR (400 MHz, CDCl_3) δ 7.90 (t, $J = 9.0$ Hz, 4H), 7.61 (dd, $J = 8.5, 1.8$ Hz, 2H), 7.51 (dd, $J = 8.4, 2.5$ Hz, 2H), 7.17–6.97 (m, 26H), 6.92 (d, $J = 8.2$ Hz, 4H), 2.28 (s, 6H). ^{31}P NMR (162 MHz, CDCl_3) δ -15.7. ^{13}C NMR (101 MHz, CDCl_3) δ 145.8 (d, $J = 42.7$ Hz), 138.7 (s), 138.6 (d, $J = 12.2$ Hz), 138.0 (s), 137.5 (d, $J = 13.9$ Hz), 136.8 (s), 136.0 (d, $J = 7.3$ Hz), 134.6 – 133.8 (br), 132.6 (d, $J = 21.6$ Hz), 130.6 (s), 129.0 (s), 128.7 (s), 128.4 (s), 128.1 (d, $J = 10.5$ Hz), 127.4 (s), 127.3 (s), 126.4 (s), 125.3 (s), 21.0 (s). HRMS found for $[\text{C}_{58}\text{H}_{44}\text{P}_2]^+\text{H}^+$: $m/z = 803.2996$, calcd for $[\text{C}_{58}\text{H}_{44}\text{P}_2]^+\text{H}^+$: $m/z = 803.2976$.

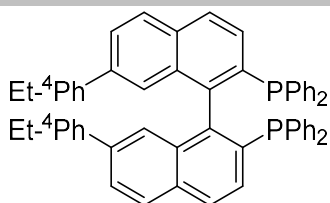


Synthesis of substituted (*Rac*)-2c1: Prepared by general method with 90% yield. ^1H NMR (400 MHz, CDCl_3) δ 7.97 (dd, $J = 15.2, 8.7$ Hz, 4H), 7.62 (dd, $J = 8.4, 1.8$ Hz, 2H), 7.40–7.31 (m, 8H), 7.15 (d, $J = 8.2$ Hz, 4H), 5.11 (s, 2H), 2.61 (q, $J = 7.6$ Hz, 4H), 1.20 (t, $J = 7.6$ Hz, 6H).

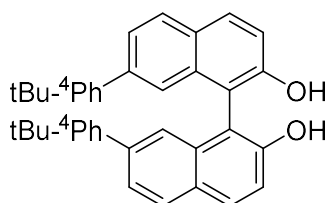


Synthesis of substituted (*Rac*)-2c2 (-OTf): Prepared by general method with 97% yield. ^1H NMR (400 MHz, CDCl_3) δ 8.14 (d, $J = 9.1$ Hz, 2H), 8.04 (d, $J = 8.6$ Hz, 2H), 7.80 (dd, $J = 8.5, 1.7$ Hz, 2H), 7.60 (d, $J = 9.0$ Hz, 2H), 7.41 (d, $J = 0.6$ Hz, 2H), 7.30 (d, $J = 8.2$ Hz, 4H), 7.14 (d, $J = 8.2$ Hz, 4H), 2.59 (q, $J = 7.6$ Hz, 4H), 1.18 (t, $J = 7.6$ Hz, 6H).

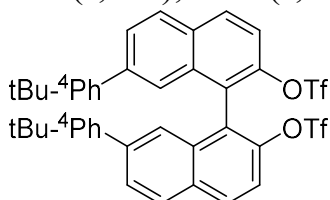
Supporting information



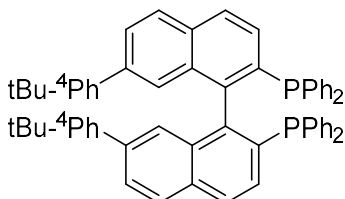
Synthesis of substituted (*Rac*)-1c3 (-PPh₂): Prepared by general method with 58% yield. ¹H NMR (400 MHz, CDCl₃) δ 7.91 (t, *J* = 8.2 Hz, 4H), 7.62 (dd, *J* = 8.5, 1.7 Hz, 2H), 7.51 (dd, *J* = 8.4, 1.4 Hz, 2H), 7.16–6.95 (m, 30H), 2.59 (q, *J* = 7.6 Hz, 4H), 1.19 (t, *J* = 7.6 Hz, 6H). ³¹P NMR (162 MHz, CDCl₃) δ -15.7. ¹³C NMR (101 MHz, CDCl₃) δ 145.8 (d, *J* = 42.8 Hz), 143.2 (s), 138.5 (d, *J* = 45.4 Hz), 137.6 (d, *J* = 14.1 Hz), 136.0 (d, *J* = 6.1 Hz), 134.5 – 133.8 (br), 133.5 (d, *J* = 2.6 Hz), 132.6 (d, *J* = 20.8 Hz), 130.6 (s), 128.5 (d, *J* = 19.9 Hz), 128.6 – 127.6 (br), 127.4 (s), 126.5 (s), 125.4 (s), 124.7 (d, *J* = 50.7 Hz), 28.5 (s), 15.6 (s). HRMS found for [C₆₀H₄₈P₂]+H⁺: *m/z* = 831.3309, calcd for [C₅₈H₄₄P₂]+H⁺: *m/z* = 831.3315.



Synthesis of substituted (*Rac*)-3c1: Prepared by general method with 91% yield. ¹H NMR (400 MHz, CDCl₃) δ 7.99 (d, *J* = 8.9 Hz, 2H), 7.95 (d, *J* = 8.5 Hz, 2H), 7.63 (dd, *J* = 8.4, 1.8 Hz, 2H), 7.41–7.31 (m, 12H), 5.11 (s, 2H), 1.28 (s, 18H).

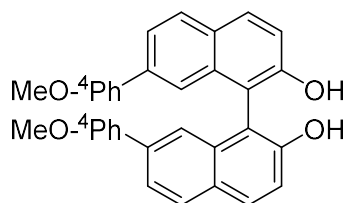


Synthesis of substituted (*Rac*)-3c2 (-OTf): Prepared by general method with 98% yield. ¹H NMR (400 MHz, CDCl₃) δ 8.14 (d, *J* = 9.0 Hz, 2H), 8.05 (d, *J* = 8.5 Hz, 2H), 7.81 (dd, *J* = 8.5, 1.7 Hz, 2H), 7.60 (d, *J* = 9.0 Hz, 2H), 7.46–7.40 (m, 2H), 7.33 (s, 8H), 1.28–1.26 (m, 18H).

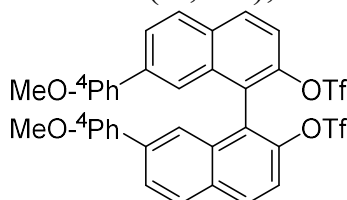


Synthesis of substituted (*Rac*)-3c3 (-PPh₂): Prepared by general method with 47% yield. ¹H NMR (400 MHz, CDCl₃) δ 7.91 (dd, *J* = 8.4, 5.4 Hz, 4H), 7.64 (dd, *J* = 8.5, 1.8 Hz, 2H), 7.53–7.48 (m, 2H), 7.25–7.21 (m, 4H), 7.17–7.03 (m, 18H), 7.04–6.96 (m, 8H), 1.28 (s, 18H). ³¹P NMR (162 MHz, CDCl₃) δ -15.8. ¹³C NMR (101 MHz, CDCl₃) δ 150.0 (d, *J* = 43.1 Hz), 145.9 (d, *J* = 42.7 Hz), 138.6 (s), 138.5 (d, *J* = 11.6 Hz), 138.0 (s), 137.6 (d, *J* = 14.0 Hz), 135.9 (d, *J* = 6.9 Hz), 134.1 (d, *J* = 14.4 Hz), 132.6 (d, *J* = 19.6 Hz), 130.6 (s), 128.5 (d, *J* = 13.6 Hz), 128.3 – 127.7 (br), 127.4 (s), 127.1 (s), 126.5 (s), 125.4 (s), 125.3 (s), 34.5 (s), 31.3 (s). HRMS found for [C₆₄H₅₆P₂]+H⁺: *m/z* = 887.3935, calcd for [C₆₄H₅₆P₂]+H⁺:

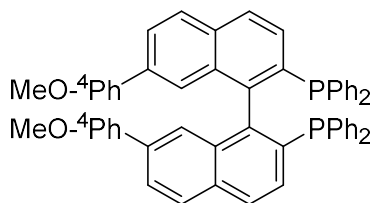
$m/z = 887.3949$.



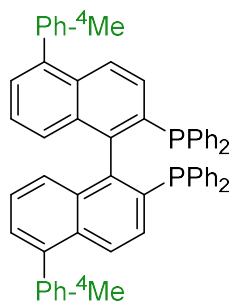
Synthesis of substituted (Rac)-4c1: Prepared by general method with 88% yield. ^1H NMR (400 MHz, CDCl_3) δ 7.99 (d, $J = 8.9$ Hz, 2H), 7.94 (d, $J = 8.5$ Hz, 2H), 7.60 (dd, $J = 8.4$, 1.8 Hz, 2H), 7.40–7.32 (m, 8H), 6.88–6.82 (m, 4H), 5.11 (s, 2H), 3.77 (s, 6H).



Synthesis of substituted (Rac)-4c2 (-OTf): Prepared by general method with 95% yield. ^1H NMR (400 MHz, CDCl_3) δ 8.14 (d, $J = 9.0$ Hz, 2H), 8.04 (d, $J = 8.5$ Hz, 2H), 7.78 (dd, $J = 8.6$, 1.7 Hz, 2H), 7.59 (d, $J = 9.0$ Hz, 2H), 7.40–7.35 (m, 2H), 7.33–7.29 (m, 4H), 6.84 (d, $J = 8.8$ Hz, 4H), 3.75 (s, 6H).



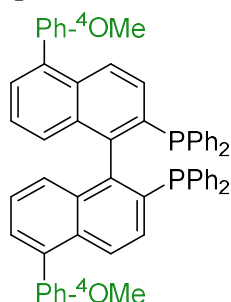
Synthesis of substituted (Rac)-4c3 (-PPh₂): Prepared by general method with 47% yield. ^1H NMR (400 MHz, CDCl_3) δ 7.90 (t, $J = 8.9$ Hz, 4H), 7.61 (dd, $J = 8.5$, 1.8 Hz, 2H), 7.52–7.48 (m, 2H), 7.15–6.96 (m, 26H), 6.77–6.71 (m, 4H), 3.76 (s, 6H). ^{31}P NMR (162 MHz, CDCl_3) δ -15.7. ^{13}C NMR (101 MHz, CDCl_3) δ 159.0 (s), 145.7 (d, $J = 42.6$ Hz), 138.5 (d, $J = 12.3$ Hz), 138.3 (s), 137.5 (d, $J = 13.7$ Hz), 136.1 (d, $J = 7.4$ Hz), 134.2 (d, $J = 22.0$ Hz), 133.4 (s), 132.7 (d, $J = 19.7$ Hz), 132.3 (s), 130.5 (s), 129.0 – 127.8 (br), 127.4 (s), 126.2 (s), 124.9 (s), 55.3 (s). HRMS found for $[\text{C}_{58}\text{H}_{44}\text{P}_2\text{O}_2]^+\text{H}^+$: $m/z = 835.2895$, calcd for $[\text{C}_{58}\text{H}_{44}\text{P}_2\text{O}_2]^+\text{H}^+$: $m/z = 835.2832$.



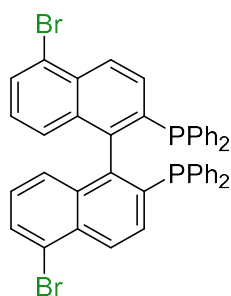
Synthesis of substituted (Rac)-5c3 (-PPh₂): Prepared by general method with 84% yield. ^1H NMR (400 MHz, CDCl_3) δ 7.97 (d, $J = 8.8$ Hz, 2H), 7.45 (d, $J = 7.9$ Hz, 4H), 7.39–7.35 (m, 2H), 7.33–7.25 (m, 8H), 7.187.05 (m, 18H), 6.95 (dd, $J = 8.5$, 7.0 Hz, 2H), 6.89 (d, $J = 8.4$ Hz, 2H), 2.45 (s, 6H). ^{31}P NMR (162 MHz, CDCl_3) δ -15.3. ^{13}C NMR (101 MHz, CDCl_3) δ 145.0 (d, $J = 20.0$ Hz), 141.3 (s), 140.8 (d, $J = 15.9$ Hz), 137.2 (s), 137.2 (s), 136.2 (s),

Supporting information

133.8 (d, $J = 11.8$ Hz), 132.7 (d, $J = 12.4$ Hz), 131.4 – 131.0 (br), 130.6 – 129.7 (br), 127.7 (s), 126.9 (s), 126.4 (s), 125.7 – 124.9 (br), 124.8 (s), 124.0 (s), 123.1 (s), 120.3 (s), 118.9 (s), 116.9 (s), 116.0 (s), 110.2 (d, $J = 33.0$ Hz), 30.6 (s). HRMS found for $[C_{58}H_{44}P_2]^+H^+$: $m/z = 803.2996$, calcd for $[C_{58}H_{44}P_2]^+H^+$: $m/z = 803.2943$.

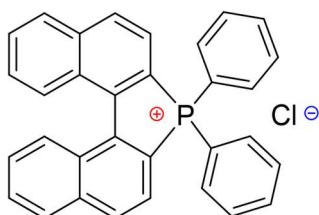


Synthesis of substituted (*Rac*)-6c3 (-PPh₂): Prepared by general method with 80 % yield. ¹H NMR (400 MHz, CDCl₃) δ 7.98 (d, $J = 8.9$ Hz, 2H), 7.51 – 7.45 (m, 4H), 7.40–7.36 (m, 2H), 7.29–7.26 (m, 2H), 7.20–7.05 (m, 20H), 7.05–7.00 (m, 4H), 6.95 (dd, $J = 8.5, 6.9$ Hz, 2H), 6.88 (d, $J = 8.4$ Hz, 2H), 3.89 (s, 6H). ³¹P NMR (162 MHz, CDCl₃) δ -15.4. ¹³C NMR (101 MHz, CDCl₃) δ 159.0 (s), 139.6 (s), 137.1 (s), 135.2 (s), 134.3 (d, $J = 21.1$ Hz), 132.9 (s), 132.0 – 130.9 (br), 130.5 (s), 129.0 – 127.2 (br), 126.2 (s), 125.3 (s), 114.2 (d, $J = 8.0$ Hz), 113.7 (s), 113.1 (s), 55.4 (s). HRMS found for $[C_{58}H_{44}P_2O_2]^+H^+$: $m/z = 835.2895$, calcd for $[C_{58}H_{44}P_2O_2]^+H^+$: $m/z = 835.2817$.

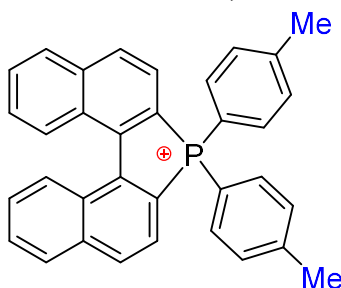


Synthesis of substituted (*Rac*)-7c3 (-PPh₂): Prepared by the general method with 47% yield. ¹H NMR (400 MHz, CDCl₃) δ 8.31 (d, $J = 8.8$ Hz, 2H), 7.60 (dd, $J = 5.3, 3.1$ Hz, 2H), 7.54 (dd, $J = 8.8, 2.6$ Hz, 2H), 7.23–7.08 (m, 16H), 7.05 – 6.98 (m, 4H), 6.69–6.65 (m, 3H). ³¹P NMR (162 MHz, CDCl₃) δ -15.2. HRMS found for $[C_{44}H_{30}P_2Br_2]^+H^+$: $m/z = 781.0247$, calcd for $[C_{44}H_{30}P_2Br_2]^+H^+$: $m/z = 781.0278$.

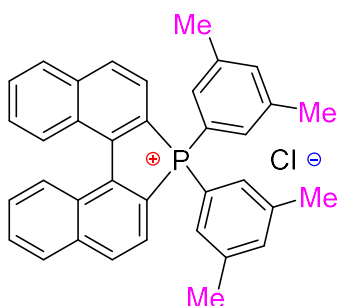
Section B: Synthetic Procedures of Phospha[5]helicene and Phosponium



Synthesis of substituted (*M*)-1b and (*P*)-1b: Prepared by general method (10) with 58% (61%, gram-scale) yield. ^1H NMR (400 MHz, CDCl_3) δ 8.40–8.24 (m, 6H), 8.13 (d, $J = 8.2$ Hz, 2H), 7.97 (dd, $J = 14.1, 7.5$ Hz, 4H), 7.81 (q, $J = 7.8$ Hz, 4H), 7.75–7.67 (m, 6H). ^{31}P NMR (162 MHz, CDCl_3) δ 25.1. ^{13}C NMR (101 MHz, CDCl_3) δ 144.9 (d, $J = 19.9$ Hz), 138.4 (s), 136.2 (d, $J = 3.2$ Hz), 133.7 (d, $J = 11.8$ Hz), 133.2 (d, $J = 12.1$ Hz), 131.1 (d, $J = 13.4$ Hz), 129.7 (d, $J = 32.0$ Hz), 125.2 (d, $J = 10.7$ Hz), 120.8 (s), 119.8 (s), 116.7 (s), 115.8 (s). HRMS found for $[\text{C}_{32}\text{H}_{22}\text{P}]^+$: $m/z = 437.1443$, calcd for $[\text{C}_{32}\text{H}_{22}\text{P}]^+$: $m/z = 437.1454$.



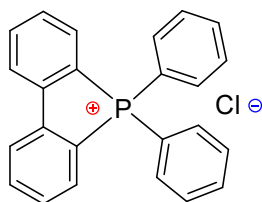
Synthesis of substituted and (*Rac*)-2b: Prepared by general method (10) with 54% (59%, gram-scale) yield. ^1H NMR (400 MHz, CDCl_3) δ 8.41–8.17 (m, 6H), 8.12 (d, $J = 8.2$ Hz, 2H), 7.81 (dt, $J = 14.9, 7.4$ Hz, 6H), 7.70–7.65 (m, 2H), 7.51 (d, $J = 8.6$ Hz, 4H), 2.45 (s, 6H). ^{31}P NMR (162 MHz, CDCl_3) δ 25.0. ^{13}C NMR (101 MHz, CDCl_3) δ 147.9 (s), 145.2–144.3 (br), 138.3 (s), 133.6 (d, $J = 12.3$ Hz), 133.0 (d, $J = 12.0$ Hz), 131.8 (d, $J = 13.8$ Hz), 129.6 (d, $J = 20.4$ Hz), 128.0 (s), 127.3 (s), 125.1 (s), 121.5 (s), 120.6 (s), 113.0 (s), 112.1 (s), 29.7 (s). HRMS found for $[\text{C}_{34}\text{H}_{26}\text{P}]^+$: $m/z = 465.1754$, calcd for $[\text{C}_{34}\text{H}_{26}\text{P}]^+$: $m/z = 465.1767$.



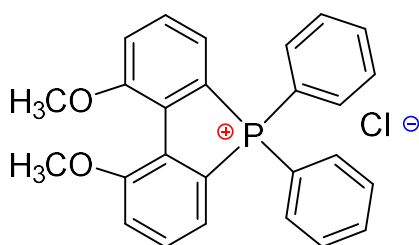
Synthesis of substituted (*M*)-3b and (*Rac*)-3b: Prepared by general method (10) with 56% yield. ^1H NMR (400 MHz, CDCl_3) δ 8.31 (d, $J = 8.5$ Hz, 4H), 8.16 (d, $J = 8.2$ Hz, 2H), 7.99 (t, $J = 8.6$ Hz, 2H), 7.86 (t, $J = 7.5$ Hz, 2H), 7.78–7.72 (m, 2H), 7.49 (s, 2H), 7.40 (d, $J = 14.6$ Hz, 4H), 2.42–2.37 (m, 12H). ^{31}P NMR (162 MHz, CDCl_3) δ 25.6. ^{13}C NMR (101 MHz, CDCl_3) δ 144.9 (d, $J = 19.7$ Hz), 141.4 (d, $J = 13.9$ Hz), 138.3 (d, $J = 2.7$ Hz), 138.2 (d, $J = 3.4$ Hz), 132.8 (d, $J = 12.5$ Hz), 130.4 (d, $J = 11.7$ Hz), 130.0 (s), 129.5 (d, $J = 11.3$ Hz), 129.4 (s), 127.8 (d, $J = 42.1$ Hz), 124.1 (d, $J = 10.4$ Hz), 120.8 (s), 119.8 (s), 116.4 (s), 115.5

Supporting information

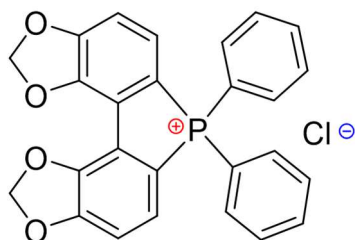
(s), 21.2 (s). HRMS found for $[\text{C}_{36}\text{H}_{30}\text{P}]^+$: $m/z = 493.2073$, calcd for $[\text{C}_{36}\text{H}_{30}\text{P}]^+$: $m/z = 493.2080$.



Synthesis of 4b: Prepared by general method (10) with 57% yield. ^1H NMR (400 MHz, CDCl_3) δ 8.30 (t, $J = 8.6$ Hz, 2H), 8.22 (dd, $J = 7.7, 3.1$ Hz, 2H), 7.96–7.70 (m, 14H). ^{31}P NMR (162 MHz, CDCl_3) δ 22.1. ^{13}C NMR (101 MHz, CDCl_3) δ 144.1 (d, $J = 19.4$ Hz), 136.8 (d, $J = 1.9$ Hz), 136.0 (d, $J = 3.3$ Hz), 133.5 (d, $J = 11.8$ Hz), 132.8 (d, $J = 9.9$ Hz), 131.8 (d, $J = 11.9$ Hz), 131.0 (d, $J = 13.6$ Hz), 124.0 (d, $J = 9.9$ Hz), 121.3 (s), 120.4 (s), 116.8 (s), 115.9 (s). HRMS found for $[\text{C}_{24}\text{H}_{18}\text{P}]^+$: $m/z = 337.1185$, calcd for $[\text{C}_{24}\text{H}_{18}\text{P}]^+$: $m/z = 337.1141$.

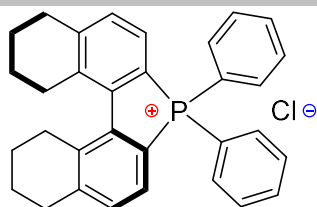


Synthesis of (Rac)-5b: Prepared by general method (10) with 61% yield. ^1H NMR (400 MHz, CDCl_3) δ 7.87–7.61 (br, 14H), 7.46 (d, $J = 8.1$ Hz, 2H), 4.05 (s, 6H). ^{31}P NMR (162 MHz, CDCl_3) δ 22.7. ^{13}C NMR (101 MHz, CDCl_3) δ 157.6 (d, $J = 14.4$ Hz), 136.1 (d, $J = 2.8$ Hz), 133.6 (d, $J = 11.5$ Hz), 132.8 (d, $J = 14.7$ Hz), 131.6 (d, $J = 20.5$ Hz), 131.0 (d, $J = 13.6$ Hz), 124.6 (d, $J = 9.6$ Hz), 123.5 (s), 122.4 (s), 121.5 (s), 117.3 (s), 116.5 (s), 57.1 (s). HRMS found for $[\text{C}_{26}\text{H}_{22}\text{P}]^+$: $m/z = 397.1349$, calcd for $[\text{C}_{26}\text{H}_{22}\text{P}]^+$: $m/z = 397.1352$.

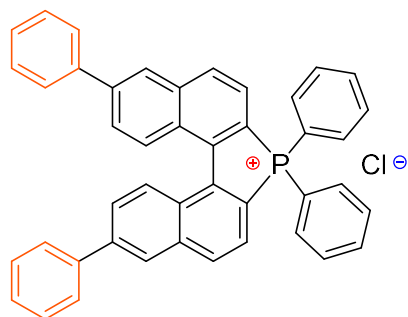


Synthesis of (S)-6b: Prepared by general method (10) with 47% yield. ^1H NMR (400 MHz, CDCl_3) δ 7.86–7.79 (m, 6H), 7.77–7.68 (m, 6H), 7.17 (dd, $J = 7.9, 3.6$ Hz, 2H), 6.28 (s, 4H). ^{31}P NMR (162 MHz, CDCl_3) δ 20.9. ^{13}C NMR (101 MHz, CDCl_3) δ 155.6 (s), 144.8 (d, $J = 15.6$ Hz), 135.7 (d, $J = 3.1$ Hz), 133.3 (d, $J = 11.8$ Hz), 130.8 (d, $J = 13.7$ Hz), 129.1 (d, $J = 11.0$ Hz), 121.1 (d, $J = 22.6$ Hz), 118.5 (s), 117.6 (s), 113.3 (s), 112.3 (s), 111.2 (d, $J = 15.0$ Hz), 103.1 (s). HRMS found for $[\text{C}_{26}\text{H}_{18}\text{O}_4\text{P}]^+$: $m/z = 465.0925$, calcd for $[\text{C}_{26}\text{H}_{18}\text{O}_4\text{P}]^+$: $m/z = 465.0937$.

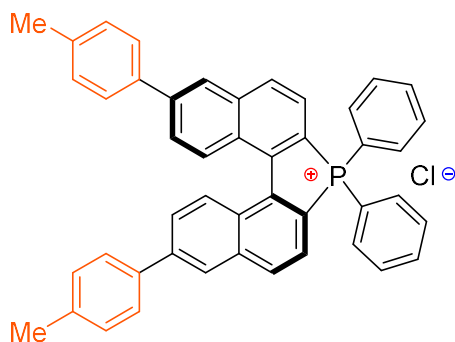
Supporting information



Synthesis of substituted (*S*)-7b: Prepared by general method (10) with 39% yield. ^1H NMR (400 MHz, CDCl_3) δ 8.41 (d, $J = 9.0$ Hz, 2H), 8.37 (dd, $J = 8.0, 4.2$ Hz, 2H), 8.31 (d, $J = 1.6$ Hz, 2H), 8.24 (t, $J = 8.6$ Hz, 2H), 8.02 – 7.89 (br, 6H), 7.87 – 7.66 (br, 10H), 7.56 (t, $J = 7.5$ Hz, 4H), 7.51 – 7.47 (t, $J = 7.3$ Hz, 2H), 2.96 (t, $J = 7.1$ Hz, 4H), 2.84 (t, $J = 6.0$ Hz, 4H), 1.99 – 1.86 (quint, 4H), 1.75 – 1.59 (quint, 4H). ^{31}P NMR (162 MHz, CDCl_3) δ 21.6. ^{13}C NMR (101 MHz, CDCl_3) δ 149.4 (s), 143.9 (d, $J = 19.3$ Hz), 140.2 (d, $J = 10.2$ Hz), 135.8 (d, $J = 3.0$ Hz), 133.3 (d, $J = 11.7$ Hz), 131.5 (d, $J = 13.0$ Hz), 130.9 (d, $J = 13.5$ Hz), 130.0 (d, $J = 9.9$ Hz), 118.9 (d, $J = 49.7$ Hz), 118.0 (d, $J = 42.5$ Hz), 30.8 (s), 29.1 (s), 21.8 (s), 21.0 (s). HRMS found for $[\text{C}_{32}\text{H}_{30}\text{P}]^+$: $m/z = 445.2089$, calcd for $[\text{C}_{32}\text{H}_{30}\text{P}]^+$: $m/z = 445.2080$.



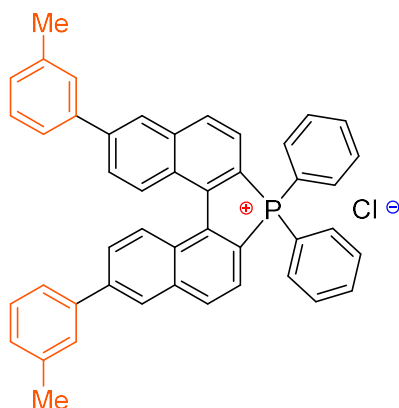
Synthesis of substituted (*Rac*)-9b: Prepared by general method (10) with 53% yield. ^1H NMR (400 MHz, CDCl_3) δ 8.49–8.27 (m, 8H), 7.99 (t, $J = 8.0$ Hz, 6H), 7.85–7.71 (m, 10H), 7.58–7.46 (m, 6H). ^{31}P NMR (162 MHz, CDCl_3) δ 24.9. ^{13}C NMR (101 MHz, CDCl_3) δ 144.8 (d, $J = 19.9$ Hz), 142.4 (s), 139.1 (s), 138.9 (s), 136.2 (s), 133.8 (d, $J = 11.7$ Hz), 133.4 (d, $J = 12.0$ Hz), 131.1 (d, $J = 13.6$ Hz), 129.3 (s), 128.7 (d, $J = 6.5$ Hz), 128.5 (d, $J = 11.7$ Hz), 127.5 (s), 126.9 (d, $J = 26.4$ Hz), 125.8 (d, $J = 11.0$ Hz). HRMS found for $[\text{C}_{44}\text{H}_{30}\text{P}]^+$: $m/z = 589.2085$, calcd for $[\text{C}_{44}\text{H}_{30}\text{P}]^+$: $m/z = 589.2080$.



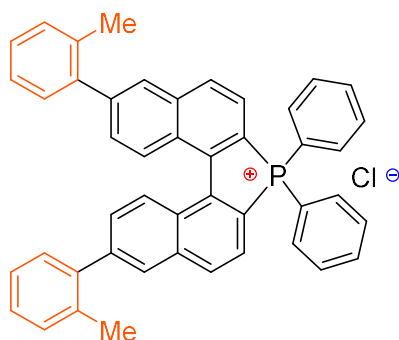
Synthesis of substituted (*P*)-10b: Prepared by general method (10) with 38% yield (40%, gram-scale). ^1H NMR (400 MHz, CDCl_3) δ 8.45–8.24 (m, 8H), 7.97 (d, $J = 8.7$ Hz, 6H), 7.84 (s, 2H), 7.71 (d, $J = 7.9$ Hz, 8H), 7.37 (d, $J = 7.8$ Hz, 4H), 2.46 (s, 6H). ^{31}P NMR (162 MHz, CDCl_3) δ 24.9. ^{13}C NMR (101 MHz, CDCl_3) δ 142.4 (s), 138.9 (d, $J = 8.6$ Hz), 136.19 (s), 133.7 (d, $J = 11.7$ Hz), 133.2 (d, $J = 12.5$ Hz), 131.1 (d, $J = 13.5$ Hz), 130.0 (s), 129.3

Supporting information

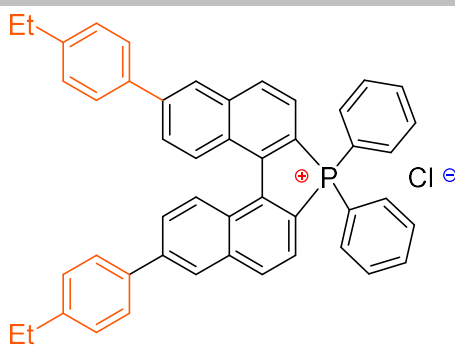
(s), 128.7 (s), 127.5 (s), 127.3 (s), 126.9 (s), 125.7 (d, $J = 10.8$ Hz), 119.3 (s), 116.9 (s), 116.0 (s), 29.7 (s). HRMS found for $[C_{46}H_{34}P]^+$: $m/z = 617.2337$, calcd for $[C_{46}H_{34}P]^+$: $m/z = 617.2393$.



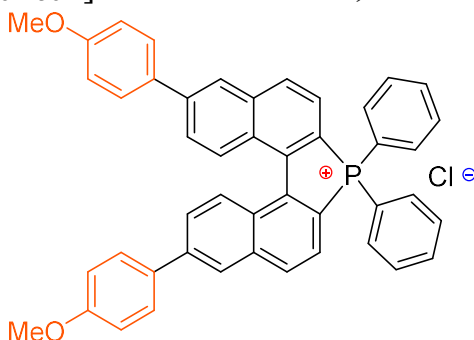
Synthesis of substituted (Rac)-11b: Prepared by general method (10) with 37% yield. ¹H NMR (400 MHz, CDCl₃) δ 8.38 (ddd, $J = 13.9, 10.9, 5.3$ Hz, 6H), 8.13–8.07 (m, 2H), 8.03 (dd, $J = 9.0, 1.8$ Hz, 2H), 7.94–7.87 (m, 6H), 7.75 (td, $J = 7.8, 3.7$ Hz, 4H), 7.63 (d, $J = 8.9$ Hz, 4H), 7.46 (t, $J = 7.6$ Hz, 2H), 7.32 (d, $J = 7.5$ Hz, 2H), 2.51 (s, 6H). ³¹P NMR (162 MHz, CDCl₃) δ 25.1. ¹³C NMR (101 MHz, CDCl₃) δ 145.0 (d, $J = 20.0$ Hz), 142.9 (s), 138.9 (d, $J = 10.6$ Hz), 136.4 (s), 133.4 (d, $J = 11.5$ Hz), 133.1 (d, $J = 12.6$ Hz), 129.5 (s), 129.1 (s), 128.5 (d, $J = 10.3$ Hz), 128.1 (s), 127.3 (s), 126.5 (s), 124.7 (d, $J = 10.6$ Hz), 124.5 (s), 120.0 (s), 119.0 (s), 116.8 (s), 115.9 (s), 21.4 (s). HRMS found for $[C_{46}H_{34}P]^+$: $m/z = 617.2349$, calcd for $[C_{46}H_{34}P]^+$: $m/z = 617.2393$.



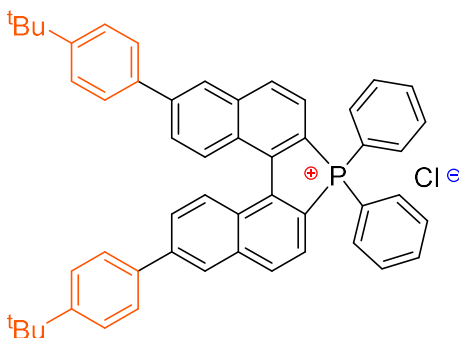
Synthesis of substituted (Rac)-12b: Prepared by general method (10) with 42% yield. ¹H NMR (400 MHz, CDCl₃) δ 8.50–8.31 (m, 4H), 8.27–8.04 (m, 4H), 7.93 (dt, $J = 15.7, 8.0$ Hz, 6H), 7.77 (m, 6H), 7.37 (m, 8H), 2.39 (s, 6H). ³¹P NMR (162 MHz, CDCl₃) δ 25.3. ¹³C NMR (101 MHz, CDCl₃) δ 145.0 (d, $J = 19.9$ Hz), 143.9 (s), 139.8 (s), 138.5 (s), 136.4 (s), 135.3 (s), 133.6 (d, $J = 11.8$ Hz), 133.0 (d, $J = 12.4$ Hz), 131.1 (d, $J = 13.5$ Hz), 130.8 (s), 129.8 (s), 129.3 (d, $J = 40.5$ Hz), 128.3 (d, $J = 15.6$ Hz), 127.8 (s), 126.2 (s), 124.9 (d, $J = 10.9$ Hz), 120.3 (s), 119.4 (s), 116.7 (s), 115.8 (s), 20.4 (s). HRMS found for $[C_{46}H_{34}P]^+$: $m/z = 617.2358$, calcd for $[C_{46}H_{34}P]^+$: $m/z = 617.2393$.



Synthesis of substituted (*Rac*)-13b: Prepared by general method (10) with 70% yield. ^1H NMR (400 MHz, CDCl_3) δ 8.46–8.28 (m, 8H), 8.00 (dd, $J = 15.8, 8.2$ Hz, 6H), 7.84 (t, $J = 6.6$ Hz, 2H), 7.74 (d, $J = 8.1$ Hz, 8H), 7.39 (d, $J = 8.1$ Hz, 4H), 2.76 (q, $J = 7.6$ Hz, 4H), 1.31 (d, $J = 7.6$ Hz, 6H). ^{31}P NMR (162 MHz, CDCl_3) δ 24.8 (s). ^{13}C NMR (101 MHz, CDCl_3) δ 145.2 (s), 144.9 (d, $J = 20.0$ Hz), 142.4 (s), 138.9 (s), 136.5 (s), 136.2 (s), 133.8 (d, $J = 11.7$ Hz), 133.2 (d, $J = 12.2$ Hz), 131.1 (d, $J = 13.4$ Hz), 128.9 (s), 128.6 (s), 128.4 (s), 127.4 (s), 127.0 (s), 126.3 (s), 125.7 (d, $J = 10.6$ Hz), 120.3 (s), 119.3 (s), 116.9 (s), 116.0 (s), 28.6 (s), 15.5 (s). HRMS found for $[\text{C}_{48}\text{H}_{38}\text{P}]^+$: $m/z = 645.2719$, calcd for $[\text{C}_{48}\text{H}_{38}\text{P}]^+$: $m/z = 645.2706$.



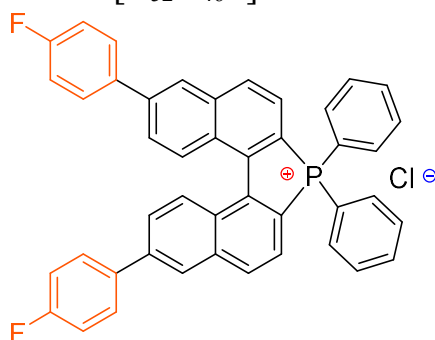
Synthesis of substituted (*P*)-14b: Prepared by general method (10) with 63% yield. ^1H NMR (400 MHz, CDCl_3) δ 8.34 (dq, $J = 17.2, 8.7$ Hz, 6H), 8.26 (d, $J = 1.6$ Hz, 2H), 8.04–7.93 (m, 6H), 7.84 (dd, $J = 8.1, 6.4$ Hz, 2H), 7.75 (ddd, $J = 11.1, 7.2, 2.8$ Hz, 8H), 7.09 (d, $J = 8.8$ Hz, 4H), 3.91 (s, 6H). ^{31}P NMR (162 MHz, CDCl_3) δ 24.8. ^{13}C NMR (101 MHz, CDCl_3) δ 160.3 (s), 144.8 (s), 142.0 (s), 139.0 (s), 136.1 (s), 133.7 (d, $J = 11.8$ Hz), 133.1 (d, $J = 12.0$ Hz), 131.43 (s), 131.09 (d, $J = 13.6$ Hz), 128.63 (s), 128.22 (d, $J = 11.4$ Hz), 126.8 (s), 125.8 (s), 125.6 (d, $J = 10.8$ Hz), 119.9 (d, $J = 10.0$ Hz), 119.0 (s), 116.0 (s), 116.1 (s), 114.8 (s), 55.5 (s). HRMS found for $[\text{C}_{46}\text{H}_{34}\text{P}]^+$: $m/z = 649.2261$, calcd for $[\text{C}_{46}\text{H}_{34}\text{O}_2\text{P}]^+$: $m/z = 649.2291$.



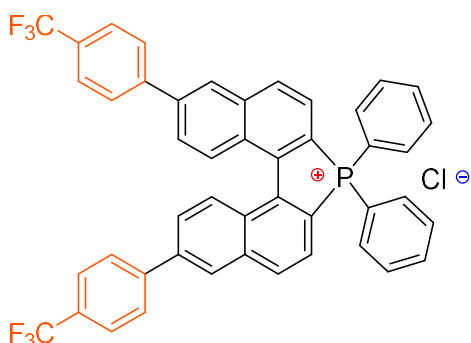
Synthesis of substituted (*Rac*)-15b: Prepared by general method (10) with 61% yield. ^1H NMR (400 MHz, CDCl_3) δ 8.44–8.30 (m, 6H), 8.13–8.00 (m, 4H), 7.90 (dt, $J = 13.0, 6.2$

Supporting information

Hz, 6H), 7.81–7.71 (m, 8H), 7.59 (dd, $J = 8.0, 5.6$ Hz, 4H), 1.41 (s, 18H). ^{31}P NMR (162 MHz, CDCl_3) δ 25.1. ^{13}C NMR (101 MHz, CDCl_3) δ 152.2 (s), 145.1 (d, $J = 20.0$ Hz), 142.5 (s), 139.0 (s), 136.4 (s), 136.0 (s), 133.4 (d, $J = 11.8$ Hz), 133.0 (d, $J = 12.3$ Hz), 131.1 (d, $J = 13.5$ Hz), 128.6 (s), 128.5 (d, $J = 11.7$ Hz), 127.2 (s), 127.1 (s), 126.2 (s), 124.8 (d, $J = 10.6$ Hz), 119.8 (s), 118.9 (s), 116.8 (s), 115.9 (s), 34.7 (s), 31.2 (s). HRMS found for $[\text{C}_{52}\text{H}_{46}\text{P}]^+$: $m/z = 701.3364$, calcd for $[\text{C}_{52}\text{H}_{46}\text{P}]^+$: $m/z = 701.3332$.

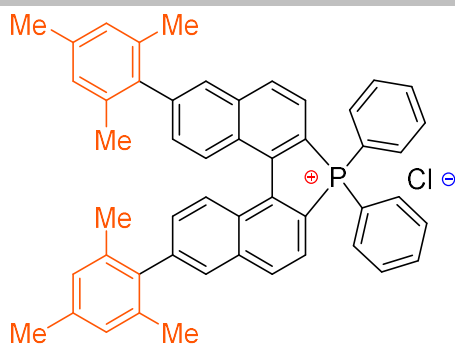


Synthesis of substituted (*Rac*)-16b: Prepared by general method (7) with 85% yield. ^1H NMR (400 MHz, MeOD) δ 8.45 (m, 6H), 8.30 (d, $J = 9.2$ Hz, 2H), 8.10–7.99 (m, 6H), 7.97–7.86 (m, 6H), 7.80–7.74 (m, 4H), 7.33–7.23 (m, 4H). ^{31}P NMR (162 MHz, MeOD) δ 25.4. ^{13}C NMR (101 MHz, MeOD) δ 164.5 (s), 162.0 (s), 141.1 (s), 138.9 (s), 135.9 (s), 135.3 (s), 133.4 (d, $J = 11.9$ Hz), 131.5 (t, $J = 7.3$ Hz), 130.6 (d, $J = 13.6$ Hz), 129.0 (d, $J = 8.3$ Hz), 128.6 (s), 126.5 (s), 126.1 (s), 125.1 (s), 119.9 (s), 117.2 (s), 116.7 (d, $J = 87.4$ Hz), 115.7 (d, $J = 22.0$ Hz). HRMS found for $[\text{C}_{44}\text{H}_{28}\text{P}]^+$: $m/z = 625.1905$, calcd for $[\text{C}_{44}\text{H}_{28}\text{F}_2\text{P}]^+$: $m/z = 625.1891$.

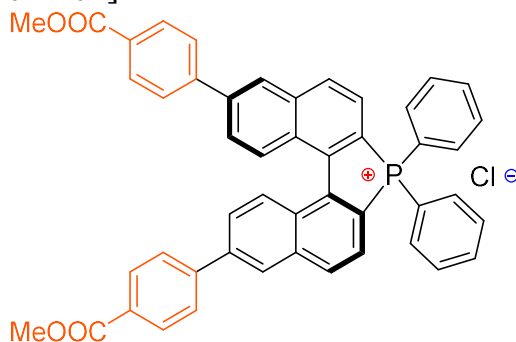


Synthesis of substituted (*Rac*)-17b: Prepared by general method (10) with 78% yield. ^1H NMR (400 MHz, CDCl_3) δ 8.56–8.29 (m, 8H), 8.09–7.88 (m, 10H), 7.87–7.79 (m, 6H), 7.77–7.72 (m, 4H). ^{31}P NMR (162 MHz, CDCl_3) δ 25.2. ^{13}C NMR (101 MHz, CDCl_3) δ 144.6 (d, $J = 19.9$ Hz), 142.7 (s), 140.8 (s), 138.8 (s), 136.3 (s), 134.3 – 133.3 (br), 131.2 (d, $J = 13.6$ Hz), 128.8 (s), 127.9 (s), 127.5 (s), 126.8 (s), 126.2 (d, $J = 3.5$ Hz), 121.3 (s), 120.3 (s), 116.5 (s), 115.7 (s), 29.7 (s). HRMS found for $[\text{C}_{46}\text{H}_{28}\text{F}_6\text{P}]^+$: $m/z = 725.1891$, calcd for $[\text{C}_{52}\text{H}_{46}\text{F}_6\text{P}]^+$: $m/z = 725.1827$.

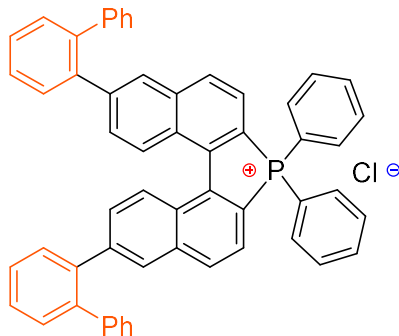
Supporting information



Synthesis of substituted (*Rac*)-18b: Prepared by general method (10) with 75% yield. ^1H NMR (400 MHz, CDCl_3) δ 8.47–8.28 (m, 6H), 8.06 (dd, $J = 14.0, 7.4$ Hz, 4H), 7.93–7.73 (m, 9H), 7.54 (dd, $J = 8.8, 1.4$ Hz, 2H), 7.01 (s, 4H), 2.37 (s, 6H), 2.08 (s, 12H). ^{31}P NMR (162 MHz, CDCl_3) δ 25.1. ^{13}C NMR (101 MHz, CDCl_3) δ 144.9 (d, $J = 19.9$ Hz), 143.2 (s), 138.7 (s), 137.6 (s), 137.0 (s), 136.2 (s), 135.6 (s), 133.8 (d, $J = 11.8$ Hz), 133.0 (d, $J = 12.1$ Hz), 131.1 (d, $J = 13.6$ Hz), 129.6 (d, $J = 11.8$ Hz), 128.9 – 127.8 (br), 125.7 (d, $J = 11.1$ Hz), 120.6 (s), 119.6 (s), 116.9 (s), 116.0 (s), 21.1 (s), 20.9 (s). HRMS found for $[\text{C}_{50}\text{H}_{42}\text{P}]^+$: $m/z = 673.3011$, calcd for $[\text{C}_{52}\text{H}_{46}\text{P}]^+$: $m/z = 673.3019$.



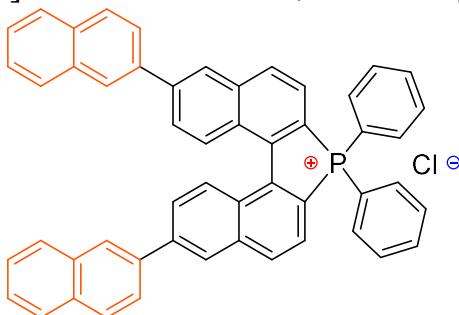
Synthesis of substituted (*P*)-19b: Prepared by general method (10) with 53% yield. ^1H NMR (400 MHz, CDCl_3) δ 8.55–8.35 (m, 8H), 8.22 (d, $J = 8.4$ Hz, 4H), 8.09–7.97 (m, 6H), 7.92–7.82 (m, 6H), 7.75 (dt, $J = 11.0, 5.6$ Hz, 4H), 3.98 (s, 6H). ^{31}P NMR (162 MHz, CDCl_3) δ 25.1. ^{13}C NMR (101 MHz, CDCl_3) δ 166.7 (s), 144.7 (d, $J = 19.9$ Hz), 143.4 (s), 141.2 (s), 138.8 (s), 136.3 (d, $J = 2.8$ Hz), 133.8 (d, $J = 11.8$ Hz), 133.7 – 133.2 (br), 131.1 (d, $J = 13.6$ Hz), 130.5 (s), 130.2 (s), 128.8 (s), 127.5 (s), 126.8 (s), 126.2 (d, $J = 10.8$ Hz), 121.2 (s), 120.3 (s), 116.6 (s), 115.7 (s), 52.3 (s), 29.7 (s). HRMS found for $[\text{C}_{48}\text{H}_{34}\text{O}_4\text{P}]^+$: $m/z = 705.2181$, calcd for $[\text{C}_{52}\text{H}_{46}\text{O}_4\text{P}]^+$: $m/z = 705.2189$.



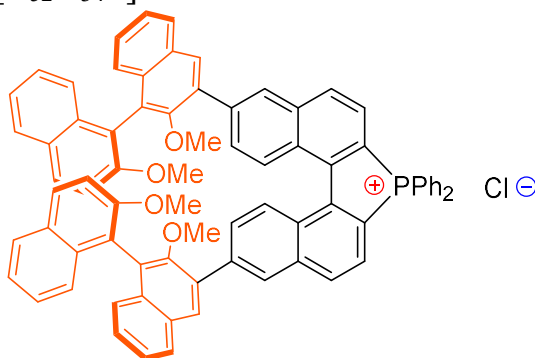
Synthesis of substituted (*Rac*)-20b: Prepared by general method (10) with 42% yield. ^1H NMR (400 MHz, CDCl_3) δ 8.28 (dt, $J = 12.3, 8.0$ Hz, 4H), 8.09–7.96 (m, 6H), 7.84 (t, $J = 6.9$ Hz, 2H), 7.78–7.69 (m, 6H), 7.65–7.59 (m, 2H), 7.54 (d, $J = 2.8$ Hz, 6H), 7.17 (m, 10H),

Supporting information

7.06 (dd, $J = 8.9, 1.4$ Hz, 2H). ^{31}P NMR (162 MHz, CDCl_3) δ 24.8. ^{13}C NMR (101 MHz, CDCl_3) δ 144.7 (s), 144.5 (s), 143.4 (s), 140.9 (d, $J = 5.2$ Hz), 138.6 (s), 138.4 (d, $J = 1.7$ Hz), 136.2 (s), 133.7 (d, $J = 11.8$ Hz), 132.8 (d, $J = 12.5$ Hz), 131.1 (d, $J = 13.6$ Hz), 130.9 (s), 130.5 (s), 130.0 (s), 129.8 (s), 128.9 (d, $J = 22.5$ Hz), 128.1 (d, $J = 7.4$ Hz), 127.8 (d, $J = 11.2$ Hz), 126.9 (d, $J = 1.9$ Hz), 125.5 (d, $J = 10.6$ Hz), 120.2 (s), 119.3 (s), 116.9 (s), 116.0 (s). HRMS found for $[\text{C}_{56}\text{H}_{38}\text{P}]^+$: $m/z = 741.2728$, calcd for $[\text{C}_{56}\text{H}_{38}\text{P}]^+$: $m/z = 741.2706$.

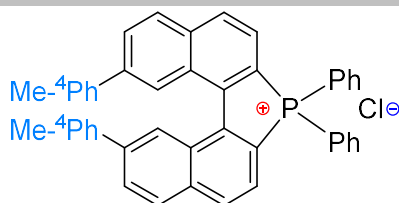


Synthesis of substituted (*Rac*)-21b: Prepared by general method (10) with 47% yield. ^1H NMR (400 MHz, CDCl_3) δ 8.44 (dd, $J = 24.9, 8.5$ Hz, 8H), 8.29 (s, 2H), 8.14 (dd, $J = 9.0, 1.4$ Hz, 2H), 8.07–7.91 (m, 12H), 7.85 (t, $J = 6.9$ Hz, 2H), 7.75 (d, $J = 3.2$ Hz, 4H), 7.61–7.53 (m, 4H). ^{31}P NMR (162 MHz, CDCl_3) δ 24.9. ^{13}C NMR (101 MHz, CDCl_3) δ 144.9 (d, $J = 19.9$ Hz), 142.3 (s), 139.0 (d, $J = 2.1$ Hz), 136.3 (s), 136.2 (d, $J = 3.0$ Hz), 133.8 (d, $J = 11.8$ Hz), 133.7 (s), 133.4 (d, $J = 12.2$ Hz), 133.2 (s), 131.1 (d, $J = 13.6$ Hz), 129.1 (s), 128.7 (s), 128.58 (d, $J = 11.8$ Hz), 128.5 (s), 127.8 (s), 127.1 (d, $J = 15.1$ Hz), 126.8 (s), 125.9 (d, $J = 10.7$ Hz), 125.1 (s), 120.6 (s), 119.6 (s), 116.8 (s), 116.0 (s). HRMS found for $[\text{C}_{52}\text{H}_{34}\text{P}]^+$: $m/z = 689.2416$, calcd for $[\text{C}_{52}\text{H}_{34}\text{P}]^+$: $m/z = 689.2393$.

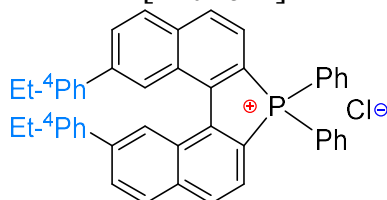


Synthesis of substituted (*S,S*)-22b: Prepared by general method (10) with 44% yield. ^1H NMR (400 MHz, CDCl_3) δ 8.53 (s, 2H), 8.47–8.33 (m, 6H), 8.20–8.14 (m, 4H), 8.07–7.98 (m, 8H), 7.91–7.83 (m, 4H), 7.76 (td, $J = 7.6, 3.7$ Hz, 4H), 7.52–7.44 (m, 4H), 7.37–7.28 (m, 6H), 7.24 (s, 2H), 7.19 (d, $J = 8.4$ Hz, 2H), 3.84 (s, 6H), 3.18 (s, 6H). ^{31}P NMR (162 MHz, CDCl_3) δ 25.1. ^{13}C NMR (101 MHz, CDCl_3) δ 154.9 (s), 153.8 (s), 145.0 (s), 144.8 (s), 143.5 (s), 140.8 (s), 138.7 (d, $J = 1.5$ Hz), 136.2 (d, $J = 3.1$ Hz), 134.1 (d, $J = 14.1$ Hz), 133.8 (d, $J = 11.8$ Hz), 133.2 (d, $J = 12.5$ Hz), 133.0 (s), 131.2 (s), 131.0 (d, $J = 11.1$ Hz), 130.0 (s), 129.5 (s), 129.2 (s), 128.6 (d, $J = 11.6$ Hz), 128.2 (d, $J = 24.0$ Hz), 127.8 (s), 126.9 (d, $J = 15.6$ Hz), 126.3 (s), 125.9 – 125.3 (br), 125.0 (s), 123.7 (s), 120.5 (s), 119.6 (s), 119.0 (s), 116.9 (s), 116.1 (s), 113.6 (s), 60.8 (s), 56.6 (s). HRMS found for $[\text{C}_{46}\text{H}_{34}\text{P}]^+$: $m/z = 1061.3708$, calcd for $[\text{C}_{46}\text{H}_{34}\text{P}]^+$: $m/z = 1061.3754$.

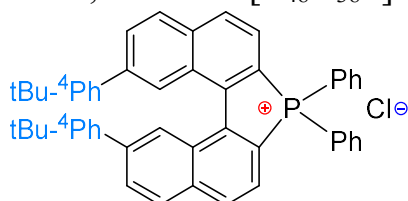
Supporting information



Synthesis of substituted (*Rac*)-1c: Prepared by general method (10) with 68% yield. ^1H NMR (400 MHz, CDCl_3) δ 8.55 (s, 2H), 8.35 (dd, $J = 17.3, 6.7$ Hz, 4H), 8.19 (d, $J = 8.6$ Hz, 2H), 8.05–7.97 (m, 6H), 7.84 (dd, $J = 8.0, 6.0$ Hz, 2H), 7.75 (dd, $J = 7.8, 3.7$ Hz, 4H), 7.33 (d, $J = 8.1$ Hz, 4H), 7.12 (d, $J = 7.9$ Hz, 4H), 2.34 (s, 6H). ^{31}P NMR (162 MHz, CDCl_3) δ 24.8. ^{13}C NMR (101 MHz, CDCl_3) δ 144.9 (d, $J = 19.7$ Hz), 140.6 (s), 138.4 (s), 137.4 (d, $J = 1.6$ Hz), 136.7 (s), 136.2 (d, $J = 3.0$ Hz), 133.7 (d, $J = 11.8$ Hz), 132.9 (d, $J = 12.2$ Hz), 131.1 (d, $J = 13.6$ Hz), 130.6 – 130.5 (br), 130.1 (s), 129.8 (s), 129.7 (s), 127.3 (s), 125.6 (s), 125.1 (d, $J = 10.3$ Hz), 121.3 (s), 120.3 (s), 116.7 (s), 115.9 (s), 21.2 (s). HRMS found for $[\text{C}_{46}\text{H}_{34}\text{P}]^+$: $m/z = 617.2397$, calcd for $[\text{C}_{46}\text{H}_{34}\text{P}]^+$: $m/z = 617.2393$.

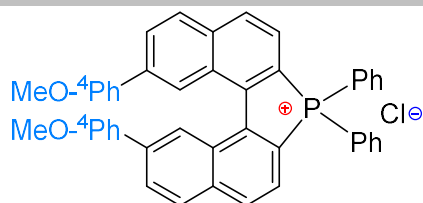


Synthesis of substituted (*Rac*)-2c: Prepared by general method (10) with 92% yield. ^1H NMR (400 MHz, MeOD) δ 8.54 (s, 2H), 8.36 (dd, $J = 8.2, 4.3$ Hz, 2H), 8.29–8.21 (m, 4H), 8.10–8.02 (m, 6H), 7.94 (ddd, $J = 7.6, 2.0, 1.0$ Hz, 2H), 7.80–7.75 (m, 4H), 7.10 (d, $J = 8.1$ Hz, 4H), 2.59 (q, $J = 7.6$ Hz, 4H), 1.17 (t, $J = 7.6$ Hz, 6H). ^{31}P NMR (162 MHz, MeOD) δ 25.0. ^{13}C NMR (101 MHz, MeOD) δ 145.0 (d, $J = 19.9$ Hz), 144.5 (s), 140.2 (s), 137.7 – 136.7 (br), 136.7 (s), 135.9 (d, $J = 2.9$ Hz), 133.5 (d, $J = 11.8$ Hz), 132.2 (d, $J = 12.3$ Hz), 130.6 (d, $J = 13.6$ Hz), 129.8 (d, $J = 11.9$ Hz), 129.7 (s), 129.1 (s), 128.3 (s), 126.9 (s), 125.1 (s), 124.4 (d, $J = 10.8$ Hz), 121.6 (s), 120.6 (s), 117.1 (s), 116.2 (s), 28.0 (s), 14.7 (s). HRMS found for $[\text{C}_{48}\text{H}_{38}\text{P}]^+$: $m/z = 645.2719$, calcd for $[\text{C}_{48}\text{H}_{38}\text{P}]^+$: $m/z = 645.2706$.

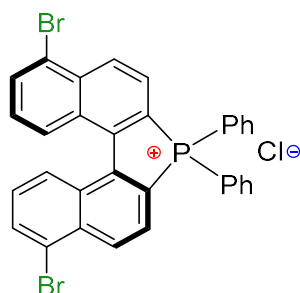


Synthesis of substituted (*Rac*)-3c: Prepared by general method (10) with 84% yield. ^1H NMR (400 MHz, MeOD) δ 8.61 (s, 2H), 8.38 (dd, $J = 8.2, 4.3$ Hz, 2H), 8.30–8.23 (m, 4H), 8.14–8.03 (m, 6H), 7.98–7.91 (m, 2H), 7.78 (td, $J = 7.9, 3.7$ Hz, 4H), 7.43–7.31 (m, 8H), 1.28 (s, 18H). ^{31}P NMR (162 MHz, MeOD) δ 25.0. ^{13}C NMR (101 MHz, MeOD) δ 149.7 (s), 143.6 (d, $J = 19.9$ Hz), 138.7 (s), 135.97 (d, $J = 1.7$ Hz), 135.1 (s), 134.4 (d, $J = 3.2$ Hz), 132.0 (d, $J = 12.0$ Hz), 130.8 (d, $J = 12.1$ Hz), 129.1 (d, $J = 13.6$ Hz), 128.3 (s), 128.2 (s), 127.7 (s), 125.2 (s), 124.2 (s), 123.7 (s), 122.9 (d, $J = 10.5$ Hz), 120.1 (s), 119.2 (s), 115.6 (s), 114.7 (s), 32.5 (s), 28.8 (s). HRMS found for $[\text{C}_{52}\text{H}_{46}\text{P}]^+$: $m/z = 701.3297$, calcd for $[\text{C}_{52}\text{H}_{46}\text{P}]^+$: $m/z = 701.3332$.

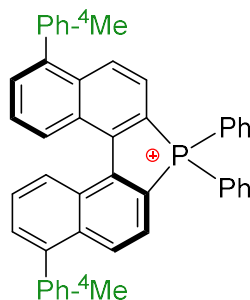
Supporting information



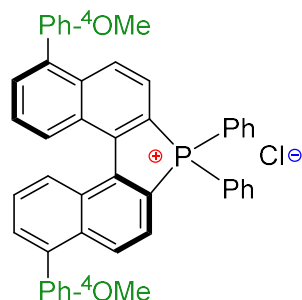
Synthesis of substituted (*Rac*)-4c: Prepared by general method (10) with 90% yield. ^1H NMR (400 MHz, MeOD) δ 8.56 (s, 2H), 8.37 (dd, $J = 8.1, 4.3$ Hz, 2H), 8.25 (t, $J = 8.8$ Hz, 4H), 8.14–8.02 (m, 6H), 7.99–7.88 (m, 2H), 7.78 (td, $J = 7.9, 3.7$ Hz, 4H), 7.48–7.41 (m, 4H), 6.90–6.80 (m, 4H), 3.78 (s, 6H). ^{31}P NMR (162 MHz, MeOD) δ 25.1. ^{13}C NMR (101 MHz, CDCl_3) δ 159.9 (s), 144.9 (d, $J = 20.0$ Hz), 140.1 (s), 137.2 (s), 136.2 (d, $J = 3.1$ Hz), 133.8 (d, $J = 11.4$ Hz), 132.8 (d, $J = 13.0$ Hz), 132.0 (s), 131.1 (s), 130.1 (d, $J = 23.0$ Hz), 129.5 (s), 128.5 (s), 125.2 (s), 114.6 (s), 55.4 (s). HRMS found for $[\text{C}_{46}\text{H}_{34}\text{P}]^+$: $m/z = 649.2308$, calcd for $[\text{C}_{46}\text{H}_{34}\text{O}_2\text{P}]^+$: $m/z = 649.2291$.



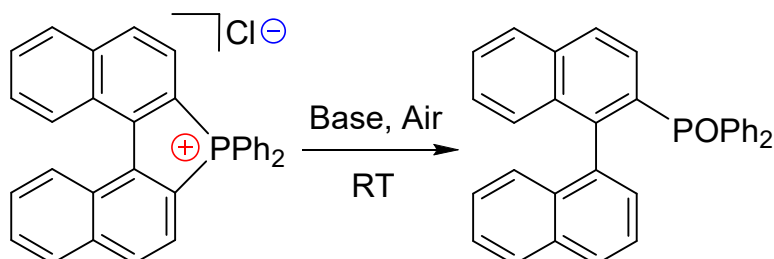
Synthesis of substituted (*Rac*)-5c: Prepared by general method (10) with 40% yield. ^1H NMR (400 MHz, CDCl_3) δ 8.81 (dd, $J = 8.5, 4.1$ Hz, 2H), 8.64 (t, $J = 8.8$ Hz, 2H), 8.16–8.05 (m, 8H), 7.86–7.82 (m, 2H), 7.74 (td, $J = 7.6, 3.8$ Hz, 4H), 7.51 (dd, $J = 10.3, 5.8$ Hz, 2H). ^{31}P NMR (162 MHz, CDCl_3) δ 25.4. ^{13}C NMR (101 MHz, CDCl_3) δ 136.9 (s), 136.4 (s), 134.0 (d, $J = 10.8$ Hz), 132.7 (d, $J = 11.9$ Hz), 131.2 (d, $J = 13.7$ Hz), 130.5 (d, $J = 11.0$ Hz), 127.5 (d, $J = 10.1$ Hz), 127.1 (d, $J = 10.8$ Hz), 124.2 (s), 121.9 (s). HRMS found for $[\text{C}_{32}\text{H}_{20}\text{Br}_2\text{P}]^+$: $m/z = 594.9671$, calcd for $[\text{C}_{32}\text{H}_{20}\text{Br}_2\text{P}]^+$: $m/z = 594.9643$.



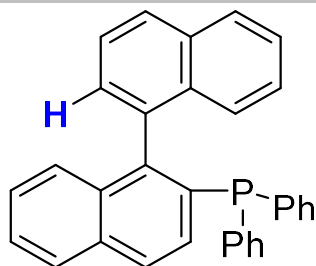
Synthesis of substituted (*Rac*)-6c: Prepared by general method (10) with 57% yield. ^1H NMR (400 MHz, CDCl_3) δ 8.28 (dd, $J = 25.0, 16.9$ Hz, 6H), 8.00 (s, 4H), 7.85–7.68 (m, 10H), 7.42 (d, $J = 7.8$ Hz, 4H), 7.36 (d, $J = 7.4$ Hz, 4H), 2.49 (s, 6H). ^{31}P NMR (162 MHz, CDCl_3) δ 25.2. ^{13}C NMR (101 MHz, CDCl_3) δ 159.0 (s), 139.6 (s), 137.1 (s), 135.2 (s), 134.3 (d, $J = 21.1$ Hz), 132.9 (s), 132.0 – 130.9 (m), 130.5 (s), 129.0 – 127.2 (br), 126.2 (s), 125.3 (s), 114.2 (d, $J = 8.0$ Hz), 113.7 (s), 113.1 (s), 55.4 (s). HRMS found for $[\text{C}_{46}\text{H}_{34}\text{P}]^+$: $m/z = 617.2404$, calcd for $[\text{C}_{46}\text{H}_{34}\text{P}]^+$: $m/z = 617.2393$.



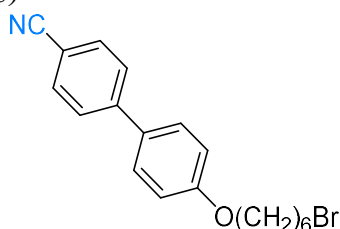
Synthesis of substituted (*P*)-7c: Prepared by general method (**10**) with 73% yield. ^1H NMR (400 MHz, CDCl_3) δ 8.35 (dd, $J = 8.4, 4.4$ Hz, 2H), 8.26 (d, $J = 8.1$ Hz, 2H), 8.20 (t, $J = 8.8$ Hz, 2H), 7.99 (dd, $J = 14.1, 7.6$ Hz, 4H), 7.83 (dd, $J = 7.9, 6.2$ Hz, 2H), 7.76–7.68 (m, 8H), 7.45 (d, $J = 8.6$ Hz, 4H), 7.09 (d, $J = 8.7$ Hz, 4H), 3.92 (s, 6H). ^{31}P NMR (162 MHz, CDCl_3) δ 25.2. ^{13}C NMR (101 MHz, CDCl_3) δ 159.8 (s), 145.2 (d, $J = 19.8$ Hz), 141.6 (s), 137.1 (s), 136.3 (d, $J = 3.2$ Hz), 133.7 (d, $J = 11.8$ Hz), 132.0 – 130.9 (br), 130.4 (s), 130.2 (d, $J = 11.5$ Hz), 127.0 (d, $J = 35.8$ Hz), 125.0 (d, $J = 10.6$ Hz), 120.9 (s), 120.0 (s), 116.6 (s), 115.8 (s), 114.3 (s), 55.5 (s). HRMS found for $[\text{C}_{46}\text{H}_{34}\text{P}]^+$: $m/z = 649.2308$, calcd for $[\text{C}_{46}\text{H}_{34}\text{O}_2\text{P}]^+$: $m/z = 649.2291$.



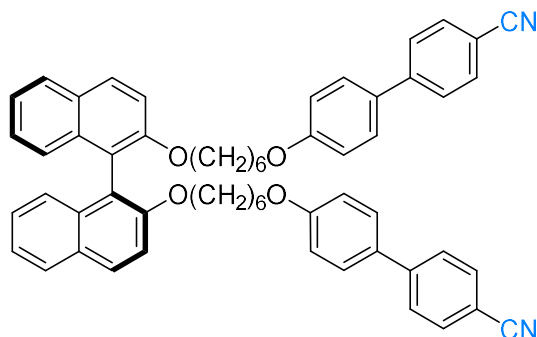
Synthesis of substituted (*Rac*)-1d: In a 50 mL Schlenk tube were placed $[(\text{Rac})\text{-1b}]^+[\text{Cl}]^-$ 50 mg (1.0 eq), NaOH (2.0 eq), and a 20 mL of CH_3OH solvent. The mixture solution was reacted at room temperature under an air atmosphere for about 5 min. The organic phase was extracted successively with dilute hydrochloric acid and dichloromethane. The organic phase was dried with anhydrous MgSO_4 and filtered. The solvent was removed by decompressing vaporization. The resulting residue was purified by column chromatography with EA: CH_2Cl_2 (1:3), and then the white solid powder was obtained with 91% yield. ^1H NMR (400 MHz, CDCl_3) δ 7.97 (dd, $J = 8.6, 2.0$ Hz, 1H), 7.92 (d, $J = 8.2$ Hz, 1H), 7.84 (dd, $J = 11.6, 8.6$ Hz, 1H), 7.61 (dd, $J = 15.8, 8.2$ Hz, 2H), 7.56–7.45 (m, 4H), 7.33 (ddd, $J = 9.7, 6.6, 5.4$ Hz, 3H), 7.28–7.15 (m, 5H), 7.11 (d, $J = 8.5$ Hz, 1H), 7.09–7.02 (m, 2H), 6.92 (ddd, $J = 21.3, 10.8, 5.7$ Hz, 3H). ^{31}P NMR (162 MHz, CDCl_3) δ 28.0. ^{13}C NMR (101 MHz, CDCl_3) δ 144.2 (d, $J = 9.1$ Hz), 135.0 – 134.3 (br), 133.5 (d, $J = 11.1$ Hz), 133.3 (s), 132.7 (d, $J = 7.9$ Hz), 132.6 (s), 132.2 (s), 131.8 (d, $J = 9.3$ Hz), 131.5 (s), 130.9 (d, $J = 2.6$ Hz), 130.8 (d, $J = 9.9$ Hz), 130.4 (d, $J = 2.7$ Hz), 130.2 (s), 129.7 (s), 128.9 (s), 128.8 (s), 128.2 – 127.6 (br), 127.4 (d, $J = 12.2$ Hz), 126.8 (d, $J = 5.1$ Hz), 125.5 (d, $J = 29.7$ Hz), 124.7 (s).



Synthesis of substituted (*Rac*)-1c: In a 50 mL Schlenk tube were placed (*Rac*)-1d 100 mg (1.0 eq), HSiCl_3 (2.0 eq), and a 20 mL of dry toluene solvent. The mixture solution was reacted at 100 °C under an Ar atmosphere for about 12 h. The organic phase was extracted successively with water and dichloromethane. The organic phase was dried with anhydrous MgSO_4 and filtered. The solvent was removed by decompressing vaporization. The resulting residue was purified by column chromatography with PE: CH_2Cl_2 (4:1), and then the white solid powder was obtained with 84% yield. ^1H NMR (400 MHz, CDCl_3) δ 7.92 (dd, $J = 8.2, 4.4$ Hz, 2H), 7.87 (t, $J = 9.0$ Hz, 2H), 7.49 – 7.39 (m, 3H), 7.35–7.29 (m, 6H), 7.24–7.11 (m, 10H). ^{31}P NMR (162 MHz, CDCl_3) δ -14.1.



Synthesis of 4'-((6-bromohexyl)oxy)-[1,1'-biphenyl]-4-carbonitrile: In a 50 mL Schlenk tube were placed 4'-hydroxy-[1,1'-biphenyl]-4-carbonitrile 1.0 g (5.1 mmol), K_2CO_3 (2.0 eq), 1,6-dibromohexane (1.0 eq), and a 25 mL of dry DMF solvent. The mixture solution was reacted at 80 °C under an Ar atmosphere for about 5 h. The organic phase was extracted successively with water and dichloromethane. The organic phase was dried with anhydrous MgSO_4 and filtered. The solvent was removed by decompressing vaporization. The resulting residue was purified by column chromatography with PE: CH_2Cl_2 (1:1), and then the white solid powder was obtained with 57% yield. ^1H NMR (600 MHz, CDCl_3 , TMS) δ 7.7 (2H d, $J = 8.5$ Hz), 7.65 (2H d, $J = 8.5$ Hz), 7.52 (2H dd, $J = 9.3, 2.4$ Hz), 6.98 (2H t, $J = 5.8$ Hz), 4.01 (2H t, $J = 6.4$ Hz), 3.44 (2H t, $J = 6.8$ Hz), 1.95–1.87 (2H m), 1.84 (2H dd, $J = 13.4, 6.9$ Hz), 1.57–1.49 (4H m).



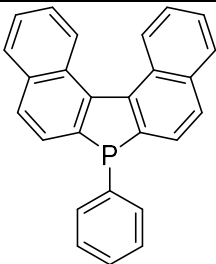
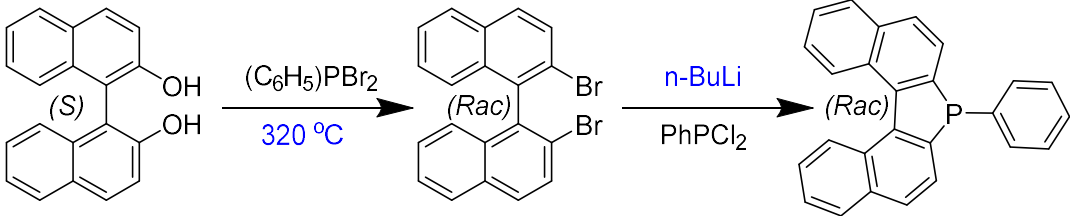
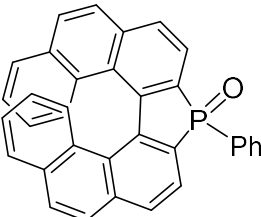
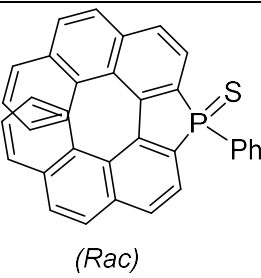
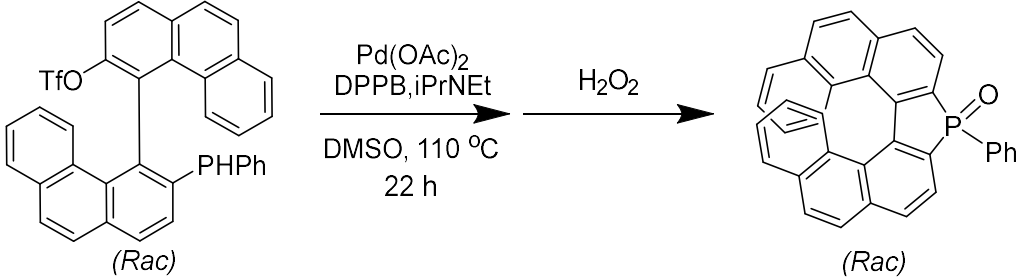
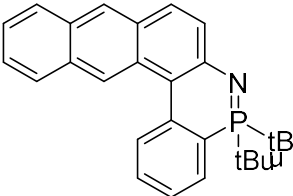
Synthesis of (*S*)-4',4'''-(((1,1'-binaphthalene]-2,2'-diylbis(oxy))bis(hexane-6,1-diyl))bis(oxy))bis([1,1'-biphenyl]-4-carbonitrile): In a 50 mL Schlenk tube were placed 4'-((6-bromohexyl)oxy)-[1,1'-biphenyl]-4-carbonitrile 0.5 g (1.4 mmol), K_2CO_3 (2.0 eq), (*S*)-[1,1'-binaphthalene]-2,2'-diol (0.5 eq), and 25 mL of dry DMF solvent. The mixture

Supporting information

solution was reacted at 80 °C under an Ar atmosphere for about 5 h. The organic phase was extracted successively with water and dichloromethane. The organic phase was dried with anhydrous MgSO₄ and filtered. The solvent was removed by decompressing vaporization. The resulting residue was purified by column chromatography with PE:CH₂Cl₂ (1:1), and then the white solid powder was obtained with 87% yield. ¹H NMR (400 MHz, CDCl₃) δ 7.91 (d, J = 8.9 Hz, 2H), 7.83 (d, J = 8.1 Hz, 2H), 7.71–7.66 (m, 4H), 7.65–7.60 (m, 4H), 7.55–7.48 (m, 4H), 7.40 (d, J = 9.0 Hz, 2H), 7.29 (ddd, J = 8.1, 6.4, 1.5 Hz, 2H), 7.23–7.12 (m, 4H), 4.00 (dt, J = 9.3, 6.0 Hz, 2H), 3.90 (dt, J = 9.3, 6.3 Hz, 2H), 3.78 (t, J = 6.6 Hz, 4H).

Supporting information

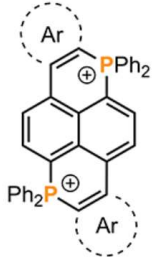
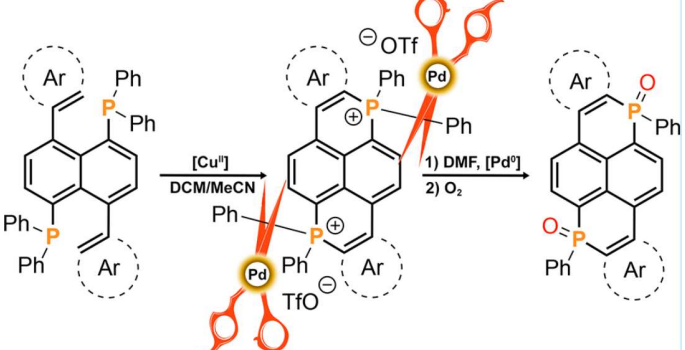
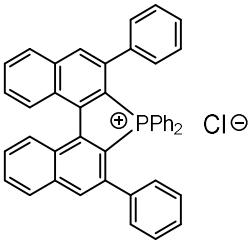
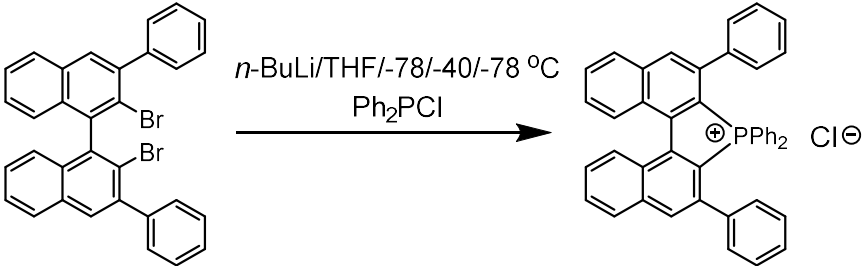
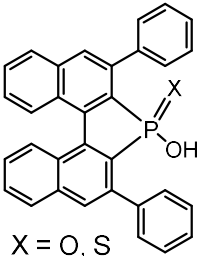
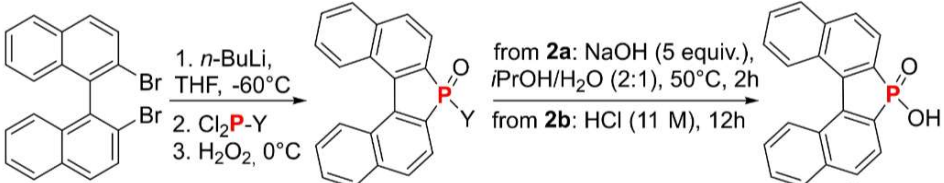
Table S1. Photoelectric and chiral chiroptoelectronic properties of reported organic phospha[n]helicenes or achiral phosphonium salts

π-Extended Neutral Phospha[n]helicenes				
Structure	λ_{PL} (nm)	PLQY (%)	$^a g_{\text{lum}} / ^b g_{\text{abs}}$	Reference
	Not emissive	-	-	6
				
	462	7.8 / 0.1	+ 3014 (c = 0.10, CHCl ₃)	7
	460	0.1	+3198 (c = 0.10, CHCl ₃)	7
				
	535	~12	-	8

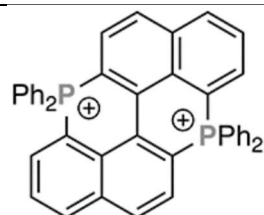
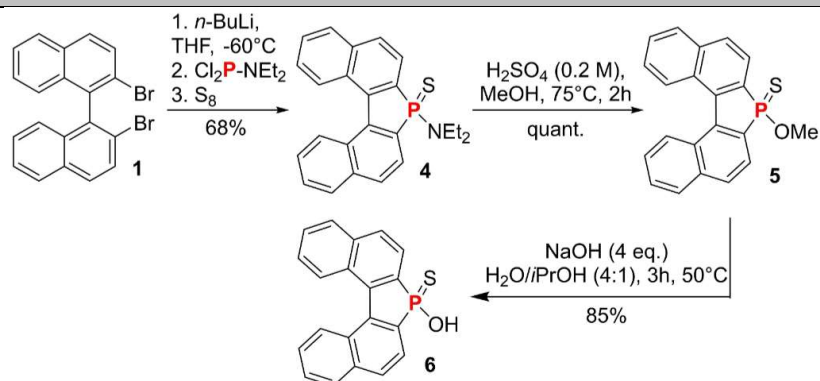
Supporting information

	446, 572	1	2.48×10^{-2}	9
	Unknown	-	-	10
	Unknown	-	-	11
	375-482	-	-	12
	371 epimerization	18	2×10^{-3}	13
	441, 449	6, 5.7	$1.3-1.9 \times 10^{-3}$	14
π-Extended Phosponium Salts				

Supporting information

 <p style="text-align: center;">Achirality</p>	<p>3: 483, 506 4: 439, 460</p>	<p>3: 16 4: 7</p>	<p style="text-align: center;">-</p>	<p style="text-align: center;">15</p>
				
	<p style="text-align: center;">Unknown</p>	<p style="text-align: center;">Unknown</p>	<p style="text-align: center;">Unknown</p>	<p style="text-align: center;">16</p>
				
 <p style="text-align: center;">X = O, S</p>	<p>464 (X=O), 485 (X=S)</p>	<p>14 (X=O), 2 (X=S)</p>	<p style="text-align: center;">-</p>	<p style="text-align: center;">17</p>
				

Supporting information



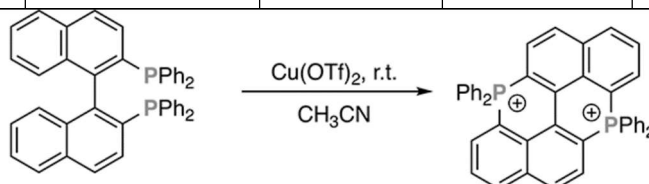
$E_{1/2}^* = +2.17$ V vs. SCE
 $E_{1/2} = -0.55$ V vs. SCE

456

-

-

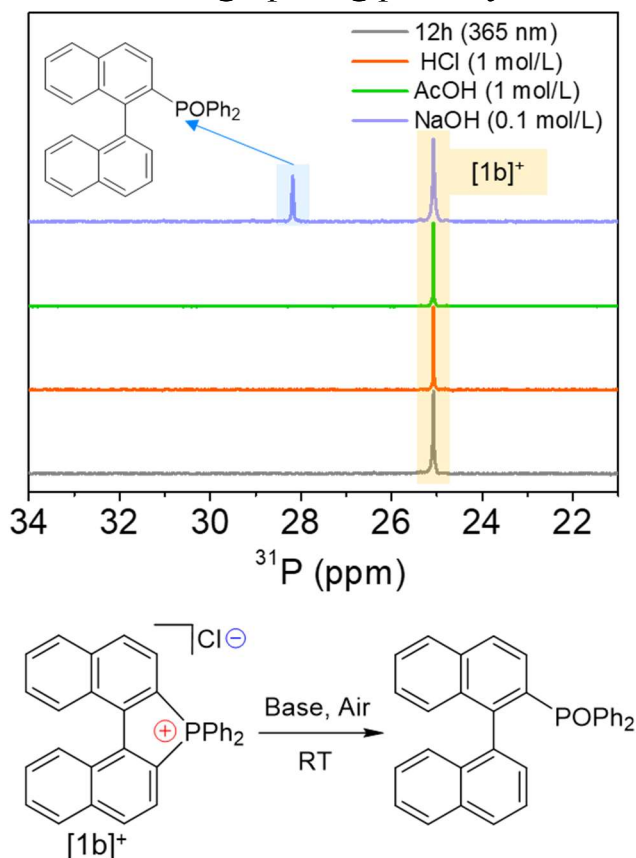
18,19



^an Asymmetry factor for circularly polarized luminescence (CPL), and ^b Asymmetry absorption factor for circular dichroism (CD).

Section C: Chemical structure stability of compound [1b]⁺[Cl]⁻ and kinetic study of racemization of [2b]⁺[Cl]⁻**1. Chemical structure stability**

These phosphahelicens (i.e. compound [1b]⁺[Cl]⁻) have good solubility and stability in many polar organic solvents (including chloroalkane, alcohols solvent, DMF, DMSO) and acid conditions as well as UV-radiation. However, the structure could be transformed into monophosphine oxide via a ring-opening passway under base conditions in the air.



Scheme S1. Monitored ³¹P-NMR spectra of [1b]⁺[Cl]⁻ with different acids, base additives, or radiation (365 nm) in CD₃OD.

2. Kinetic study of [2b]⁺[Cl]⁻

For helicene [2b]⁺[Cl]⁻, the highly enantiomeric pure single crystals could be used for racemization kinetic study. The pure single crystals were synthesized from enantiomeric BINAPs at low temperatures (see Section B in SI). The single crystals were grown in a supersaturated solution (DCM/n-hexane=1/2) at 10-15 °C. The regular single crystals were dissolved in cold DCM at -15±2 °C, and the circular dichroism (CD) spectra of both enantiomers were rapidly and successfully recorded in DCM at different temperature conditions.

We assumed that the racemization process obeys first-order kinetic. Because of the linear relationship between CD intensity and concentration of excess enantiomer, equation 1) can be replaced by ellipticity experimentally measured by CD spectroscopy at a certain wavelength (at 370 nm).

$$A = A_0 e^{-kt} \quad 1)$$

By plotting the natural logarithm of [Int₃₇₀]_t/[Int₃₇₀]₀ values, we performed Eyring plots to determine experimental ΔH^\ddagger (12.5 kcal/mol), ΔS^\ddagger (-25.4 cal/mol·K), ΔG_{exp}^\ddagger (20.1 kcal/mol) and rate constant (k) = $1.50 \times 10^{-4} \text{ sec}^{-1}$, racemization half-life ($t_{1/2}$) = 77.5 min at 298.15 K were estimated by the following equations (1)–(5):

$$k = \frac{k_B T}{h} \times \exp\left(\frac{-\Delta H^\ddagger}{RT}\right) \times \exp\left(\frac{\Delta S^\ddagger}{R}\right) \quad 2)$$

$$\ln\left(\frac{k}{T}\right) = \left(\frac{-\Delta H^\ddagger}{R}\right)\frac{1}{T} + \ln\left(\frac{k_B}{h}\right) + \frac{\Delta S^\ddagger}{R} \quad 3)$$

$$\Delta G_{exp}^\ddagger = \Delta H^\ddagger - T \cdot \Delta S^\ddagger \quad 4)$$

$$t_{\frac{1}{2}} = \frac{\ln 2}{k} \quad 5)$$

where k_B , h and R are Boltzmann constant ($1.380649 \times 10^{-23} \text{ J}\cdot\text{K}^{-1}$), Planck's constant ($6.62607015 \times 10^{-34} \text{ J}\cdot\text{sec}$), and molar gas constant ($8.314462618 \text{ J}\cdot\text{K}^{-1}\cdot\text{mol}^{-1}$), respectively.^{20,21}

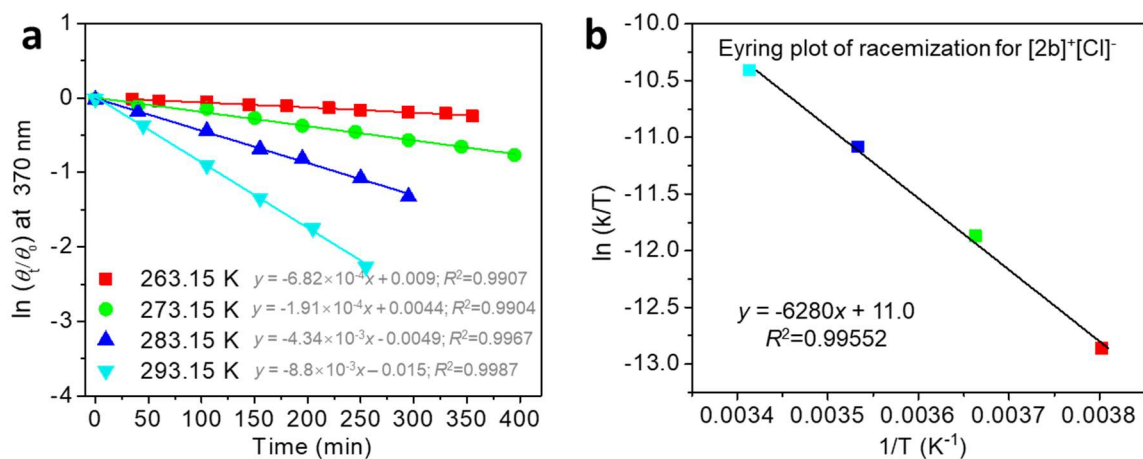


Fig S1. (a) Temperature and time-dependent decay of intensities of ellipticity in CD spectra at 370 nm for $[2b]^+[Cl]^-$ and (b) its Eyring plots.

Section D: X-ray crystallographic data

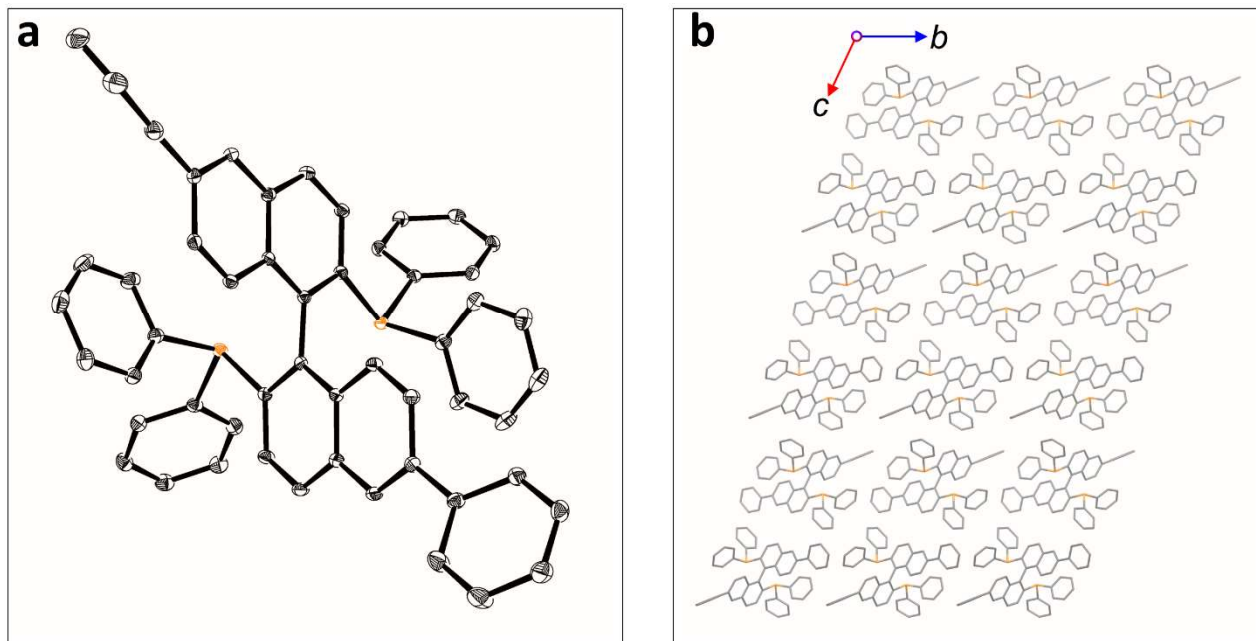


Fig. S2 (a) ORTEP representation of the single-crystal structure of isomer (*S*)-9b3 with thermal ellipsoids at 50% probability. (b) Molecular packing model of (*Rac*)-9b3 along the *a*-axis in crystal. The H-atoms were omitted for clarity.

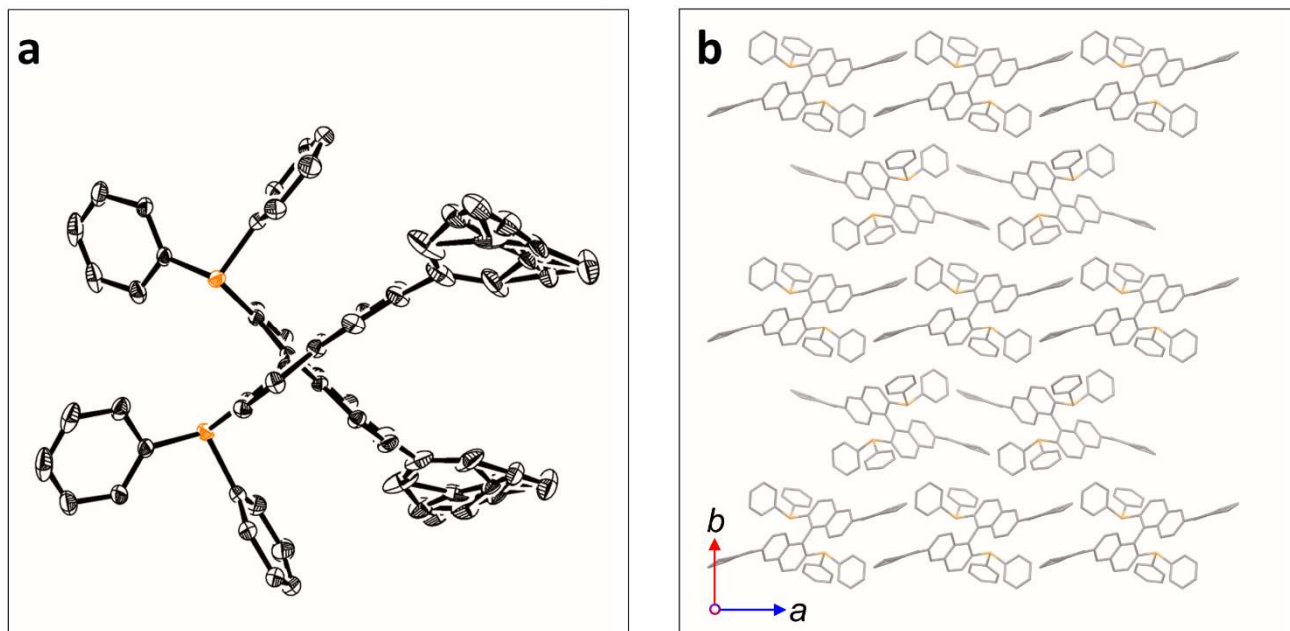


Fig. S3 (a) ORTEP representation of the single-crystal structure of compound (*S*)-11b3 with thermal ellipsoids at 50% probability. (b) Molecular packing model of (*S*)-11b3 along the *c*-axis in crystal. Some disorders were observed in phenyl rings. The H-atoms were omitted for clarity.

Supporting information

Table S2. Crystallographic Data and Structure Refinement for (Rac)-9b3, (S)-11b3, (S)-14b3, (Rac)-15b3, (S)-6c3

Name	(Rac)-9b3	(S)-11b3	(S)-14b3	(Rac)-15b3	(S)-6c3
CCDC number	2225472	2225477	2225478	2225473	2225474
Empirical formula	C ₅₆ H ₄₀ P ₂	C ₅₈ H ₄₄ P ₂	C ₅₈ H ₄₄ O ₂ P ₂	C ₆₄ H ₅₆ P ₂	C ₅₈ H ₄₄ P ₂
Formula weight	774.82	802.87	834.87	887.03	887.80
Crystal system	triclinic	orthorhombic	triclinic	monoclinic	orthorhombic
Space group	$P\bar{1}$	$P2_12_12$	$P1$	$C2/c$	$P2_12_12_1$
$a/\text{Å}$	8.1589(6)	13.5549(15)	9.2214(9)	32.764(3)	12.2007(7)
$b/\text{Å}$	13.3454(11)	18.4613(18)	13.2109(12)	8.5089(8)	18.1269(12)
$c/\text{Å}$	20.1127(15)	8.6468(9)	18.8909(16)	19.653(2)	20.8115(11)
$\alpha/^\circ$	105.202(3)	90	95.700(3)	90	90
$\beta/^\circ$	99.249(3)	90	99.414(3)	118.644(6)	90
$\gamma/^\circ$	92.305(4)	90	101.148(4)	90	90
Volume/Å ³	2078.0(3)	2163.8(4)	2207.0(4)	4808.5(8)	4602.7(5)
Z	2	2	2	4	4
$\rho_{\text{calc}}(\text{g}/\text{cm}^3)$	1.238	1.232	1.256	1.225	1.281
μ/mm^{-1}	0.143	0.140	0.143	0.132	0.251
F(000)	812.0	844.0	876	1880	1856
Crystal size/mm ³	0.2*0.2*0.1	0.15*0.2*0.1	0.1*0.1*0.1	0.12*0.1*0.1	0.2*0.2*0.05
Radiation (Å)	MoK α ($\lambda = 0.71073$)	MoK α ($\lambda = 0.71073$)	MoK α ($\lambda = 0.71073$)	MoK α ($\lambda = 0.71073$)	MoK α ($\lambda = 0.71073$)
2 θ range for data collection/ $^\circ$	8.082 to 107.762	5.202 to 46.431	4.583 to 55.047	4.723 to 54.921	4.470 to 49.418
Index ranges	-9 $\leq h \leq 9$, -15 $\leq k \leq 15$, -23 $\leq l \leq 22$	-17 $\leq h \leq 17$, -22 $\leq k \leq 23$, -11 $\leq l \leq 11$	-11 $\leq h \leq 12$, -16 $\leq k \leq 17$, -24 $\leq l \leq 22$	-33 $\leq h \leq 41$, -10 $\leq k \leq 10$, -25 $\leq l \leq 24$	-15 $\leq h \leq 15$, -23 $\leq k \leq 22$, -26 $\leq l \leq 27$
Reflections collected	17502	20546	20889	20104	43979
Independent reflections	7146 [$R_{\text{int}} = 0.049$, $R_{\text{sigma}} = 0.0578$]	4964 [$R_{\text{int}} = 0.079$, $R_{\text{sigma}} = 0.0731$]	9648 [$R_{\text{int}} = 0.042$, $R_{\text{sigma}} = 0.0709$]	5316 [$R_{\text{int}} = 0.084$, $R_{\text{sigma}} = 0.0726$]	6589 [$R_{\text{int}} = 0.086$, $R_{\text{sigma}} = 0.0831$]
Goodness-of-fit on F^2	1.121	1.027	1.035	0.990	1.063
Final R indexes [$I \geq 2\sigma(I)$]	$R_1 = 0.0486$, $wR_2 = 0.1513$	$R_1 = 0.0598$, $wR_2 = 0.1470$	$R_1 = 0.0461$, $wR_2 = 0.1212$	$R_1 = 0.0632$, $wR_2 = 0.1654$	$R_1 = 0.0675$, $wR_2 = 0.1655$
Final R indexes [all data]	$R_1 = 0.0629$, $wR_2 = 0.1723$	$R_1 = 0.0873$, $wR_2 = 0.1638$	$R_1 = 0.0556$, $wR_2 = 0.1313$	$R_1 = 0.1063$, $wR_2 = 0.1979$	$R_1 = 0.1393$, $wR_2 = 0.2257$
Largest diff. peak/hole / e Å ⁻³	0.369 / -0.457	0.378 / -0.282	0.797 / -0.258	0.487 / -0.484	0.700 / -0.637
Flack parameter	-	0.09(8)	0.07(5)	-	0.01(5)

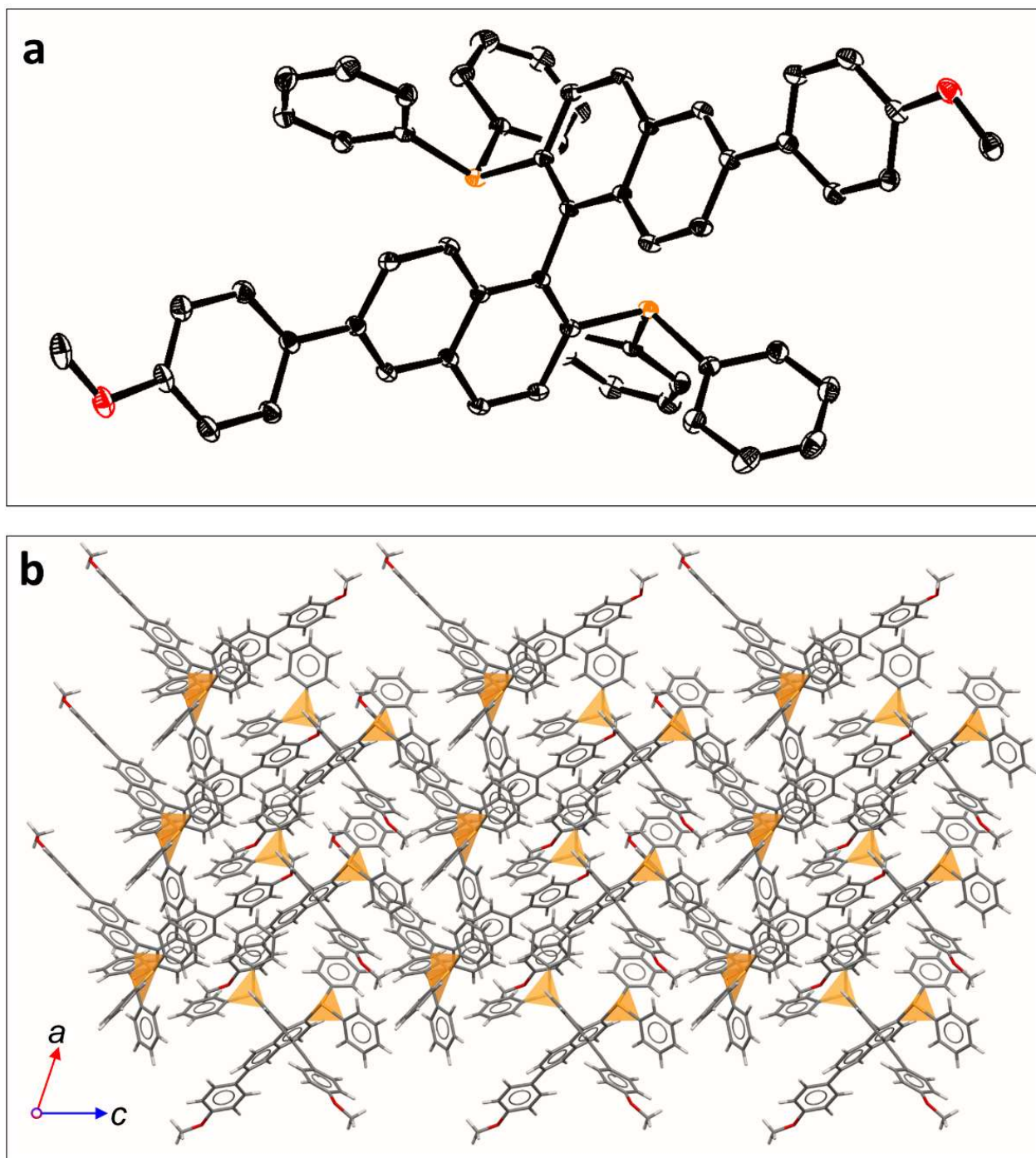


Fig. S4 (a) ORTEP representation of the single-crystal structure of compound (*S*)-14b3. The H-atoms were omitted for clarity. (b) Molecular packing model of (*S*)-14b3 along the *b*-axis in crystal.

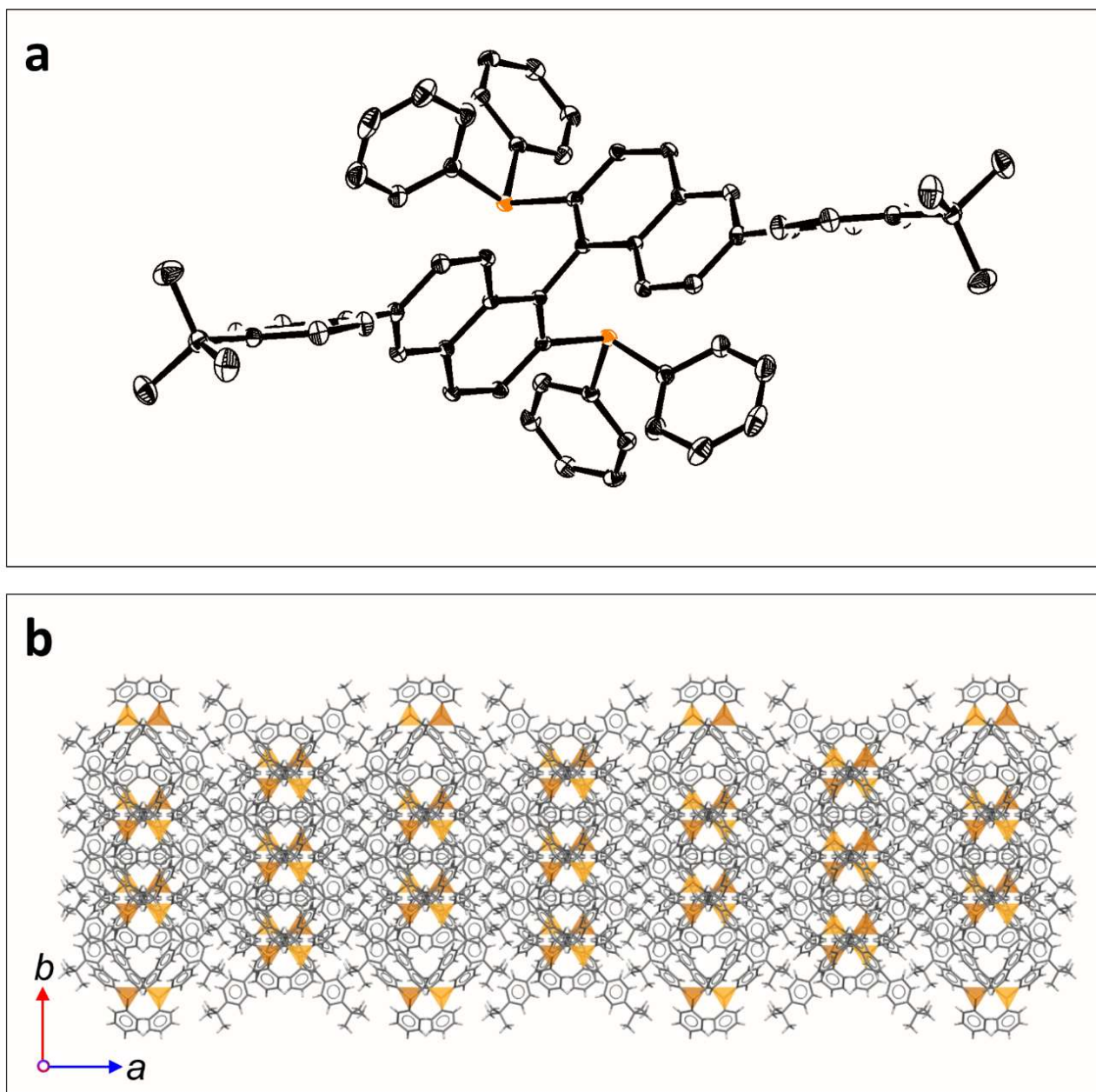


Fig. S5 (a) ORTEP representation of the single-crystal structure of isomer (*S*)-15b3 with thermal ellipsoids at 50% probability. The H-atoms were omitted for clarity. (b) Molecular packing model of (*Rac*)-15b3 along the *c*-axis in crystal.

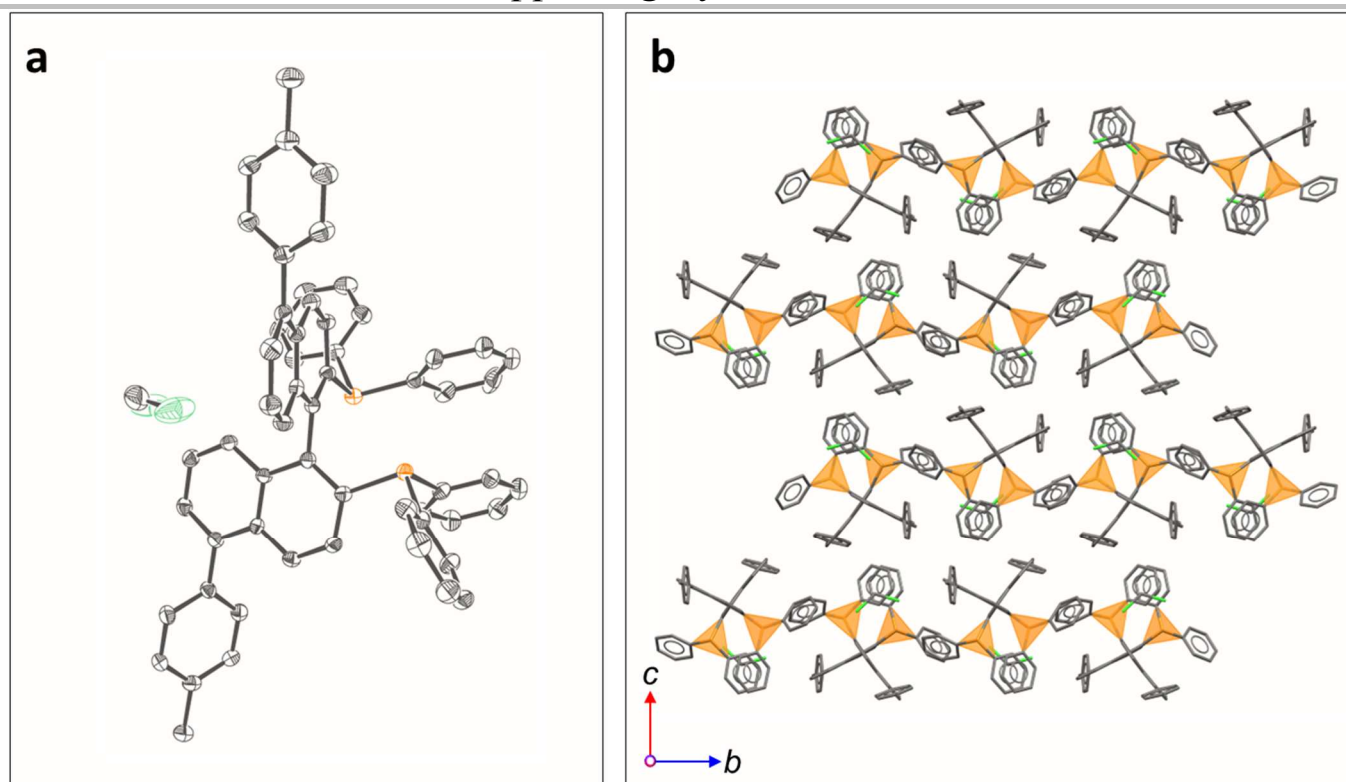


Fig. S6 (a) ORTEP representation of the single-crystal structure of (*S*)-6c3 with thermal ellipsoids at 50% probability. (b) Molecular packing model of (*Rac*)-6c3 along the *a*-axis in crystal. The H-atoms were omitted for clarity.

Supporting information

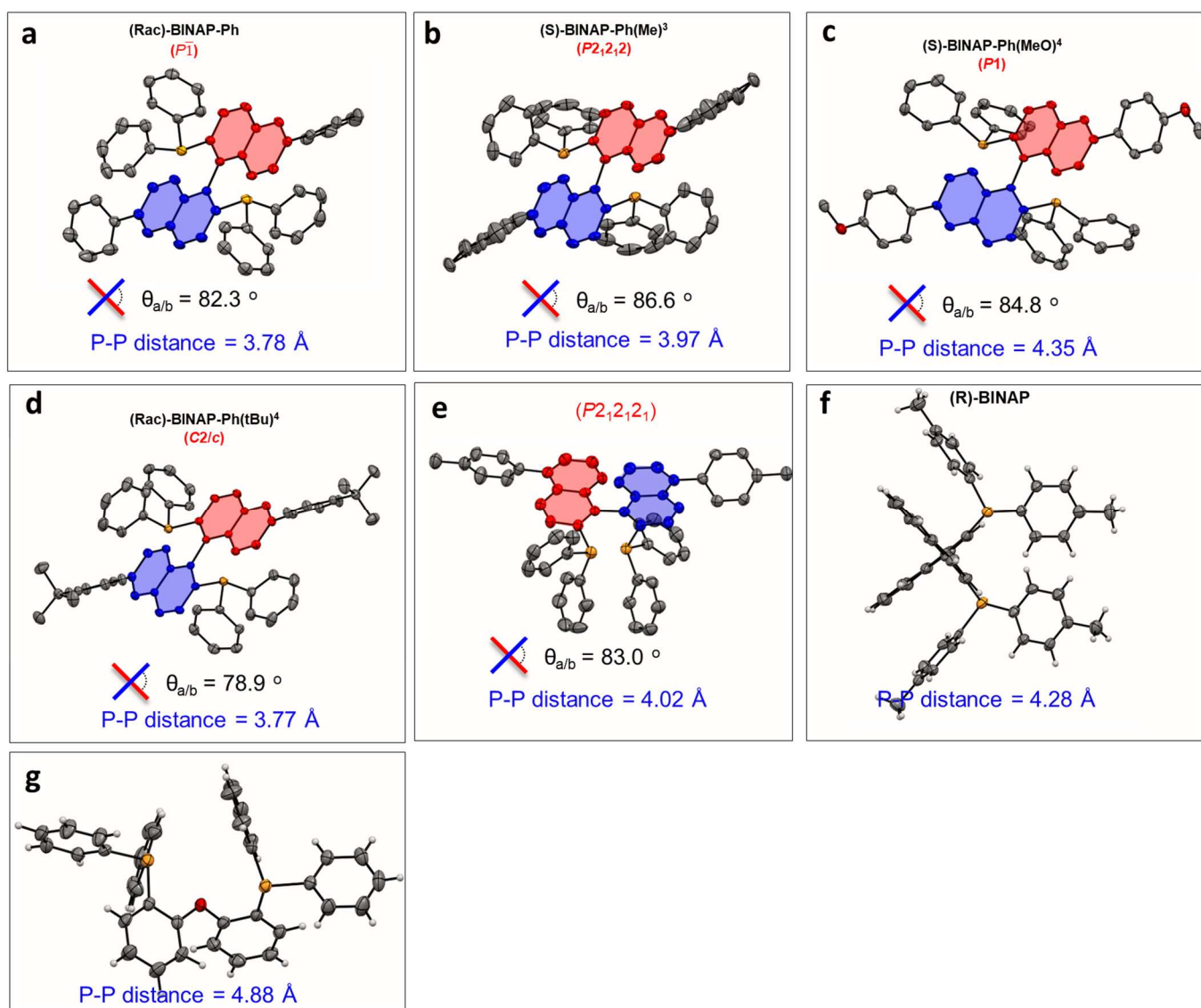


Fig. S7 (a-d) Structural analysis and comparison of the single-crystal structure of the derived BINAP substrates (*Rac*)-9b3, (*S*)-11b3, (*S*)-14b3, (*Rac*)-15b3, (*R*)-BINAP-Me, and Bis(2-diphenylphosphinophenyl)ether (DPEPhos). The dihedral angles of binaphthyl and P-P distances are inserted in the Figures.

Supporting information

Table S3. Crystallographic Data and Structure Refinement for Phospha[5]helicene

Name	[(<i>M</i>)-2b] ⁺ [Cl] ⁻ & CH ₂ Cl ₂	[(<i>P</i>)-2b] ⁺ [Cl] ⁻ & CH ₂ Cl ₂	^a [(<i>Rac</i>)-2b] ⁺ [Br] ⁻ & EtOH/MeOH/H ₂ O	^b [(<i>P</i>)-2b] ⁺ [Br] ⁻ & CH ₂ Cl ₂ <i>Y</i> _(<i>P</i>-isomer) =60.4 %
CCDC	2130476	2130479	2130454	2130459
Empirical formula	C ₃₅ H ₂₈ Cl ₃ P	C ₃₅ H ₂₈ Cl ₃ P	C ₃₇ H ₃₇ BrO _{2.5} P	C ₃₅ H ₂₈ BrCl ₂ P
Formula weight	585.89	585.89	632.54	630.34
Crystal system	orthorhombic	orthorhombic	monoclinic	orthorhombic
Space group	<i>P</i> 2 ₁ 2 ₁ 2 ₁	<i>P</i> 2 ₁ 2 ₁ 2 ₁	<i>C</i> 2/ <i>c</i>	<i>P</i> 2 ₁ 2 ₁ 2 ₁
<i>a</i> /Å	12.230(2)	12.200(4)	25.8430(19)	12.280(4)
<i>b</i> /Å	12.471(3)	12.614(3)	11.7629(8)	12.550(4)
<i>c</i> /Å	19.360(5)	19.437(5)	22.1155(17)	19.659(6)
α /°	90	90	90	90
β /°	90	90	114.085(3)	90
γ /°	90	90	90	90
Volume/Å ³	2952.9(11)	2991.1(14)	6137.6(8)	3029.7(16)
<i>Z</i>	4	4	8	4
ρ_{calc} (g/cm ³)	1.318	1.301	1.369	1.382
μ /mm ⁻¹	0.388	0.383	1.426	1.609
<i>F</i> (000)	1216.0	1216.0	2632.0	1288.0
Crystal size/mm ³	0.2*0.2*0.08	0.4*0.3*0.11	0.12*0.1*0.1	0.2*0.3*0.1
Radiation (Å)	MoK α (λ =0.71073)	MoK α (λ =0.71073)	MoK α (λ =0.71073)	MoK α (λ =0.71073)
2 θ range for data collection/°	4.668 to 55.123	4.661 to 53.715	6.519 to 107.860	3.692 to 53.748
Index ranges	-14 ≤ <i>h</i> ≤ 14, -14 ≤ <i>k</i> ≤ 11, -22 ≤ <i>l</i> ≤ 22	-11 ≤ <i>h</i> ≤ 14, -15 ≤ <i>k</i> ≤ 15, -23 ≤ <i>l</i> ≤ 22	-31 ≤ <i>h</i> ≤ 29, -14 ≤ <i>k</i> ≤ 13, -26 ≤ <i>l</i> ≤ 26	-12 ≤ <i>h</i> ≤ 14, -15 ≤ <i>k</i> ≤ 15, -23 ≤ <i>l</i> ≤ 23
Reflections collected	20197	22731	25132	16472
Independent reflections	5601 [<i>R</i> _{int} = 0.080, <i>R</i> _{sigma} = 0.0880]	5129 [<i>R</i> _{int} = 0.080, <i>R</i> _{sigma} = 0.0696]	9952 [<i>R</i> _{int} = 0.068, <i>R</i> _{sigma} = 0.0500]	9281 [<i>R</i> _{int} = 0.065, <i>R</i> _{sigma} = 0.0556]
Goodness-of-fit on <i>F</i> ²	1.074	1.063	1.069	0.1058
Final <i>R</i> indexes [<i>I</i> ≥ 2 σ (<i>I</i>)]	<i>R</i> ₁ = 0.0850, <i>wR</i> ₂ = 0.1952	<i>R</i> ₁ = 0.0587, <i>wR</i> ₂ = 0.1536	<i>R</i> ₁ = 0.0559, <i>wR</i> ₂ = 0.1604	<i>R</i> ₁ = 0.0427, <i>wR</i> ₂ = 0.1165
Final <i>R</i> indexes [all data]	<i>R</i> ₁ = 0.1147, <i>wR</i> ₂ = 0.2110	<i>R</i> ₁ = 0.0837, <i>wR</i> ₂ = 0.1693	<i>R</i> ₁ = 0.0678, <i>wR</i> ₂ = 0.1708	<i>R</i> ₁ = 0.0451, <i>wR</i> ₂ = 0.1194
Largest diff. peak/hole / e Å ⁻³	0.650 / -0.561	0.399 / -0.391	0.610 / -0.974	0.424 / -0.519
Flack parameter	0.05(5)	0.03(5)	-	0.395(12) ^b

^aCrystal sample was grown from a completely racemic mother liquid (The (*P*)-isomer mixed with (*M*)-isomer at a 1:1 ratio). ^bInversion twinning crystal sample was obtained from a partial racemic mother liquid (solution reacted at 50 °C for 30 min). The proportion of (*P*)-isoform (*Y*_(*P*-isomer)=60.4 %) was estimated by the equation of *Y*_(*P*-isomer)=100(1-flack parameter)%, indicating isomerization existed at the high temperature.

Supporting information

Table S4. Crystallographic Data and Structure Refinement for Hybrid P(III)/Mn(II) Complexes

Name	$[(6b)]^+[\text{MnCl}_4]^{2-}$	$[(6b)_2]^{2+}[(\text{MnCl}_3\text{EtOH})][(\text{MnCl}_3\text{THF})]^-$
CCDC	2225470	2225471
Empirical formula	$\text{C}_{52}\text{H}_{38}\text{Cl}_4\text{MnO}_9\text{P}_2$	$\text{C}_{58}\text{H}_{50}\text{Cl}_6\text{Mn}_2\text{O}_{10}\text{P}_2$
Formula weight	1065.50	1291.50
Crystal system	monoclinic	triclinic
Space group	$P2_1/n$	$P\bar{1}$
$a/\text{\AA}$	11.7291(11)	8.6233(14)
$b/\text{\AA}$	21.4215(19)	18.799(3)
$c/\text{\AA}$	19.3277(19)	19.623(3)
$\alpha/^\circ$	90	113.171(5)
$\beta/^\circ$	106.219(4)	95.078(6)
$\gamma/^\circ$	90	93.304(5)
Volume/ \AA^3	4662.9(8)	2898.1(8)
Z	4	2
$\rho_{\text{calc}}(\text{g}/\text{cm}^3)$	1.518	1.480
μ/mm^{-1}	0.640	0.825
$F(000)$	2180.0	1320.0
Crystal size/ mm^3	0.2*0.2*0.1	0.3*0.1*0.1
Radiation (\AA)	MoK α ($\lambda = 0.71073$)	MoK α ($\lambda = 0.71073$)
2 θ range for data collection/ $^\circ$	5.482 to 107.589	4.738 to 54.909
Index ranges	$-14 \leq h \leq 14, -25 \leq k \leq 25, -21 \leq l \leq 23$	$-10 \leq h \leq 10, -21 \leq k \leq 22, -23 \leq l \leq 23$
Reflections collected	29732	21215
Independent reflections	19293 [$R_{\text{int}} = 0.050, R_{\text{sigma}} = 0.0460$]	7310 [$R_{\text{int}} = 0.063, R_{\text{sigma}} = 0.0837$]
Goodness-of-fit on F^2	1.052	1.128
Final R indexes [$I \geq 2\sigma(I)$]	$R_1 = 0.0438, wR_2 = 0.1069$	$R_1 = 0.0738, wR_2 = 0.2056$
Final R indexes [all data]	$R_1 = 0.0525, wR_2 = 0.1123$	$R_1 = 0.1052, wR_2 = 0.2322$
Largest diff. peak/hole / $e \text{\AA}^{-3}$	0.473 / -0.706	1.266 / -1.158

^aThe crystalline $[(6b)^+]_2[\text{MnCl}_4]^{2-}$ and $[(6b)^+]_2[(\text{MnCl}_3(\text{EtOH}))][(\text{MnCl}_3(\text{THF}))]^-$ could be obtained from the reaction mixture in the schlenk tube after slow cooling.

Supporting information

Table S5. Crystallographic Data and Structure Refinement for Phospha[5]helicene				
Name	^a [(<i>Rac</i>)-1b] ⁺ [BF ₄] ⁻	^a [(<i>Rac</i>)-1b] ⁺ [PF ₆] ⁻	^b [(<i>P</i>)-2b] ⁺ [BF ₄] ⁻	[(<i>M</i>)-2b] ⁺ [BF ₄] ⁻ & CH ₂ Cl ₂ & 2H ₂ O
CCDC	2225467	2225468	2225466	2225461
Empirical formula	C ₃₂ H ₂₂ PBF ₄	C ₃₂ H ₂₂ P ₂ F ₆	C ₃₄ H ₂₆ BF ₄ P	C ₃₅ H ₃₂ BCl ₂ F ₄ O ₂ P
Formula weight	524.28	582.44	552.33	673.29
Crystal system	monoclinic	monoclinic	orthorhombic	orthorhombic
Space group	<i>P</i> 2 ₁ / <i>n</i>	<i>P</i> 2 ₁ / <i>n</i>	<i>P</i> 2 ₁ 2 ₁ 2 ₁	<i>P</i> 2 ₁ 2 ₁ 2 ₁
<i>a</i> /Å	11.3669(7)	11.8054(4)	11.0745(7)	11.0759(8)
<i>b</i> /Å	11.7224(7)	11.5114(4)	11.4366(8)	11.4222(8)
<i>c</i> /Å	18.4484(12)	19.2346(7)	27.0879(17)	27.0428(17)
<i>α</i> /°	90	90	90	90
<i>β</i> /°	92.265(2)	93.387(1)	90	90
<i>γ</i> /°	90	90	90	90
Volume/Å ³	2456.3(3)	2609.35(16)	3430.8(4)	3421.2(4)
<i>Z</i>	4	4	4	4
ρ_{calc} (g/cm ³)	1.418	1.483	1.069	1.307
μ /mm ⁻¹	0.164	0.232	0.120	0.288
<i>F</i> (000)	1080.0	1192.0	1144.0	1392.0
Crystal size/mm ³	0.2*0.2*0.2	0.3*0.2*0.2	0.3*0.3*0.1	0.3*0.2*0.1
Radiation (Å)	MoK α (λ = 0.71073)	MoK α (λ = 0.71073)	MoK α (λ = 0.71073)	MoK α (λ = 0.71073)
2 θ range for data collection/°	4.994 to 54.961	4.947 to 54.742	4.662 to 43.826	4.667 to 49.318
Index ranges	-13 ≤ <i>h</i> ≤ 14, -15 ≤ <i>k</i> ≤ 15, -21 ≤ <i>l</i> ≤ 23	-14 ≤ <i>h</i> ≤ 15, -14 ≤ <i>k</i> ≤ 14, -24 ≤ <i>l</i> ≤ 24	-13 ≤ <i>h</i> ≤ 14, -14 ≤ <i>k</i> ≤ 14, -35 ≤ <i>l</i> ≤ 35	-10 ≤ <i>h</i> ≤ 13, -13 ≤ <i>k</i> ≤ 13, -32 ≤ <i>l</i> ≤ 32
Reflections collected	22063	24633	32383	26428
Independent reflections	9942 [<i>R</i> _{int} = 0.0532, <i>R</i> _{sigma} = 0.0470]	6305 [<i>R</i> _{int} = 0.0539, <i>R</i> _{sigma} = 0.0476]	6120 [<i>R</i> _{int} = 0.0674, <i>R</i> _{sigma} = 0.0775]	7768 [<i>R</i> _{int} = 0.0639, <i>R</i> _{sigma} = 0.0458]
Goodness-of-fit on <i>F</i> ²	1.028	1.063	0.949	1.130
Final <i>R</i> indexes [<i>I</i> ≥ 2 σ (<i>I</i>)]	<i>R</i> ₁ = 0.0469, <i>wR</i> ₂ = 0.1224	<i>R</i> ₁ = 0.0774, <i>wR</i> ₂ = 0.2140	<i>R</i> ₁ = 0.0583, <i>wR</i> ₂ = 0.1327	<i>R</i> ₁ = 0.0892, <i>wR</i> ₂ = 0.2507
Final <i>R</i> indexes [all data]	<i>R</i> ₁ = 0.0562, <i>wR</i> ₂ = 0.1300	<i>R</i> ₁ = 0.1001, <i>wR</i> ₂ = 0.2335	<i>R</i> ₁ = 0.0892, <i>wR</i> ₂ = 0.1448	<i>R</i> ₁ = 0.1029, <i>wR</i> ₂ = 0.2667
Largest diff. peak/hole / e Å ⁻³	0.465 / -0.381	1.399 / -1.244	0.216 / -0.240	1.187 / -0.489
Flack parameter	-	-	0.05(7)	0.08(5)

^aCrystal samples were grown from a completely racemic mother liquid after an ion-exchange operation at room temperature. ^bCrystal samples were grown from the enantiomerically enriched [2b]⁺[Cl]⁻ solution after an ion-exchange operation at room temperature.

Table S6. Crystallographic Data and Structure Refinement for Phospha[5]helicene

Supporting information

Name	[(<i>Rac</i>)-3c] ⁺ [BF ₄] ⁻	[(<i>M</i>)-7c] ⁺ [PF ₆] ⁻
CCDC	2225469	2225482
Empirical formula	C ₅₂ H ₄₆ BF ₄ P	C ₄₆ H ₃₄ BF ₄ O ₂ P
Formula weight	788.67	736.51
Crystal system	monoclinic	monoclinic
Space group	<i>C2/c</i>	<i>P2</i> ₁
<i>a</i> /Å	29.9808(17)	11.5658(5)
<i>b</i> /Å	29.9808(17)	14.0383(7)
<i>c</i> /Å	29.9808(17)	12.2223(6)
α /°	90	90
β /°	116.312(2)	116.441(1)
γ /°	90	90
Volume/Å ³	20938(3)	1776.88(15)
<i>Z</i>	16	2
ρ_{calc} (g/cm ³)	788.67	1.377
μ /mm ⁻¹	0.524	0.139
<i>F</i> (000)	6624.0	764.0
Crystal size/mm ³	0.4*0.1*0.2	0.2*0.2*0.2
Radiation (Å)	GaK α (λ =1.34139)	MoK α (λ =0.71073)
2 θ range for data collection/°	5.668 to 108.612	4.719 to 54.183
Index ranges	-36 \leq h \leq 36, -25 \leq k \leq 28, -28 \leq l \leq 39	-15 \leq h \leq 14, -18 \leq k \leq 18, -12 \leq l \leq 15
Reflections collected	17839	16941
Independent reflections	9964 [<i>R</i> _{int} = 0.0828, <i>R</i> _{sigma} = 0.0572]	5018 [<i>R</i> _{int} = 0.0467, <i>R</i> _{sigma} = 0.0703]
Goodness-of-fit on <i>F</i> ²	1.013	1.051
Final <i>R</i> indexes [<i>I</i> \geq 2 σ (<i>I</i>)]	<i>R</i> ₁ = 0.0981, <i>wR</i> ₂ = 0.2467	<i>R</i> ₁ = 0.0503, <i>wR</i> ₂ = 0.1125
Final <i>R</i> indexes [all data]	<i>R</i> ₁ = 0.1274, <i>wR</i> ₂ = 0.2618	<i>R</i> ₁ = 0.0851, <i>wR</i> ₂ = 0.1389
Largest diff. peak/hole / e Å ⁻³	0.432 / -0.564	0.308 / -0.294
Flack parameter	-	0.00(7)

^aCrystal samples were grown from a completely racemic mother liquid after an ion-exchange operation at room temperature.

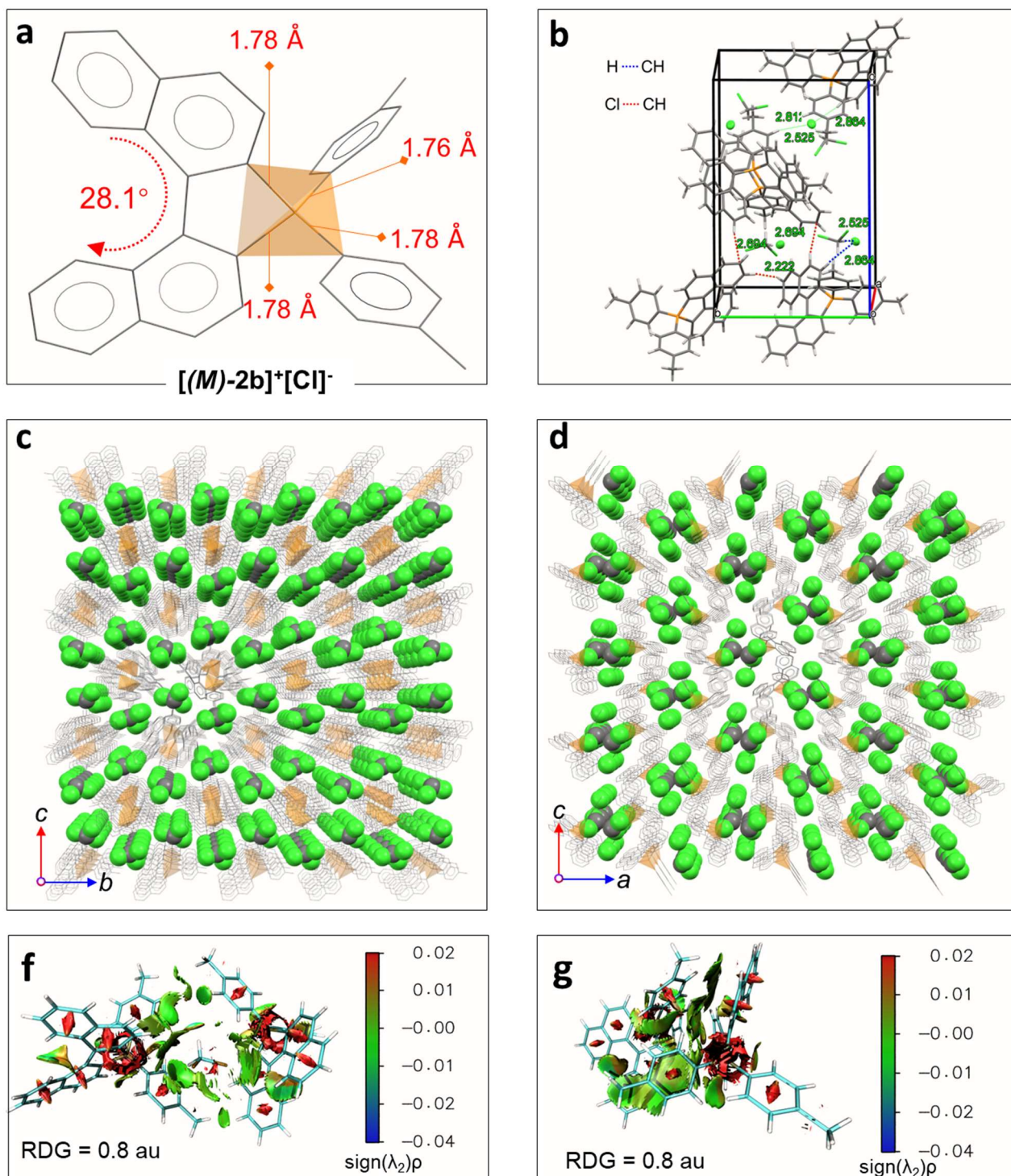


Fig. S8 (a) ORTEP representation of the single-crystal structure of compound $[(M)-2b]^+[Cl]^-$. (b) Intermolecular hydrogen bonding gridding in the cell. (c-d) Molecular packing model of $[(M)-2b]^+[Cl]^-$ along the a -axis and b -axis in crystal. (f-g) RDG maps of $[(M)-2b]^+$ dimer structure in crystal. The reduced density gradient (RDG) analysis was performed at B3LYP-D3(BJ)/6-31G(d) level.

Supporting information

Table S7. Selective Bond Lengths (Å) and Bond Angles (°) for Phospha[5]helicene and Hybrid Complexes

Compound	Bond lengths (Å)			Bond angles (°)		
	lable	^a exp	^b cal	lable	^a exp	^b cal
[(<i>M</i>)-2b] ⁺ [Cl] ⁻	C1-P1	1.779(9)	1.795	C1-P1-C21	112.2(4)	110.5
	C12-P1	1.780(8)	1.795	C12-P1-C21	111.0(4)	115.8
	C21-P1	1.788(8)	1.799	C28-P1-C21	114.0(4)	110.1
	C28-P1	1.764(9)	1.799	C1-P1-C12	94.6(4)	93.4
[(<i>P</i>)-2b] ⁺ [Cl] ⁻	C1-P1	1.788(6)	1.796	C1-CP1-C12	94.2(3)	93.4
	C12-P1	1.785(6)	1.796	C12-P1-C28	114.0(3)	113.2
	C28-P1	1.784(6)	1.796	C28-P1-C21	113.6(8)	110.3
	C21-P1	1.793(6)	1.796	C21-P1-C1	112.3(3)	113.2
[(<i>P</i>)-2b] ⁺ [Br] ⁻	C1-P1	1.785(5)	1.799	C1-P1-C11	94.0(2)	93.0
	C11-P1	1.783(4)	1.800	C11-P1-C21	113.5(2)	112.7
	C21-P1	1.781(5)	1.792	C21-P1-C28	113.3(2)	111.6
	C28-P1	1.789(5)	1.790	C28-P1-C1	112.8(2)	114.5
[(6b) ⁺] ₂ [MnCl ₄] ²⁻	Mn1-Cl1	2.362(1)	-	Cl2-Mn1-Cl1	112.6(1)	-
	Mn1-Cl2	2.3630(9)	-	Cl1-Mn1-Cl4	109.3(1)	-
	Mn1-Cl3	2.386(1)	-	Cl2-Mn1-Cl3	109.6(1)	-
	Mn1-Cl4	2.3705(8)	-	Cl4-Mn1-Cl3	109.3(1)	-
	C1-P1	1.778(3)	1.798	C1-P1-C8	94.5(1)	93.9
	C8-P1	1.783(2)	1.798	C8-P1-C21	111.1(1)	113.9
	C15-P1	1.788(2)	1.811	C21-P1-C15	112.8(1)	109.3
	C21-P1	1.784(2)	1.811	C15-P1-C1	112.8(1)	113.9
[(<i>Rac</i>)-1b] ⁺ [BF ₄] ⁻	C1-P1	1.780(2)	1.798	C12-P1-C21	114.2(1)	112.5
	C12-P1	1.780(2)	1.798	C1-P1-C12	93.9(1)	93.6
	C27-P1	1.787(2)	1.808	C1-P1-C27	112.1(1)	112.5
	C21-P1	1.785(2)	1.808	C27-P1-C21	112.6(1)	109.9
[(<i>Rac</i>)-2b] ⁺ [BF ₄] ⁻	C1-P1	1.798(4)	-	C47-P1-C1	114.7(2)	-
	C22-P1	1.776(5)	-	C1-P1-C22	95.0(2)	-
	P1-C41	1.776(5)	-	C22-P1-C41	114.3(2)	-
	P1-C47	1.800(6)	-	C41-P1-C47	108.9(2)	-
[(<i>M</i>)-7c] ⁺ [BF ₄] ⁻	P001-C009	1.784(5)	-	C00Z-P001-C009	111.7(2)	-
	P001-C00F	1.772(4)	-	C009-P001-C00F	94.0(2)	-
	P001-C00U	1.786(4)	-	C00F-P001-C00U	111.9(2)	-
	P001-C00Z	1.782(5)	-	C00U-P001-C00Z	112.5(2)	-

^aexp: Single crystal diffraction data. ^bcal: DFT optimized data by Gaussian 16. A03 (at B3LYP/6-31G(d) level).

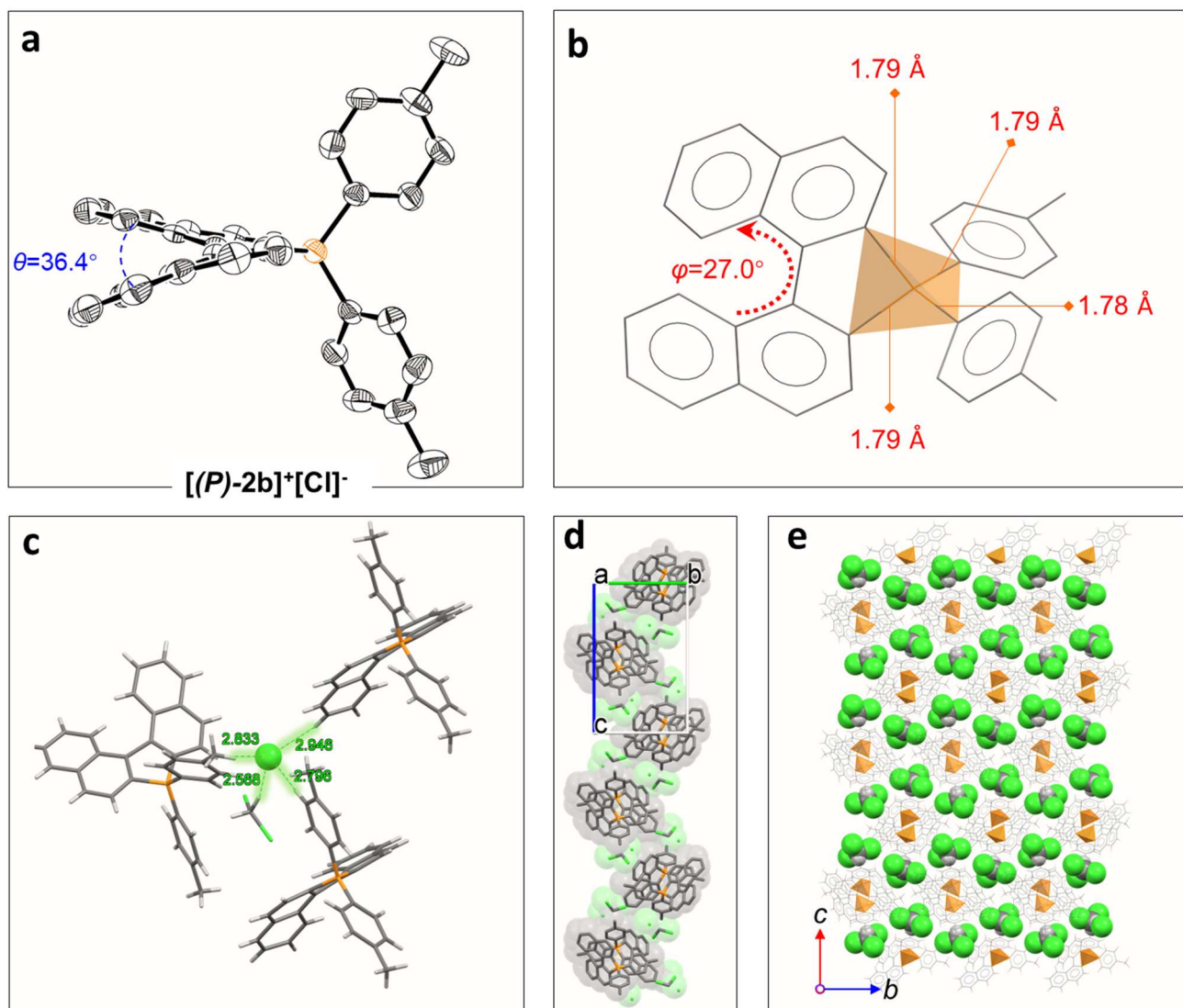


Fig. S9 (a) ORTEP representation of the single-crystal structure of compound $[(P)\text{-}2b]^+[\text{Cl}]^-$ at the 50% probability level. (b) Bond lengths and torsion angle of cationic $[(P)\text{-}2b]^+$. (c) Multiple intermolecular hydrogen bonding interactions between $[(P)\text{-}2b]^+$, CH_2Cl_2 , and $[\text{Cl}]^-$. (d) One-dimensional helical chain packing model of $[(P)\text{-}2b]^+[\text{Cl}]^-$. (e) Molecular packing model of $[(P)\text{-}2b]^+[\text{Cl}]^-$ along the a -axis in crystal.

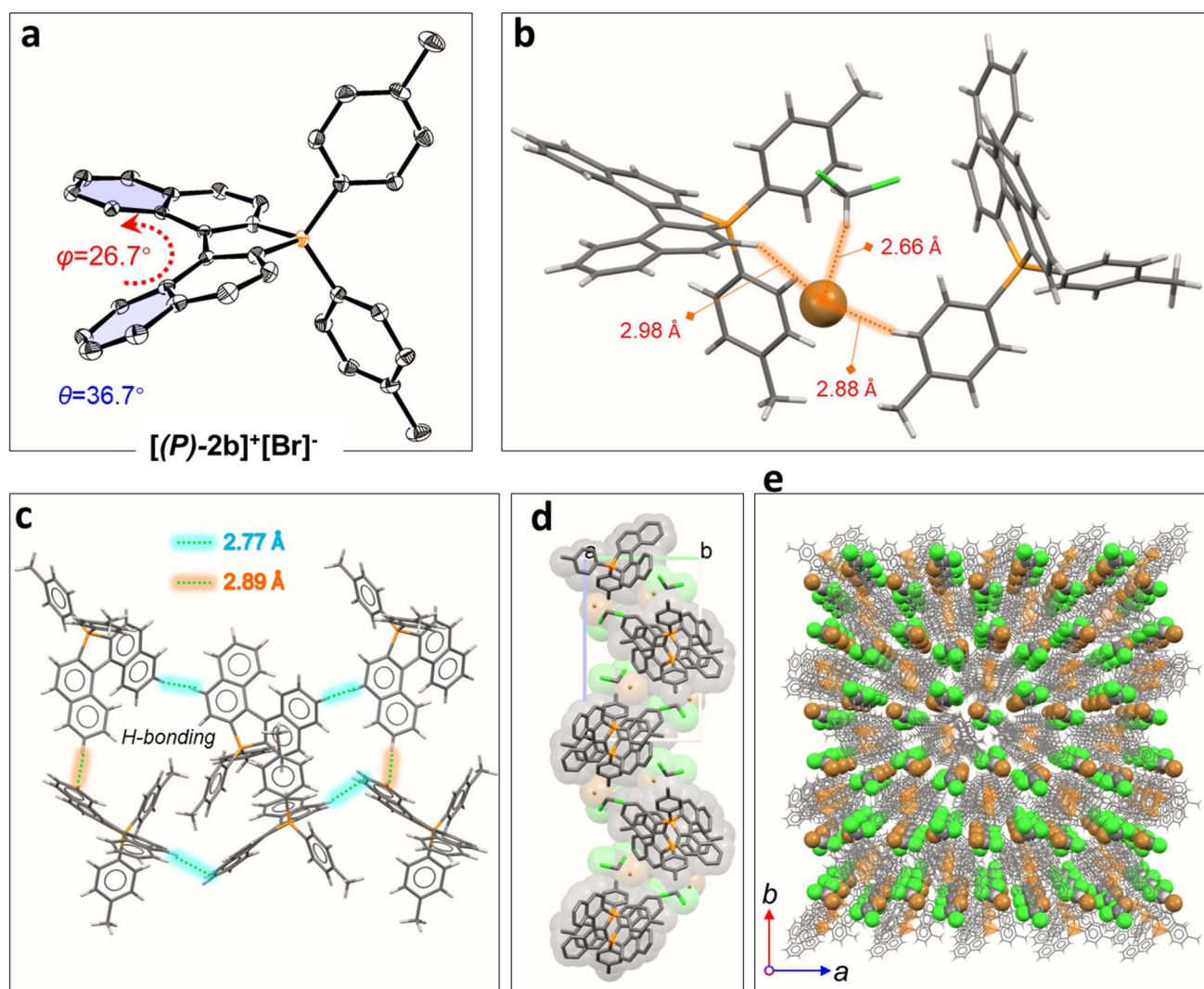


Fig. S10 (a) ORTEP representation of the single-crystal structure of compound $[(P)\text{-}2b]^+[\text{Br}]^-$ at the 50% probability level. (b) Multiple intermolecular hydrogen bonding interactions between $[(P)\text{-}2b]^+$, CH_2Cl_2 , and $[\text{Br}]^-$. (c) Intermolecular hydrogen bonding gridding of adjacent $[(P)\text{-}2b]^+$ in crystal. (d) One-dimensional helical chain packing model of $[(P)\text{-}2b]^+[\text{Br}]^-$. (e) Molecular packing model of $[(P)\text{-}2b]^+[\text{Br}]^-$ along the *c*-axis in crystal.

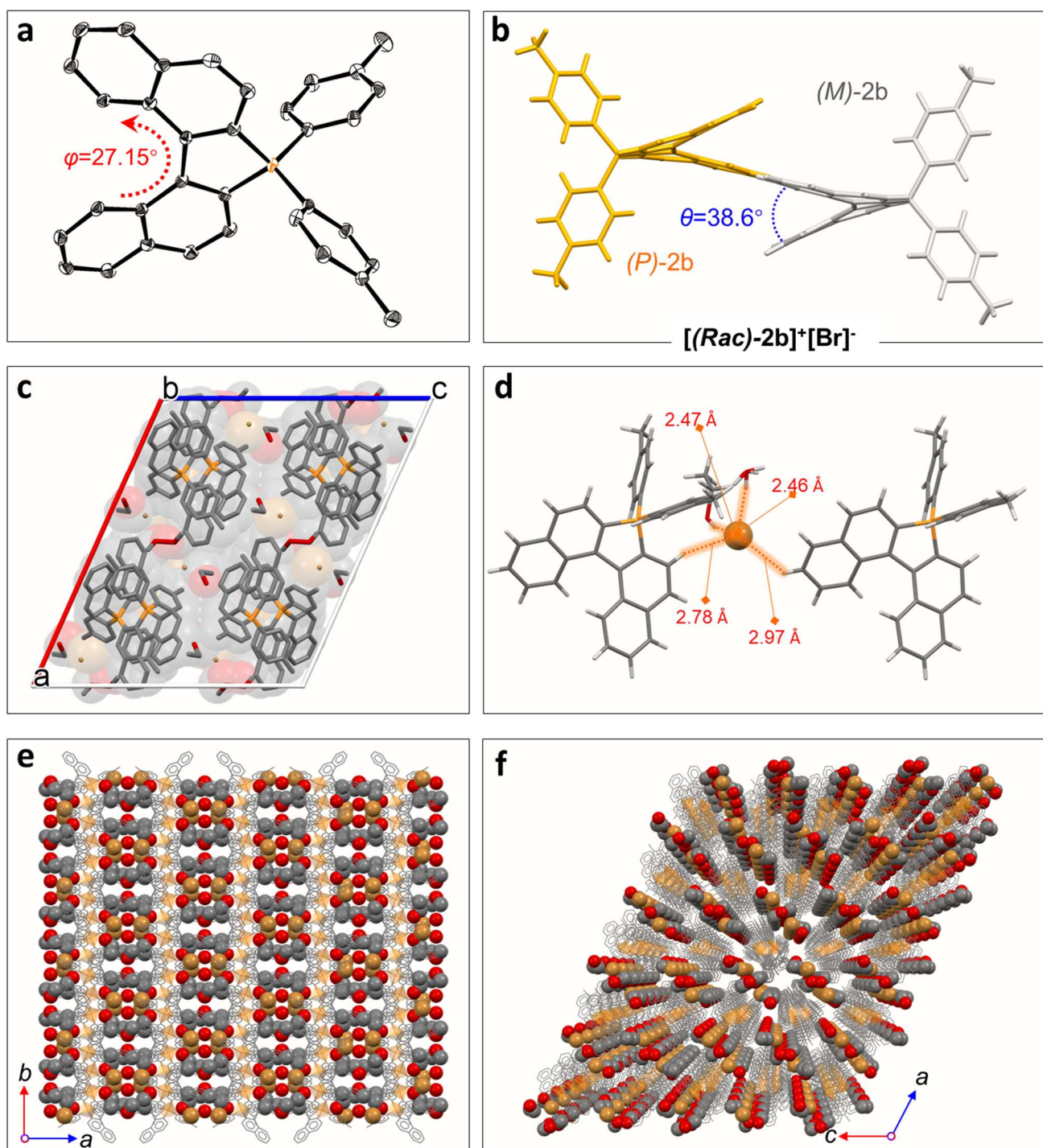


Fig. S11 (a) ORTEP representation of the single-crystal structure of *(M)*-isomer in $[(Rac)\text{-}2b]^+[\text{Br}]^-$ at the 50% probability level. The H-atoms are omitted for clarity. (b) Mirror distribution of *(M)*-isomer and *(P)*-isomer in crystal. (c) Centrosymmetric packing model of $[(Rac)\text{-}2b]^+[\text{Br}]^-$ in the cell. (d) Multiple intermolecular hydrogen bonding interactions between $[(M)\text{-}2b]^+$ isomer, EtOH, H₂O, and [Br]⁻. (e-f) Molecular packing model of $[(Rac)\text{-}2b]^+[\text{Br}]^-$ along the *c*-axis and *b*-axis in crystal. The H-atoms are omitted for clarity.

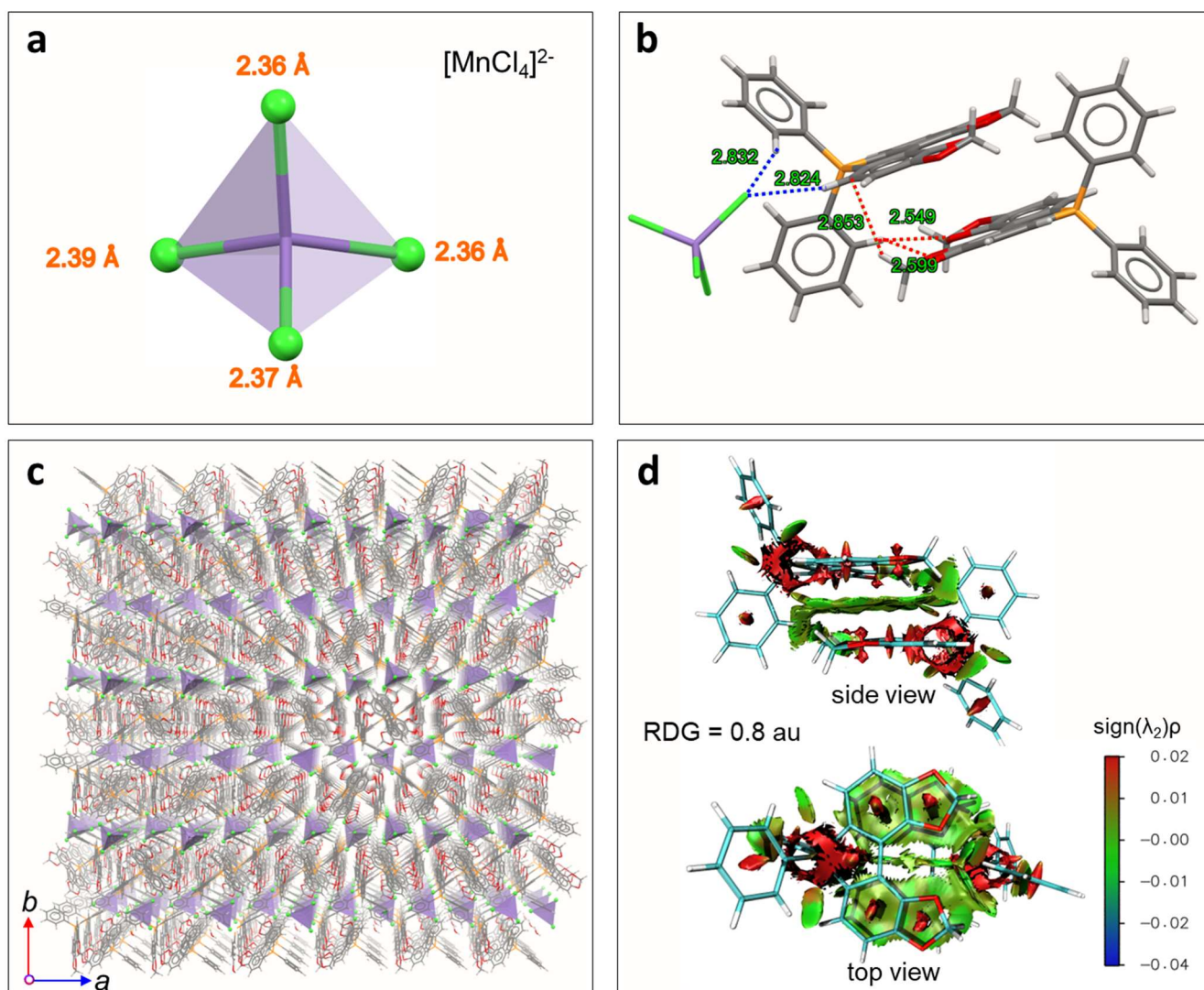


Fig. S12 (a) Representation of the crystal structure of anion $[MnCl_4]^{2-}$. (b) Cation $[6b]^+$ and anion $[MnCl_4]^{2-}$ units in hybrid $[(6b)^+]_2[MnCl_4]^{2-}$ crystal. (c) Crystal packing structure of $[(6b)^+]_2[MnCl_4]^{2-}$ complex along c -axis. (d) RDG maps of $[(6b)^+]^+$ dimer structures in crystal. The reduced density gradient (RDG) analysis was performed at B3LYP-D3(BJ)/6-31G(d) level.

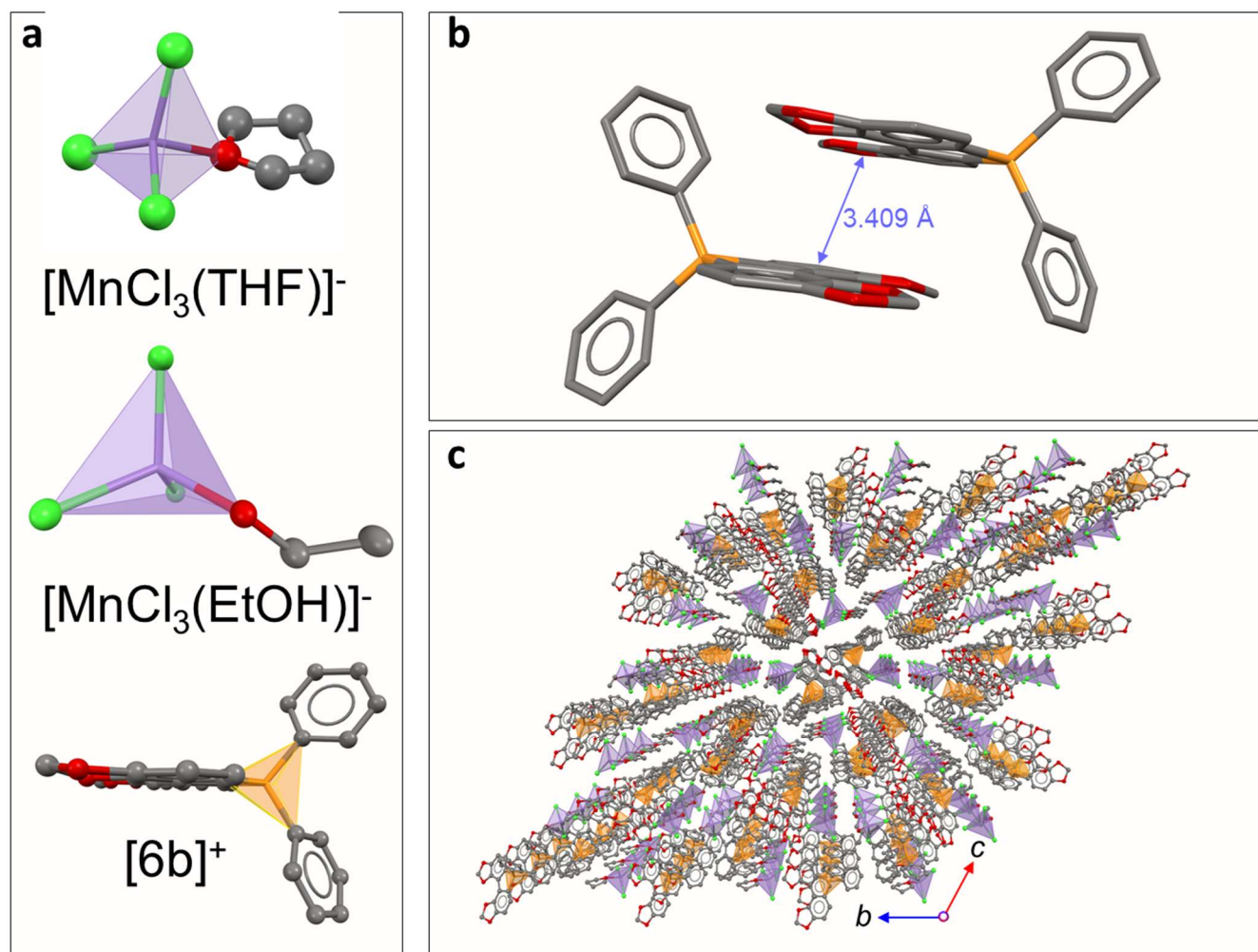


Fig. S13 (a) Crystal structure of hybrid Mn(II) and P(III) units. (b) Intermolecular π - π interactions for two neighboring $[\text{6b}]^+$ units. (c) Crystal packing structures of $[(\text{6b})^+]_2[\text{MnCl}_3(\text{EtOH})][\text{MnCl}_3(\text{THF})]^-$ complex along a -axis. The H-atoms are omitted for clarity. The reaction was performed in the mixed solvents ($V_{\text{chloroform}}:V_{\text{THF}}:V_{\text{EtOH}} = 3:1:1$).

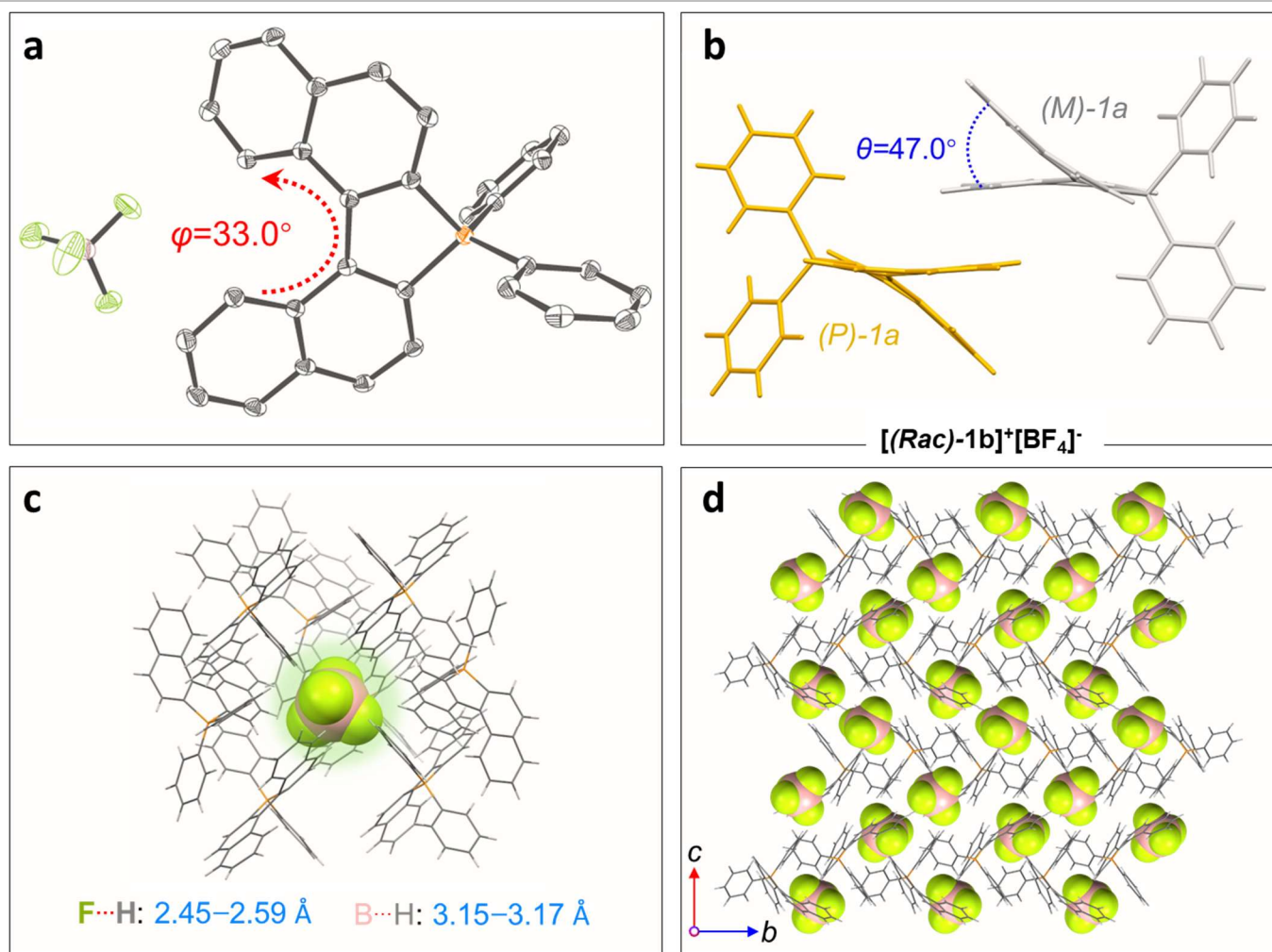


Fig. S14 (a) ORTEP structure of (*M*)-isomer in heterochiral $[(Rac)\text{-}1b]^+[\text{BF}_4]^-$ at the 50% probability level. The H-atoms are omitted for clarity. (b) Mirror distribution of (*M*)-isomer and (*P*)-isomer in crystal, the $[\text{BF}_4]^-$ anions are omitted for clarity. (c) Strong multiple intermolecular hydrogen bonding interactions ($\text{F}\cdots\text{H}$ and $\text{B}\cdots\text{H}$) between $[(M)\text{-}1b]^+$ and $[\text{BF}_4]^-$. (d) Molecular packing model of $[(Rac)\text{-}1b]^+[\text{BF}_4]^-$ along the *a*-axis in crystal.

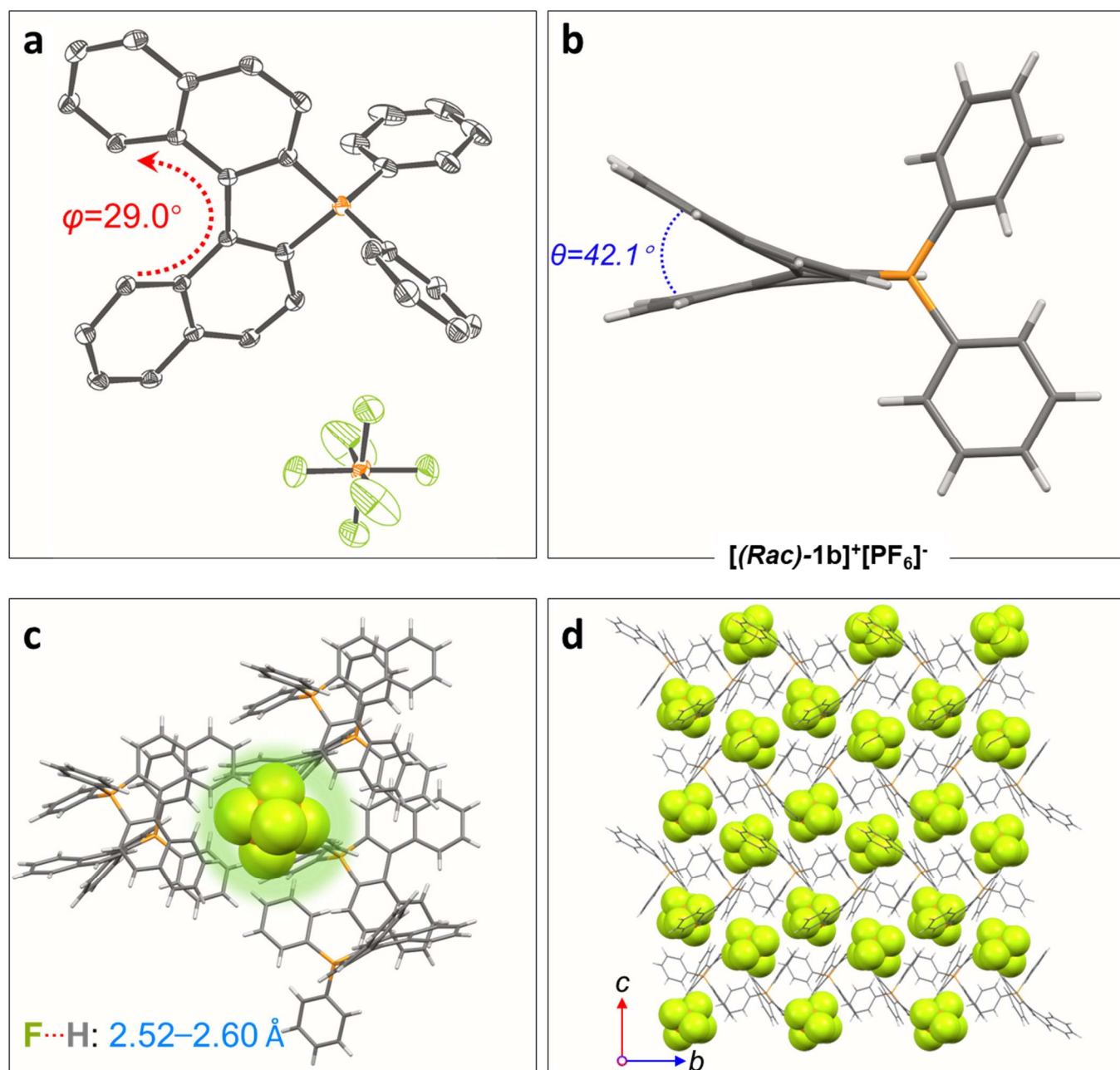


Fig. S15 (a) ORTEP structure of (*M*)-isomer in heterochiral [(*Rac*)-1b]⁺[PF₆]⁻ at the 50% probability level. The H-atoms are omitted for clarity. (b) Side view of [(*P*)-2b]⁺ unit and the dihedral angle between two phenyls in terminal naphthyls. (c) Strong multiple intermolecular hydrogen bonding interactions (F...H) between [(*M*)-1b]⁺ and [PF₆]⁻. (d) Molecular packing model of [(*Rac*)-1b]⁺[PF₆]⁻ along the *a*-axis in crystal.

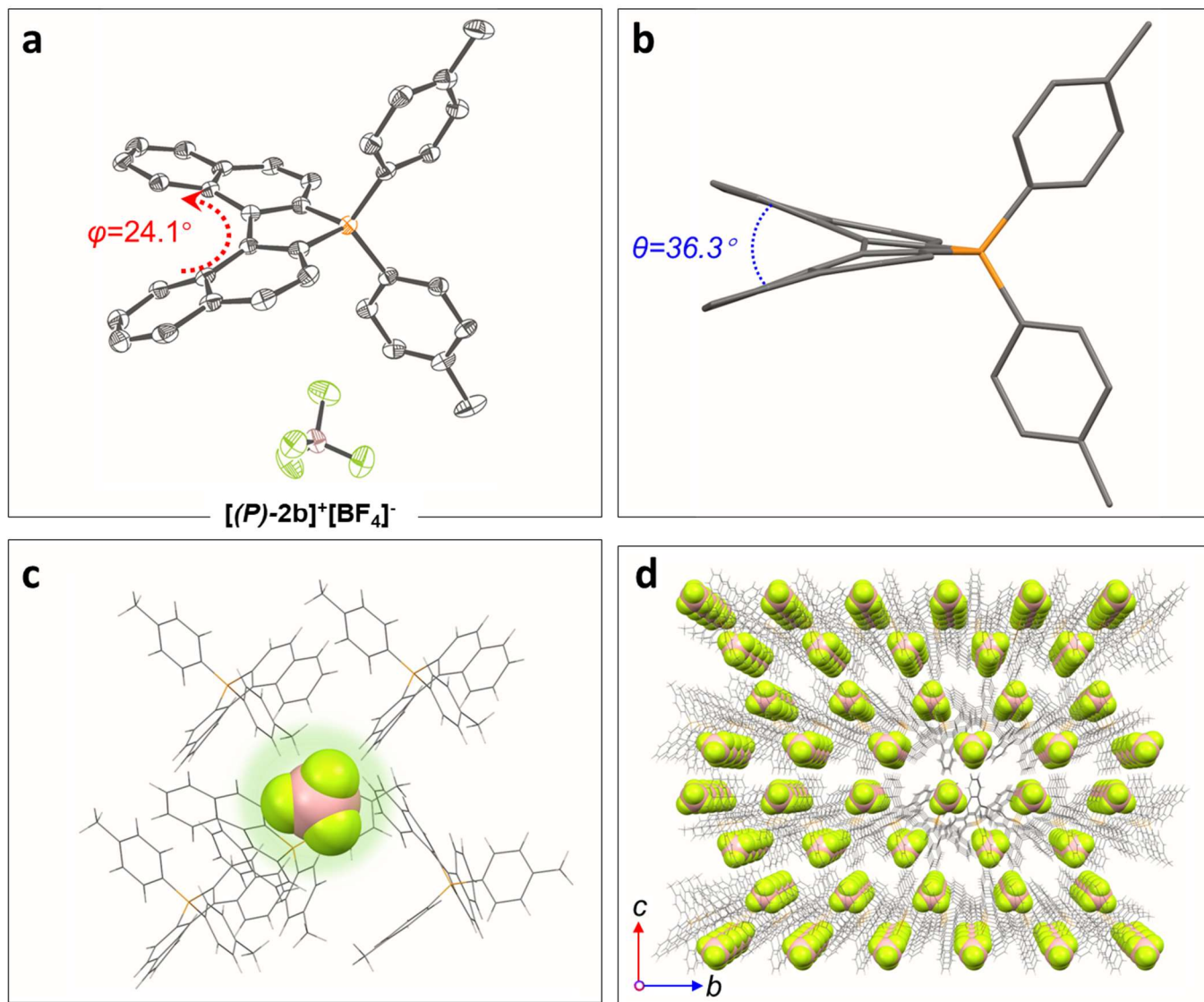


Fig. S16 (a) ORTEP structure of (P) -isomer in heterochiral $[(P)-1b]^+ [BF_4]^-$ at the 50% probability level. The H-atoms are omitted for clarity. (b) Side view of $[(P)-2b]^+$ unit and the dihedral angle between two phenyls in terminal naphthyls. (c) Strong multiple intermolecular hydrogen bonding interactions ($F \cdots H$ and $B \cdots H$) between $[(P)-2b]^+$ and $[BF_4]^-$. (d) Molecular packing model of $[(P)-2b]^+ [BF_4]^-$ along the a -axis in crystal.

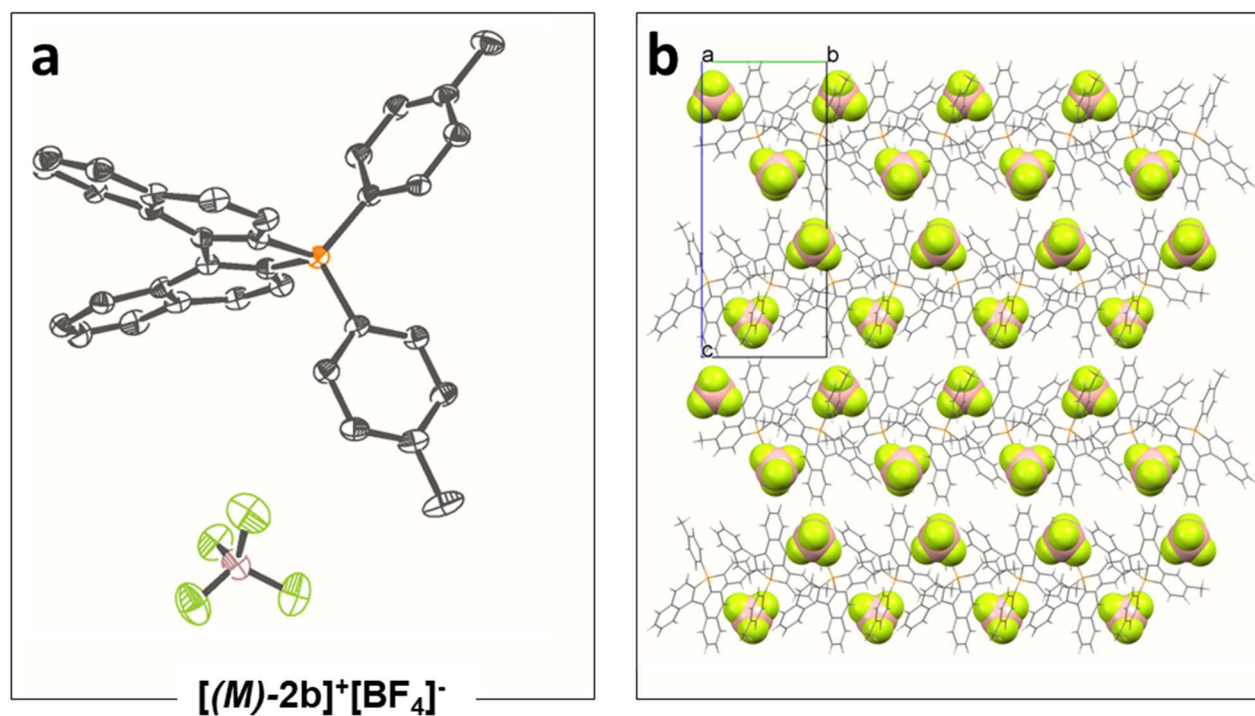


Fig. S17 (a) ORTEP structure of (P) -isomer in heterochiral $[(M)-2b]^+[\text{BF}_4]^-$ at the 50% probability level. (b) Molecular packing model of $[(M)-2b]^+[\text{BF}_4]^-$ along the a -axis in crystal.

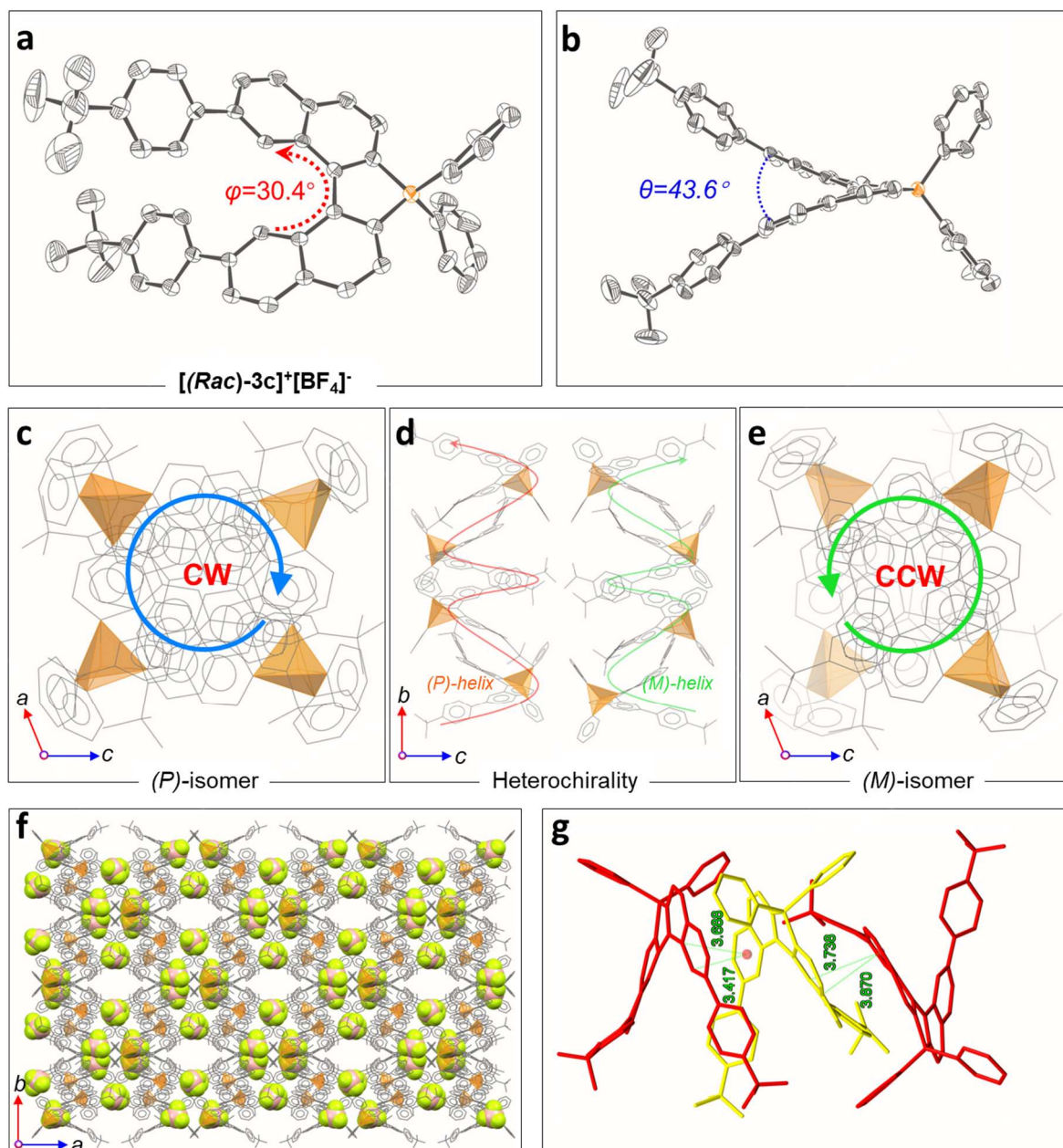


Fig. S18 (a) ORTEP structure of *(P)*-isomer in heterochiral $[(Rac)-3c]^+ [BF_4]^-$ at the 30% probability level. The H-atoms are omitted for clarity. (b) Side view of the *(P)*-isomer unit and dihedral angle between two phenyls in terminal naphthyls. The H-atoms are omitted for clarity. (c) Malposed 1-D columnar stacking in crystal with *(P)*-helix axis. (d) Heterochiral construction of $[(Rac)-3c]^+ [BF_4]^-$ of neighboring columns. The $[BF_4]^-$ are omitted for clarity. (e) Malposed 1-D columnar stacking in crystal with *(M)*-helix axis. (f) Molecular packing model of $[(Rac)-3c]^+ [BF_4]^-$ along the *c*-axis in crystal. The H-atoms are omitted for clarity. (g) Intermolecular π - π stacking interactions in crystals.

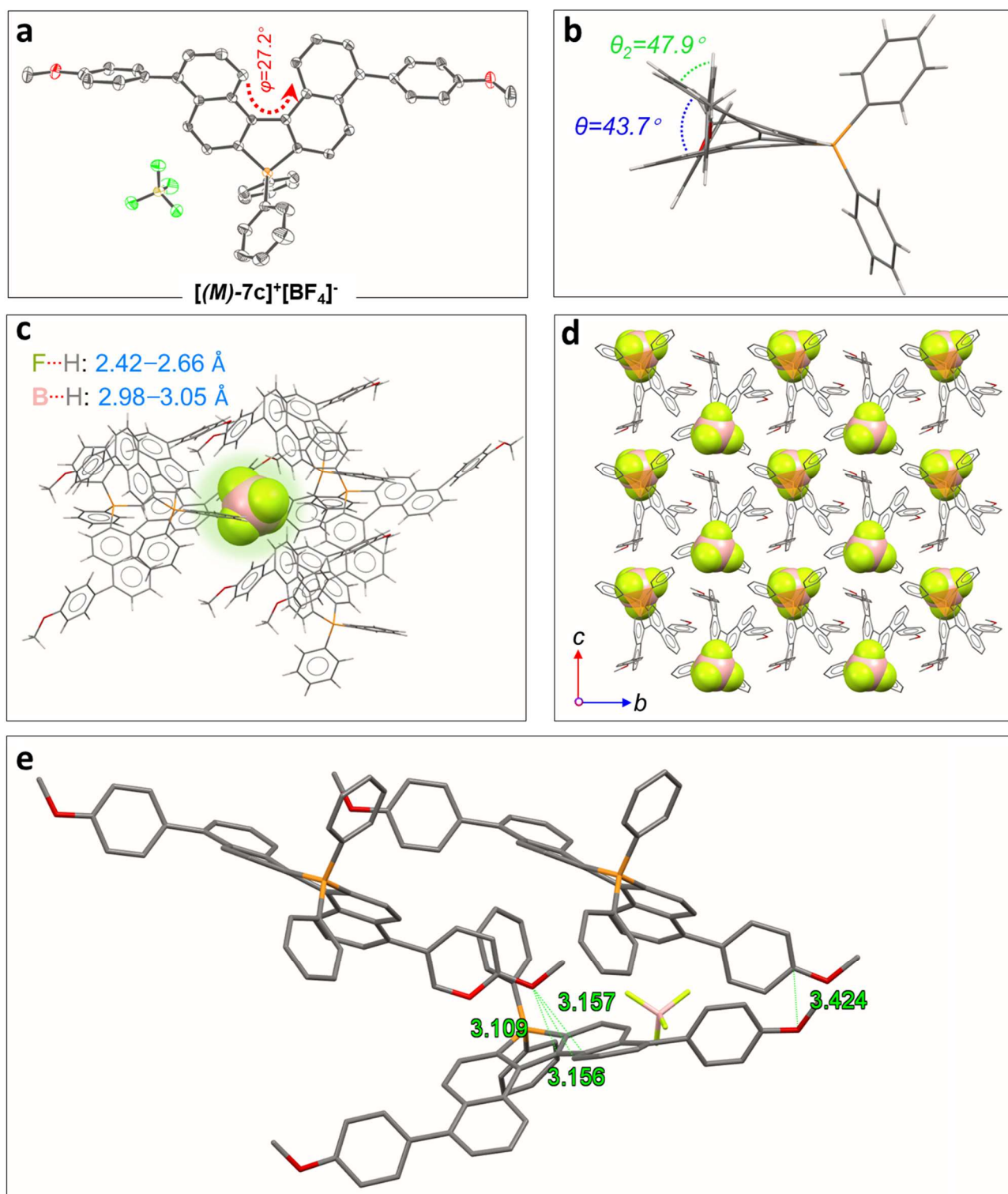


Fig. S19 (a) ORTEP structure of $[(M)-7c]^+[BF_4]^-$ at the 50% probability level. The H-atoms are omitted for clarity. (b) Side view of $[(M)-7c]^+$ unit and dihedral angle between two phenyls in terminal naphthyls. (c) Strong multiple intermolecular hydrogen bonding interactions ($F\cdots H$ and $B\cdots H$) between $[(M)-7c]^+$ and $[BF_4]^-$. (d) Molecular packing model of $[(M)-7c]^+[BF_4]^-$ along the a -axis in crystal. (e) Intermolecular hydrogen bonding interactions in crystals.

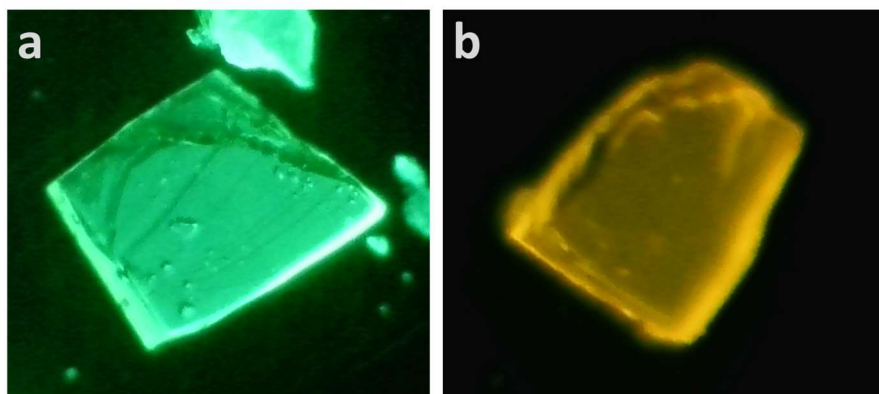


Fig. S20 (a) Fluorescence microscope image (at 365 nm) of the single crystals of [(*Rac*)-1b]⁺[BF₄]⁻ and (b) [(*Rac*)-3c]⁺[BF₄]⁻.

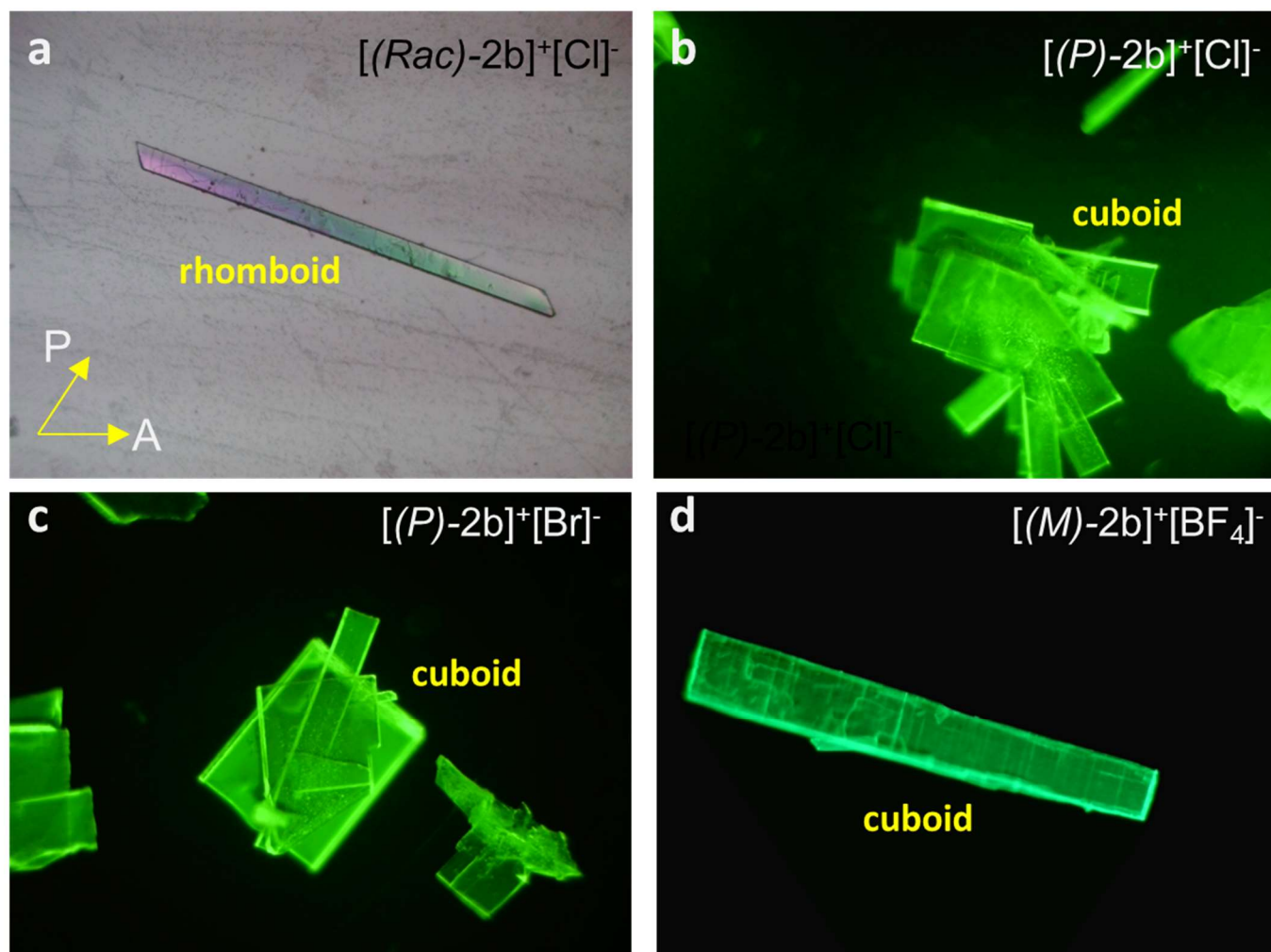


Fig. S21 (a) Polarized optical microscope of $[(M)\text{-}2b]^+[\text{Cl}]^-$. (b) Fluorescence microscope image (right, at 365 nm) of the single crystals of $[(P)\text{-}2b]^+[\text{Cl}]^-$ and (c) $[(P)\text{-}2b]^+[\text{Br}]^-$ and (d) $[(M)\text{-}2b]^+[\text{BF}_4]^-$.

Section E: Reaction mechanism study

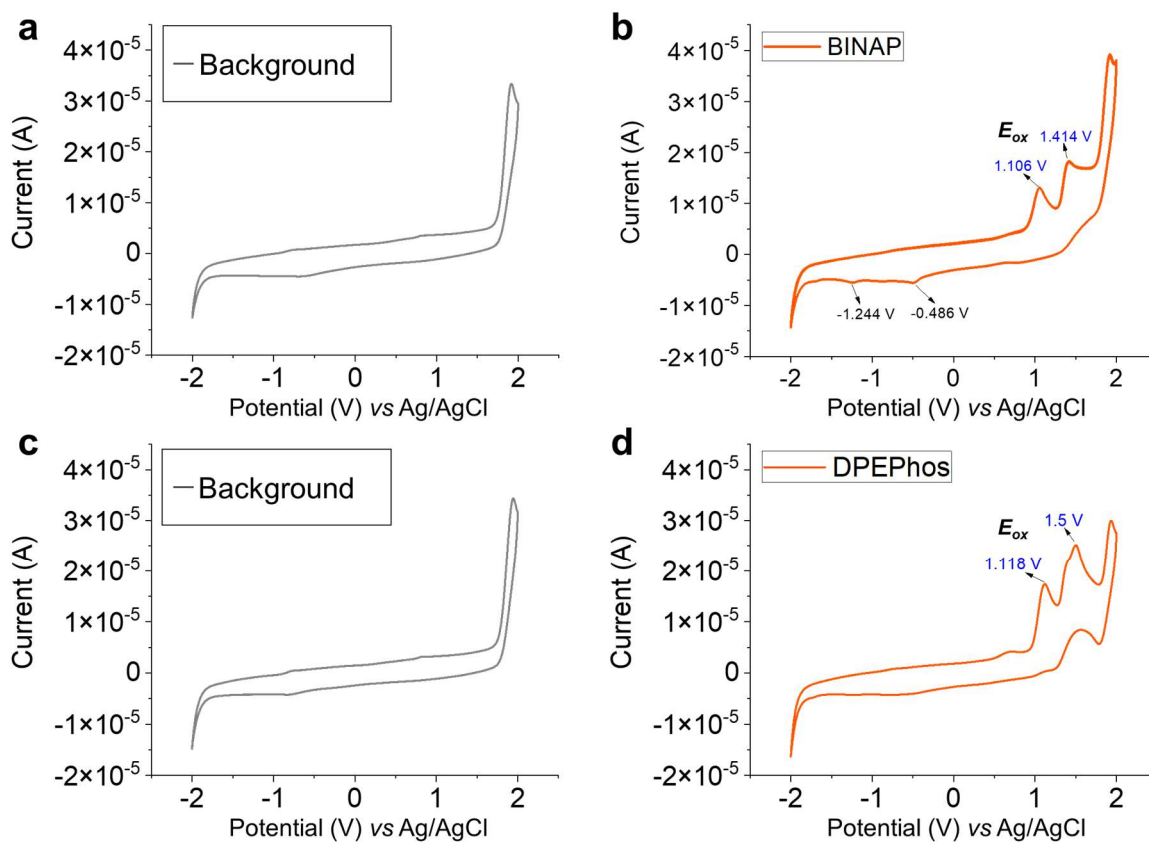


Fig. S22 Cyclic voltammetry (CV) of compounds BINAP and DPEPhos. CV experiments were measured in DCM solution ($M = 1.0 \times 10^{-3}$ mol/L) with Bu_4NPF_6 (0.1 mol/L) using Ag/AgCl as the reference electrode, glassy carbon as the working electrode, and Pt wire as the counter electrode. The scan rate was 100 mV s^{-1} .

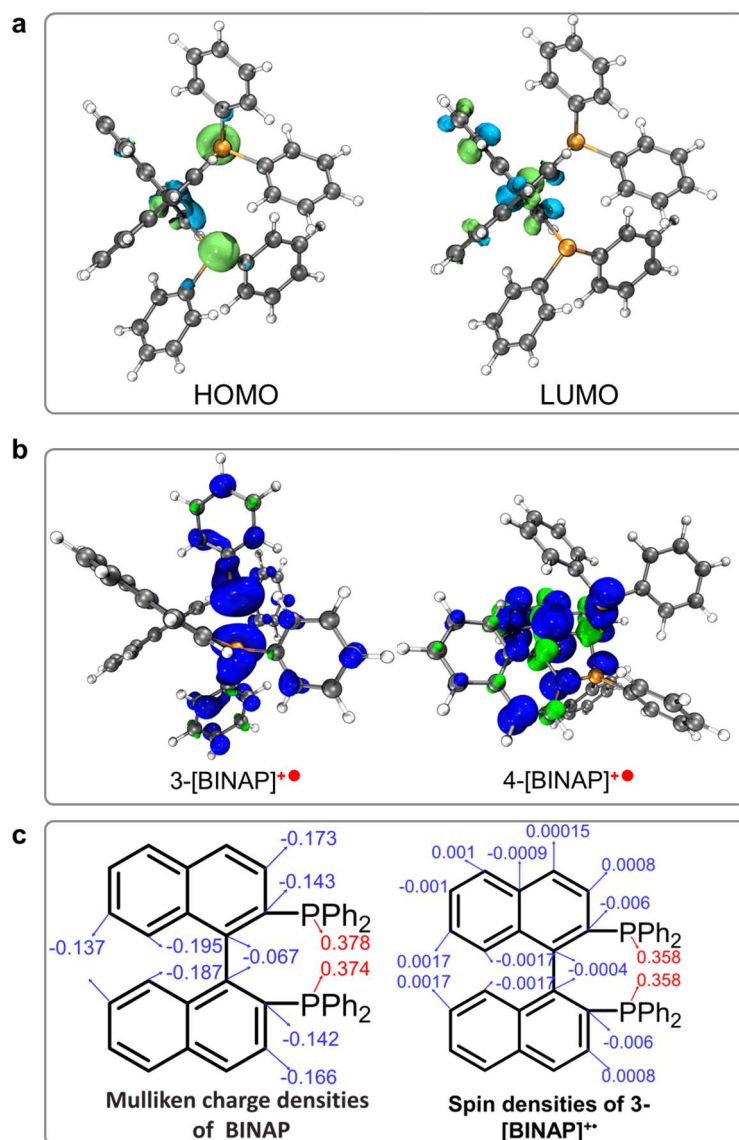


Fig. S23 (a) Calculated (at B3LYP/6-31G(d) level) frontier molecular orbital of BINAP. (b) Calculated spin density distribution map of 3-[BINAP]^{•+} and 4-[BINAP]^{•+}. (c) Calculated Mulliken charge densities and spin densities profile of the BINAP and 3-[BINAP]^{•+}, respectively.

Supporting information

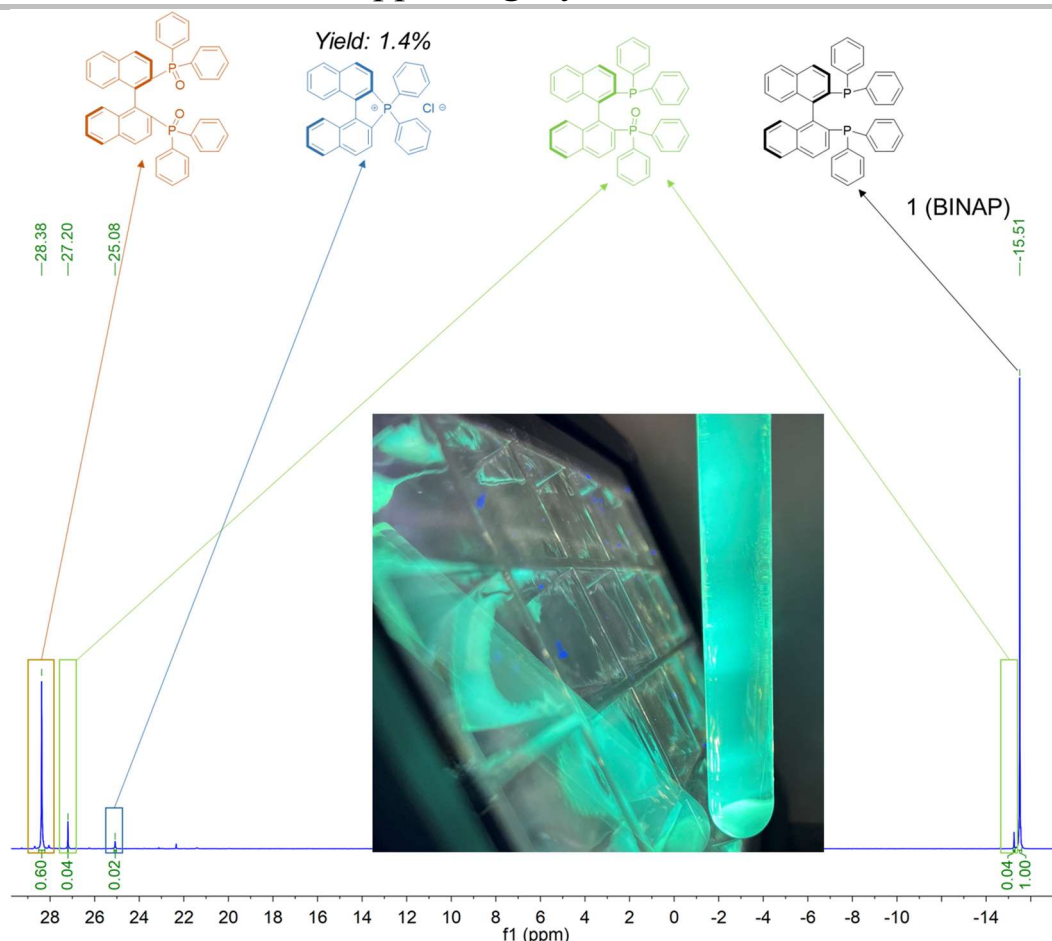


Fig. S24 Monitored ^{31}P NMR spectrum of the reaction mixture after photoinduced cyclization at room temperature (Radiation condition: at 365 nm UV light for 30 minutes).

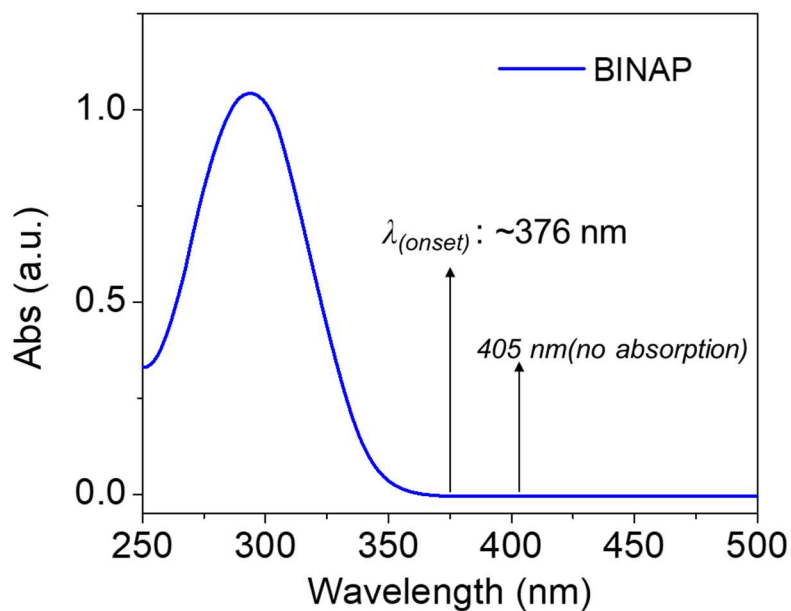


Fig. S25 Normalized UV-vis absorption spectra of BINAP in DCM ($1 \times 10^{-4} \text{ M}$).

Section F: Theoretical computation

(I) Computational methods for molecular orbitals and excited states transition: For all structures presented in this article, calculations of grid data were acquired by Multiwfn version 3.8 (dev) software.²² Isosurface maps were rendered by VMD 1.9.3 software.²³

The initial structures of the molecule were generated from single crystals by the software Mercury 2021.3.0 or built by the Gaussian View 6/ChemBioDraw Ultra 14.0 software. DFT/TD-DFT optimized structures were simulated at Gaussian 16 A.03 software in the gas phase at 298.15 K.²⁴ B3LYP exchange-correlation function and 6-31G(d) basis set for all elements.²⁵ Vibrational frequencies were computed to ensure that the geometries correspond to the true minima of the potential energy surfaces. The reduced density gradient (RDG) analysis was also performed at B3LYP-D3(BJ)/6-31G(d) level. Noncovalent interactions (NCI) have been visualized with RDG maps. The strength of the NCI was attributed to multiplying ρ and the sign of λ_2 . RDG plot was a useful tool to visualize noncovalent interactions (NCI) on a wide range of intensity from strongly attractive (blue color) to strongly repulsive (red color) through weaker interactions such as van der Waals interactions (green color).²⁶

The optimized ground structure was used for further computation tasks (frontier molecular orbital, TD-DFT/Vertical excitation energy) at a higher B3LYP/6-311G(d) or CAM-B3LYP/6-311G(d) level.²⁷ The solvent effect is based on the polarizable continuum model (PCM) for TD-DFT calculation in dichloromethane. Mulliken population analysis (MPA) was applied to obtain the electron density distribution of each atom in the HOMO/LUMO orbitals of the phospho[5]helicenes for electronic transitions. The simulated UV-vis/ECD spectra were acquired from the TD-DFT result (60 states). The UV-vis/ECD data were exported by Multiwfn version 3.8 (dev) software (the Gaussian broadening parameter/full width at half maximum (FWHM) is 0.67 eV). For the simulated emission (PL) spectrum, we assumed that the emission process obeyed the Kasha rule, the oscillator strengths of the S_2 and S_3 states were reseted as 0, and the PL curve was broadening by Gaussian type at 0.2 eV (FWHM). Based on TD-DFT simulative parameter, the dissymmetry factor (g) was calculated as follows: $g = 4R/(D + G)$, where R is the rotatory strength defined by the inner product of transition electric and magnetic dipole moments ($R = |\mu_e| \cdot |\mu_m| \cdot \cos \theta$), and D and G are the electric and magnetic dipole strengths defined by the square of transition electric and magnetic dipole moments, respectively ($D = |\mu_e|^2$; $G = |\mu_m|^2$). The MOs isosurfaces value was set at 0.025.²⁸ Moreover, additional calculations of frontier molecular orbitals were performed at CAM-B3LYP/6-311G(d) level for [(*P*)-14b]⁺, which can describe ICT behavior more precisely than B3LYP/6-311G(d) (Fig. S34, S35).^{27,29}

The optimized excited structure (S_1) was performed at B3LYP/6-31G(d) level and the further Vertical excitation energy computation and oscillator strength were simulated at B3LYP/6-311G(d) level. The

Supporting information

simulated fluorescence spectra were output by Multiwfn version 3.8 (dev) software (the Gaussian broadening parameter is 0.67 eV).

(II) The optimized ground structure was used for further computation tasks. The calculated AICD plots of cationic phosphoniums [(*P*)-1b]⁺, [(*R*)-5b]⁺, and [(*P*)-14b]⁺ by DFT at the CSGT-B3LYP/6-31G(d) level, respectively. Calculated ^aNICS(0) and ^bNICS(1) values of cationic phosphonium [(*R*)-5b]⁺ and phospho[5]helicenes [(*P*)-1b]⁺, [(*P*)-14b]⁺ by DFT at the GIAO-B3LYP/6-31G(d) level. In addition, the Anisotropy of the Induced Current Density (AICD) maps were produced by AICD 2.0 software.³⁰

(III) To reduce the computational cost, the isomerization of the transition state (TS) was searched and calculated at B3LYP-D3(BJ)/6-31G(d) level to determine the barrier of racemation. The reaction of the pivotal intermediate and transition state (TS) was also searched and calculated at B3LYP-D3(BJ)/6-31G(d) level to determine the barrier of reaction by Gibbs free energy at 298.15 K. For all TS states, frequency analyses were carried out at the same level to evaluate the vibrational energy. Only one effective virtual frequency was found. In addition, the optimized molecular conformation and their orbitals and spin densities for BINAP and 3-[BINAP]⁺⁺ were performed at B3LYP-/6-31G(d) level.

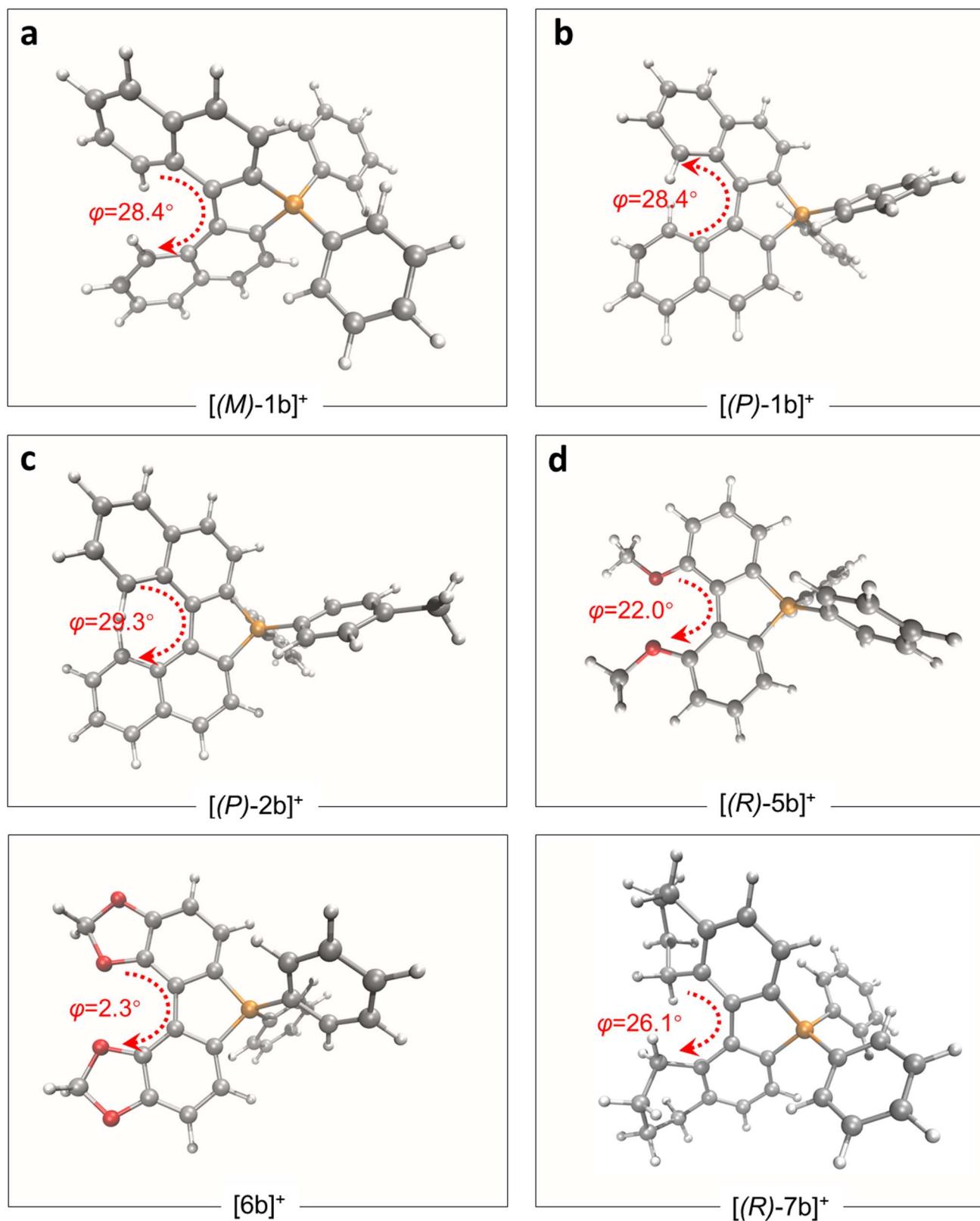


Fig. S26 Optimized molecular structures of $[(P)-1b]^+$, $[(P)-2b]^+$, $[(P)-5b]^+$, $[(P)-6b]^+$, and $[(R)-7b]^+$ at the ground state.

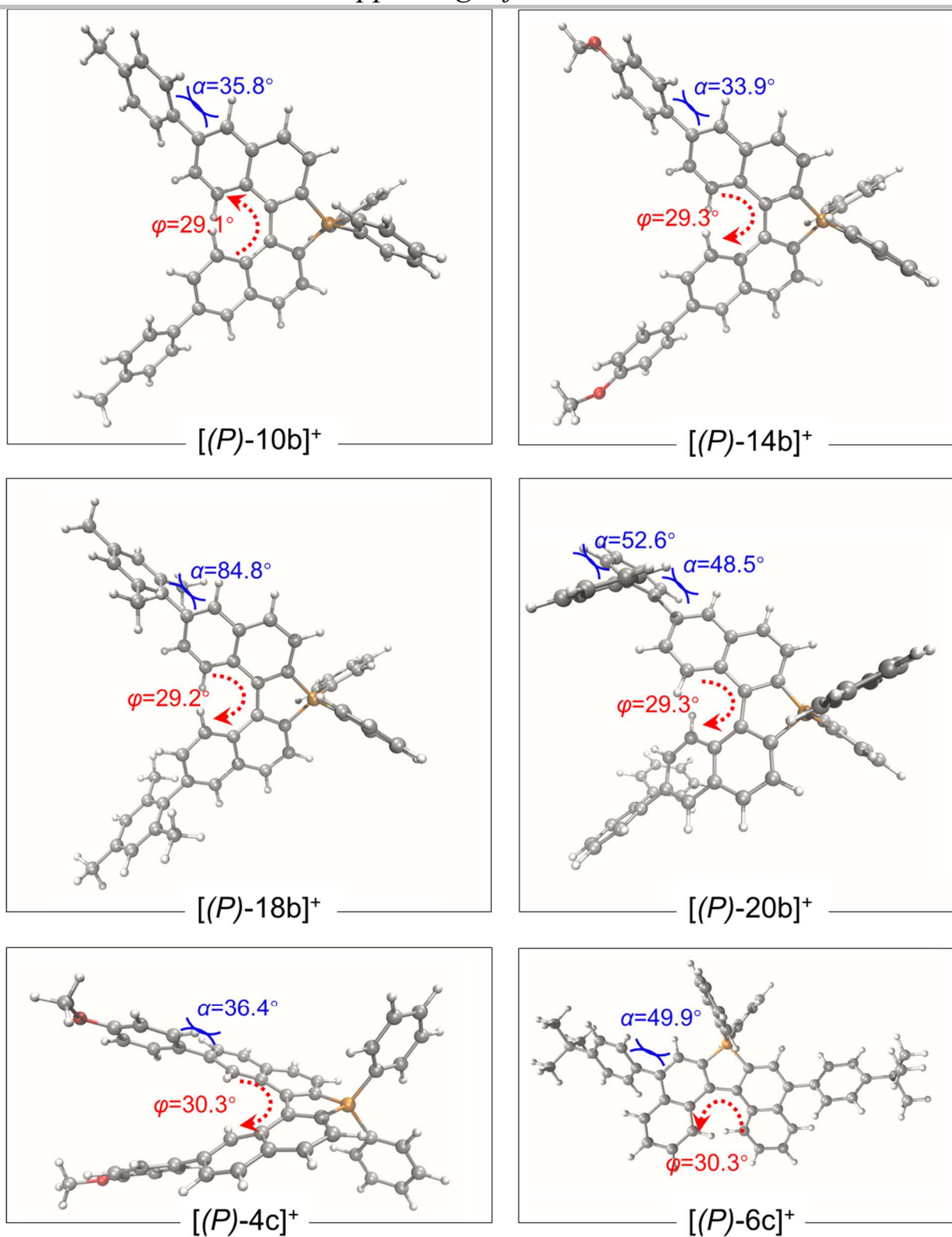


Fig. S27 Optimized molecular structures of [P]-10b⁺, [P]-14b⁺, [P]-18b⁺, [P]-20b⁺, [P]-4c⁺, and [P]-6c⁺ at the ground state.

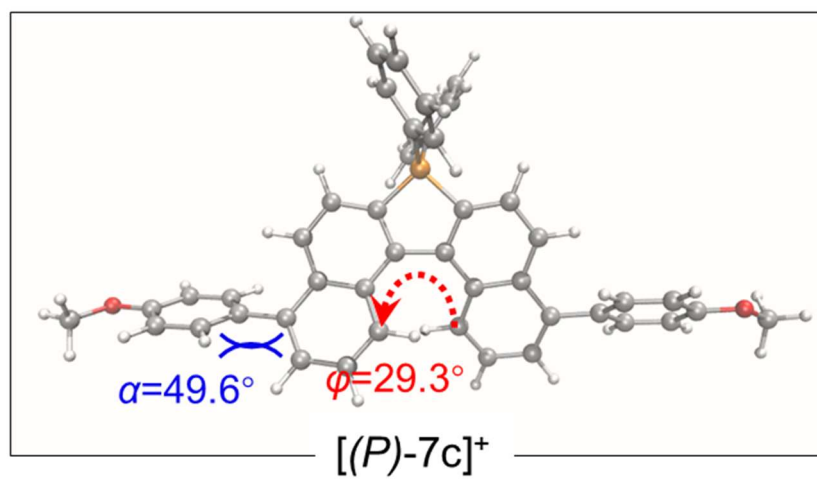


Fig. S28 Optimized molecular structure of [(P)-7c]⁺ at the ground state.

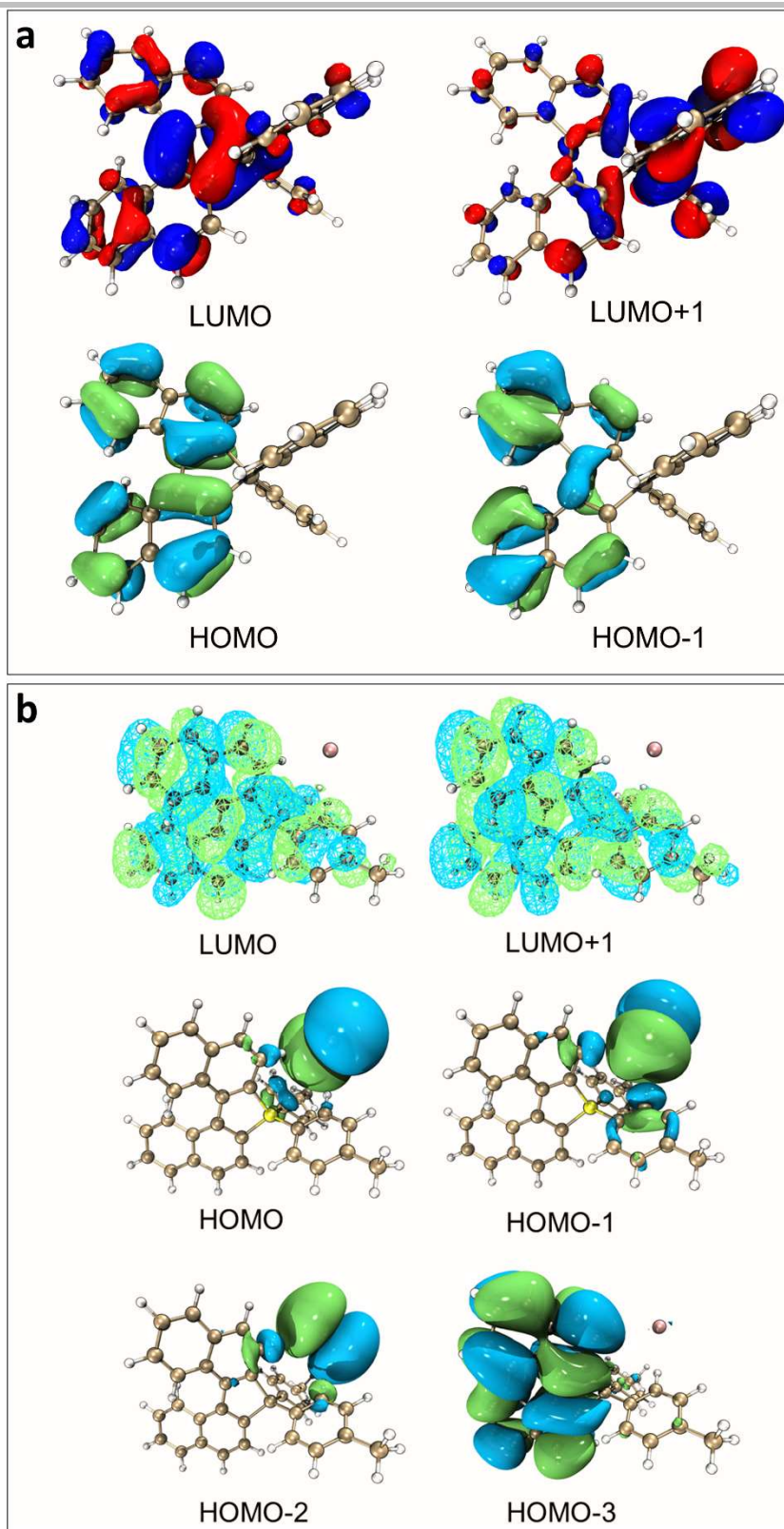


Fig. S29 Frontier molecular orbitals for $[(P)\text{-}2b]^+$ at the ground state. (b) Frontier molecular orbitals for $[(P)\text{-}2b]^+[\text{Br}]^-$ at the ground state (at B3LYP/6-311G(d) level). (isosurface value is 0.025)

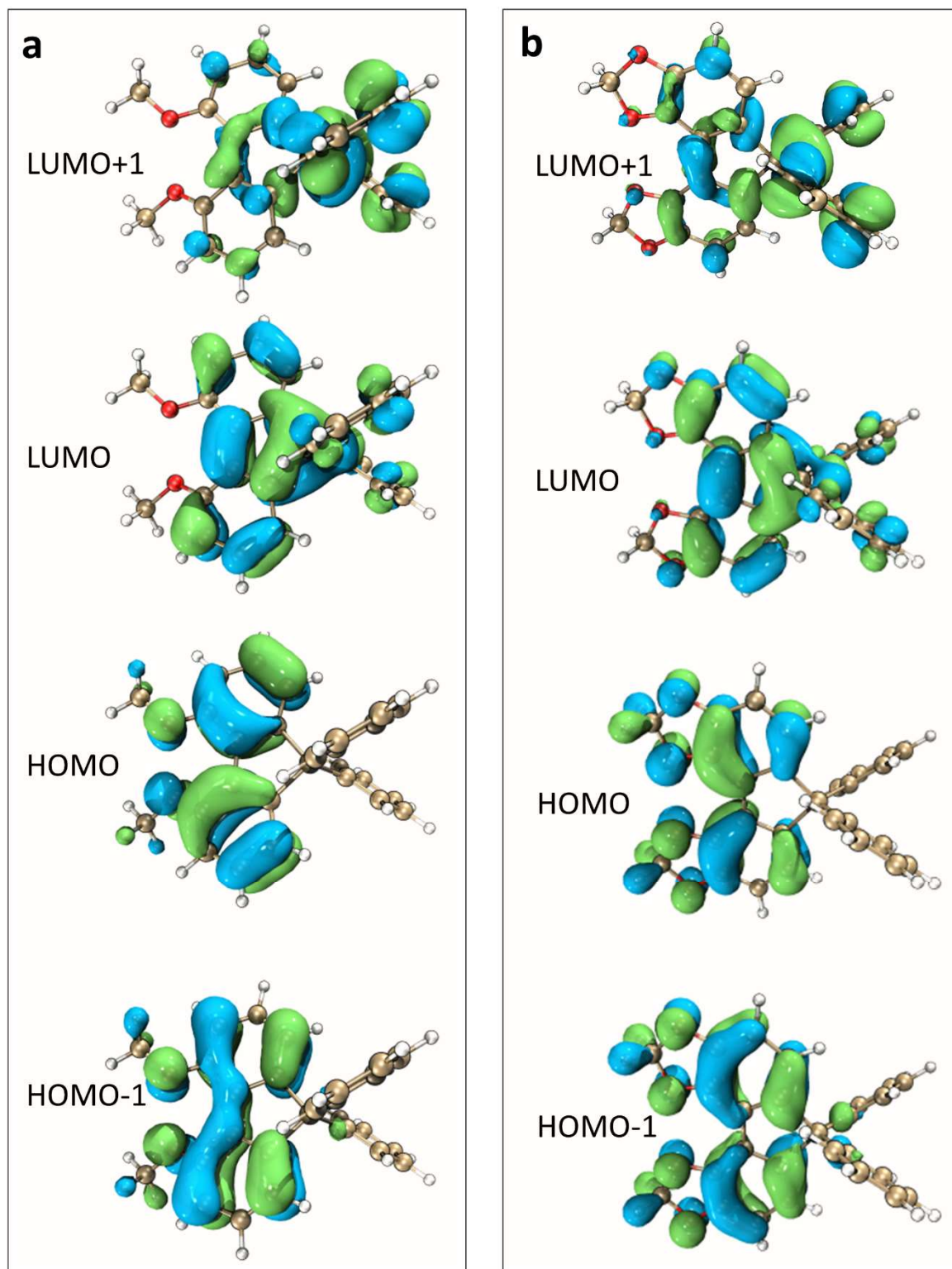


Fig. S30 Frontier molecular orbitals for $[(R)\text{-}5\text{b}]^+$ at the ground state. (b) Frontier molecular orbitals for $[6\text{b}]^+$ at the ground state (at B3LYP/6-311G(d) level). (isosurface value is 0.025)

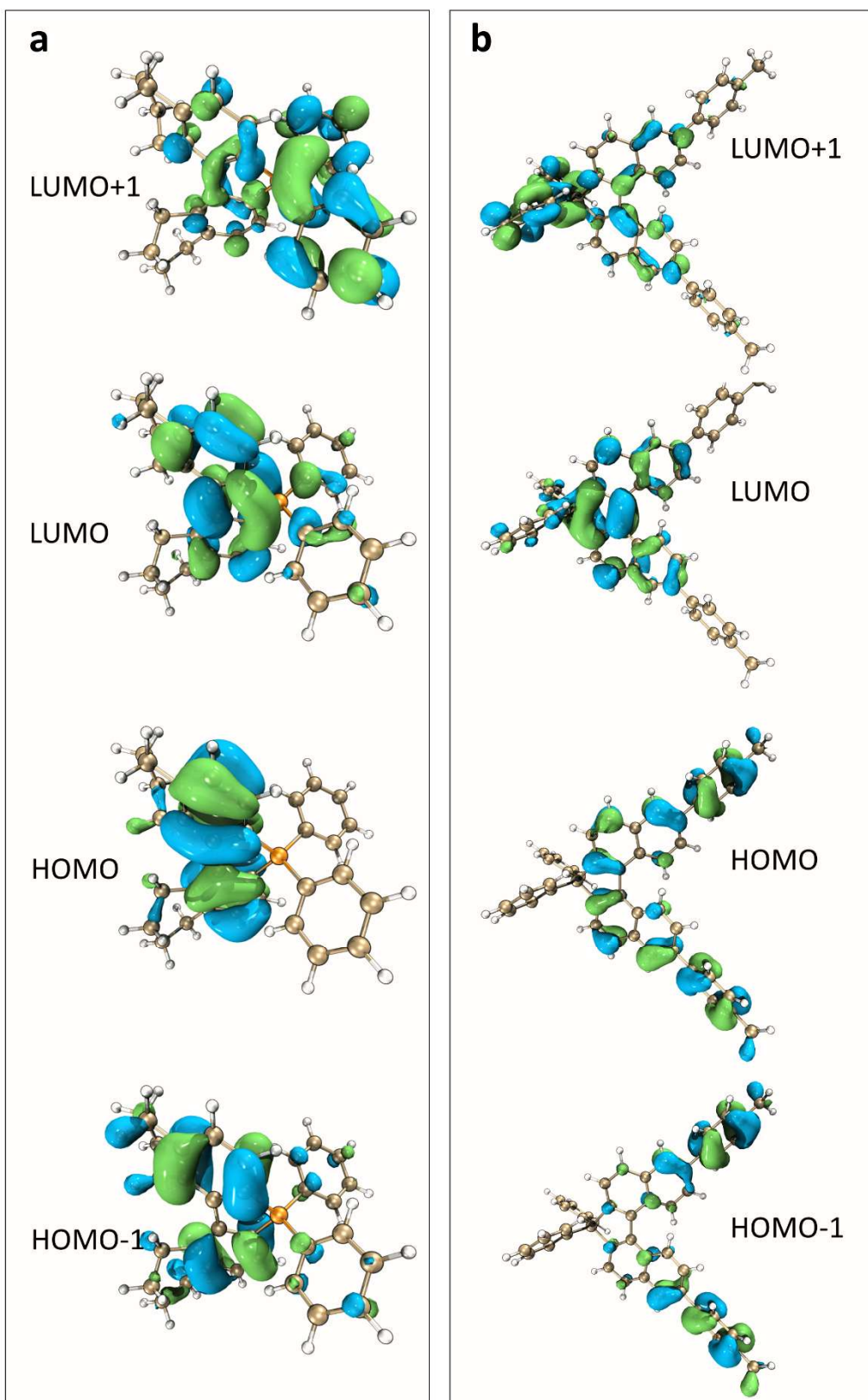


Fig. S31 Frontier molecular orbitals for $[(R)-7b]^+$ at the ground state. (b) Frontier molecular orbitals for $[(P)-10b]^+$ at the ground state (at B3LYP/6-311G(d) level). (isosurface value is 0.025)

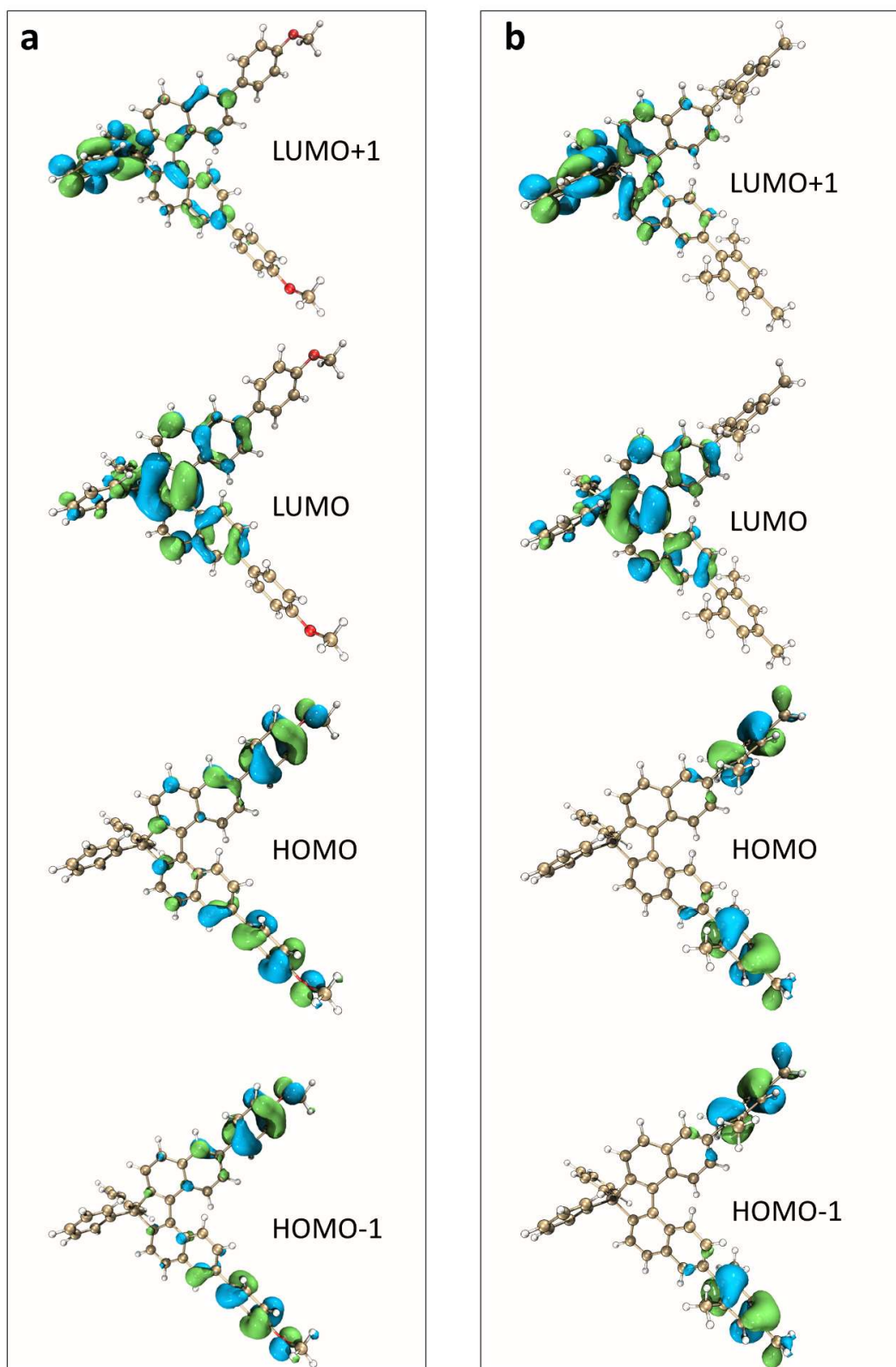


Fig. S32 (a) Frontier molecular orbitals for $[(P)\text{-}14b]^+$ at the ground state. (b) Frontier molecular orbitals for $[(P)\text{-}18b]^+$ at the ground state (at B3LYP/6-311G(d) level). (isosurface value is 0.025)

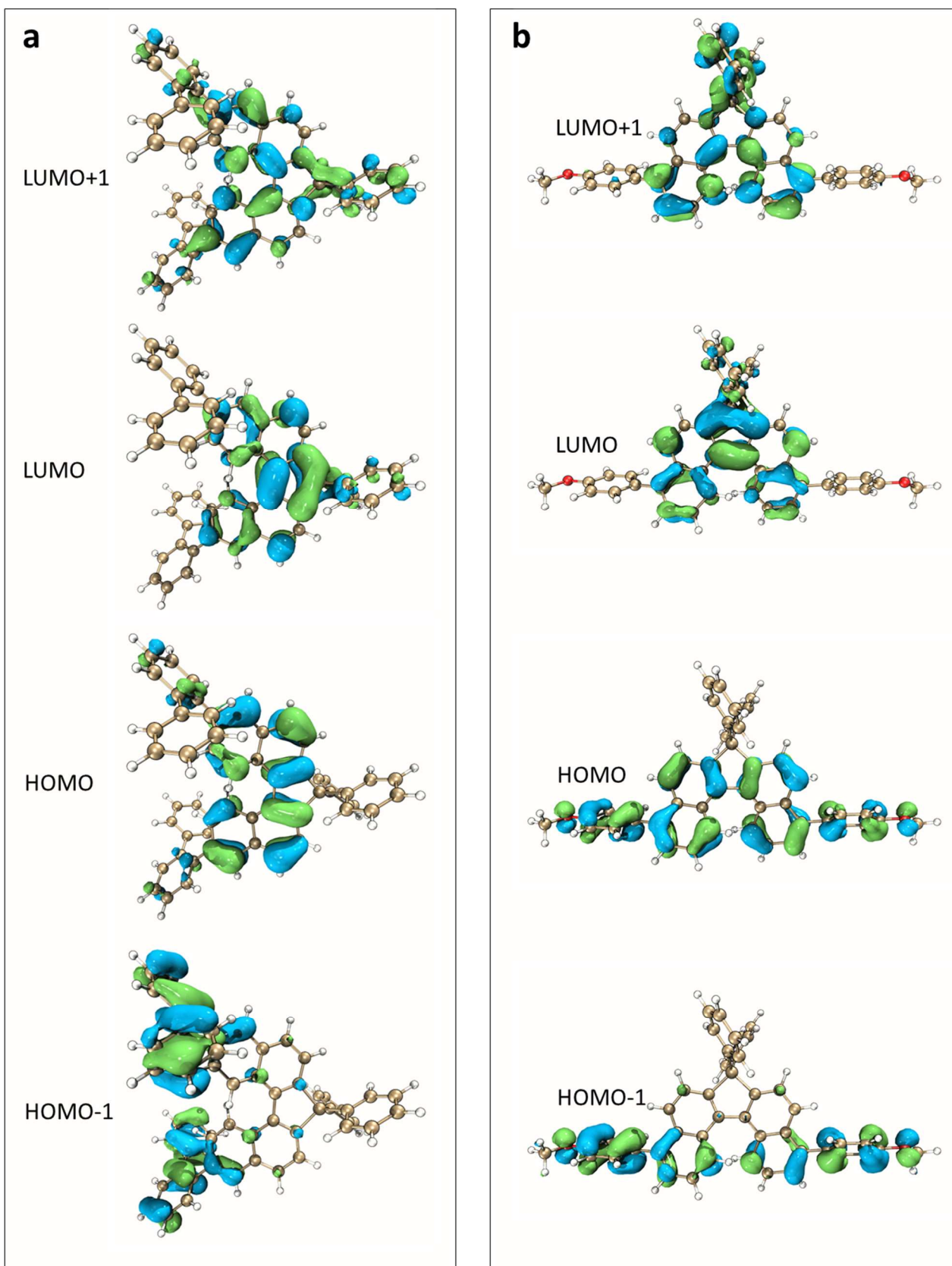


Fig. S33 (a) Frontier molecular orbitals for $[(P)\text{-}20b]^+$ at the ground state. (b) Frontier molecular orbitals for $[(P)\text{-}7c]^+$ at the ground state (at B3LYP/6-311G(d) level). (isosurface value is 0.025)

Supporting information

Note: Electronic structure analysis for bisphosphonium and phosphahelicene at CAM-B3LYP/6-311G(d) level

It was imperative to highlight the difference in electronic information between preexisting achiral bisphosphonium ($[\text{BP-1}]^{2+}$) and chiral $[(\text{Rac})\text{-1b}]^+\text{[Cl]}^-$. As shown in Fig. S34a, MOs of $[\text{BP-1}]^{2+}$ also displayed LE character (the HOMOs and LUMOs occupied in the binaphthalene skeleton), indicating common characteristics because of a similar bonding environment. But the electronic absorption spectra of compound $[\text{BP-1}]^{2+}$ revealed low energy LE band (356-450 nm, Fig. 5c, S30a) with divided peaks owing to vibronic progression. The fluorescence emission exhibited narrow FWHM (59 nm), small Stokes shift (42 nm), and high emission energy (453 nm) compared with $[(\text{Rac})\text{-1b}]^+\text{[Cl]}^-$ (Fig. 5c).³¹ These results could be assigned to a more rigid, flat scaffold, and quite different electronic level for centrosymmetric $[\text{BP-1}]^{2+}$.¹⁹

Because the CAM-B3LYP functional with long-range correction was more suitable for dealing with charge transfer excited states. Hence, additional calculations of frontier molecular orbitals for $[\text{BP-1}]^{2+}$ and (b) $[(M)\text{-7c}]^+$, $[(P)\text{-4c}]^+$, $[(P)\text{-14b}]^+$ at CAM-B3LYP/6-311G(d) level were performed to check the reliability of electronic transition behavior. As shown in Fig. S34b and S29-S33, two functionals (CAM-B3LYP / B3LYP) showed similarly separated orbitals of HOMOs/LUMOs. In short, after the introduction of the torsional electron acceptor at phosphahelicene, the LE electron transition was transformed into an ICT state.

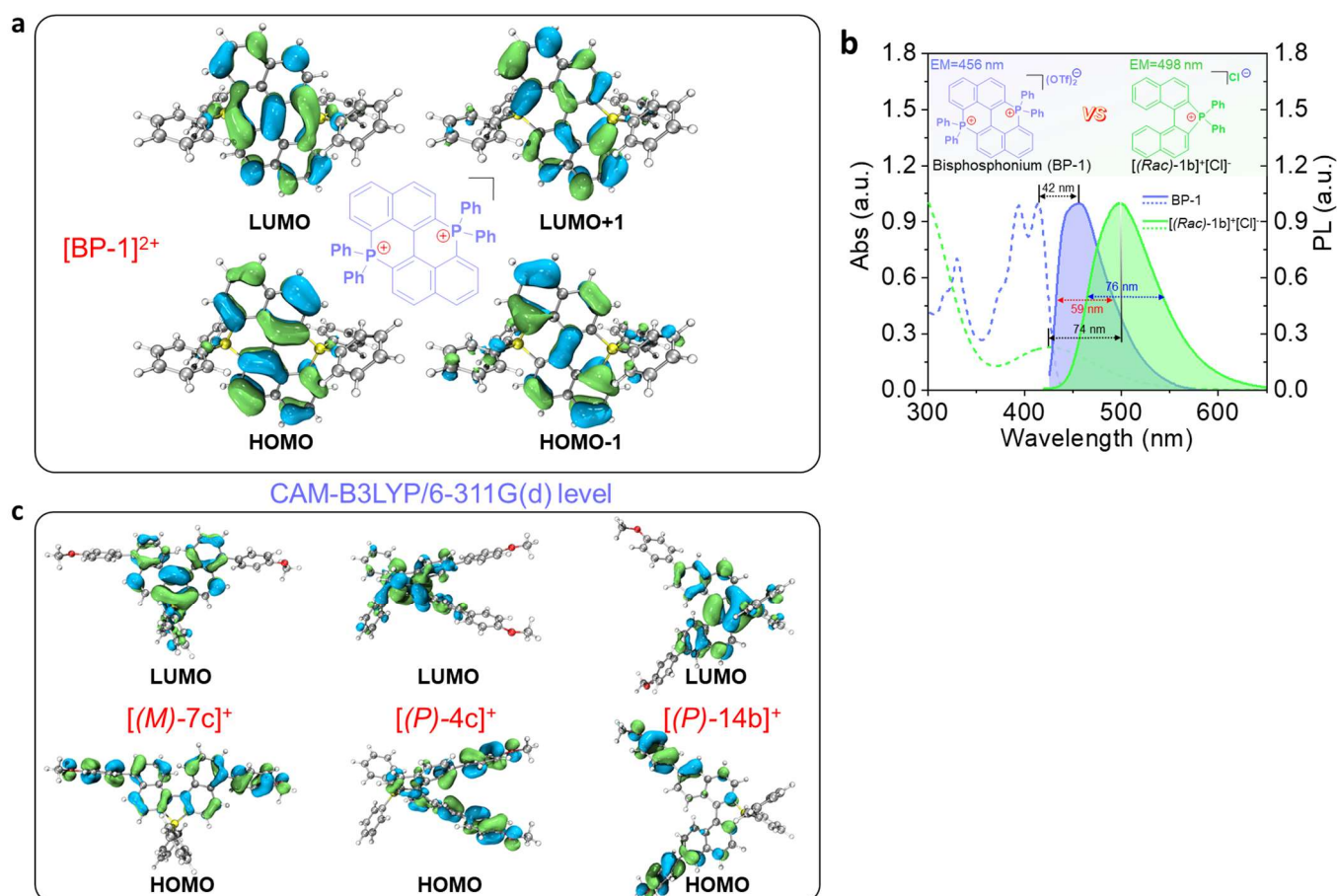


Fig. S34 (a) Additional calculations of frontier molecular orbitals for $[\text{BP-1}]^{2+}$. (b) Spectra comparison between $[\text{1b}]^+\text{[Cl]}^-$ and $[\text{BP-1}]^{2+}\text{[OTf]}_2^-$. (c) Additional calculated frontier molecular orbitals for $[(M)\text{-7c}]^+$, $[(P)\text{-4c}]^+$, $[(P)\text{-14b}]^+$ at CAM-B3LYP/6-311G(d) level, respectively (isosurface value is 0.025).

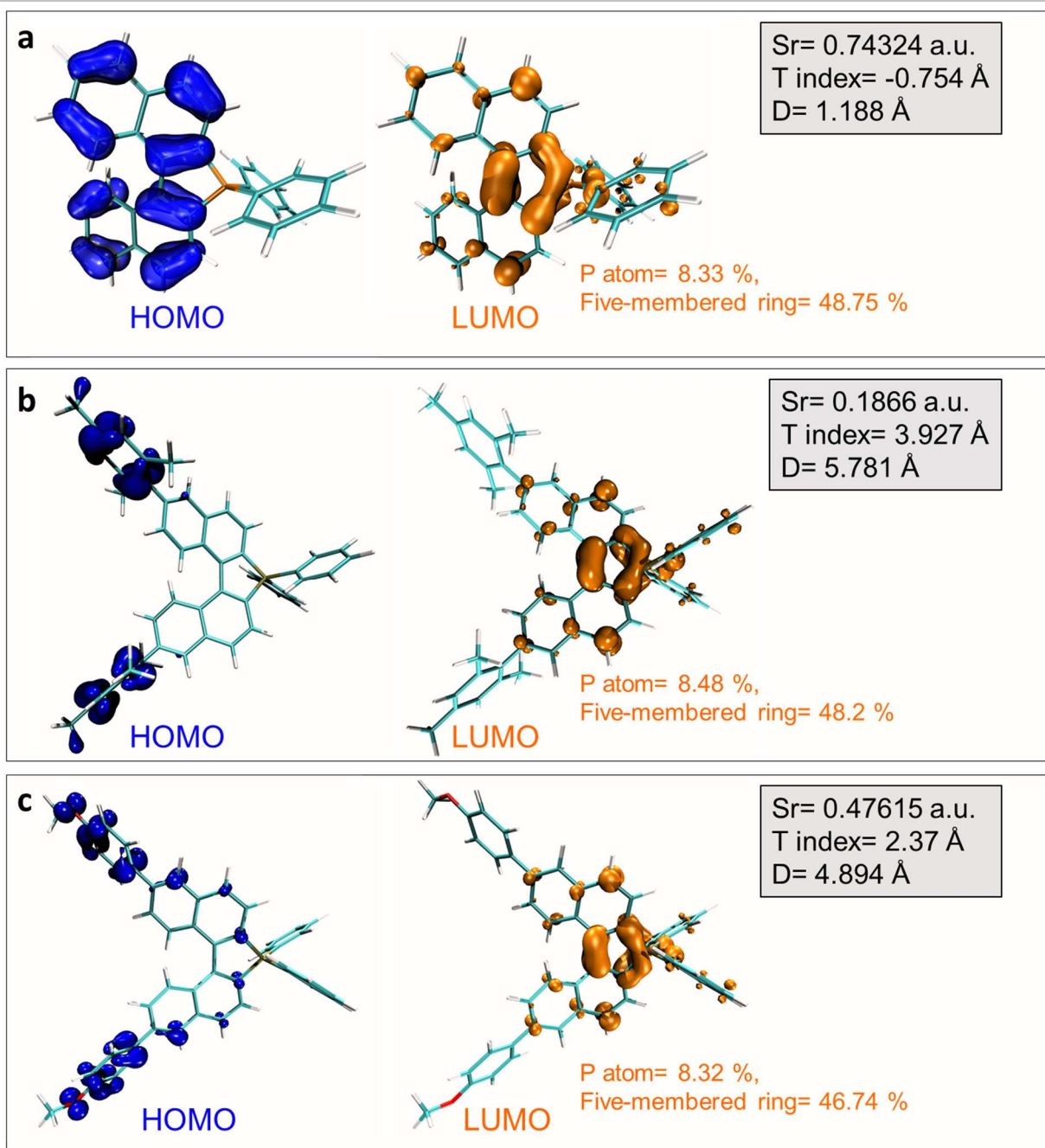


Fig. S35 Computational analysis of electron cloud distribution for (a) [(*P*)-1b]⁺, (b) [(*P*)-18b]⁺, and (c) [(*P*)-14b]⁺ at B3LYP/6-311G(d) level.

Note: The orbital analysis was adopted to confirm the ICT contribution for [(*P*)-14b]⁺ and [(*P*)-18b]⁺ in the ground state, where the HOMO-electron is distributed on the substituent-phenyls and the LUMO-electron is dominated by the P(III) pentagon with a high contribution up to 46.8-48.2%. The P-atom shows an obvious component of 8.32-8.48%, indicating electron deficiency of the quaternary P(III)-center. Compared to compound [1b]⁺ without torsional electron acceptor, the [(*P*)-18b]⁺, and (c) [(*P*)-14b]⁺ exhibited longer electron transfer distance and higher T/D index, indicating typical ICT behavior. However, [(*P*)-1b]⁺ showed a negative T index. This result could be ascribed to the LE transition of [(*P*)-1b]⁺.²²

Supporting information

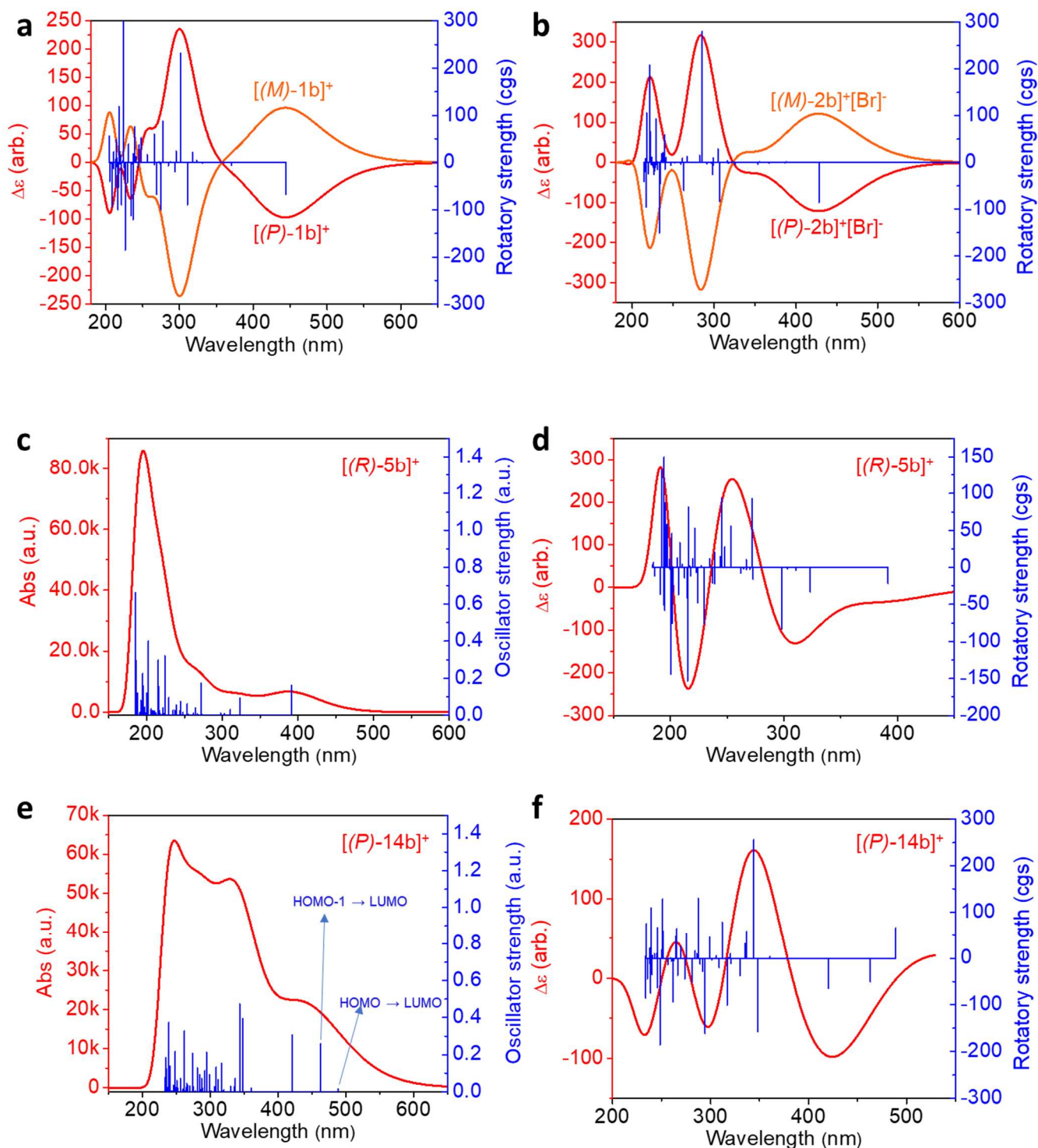


Fig. S36 (a-b) TD-DFT calculated CD spectra (left: CD absorption, Right: Rotatory strength) for enantiomeric [1b]⁺ and [2b]⁺[Br]⁻. (c) TD-DFT calculated UV-vis spectrum for [(R)-5b]⁺. (d) TD-DFT calculated CD spectrum for [(R)-5b]⁺. (e-f) TD-DFT calculated UV-vis and CD spectra for [(P)-14b]⁺.

Supporting information

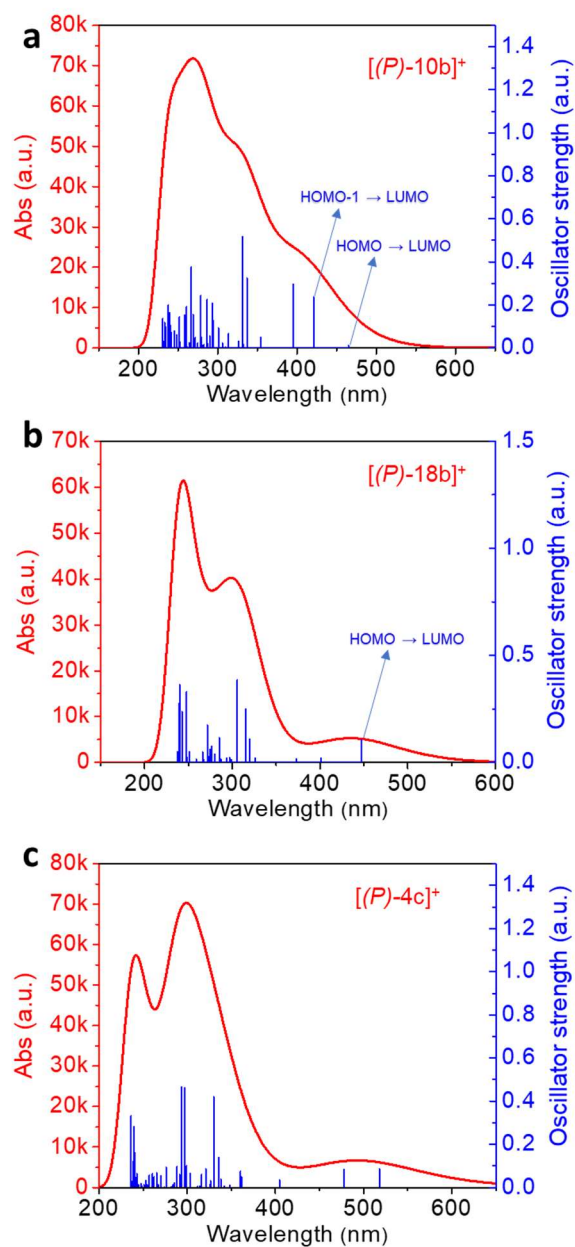


Fig. S37 (a-c) TD-DFT calculated UV-vis spectra for $[(P)-10b]^+$, $[(P)-18b]^+$, and $[(P)-4c]^+$, respectively.

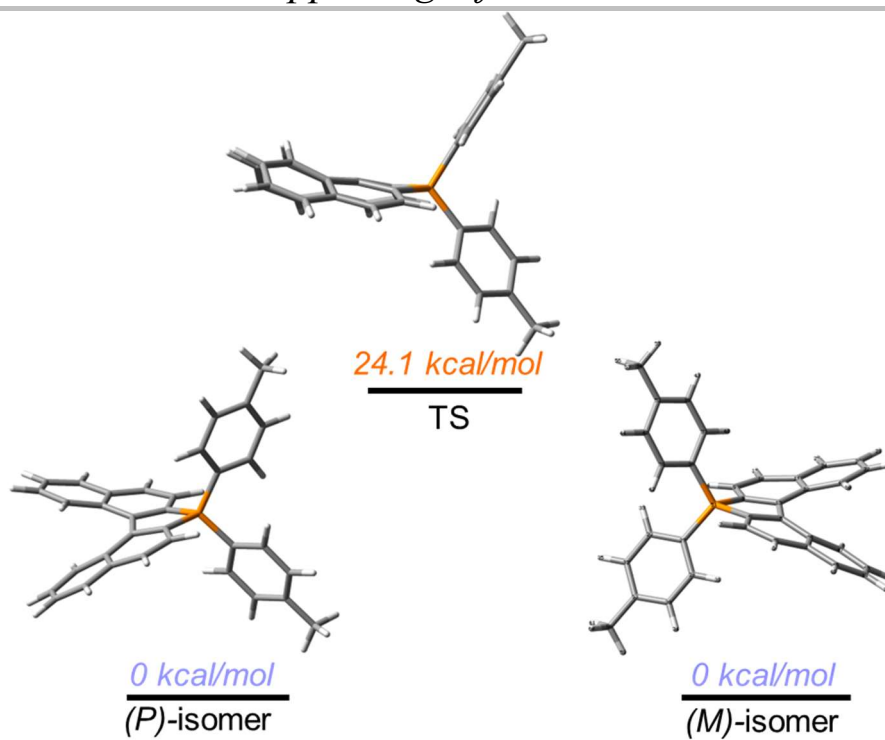


Fig. S38 Calculated isomerization energy (ΔG^\ddagger) and conformation for cation $[2b]^+$ between (M) -isomer and (P) -isomer at B3LYP/6-31G(d) level.

Supporting information

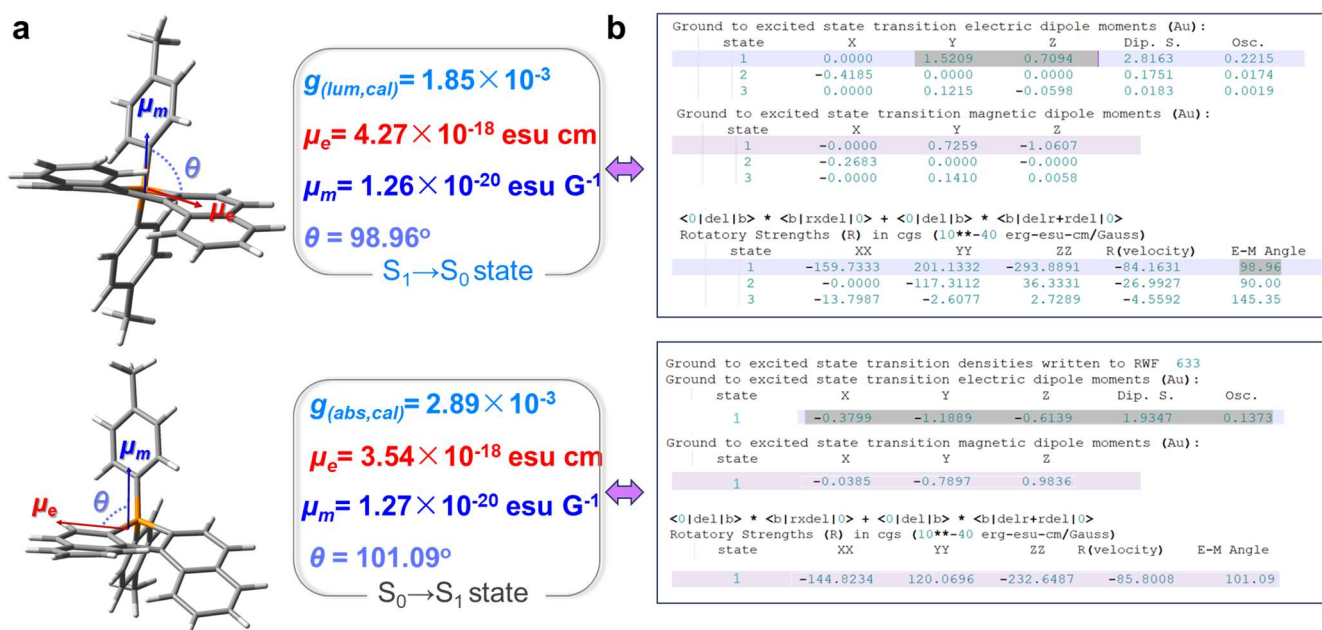


Fig. S39 (a) TD-DFT calculated electric transition dipole moments (μ_e) (red arrow), μ_m (blue arrow), θ_{e-m} , $g_{(lum,cal)}$ of $S_1 \rightarrow S_0/S_0 \rightarrow S_1$ transition for $[(P)-2b]^+$, respectively. (b) Key simulative parameters of TD-DFT results.

Supporting information

Table S9. Computed Excitation Energies and Oscillator Strengths for the $S_0 \rightarrow S_n$ Transitions of [(P)-1b]⁺			
$\lambda(\text{nm})$	E(eV)	f	transitions
444.40	2.7899	0.1184	H→L 98.8%
370.41	3.3472	0.00570	H-1→L 96.8%
331.04	3.7453	0.001	H-2→L 60.7%, H→L+3 22.6%, H→L+2 13.4%
323.04	3.8380	0.00420	H→L+1 53.8%, H-3→L 36.2%,
318.14	3.8971	0.06790	H→L+2 81.0%, H→L+3 13.6%,

Table S10. Computed Excitation Energies and Oscillator Strengths for the $S_0 \rightarrow S_n$ Transitions of [(P)-14b]⁺			
$\lambda(\text{nm})$	E(eV)	f	transitions
488.94	2.5358	0.01550	H→L 97.7%
463.04	2.6776	0.26140	H-1→L 98.3%
420.64	2.9477	0.30760	H-2→L 94.9%
360.54	3.4388	0.01830	H-3→L 89.7%,
348.25	3.5602	0.39590	H→L+1 93.5%,

Table S11. Computed Excitation Energies and Oscillator Strengths for the $S_0 \rightarrow S_n$ Transitions of [(P)-4c]⁺			
$\lambda(\text{nm})$	E(eV)	f	transitions
517	2.3949	0.08680	H→L 98.4%
477.73	2.5953	0.08310	H-1→L 98.4%
707.70	3.0636	0.03390	H-2→L 97.2%
361.35	3.4311	0.04860	H-3→L 54.7%, H→L+2 38.6
360.12	3.4429	0.07460	H→L+1 87.9%, H→L+3 5.7%

Section G: Photophysical properties

Motivated by the D-A type electronic structure of these substituted phosphahelicenes, photophysical properties were evaluated. Representative compounds were discussed main text. The optical properties derived from the ICT behavior of D-A structure units such as optical band gap and emission energy. The optical band gap and emission wavelength were decreased as the enhanced strength of the donor or π -extension. For instance, the 4-PhOMe (558 nm) and naphthyl-substituted compounds have a low-energy emission and stokes-shift, but the 4-PhCF₃ (494 nm) compounds exhibited blue shift emission. Moreover, for many compounds, the spectral shift in the solid state was inconspicuous (a few nanometers to ten nanometers), indicating restriction of π -stacking in the tetrahedral structure.

Table S12. Photophysical Data of Selective P(III) Compounds in Anhydrous Chloroform and Solid State

name	^a λ_{abs} (nm)	^b λ_{em} (nm)		^c Φ_{em} (%)		^a τ (ns)	^d k_r (ns ⁻¹)	^d k_{nr} (ns ⁻¹)
		solution	solid	solution	solid			
[(<i>M</i>)-1b] ⁺ [Cl] ⁻	271, 294, 331, 424	^e 498 (^f 509)	507	21	34	2.2	9.5×10 ⁷	3.6×10 ⁸
[(<i>P</i>)-2b] ⁺ [Cl] ⁻	268, 292, 335, 408	^e 495 (^f 506)	501	19	30	2.0	9.5×10 ⁷	4.0×10 ⁸
[(<i>Rac</i>)-5b] ⁺ [Cl] ⁻	248, 268, 320, 379	^e 456	456	77	56	1.7	4.5×10 ⁸	1.4×10 ⁸
[6b] ⁺ [Cl] ⁻	313, 327, 353, 370	^e 405	460, 545	12	NR	2.9	5.2×10 ⁷	3.0×10 ⁸
[(<i>Rac</i>)-14b] ⁺ [Cl] ⁻	296, 333, 357, 420	^e 561	558	35	57	12.9	2.7×10 ⁷	5.0×10 ⁷
[(<i>Rac</i>)-2c] ⁺ [Cl] ⁻	288, 325, 351, 431	^e 516 (^f 508)	540	39	59	5.4	7.2×10 ⁷	1.1×10 ⁸
[(<i>Rac</i>)-4c] ⁺ [Cl] ⁻	303, 334, 414, 452	^e 544	568	37	54	8.8	5.8×10 ⁷	6.0×10 ⁷
[(<i>M</i>)-7c] ⁺ [Cl] ⁻	281, 354, 422, 449	^e 542 (^f 530)	559	39	53	10.7	3.6×10 ⁷	5.7×10 ⁷
^g BP-1	330, 372, 393, 415	453	ND	11	ND	0.9	1.2×10 ⁸	9.8×10 ⁸

^aMeasured in anhydrous chloroform solution (1×10^{-5} mol L⁻¹). ^bExcitation wavelength at 360 nm. ^cAbsolute quantum yield measured using the calibrated integrating sphere system. ^d $k_r = \Phi/\tau$; ^d $k_{nr} = (1 - \Phi)/\tau$ in chloroform. NR represents not recorded due to extremely weak emission. All experimental measurements were performed at room temperature. ^eExperimental PL peak. ^fComputational PL peak value for S₁→S₀ transition at CAM-B3LYP/6-311G(d) level. ^gAccording to record references.¹⁹

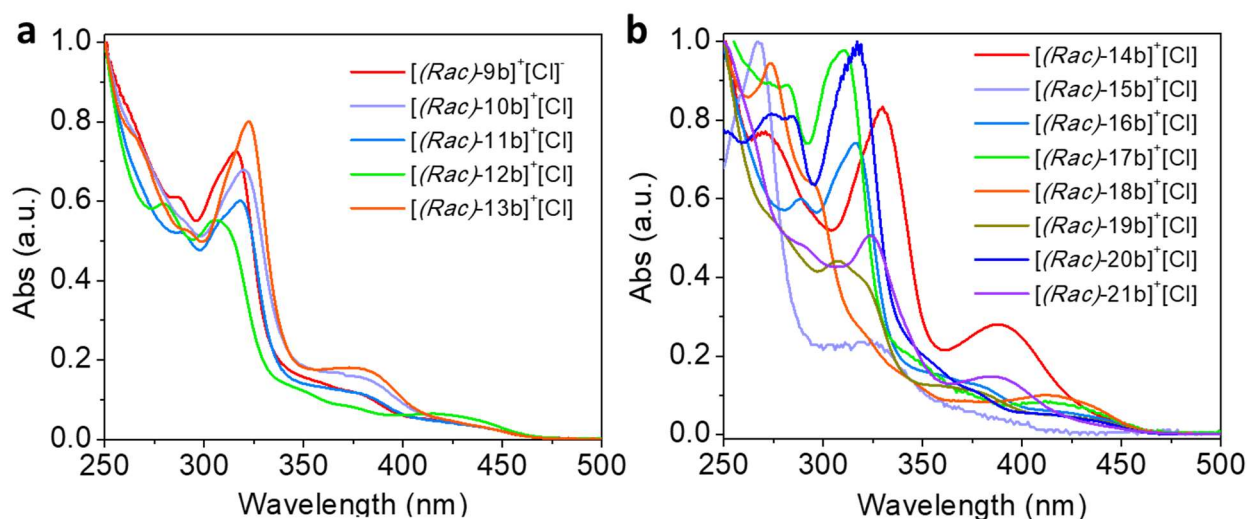


Fig. S40 (a-b) Normalized UV-vis spectra for 6,6'-substituted P(III)-helicenes in chloroform (1×10^{-4} M).

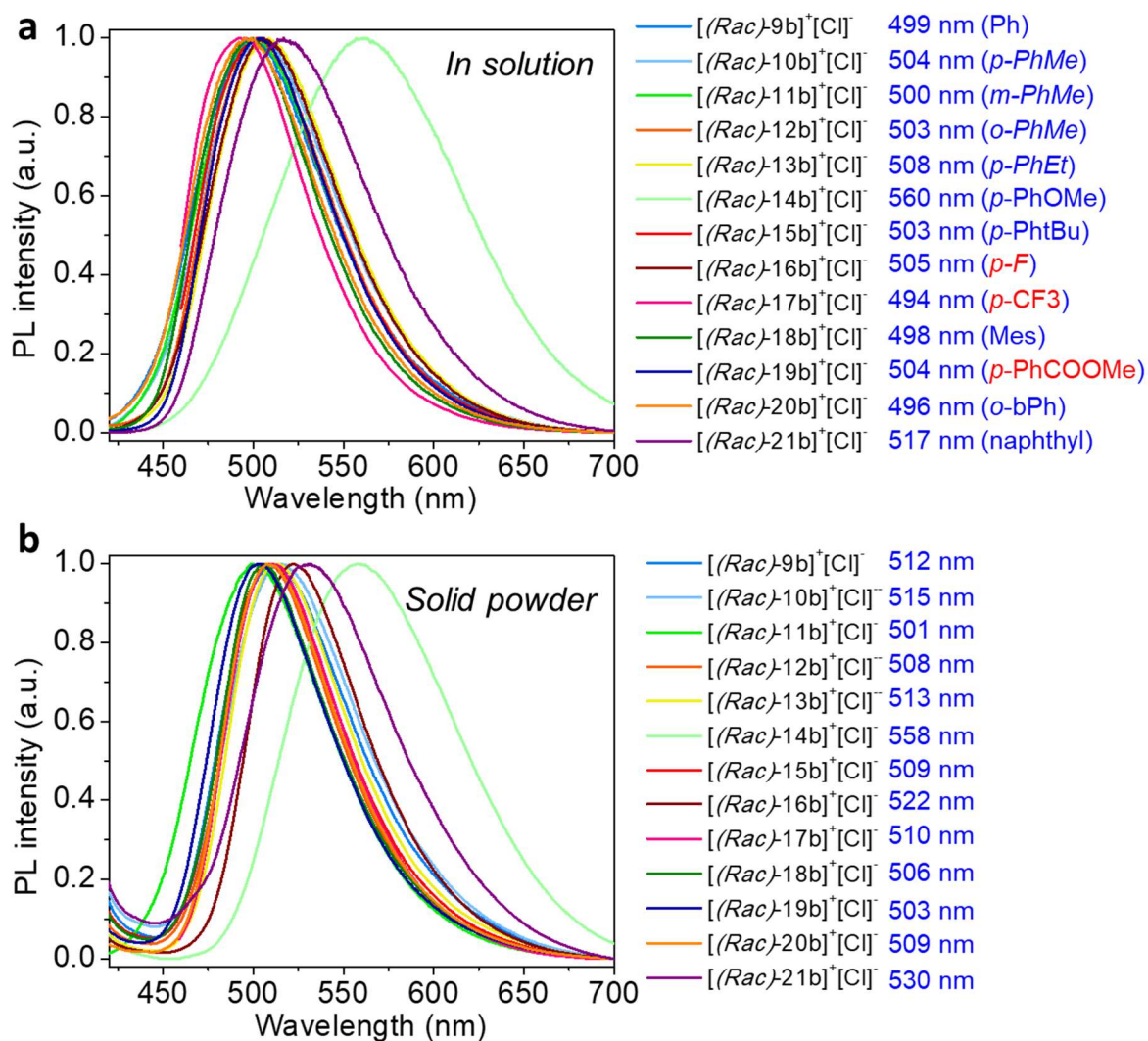


Fig. S41 (a) Normalized photoluminescence spectra for 6,6'-substituted P(III)-helicenes in chloroform (1×10^{-4} M). (b) In the solid amorphous state at room temperature.

Supporting information

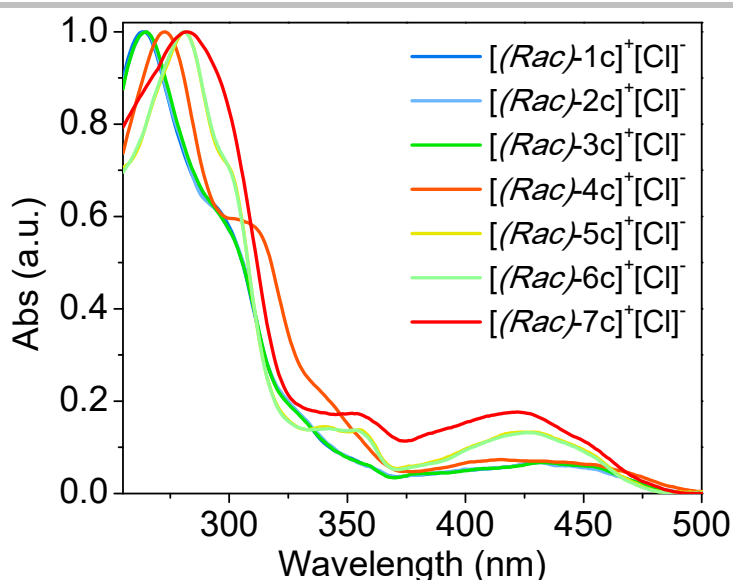


Fig. S42 Normalized UV-vis spectra for 5,5'-substituted and 7,7'-substituted P(III)-helicenes in chloroform (1×10^{-4} M).

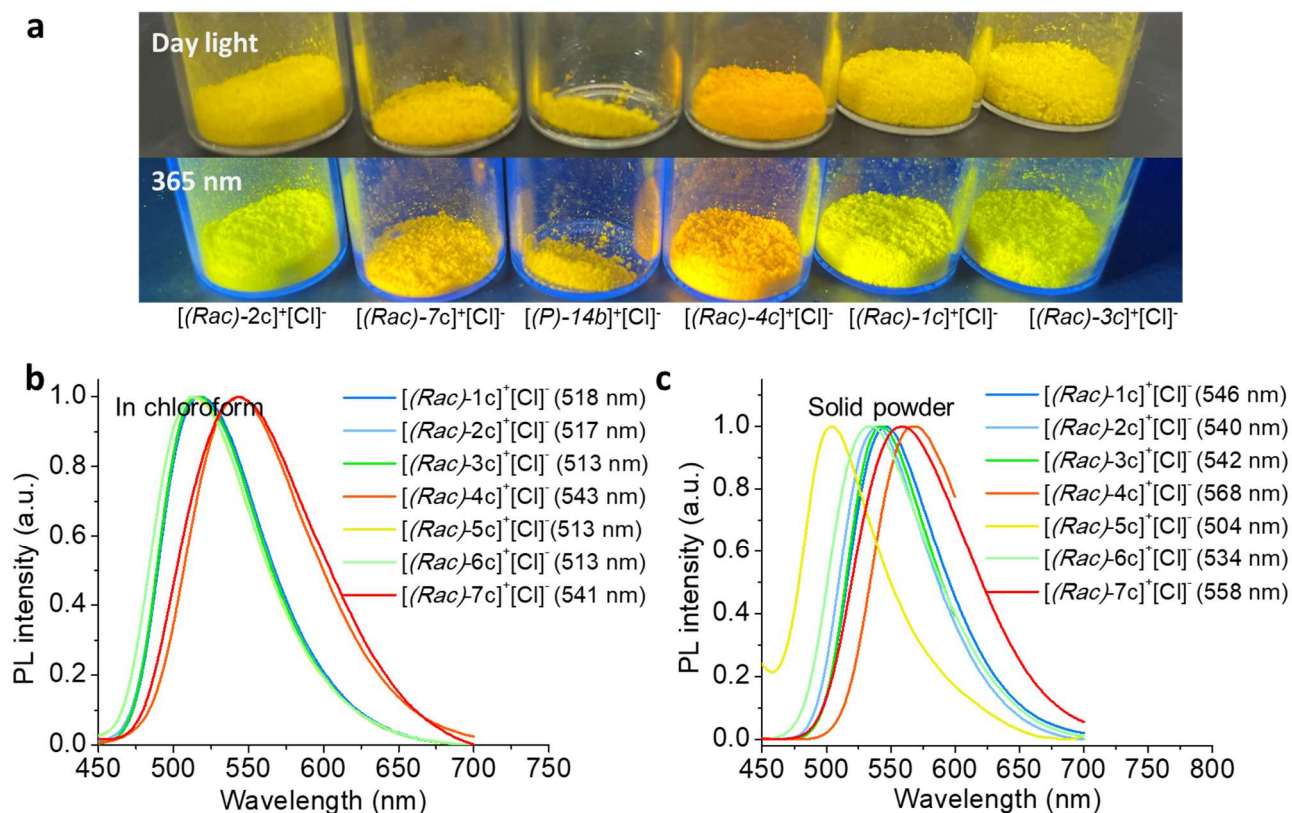


Fig. S43 (a) Photographs of cationic P(III)-helicenes in the solid powder state under day-light and UV-light ($\lambda_{\text{ex}}=365$ nm). (b) Normalized photoluminescence spectra for 5,5'-substituted and 7,7'-substituted P(III)-helicenes in chloroform (1×10^{-4} M) and (c) In the solid amorphous state at room temperature.

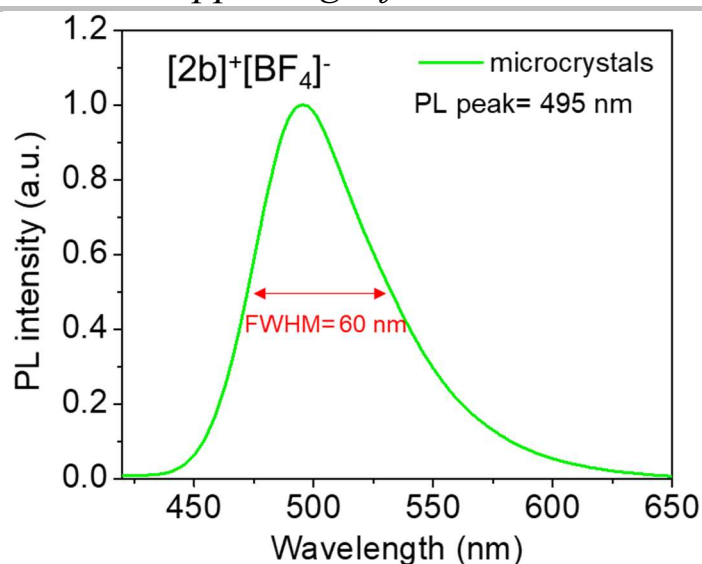


Fig. S44 Normalized photoluminescence spectra for microcrystalline sample of $[2b]^+ [BF_4]^-$.

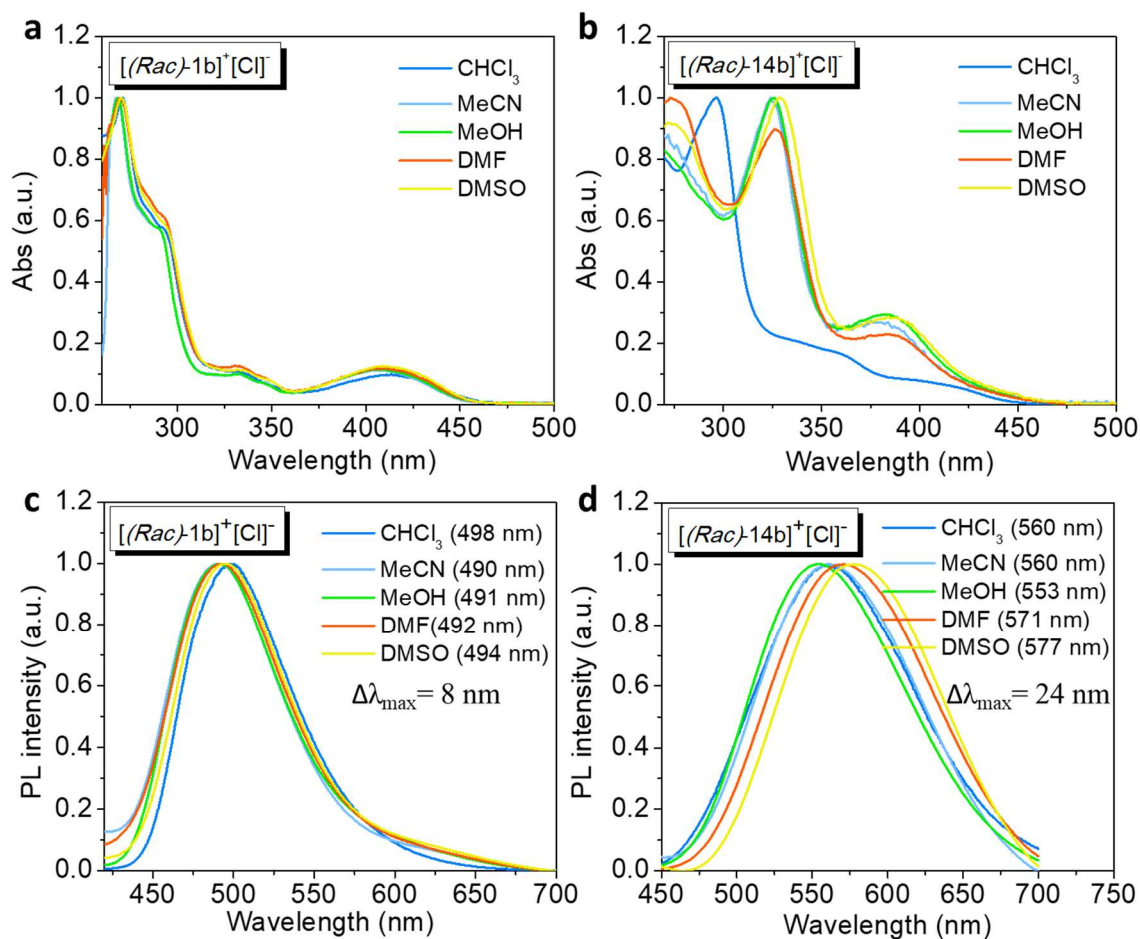


Fig. S45 (a-b) Normalized UV-vis spectra for $[1b]^+ [Cl]^-$ and $[14b]^+ [Cl]^-$ in different solutions (1×10^{-4} M). (c-d) Normalized photoluminescence spectra for $[1b]^+ [Cl]^-$ and $[14b]^+ [Cl]^-$ in different solvents (1×10^{-4} M).

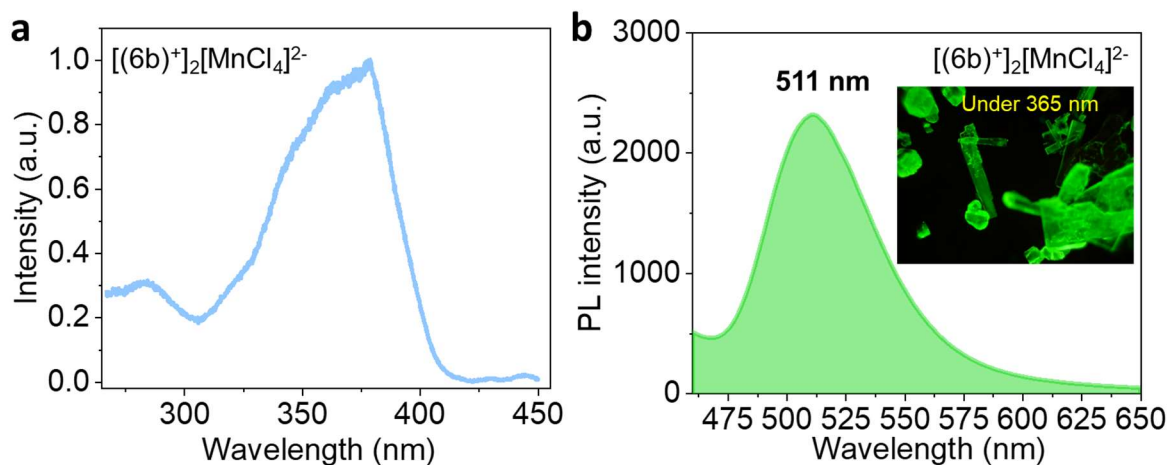


Fig. S46 (a) Excitation spectra and (b) photoluminescence spectra for hybrid $[(6b)^+]_2[MnCl_4]^{2-}$ crystals ($\lambda_{ex}=360$ nm).

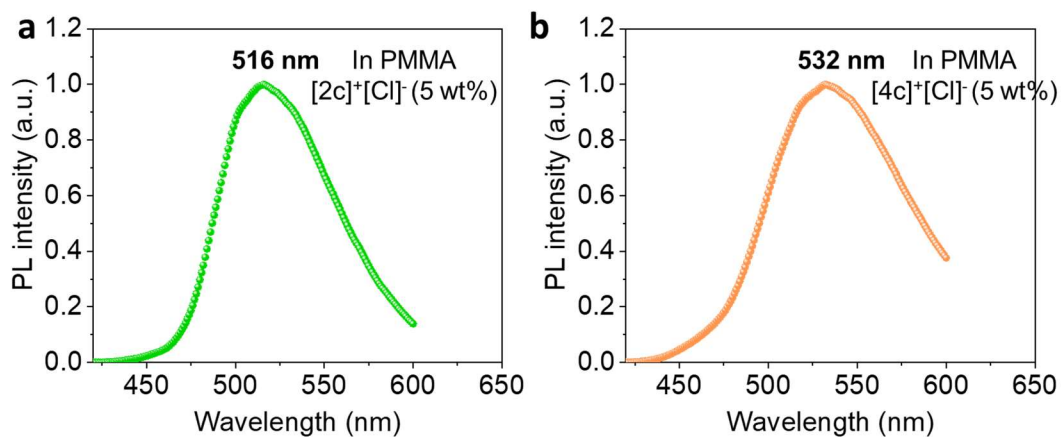


Fig. S47 Photoluminescence spectra of $[2c]^+[Cl]^-$ and $[4c]^+[Cl]^-$ in PMMA matrices ($\lambda_{ex}=360$ nm).

Section H: CD, CPL spectra data, and LCs self-assembly

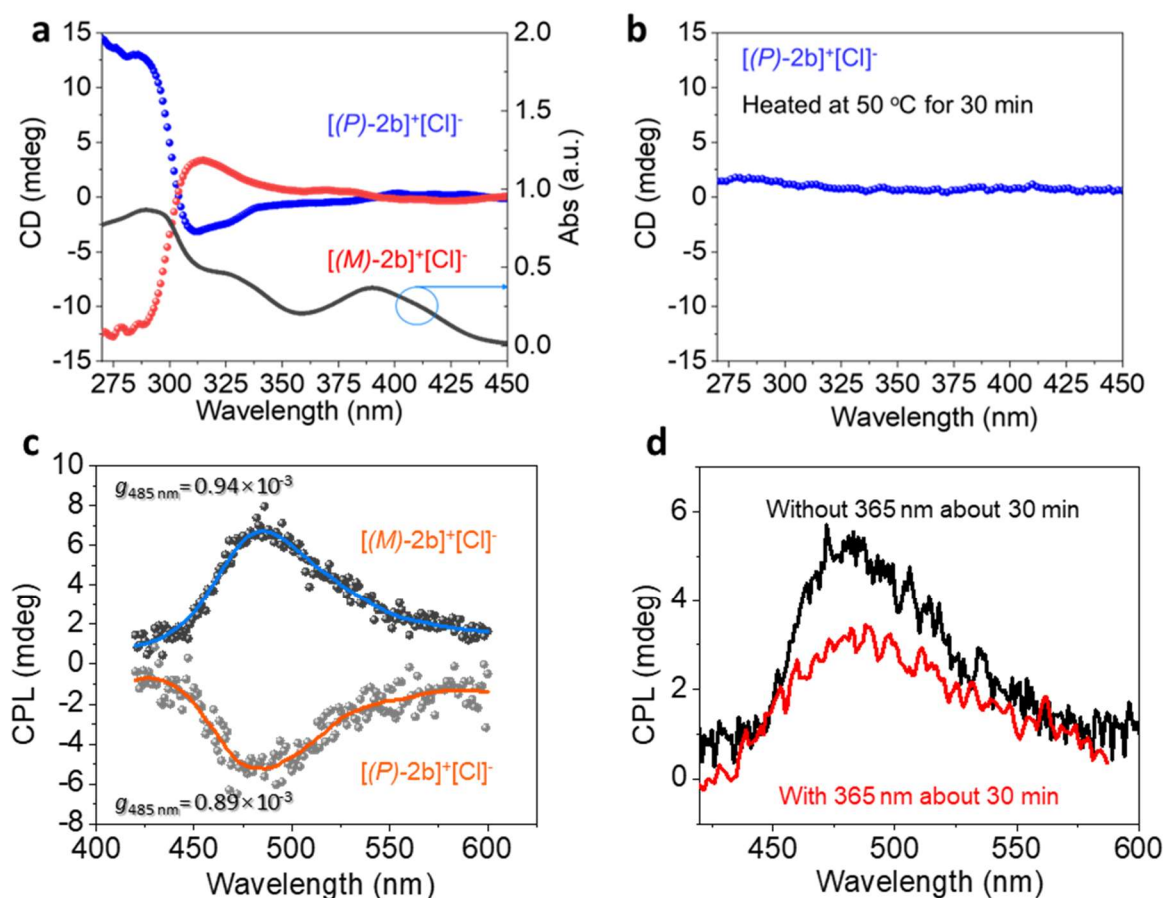


Fig. S48 (a) CD spectra of phospho[5]helicenes $[2b]^+[Cl]^-$ in CH_3OH at $-15\text{ }^\circ C$. (b) CD spectra of $[(P)-2b]^+[Cl]^-$ after heating in an EtOH/DCM (1:5) solution at $50\text{ }^\circ C$. (c) CPL spectra of phospho[5]helicene $[2b]^+[Cl]^-$ in DCM solution at $-15\text{ }^\circ C$. (d) CPL spectra of $[2b]^+[Cl]^-$ in DCM solution at $-15\text{ }^\circ C$ with/without 365 nm radiation (the CPL spectra were recorded after 30 min).

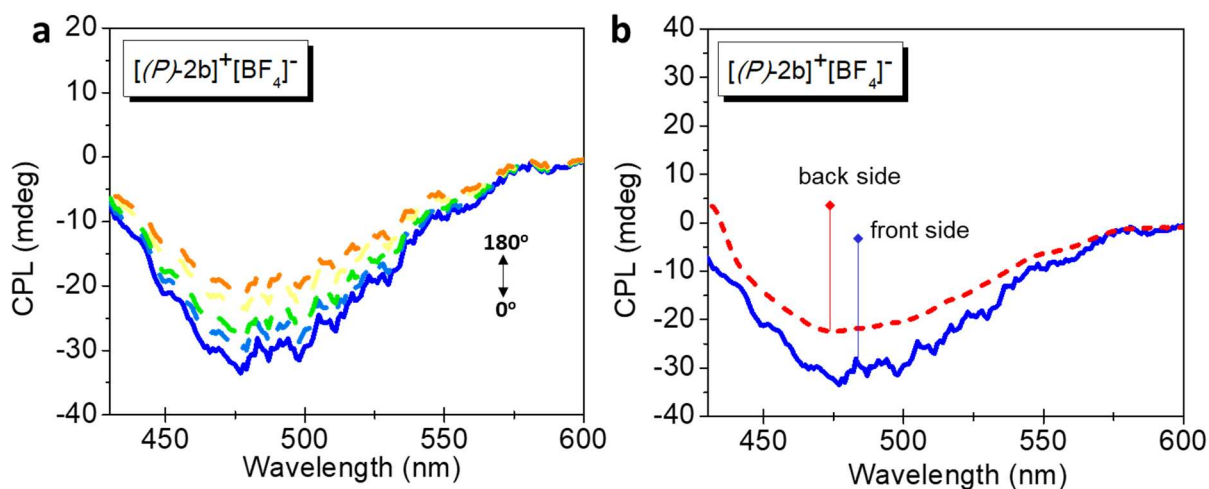


Fig. S49 Angel-dependent CPL spectra of phospho[5]helicene $[(P)-2b]^+[BF_4]^-$ in the microcrystalline state.

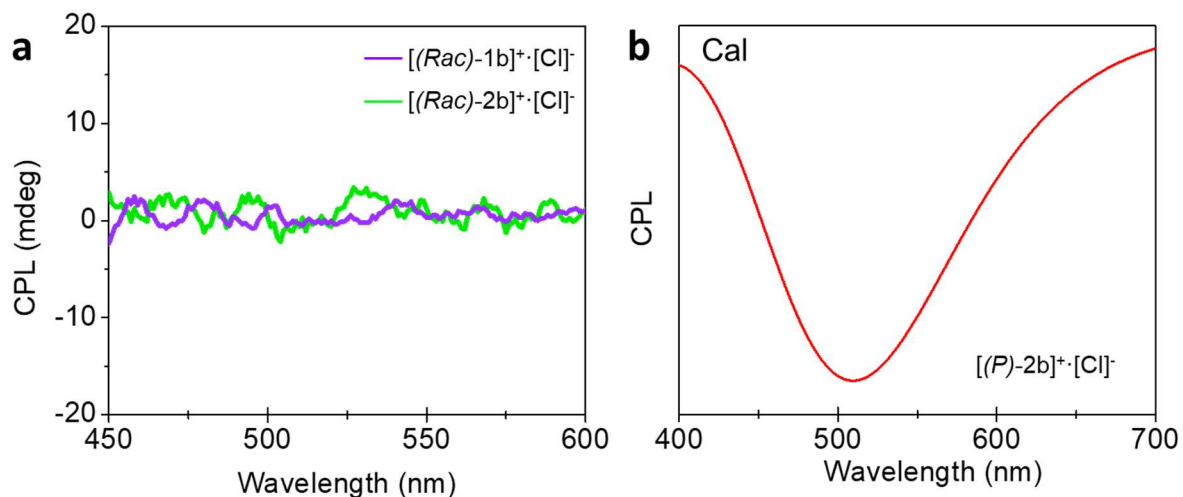


Fig. S50 (a) CPL spectra of racemic phosphahelicenes $[2b]^+[Cl]^-$ in the amorphous state (excited at 360 nm). (b) TD-DFT calculated CPL signal (negative signal) of $[(P)-2b]^+$, which is consistent with the experiment result (broadening level: 0.67 eV for FWHM).

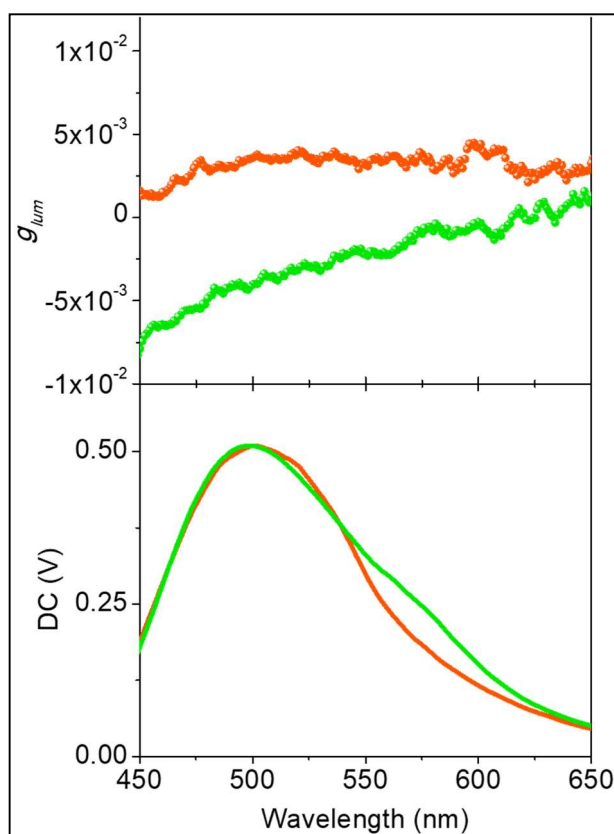


Fig. S51 CPL asymmetry factor of enantiomerically enriched phosphahelicenes $[2b]^+[BF_4]^-$ in the microcrystalline state (excited at 360 nm) and wavelength-related DC variation of CPL.

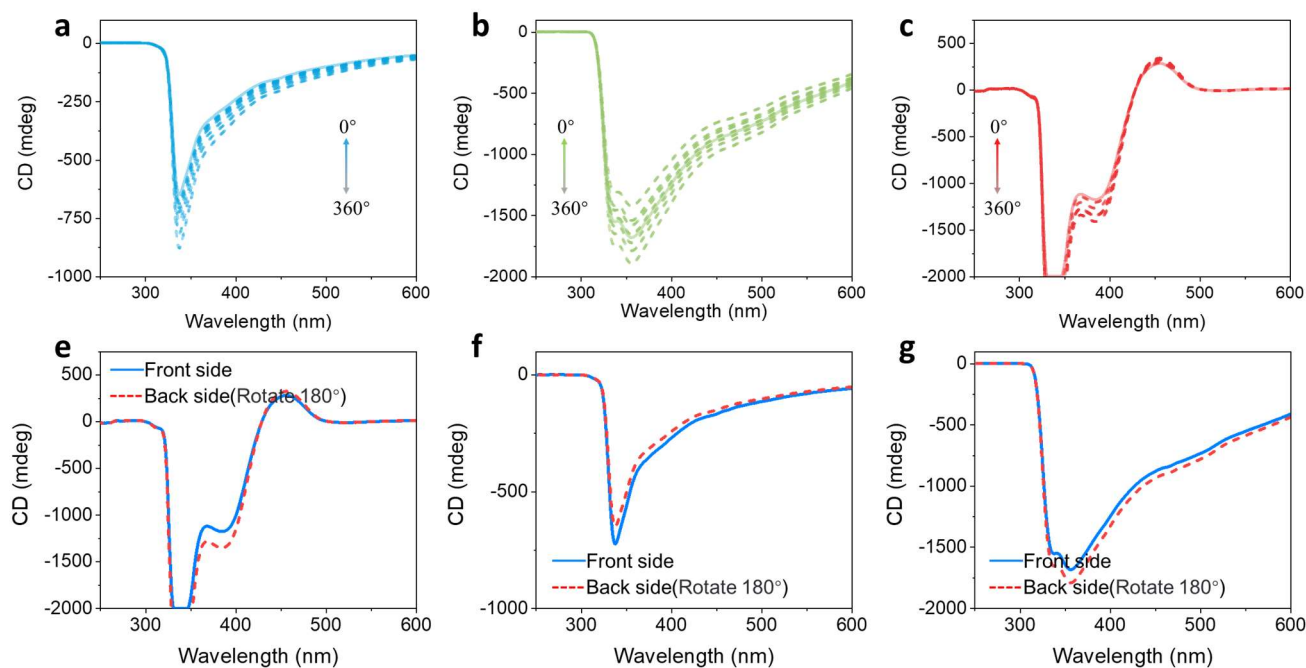


Fig. S52 Angle-dependent CD spectra of ternary cholesteric LCs films at 25 °C. (a) 4 wt% for (*S*)-guest-B and 2 wt% [(*Rac*)-5b]⁺[Cl]⁻, (b) 4 wt% for (*S*)-guest-B and 2 wt% [(*Rac*)-2c]⁺[Cl]⁻, (c) 4 wt% for (*S*)-guest-B and 2 wt% [(*Rac*)-4c]⁺[Cl]⁻.

Supporting information

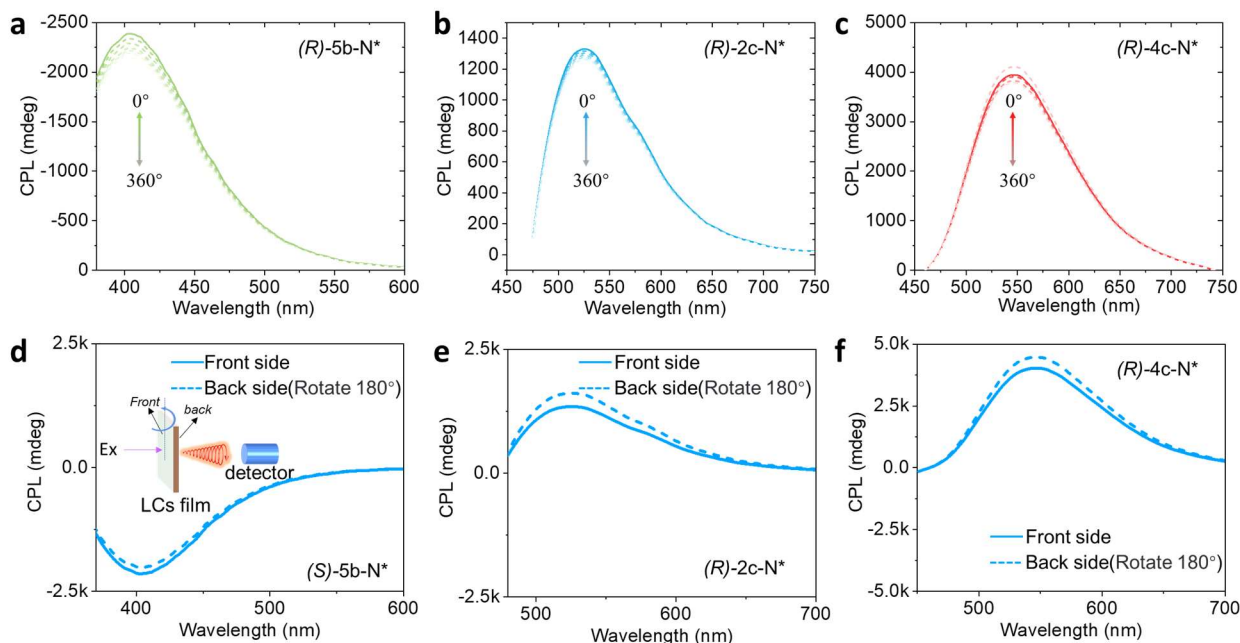


Fig. S53 Angle-dependent CPL spectra of ternary cholesteric LCs at 25 °C. (a) 4 wt% for (*S*)-guest-B and 2 wt% [(*Rac*)-5b]⁺[Cl]⁻, (b) 4 wt% for (*S*)-guest-B and 2 wt% [(*Rac*)-2c]⁺[Cl]⁻, (c) 4 wt% for (*S*)-guest-B and 2 wt% [(*Rac*)-4c]⁺[Cl]⁻.

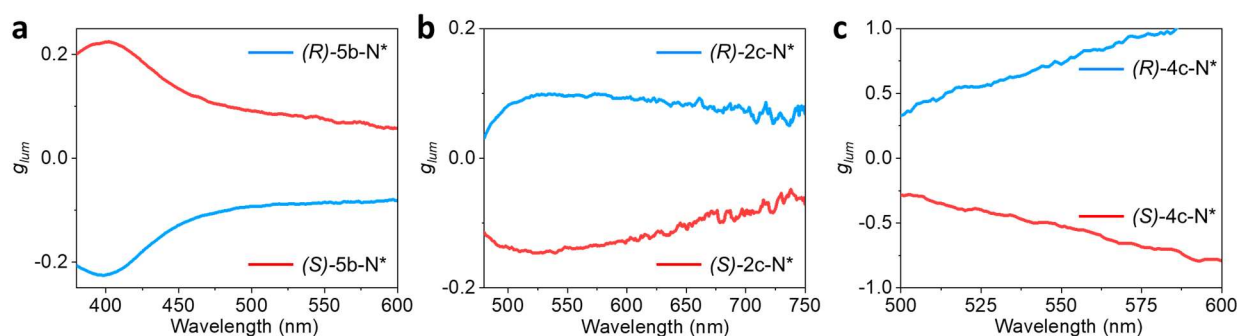


Fig. S54 Corresponding asymmetry factor for CPL of ternary cholesteric LCs at 25 °C. (a) 4 wt% for (*S*)-guest-B and 2 wt% [(*Rac*)-5b]⁺[Cl]⁻, (b) 4 wt% for (*S*)-guest-B and 2 wt% [(*Rac*)-2c]⁺[Cl]⁻, (c) 4 wt% for (*S*)-guest-B and 2 wt% [(*Rac*)-4c]⁺[Cl]⁻.

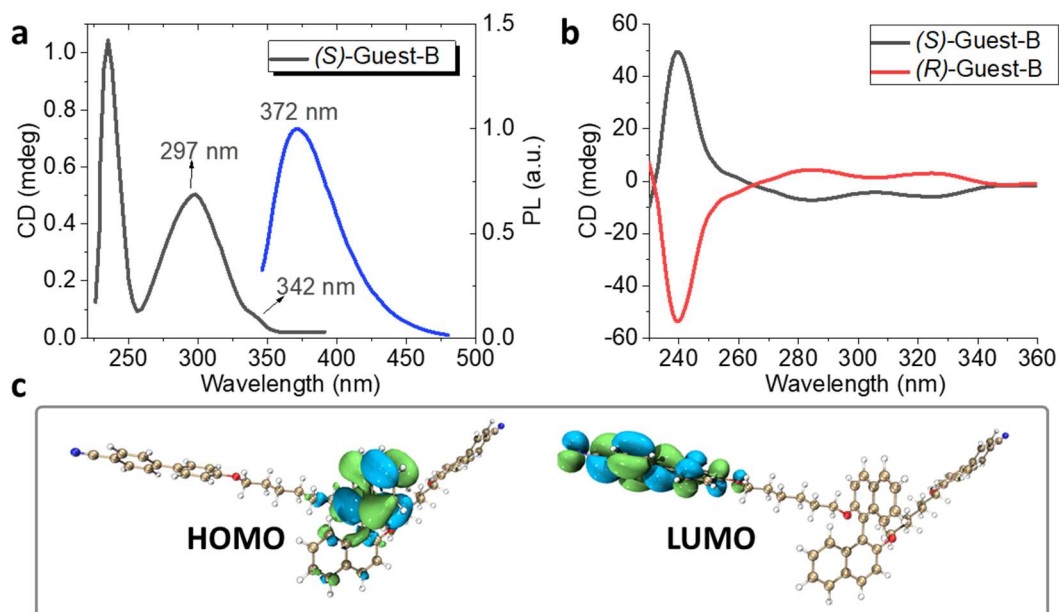


Fig. S55 (a) Experimental UV-vis and PL spectra for (S)-Guest-B in dichloromethane (1×10^{-5} M). (b) CD spectra of (S)/(R)-Guest-B in dichloromethane (1×10^{-5} M).

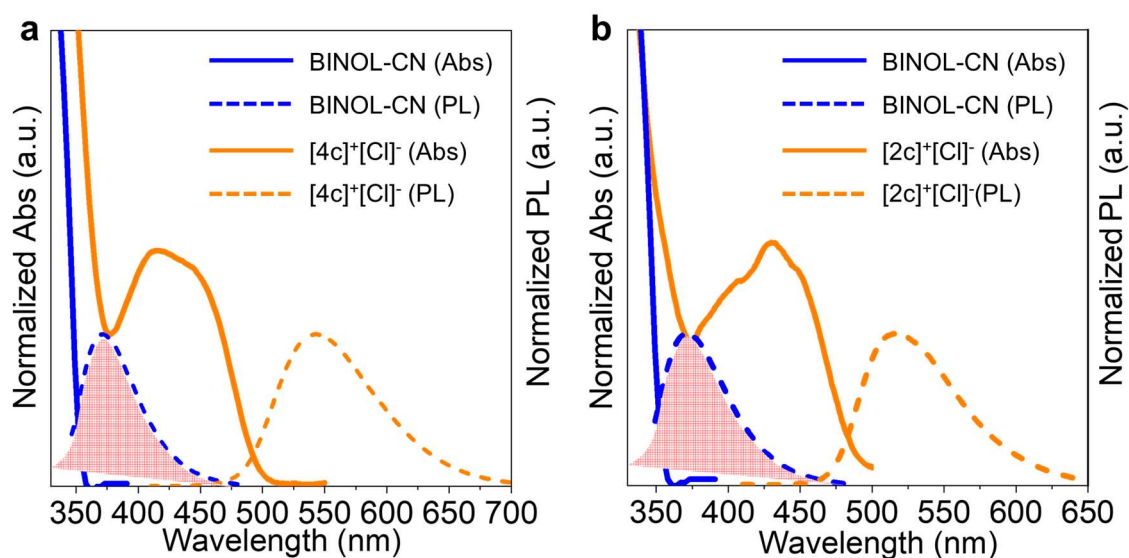


Fig. S56 The comparison of UV-vis and PL spectra for phoshahelicenes and BINOL-CN in dichloromethane (1×10^{-5} M).

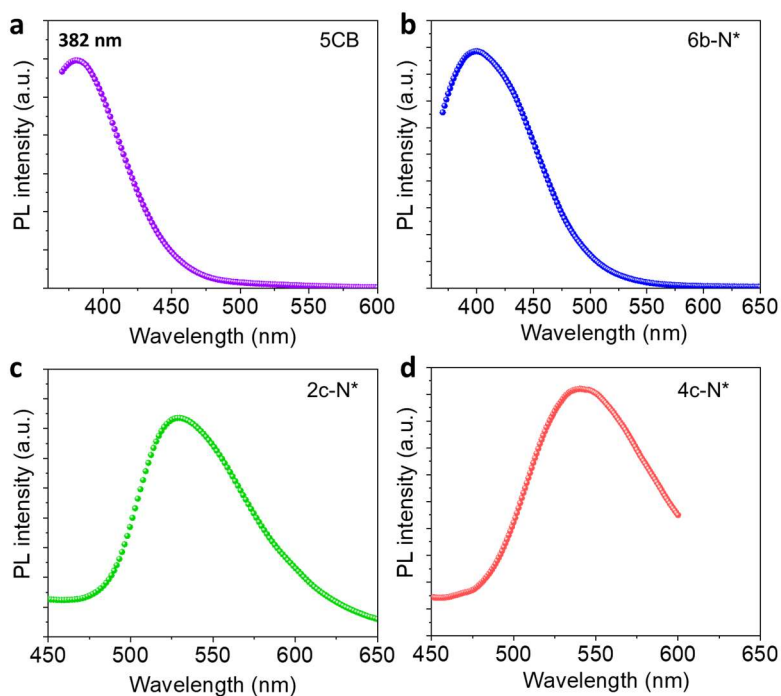


Fig. S57 (a) PL spectra of 5-CB in LCs state at room temperature ($\lambda_{\text{ex}}=350$ nm). (b-d) PL spectra of ternary N*-LCs films at room temperature ($\lambda_{\text{ex}}=350$ nm, 4 wt% for (*S*)-BINOL-CN and 2 wt% phosphahelicenes).

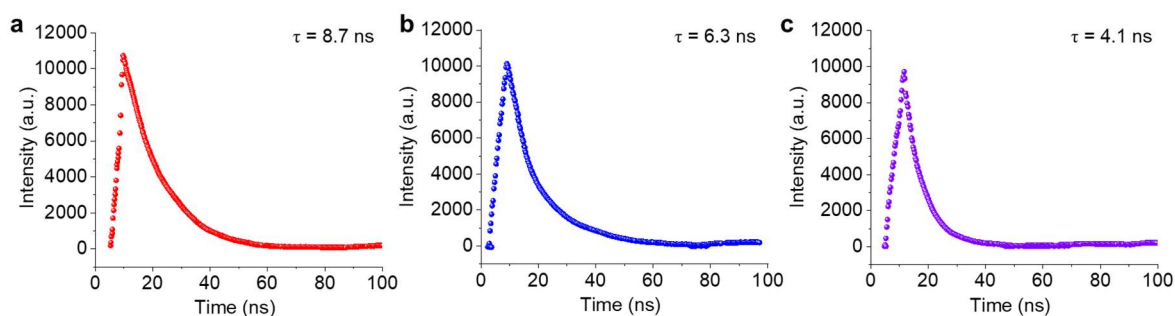


Fig. S58 Fluorescence decay for ternary N*-LCs films at room temperature (BINOL-CN/2 wt% and phosphahelicene/0.1 wt%).

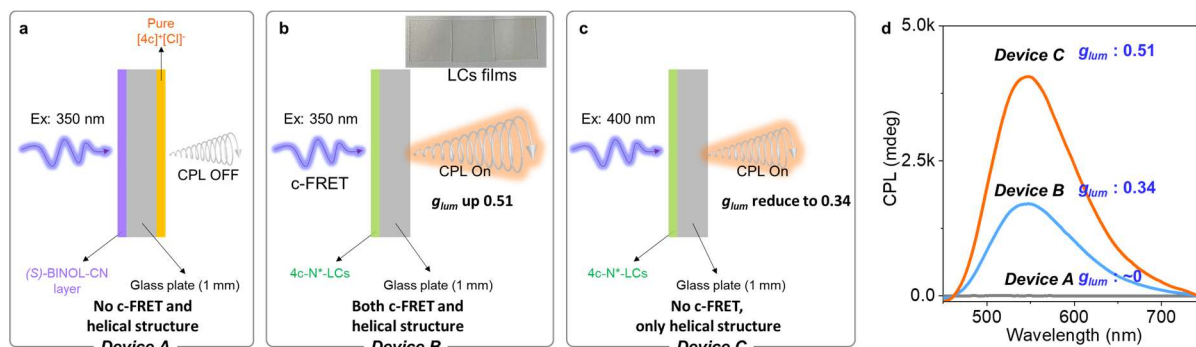


Fig. S59 Schematic of ternary N*-LCs devices for CPL measurement and corresponding CPL spectra (BINOL-CN/4 wt% and phosphahelicene/2 wt%).

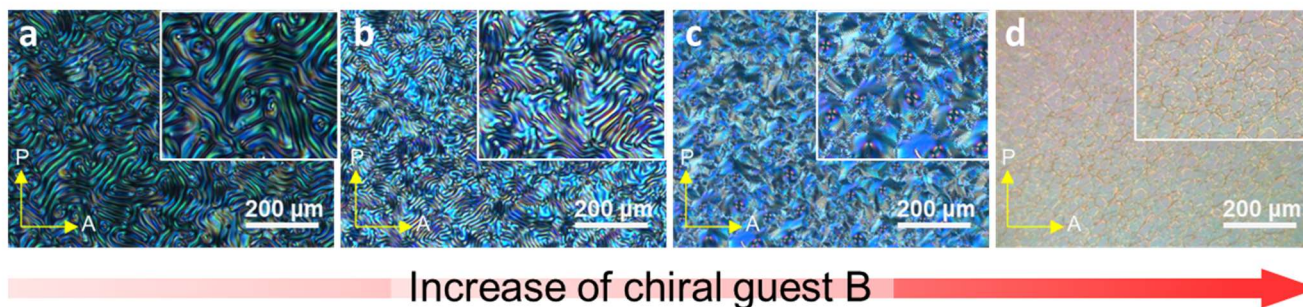


Fig. S60 POM texture of ternary cholesteric LCs at 25 °C on cooling from the isotropic phase doped with different amounts of (*S*)-BINOL-CN and 2 wt% [5b]⁺[Cl]⁻ (a) 0.5 wt% for (*S*)-BINOL-CN, (b) 1 wt%, (c), 2 wt% (d) 4 wt%.

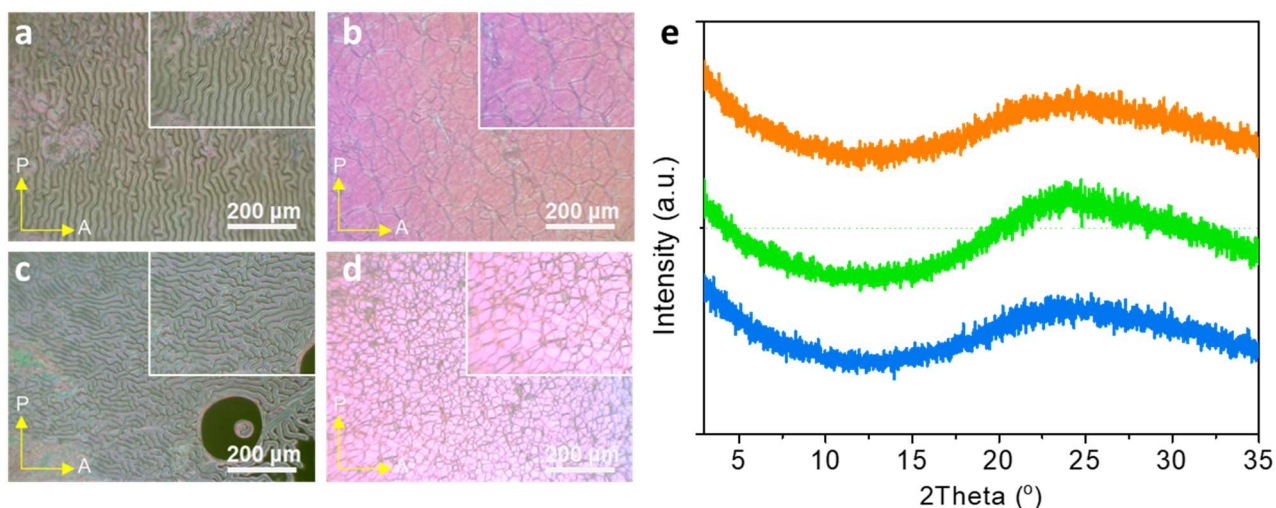
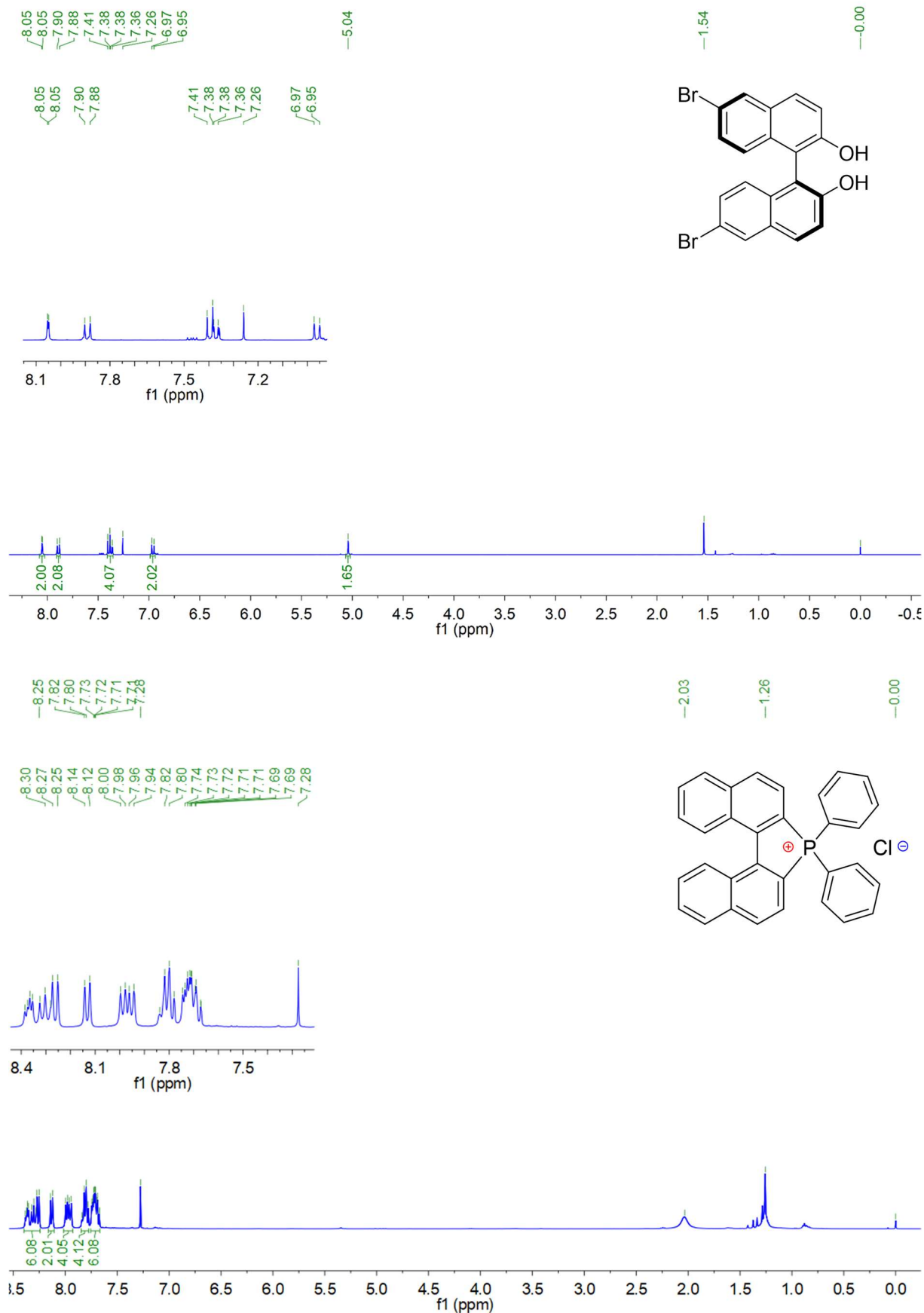


Fig. S61 POM textures of ternary cholesteric LCs films at 25 °C on cooling from the isotropic phase (doped with different amounts of (*S*)-Guest B and 2 wt% [X]⁺[Cl]⁻). (a) 0.5 wt% for (*S*)-BINOL-CN and [2c]⁺[Cl]⁻, (b) 4 wt% for (*S*)-BINOL-CN and [2c]⁺[Cl]⁻, (c) 0.5 wt% for (*S*)-BINOL-CN and [4c]⁺[Cl]⁻ (d) 4 wt% for (*S*)-BINOL-CN and [4c]⁺[Cl]⁻. (e) XRD patterns of ternary cholesteric LCs at 25 °C (blue line: 4 wt% for (*S*)-BINOL-CN and 2 wt% [5b]⁺[Cl]⁻, green line: 4 wt% for (*S*)-BINOL-CN and 2 wt% [2c]⁺[Cl]⁻, orange line: 4 wt% for (*S*)-BINOL-CN and 2 wt% [4c]⁺[Cl]⁻).

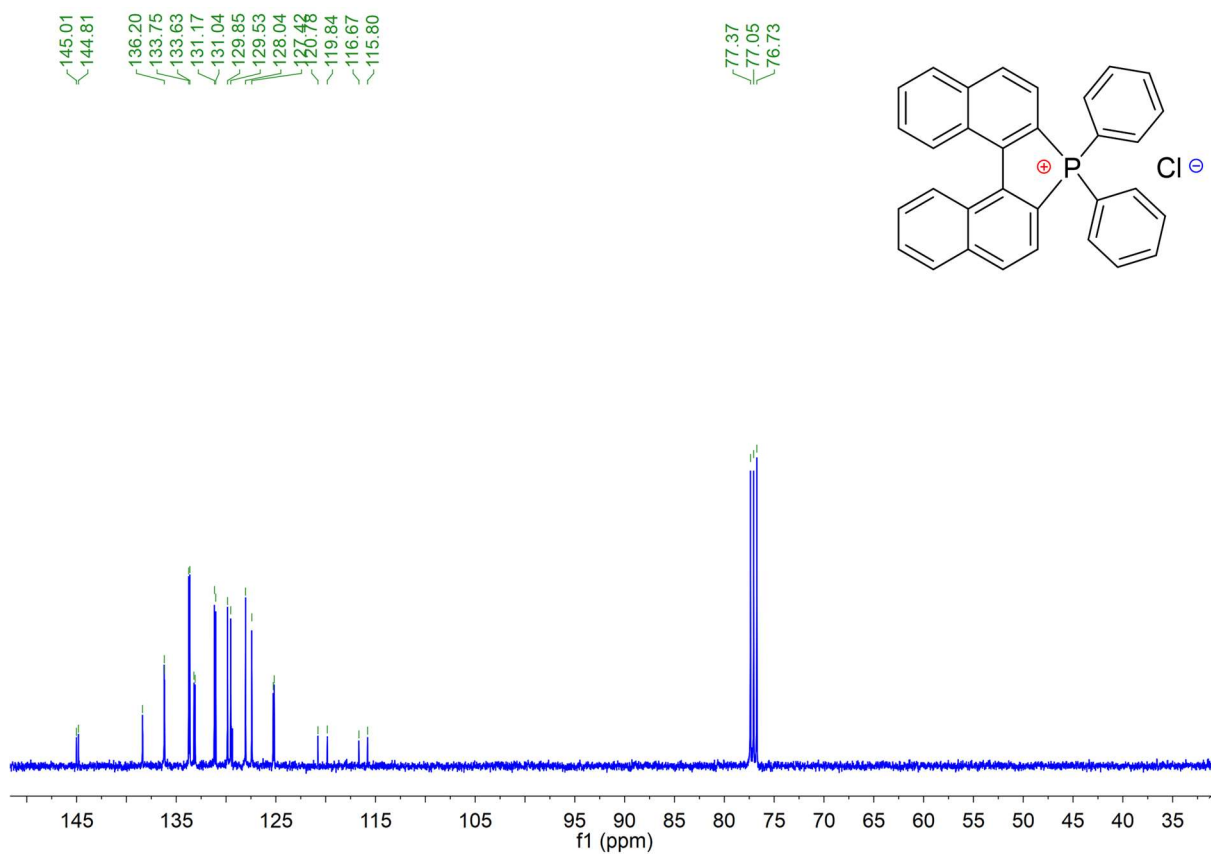
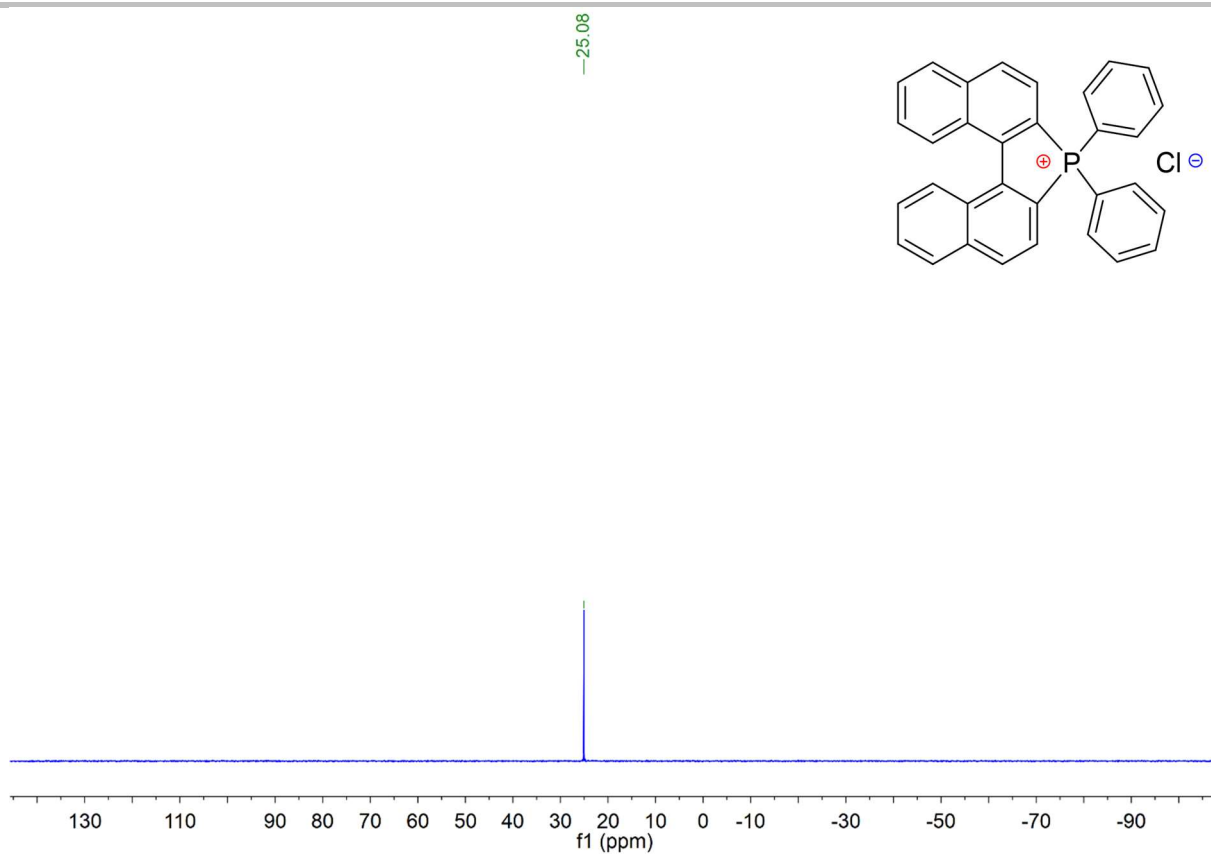
References

- 1 D. J. Ager, M. B. East, A. Eisenstadt and S. A. Laneman, *Chem. Commun.*, 1997, 2359–2360.
- 2 Y. Nojima, M. Hasegawa, N. Hara, Y. Imai and Y. Mazaki, *Chem. Commun.*, 2019, **55**, 2749–2752.
- 3 J. Bunzen, T. Bruhn, G. Bringmann and A. Lützen, *J. Am. Chem. Soc.*, 2009, **131**, 3621–3630.
- 4 M. Berthod, G. Mignani, G. Woodward and M. Lemaire, *Chem. Rev.*, 2005, **105**, 1801–1836.
- 5 M. Liu, L. Zhang and T. Wang, *Chem. Rev.*, 2015, **115**, 7304–7397.
- 6 S. Gladiali, A. Dore, D. Fabbri, O. de Lucchi and G. Valle, *J. Org. Chem.*, 1994, **59**, 6363–6371.
- 7 K. Nakano, H. Oyama, Y. Nishimura, S. Nakasako and K. Nozaki, *Angew. Chem.*, 2012, **124**, 719–723.
- 8 H. Deng, M. Wang, Y. Liang, X. Chen, T. Wang, J. J. Wong, Y. Zhao, K. N. Houk and Z. Shi, *Chem*, 2022, **8**, 569–579.
- 9 T. Beránek, M. Jakubec, J. Sýkora, I. Císařová, J. Žádný and J. Storch, *Org. Lett.*, 2022, **24**, 4756–4761.
- 10 K. Yavari, S. Moussa, B. Ben Hassine, P. Retailleau, A. Voituriez and A. Marinetti, *Angew. Chem. Int. Ed.*, 2012, **51**, 6748–6752.
- 11 Y. Sawada, S. Furumi, A. Takai, M. Takeuchi, K. Noguchi and K. Tanaka, *J. Am. Chem. Soc.*, 2012, **134**, 4080–4083.
- 12 N. Fukawa, T. Osaka, K. Noguchi and K. Tanaka, *Org. Lett.*, 2010, **12**, 1324–1327.
- 13 R. Mokrai, A. Mocanu, M. P. Duffy, T. Vives, E. Caytan, V. Dorcet, T. Roisnel, L. Nyulászi, Z. Benkő, P.-A. Bouit and M. Hissler, *Chem. Commun.*, 2021, **57**, 7256–7259.
- 14 K. Usui, N. Narita, R. Eto, S. Suzuki, A. Yokoo, K. Yamamoto, K. Igawa, N. Iizuka, Y. Mimura, T. Umeno, S. Matsumoto, M. Hasegawa, K. Tomooka, Y. Imai and S. Karasawa, *Chem. – A Eur. J.*, 2022, **28**, e202202922.
- 15 P. Hindenberg, A. Belyaev, F. Rominger, I. O. Koshevoy and C. Romero-Nieto, *Org. Lett.*, 2022, **24**, 6391–6396.
- 16 M. Widhalm, C. Aichinger and K. Mereiter, *Tetrahedron Lett.*, 2009, **50**, 2425–2429.
- 17 E. Rémond, J. Fehrentz, L. Liénart, S. Clement, J. Baneres and F. Cavelier, *Chem. Eur. J.*, 2022, **28**, e202201526.
- 18 S. Nieto, P. Metola, V. M. Lynch and E. V Anslyn, *Organometallics*, 2008, **27**, 3608–3610.
- 19 H. Cheng, X. Wang, L. Chang, Y. Chen, L. Chu and Z. Zuo, *Sci. Bull.*, 2019, **64**, 1896–1901.
- 20 F. Xu, S. Crespi, G. Pacella, Y. Fu, M. C. A. Stuart, Q. Zhang, G. Portale and B. L. Feringa, *J. Am. Chem. Soc.*, 2022, **144**, 6019–6027.
- 21 P. Osswald and F. Würthner, *J. Am. Chem. Soc.*, 2007, **129**, 14319–14326.
- 22 T. Lu and F. Chen, *J. Comput. Chem.*, 2012, **33**, 580–592.
- 23 W. Humphrey, A. Dalke and K. Schulten, *J. Mol. Graph.*, 1996, **14**, 33–38.
- 24 Gaussian 16, Revision A.03, M. J. Frisch, G. W. Trucks, H. B. Schlegel, G. E. Scuseria, M. A. Robb, J. R. Cheeseman, G. Scalmani, V. Barone, G. A. Petersson, H. Nakatsuji, X. Li, M. Caricato, A. V. Marenich, J. Bloino, B. G. Janesko, R. Gomperts, B. Mennucci, H. P. Hratchian, J. V. Ortiz, A. F. Izmaylov, J. L. Sonnenberg, D. Williams-Young, F. Ding, F. Lipparini, F. Egidi, J. Goings, B. Peng, A. Petrone, T. Henderson, D. Ranasinghe, V. G. Zakrzewski, J. Gao, N. Rega, G. Zheng, W. Liang, M. Hada, M. Ehara, K. Toyota, R. Fukuda, J. Hasegawa, M. Ishida, T. Nakajima, Y. Honda, O. Kitao, H. Nakai, T. Vreven, K. Throssell, J. A. Montgomery, Jr., J. E. Peralta, F. Ogliaro, M. J. Bearpark, J. J. Heyd, E. N. Brothers, K. N. Kudin, V. N. Staroverov, T. A. Keith, R. Kobayashi, J. Normand, K. Raghavachari, A. P. Rendell, J. C. Burant, S. S. Iyengar, J. Tomasi, M. Cossi, J. M. Millam, M. Klene, C. Adamo, R. Cammi, J. W. Ochterski, R. L. Martin, K. Morokuma, O. Farkas, J. B. Foresman, and D. J. Fox, Gaussian, Inc., Wallingford CT, 2016.
- 25 A. D. Beeke, *J. Chem. Phys.*, 1993, **98**, 5646–5648.
- 26 E. R. Johnson, S. Keinan, P. Mori-Sánchez, J. Contreras-García, A. J. Cohen and W. Yang, *J. Am. Chem. Soc.*, 2010, **132**, 6498–6506.
- 27 T. Yanai, D. P. Tew and N. C. Handy, *Chem. Phys. Lett.*, 2004, **393**, 51–57.
- 28 Z. P. Yan, L. Yuan, Y. Zhang, M. X. Mao, X. J. Liao, H. X. Ni, Z. H. Wang, Z. An, Y. X. Zheng and J. L. Zuo, *Adv. Mater.*, 2022, 2204253.
- 29 É. Brémond, M. Savarese, N. Q. Su, Á. J. Pérez-Jiménez, X. Xu, J. C. Sancho-García and C. Adamo, *J. Chem. Theory Comput.*, 2016, **12**, 459–465.
- 30 D. Geuenich, K. Hess, F. Köhler and R. Herges, *Chem. Rev.*, 2005, **105**, 3758–3772.
- 31 A. Belyaev, Y.-T. Chen, Z.-Y. Liu, P. Hindenberg, C.-H. Wu, P.-T. Chou, C. Romero-Nieto and I. O. Koshevoy, *Chem. – A Eur. J.*, 2019, **25**, 6332–6341.

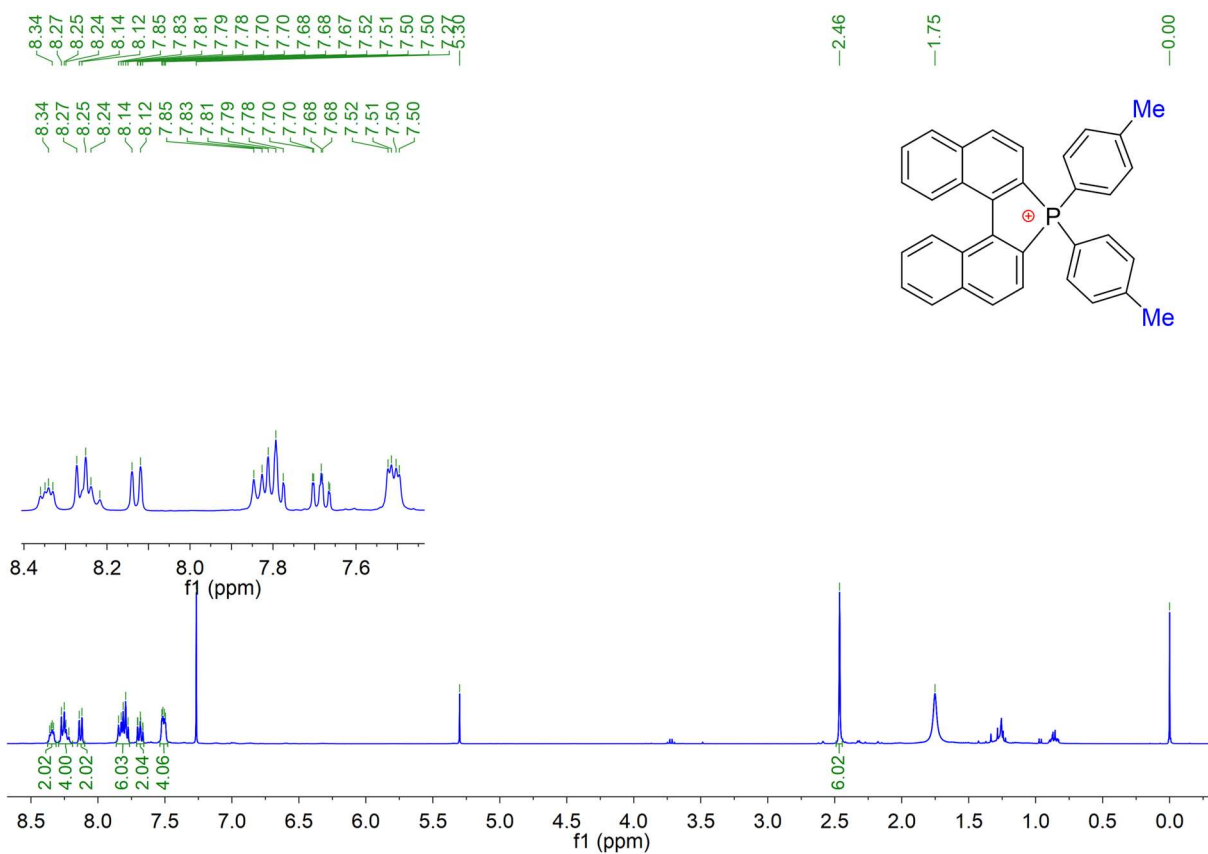
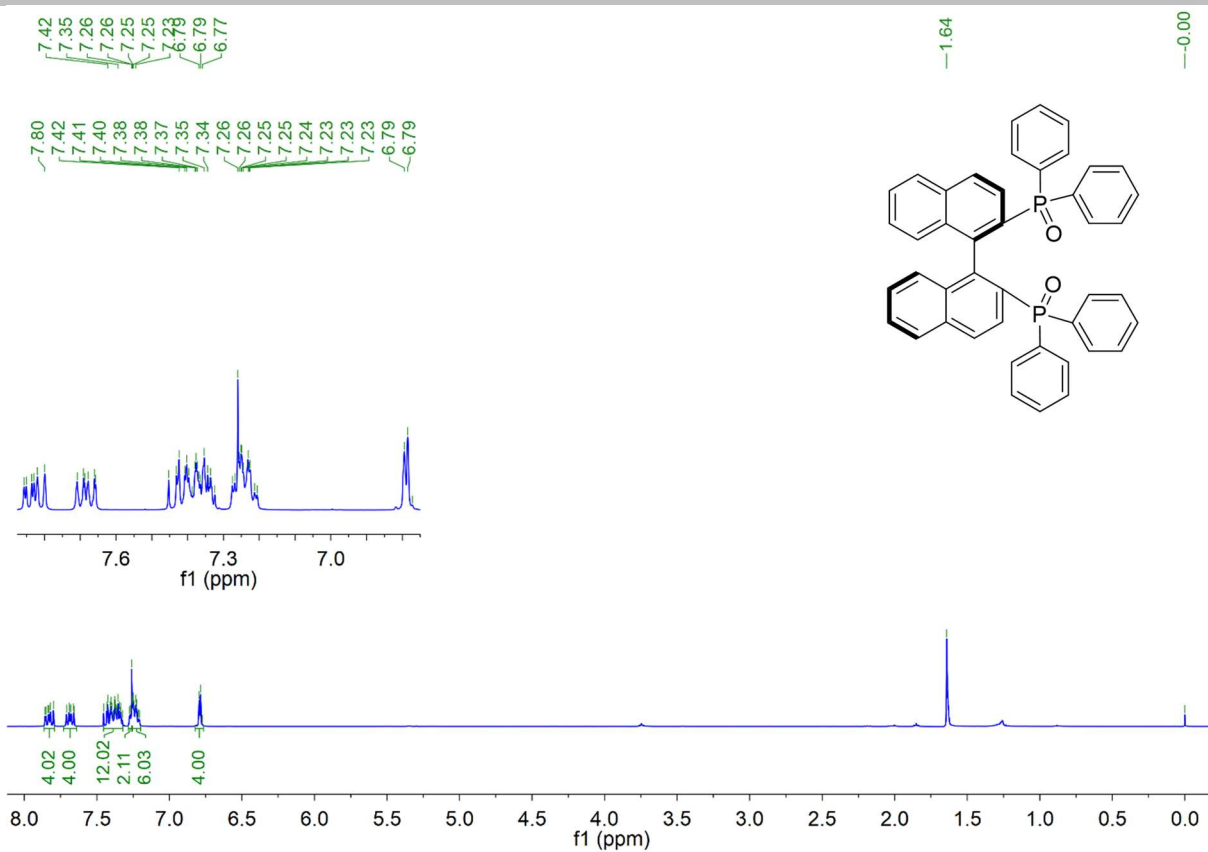
Supporting information
Section H: NMR spectra



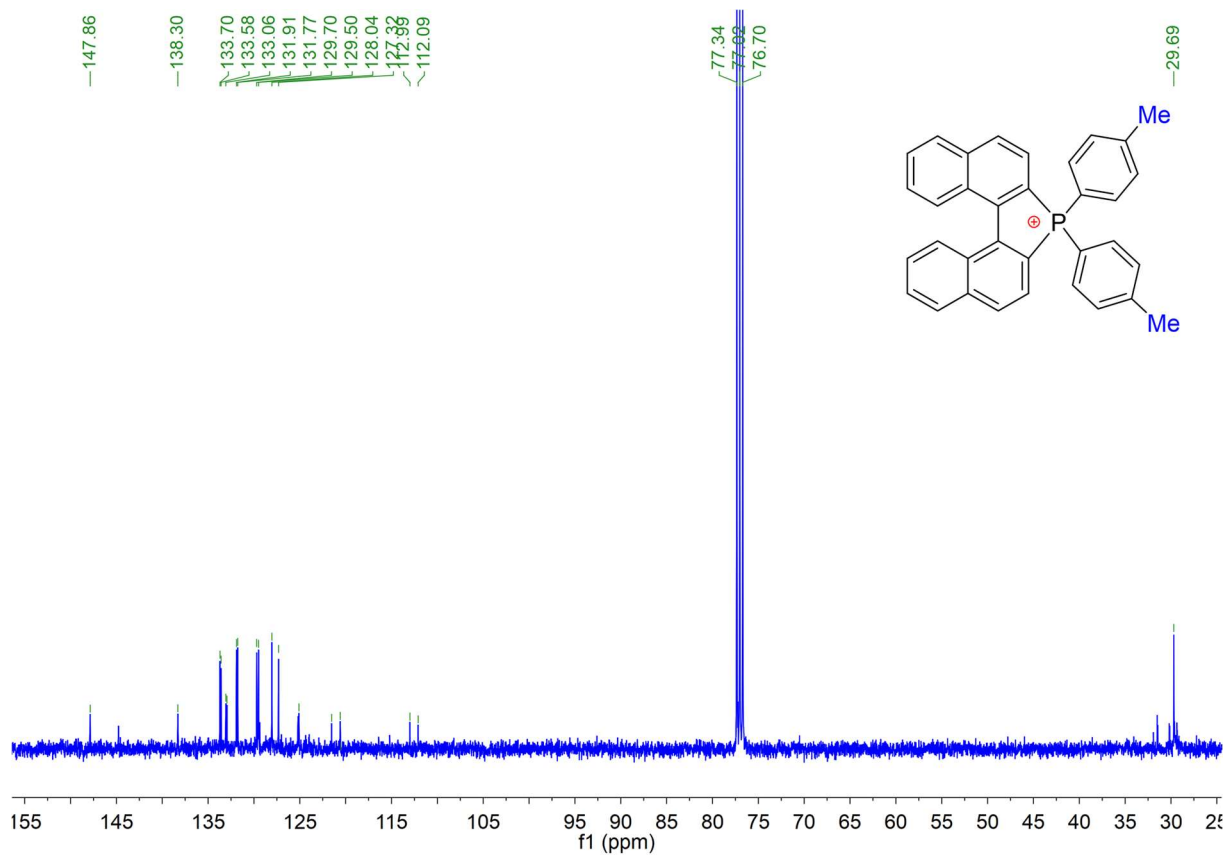
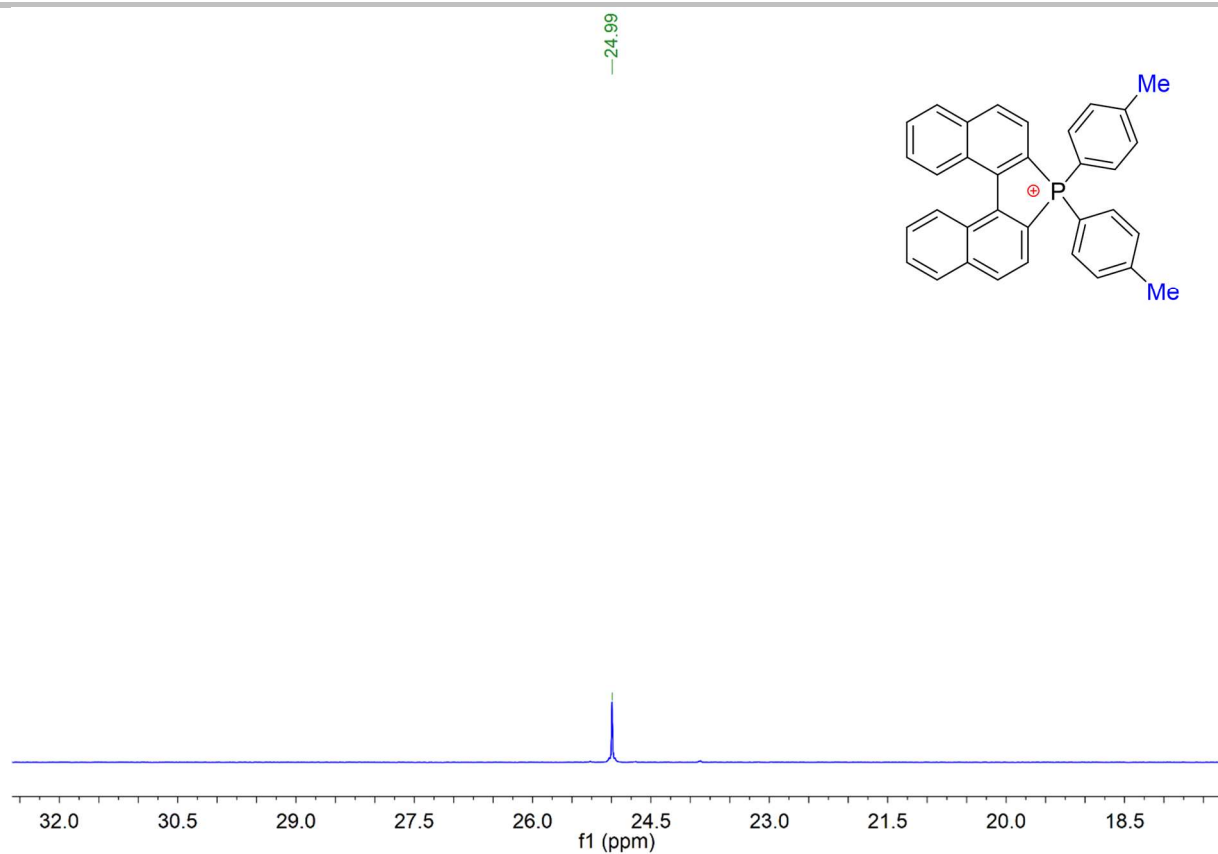
Supporting information



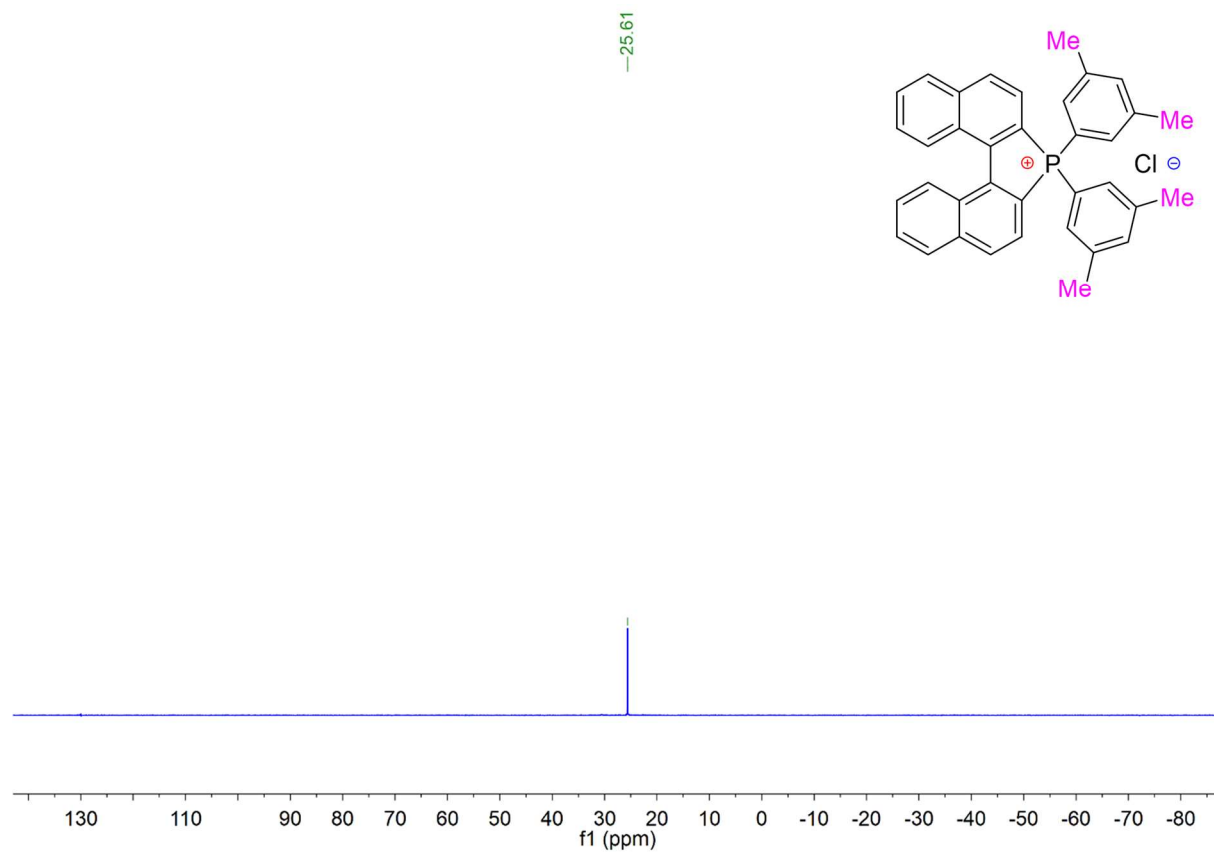
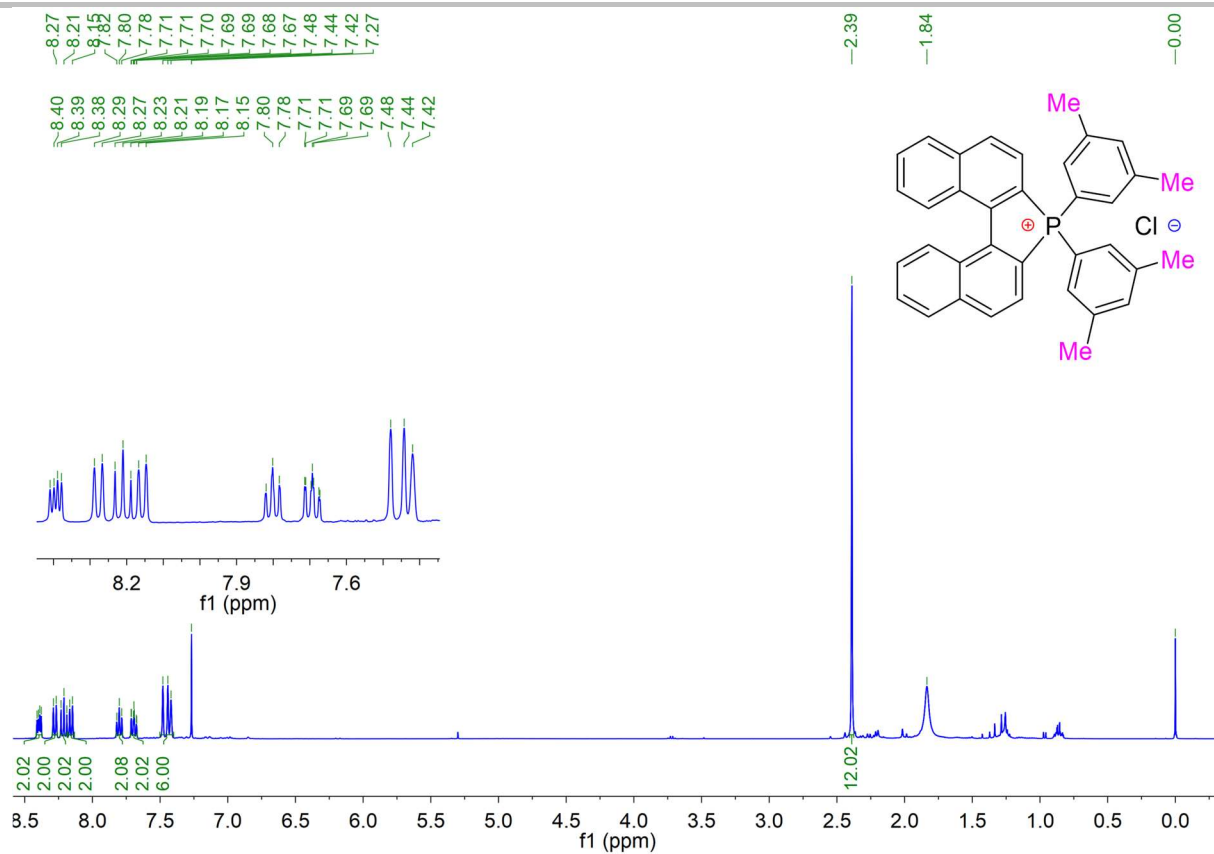
Supporting information



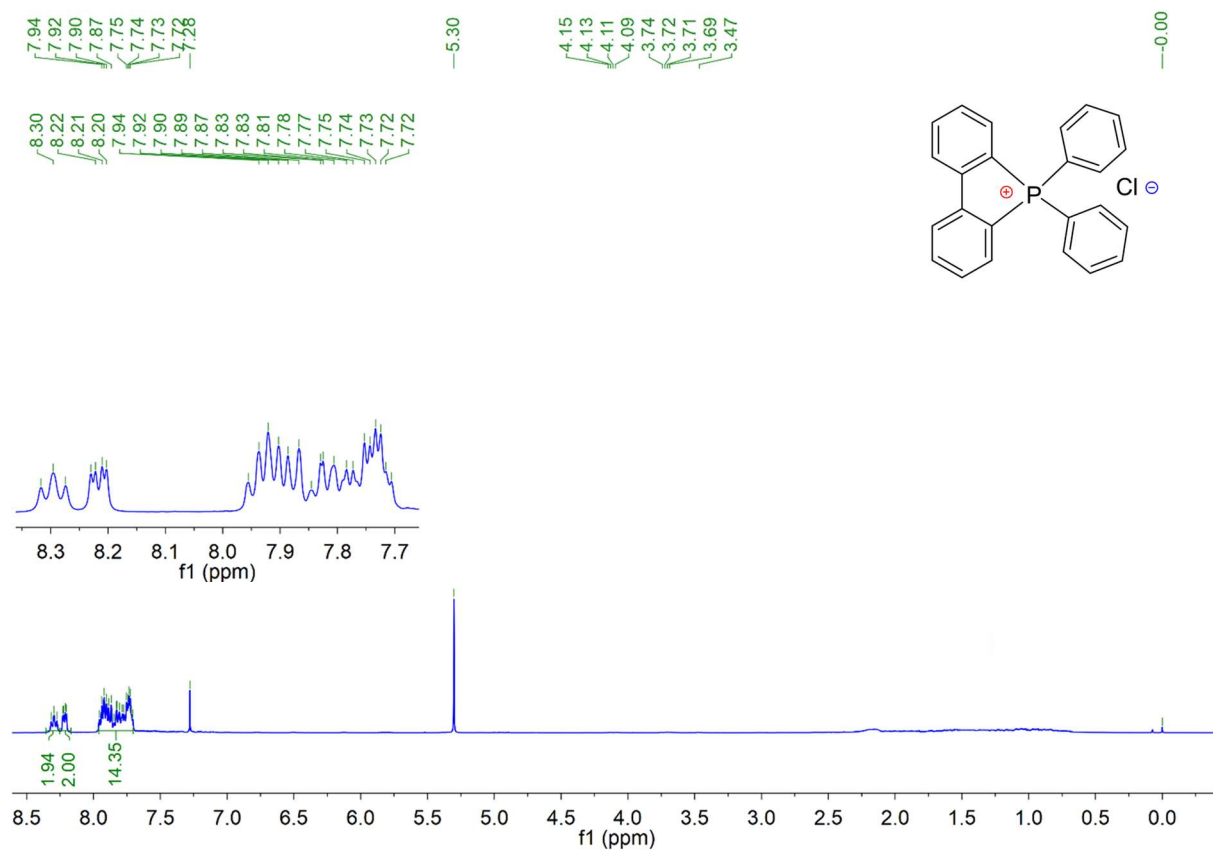
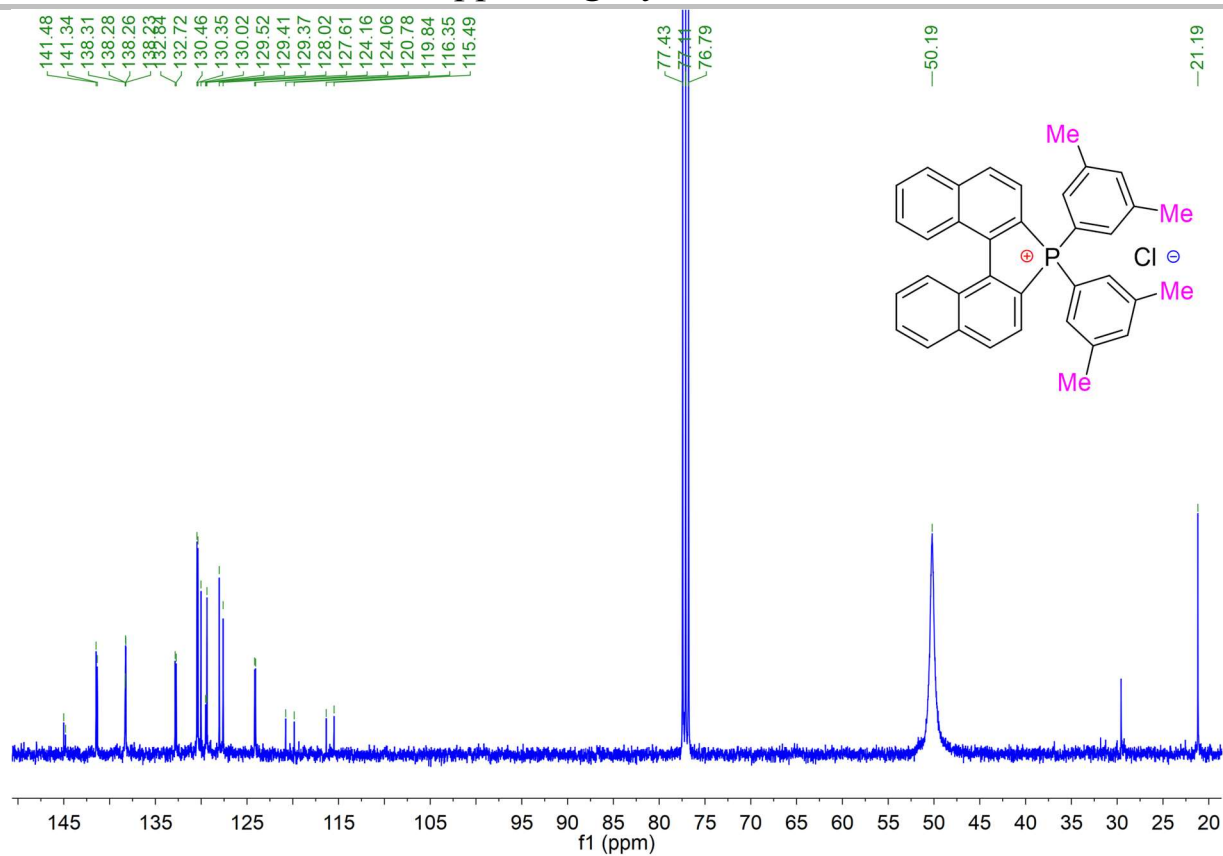
Supporting information



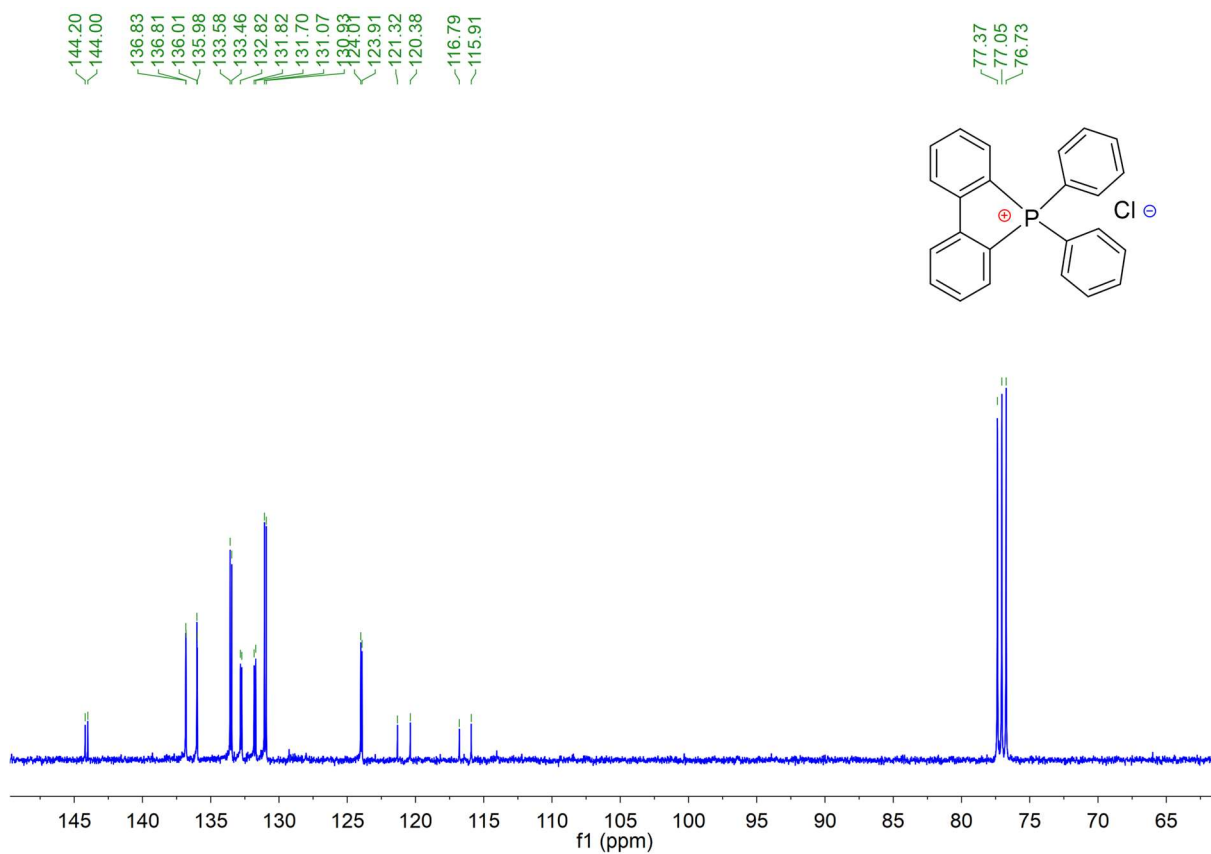
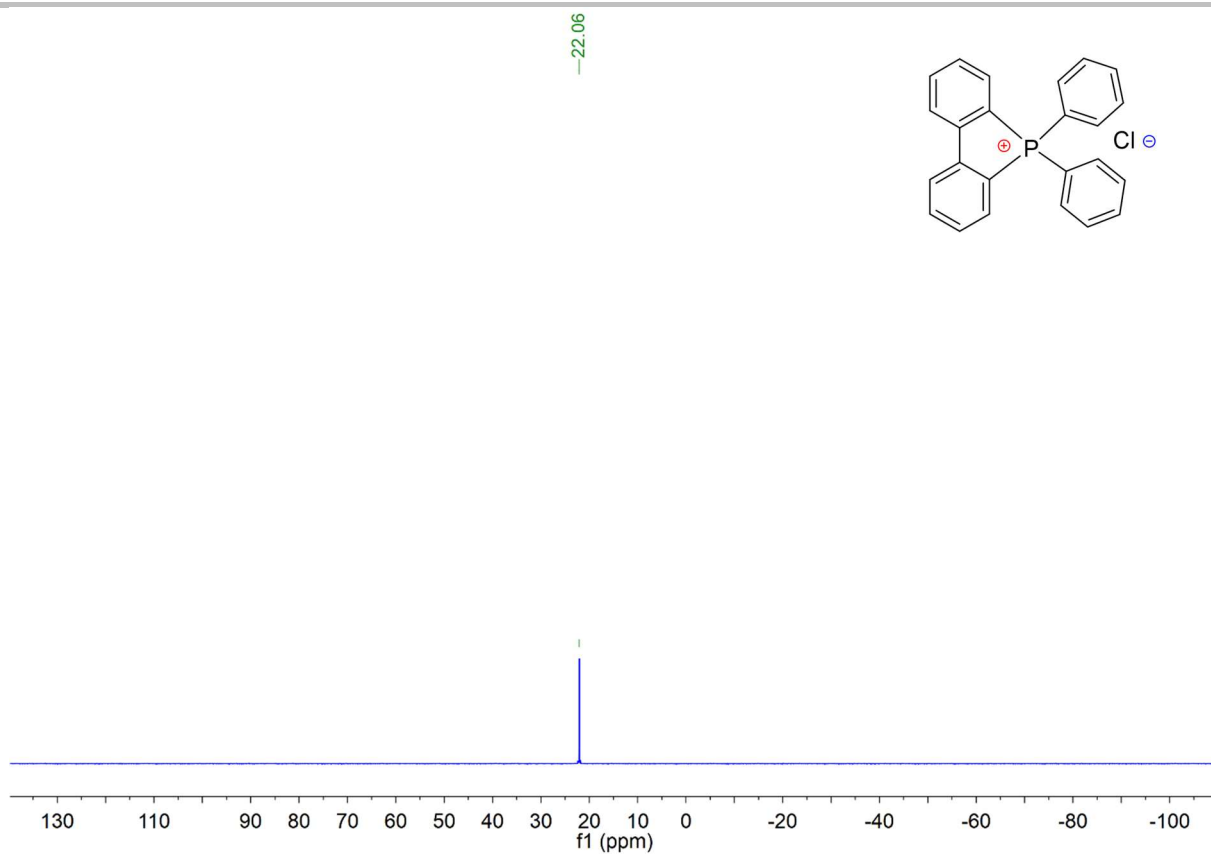
Supporting information



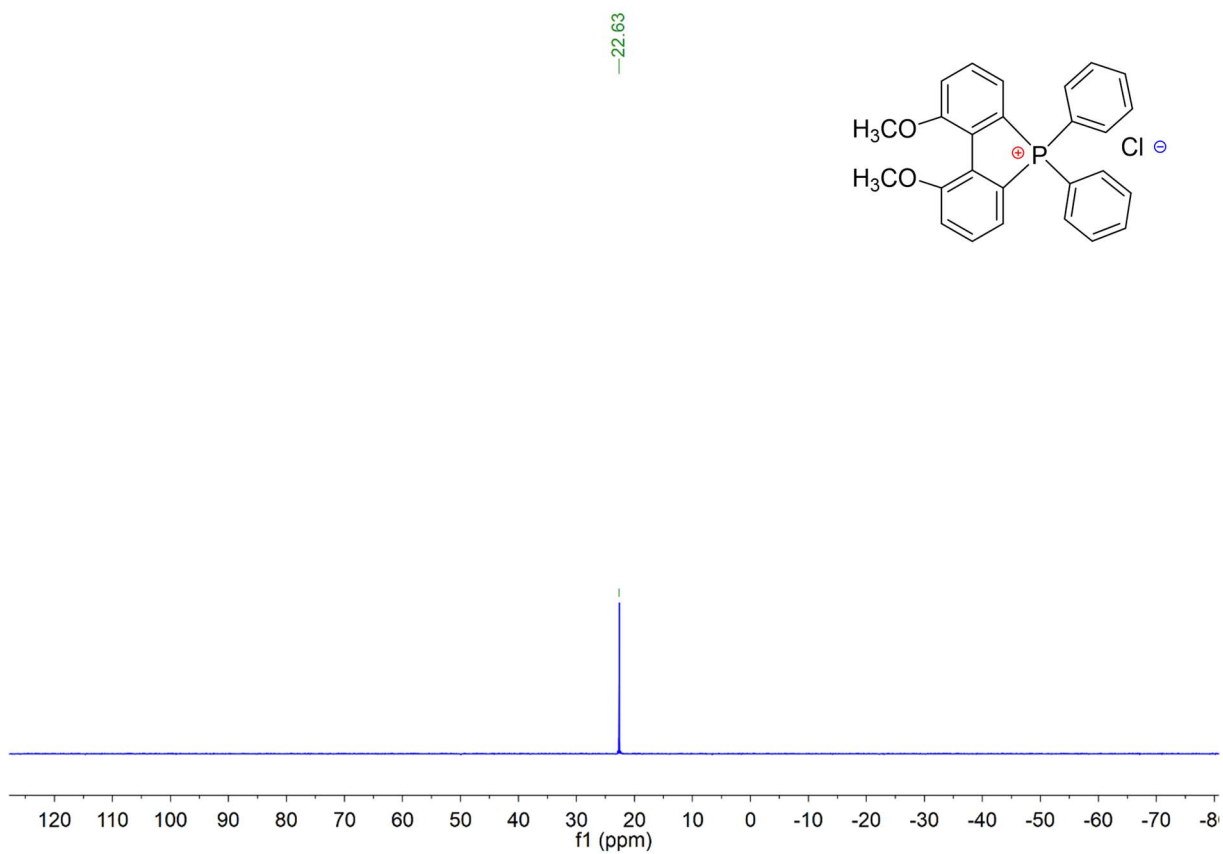
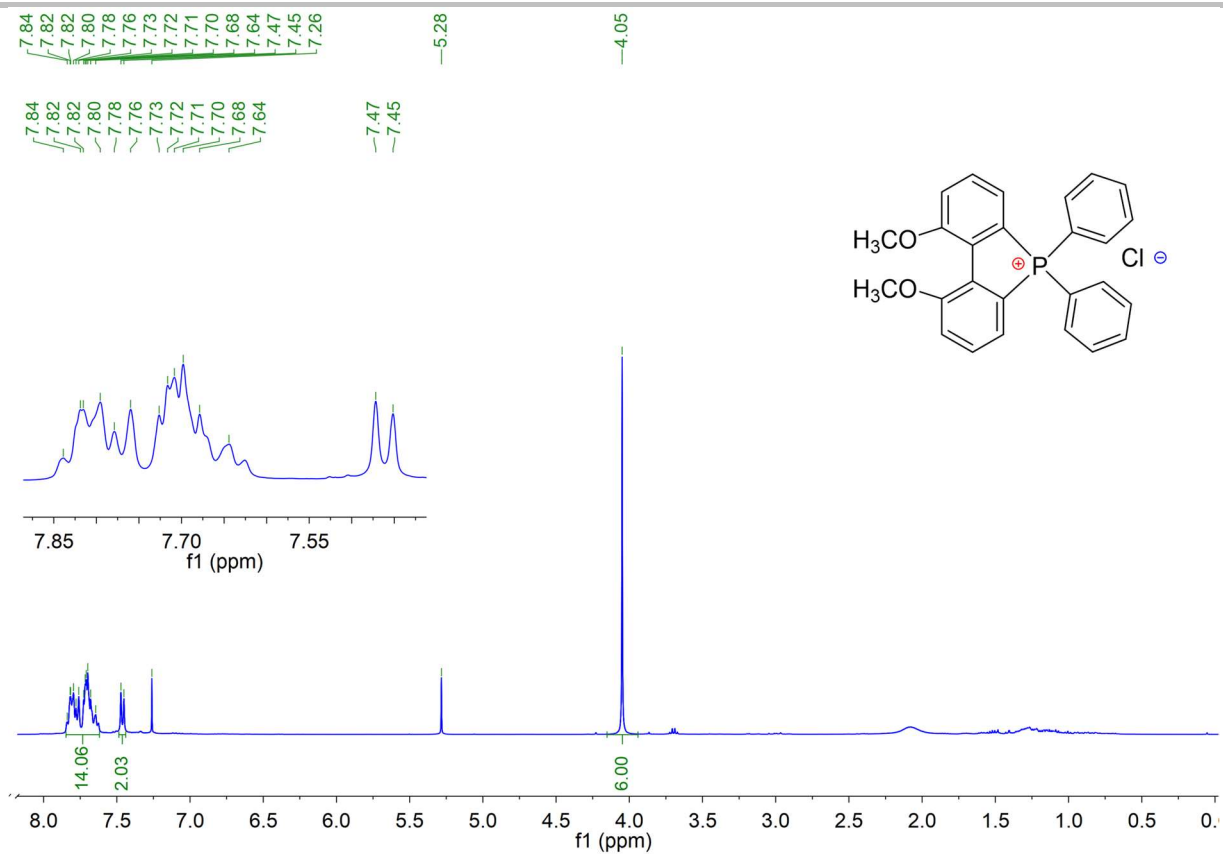
Supporting information



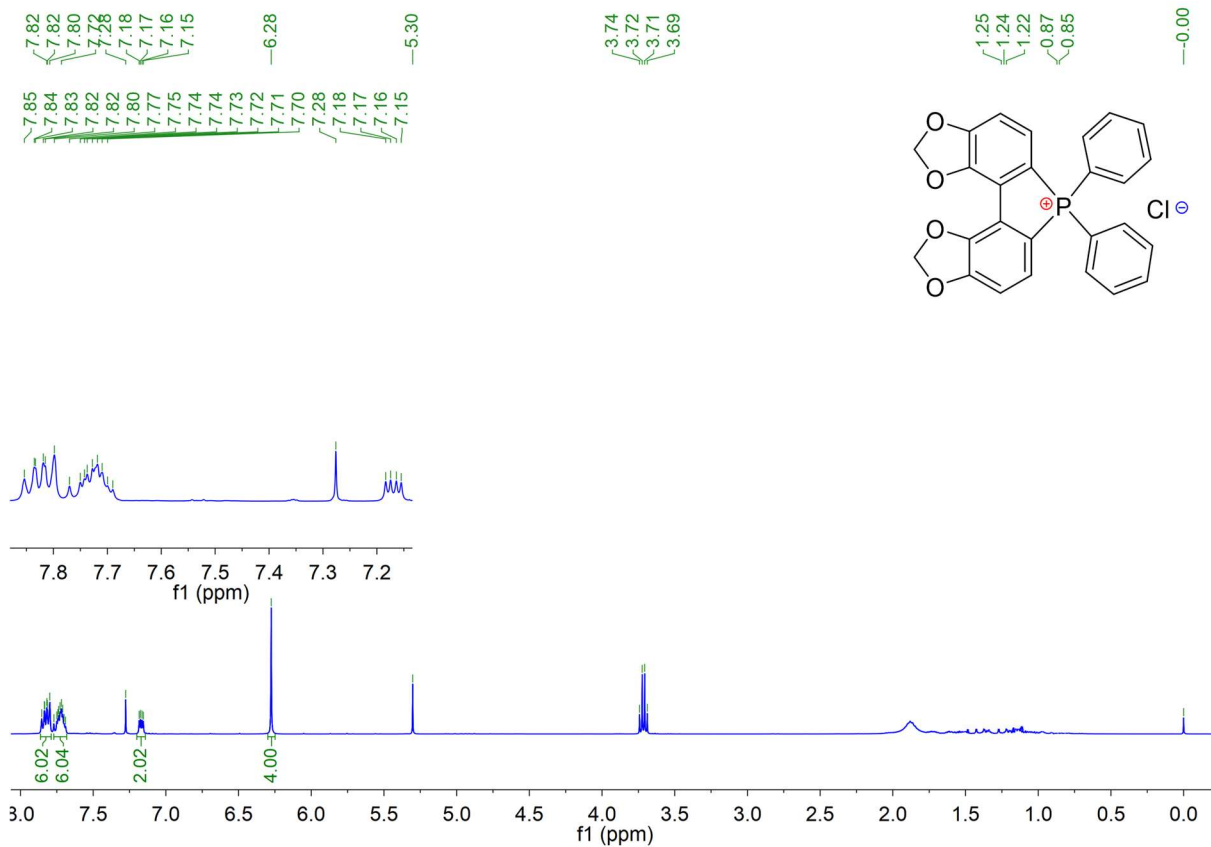
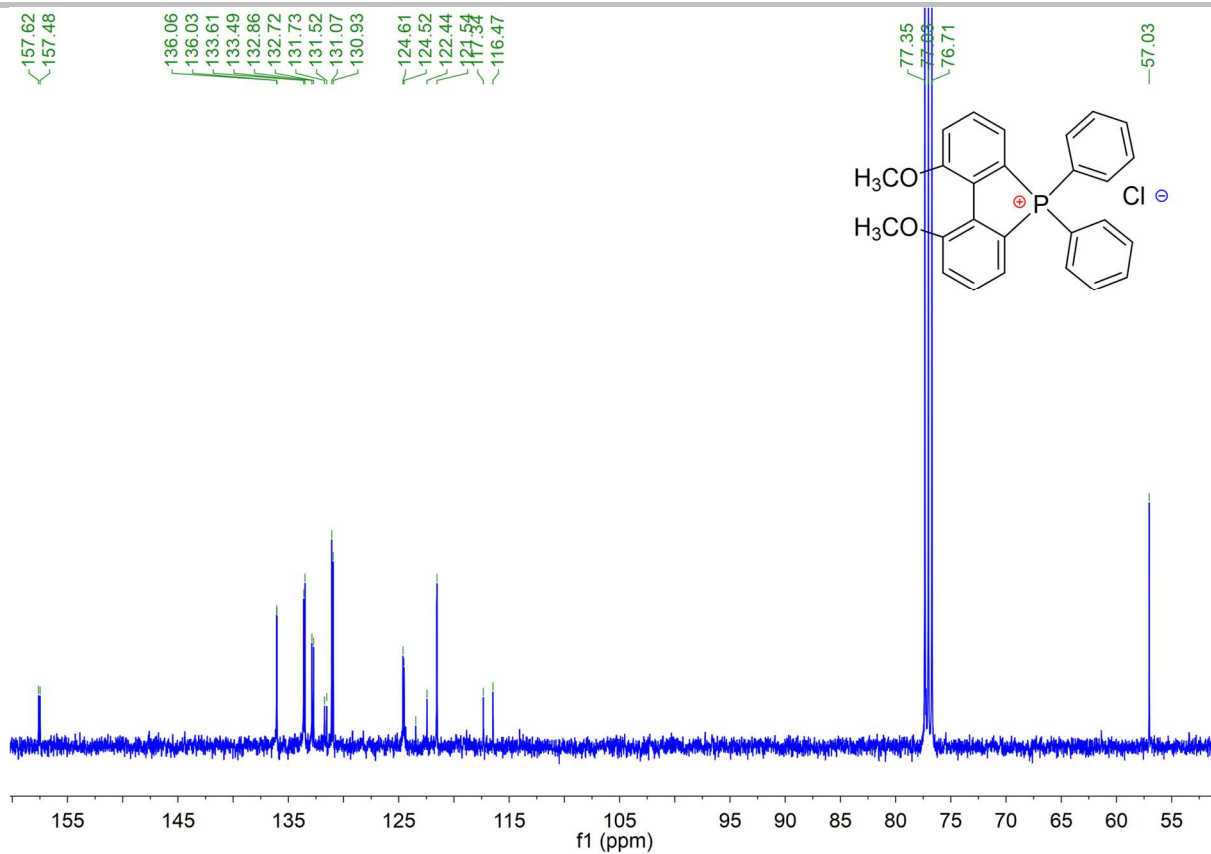
Supporting information



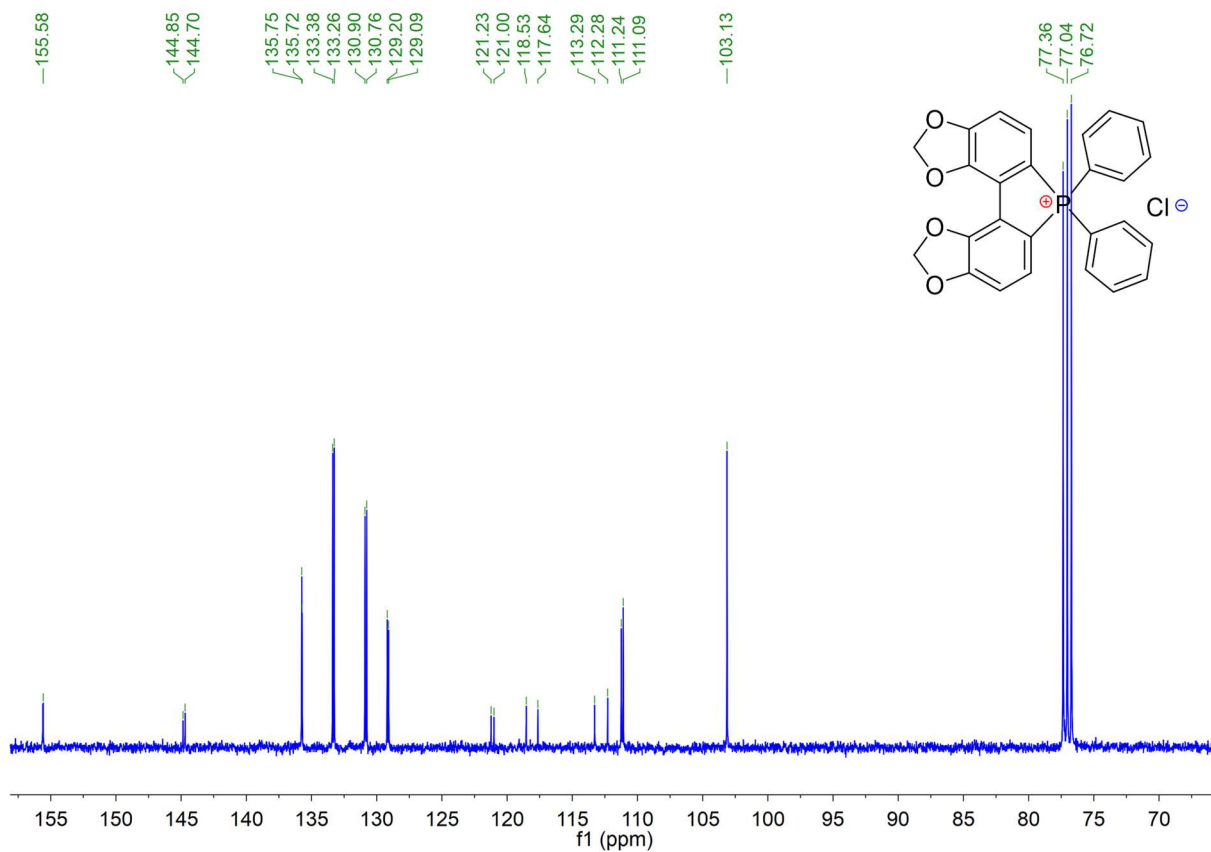
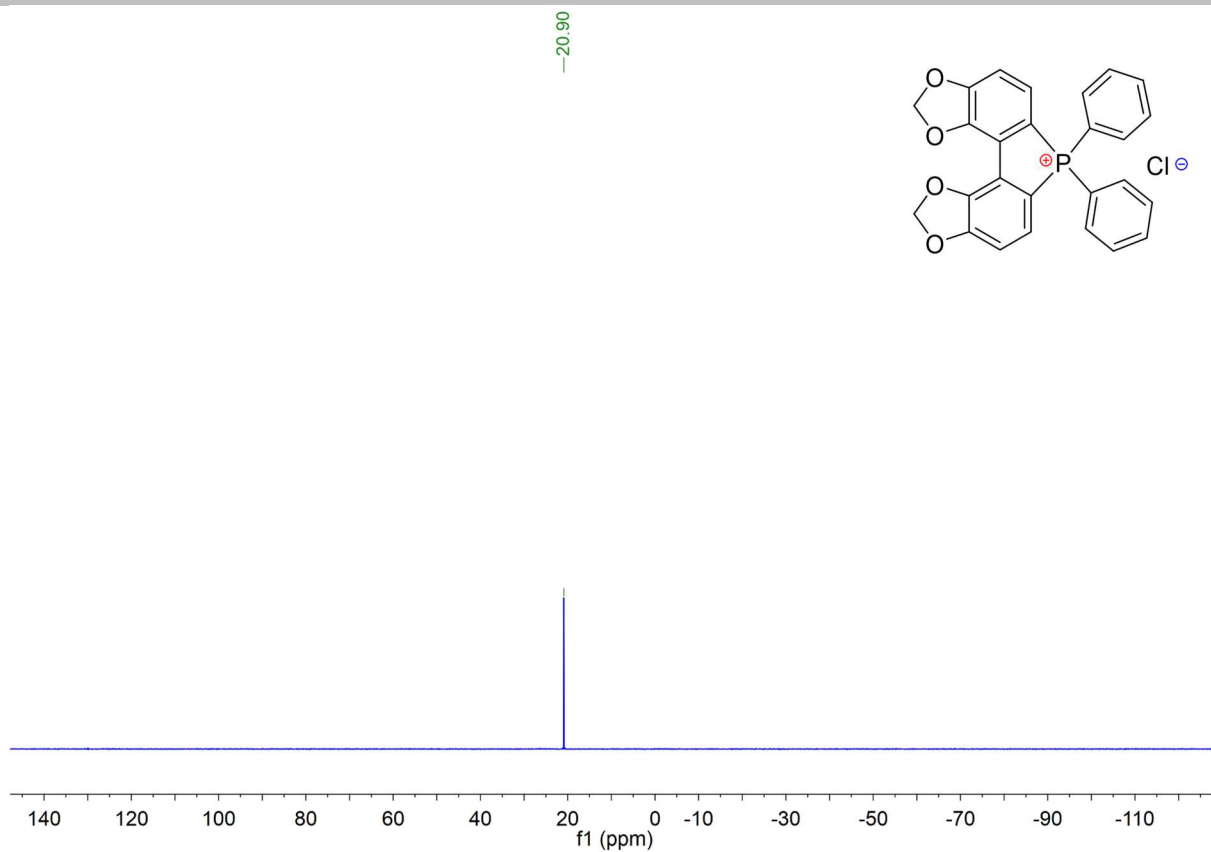
Supporting information



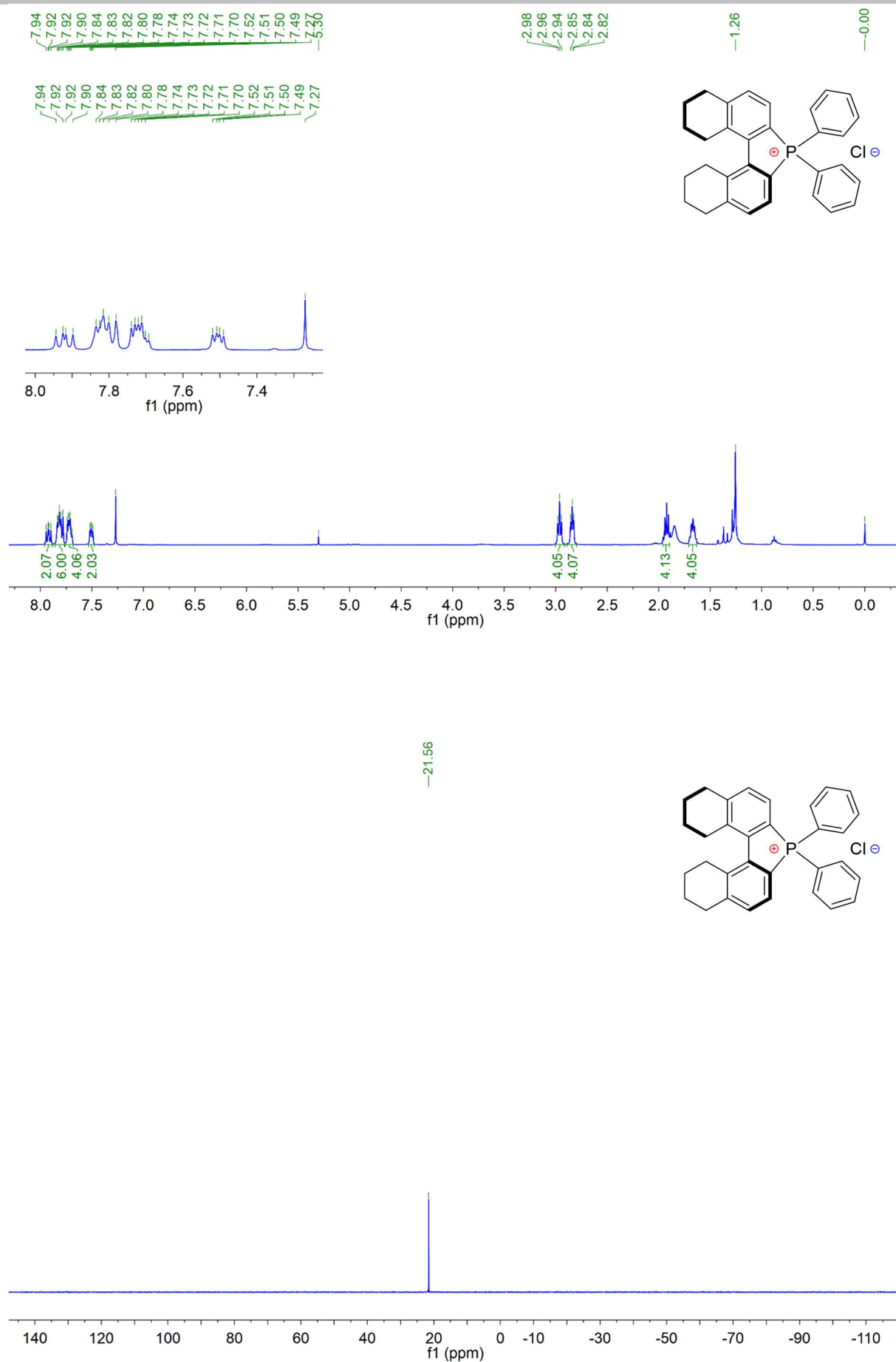
Supporting information



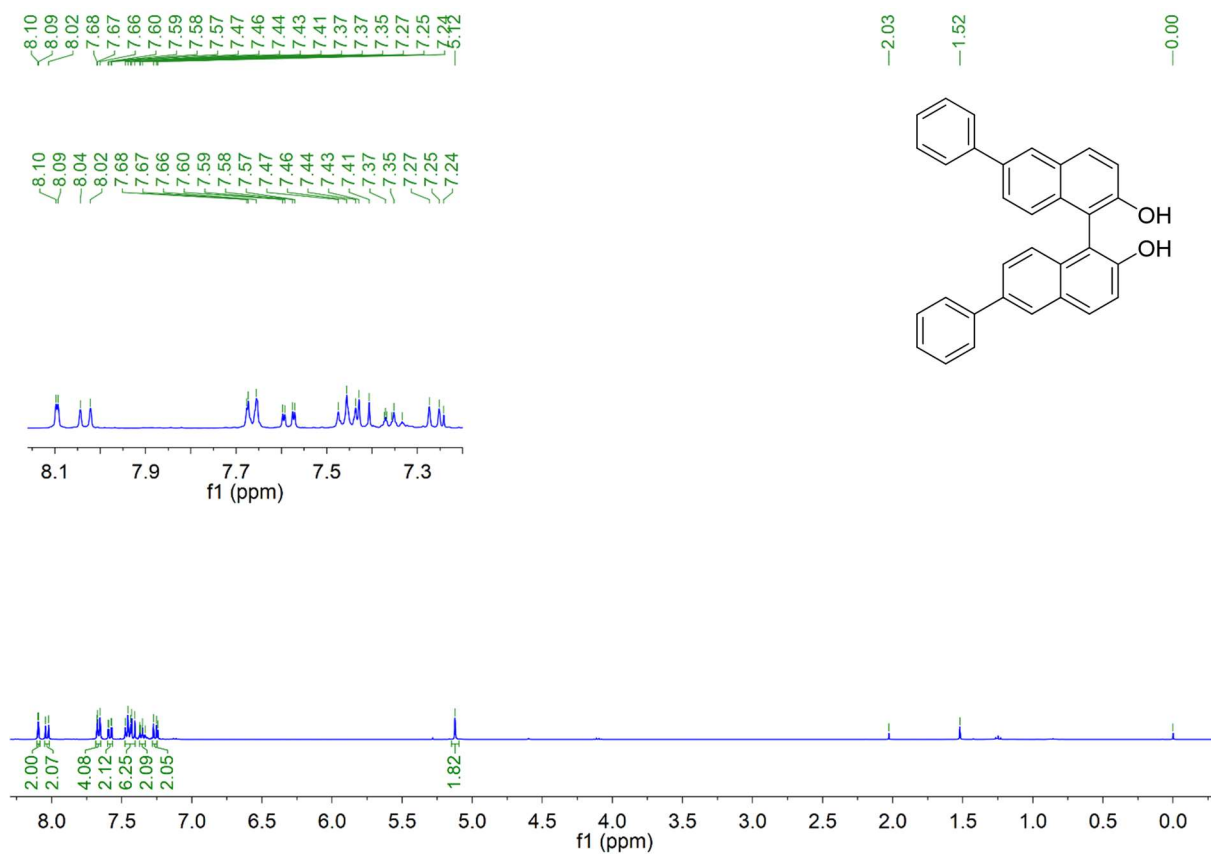
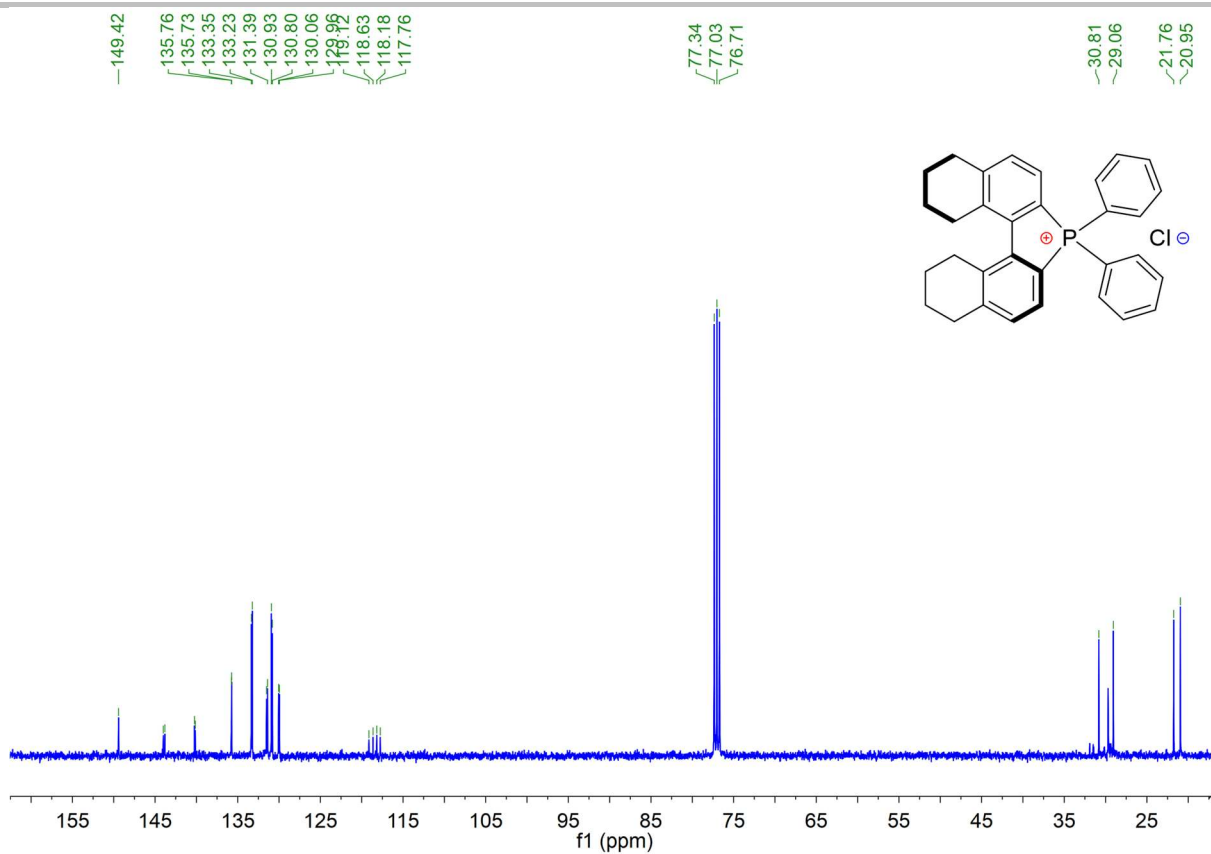
Supporting information



Supporting information



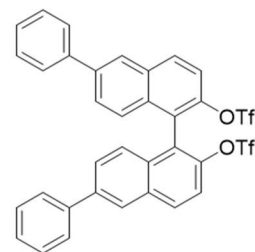
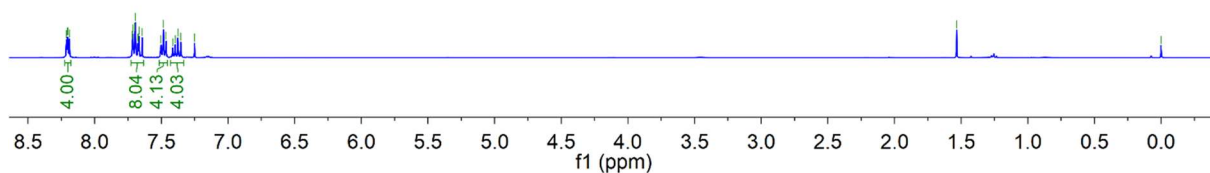
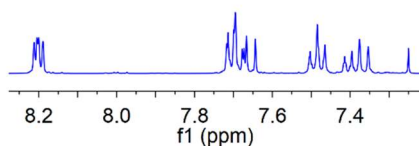
Supporting information



Supporting information

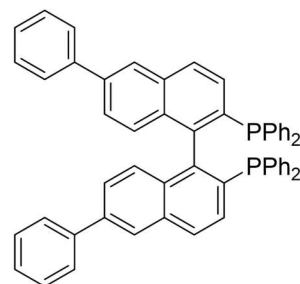
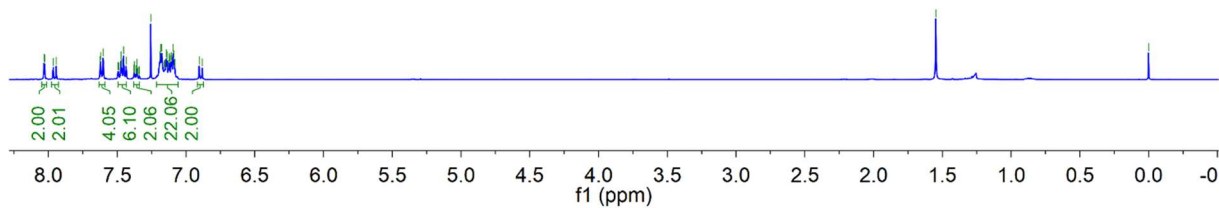
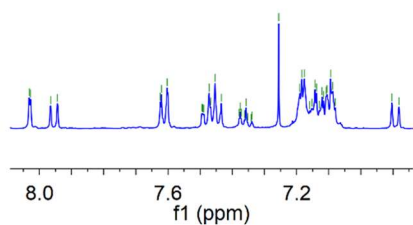
8.21
8.20
8.20
8.19
7.72
7.71
7.70
7.70
7.68
7.67
7.67
7.67
7.50
7.48
7.46
7.41
7.40
7.38
7.35
7.25

8.21
8.20
8.20
8.19
7.72
7.70
7.70
7.68
7.67
7.67
7.64
7.48
7.46
7.41
7.40
7.38
7.35
7.25

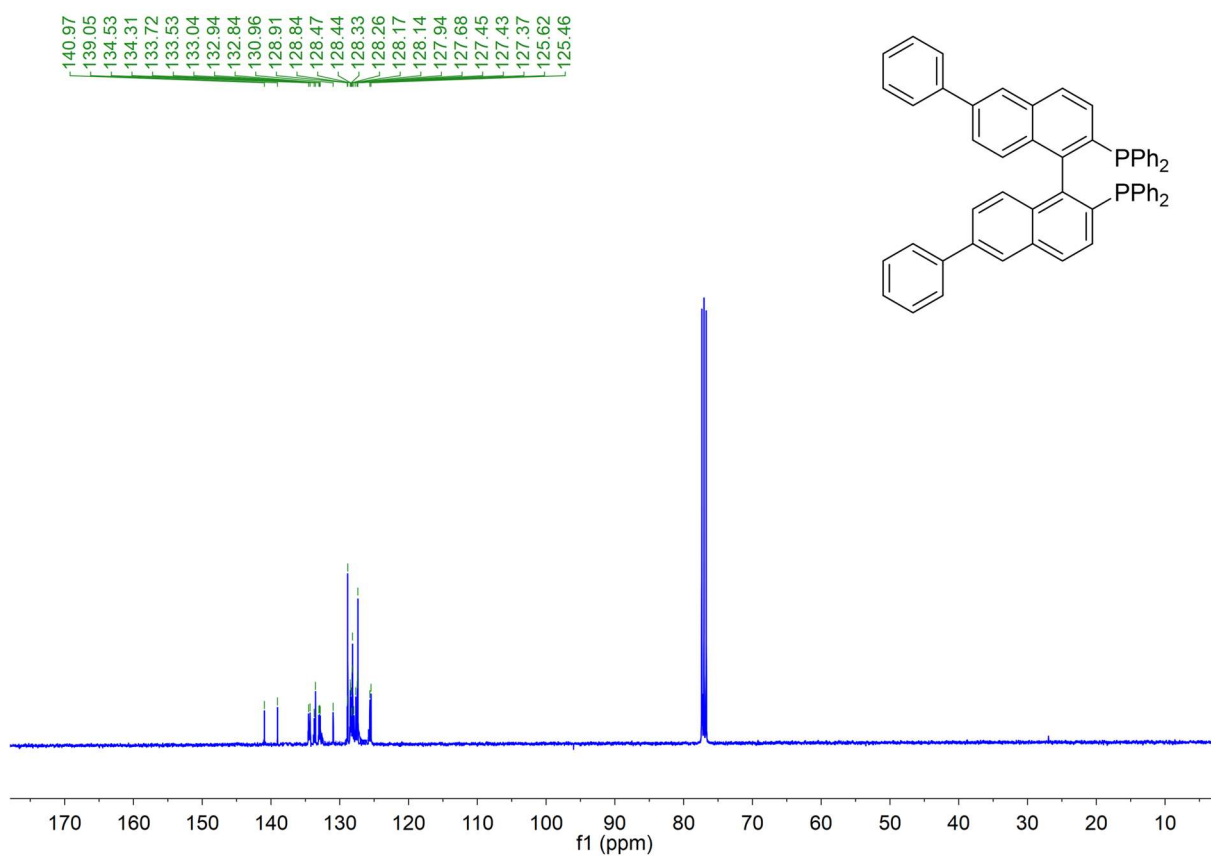
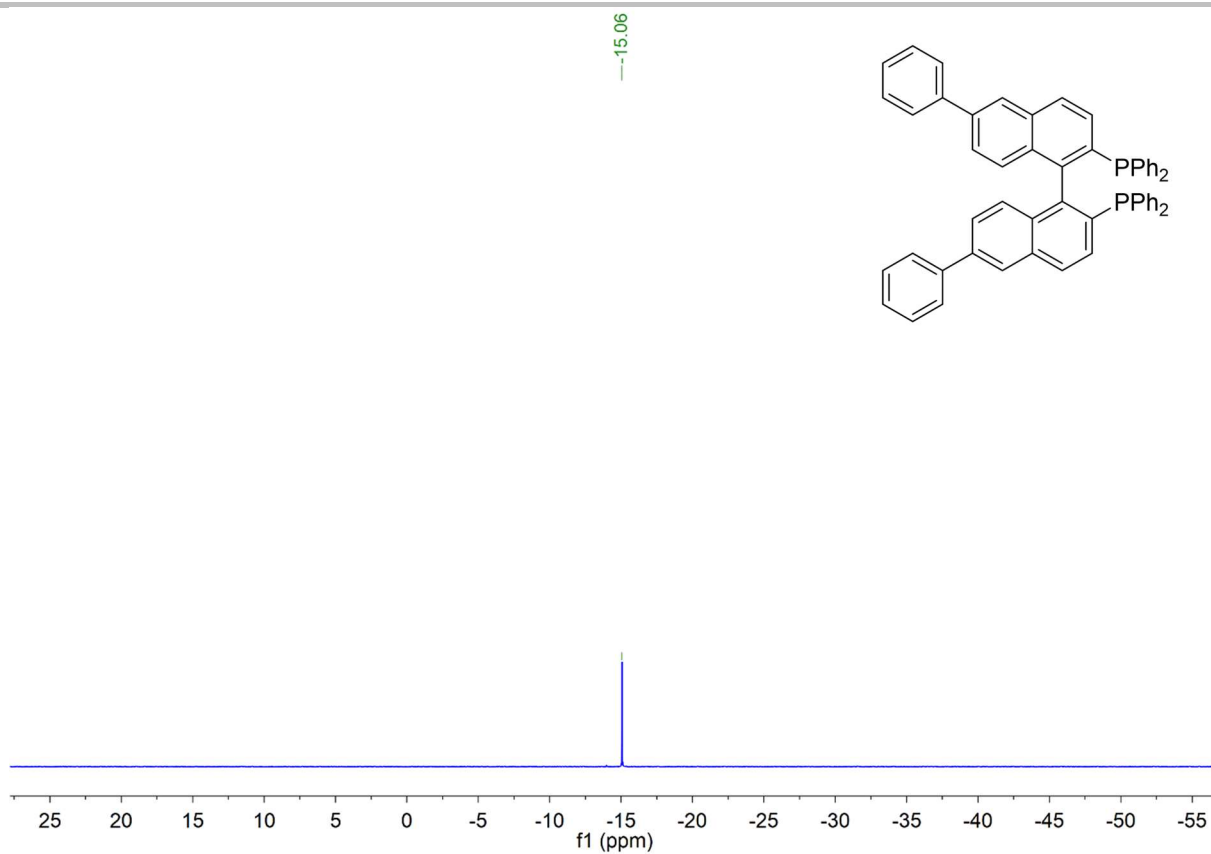


8.03
8.03
7.84
7.62
7.60
7.49
7.49
7.49
7.47
7.47
7.45
7.43
7.38
7.37
7.36
7.35
7.34
7.34
7.26
7.19
7.18
7.18
7.16
7.15
7.14
7.14
7.13
7.12
7.12
7.11
7.11
7.09
7.08
6.90
6.88

8.03
8.03
7.62
7.60
7.47
7.45
7.26
7.19
7.18
7.18
7.14
7.14
7.12
7.12
7.11
7.11
7.09
7.09



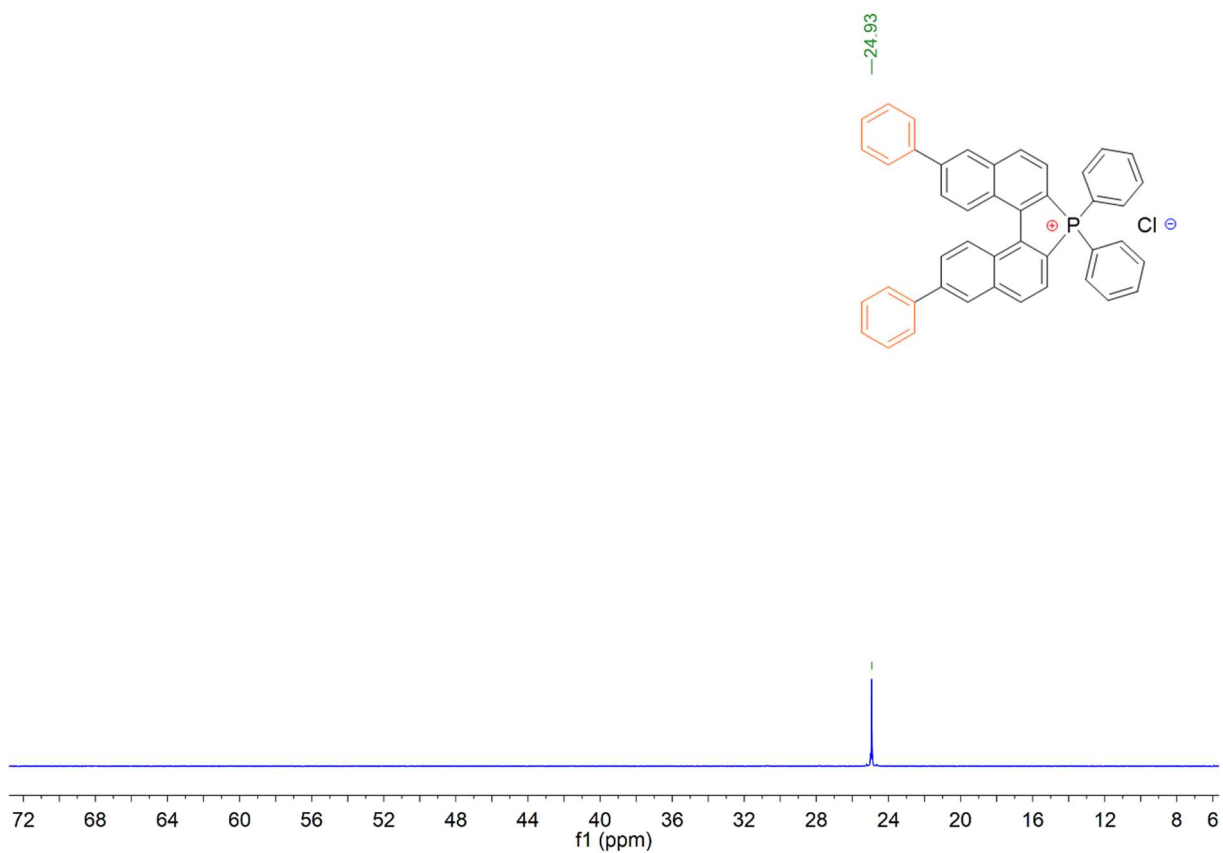
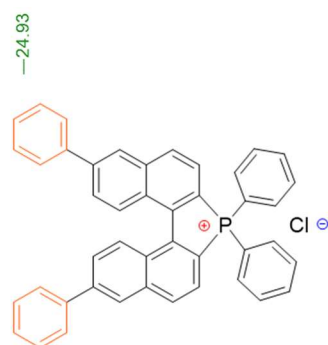
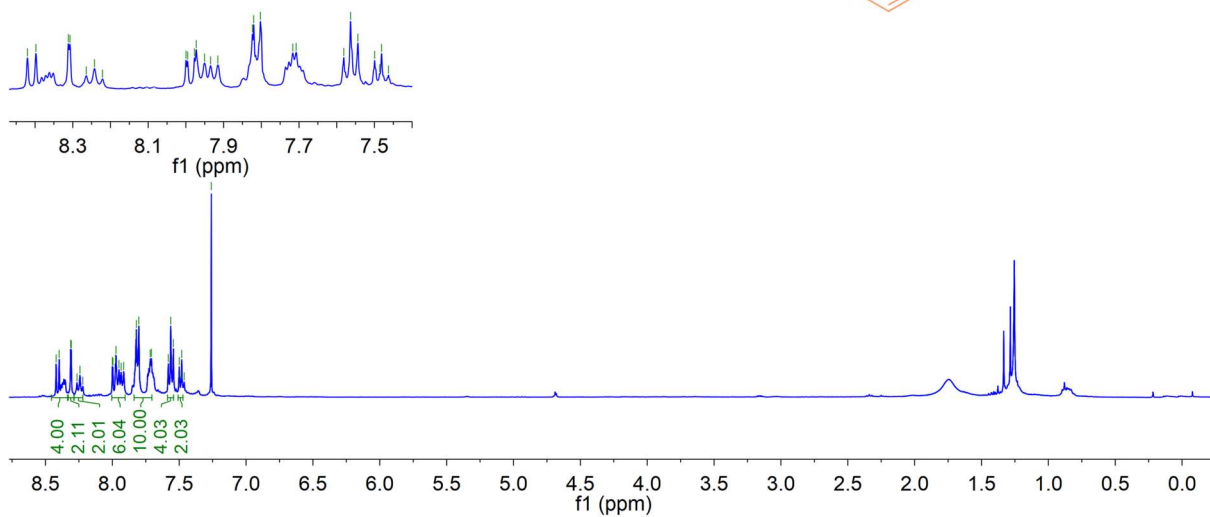
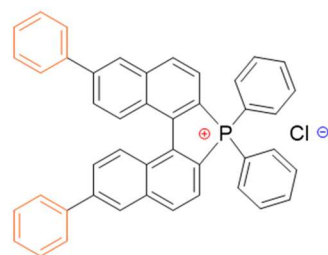
Supporting information



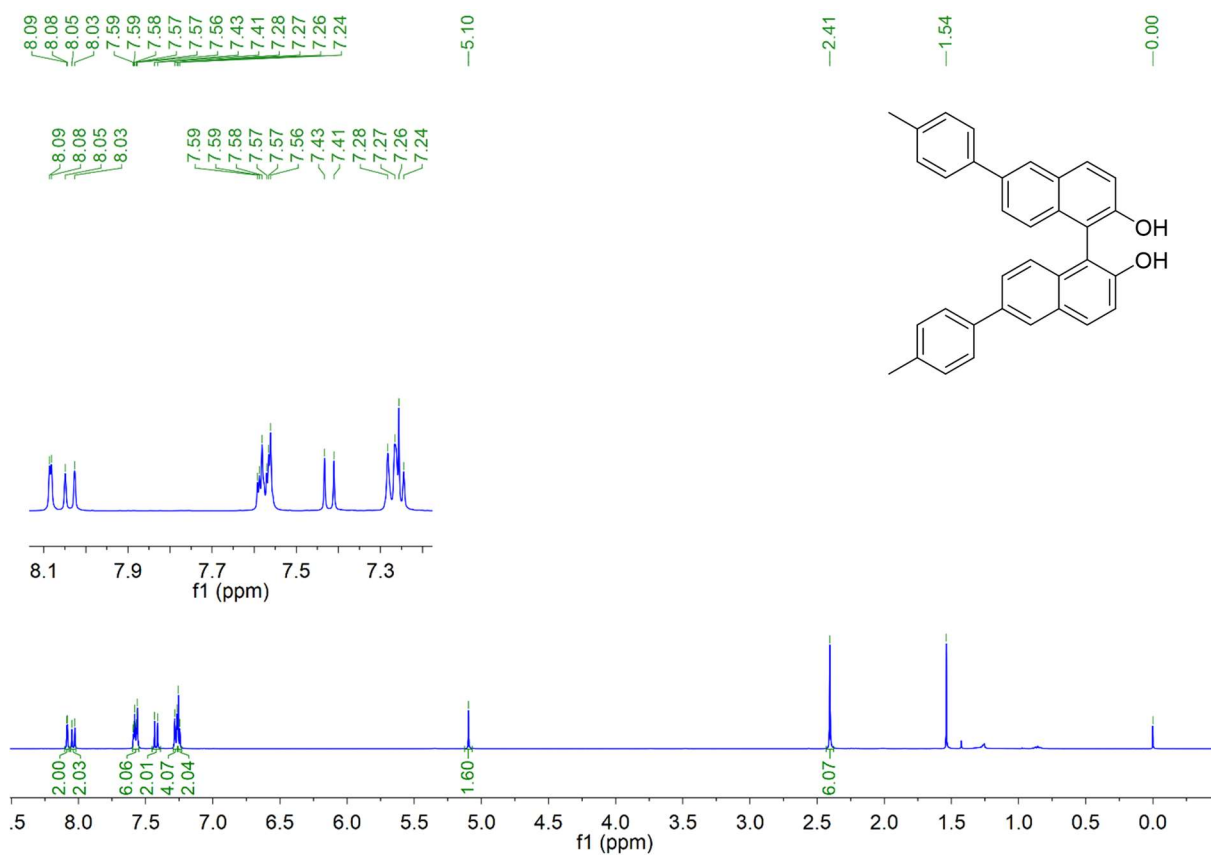
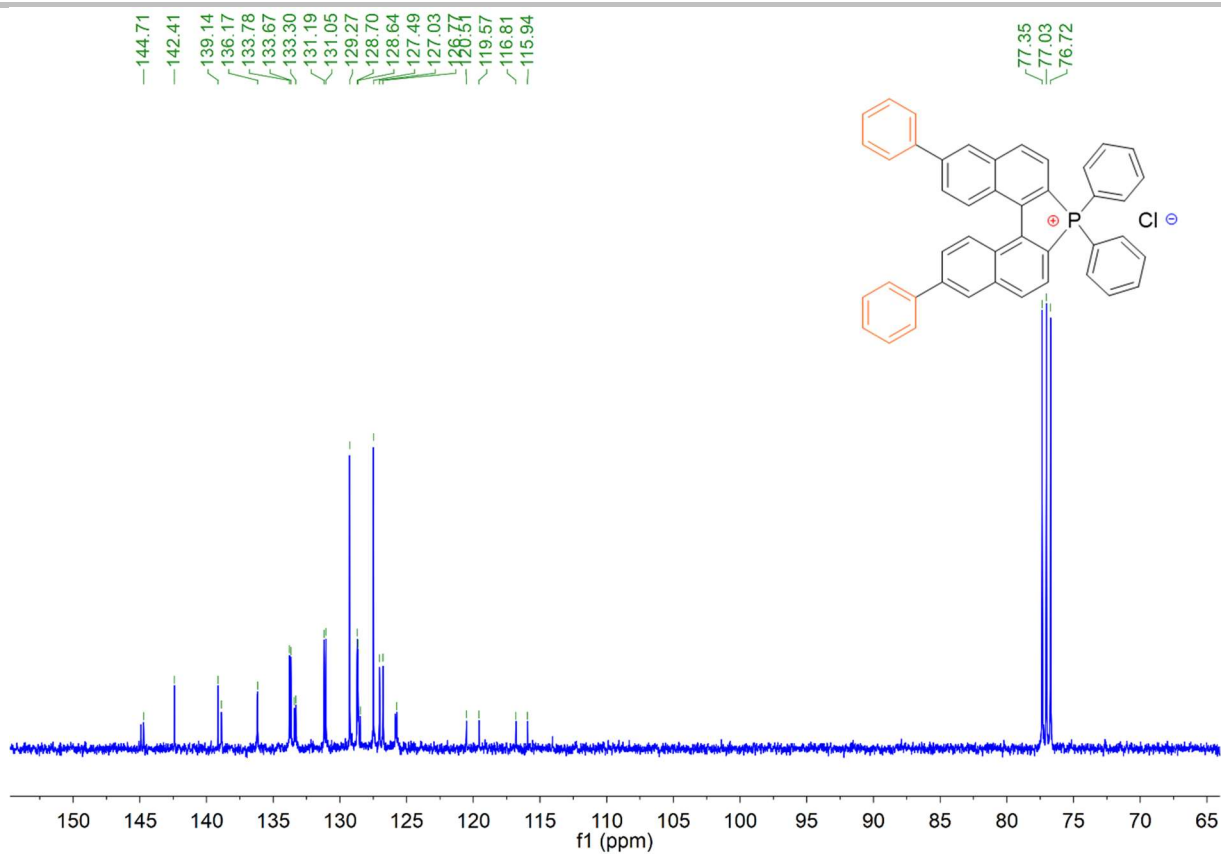
Supporting information

8.42
8.40
8.31
8.31
8.26
8.24
8.22
8.00
8.00
7.97
7.95
7.98
7.82
7.97
7.80
7.93
7.92
7.72
7.71
7.82
7.58
7.54
7.80
7.72
7.71
7.58
7.54
7.50
7.49
7.48
7.46
7.26

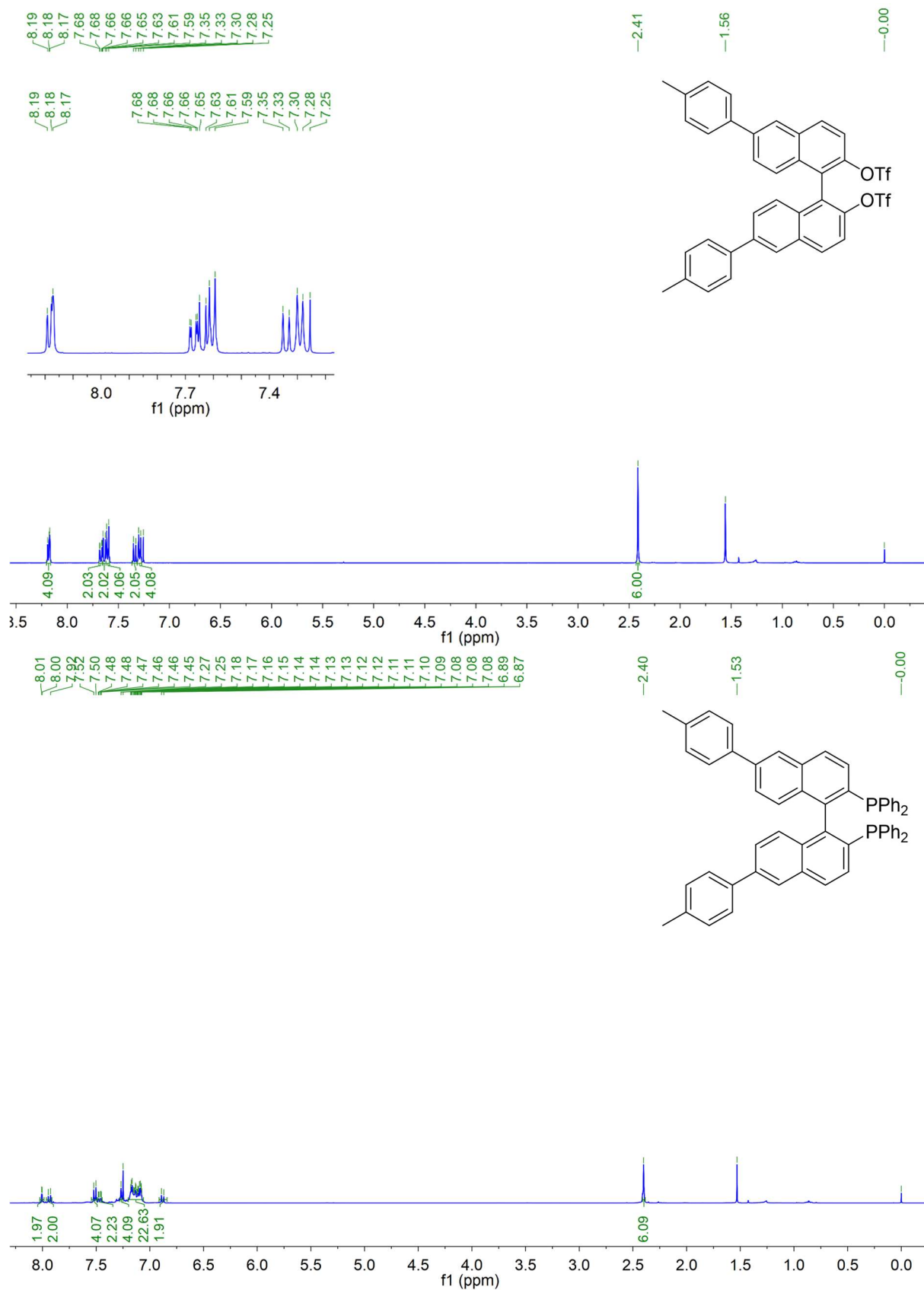
8.42
8.40
8.31
8.31
8.00
7.98
7.97
7.95
7.82
7.80
7.72
7.71
7.58
7.54
7.50
7.49
7.48
7.46
7.26



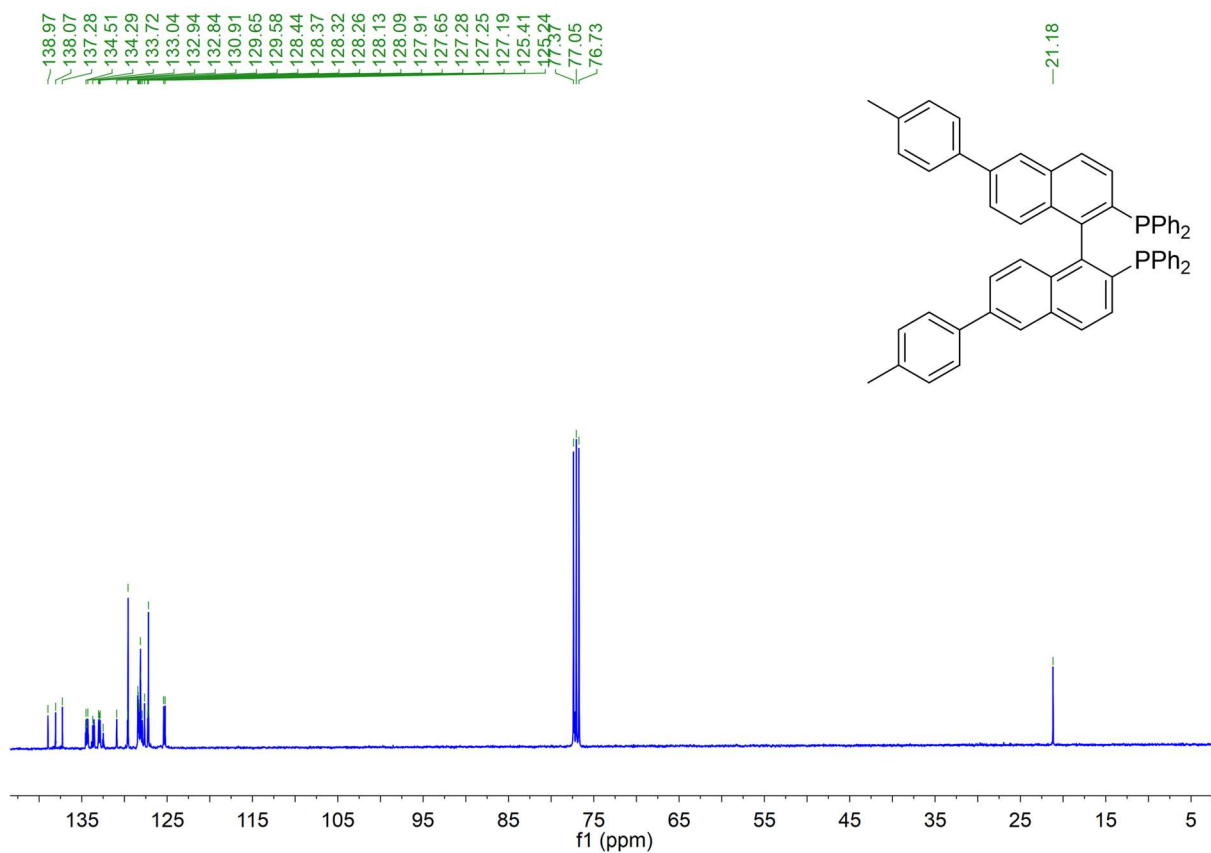
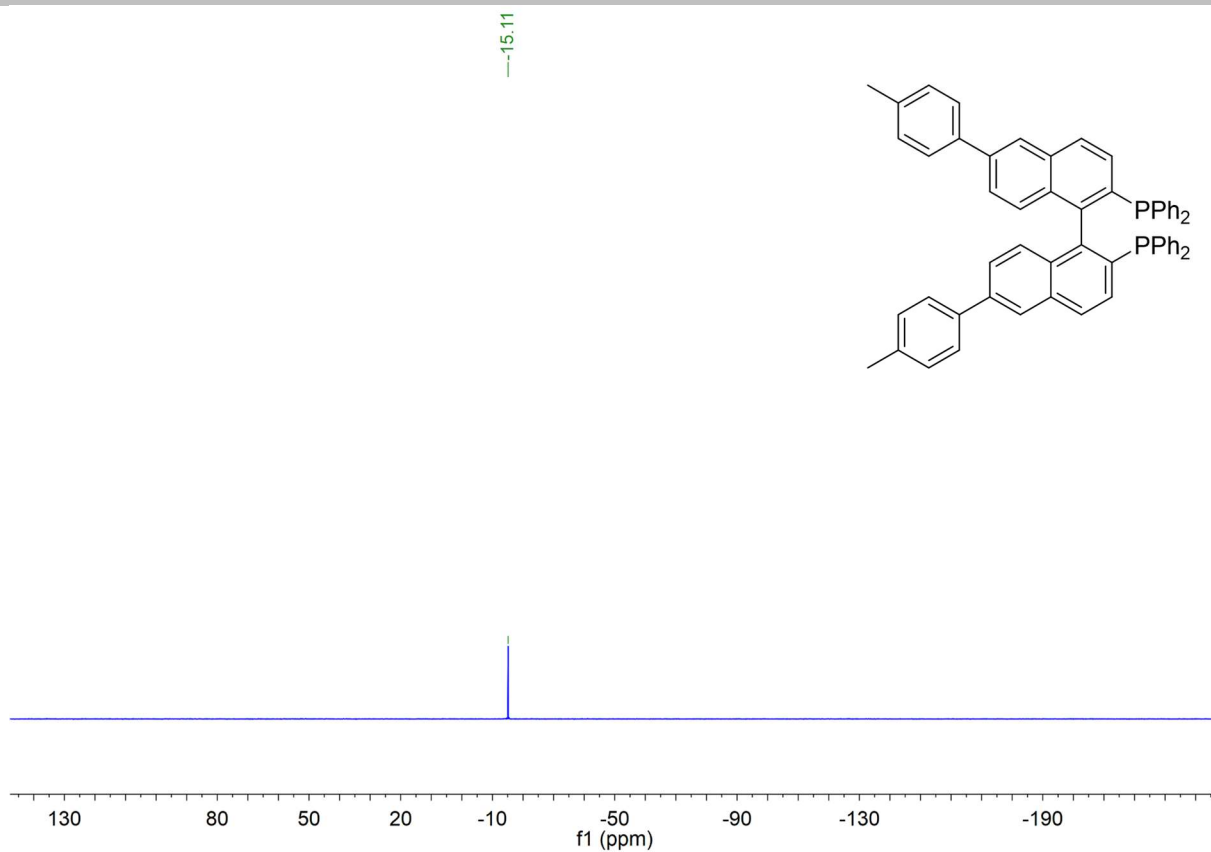
Supporting information



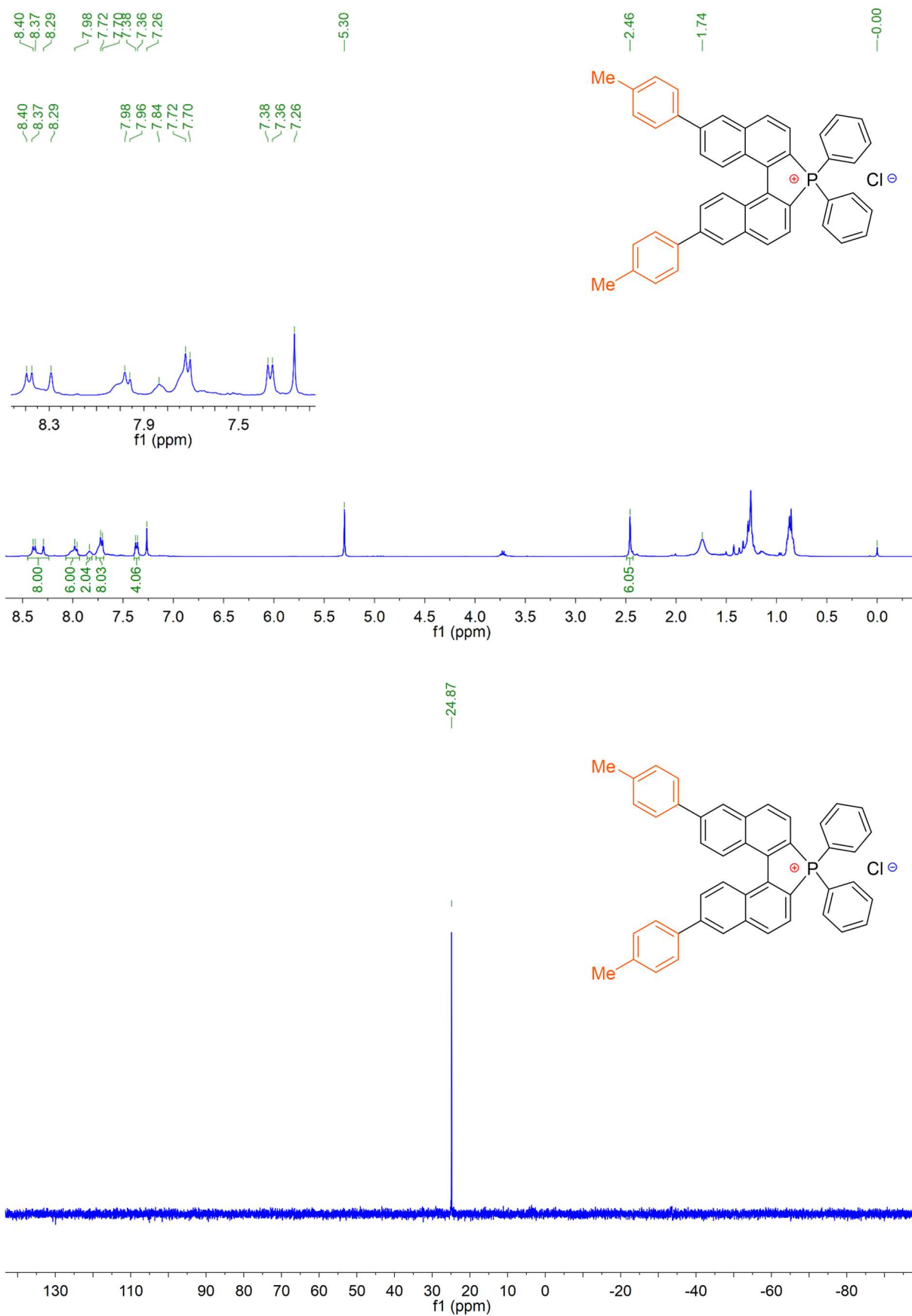
Supporting information



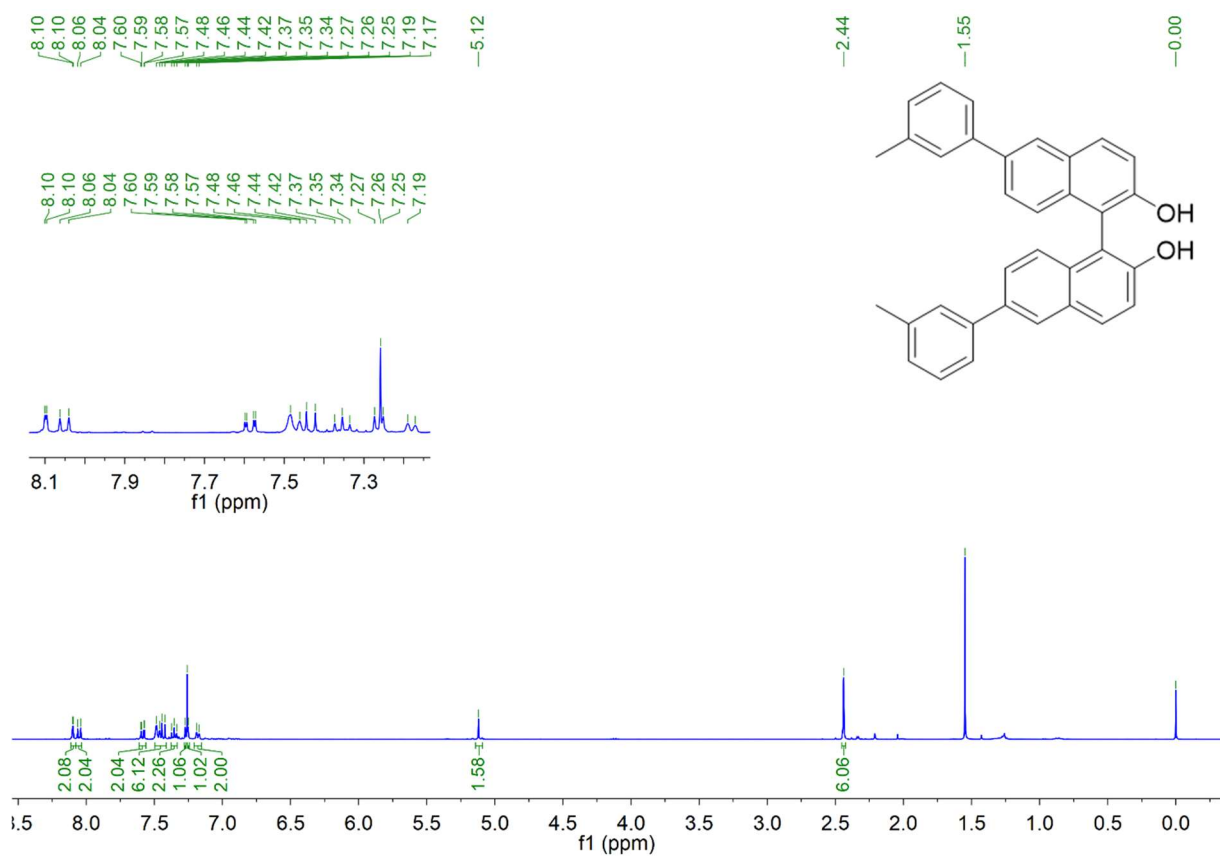
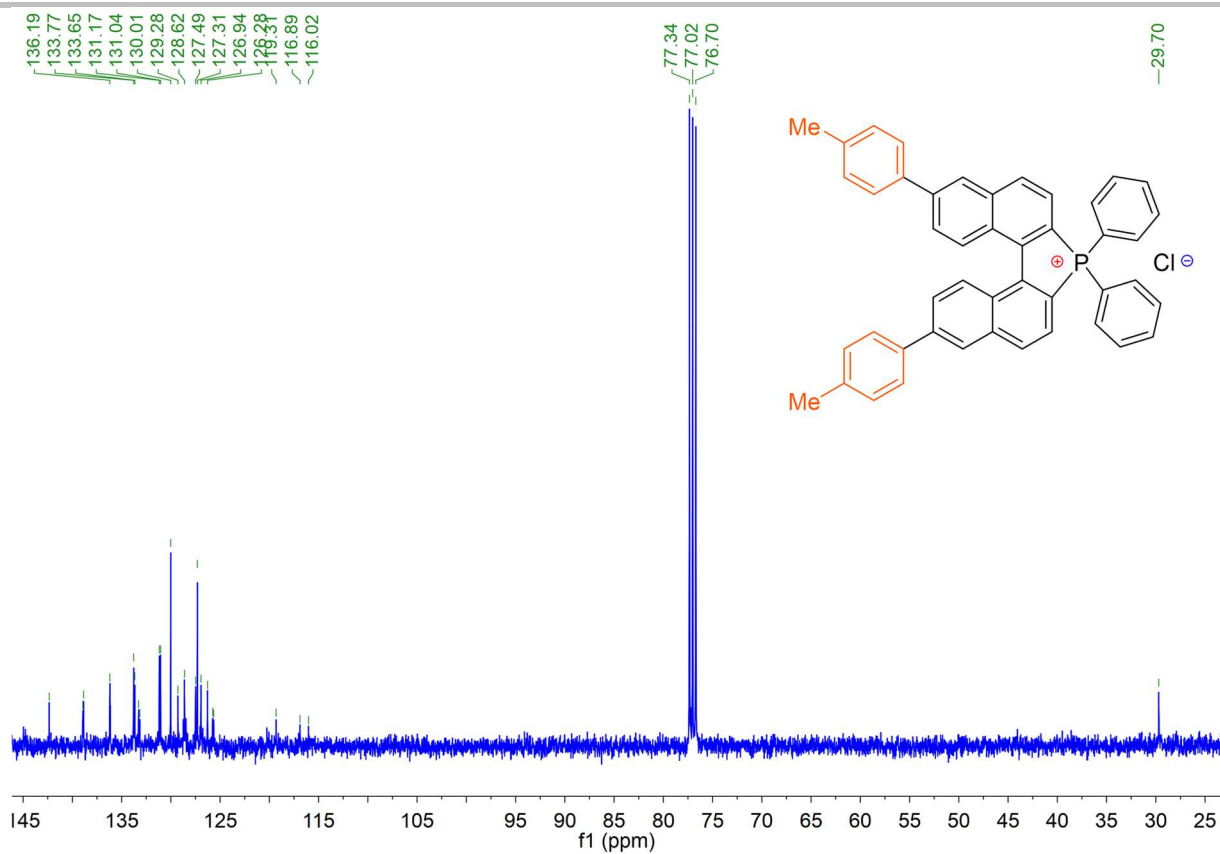
Supporting information



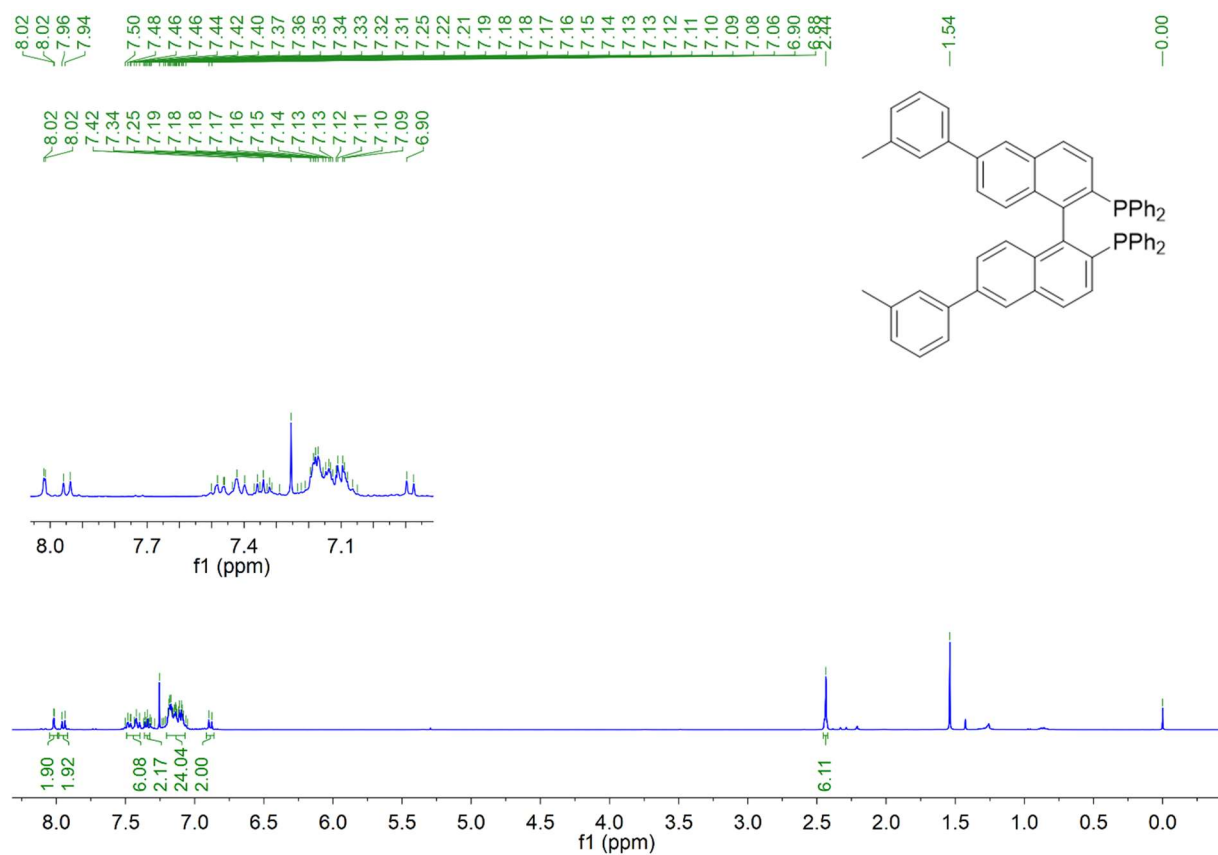
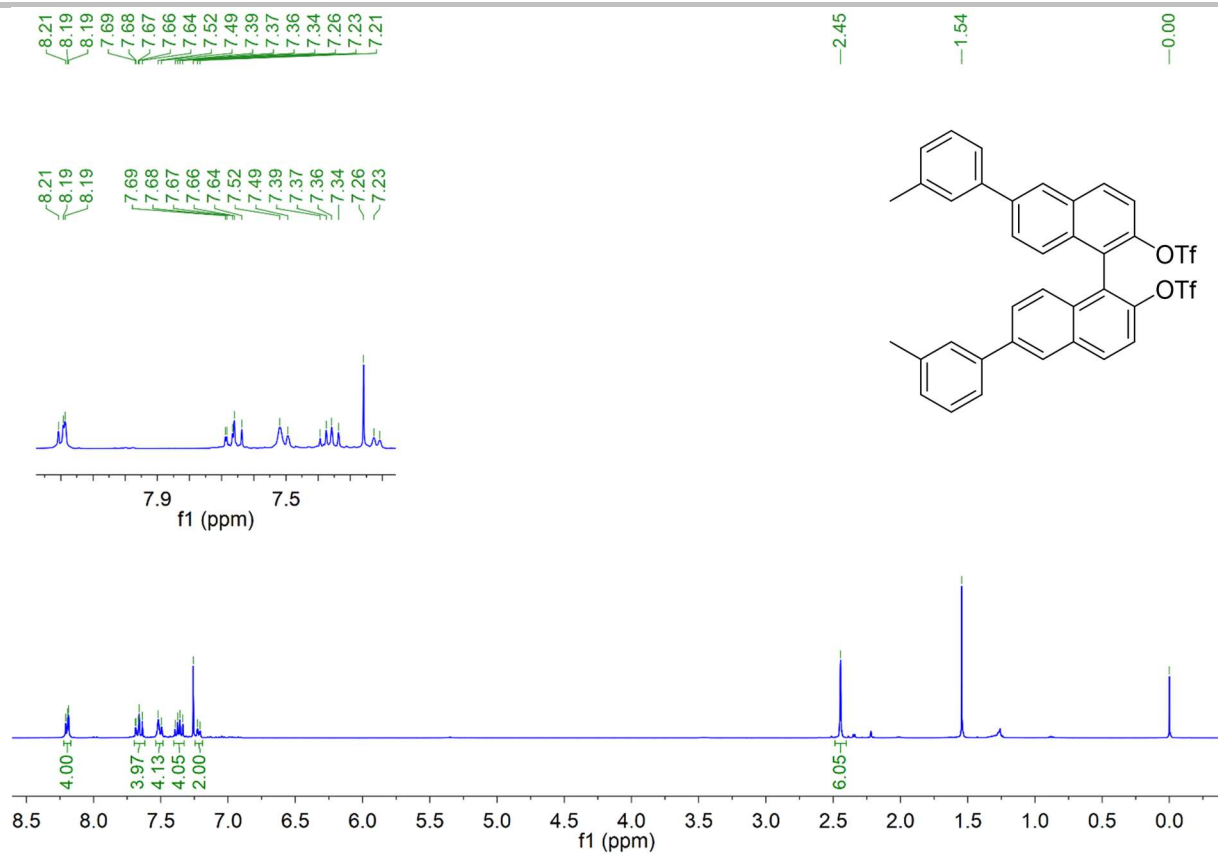
Supporting information



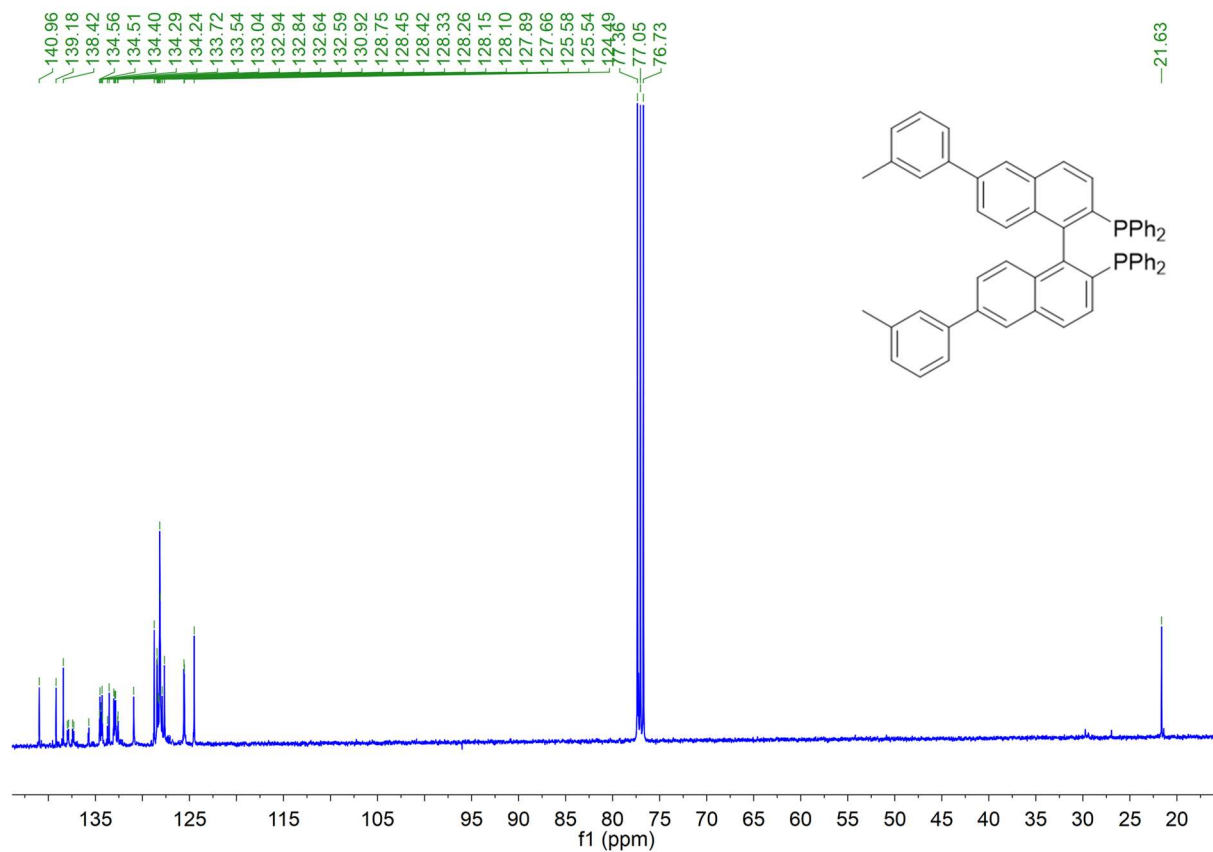
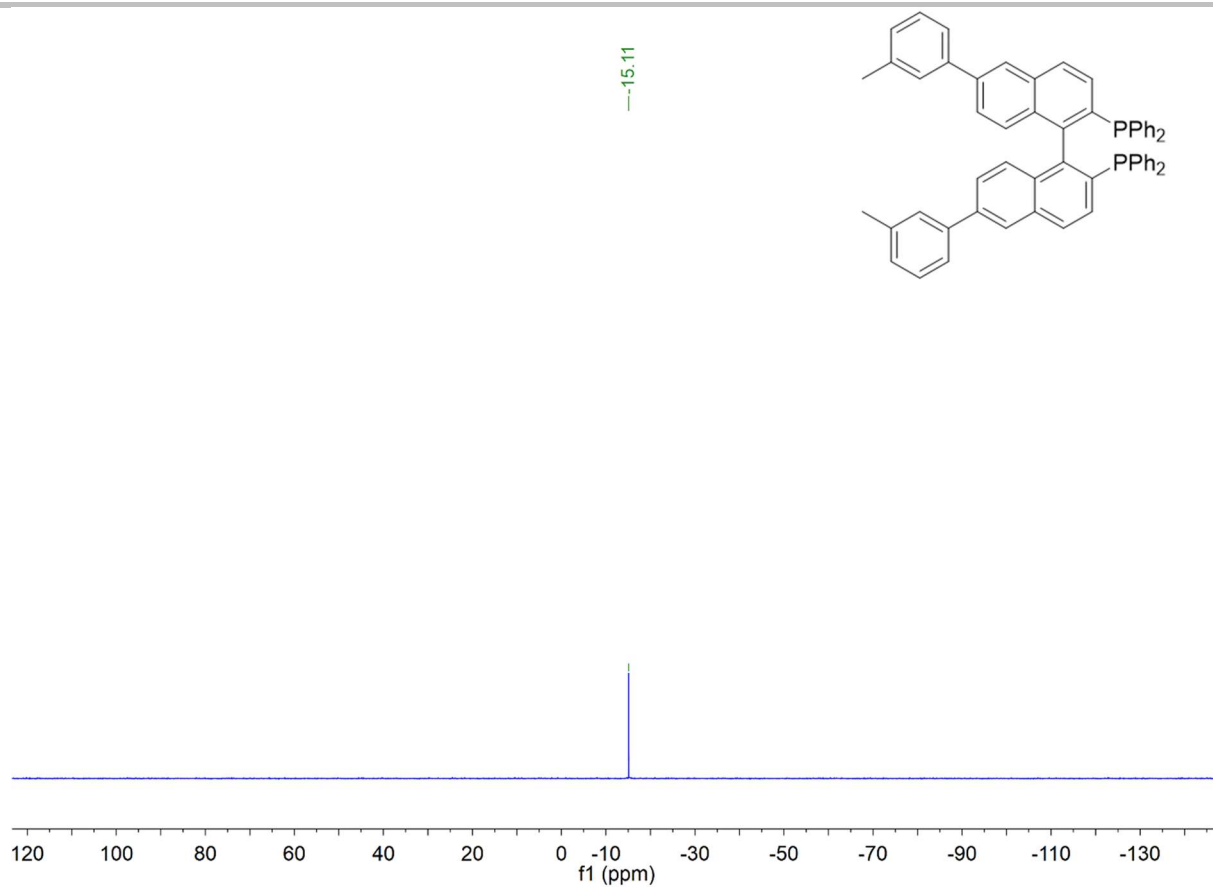
Supporting information



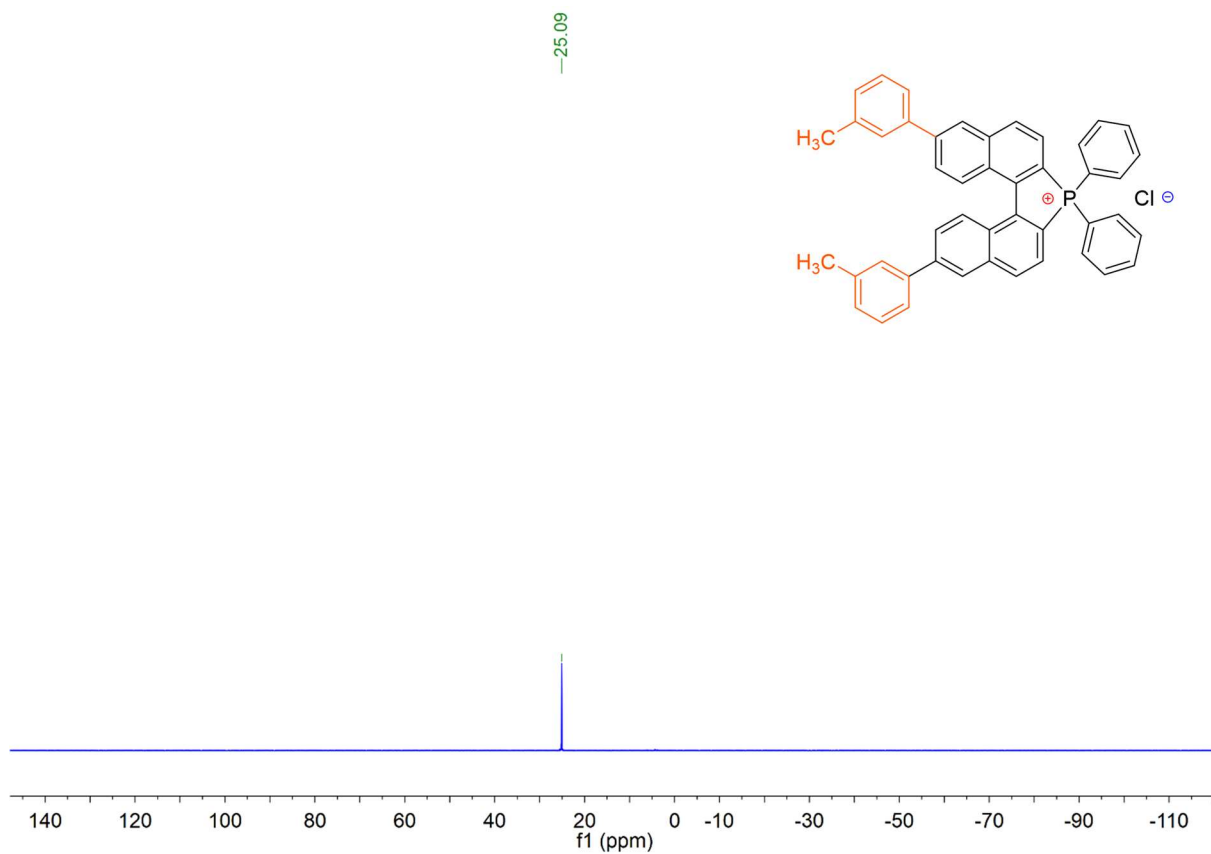
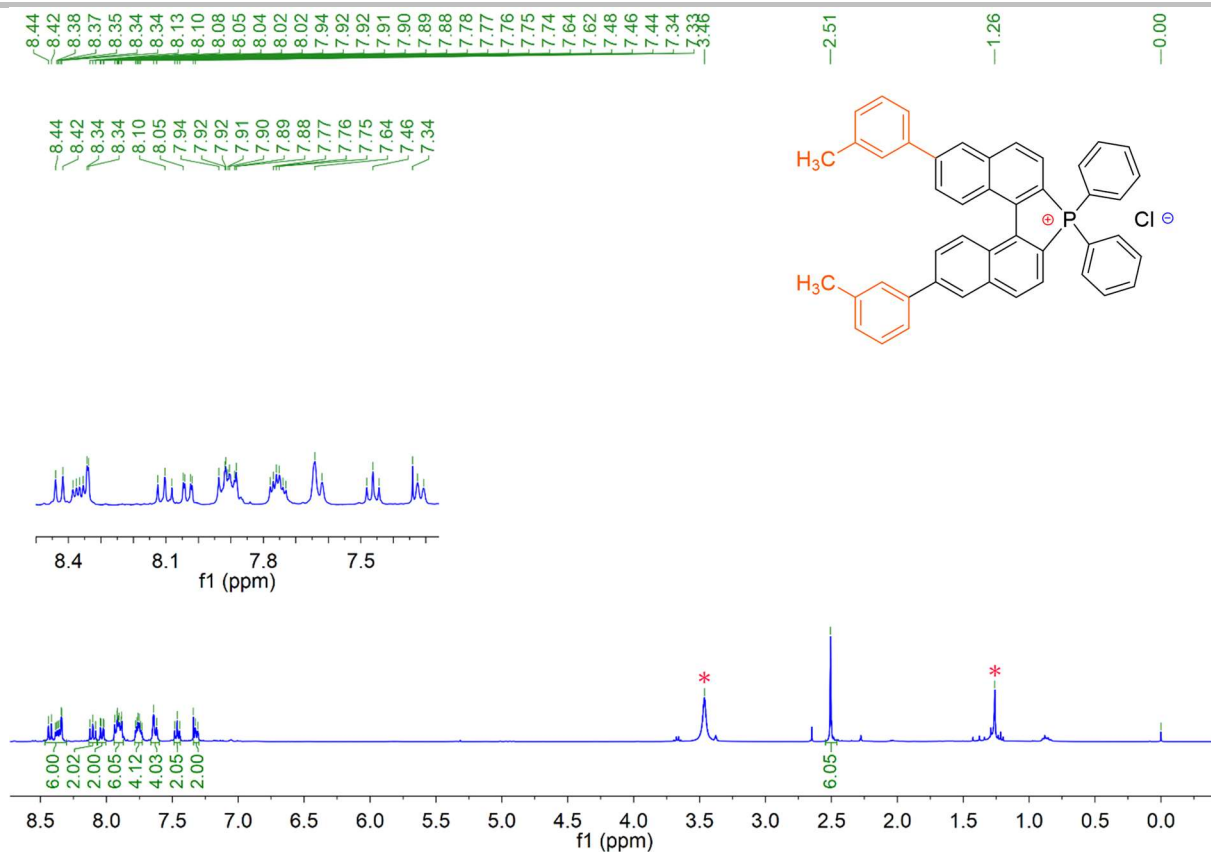
Supporting information



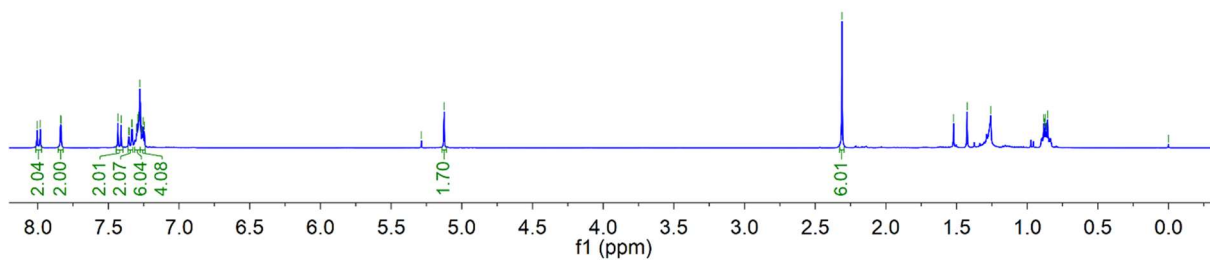
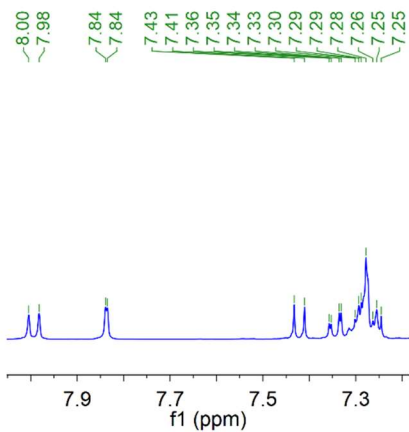
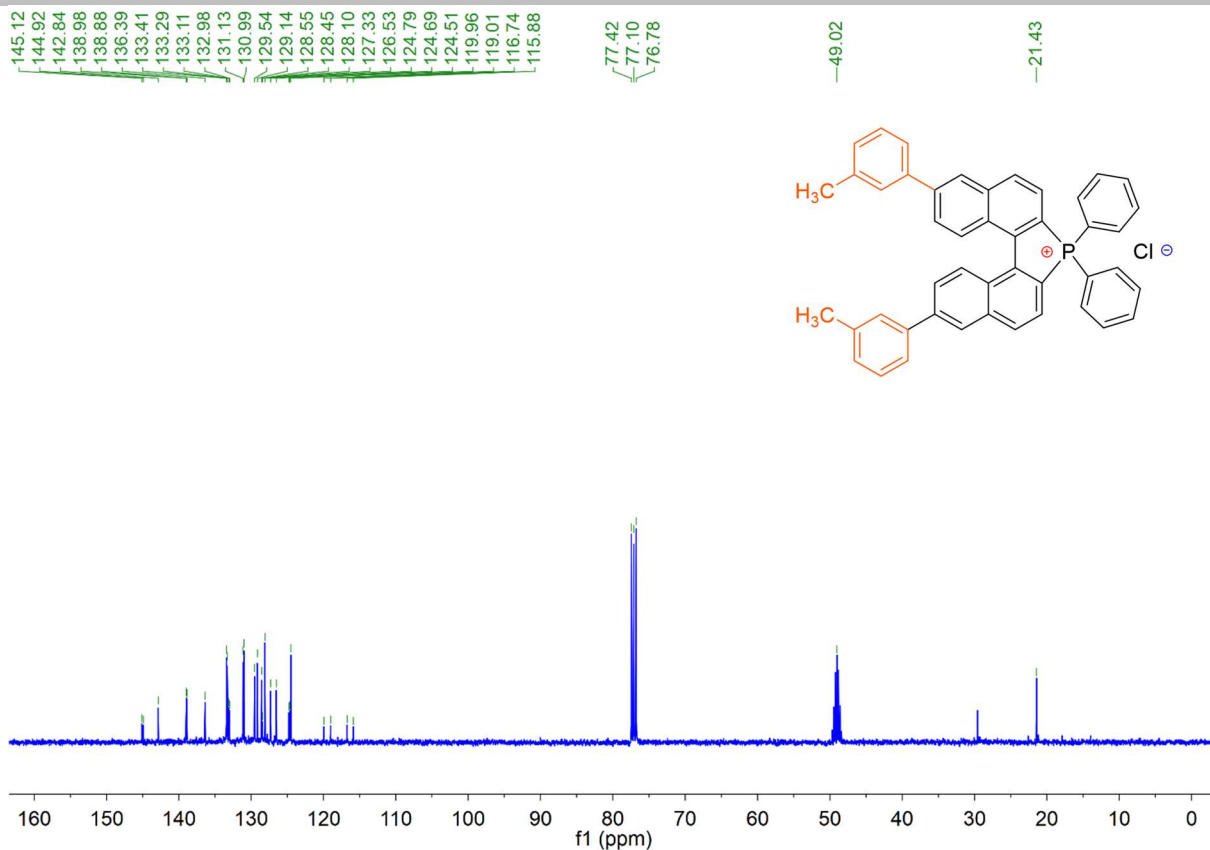
Supporting information



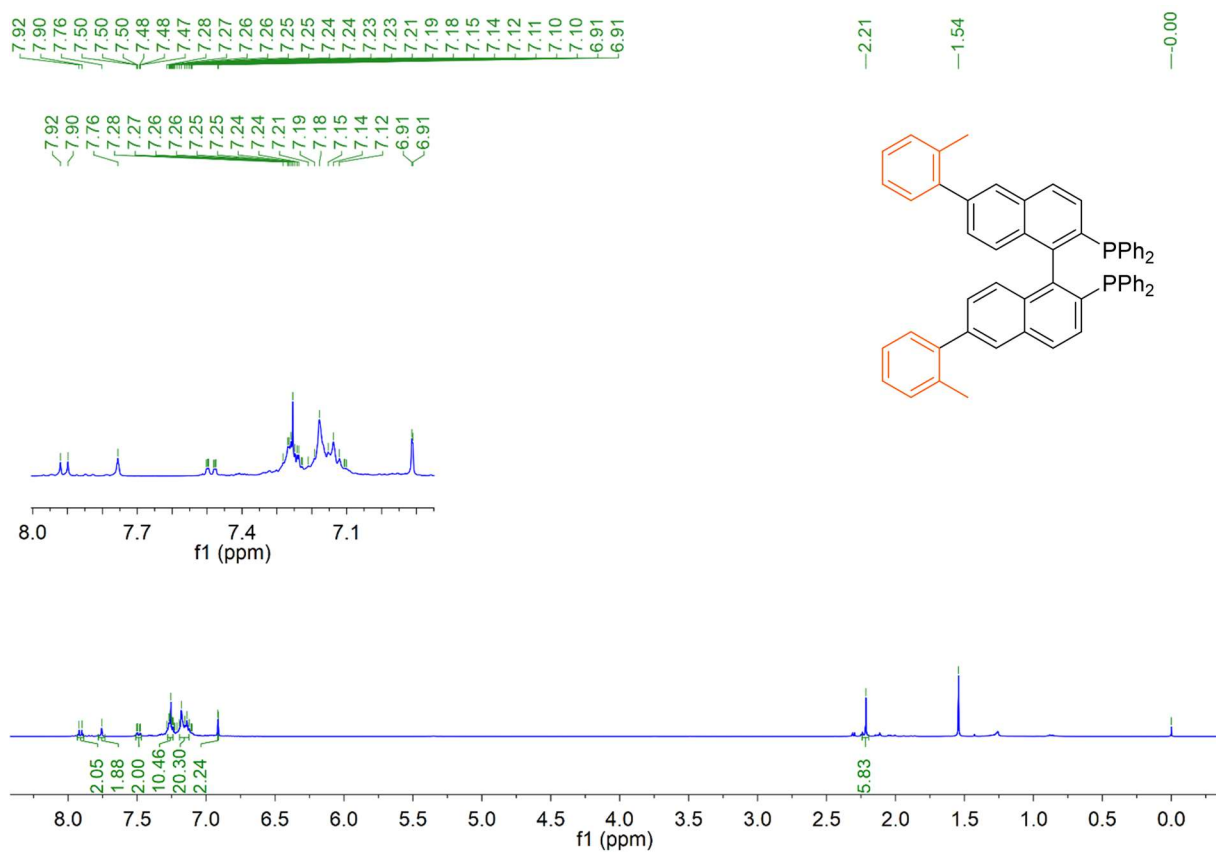
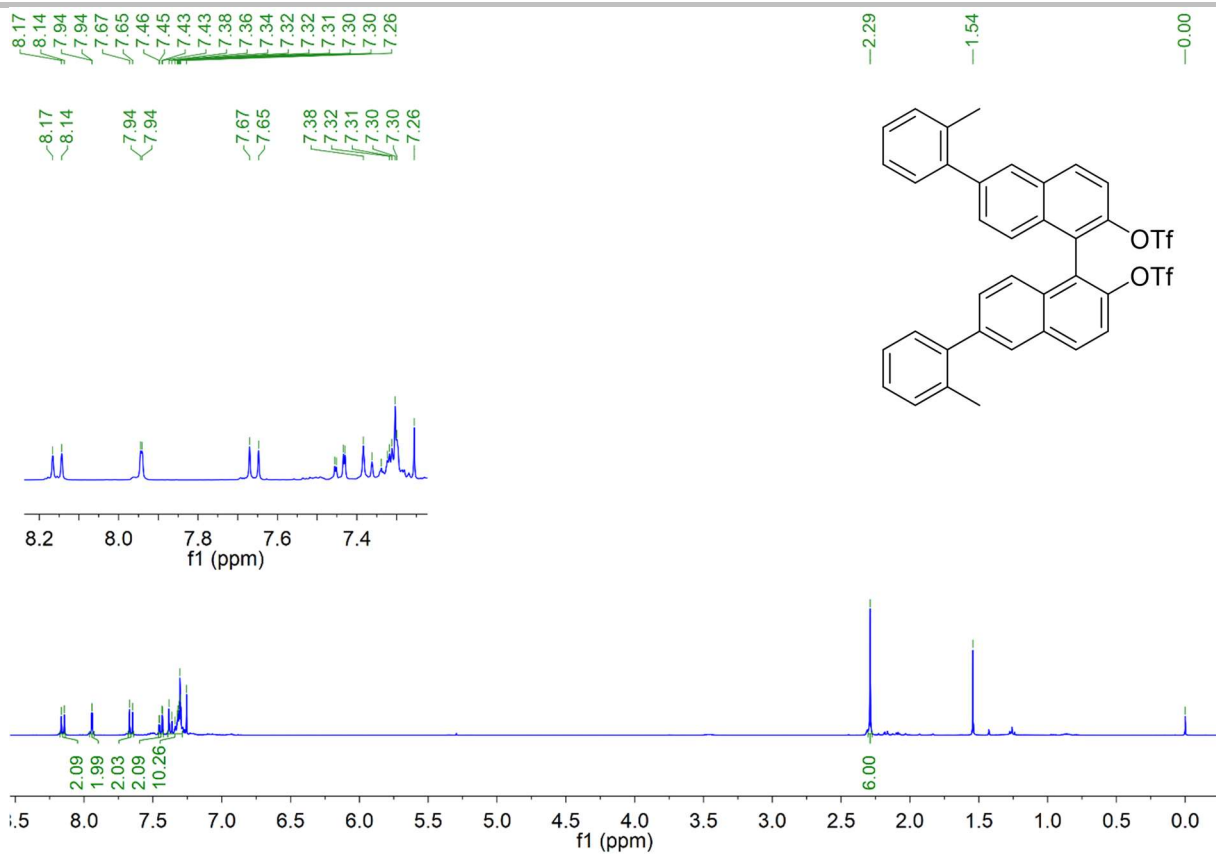
Supporting information



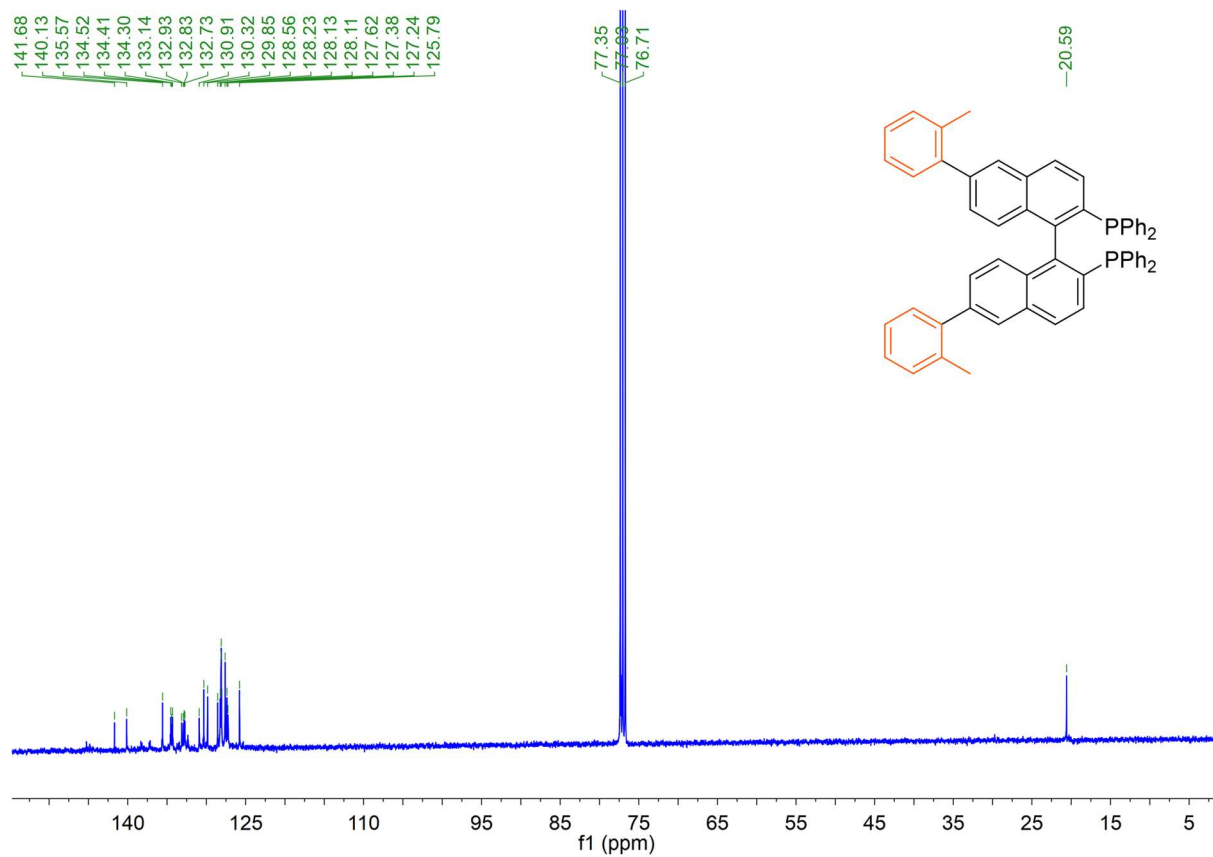
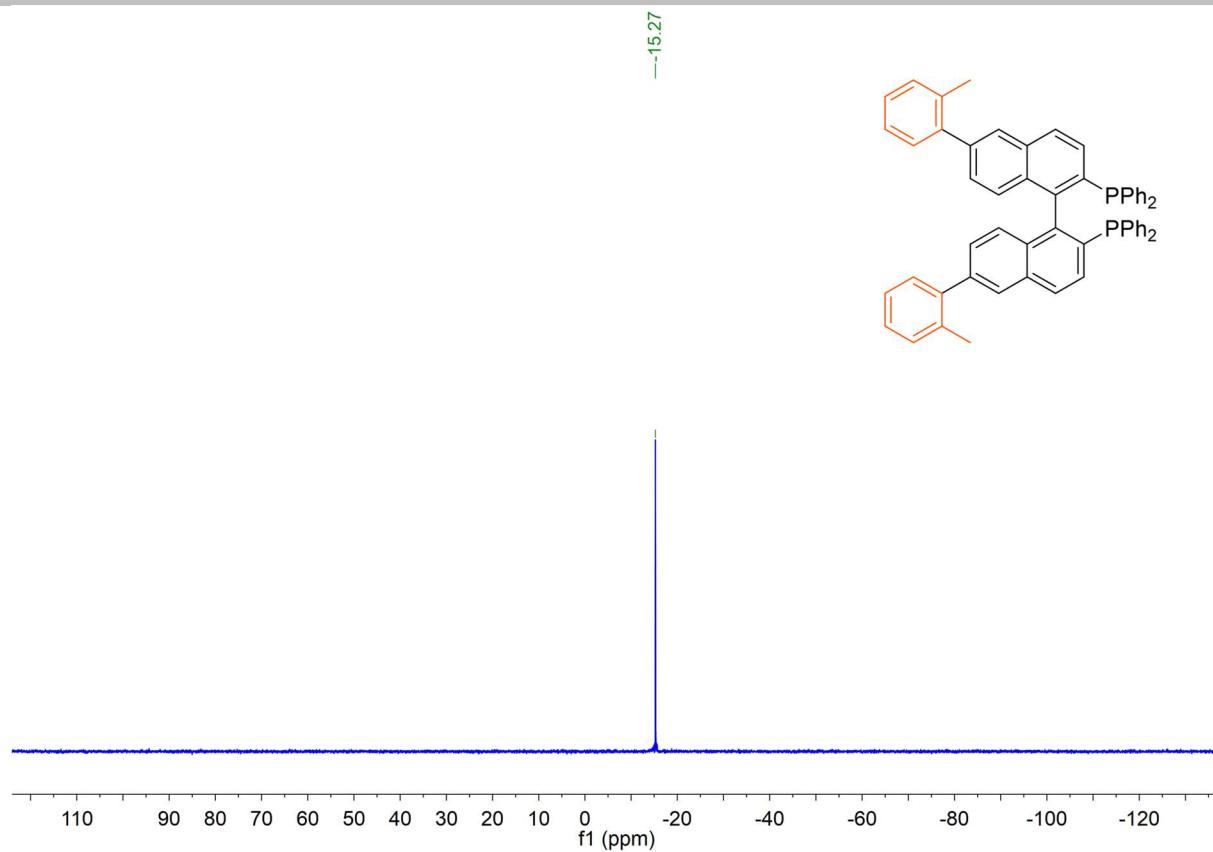
Supporting information



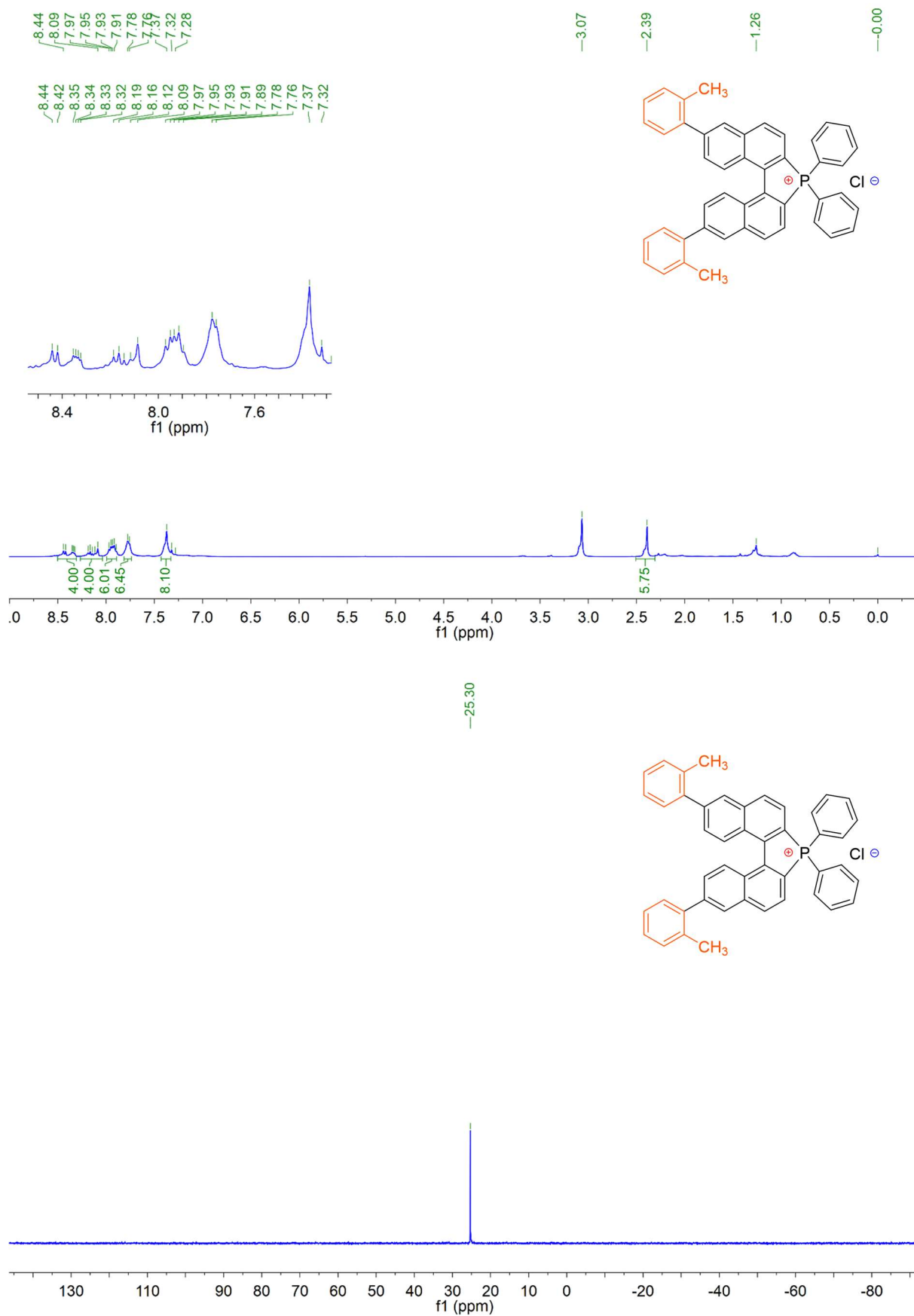
Supporting information



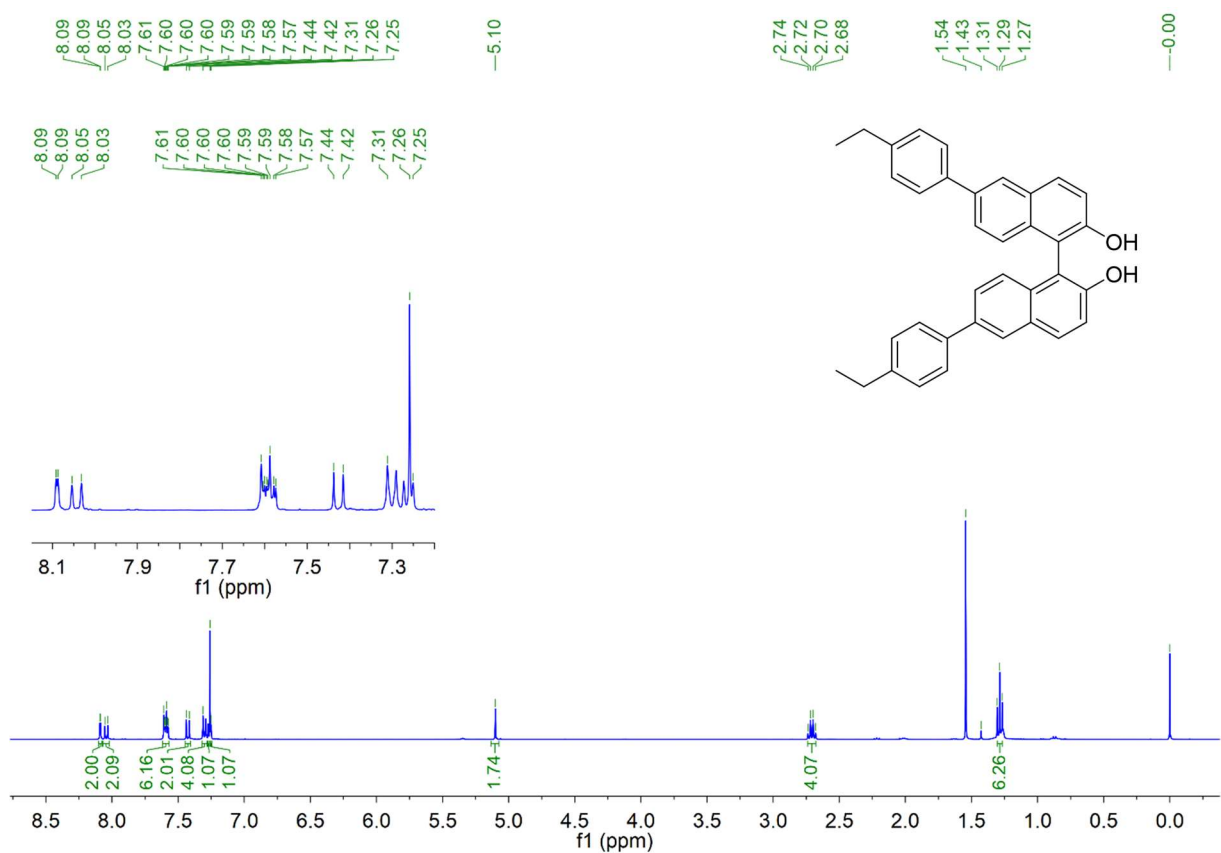
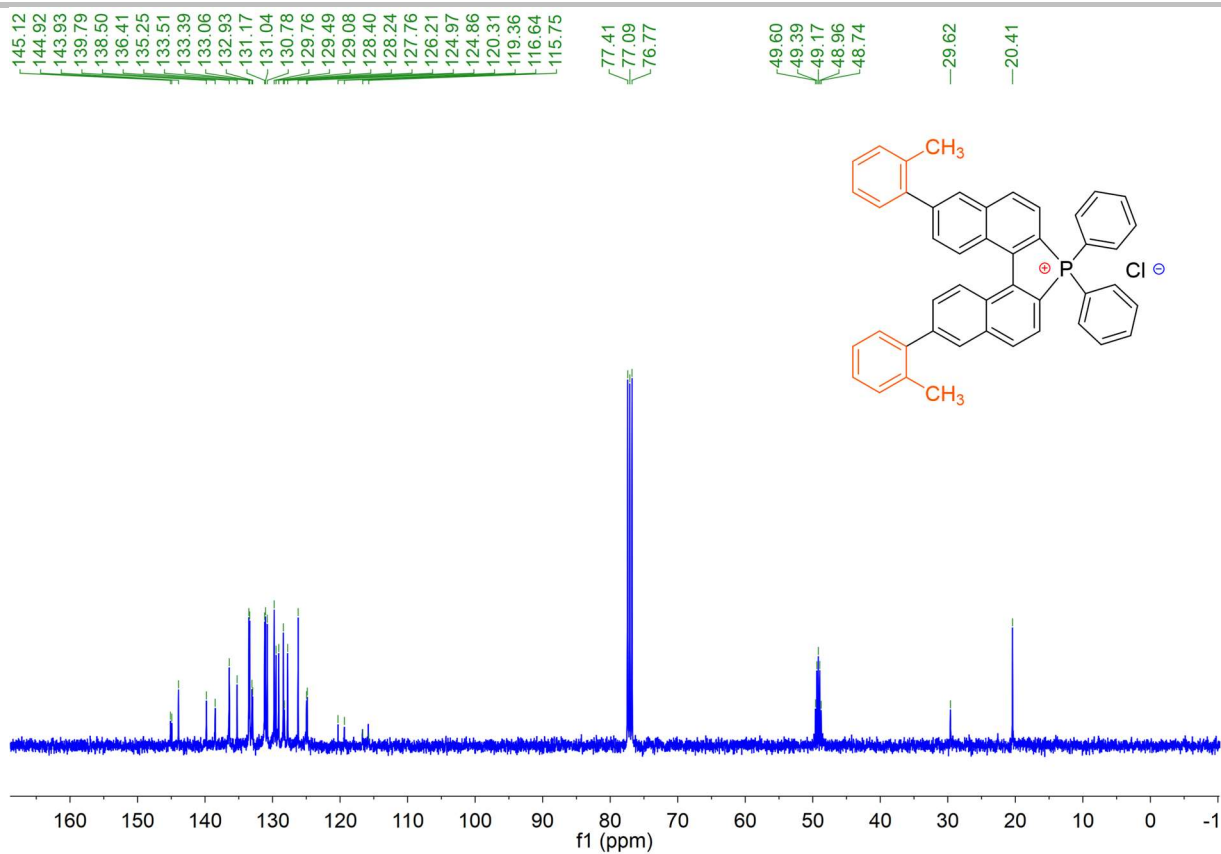
Supporting information



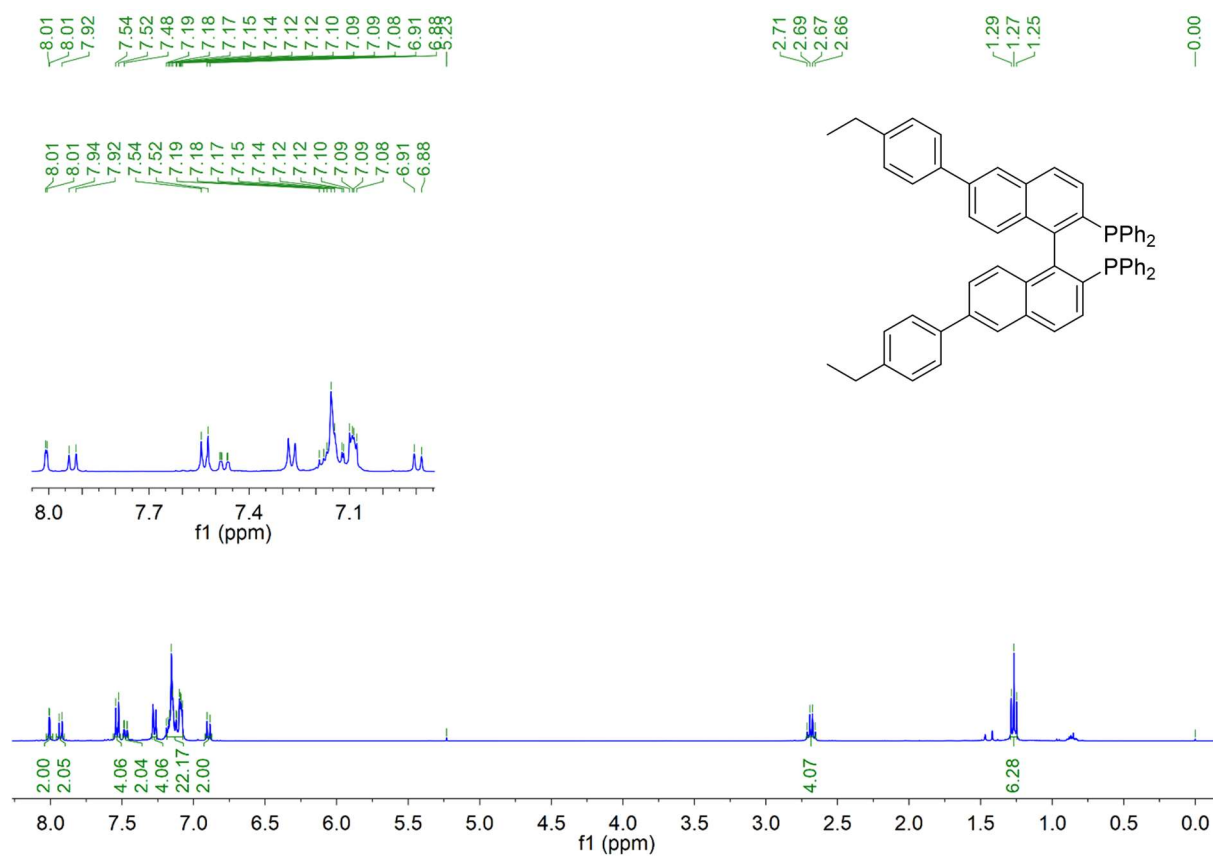
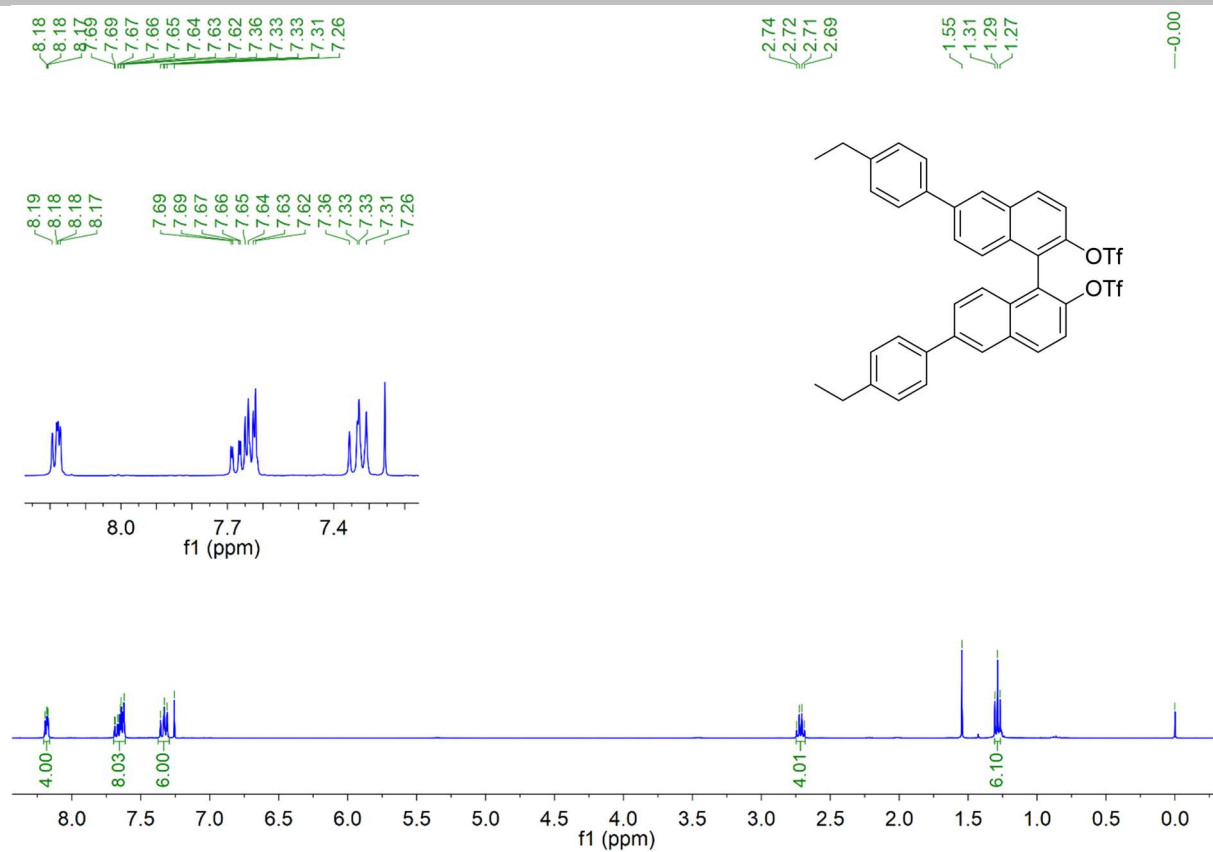
Supporting information



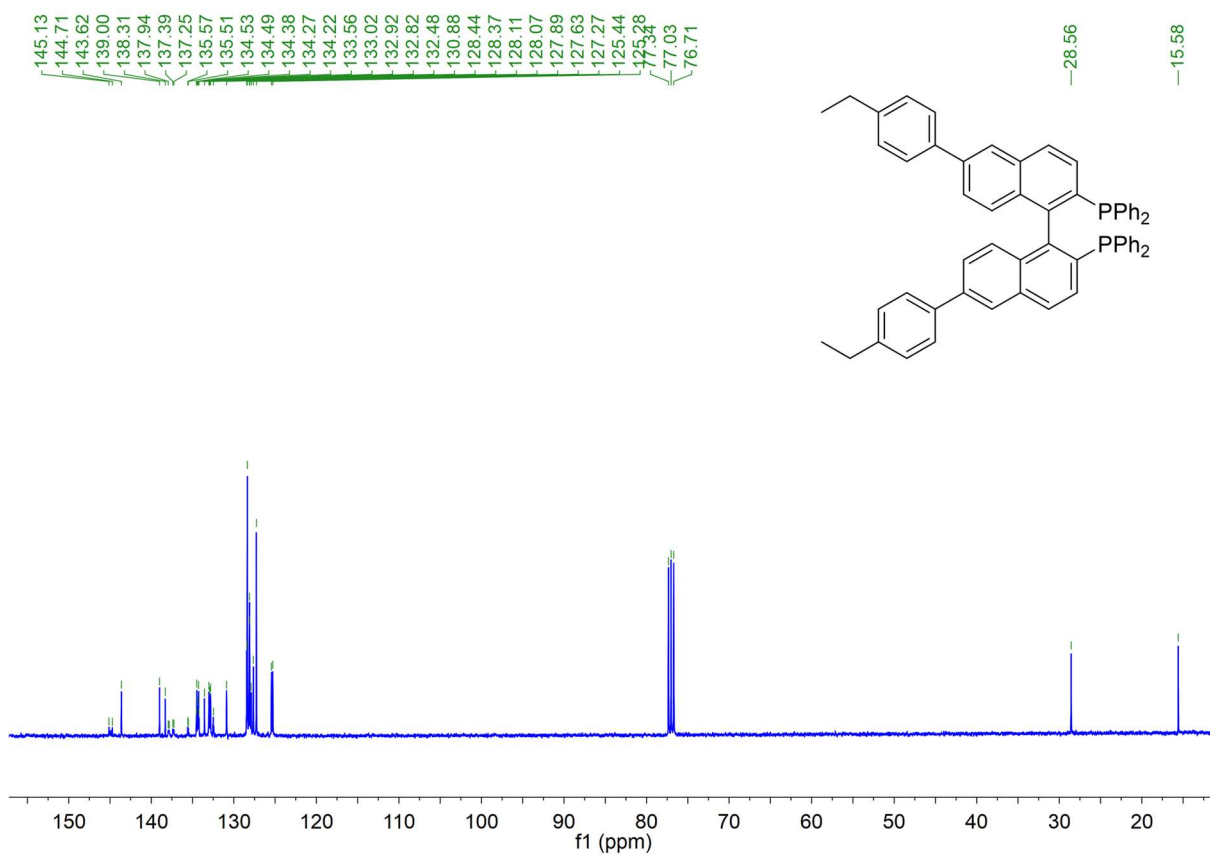
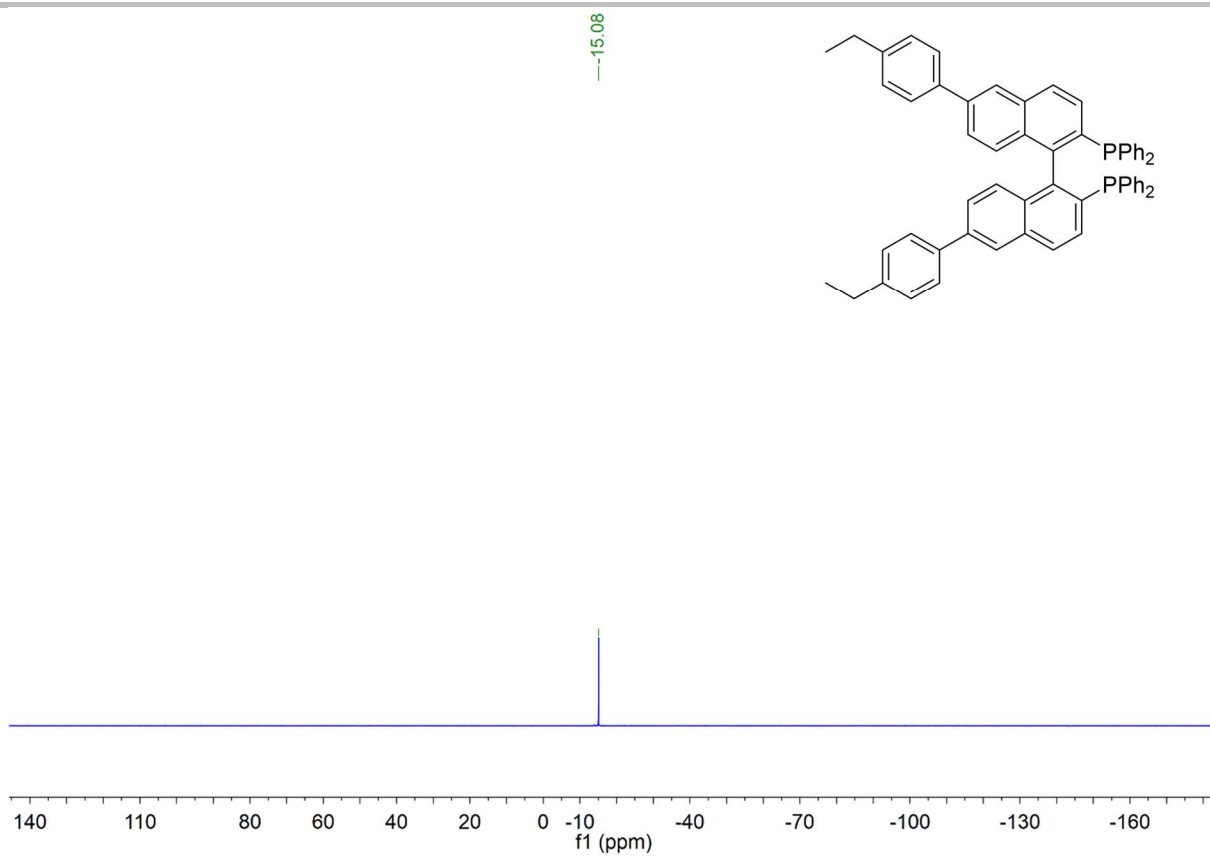
Supporting information



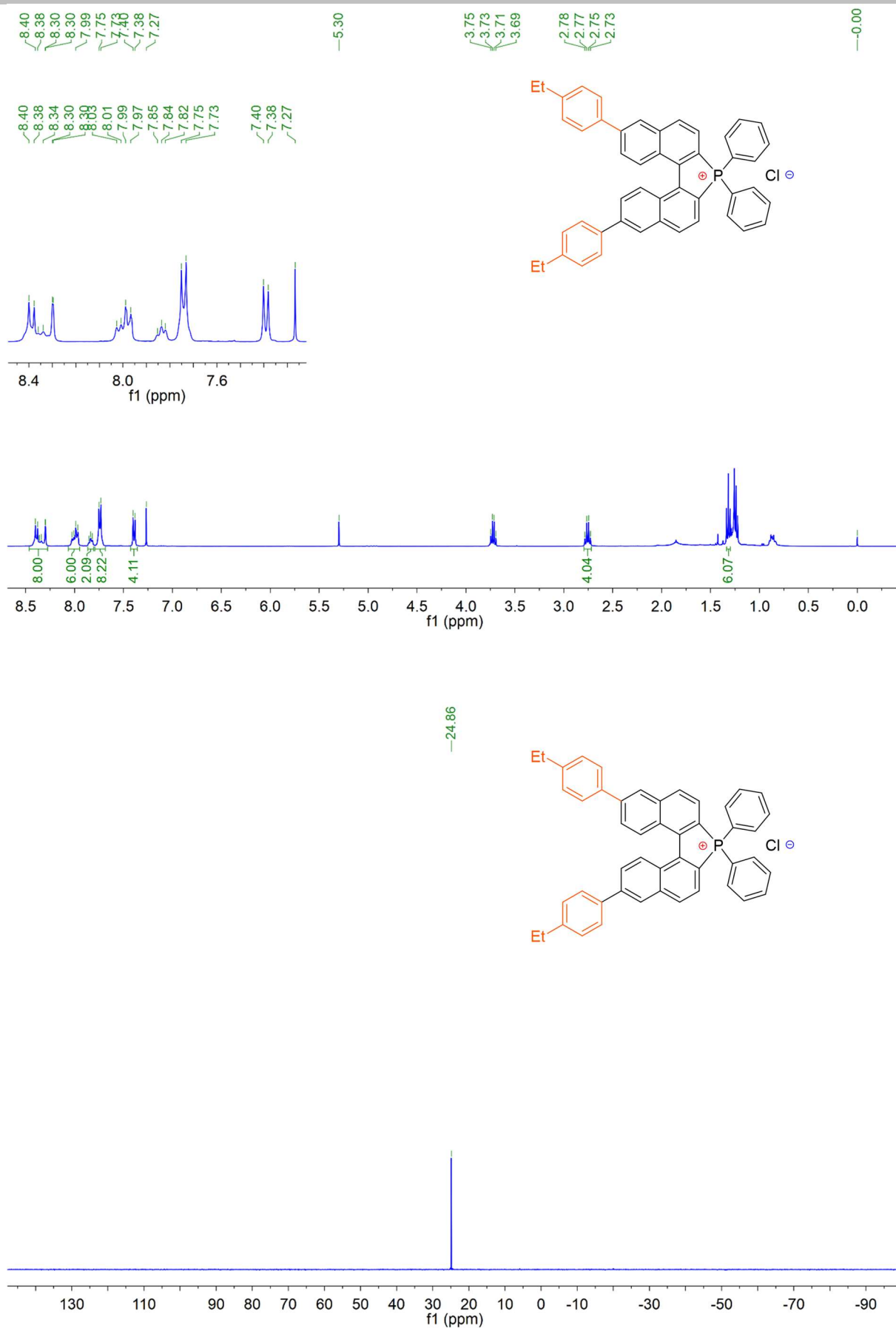
Supporting information



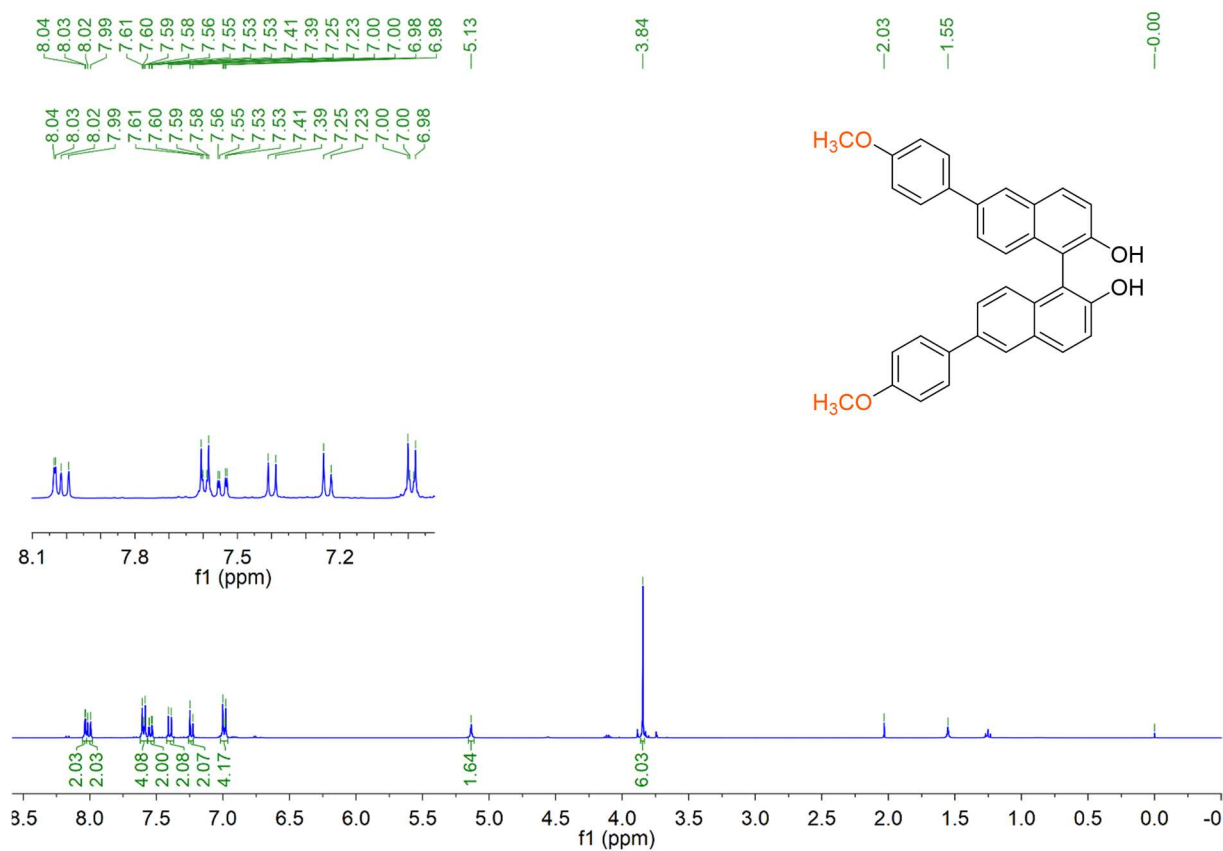
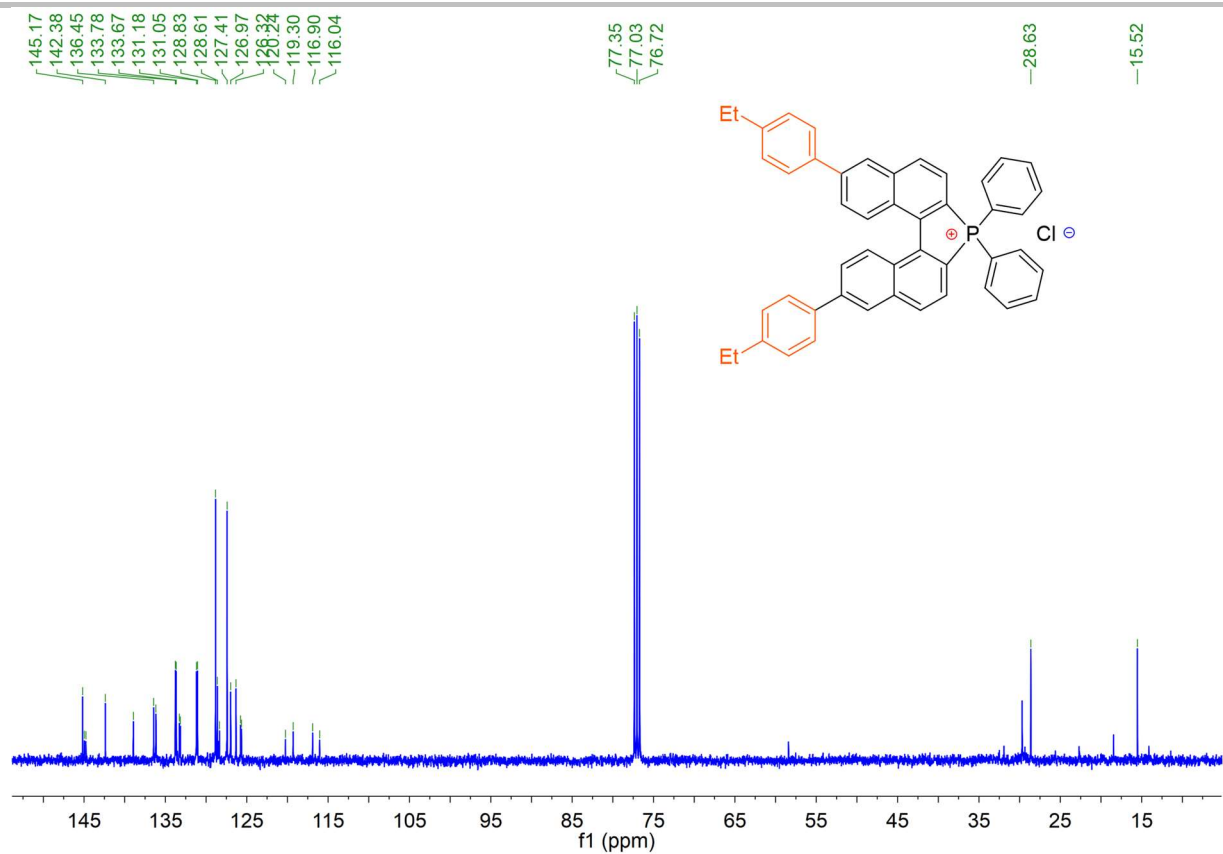
Supporting information



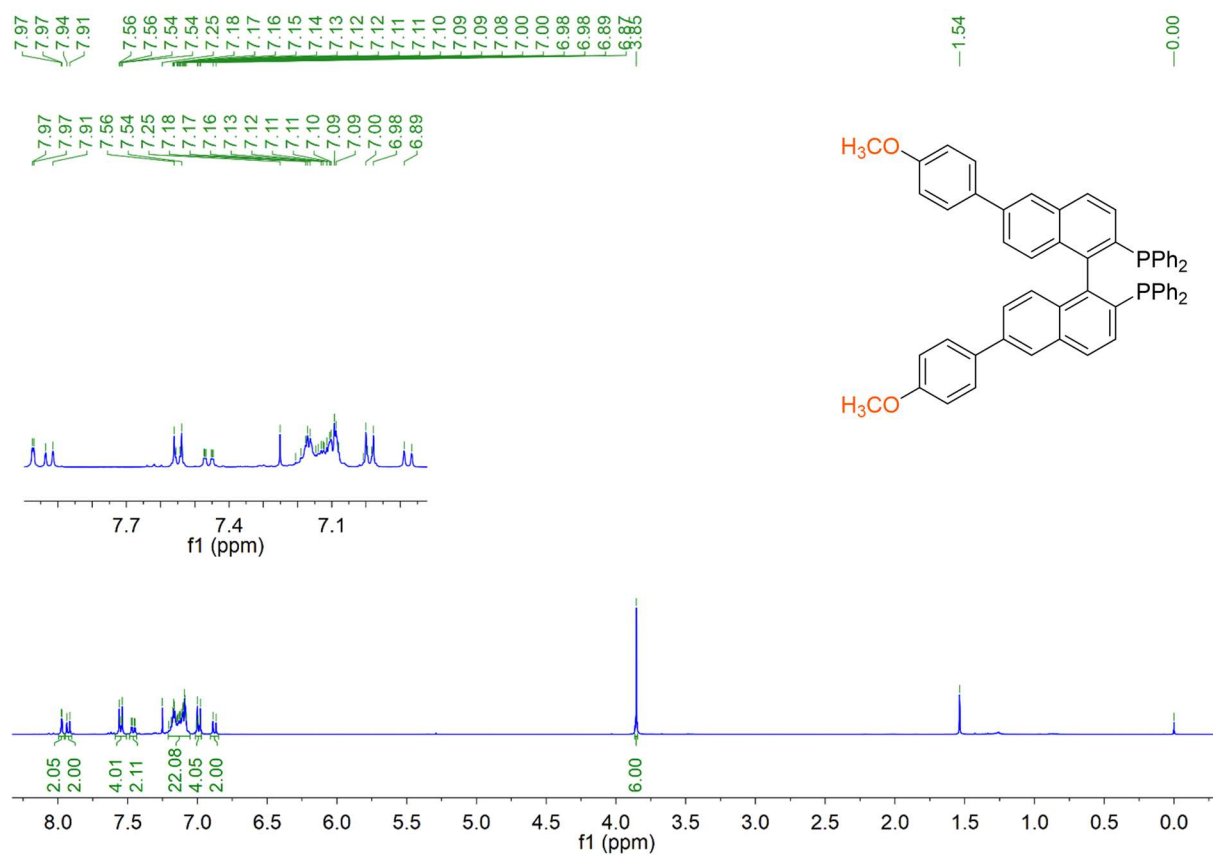
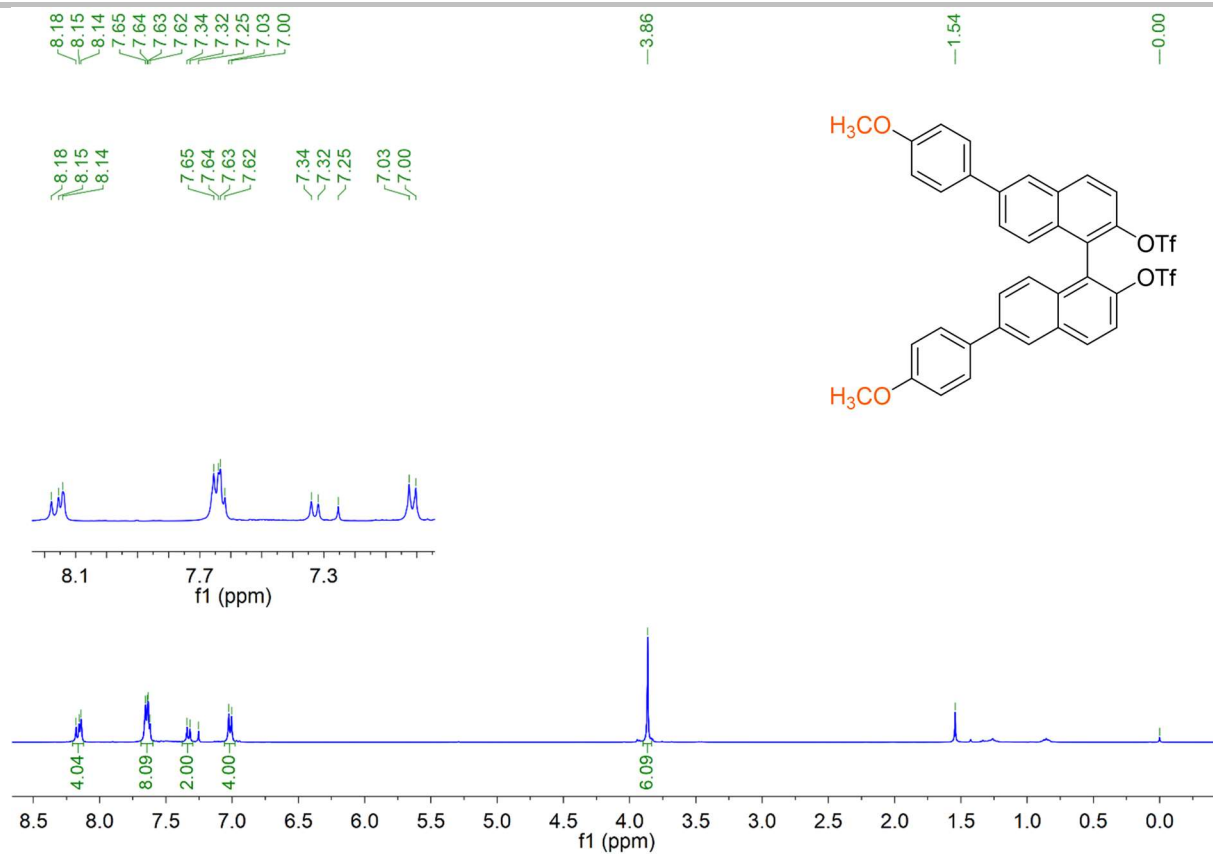
Supporting information



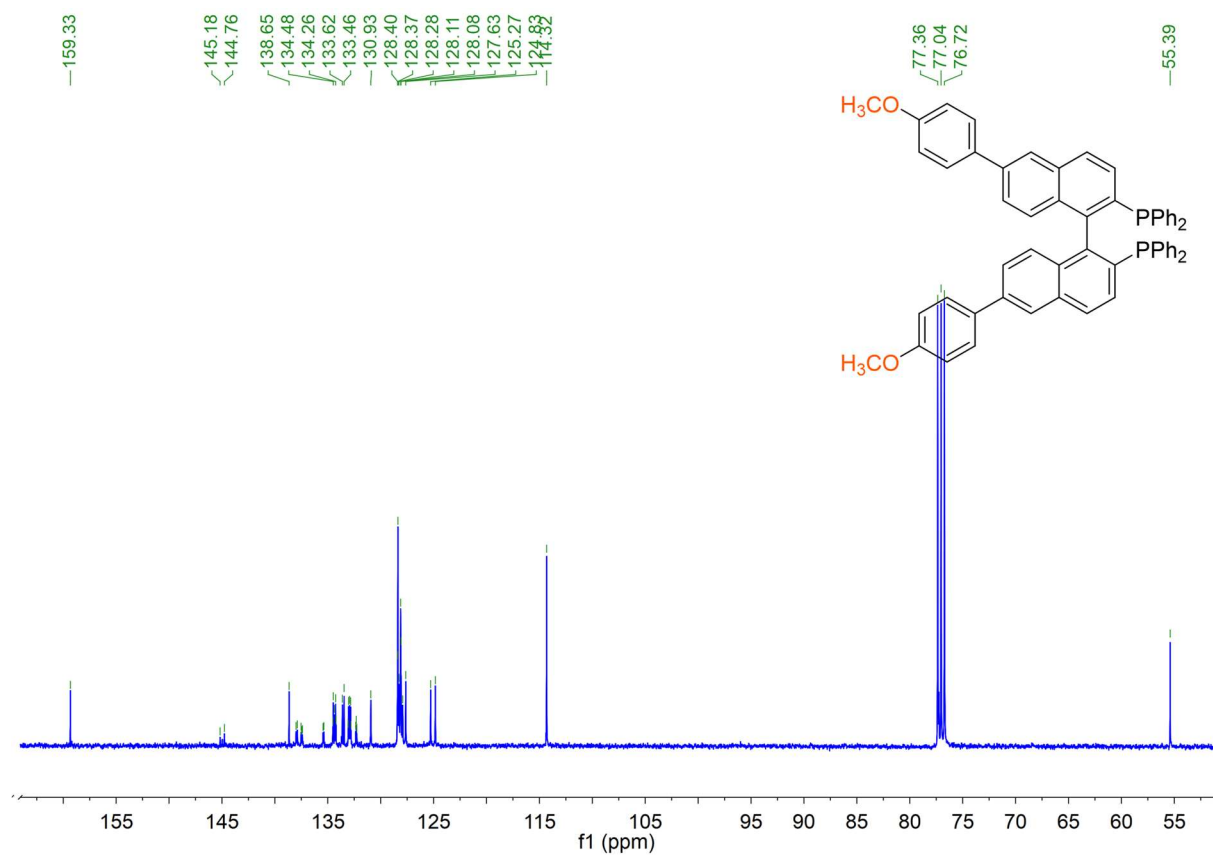
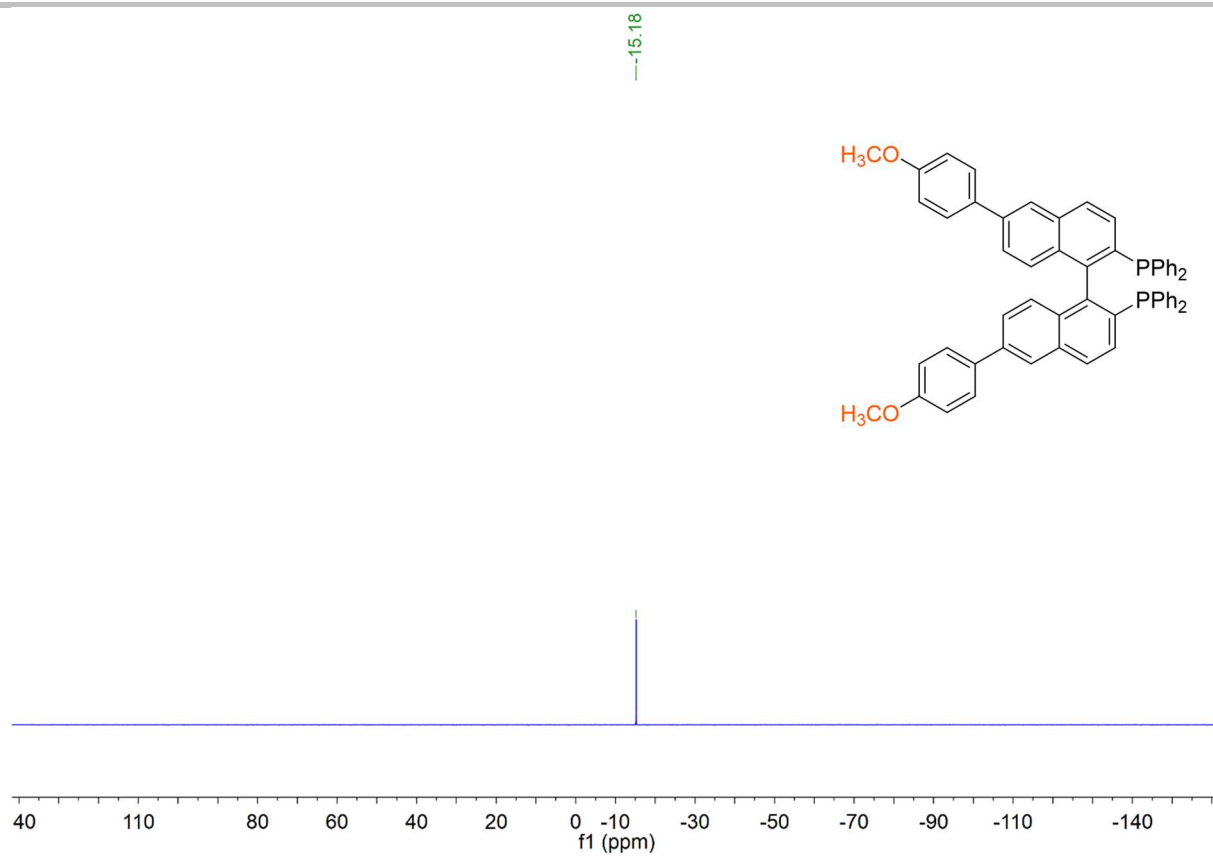
Supporting information



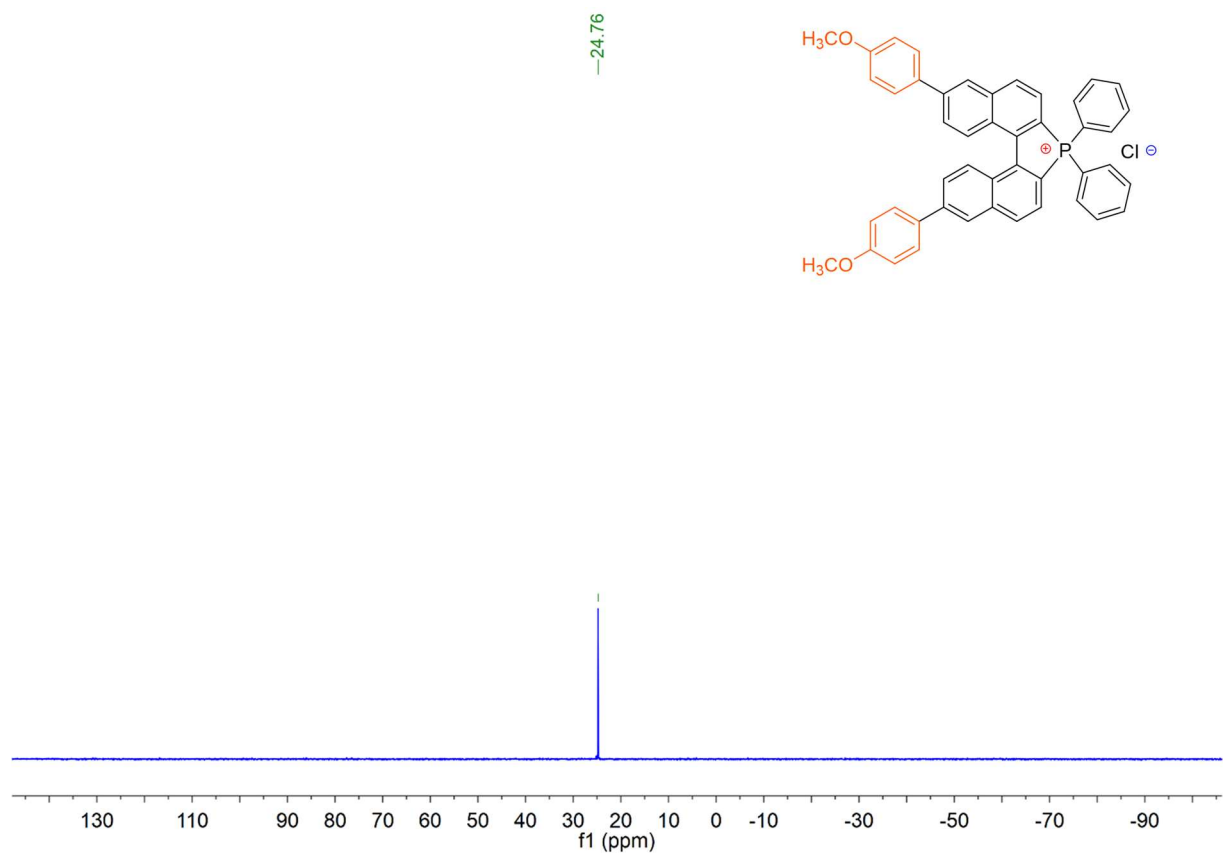
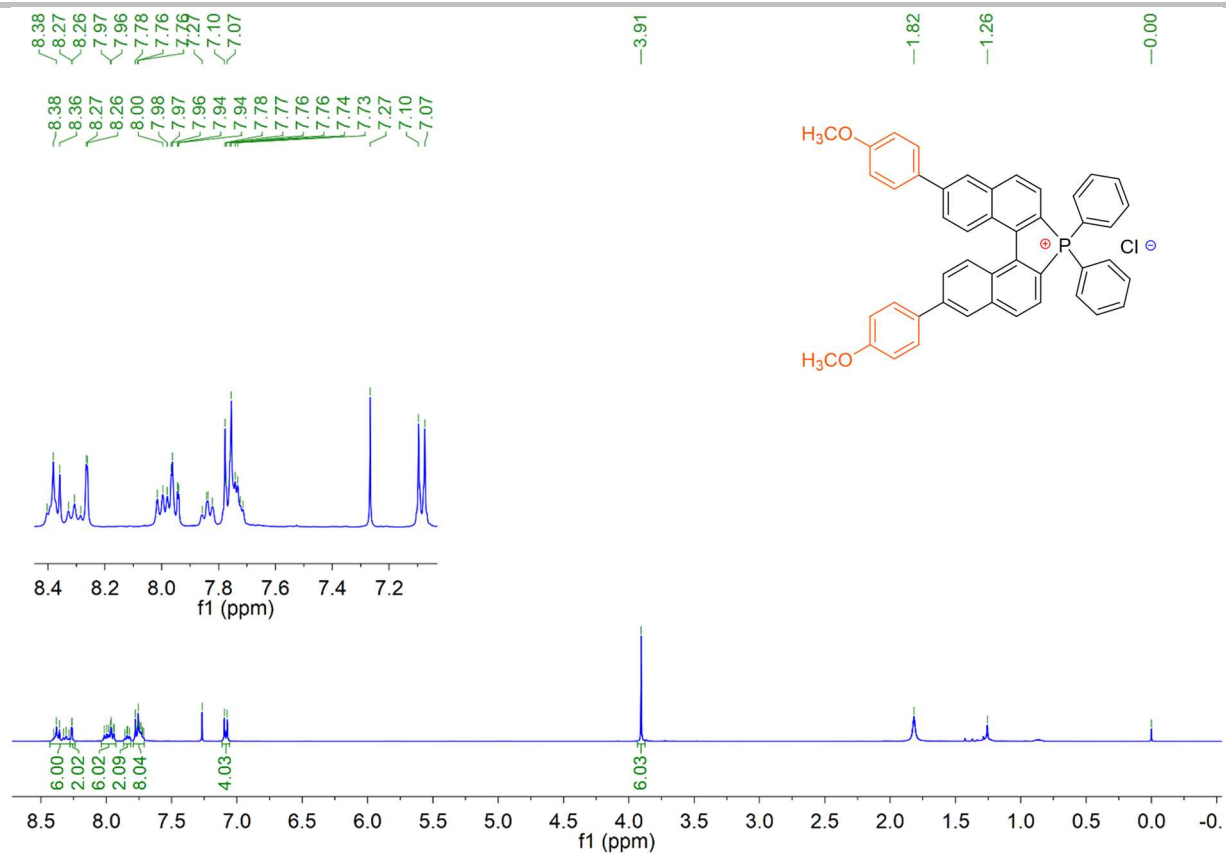
Supporting information



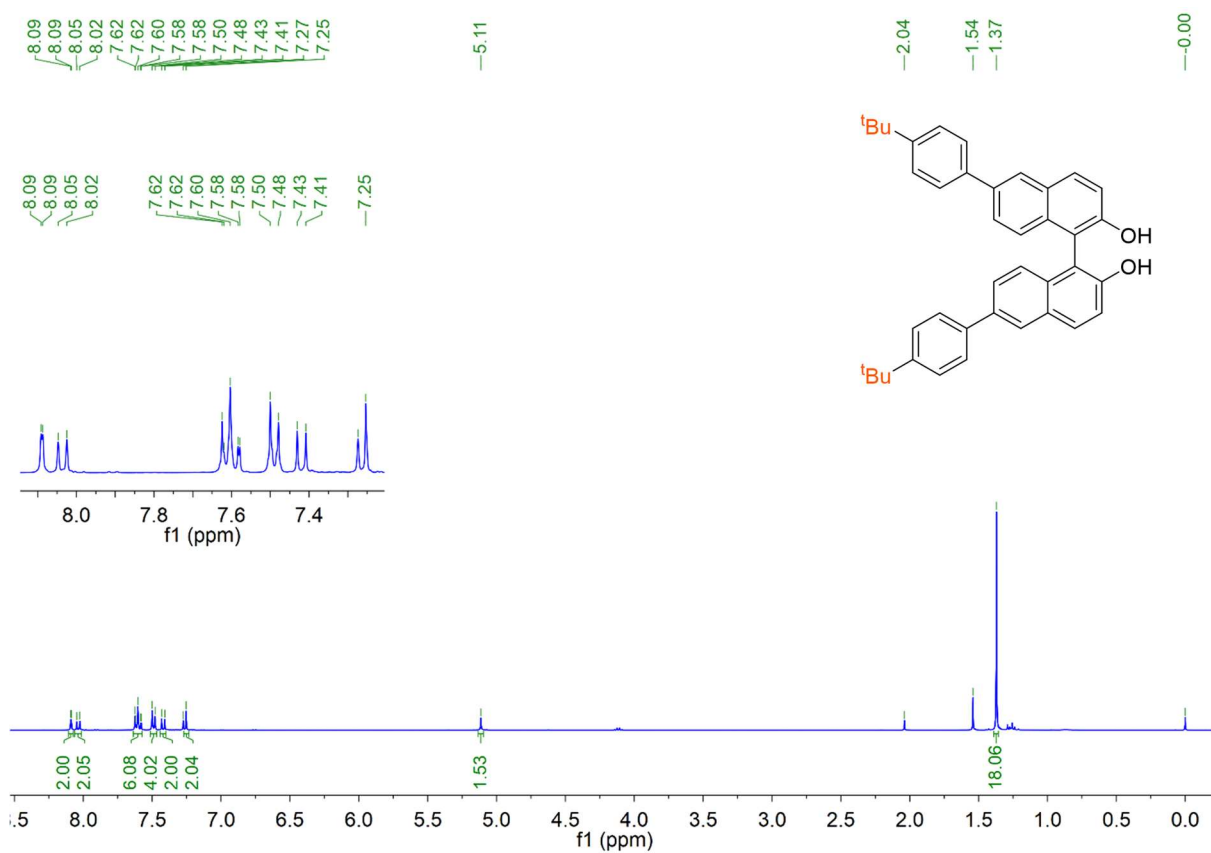
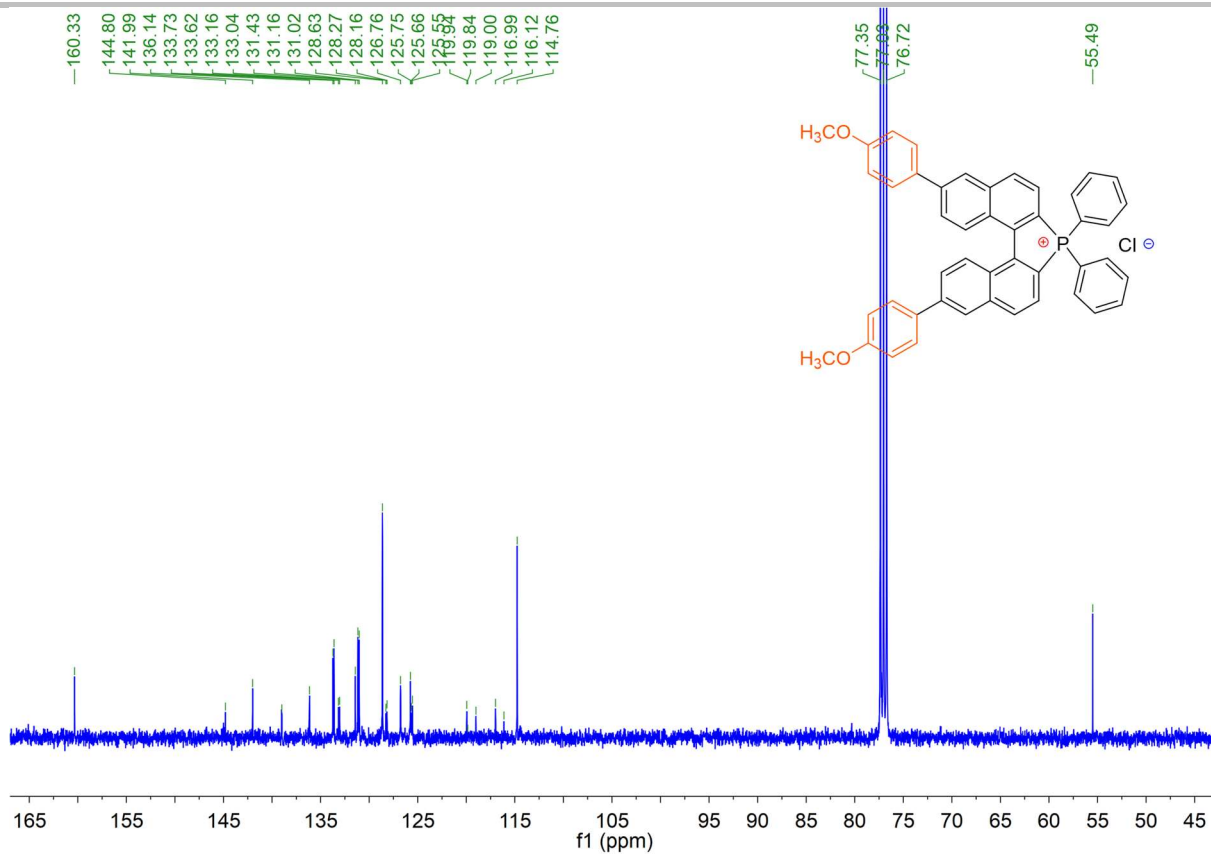
Supporting information



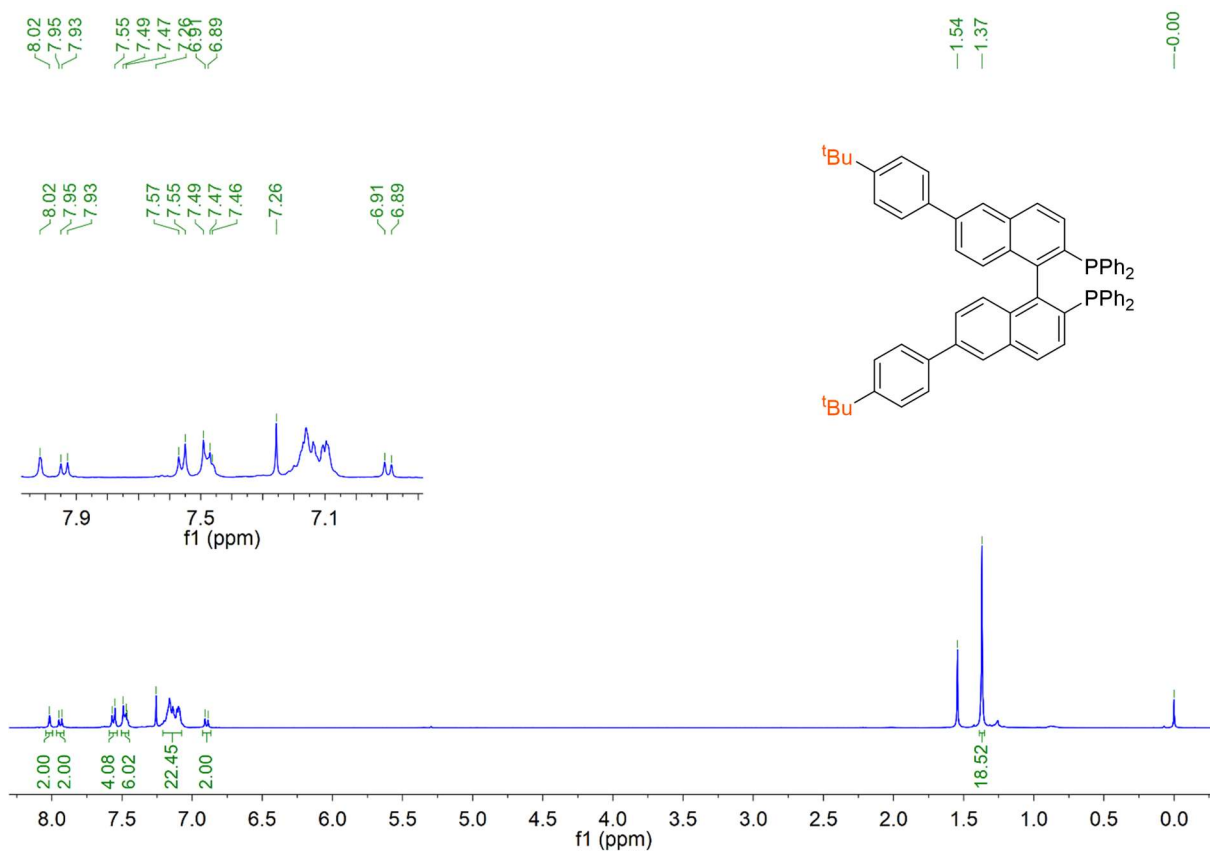
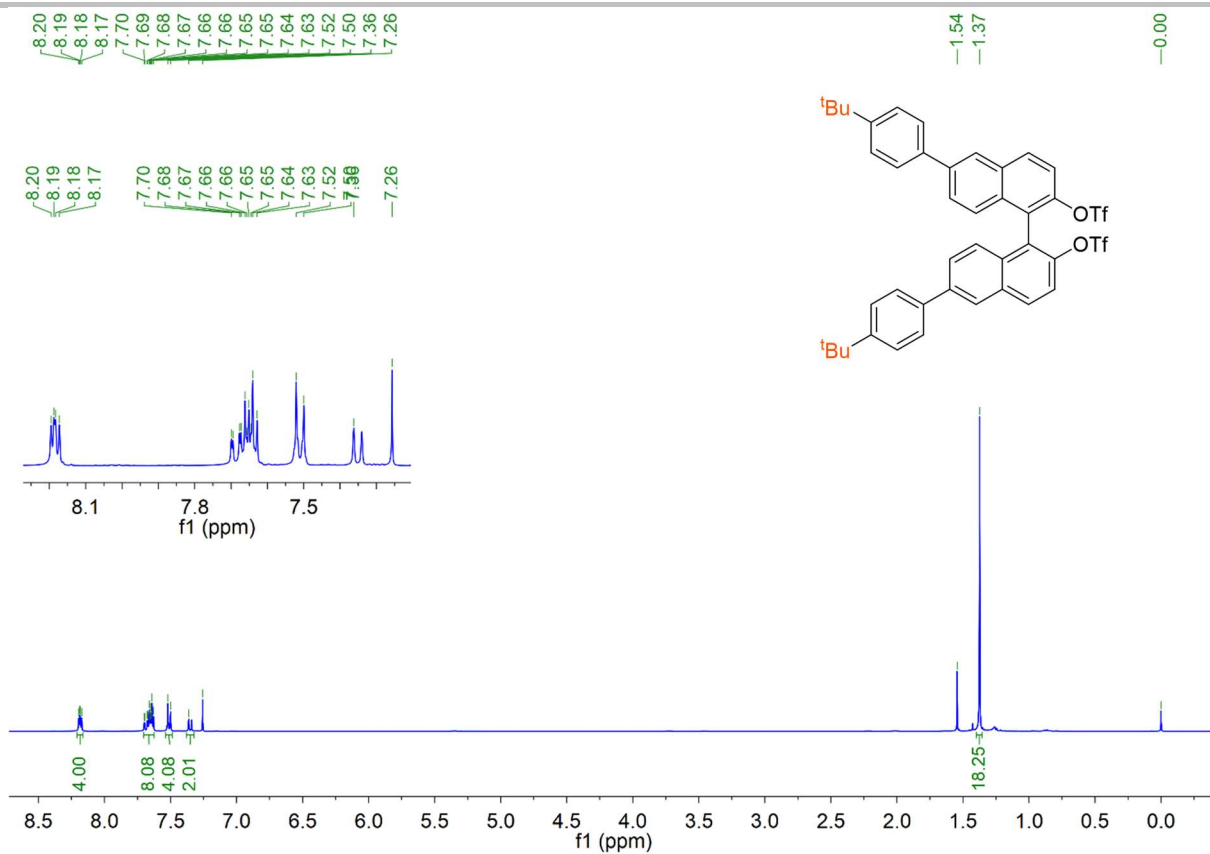
Supporting information



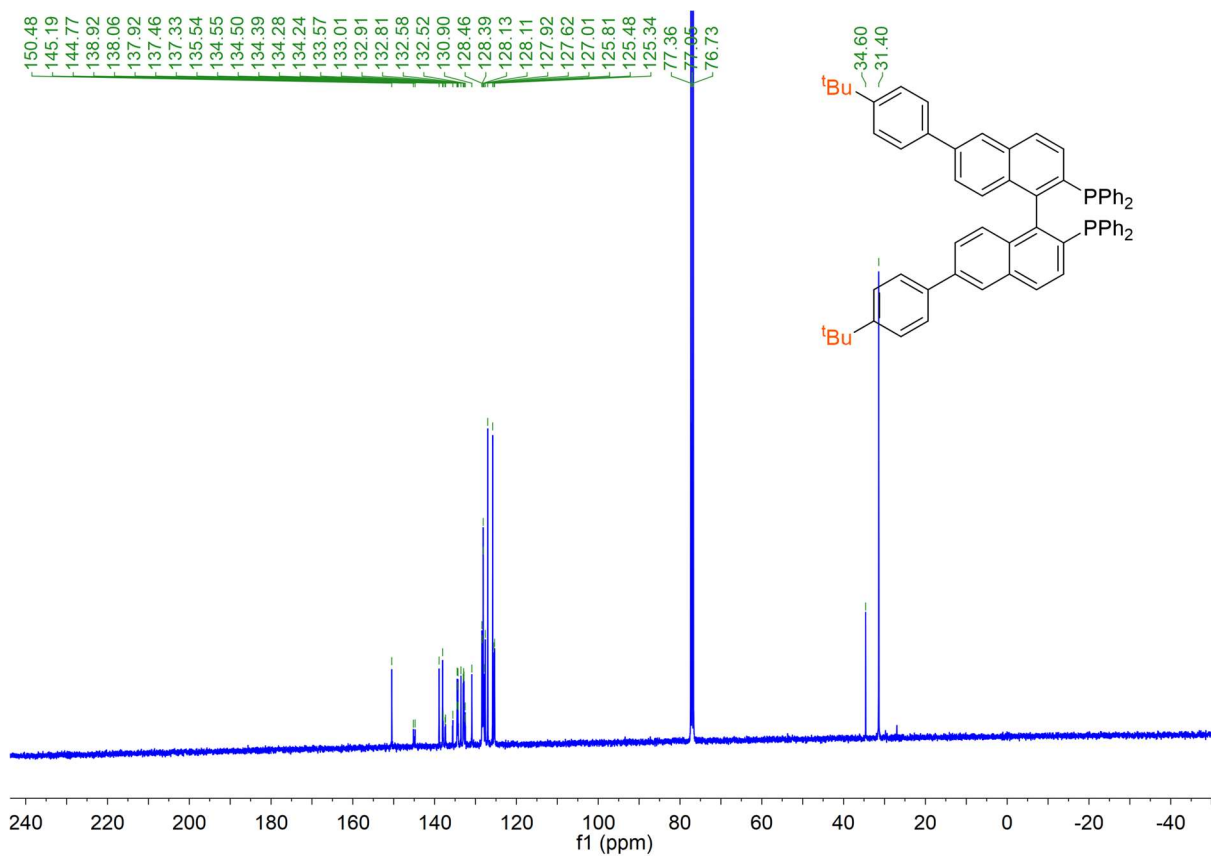
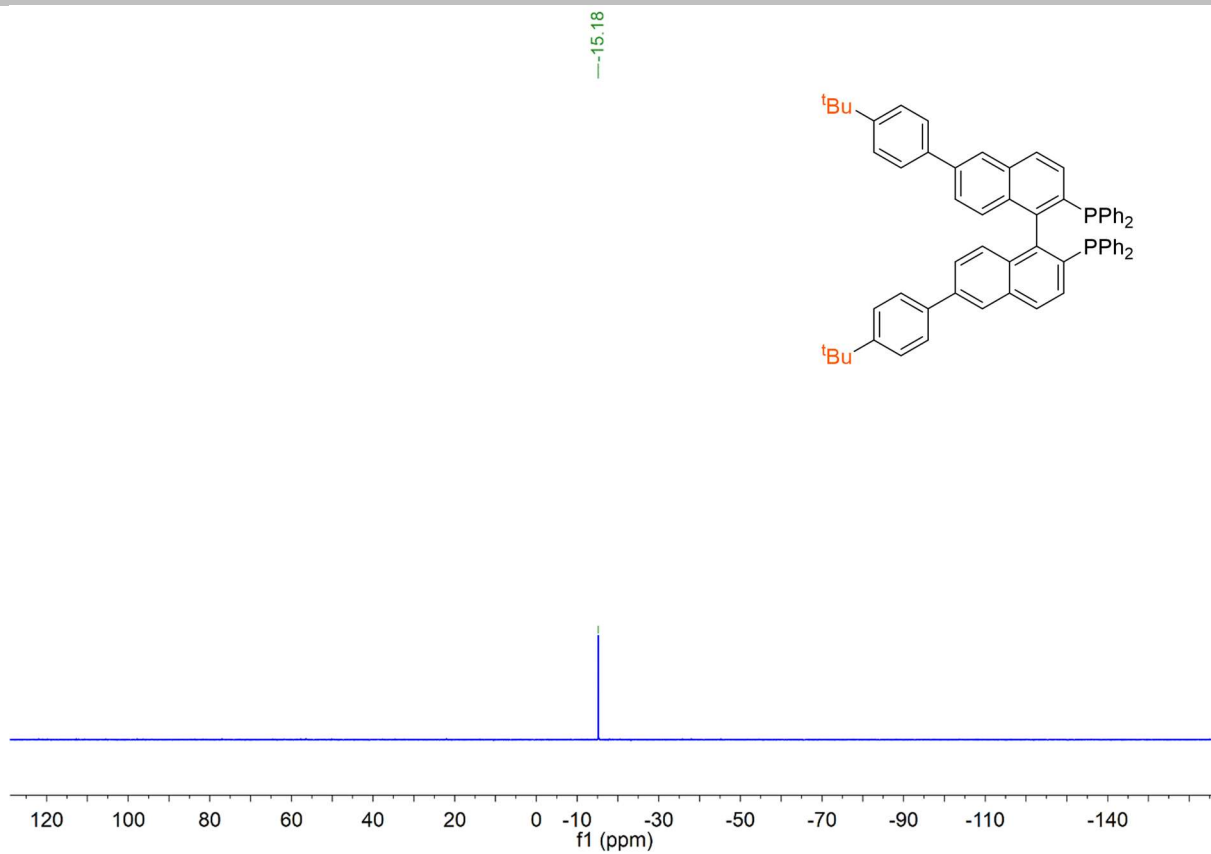
Supporting information



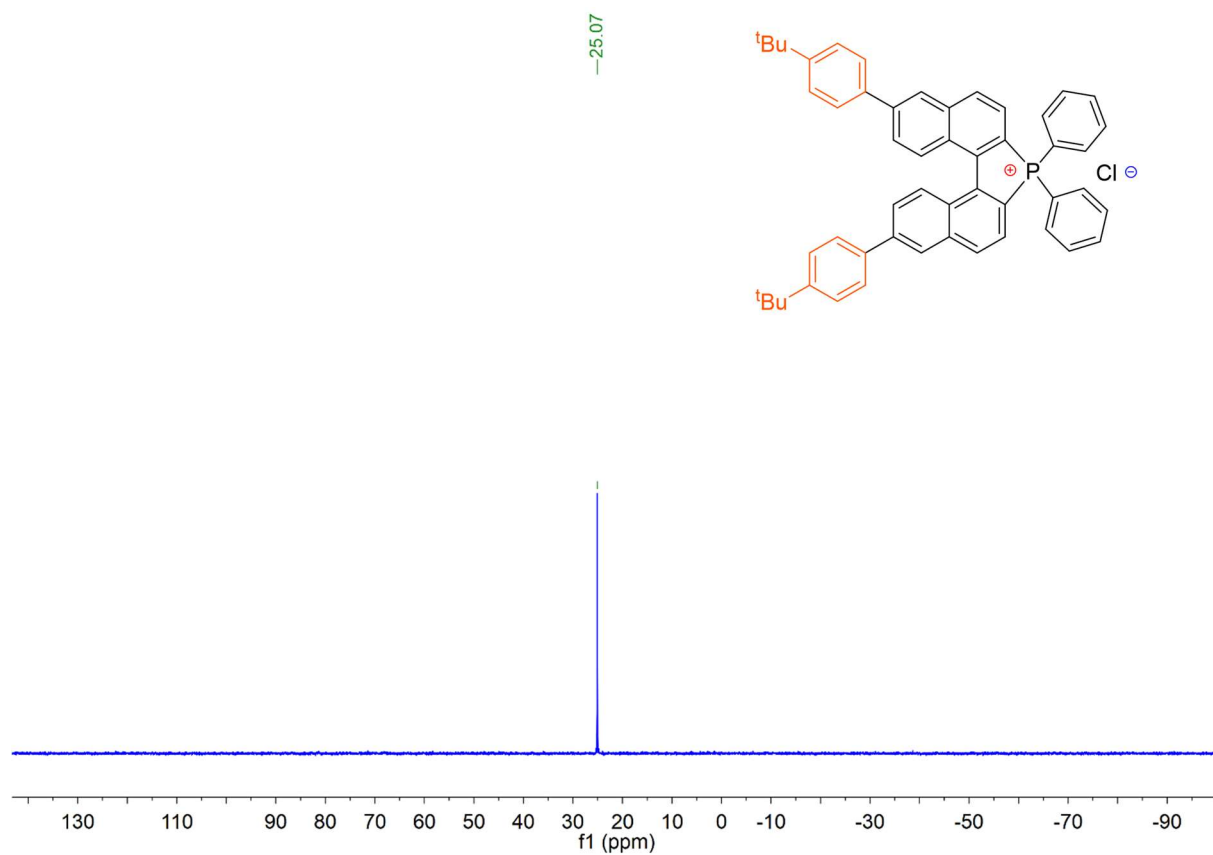
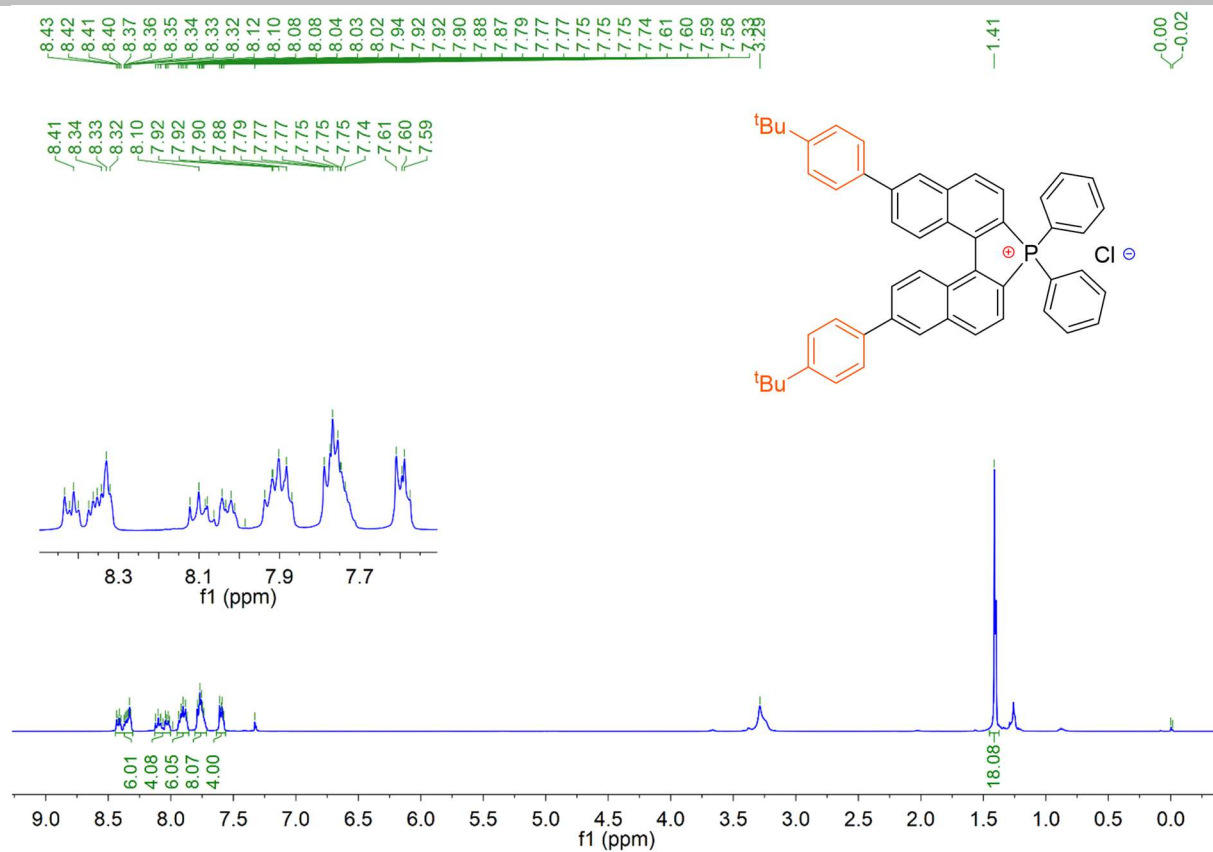
Supporting information



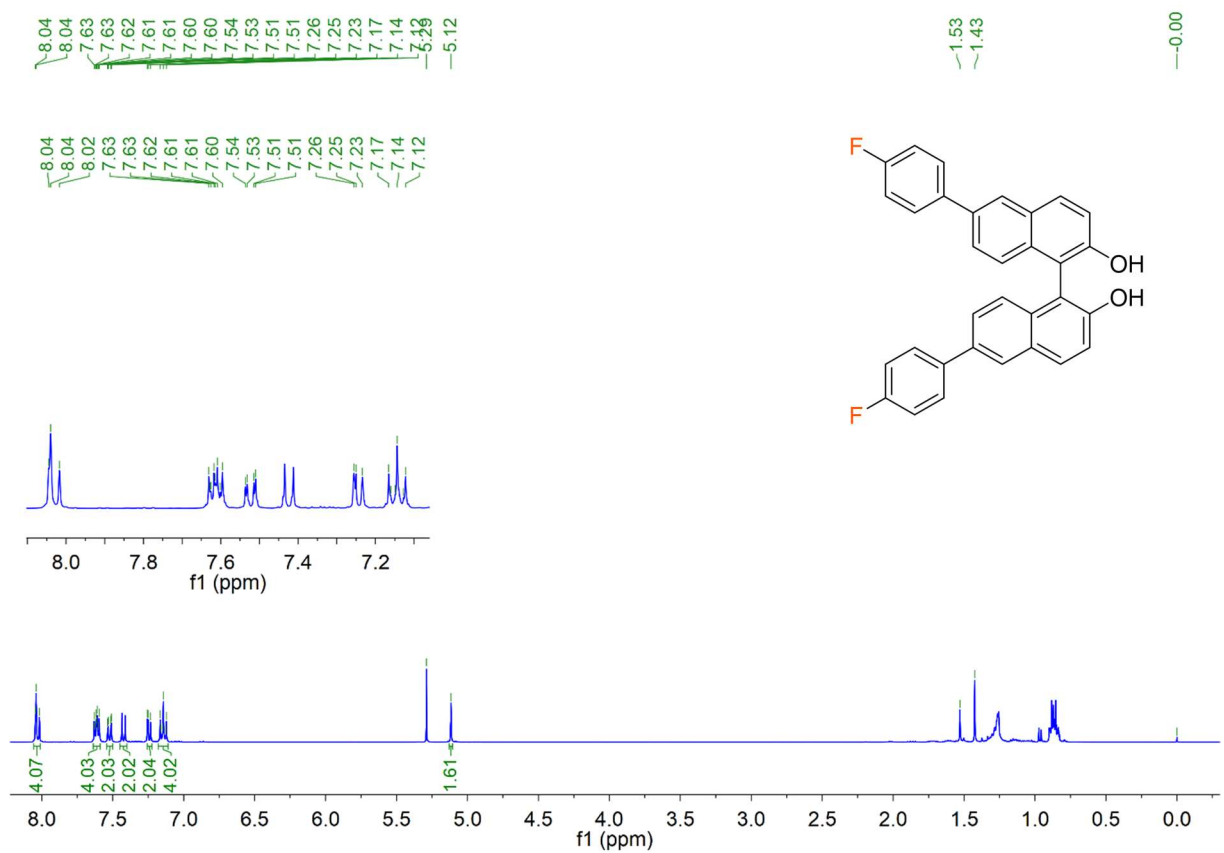
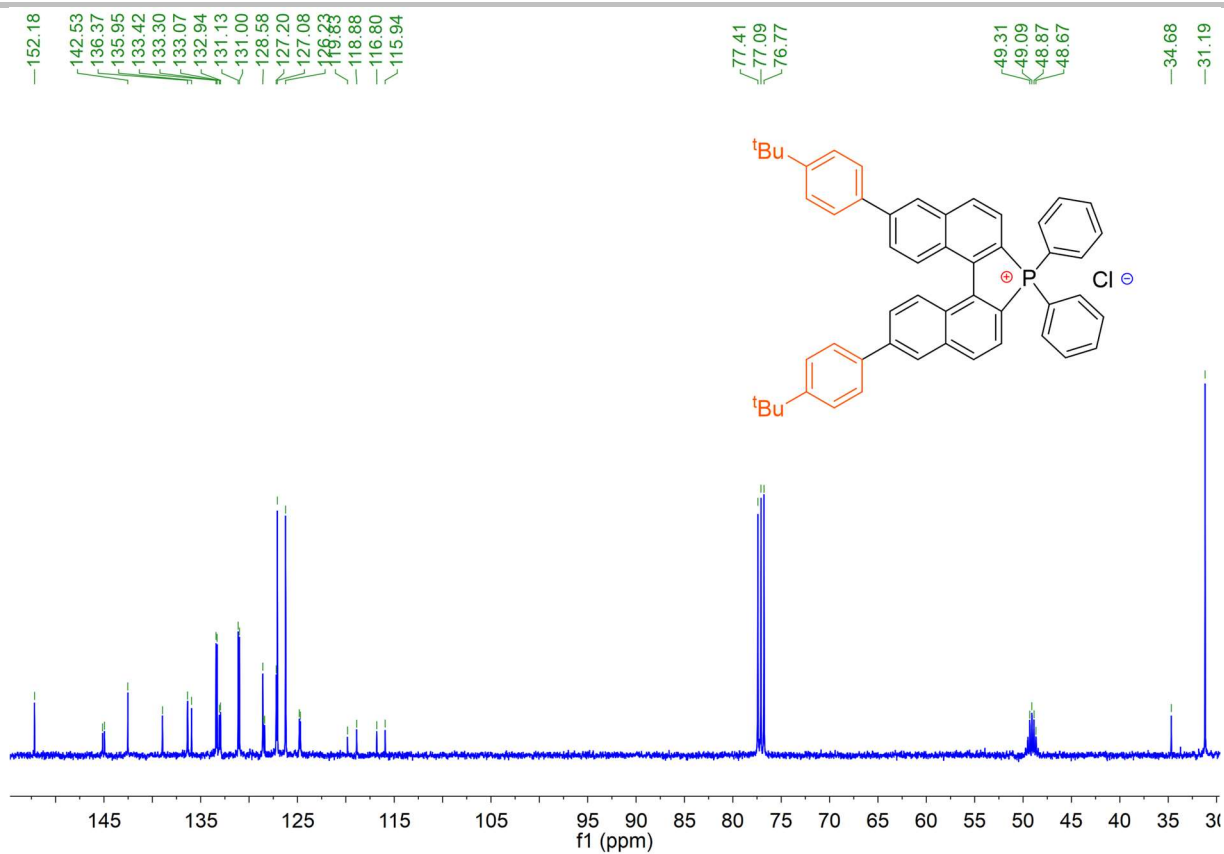
Supporting information



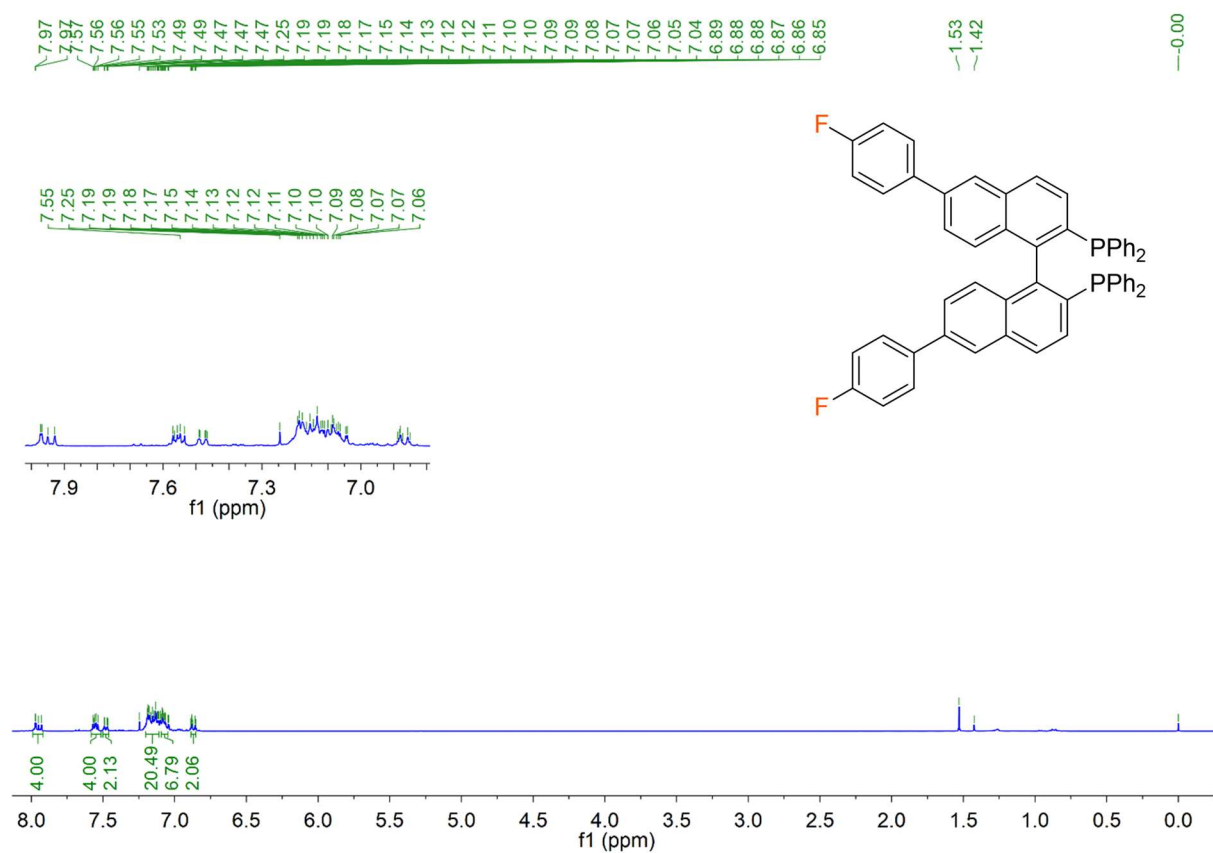
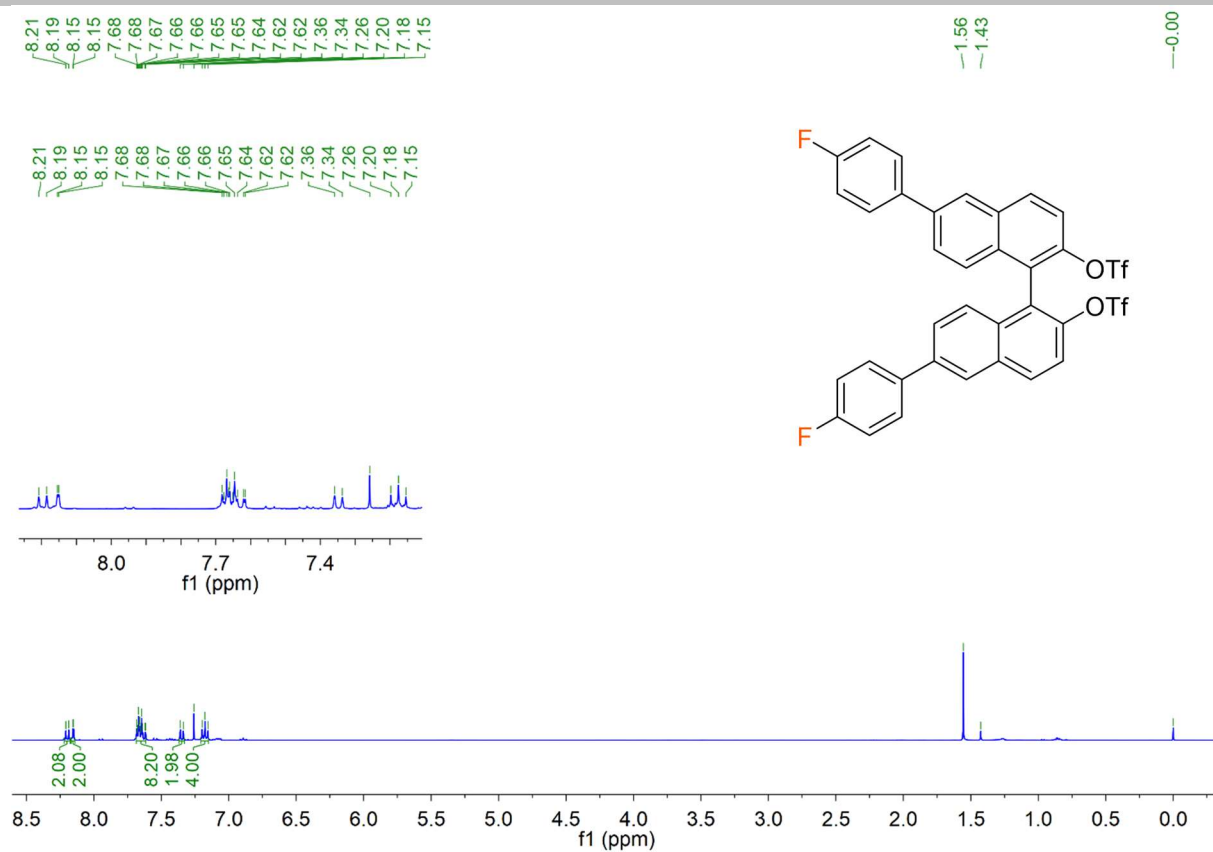
Supporting information



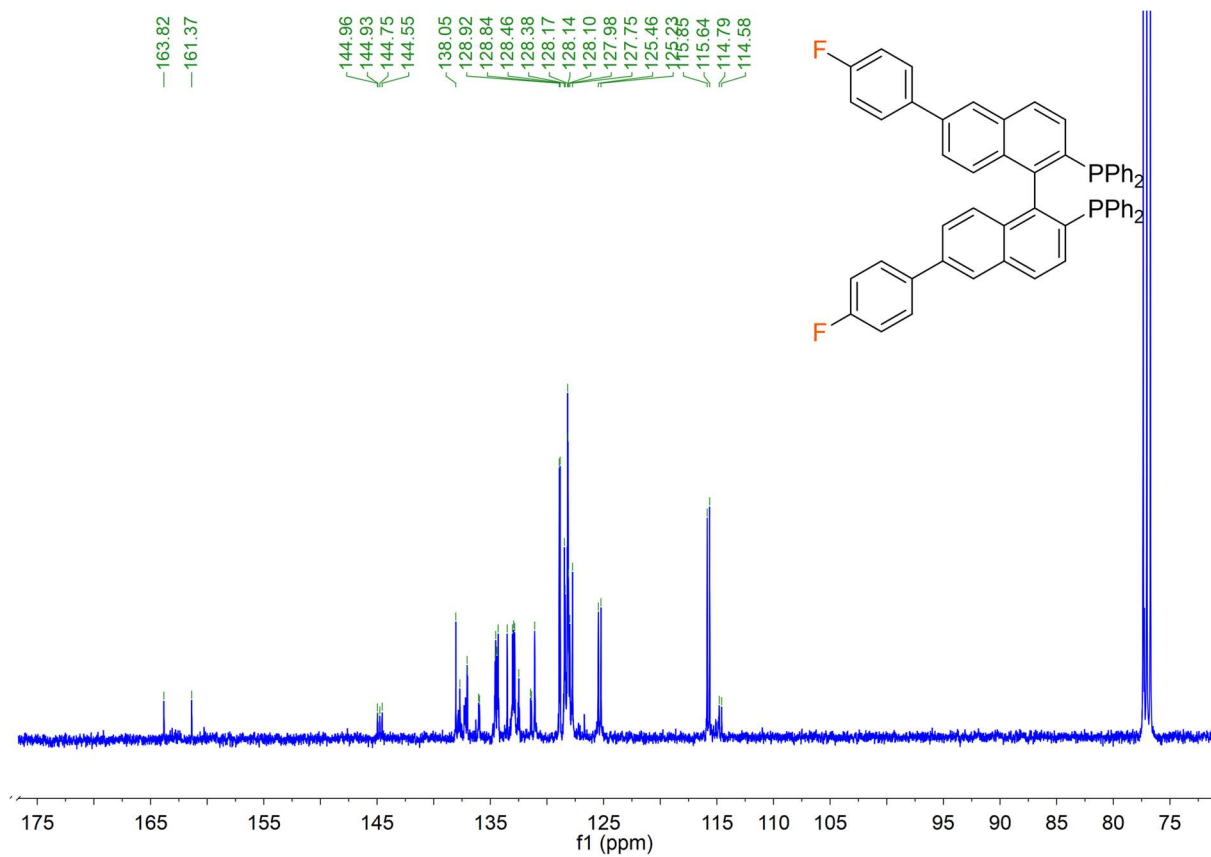
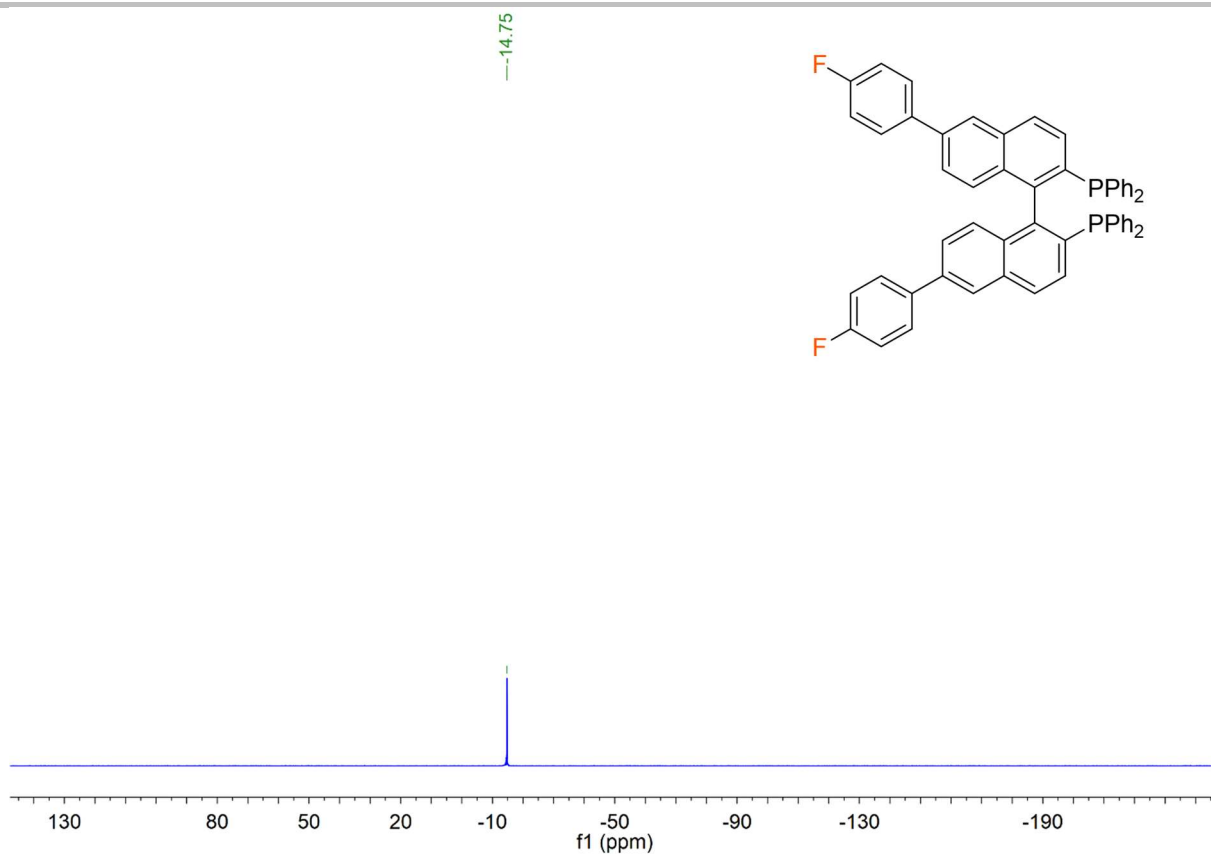
Supporting information



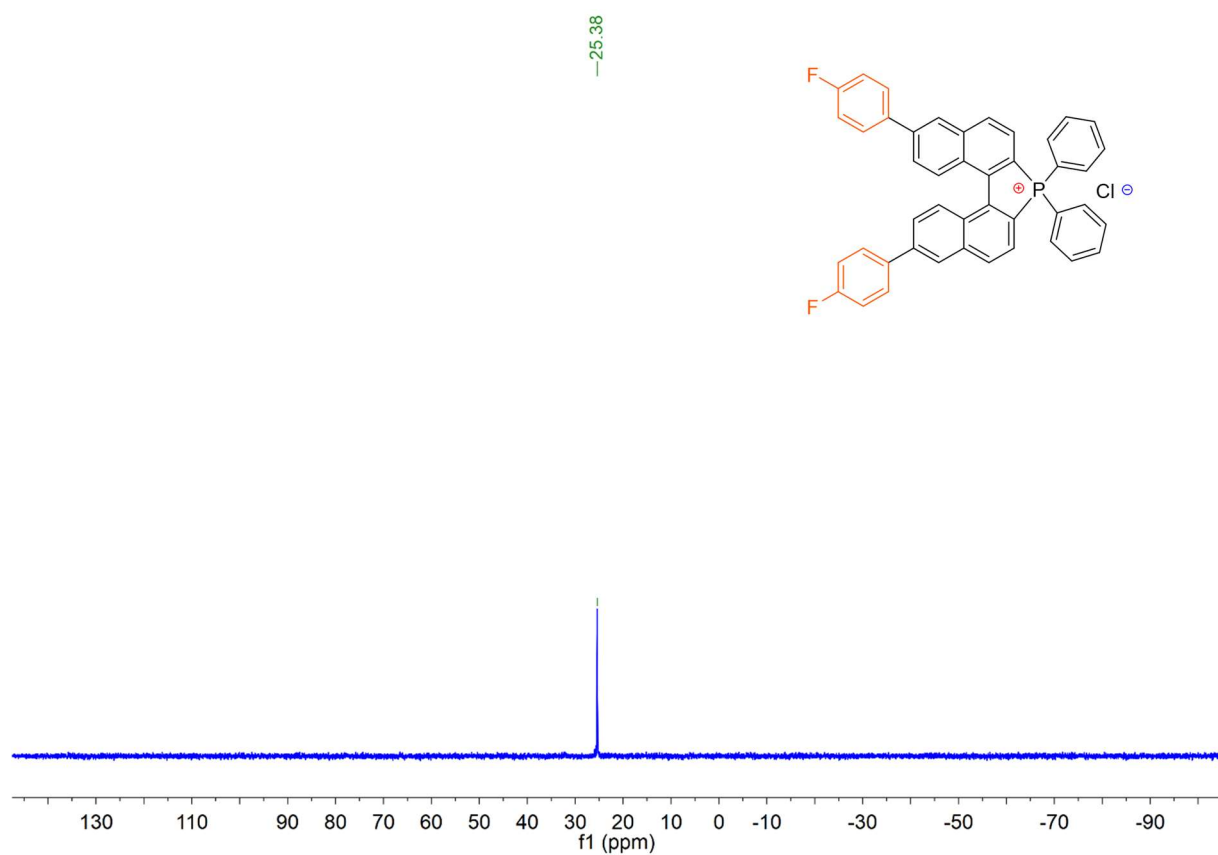
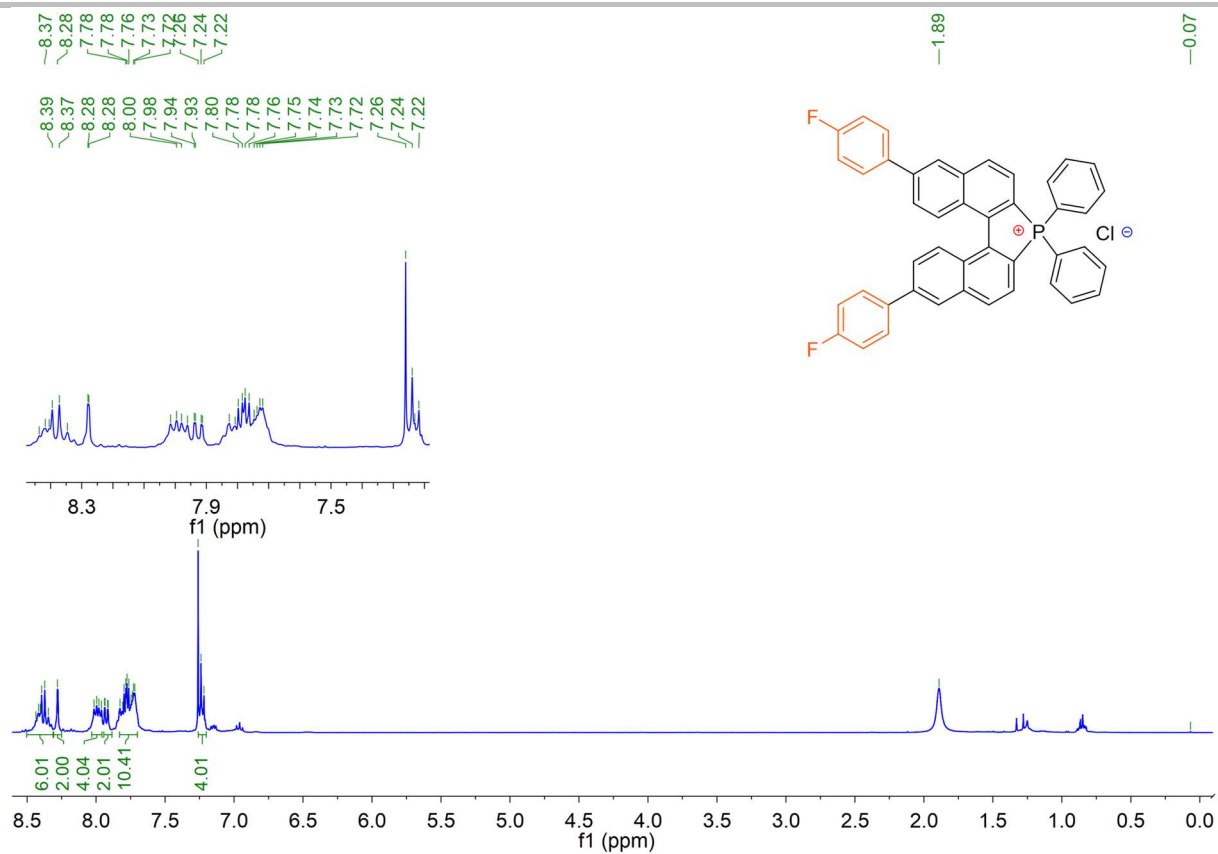
Supporting information



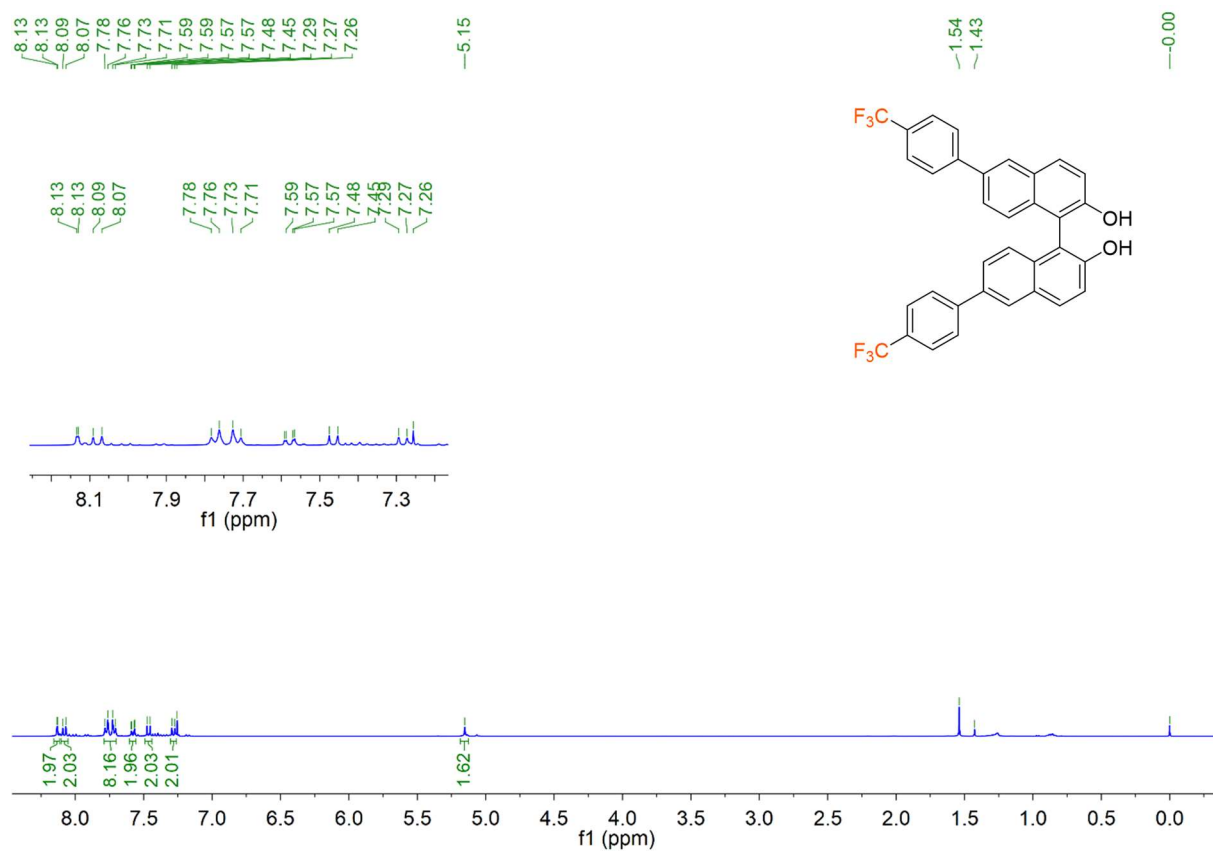
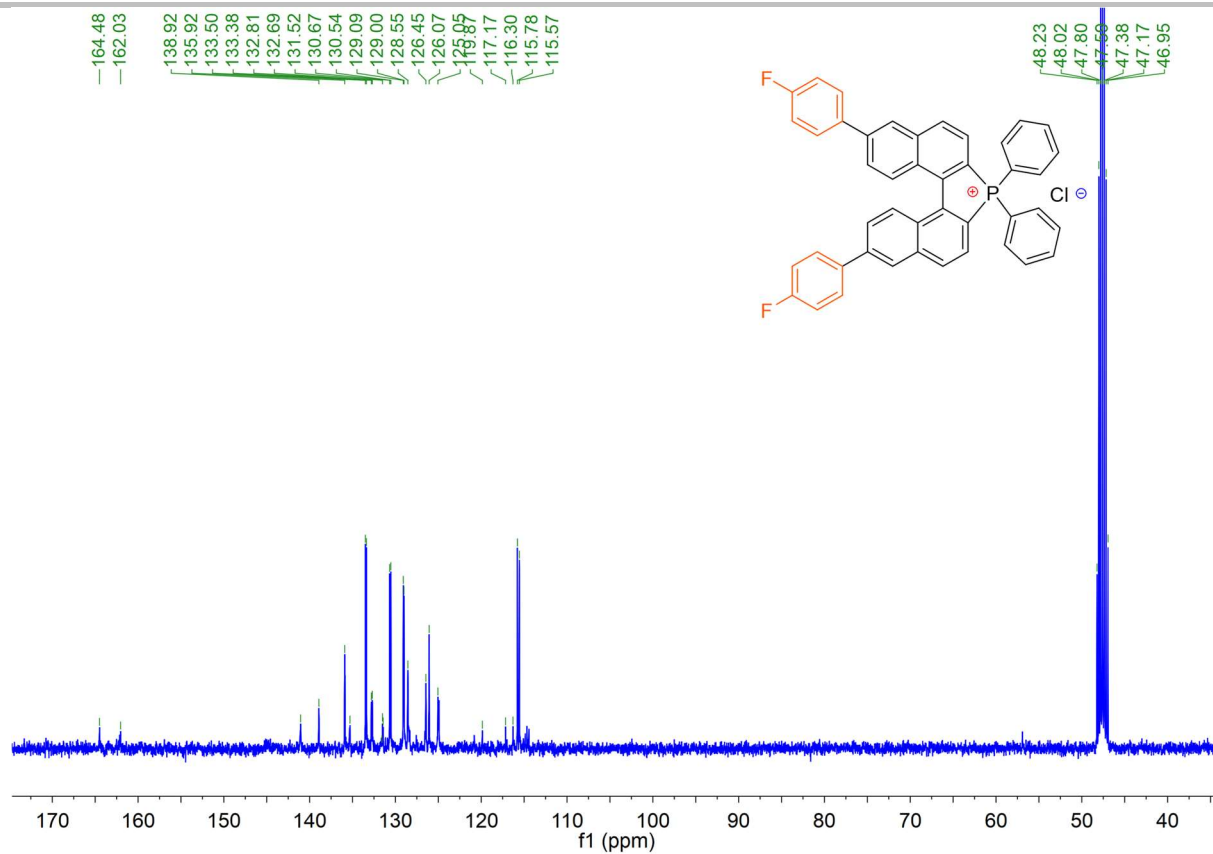
Supporting information



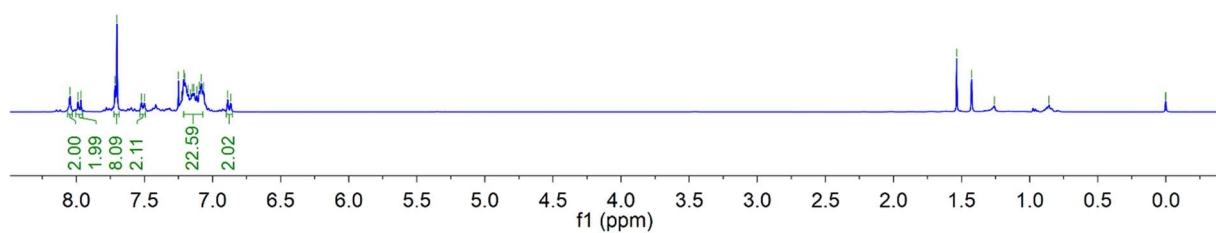
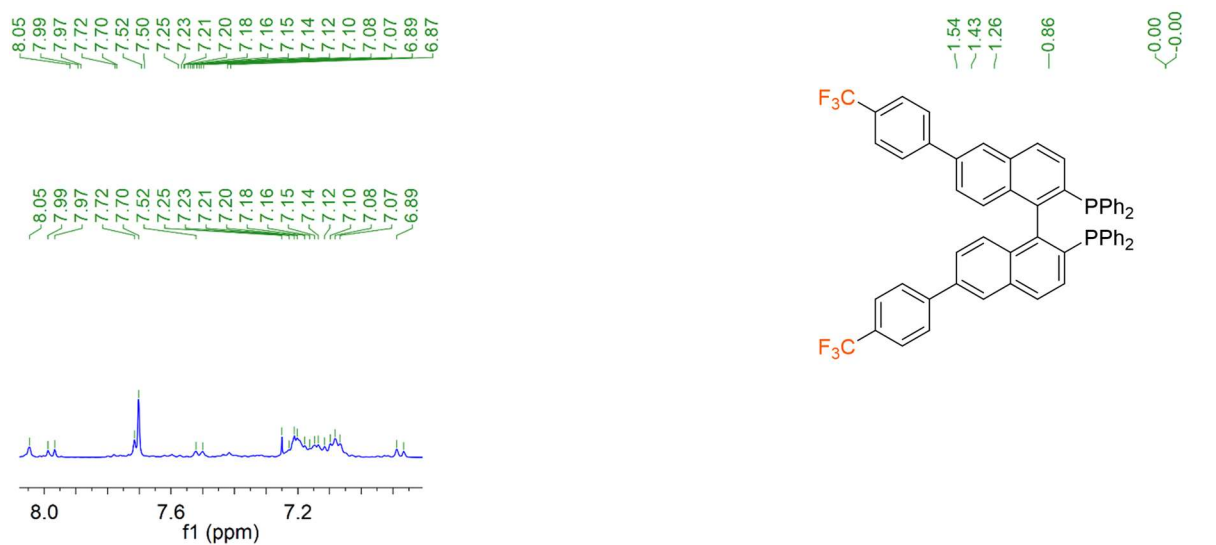
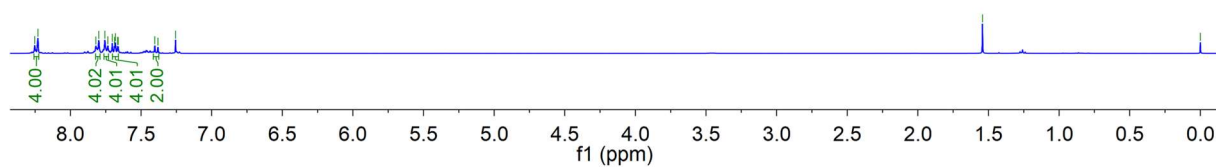
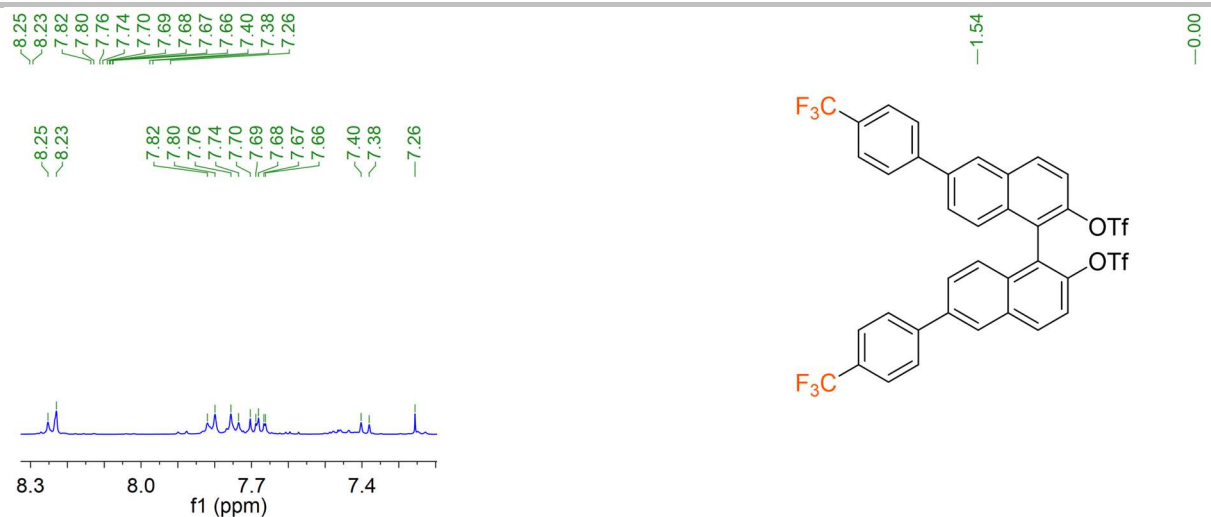
Supporting information



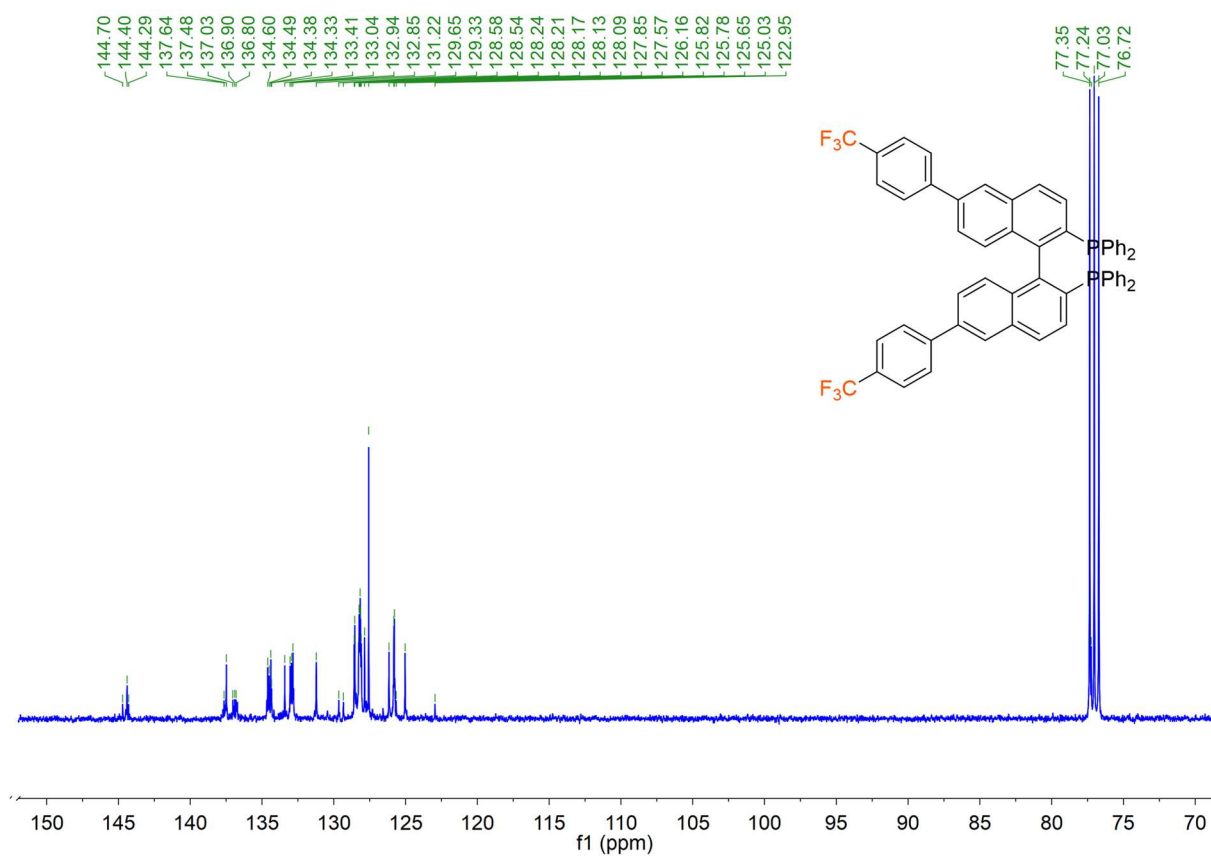
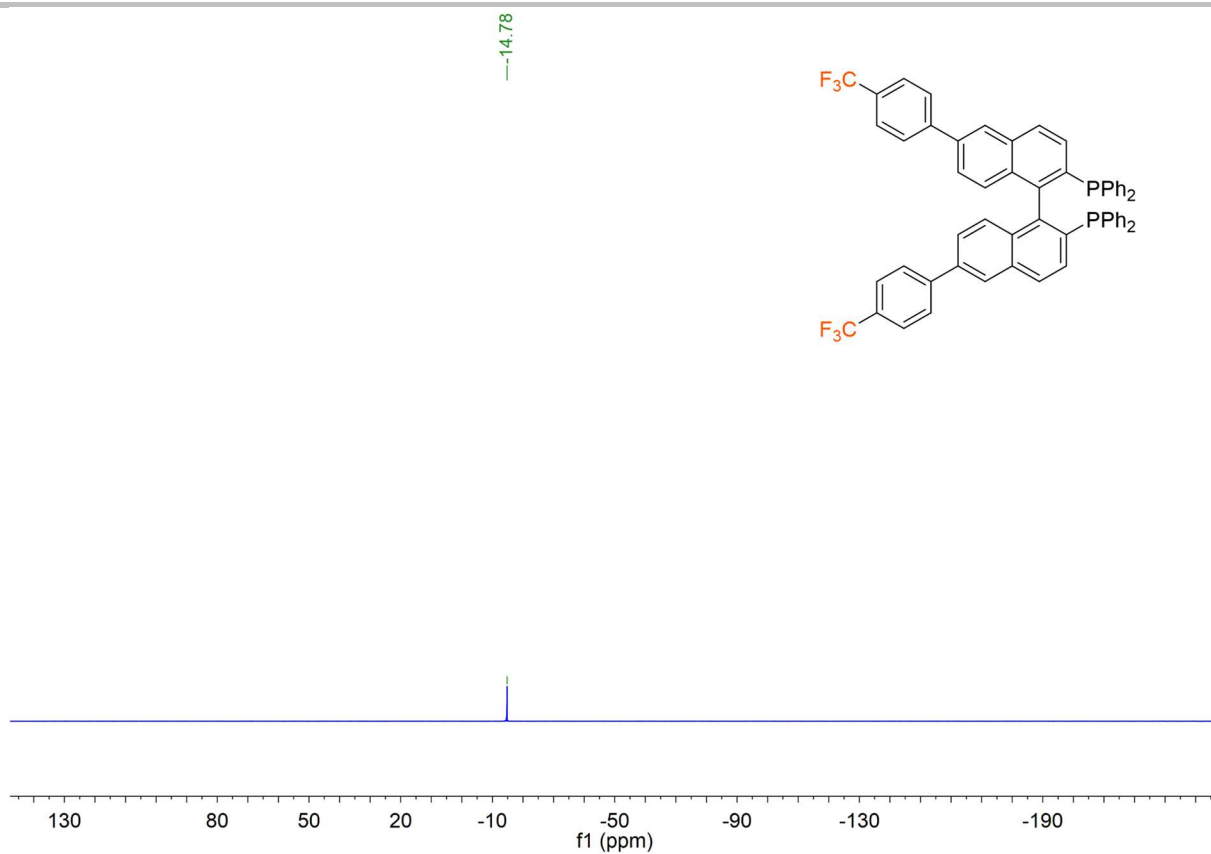
Supporting information



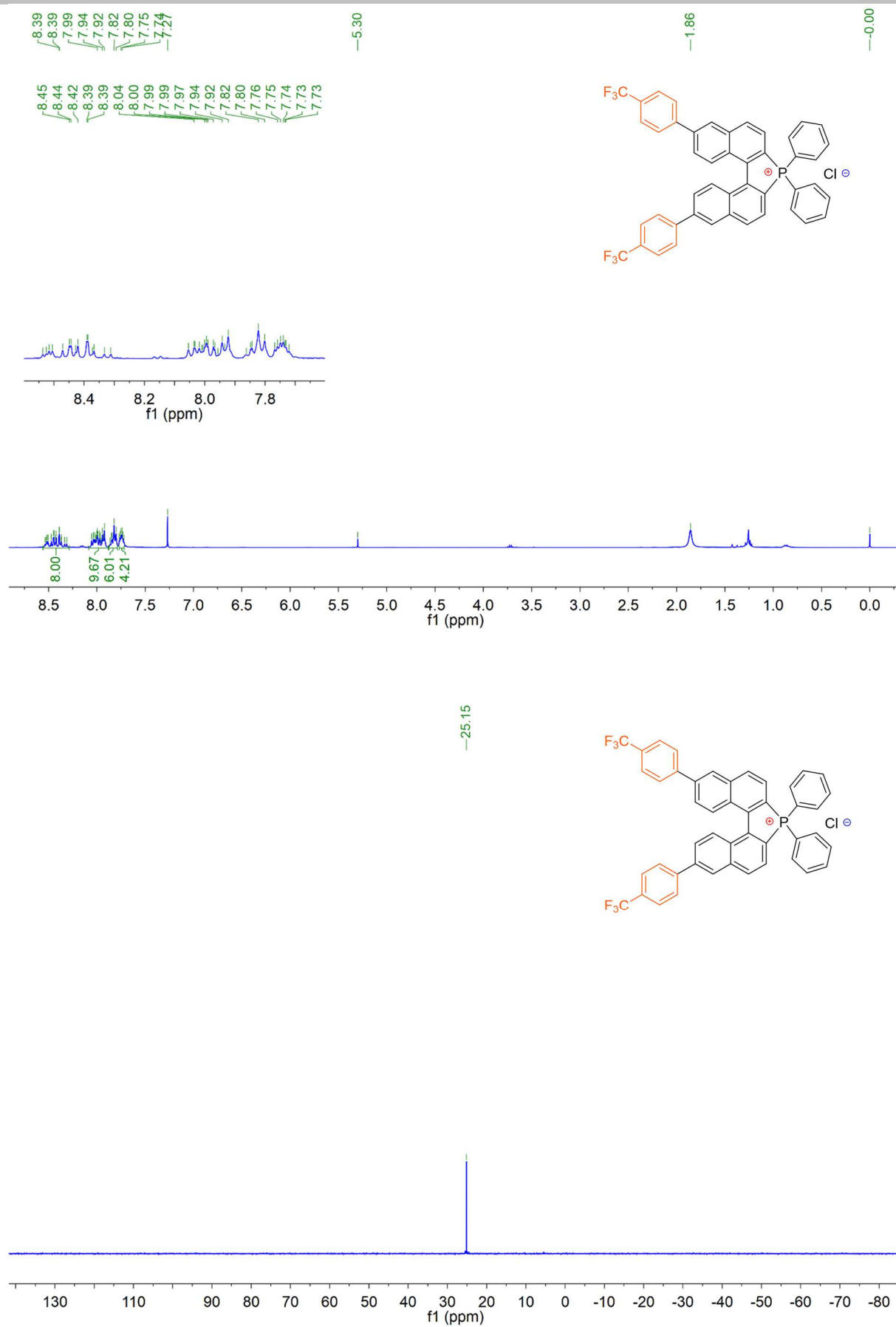
Supporting information



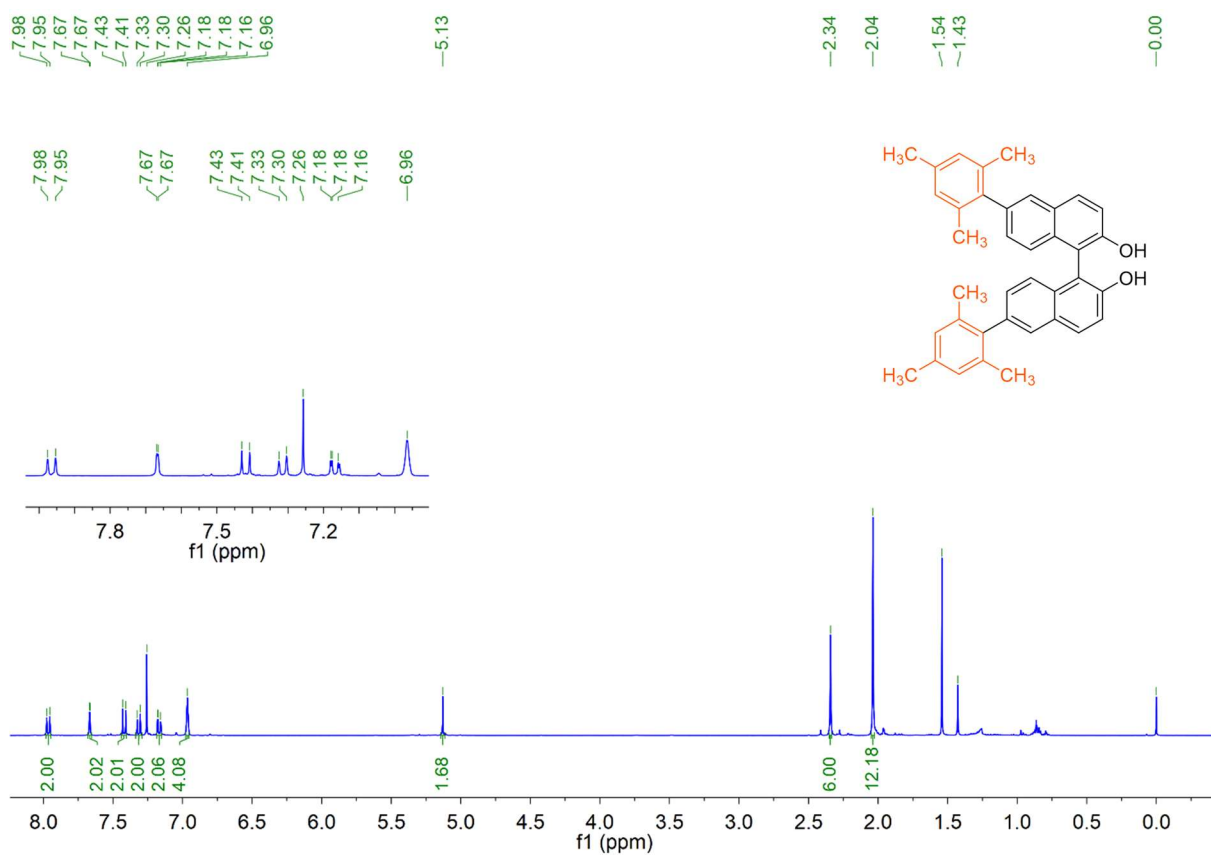
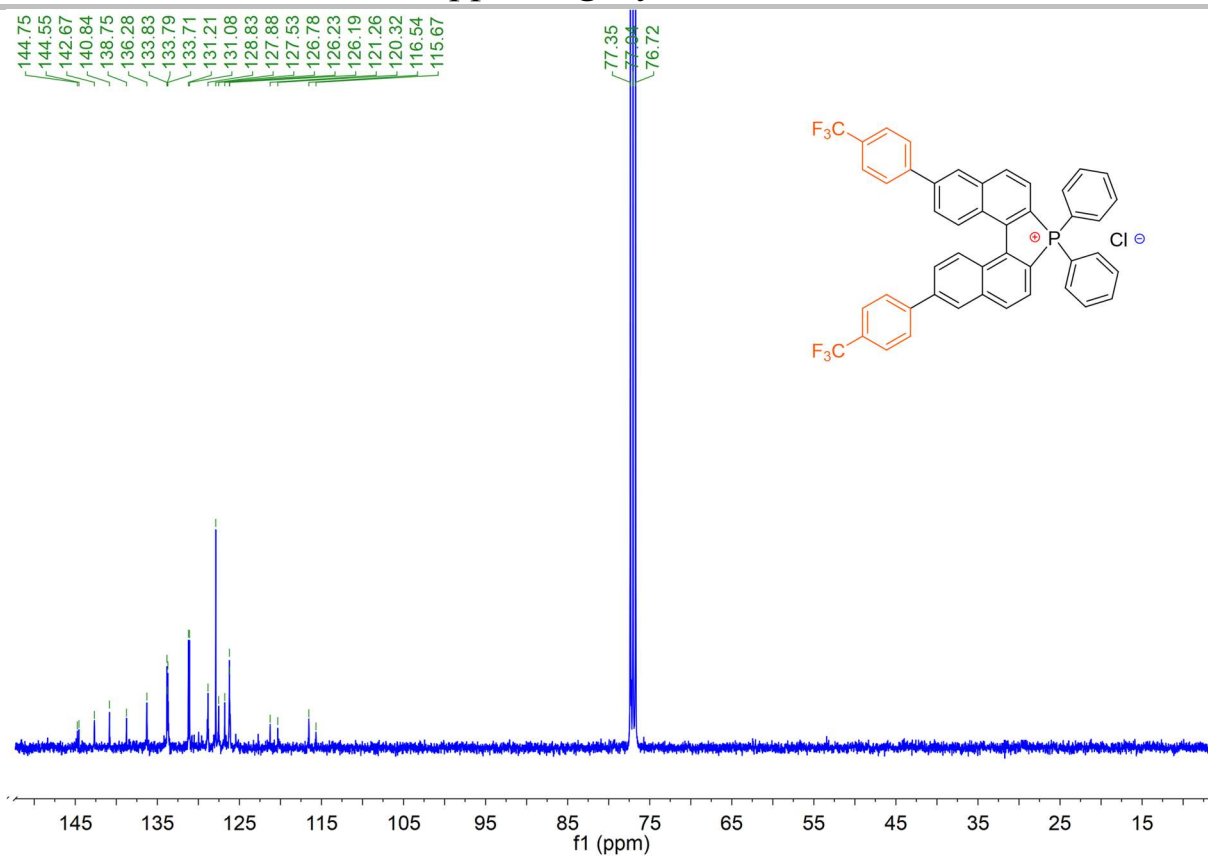
Supporting information



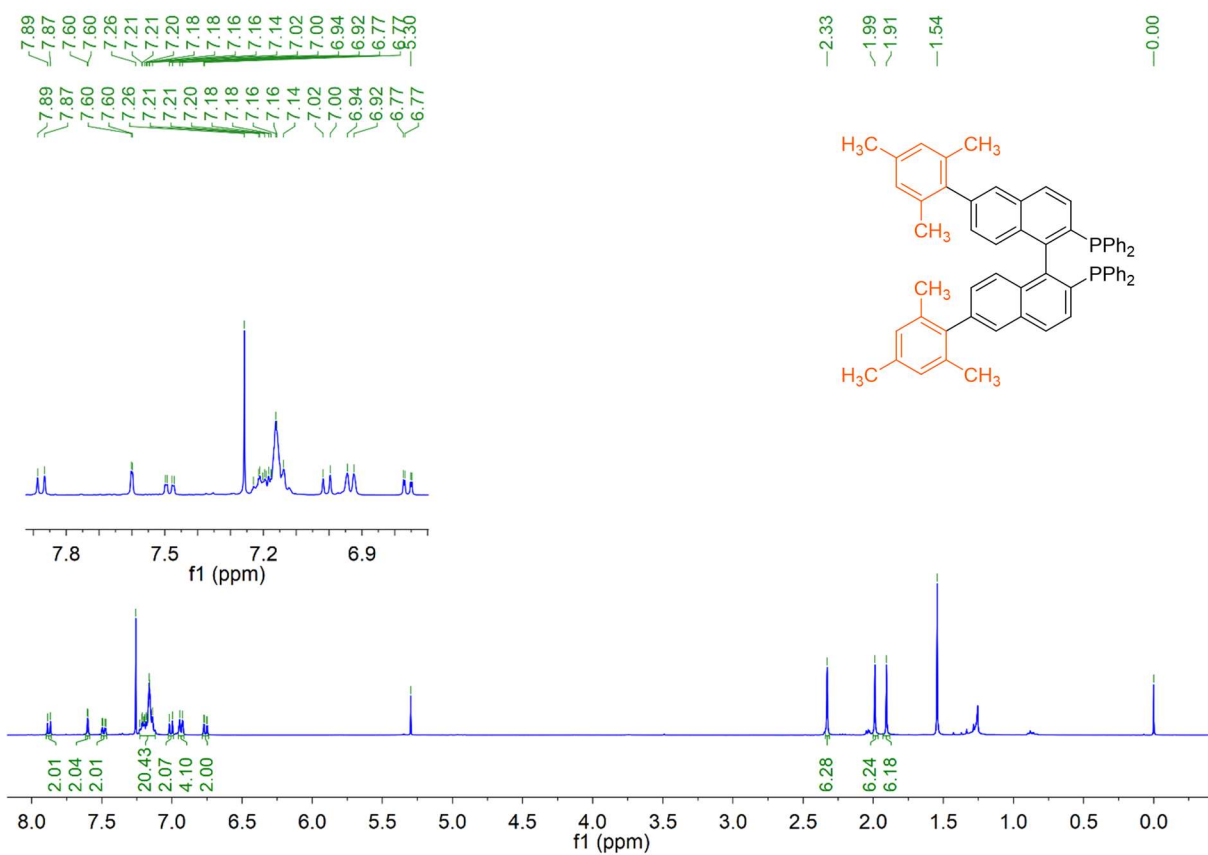
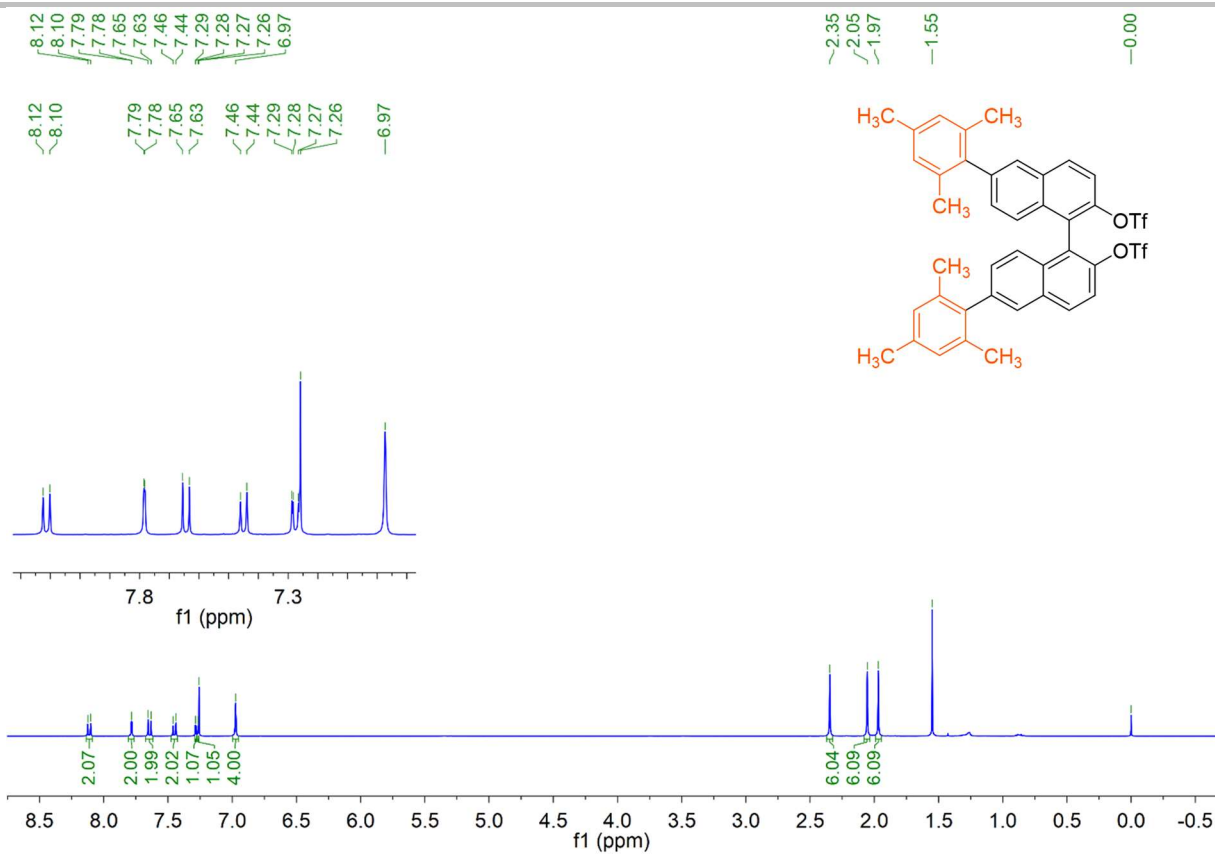
Supporting information



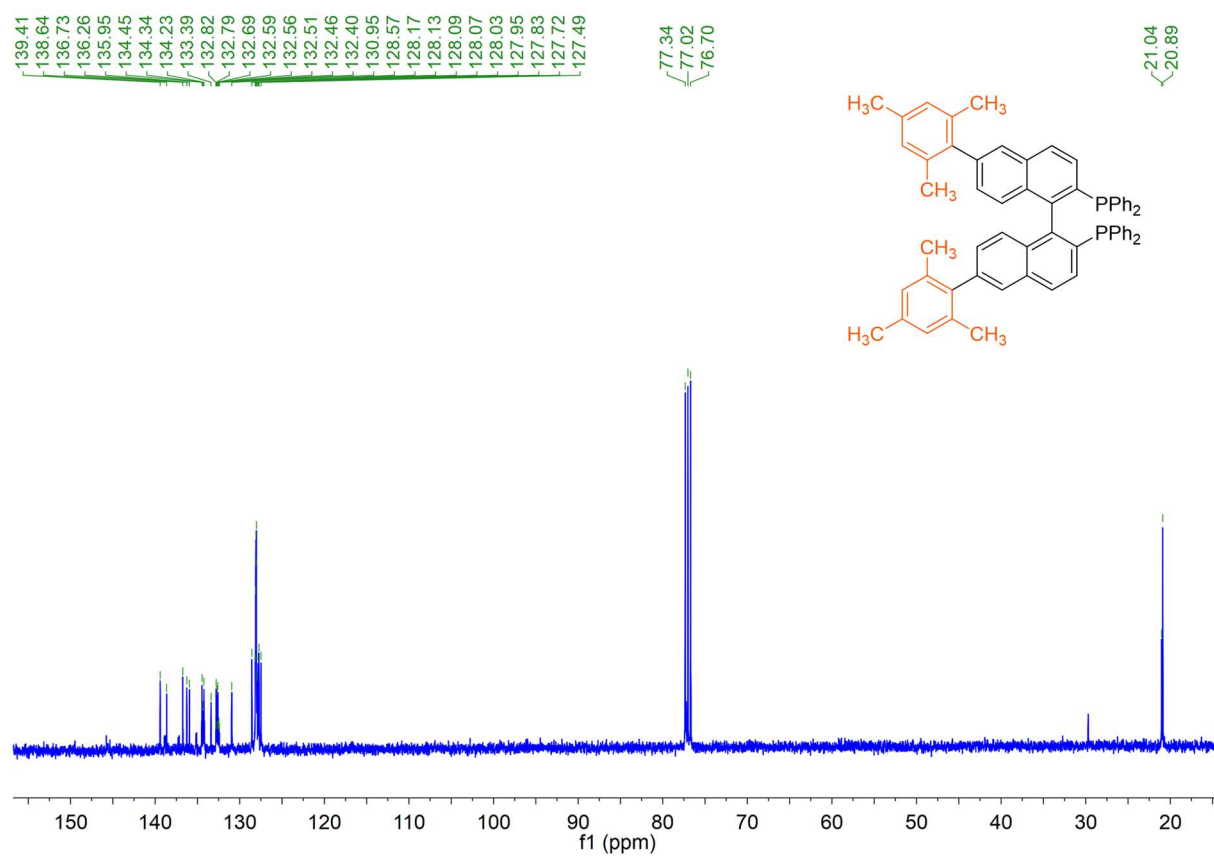
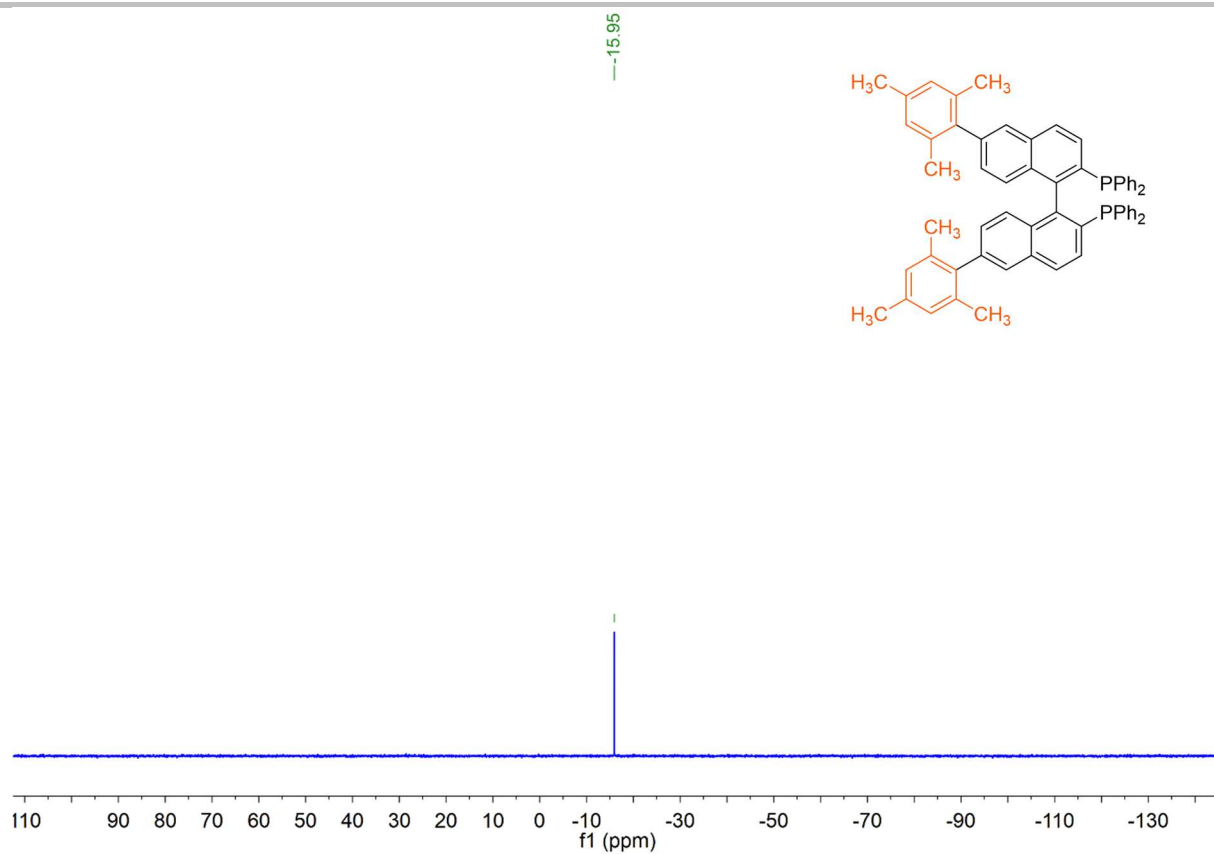
Supporting information



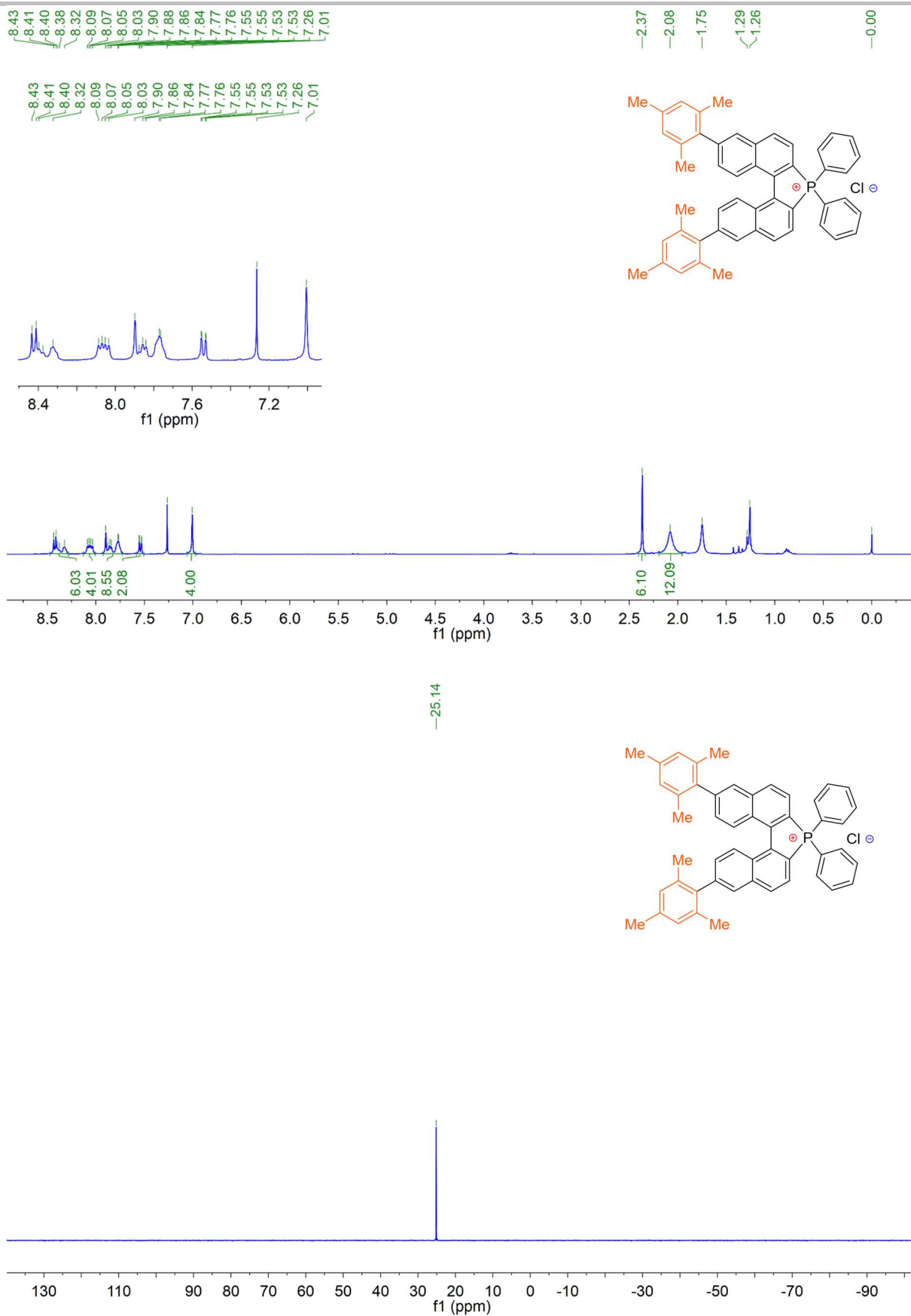
Supporting information



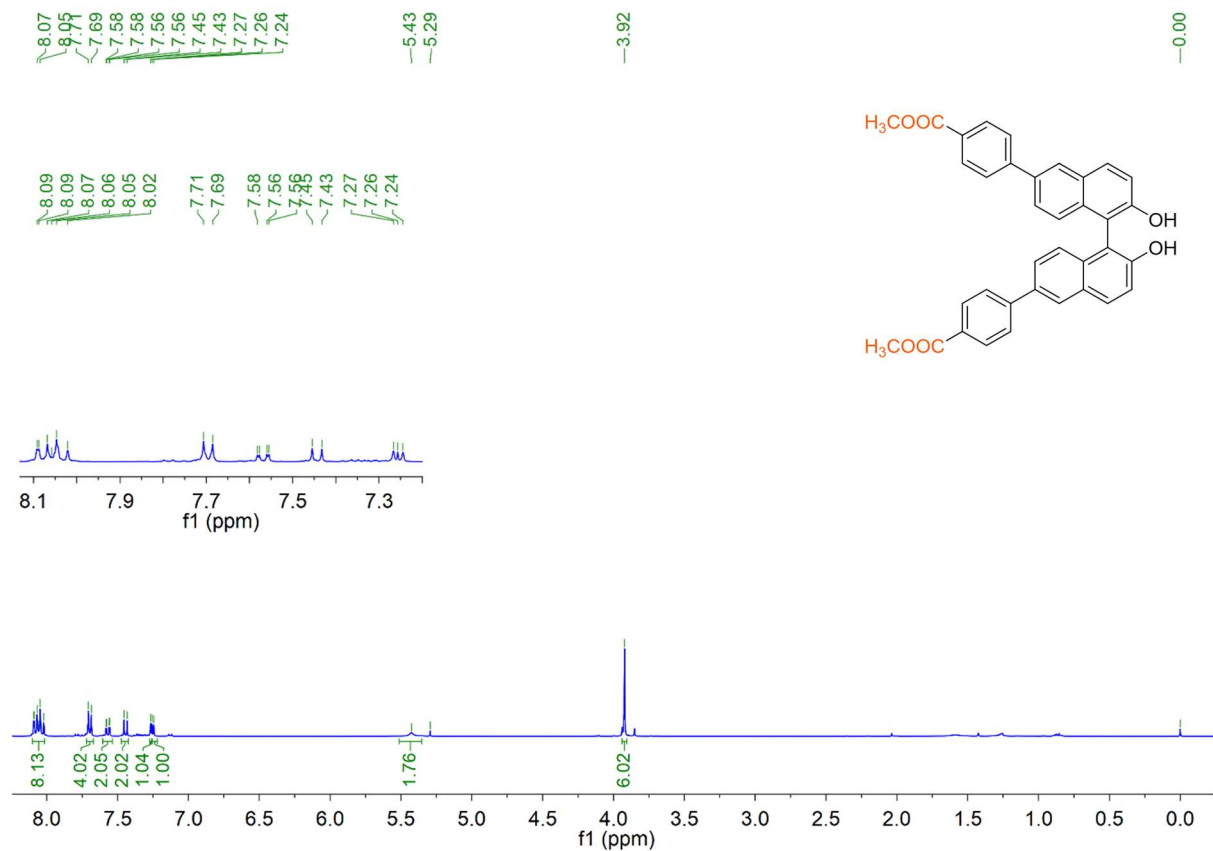
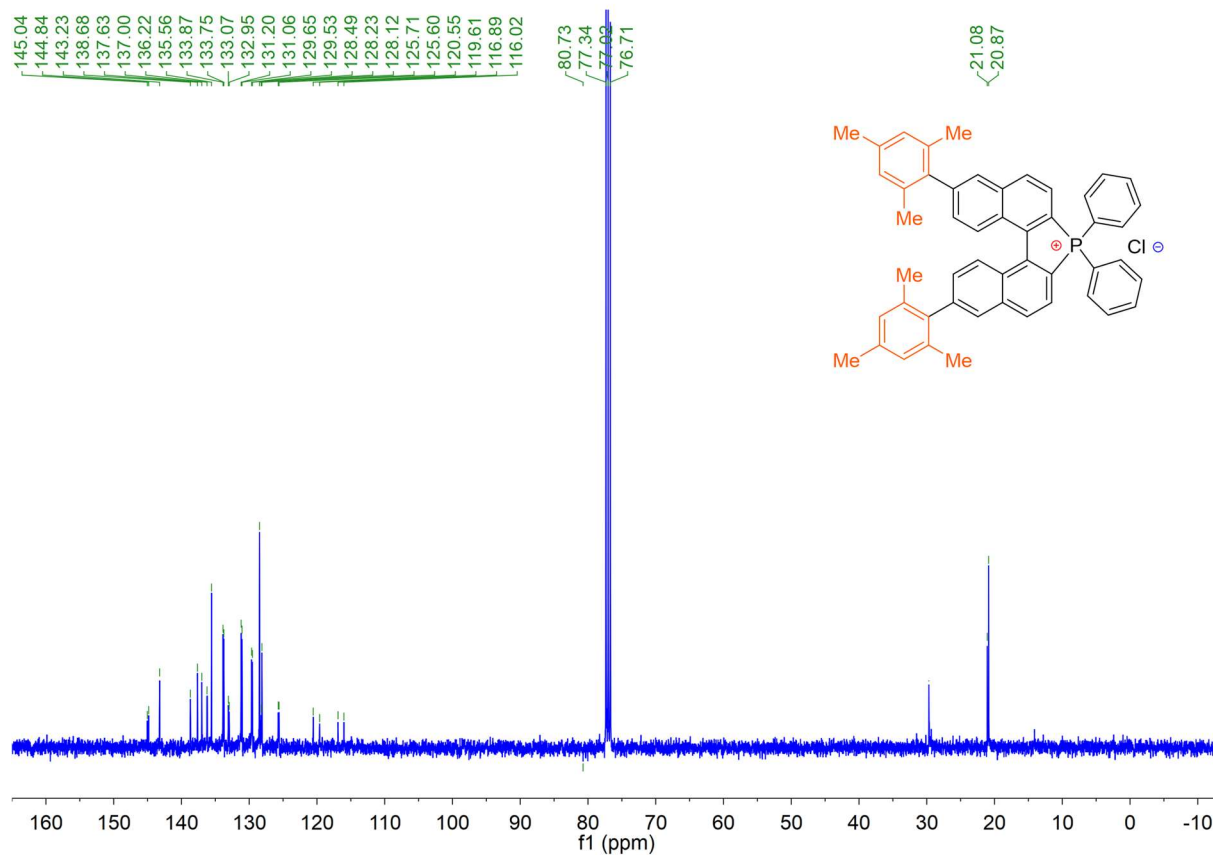
Supporting information



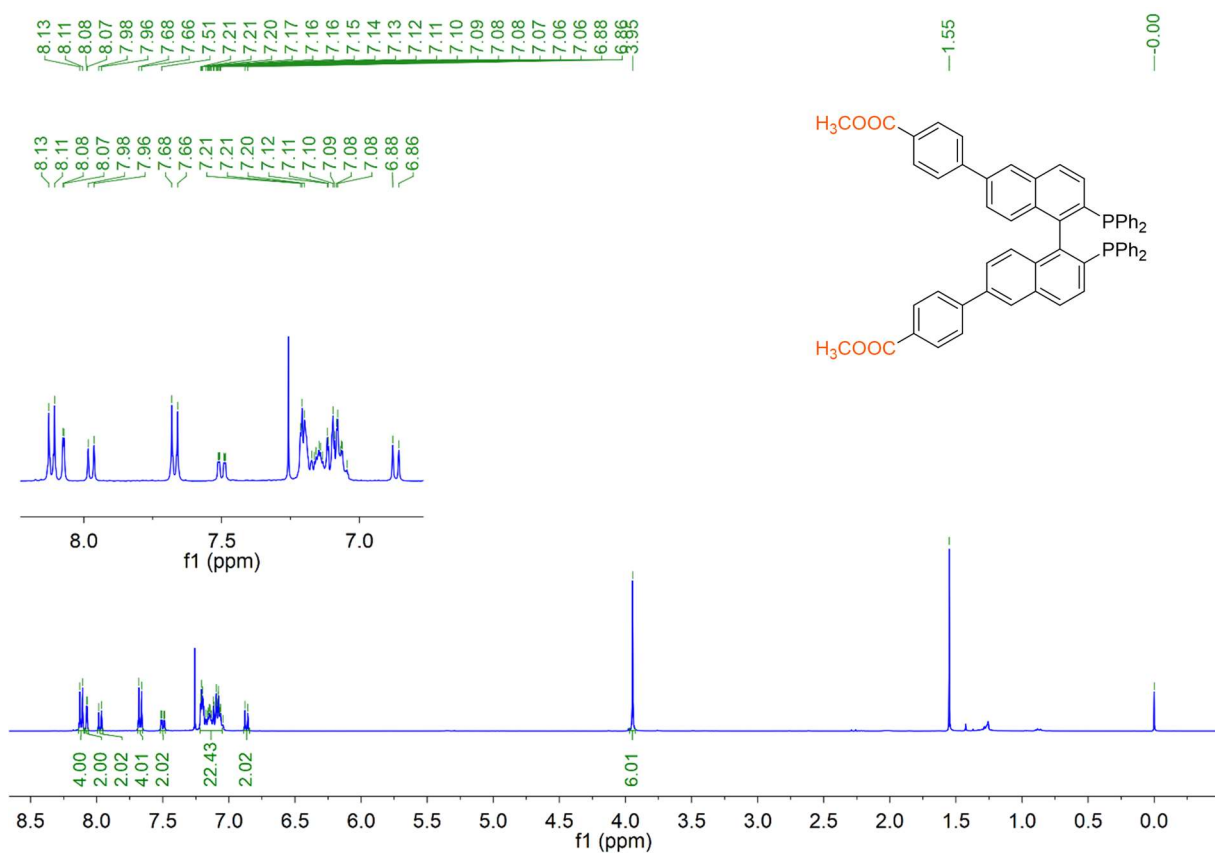
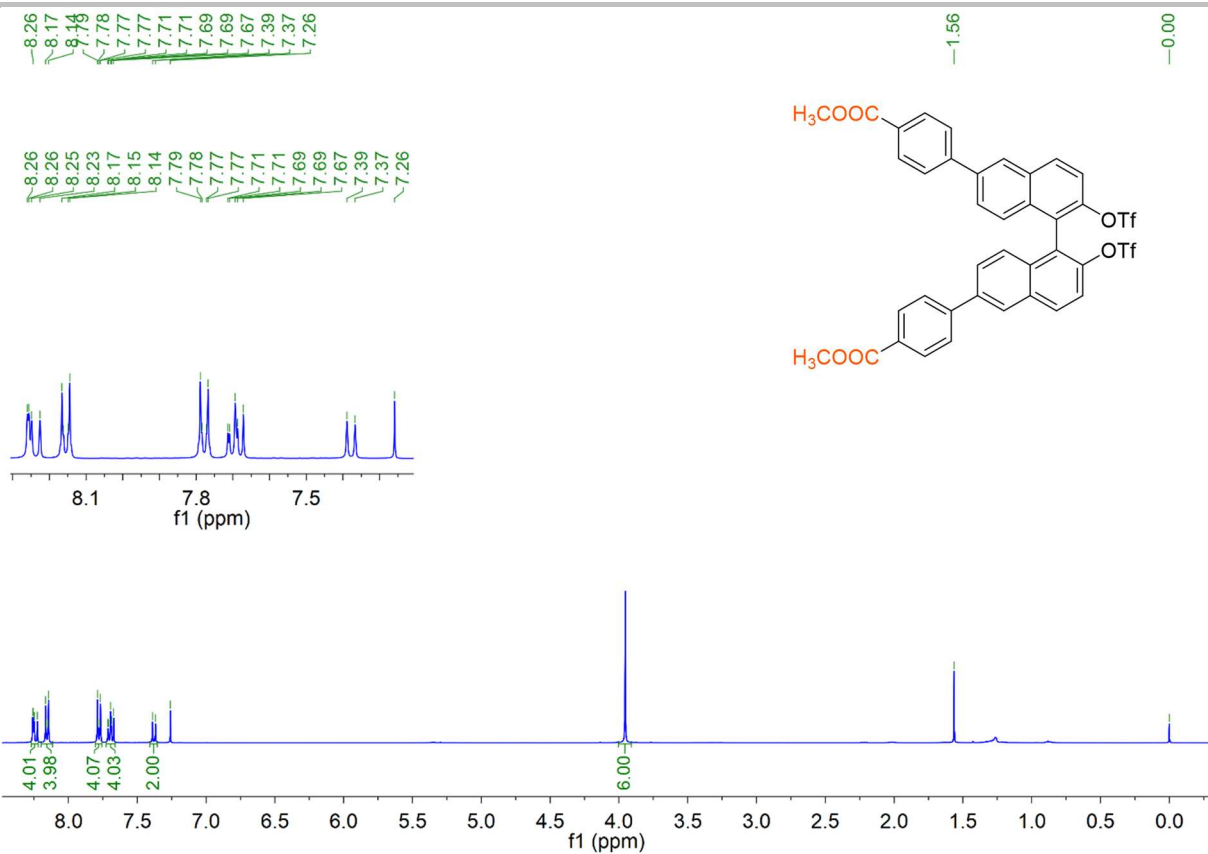
Supporting information



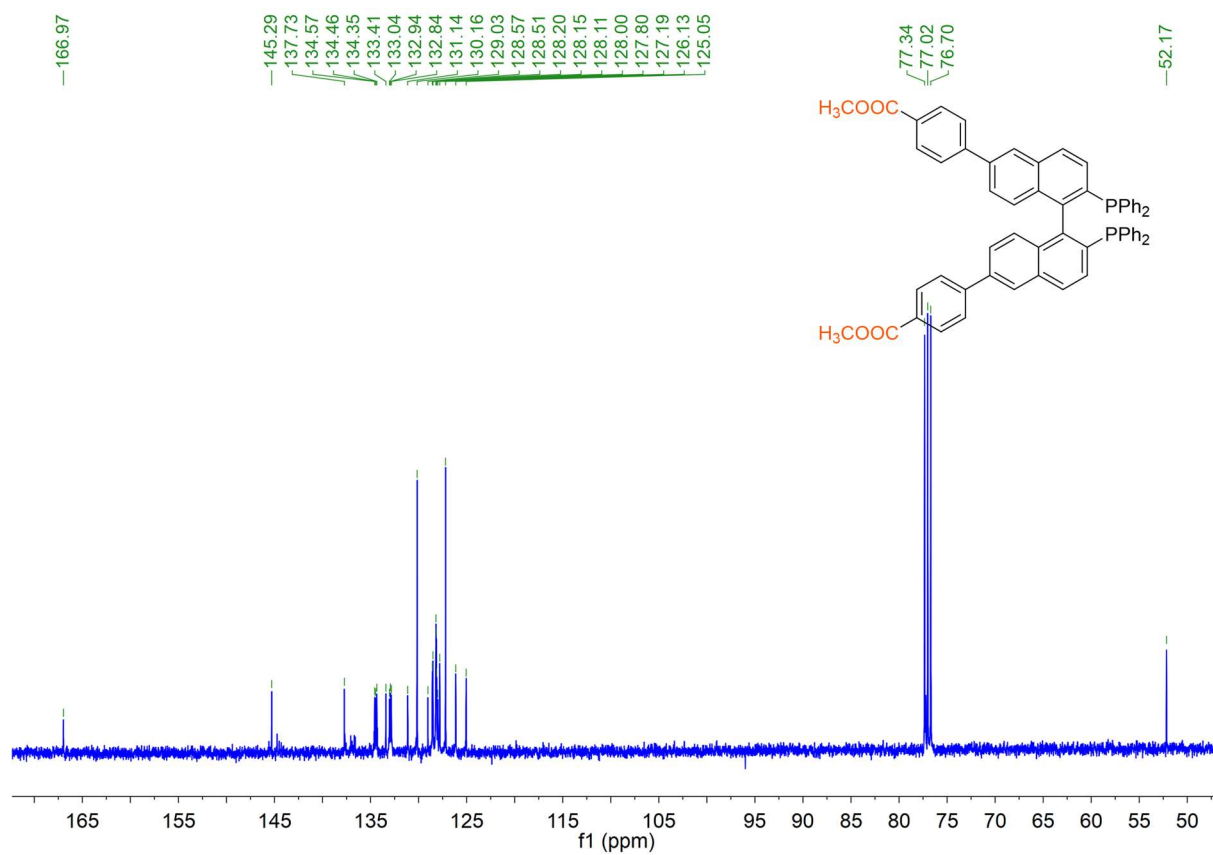
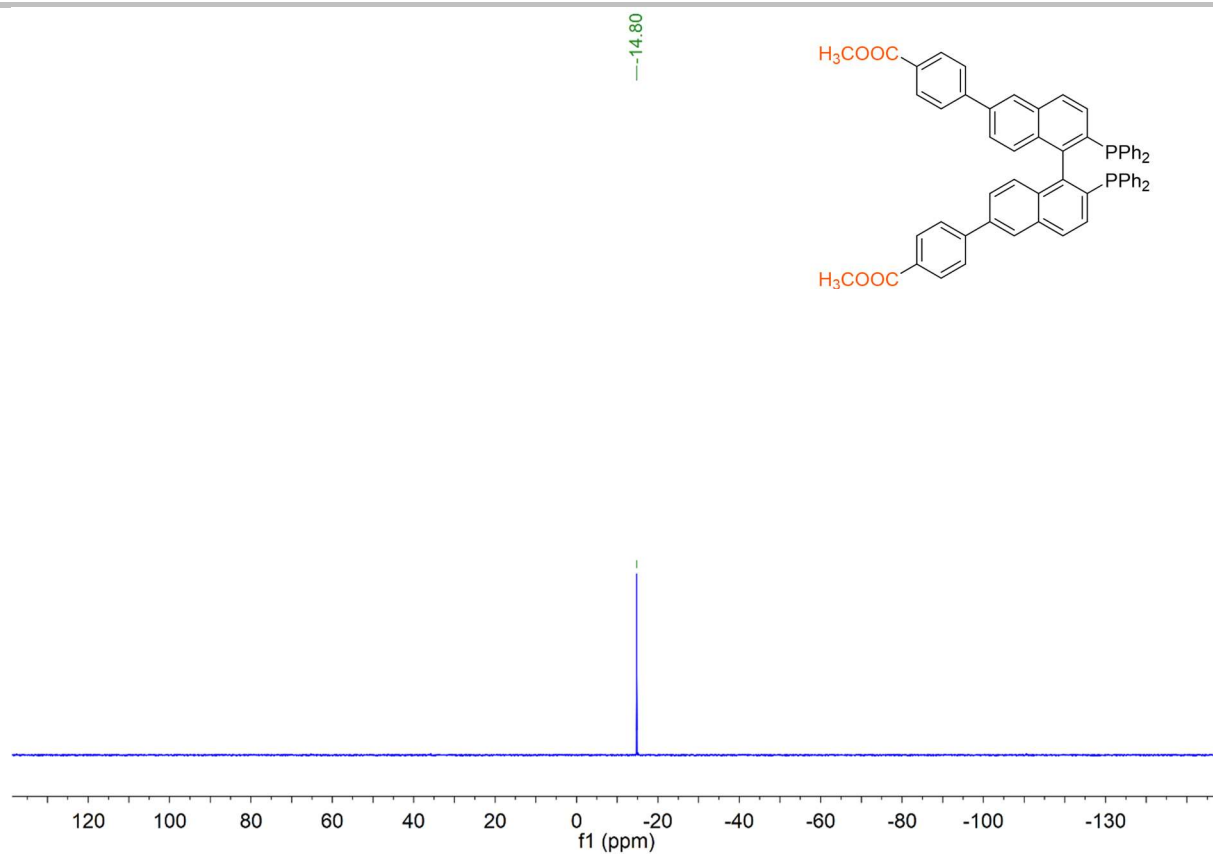
Supporting information



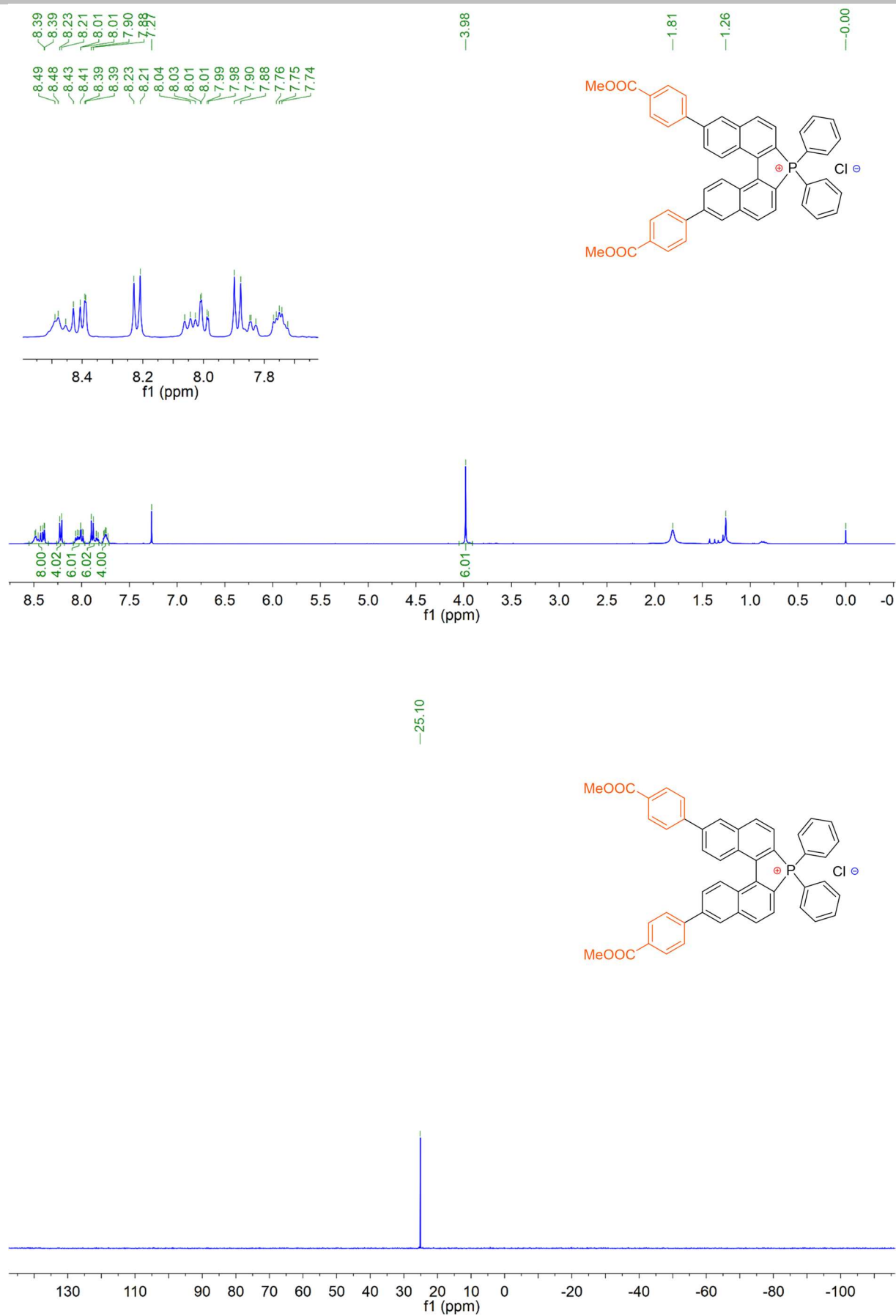
Supporting information



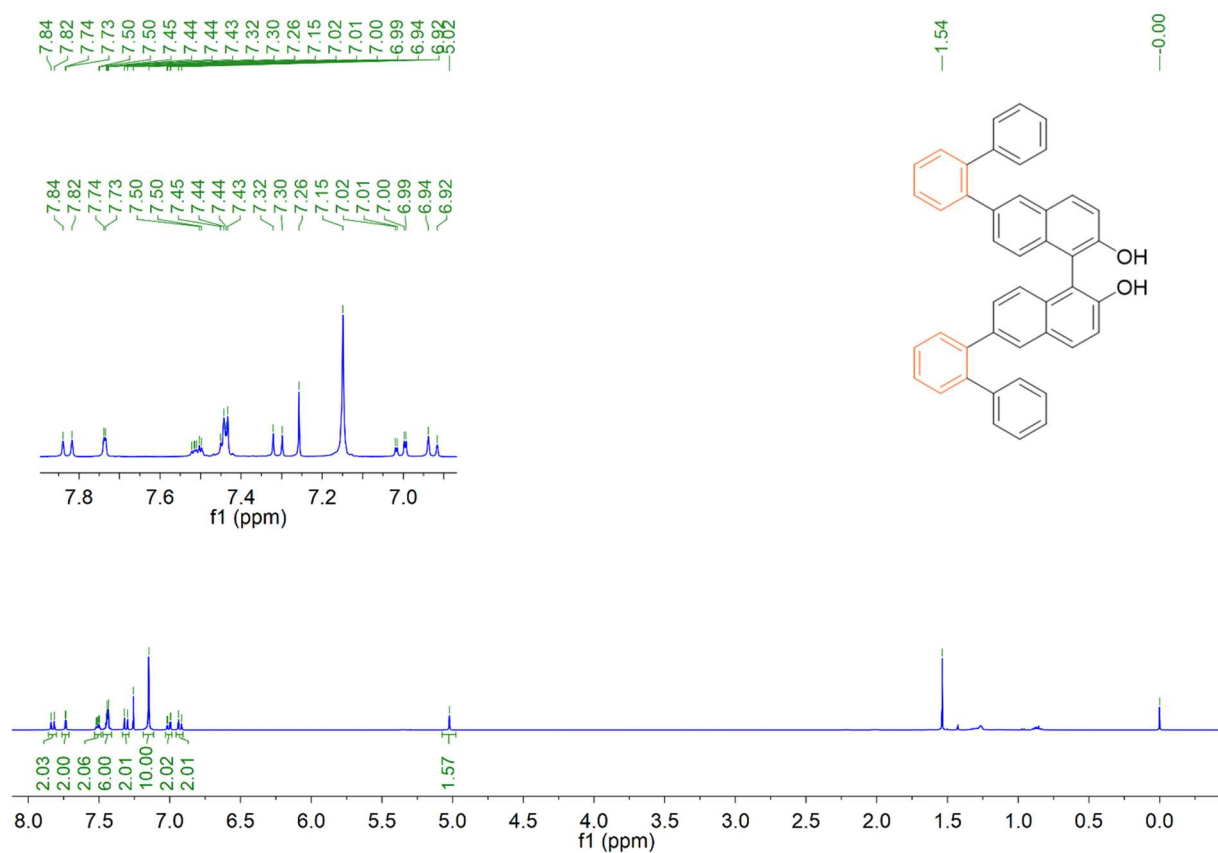
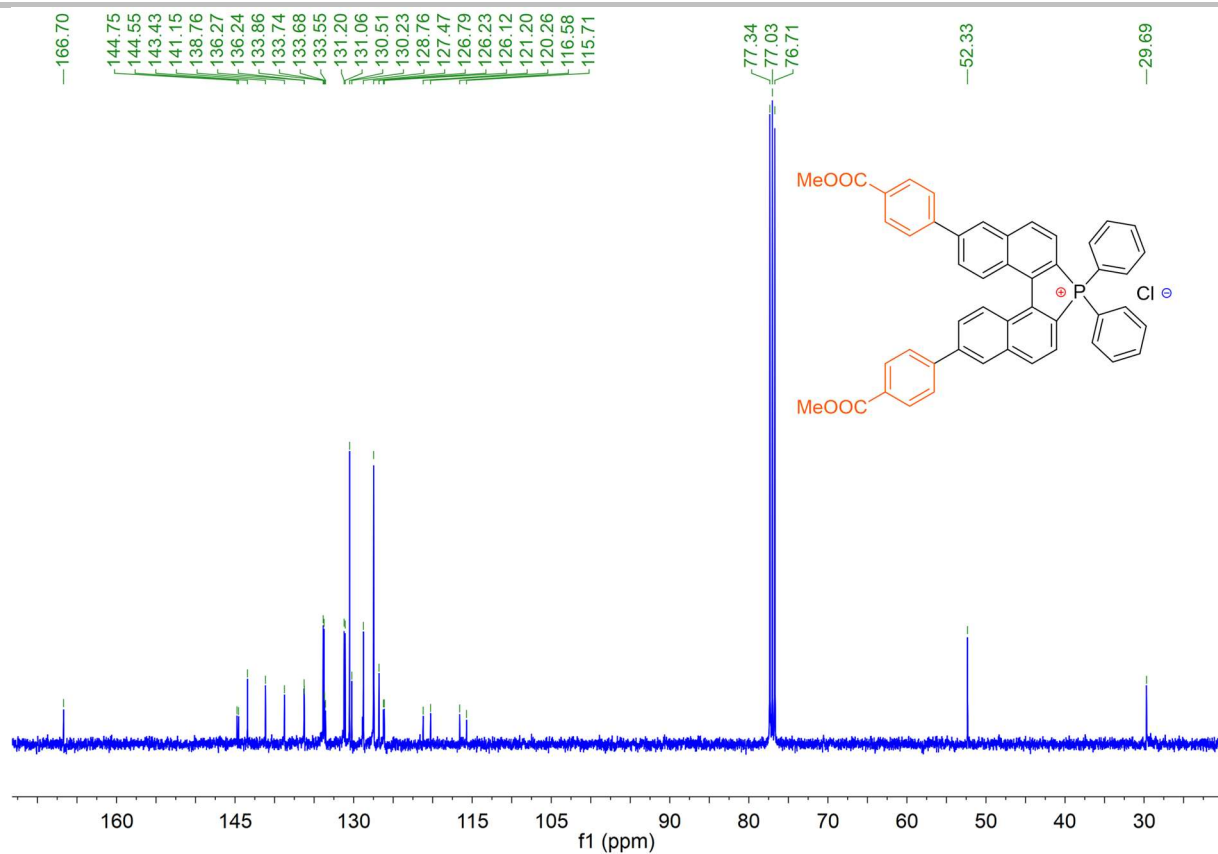
Supporting information



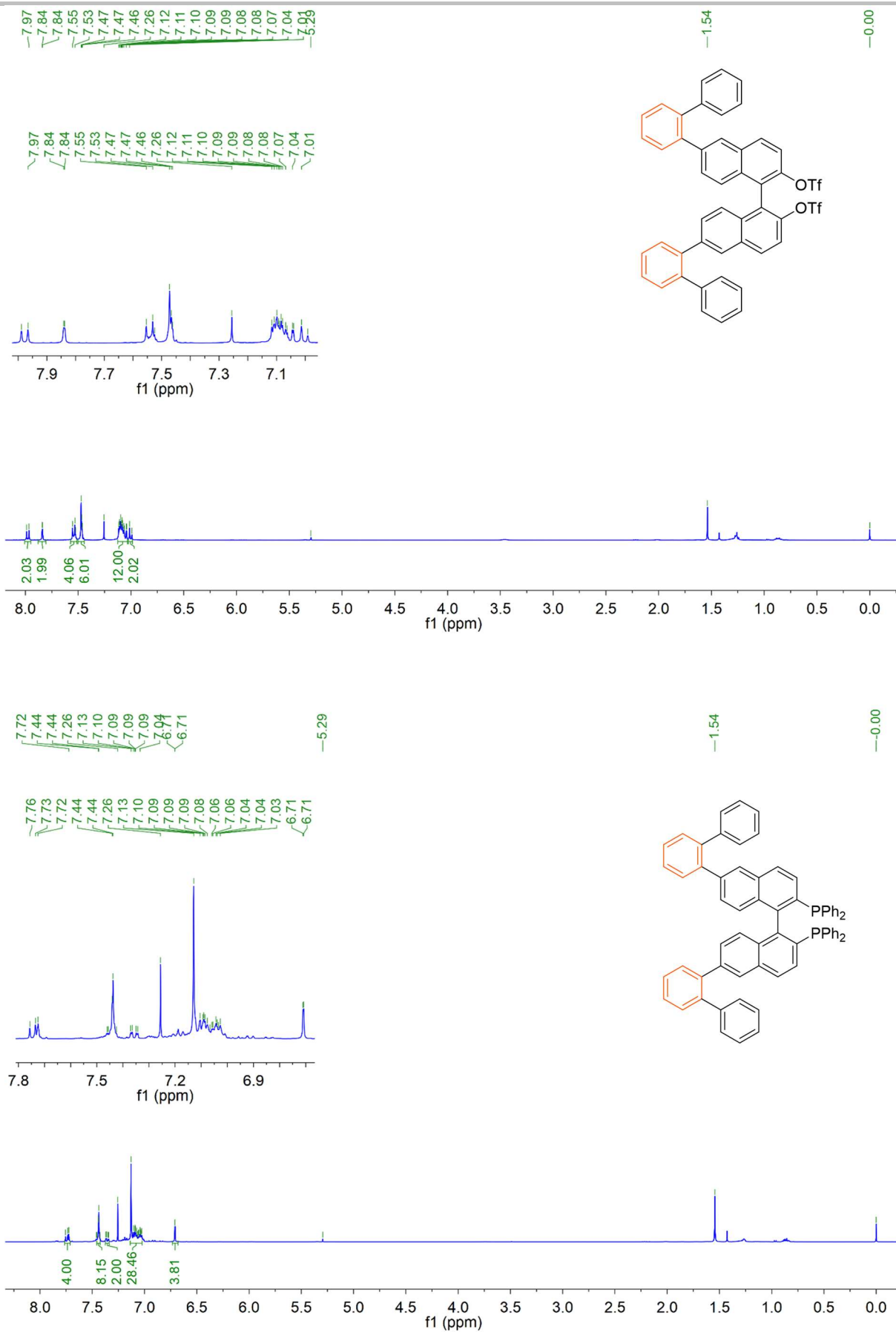
Supporting information



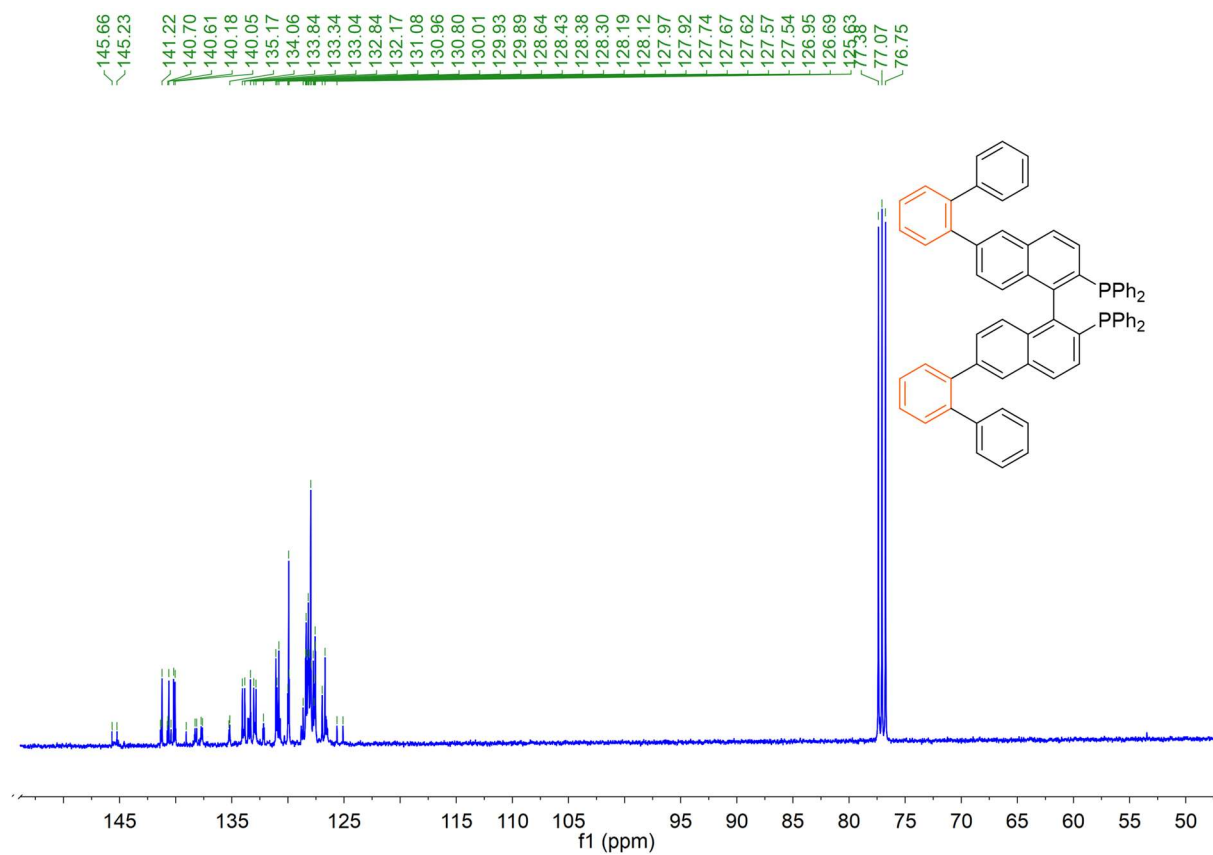
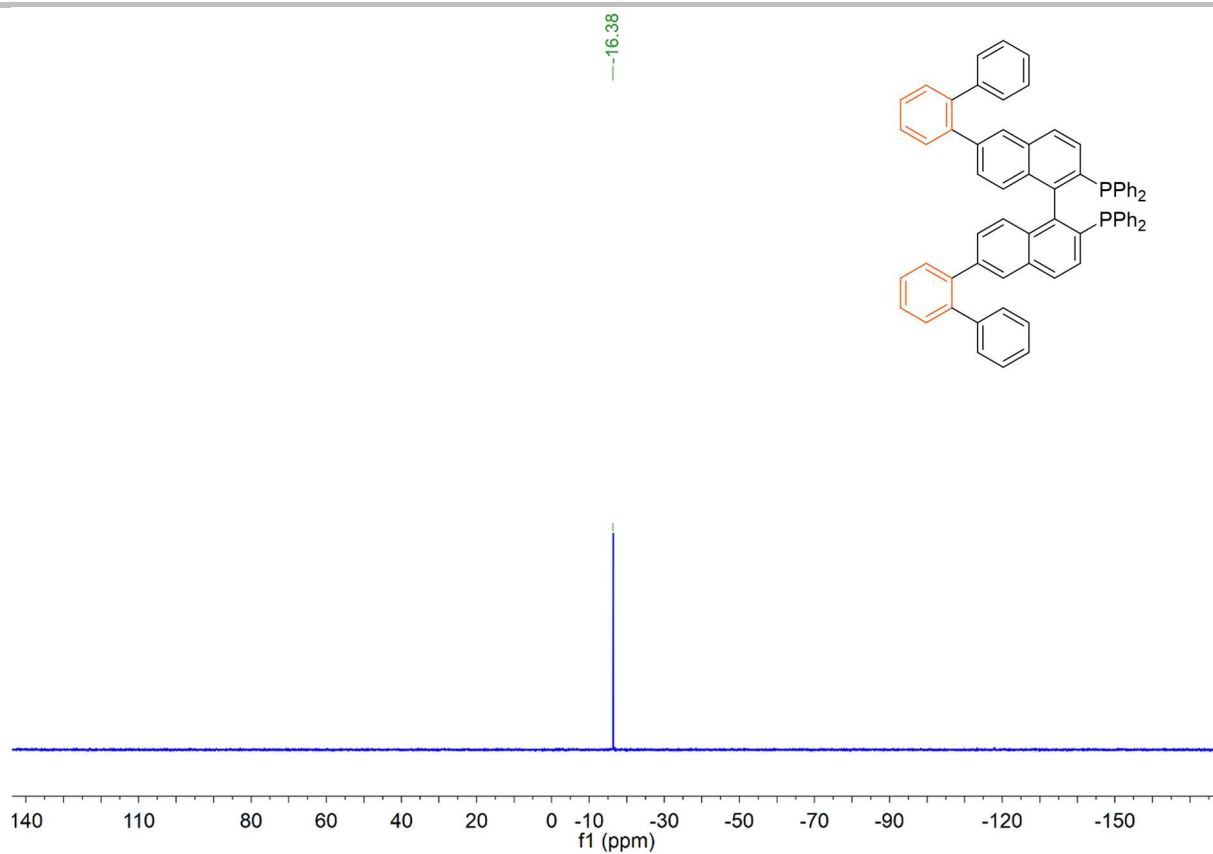
Supporting information



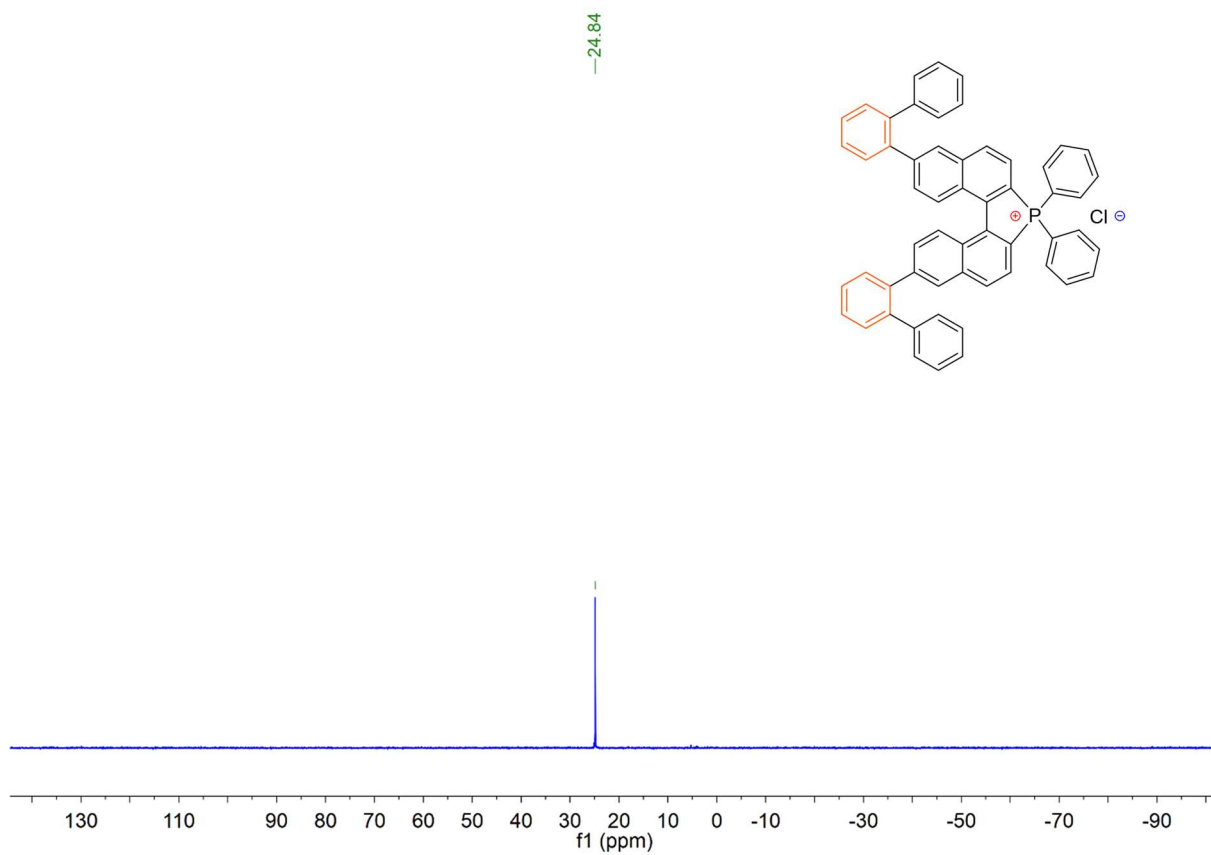
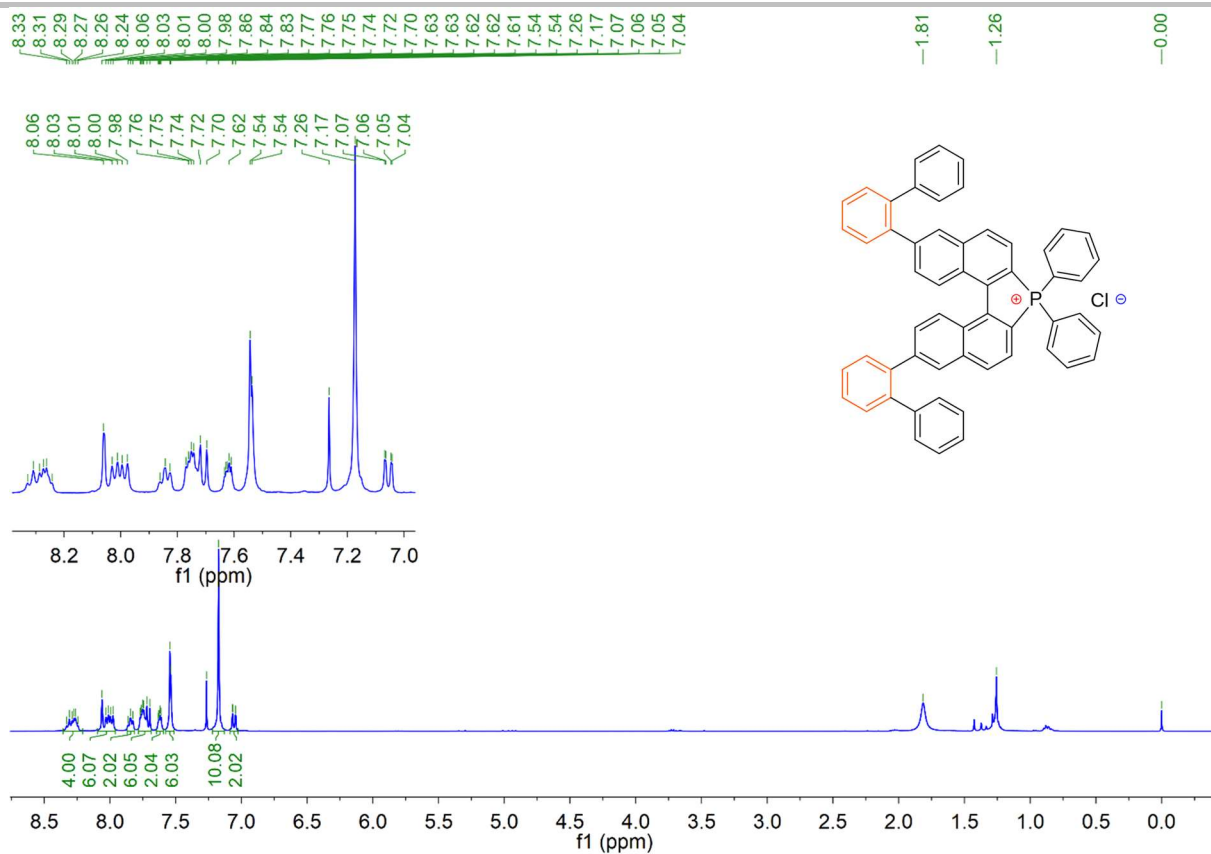
Supporting information



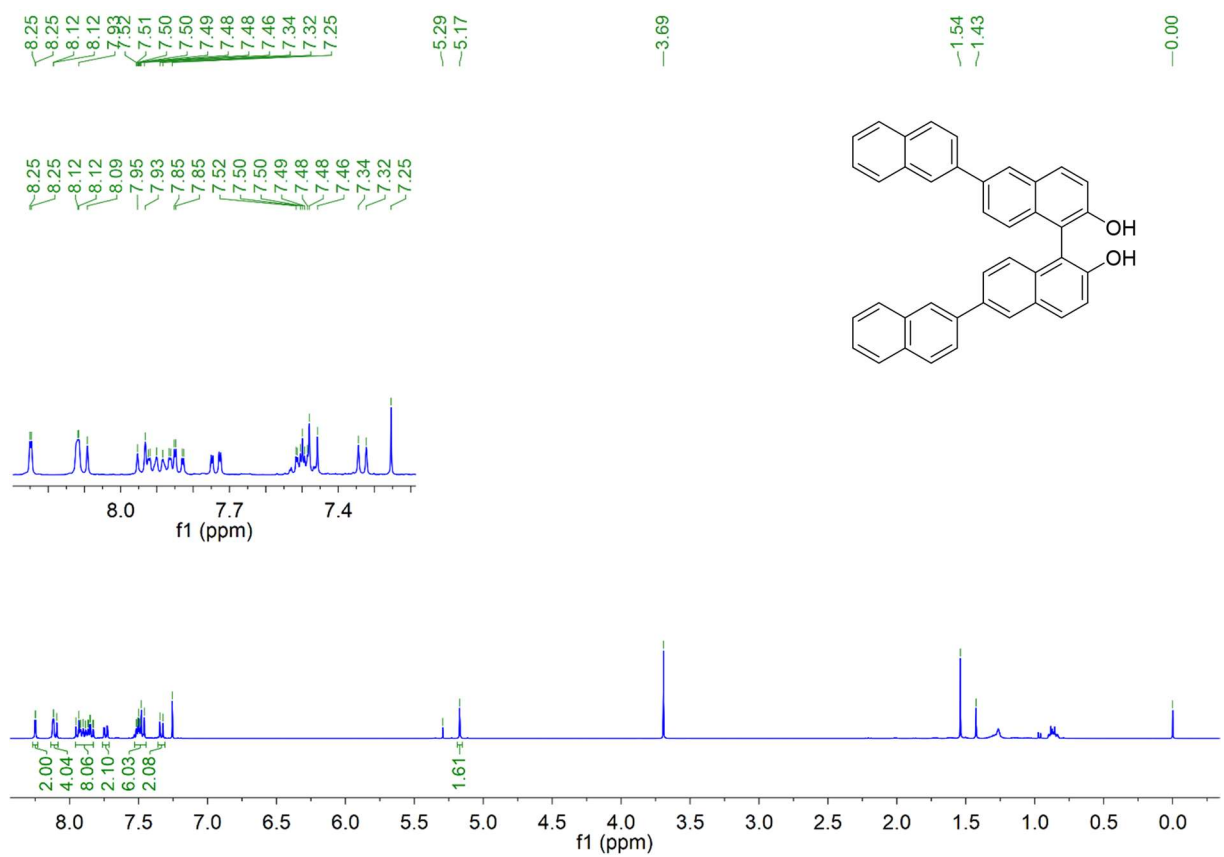
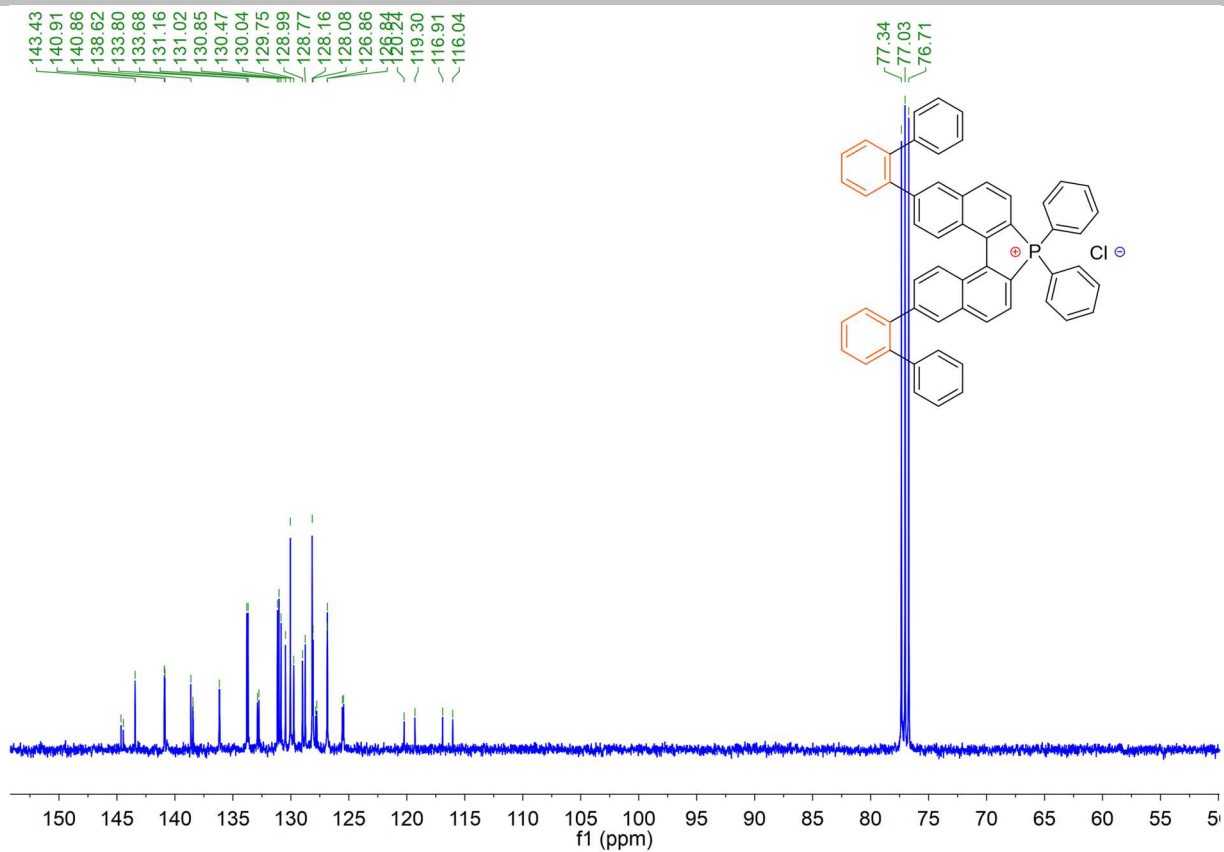
Supporting information



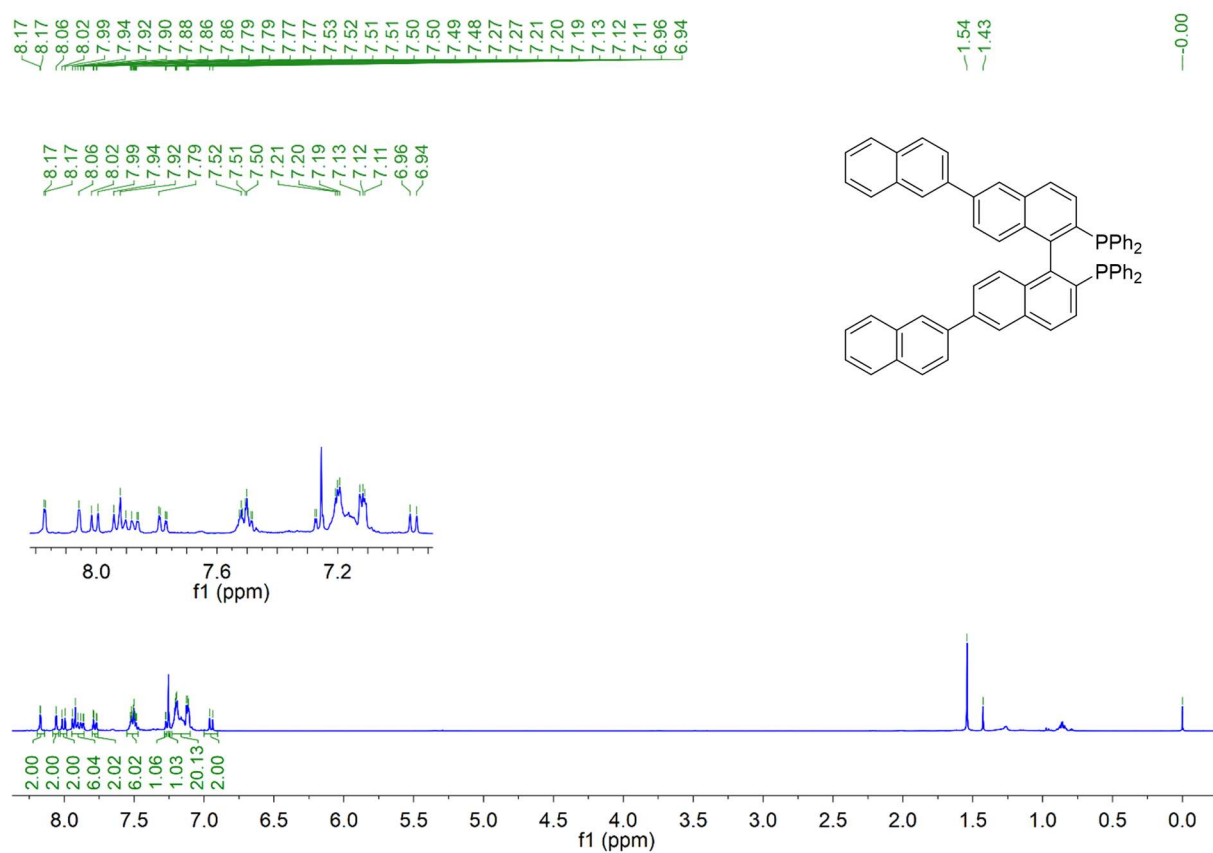
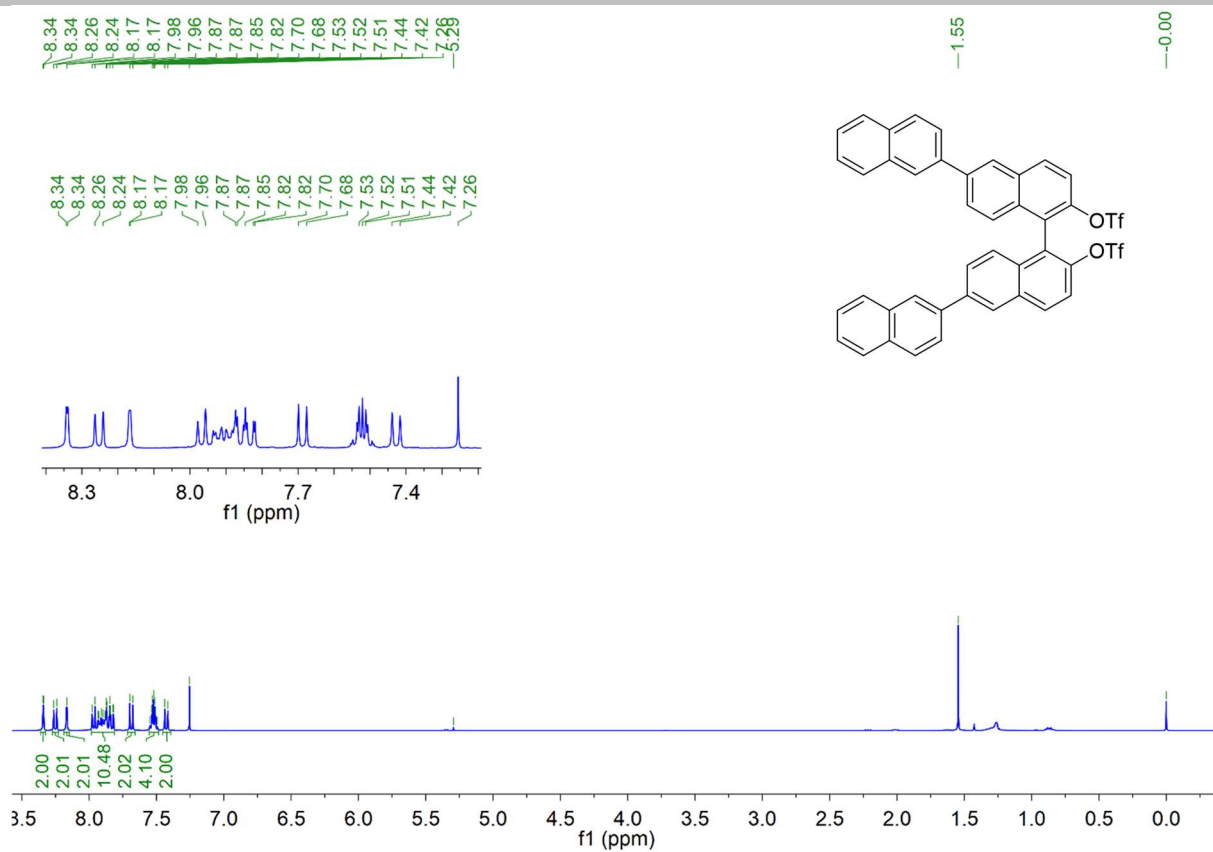
Supporting information



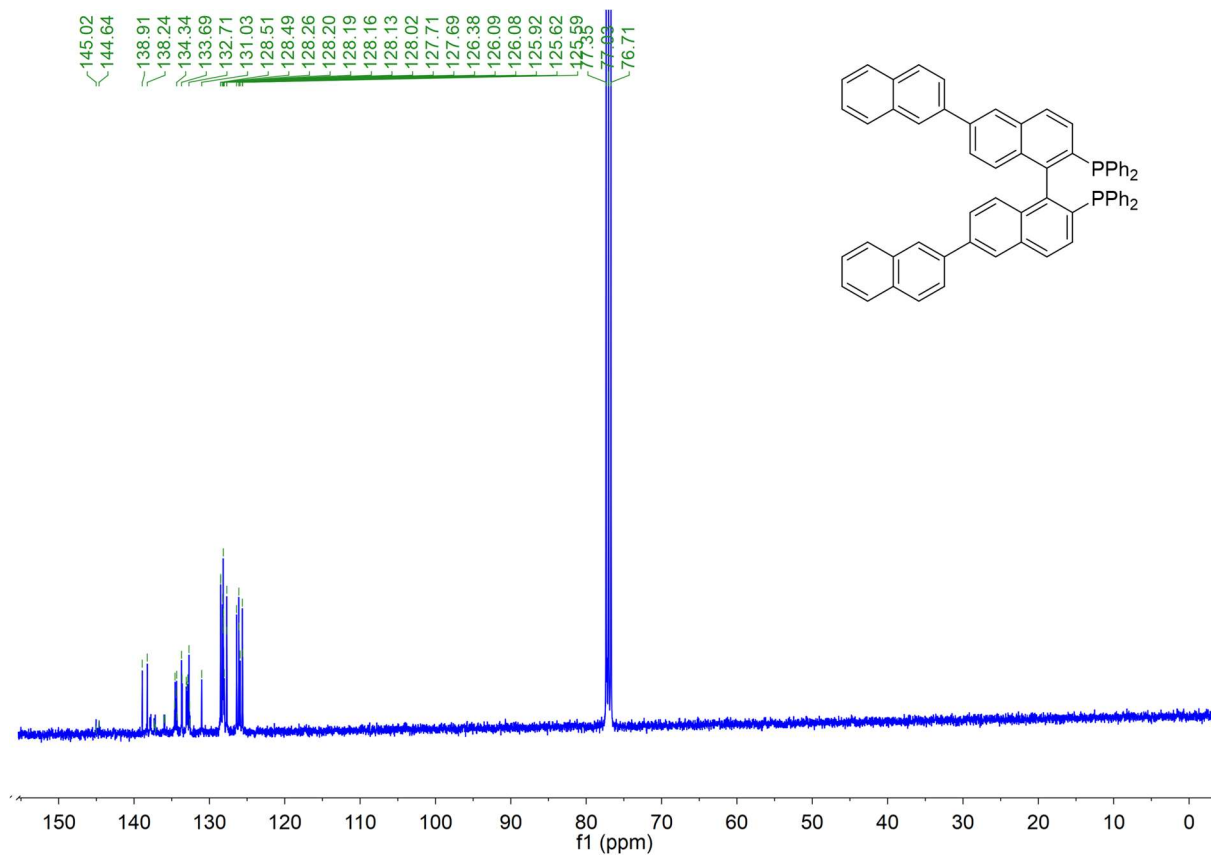
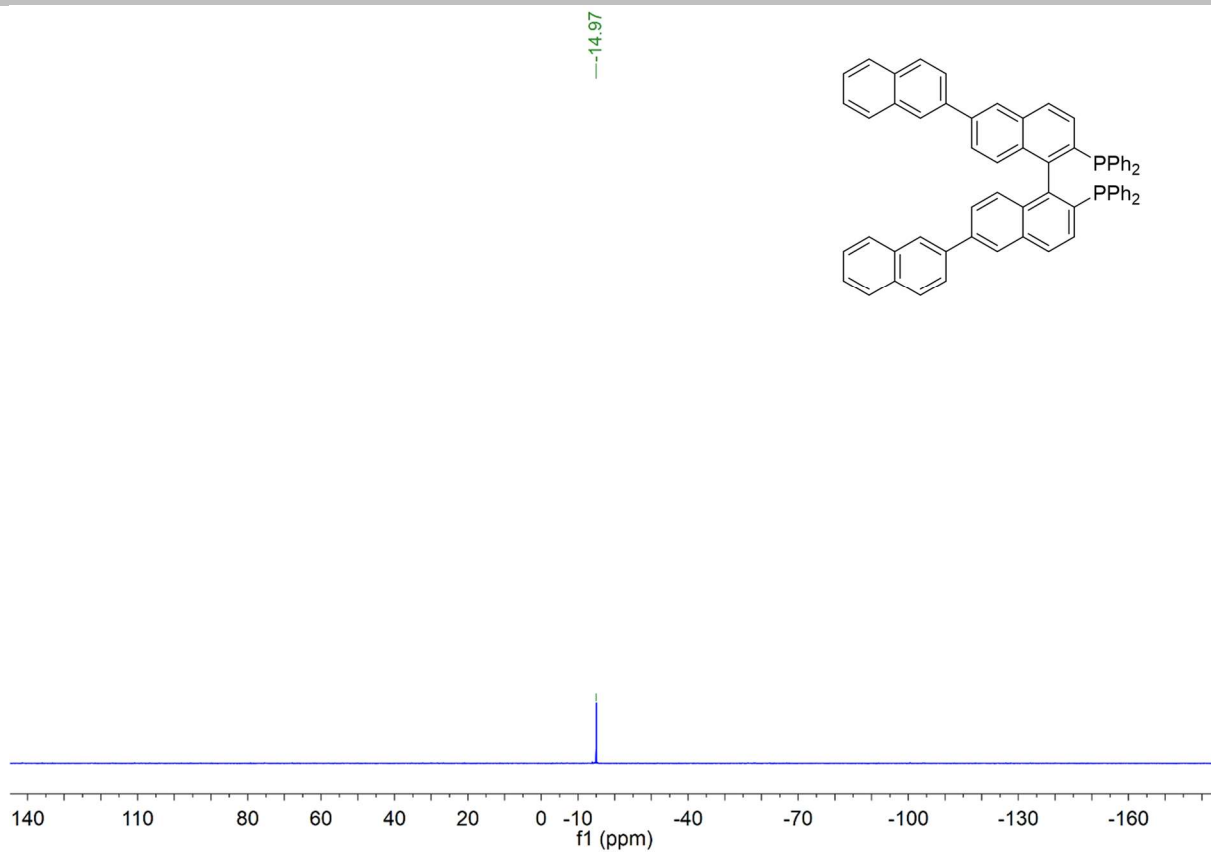
Supporting information



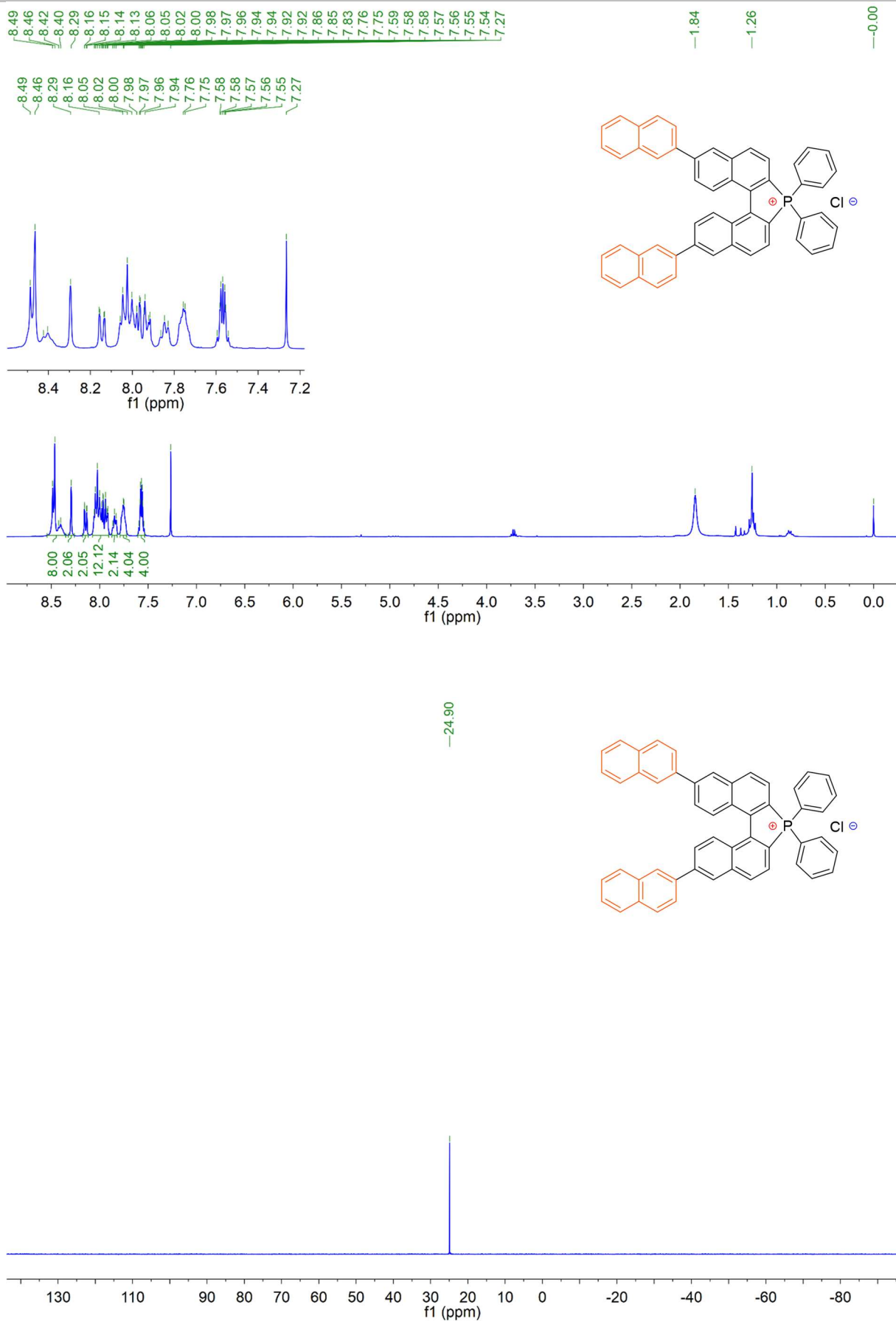
Supporting information



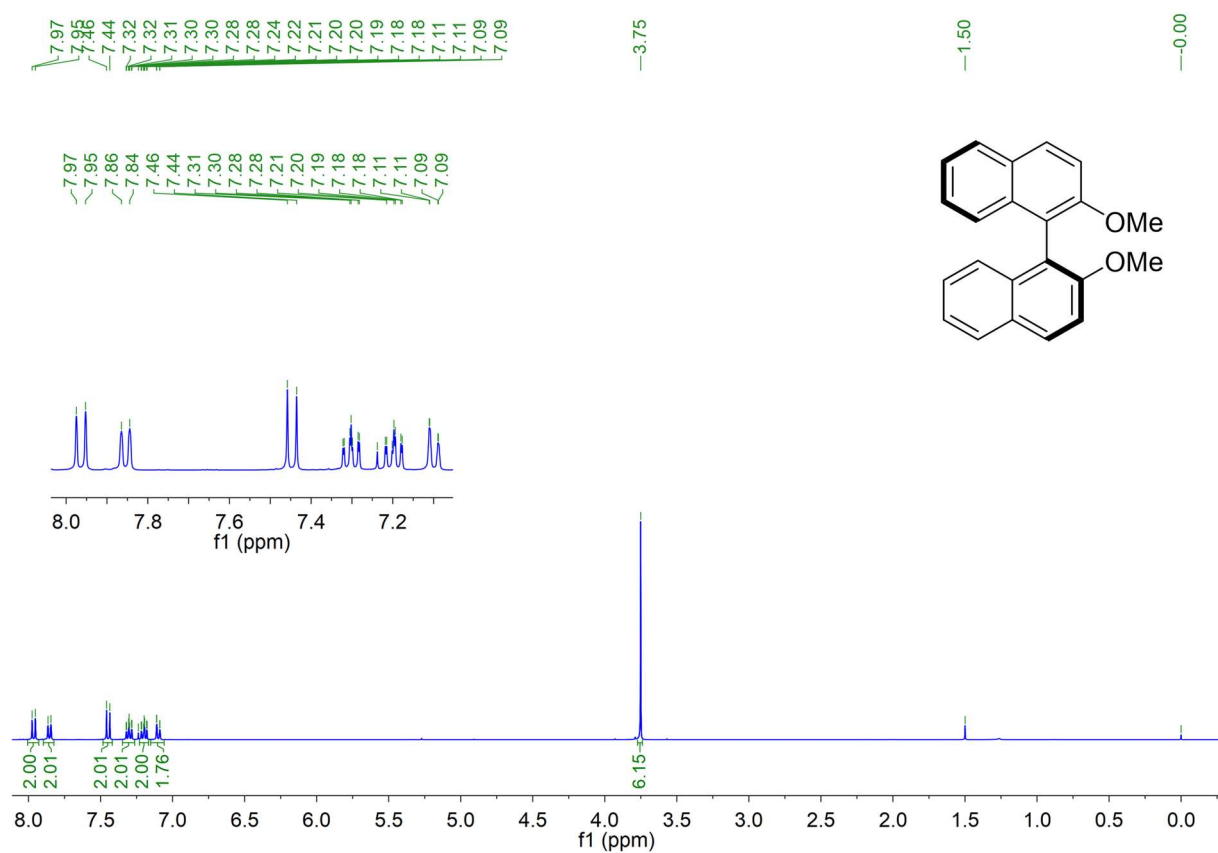
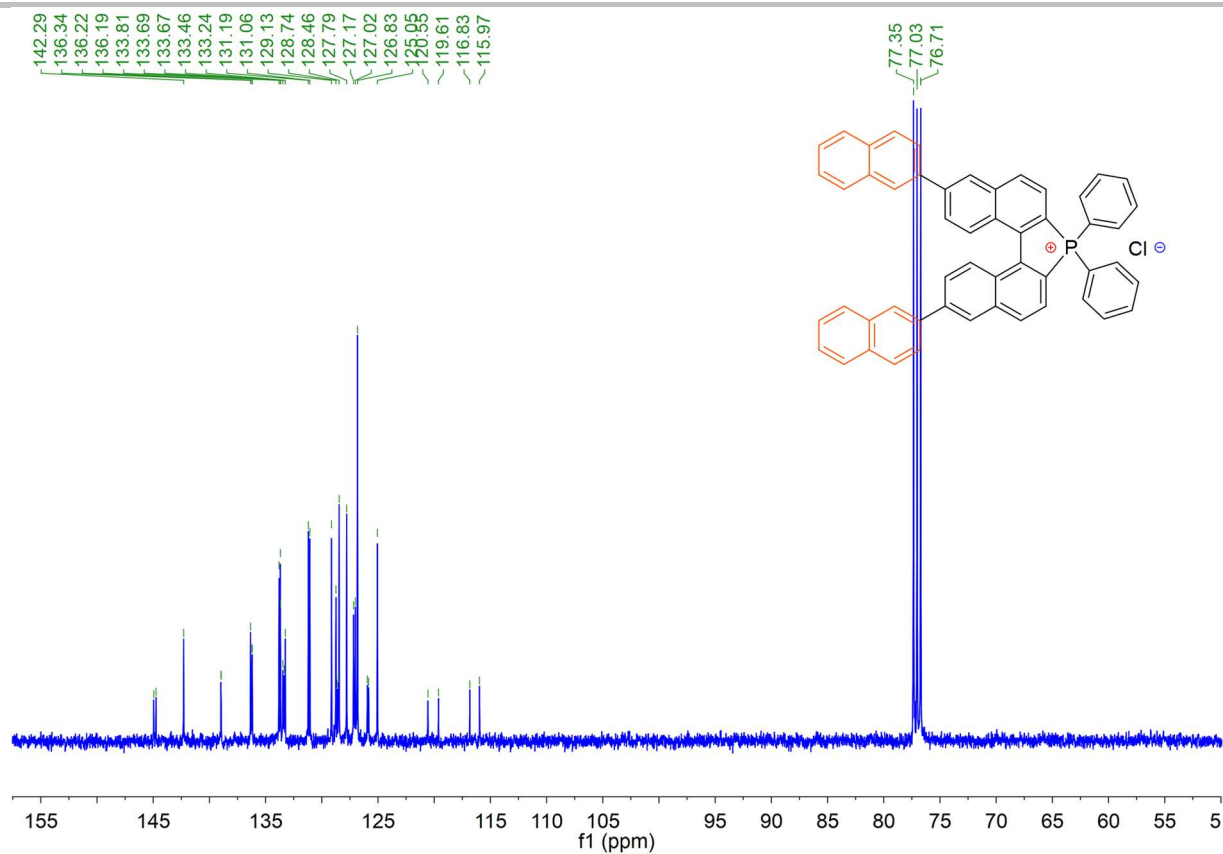
Supporting information



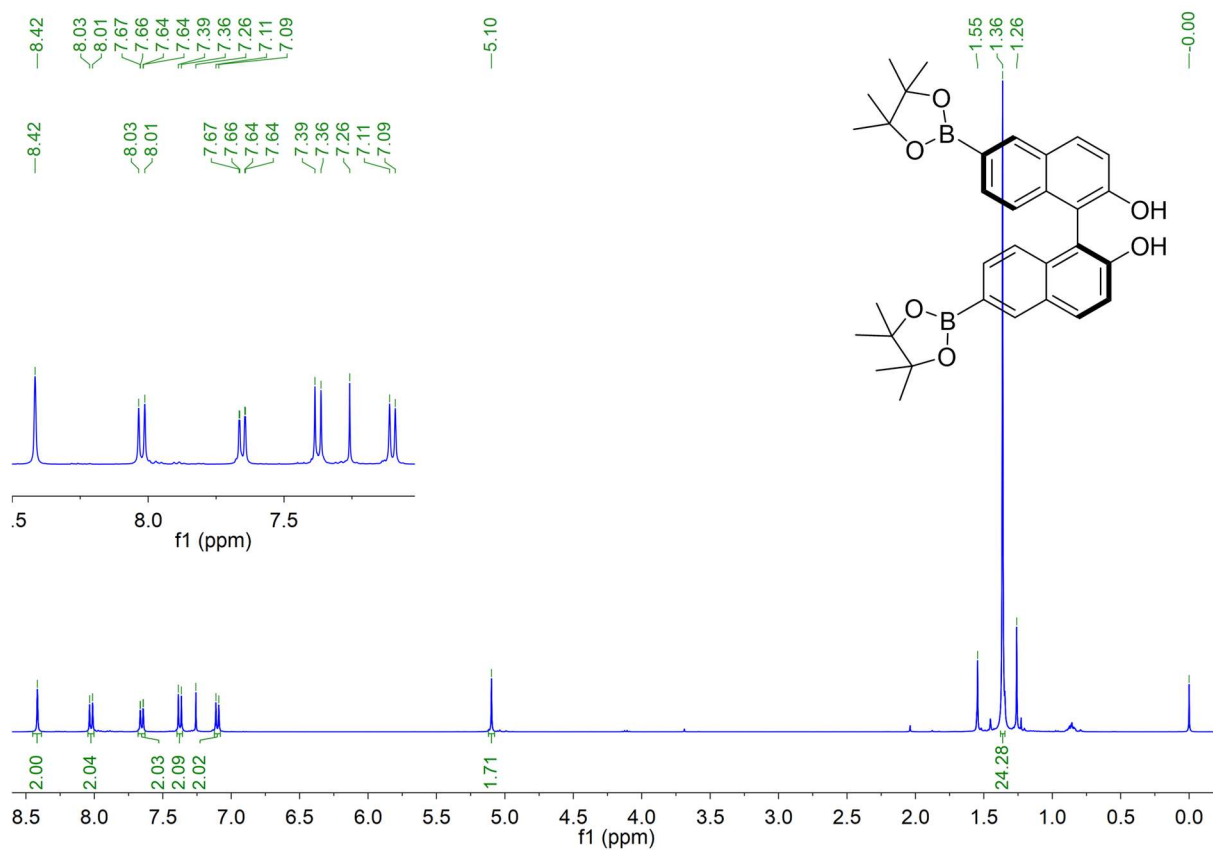
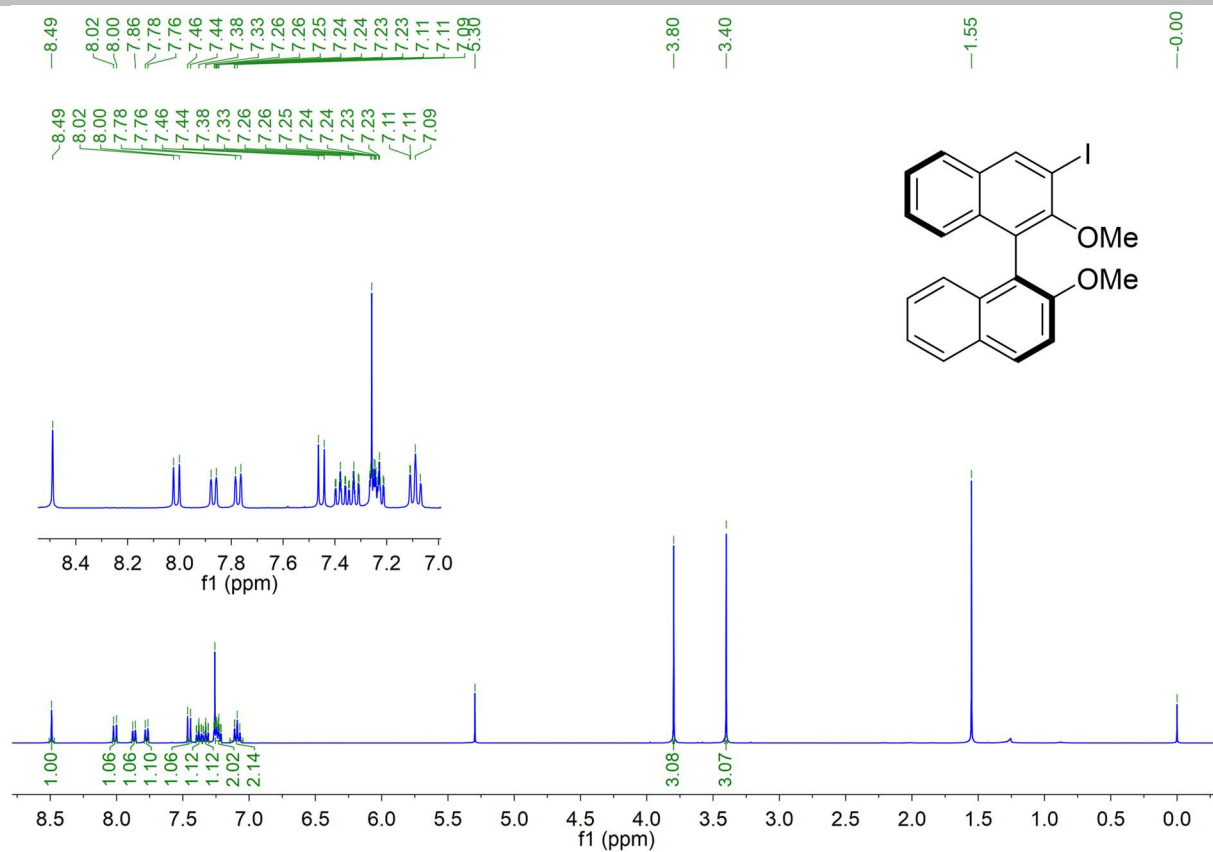
Supporting information



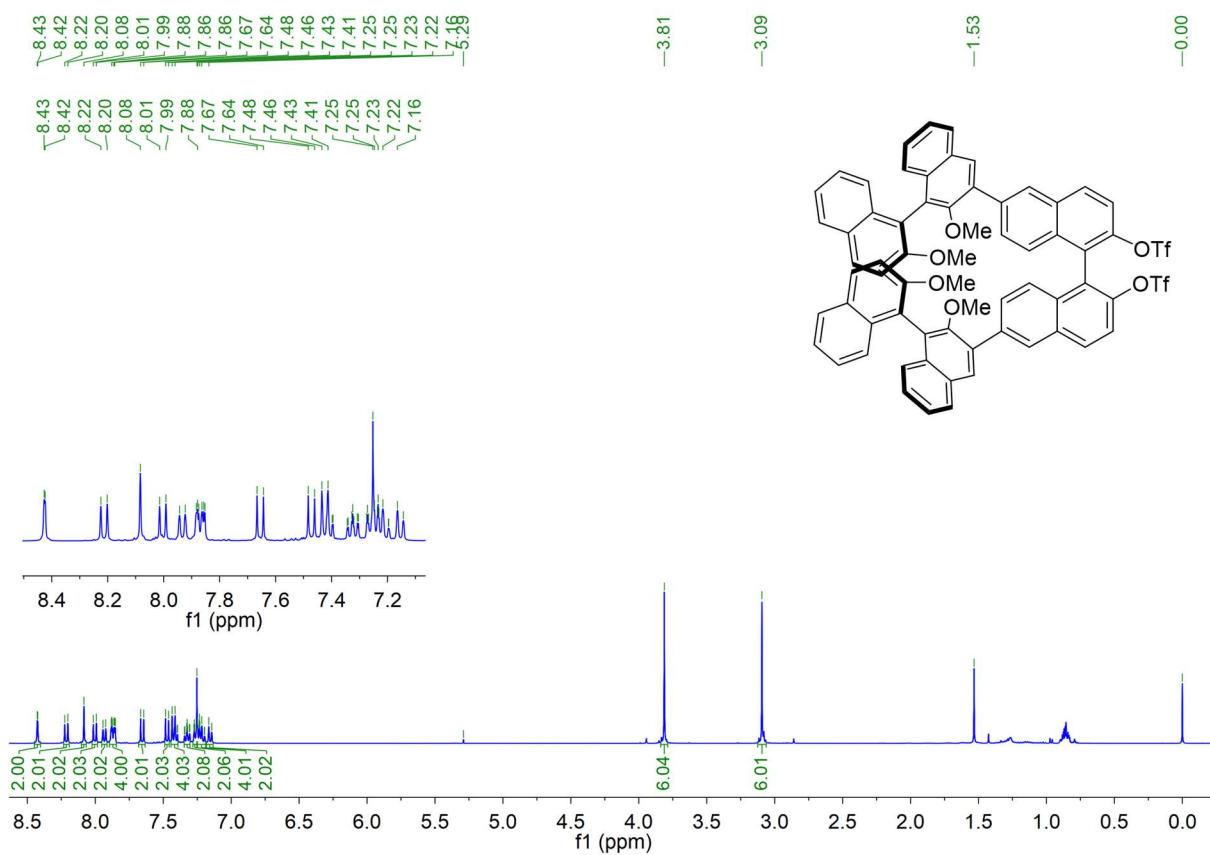
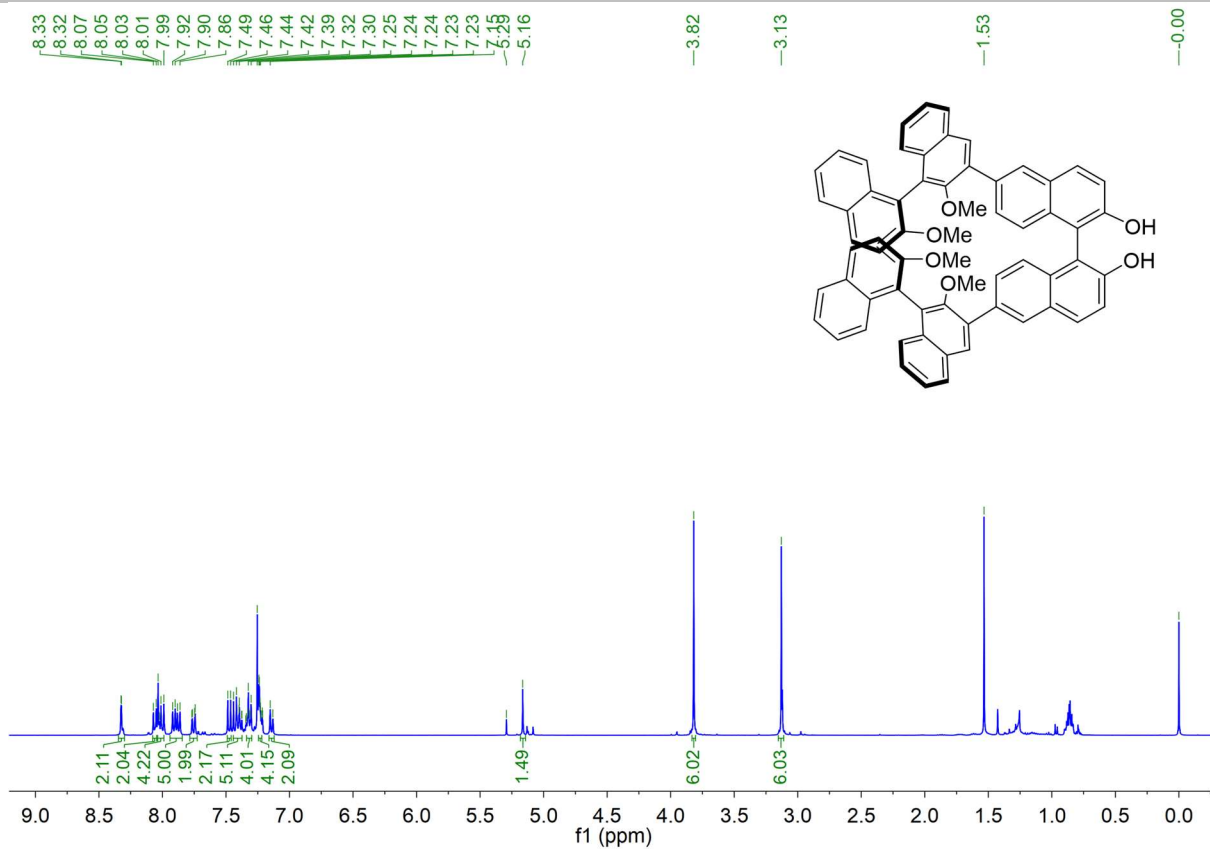
Supporting information



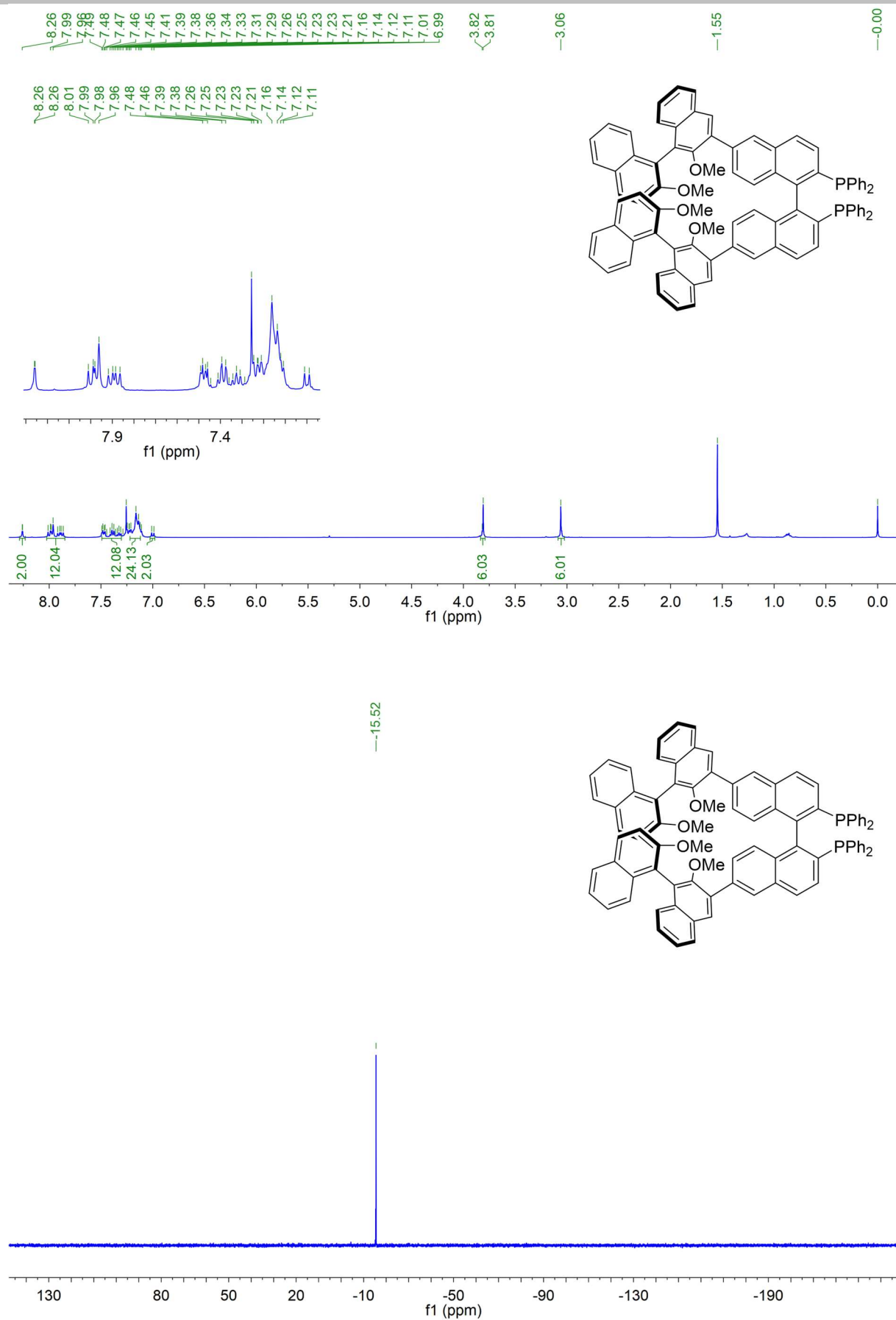
Supporting information



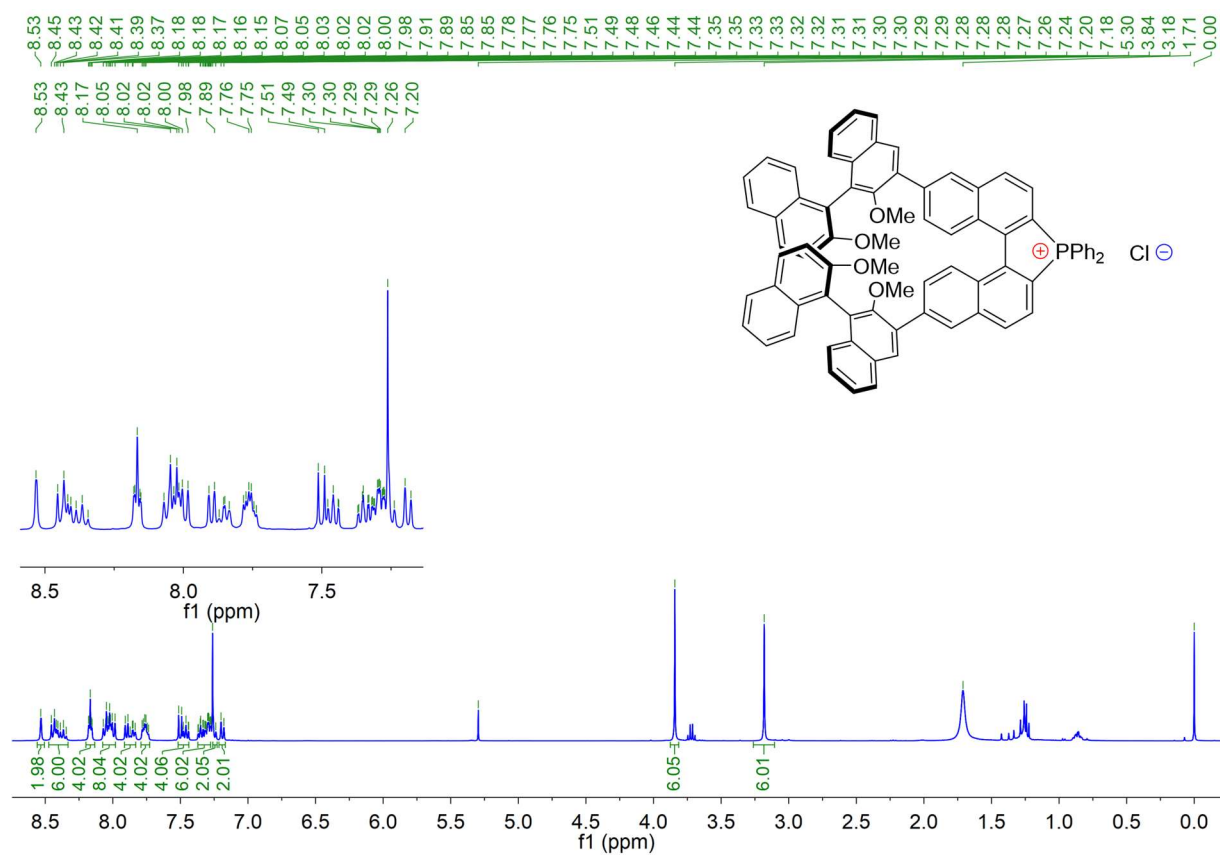
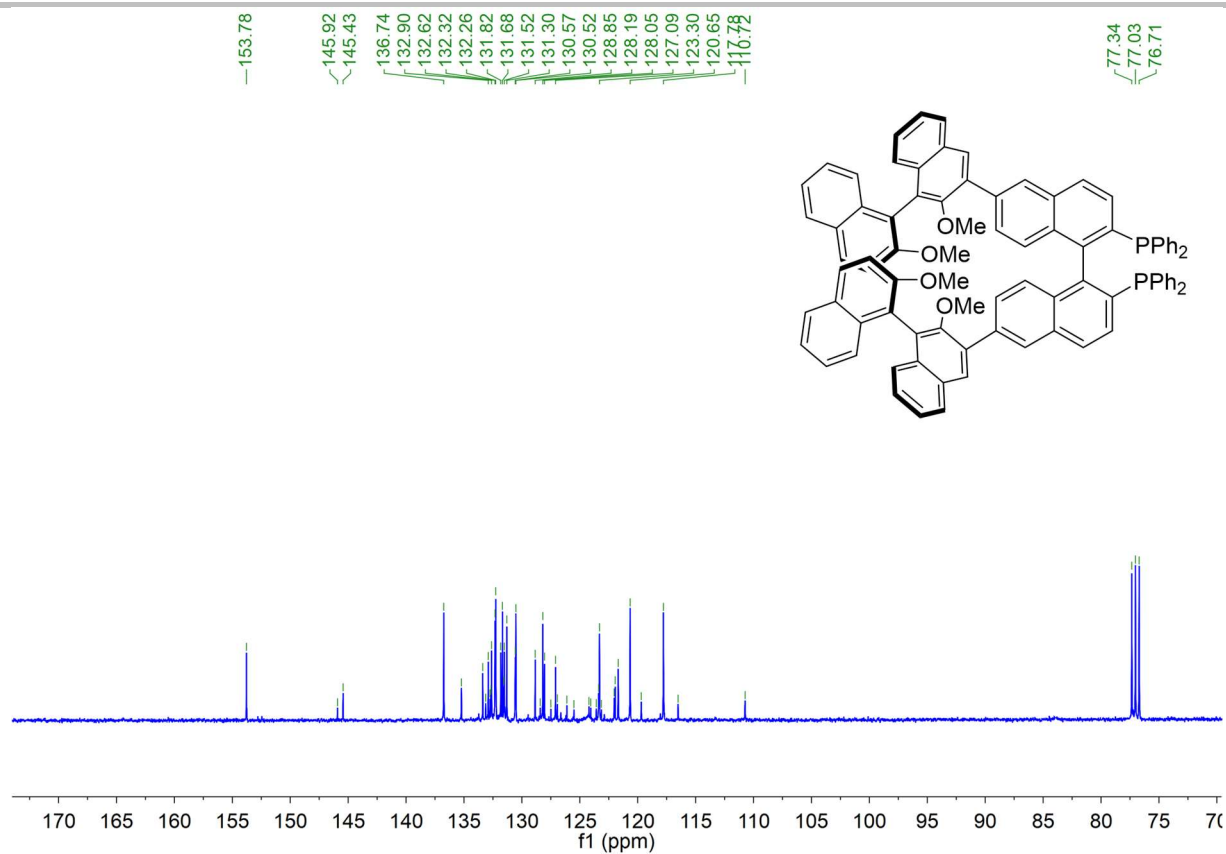
Supporting information



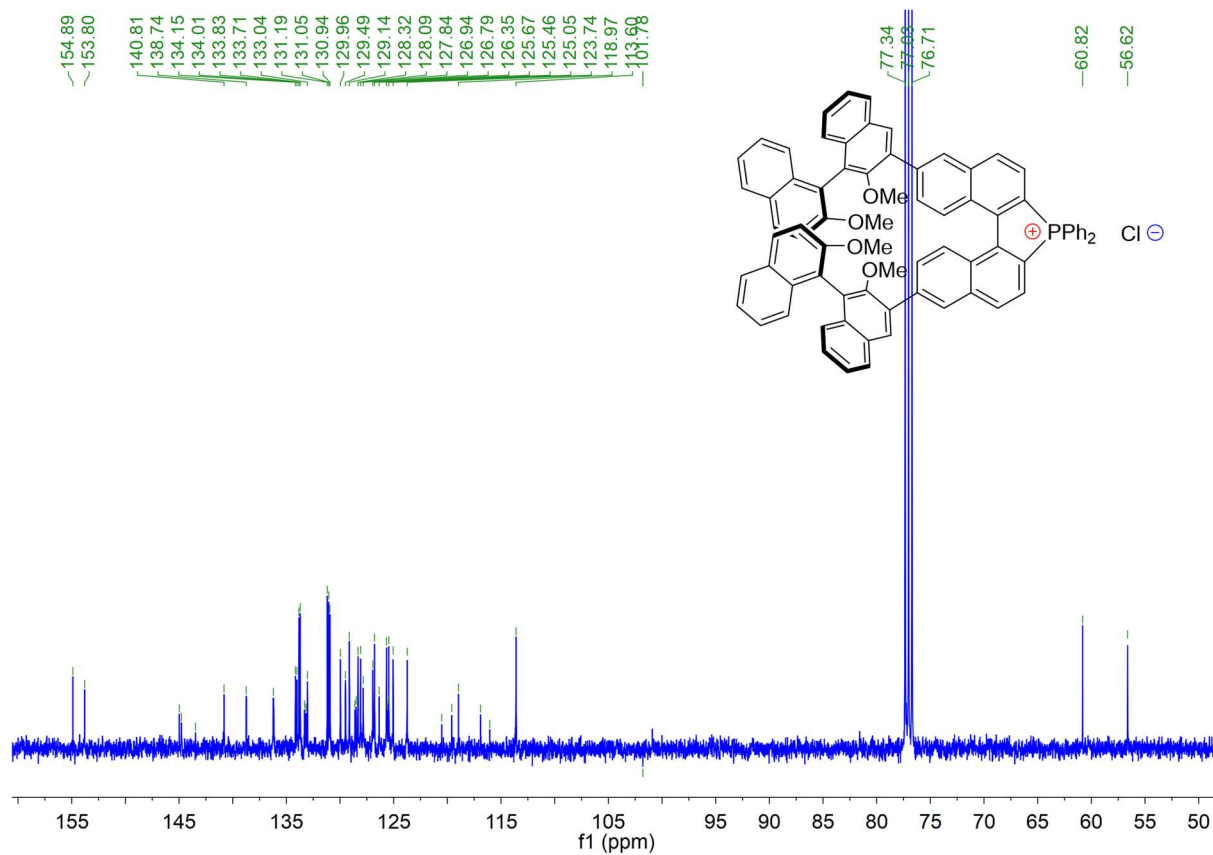
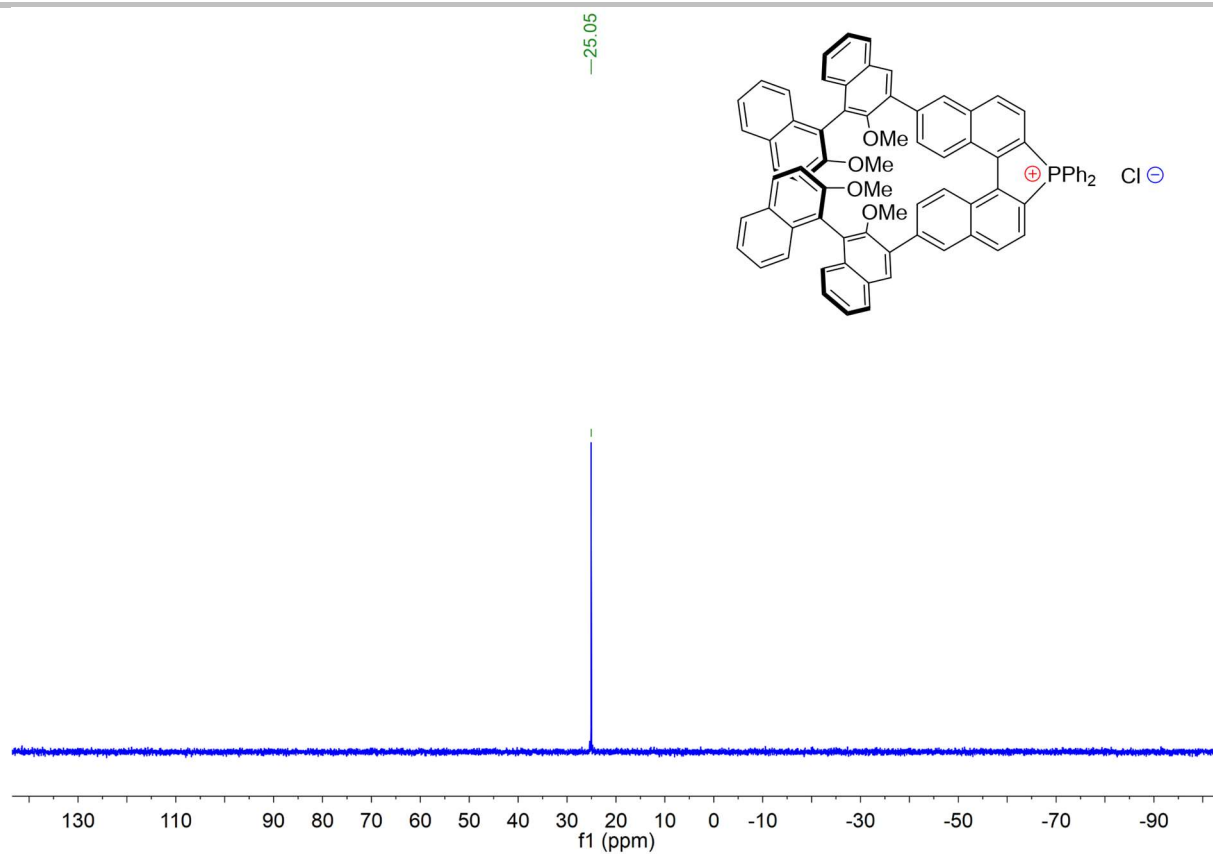
Supporting information



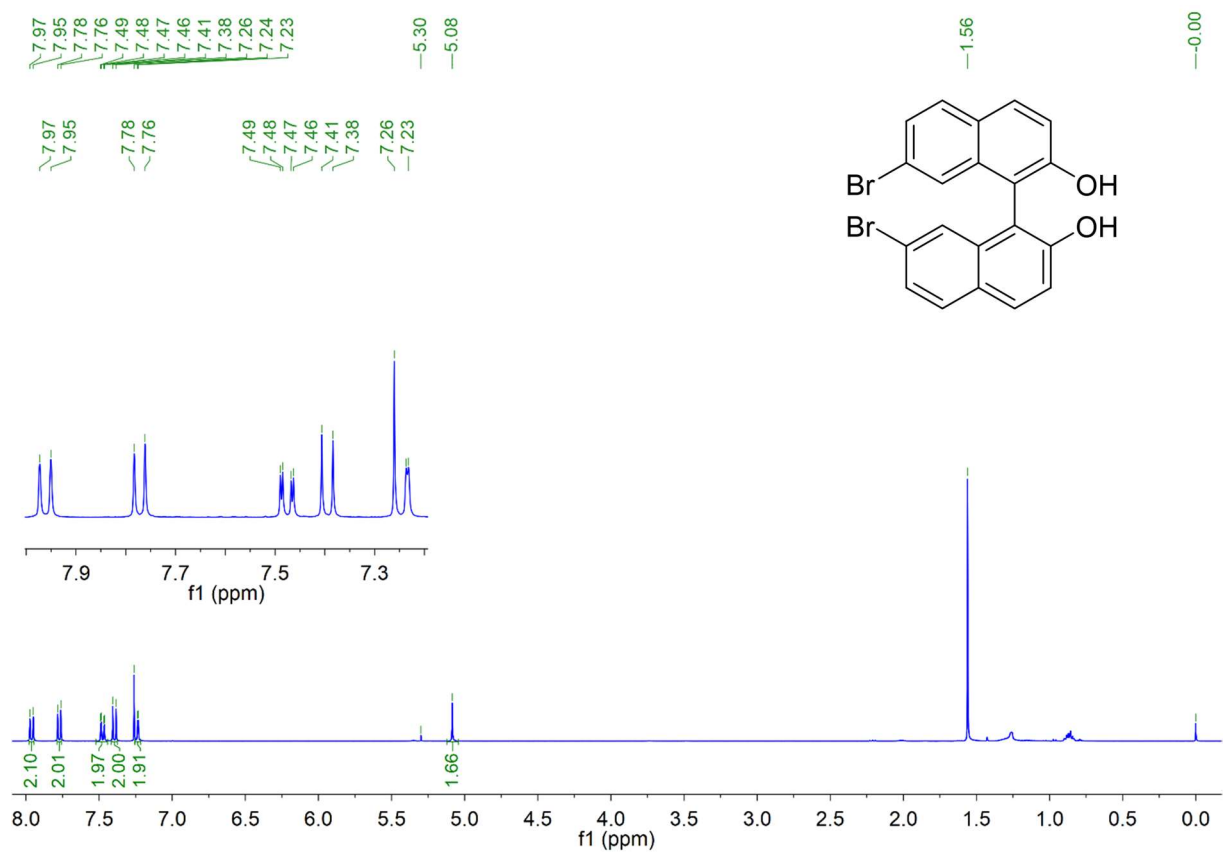
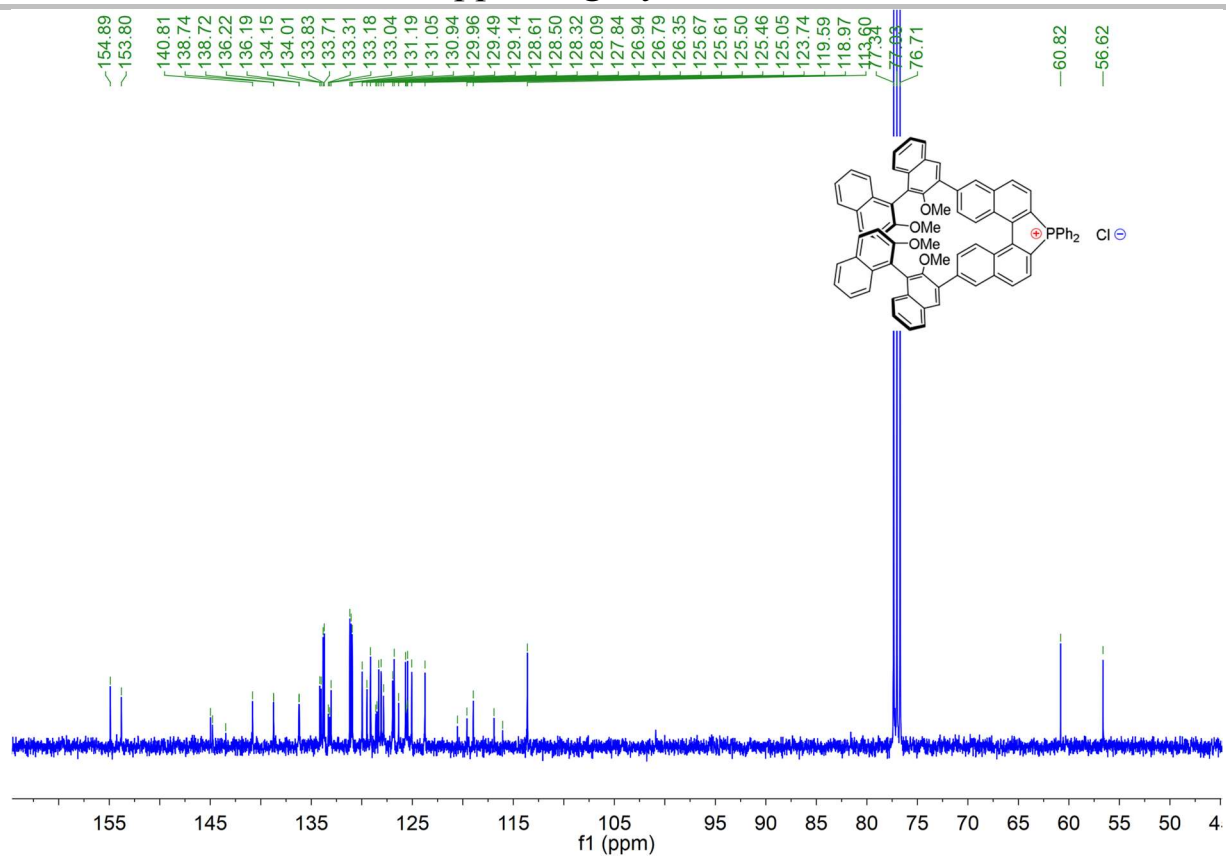
Supporting information



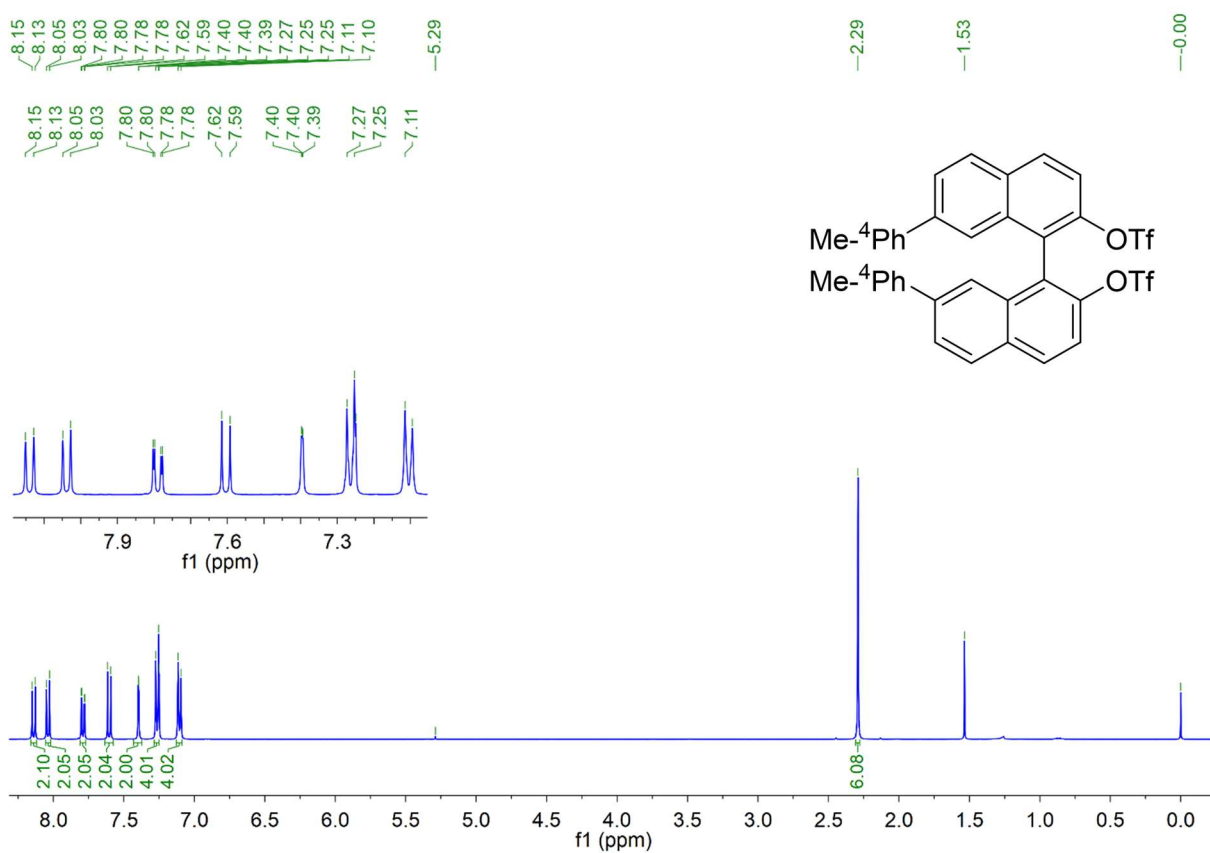
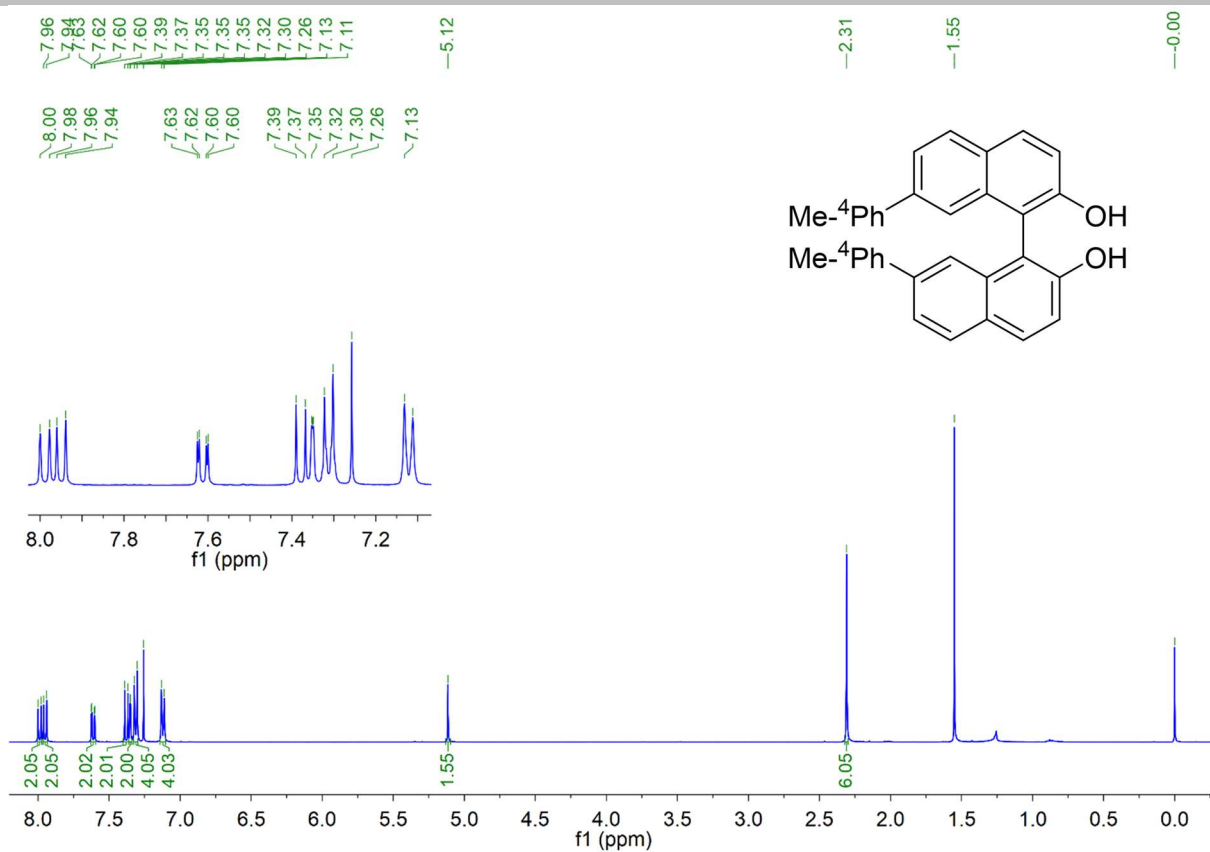
Supporting information



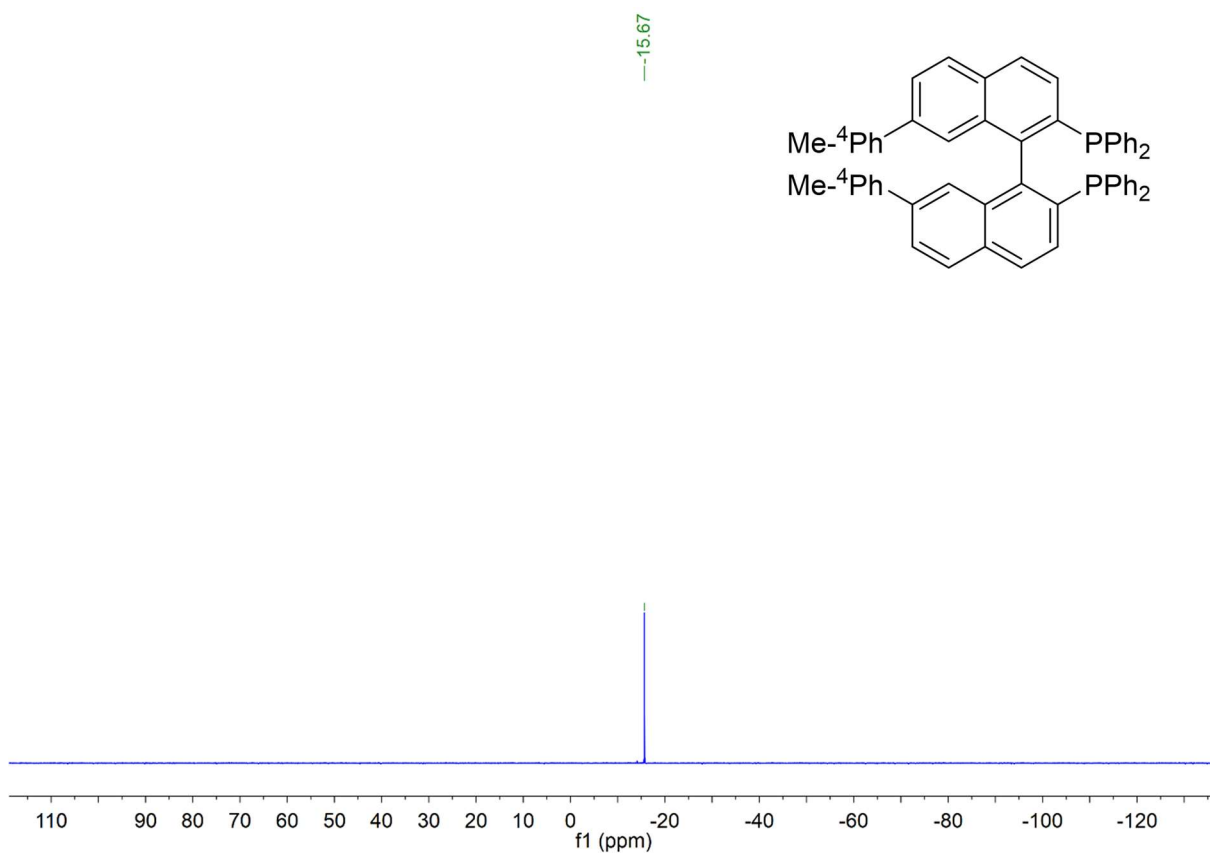
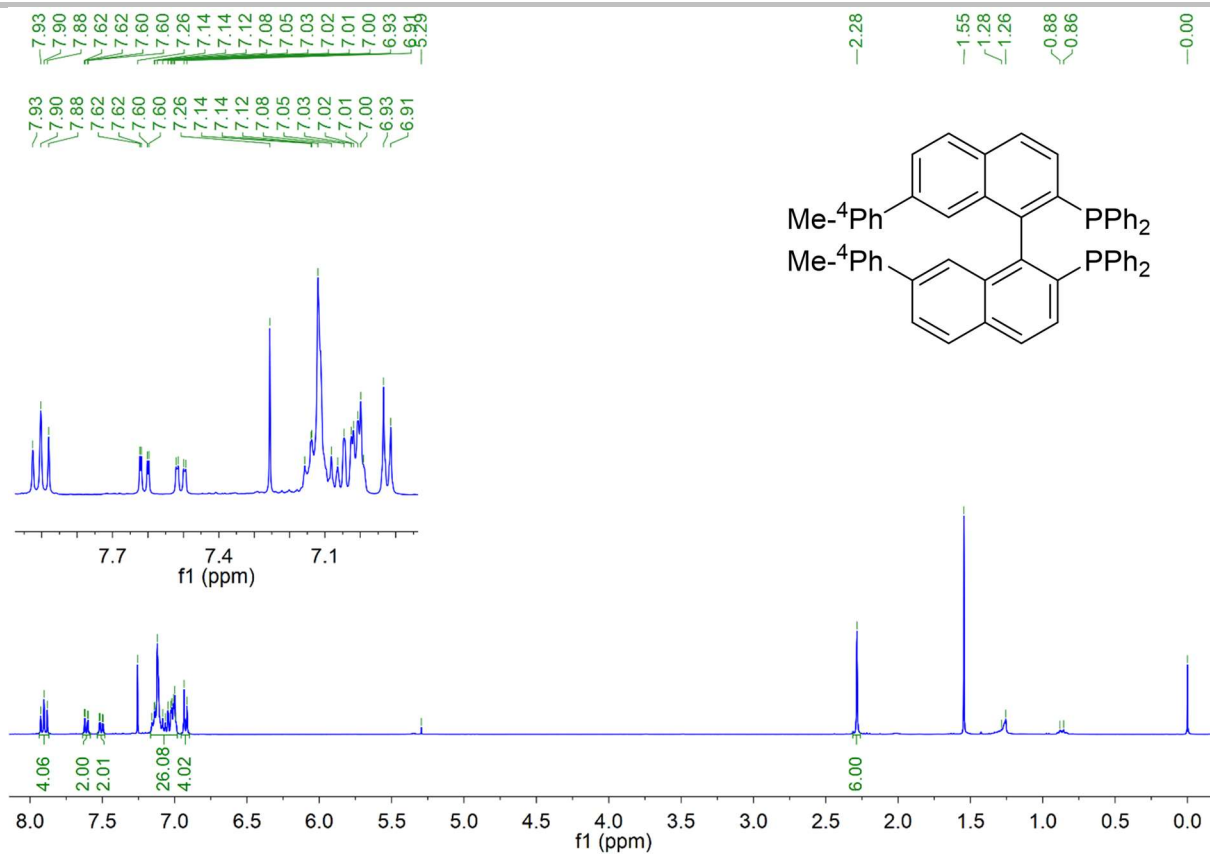
Supporting information



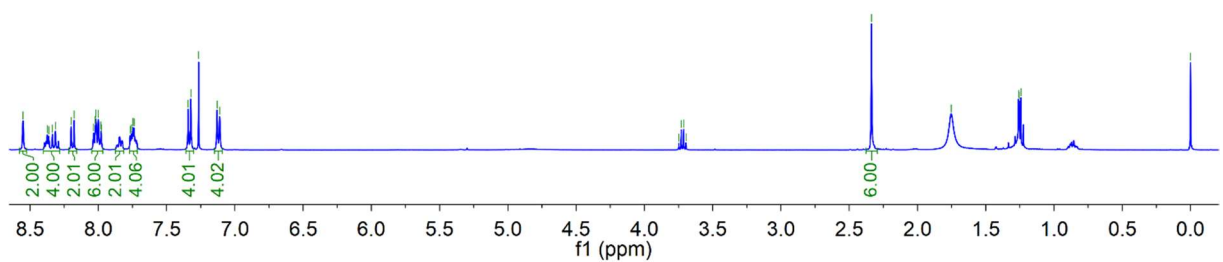
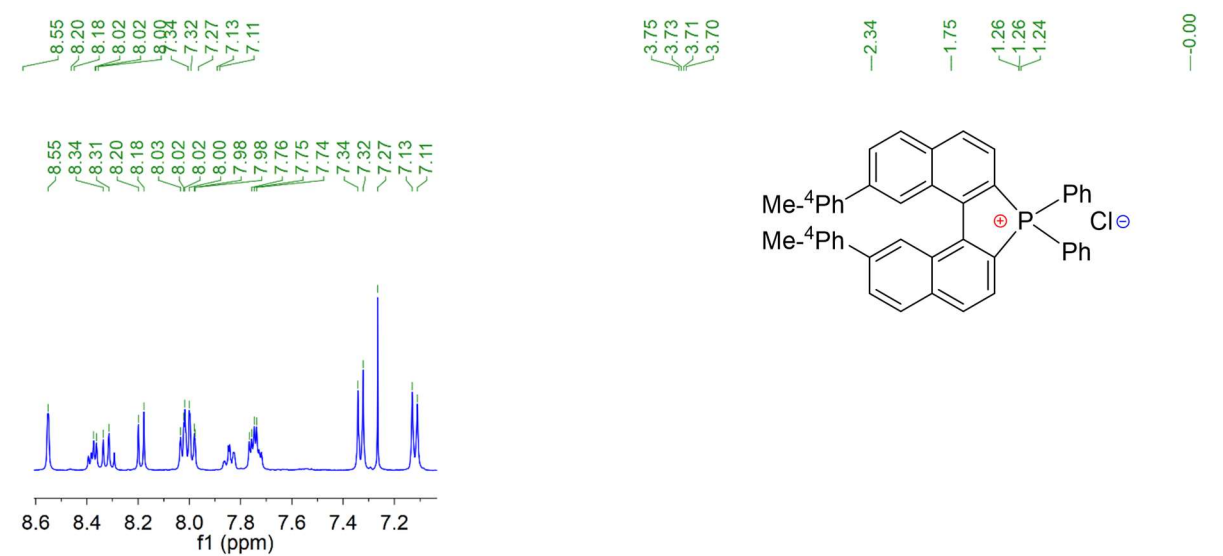
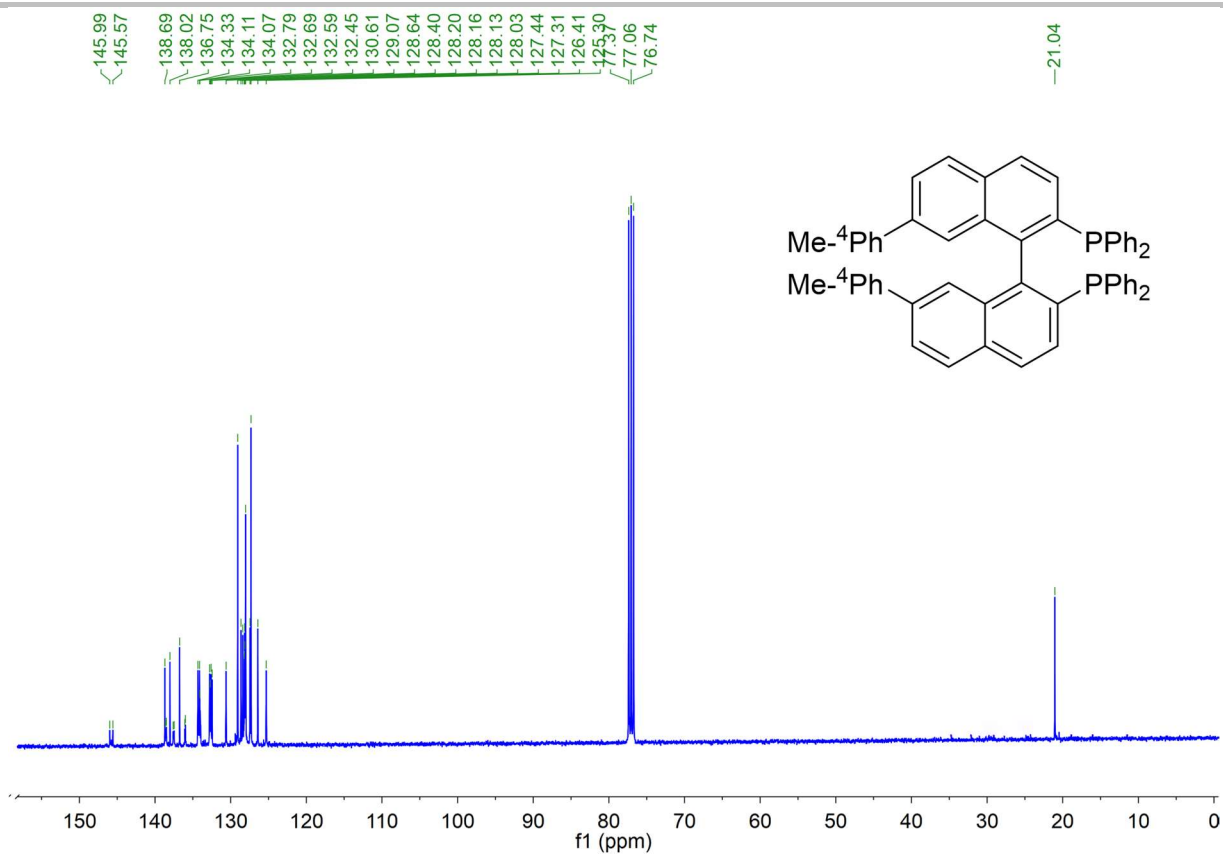
Supporting information



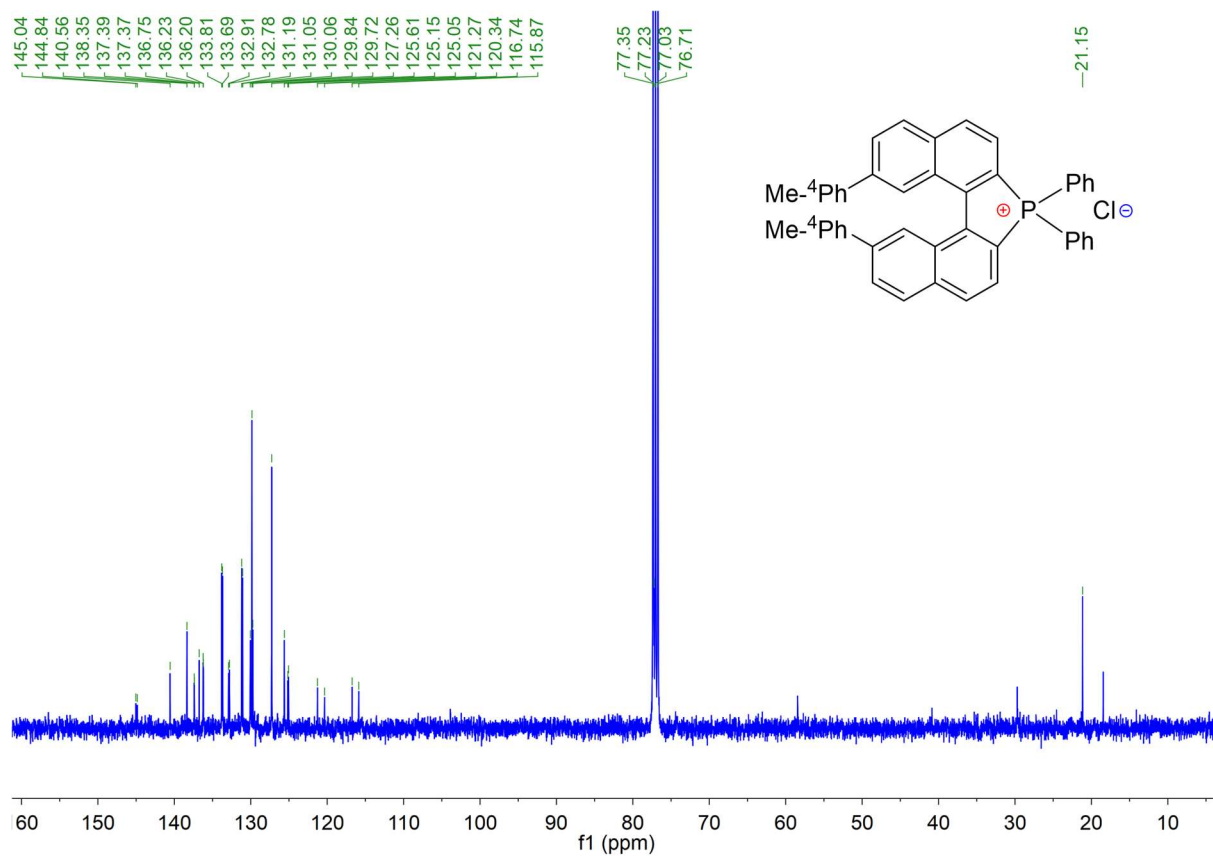
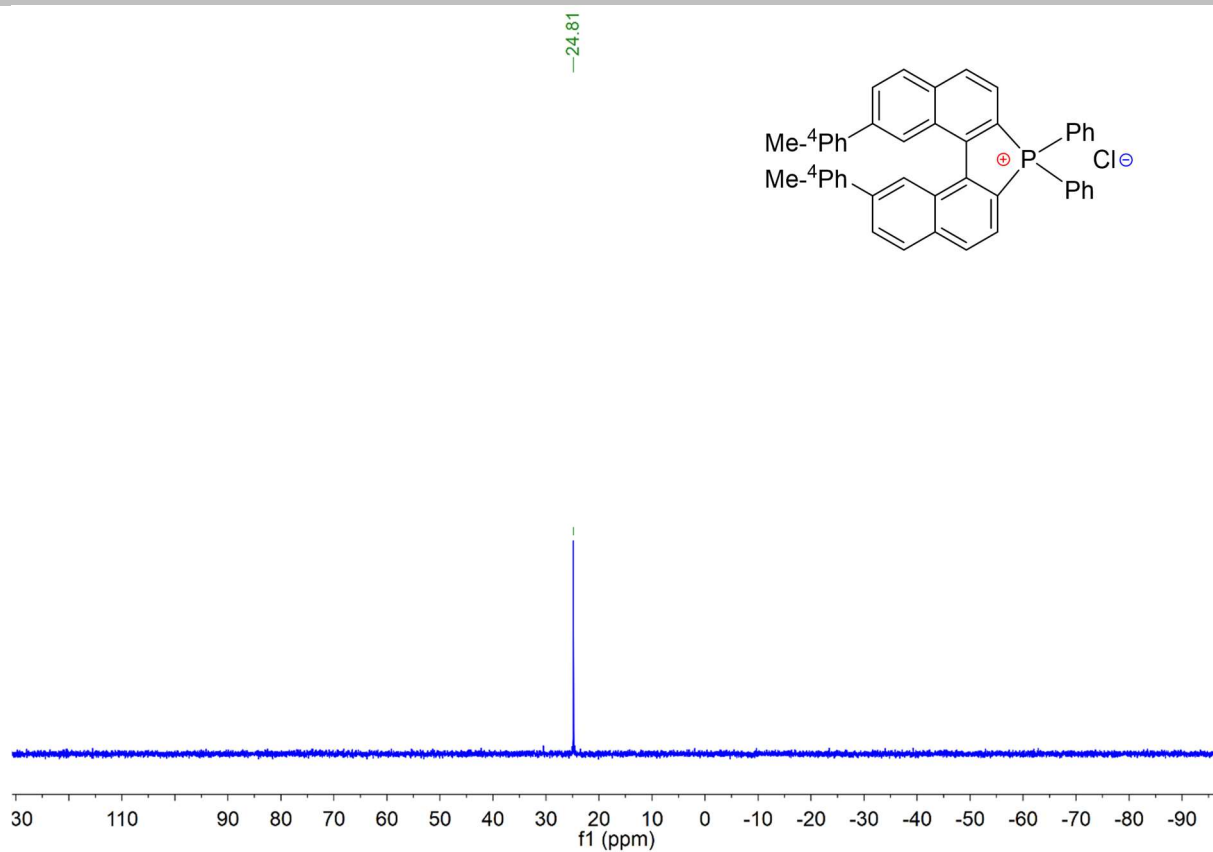
Supporting information



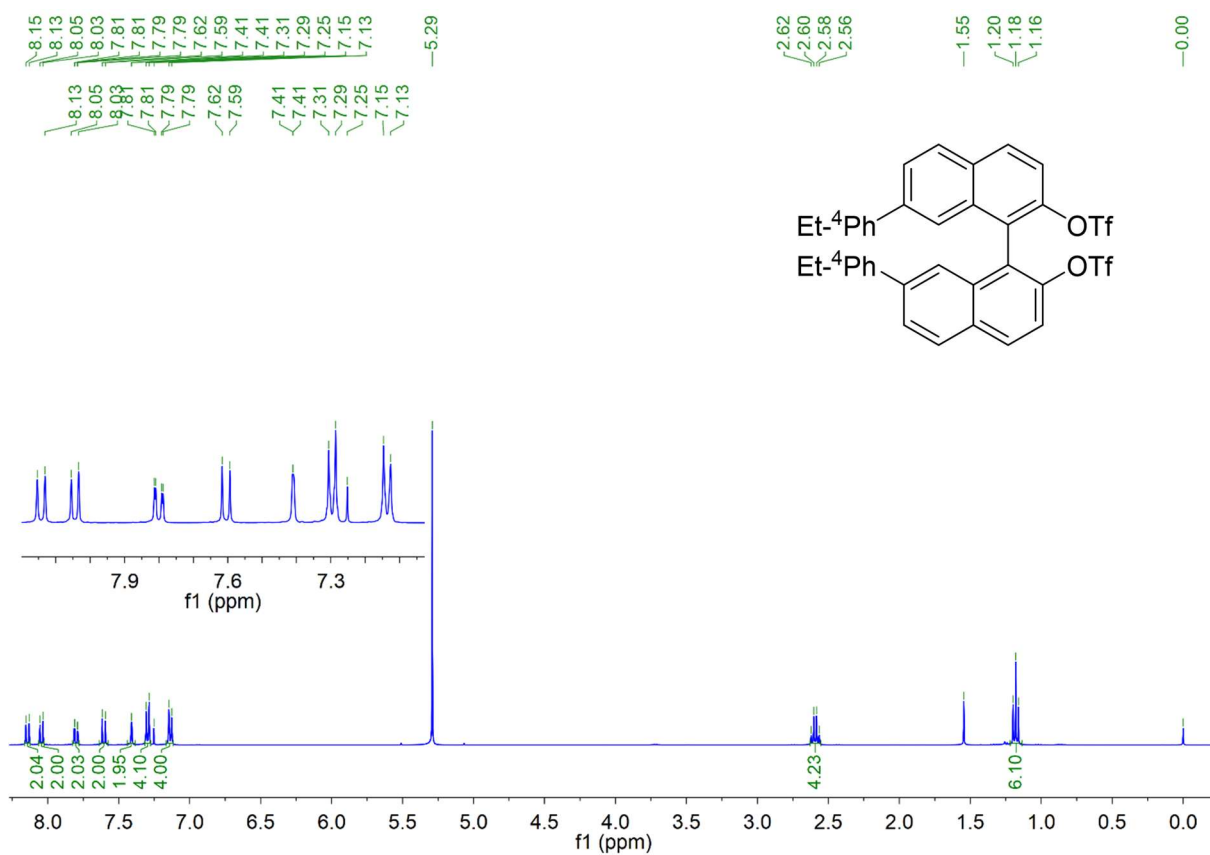
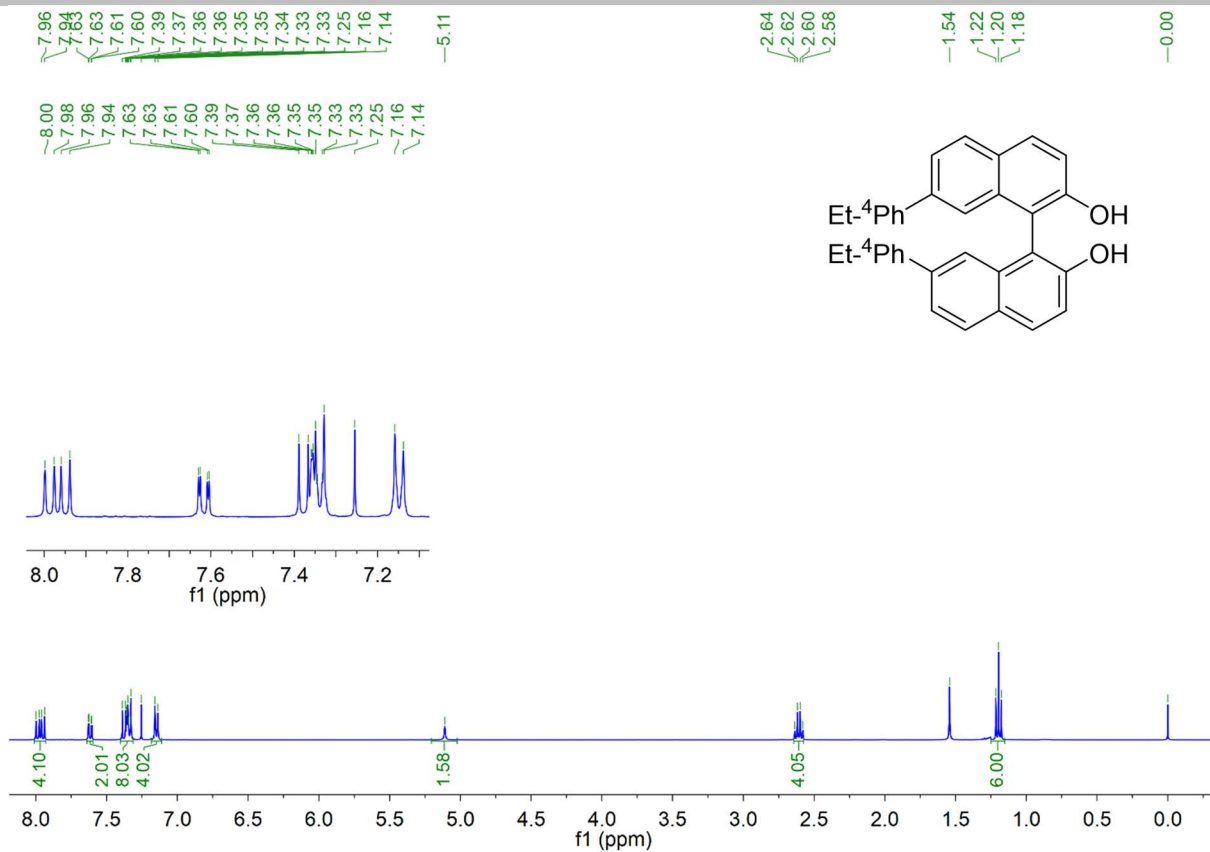
Supporting information



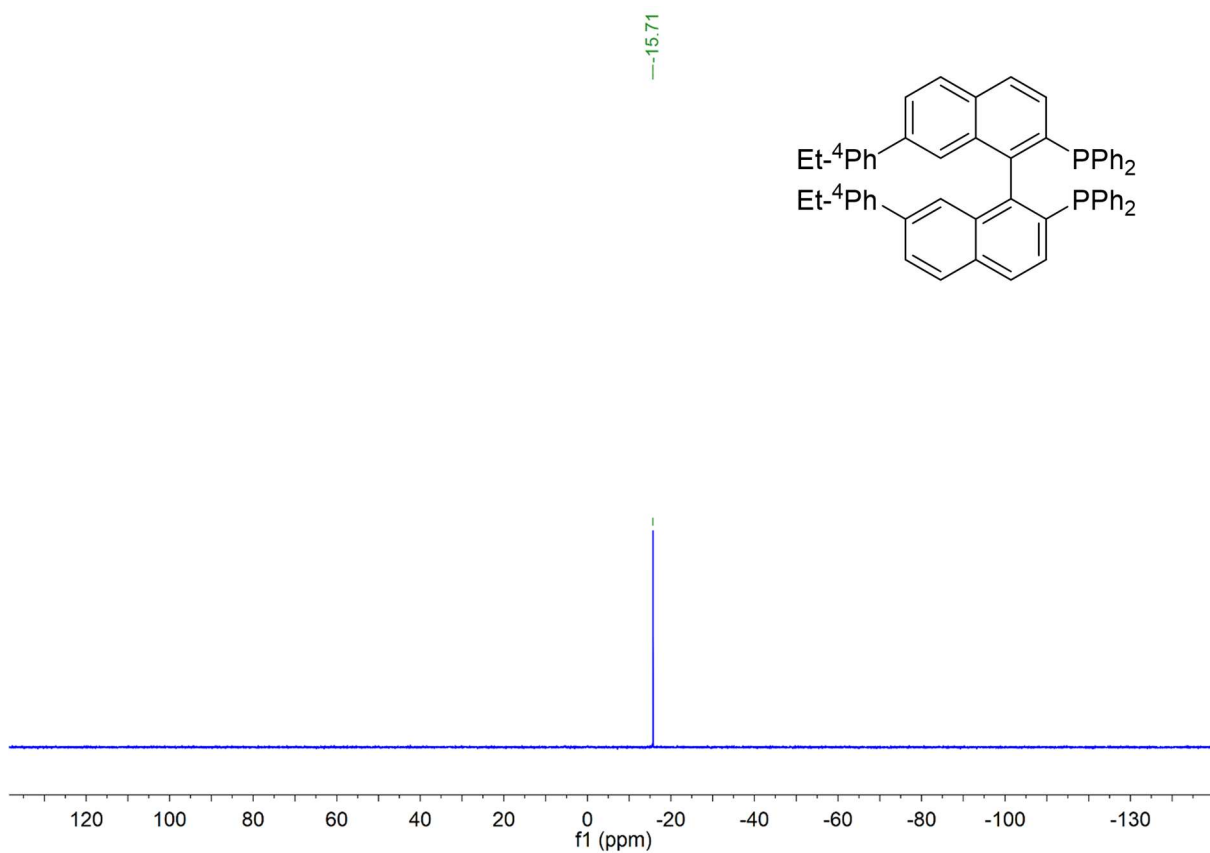
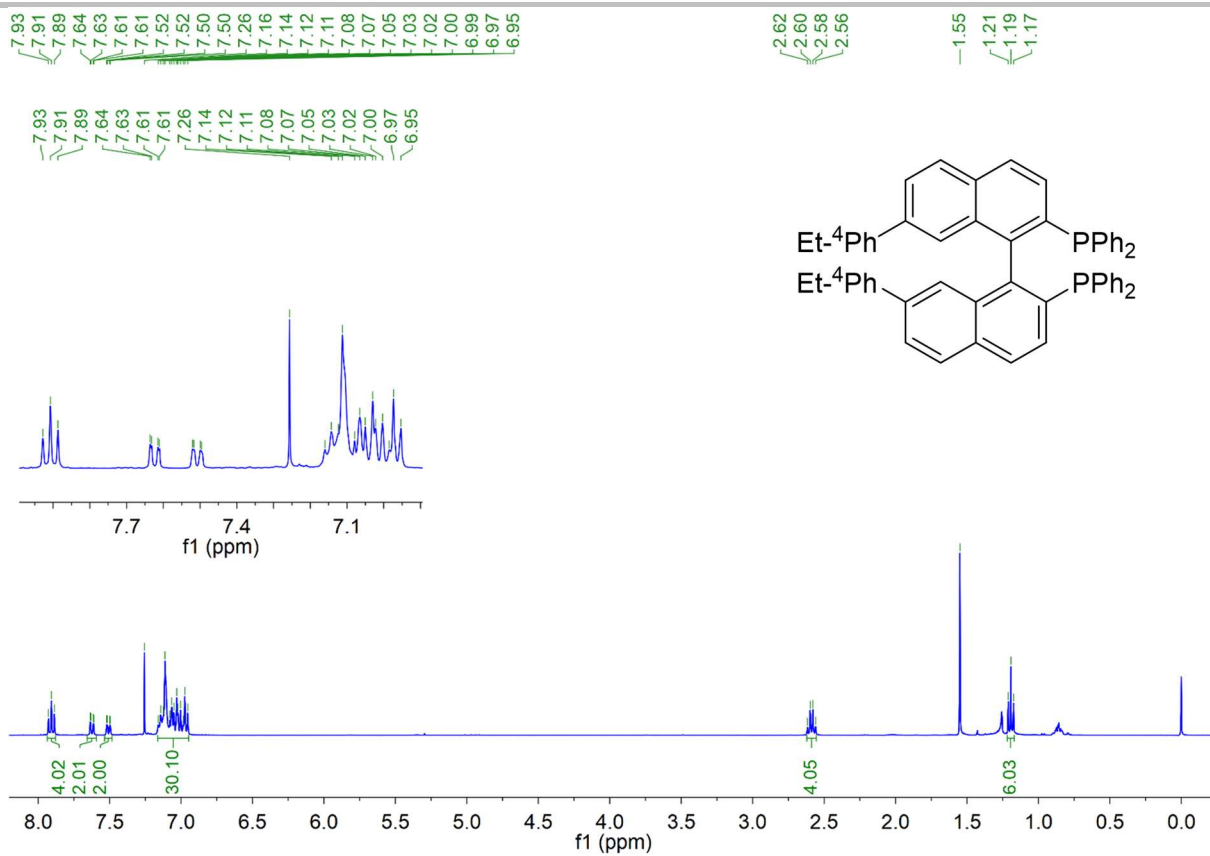
Supporting information



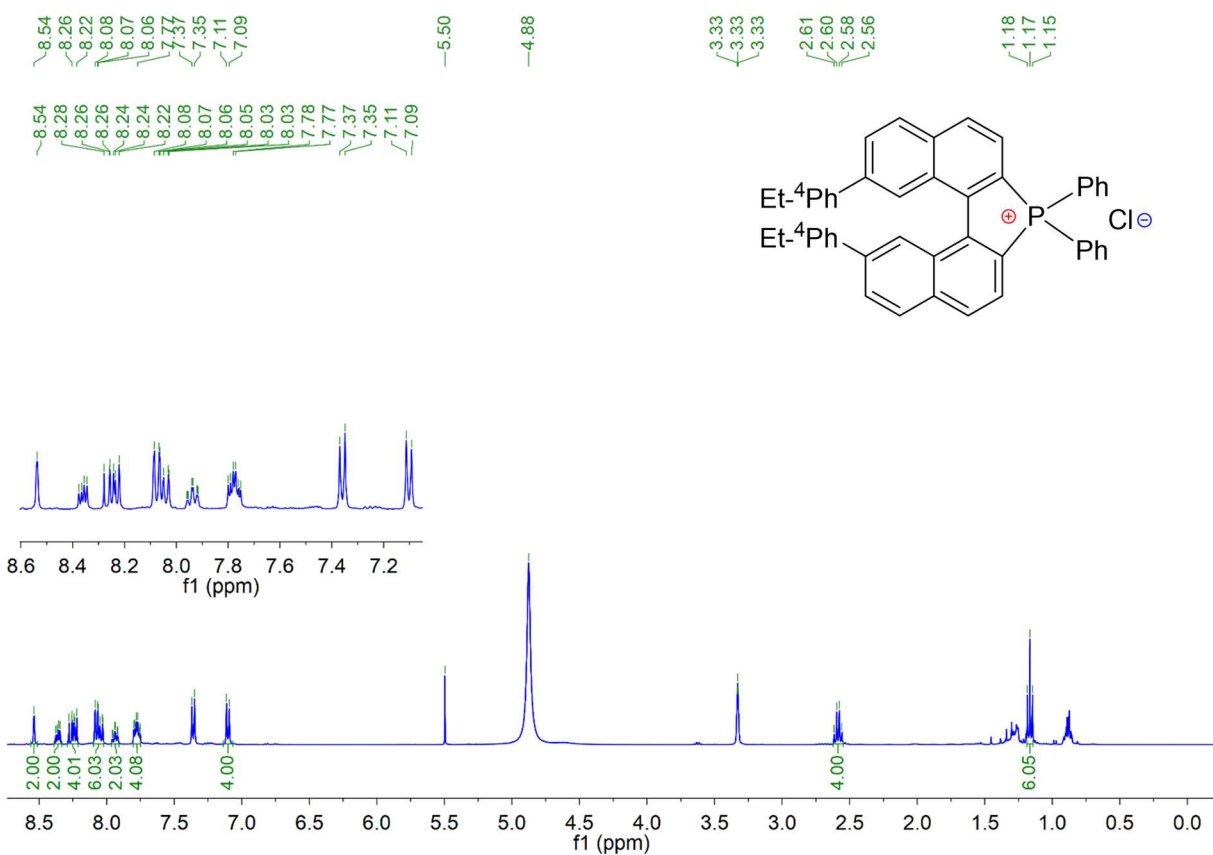
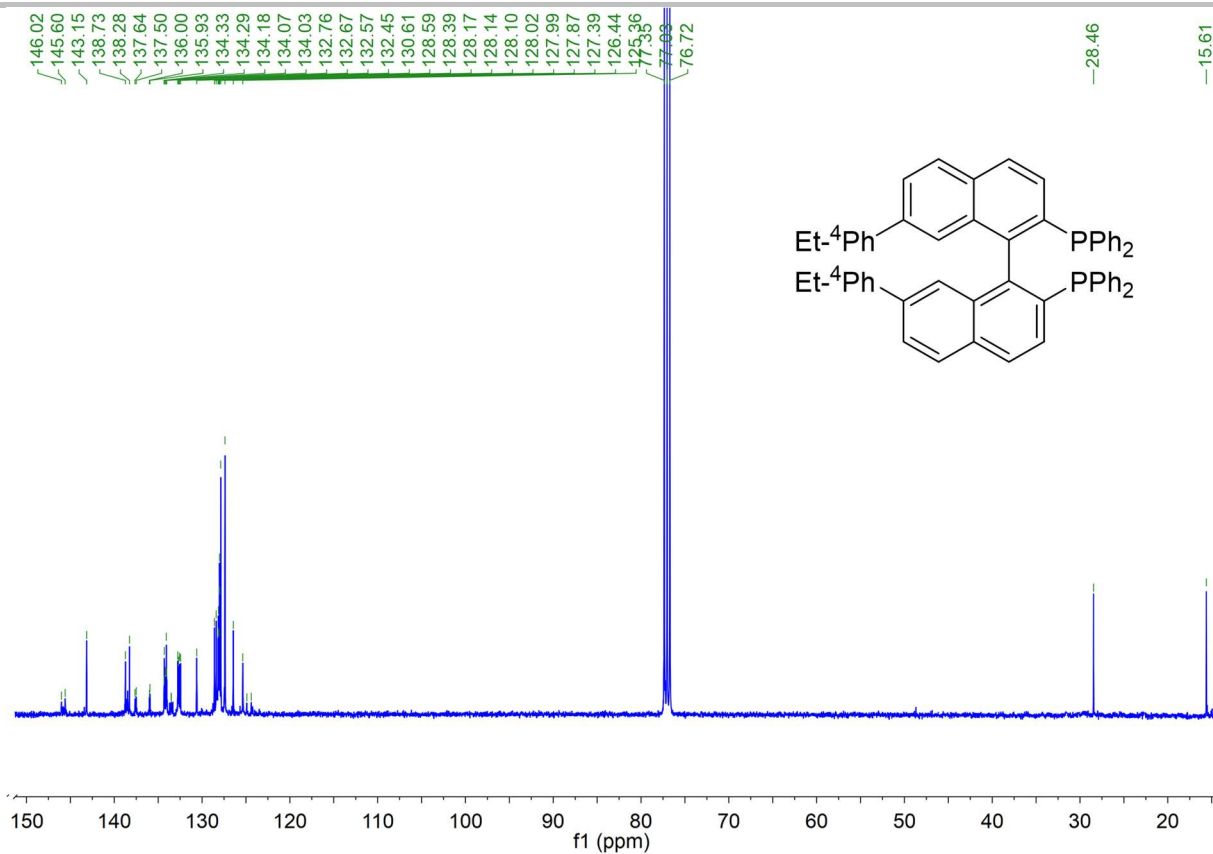
Supporting information



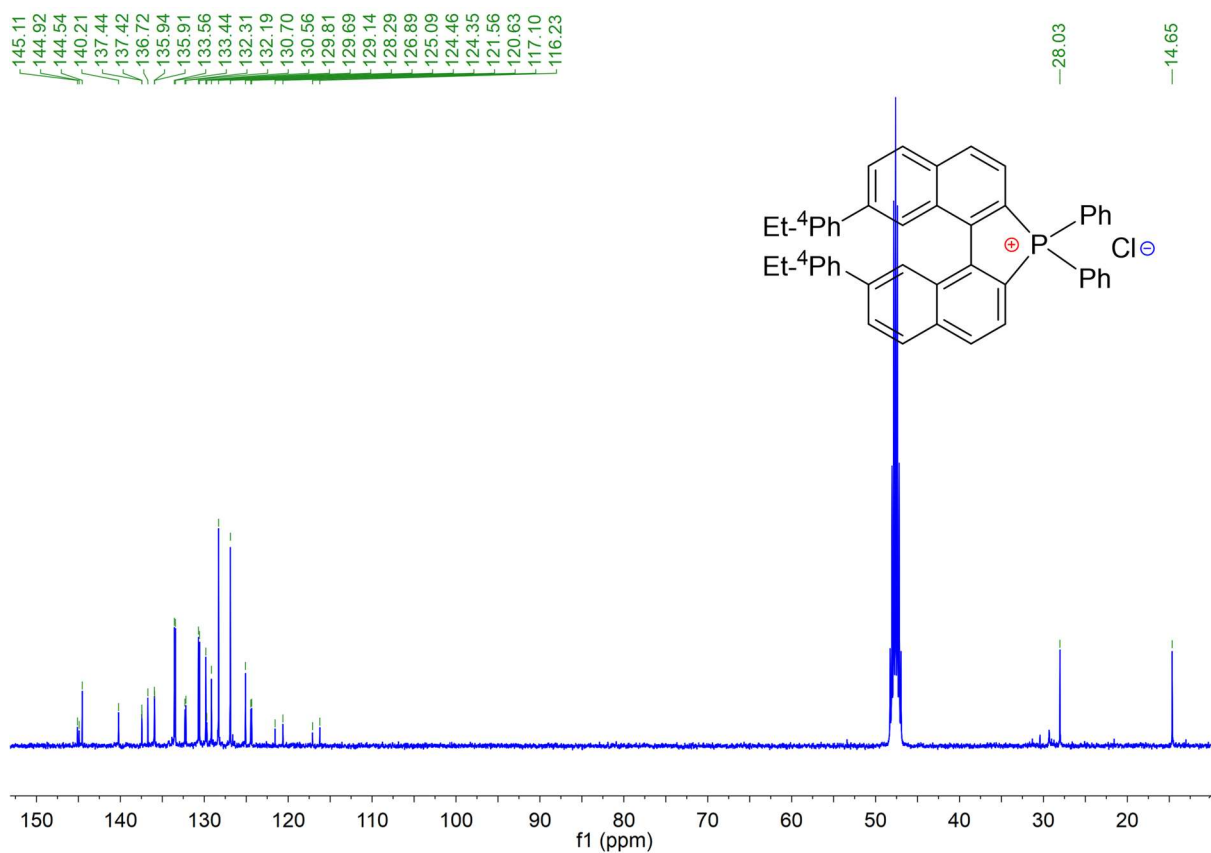
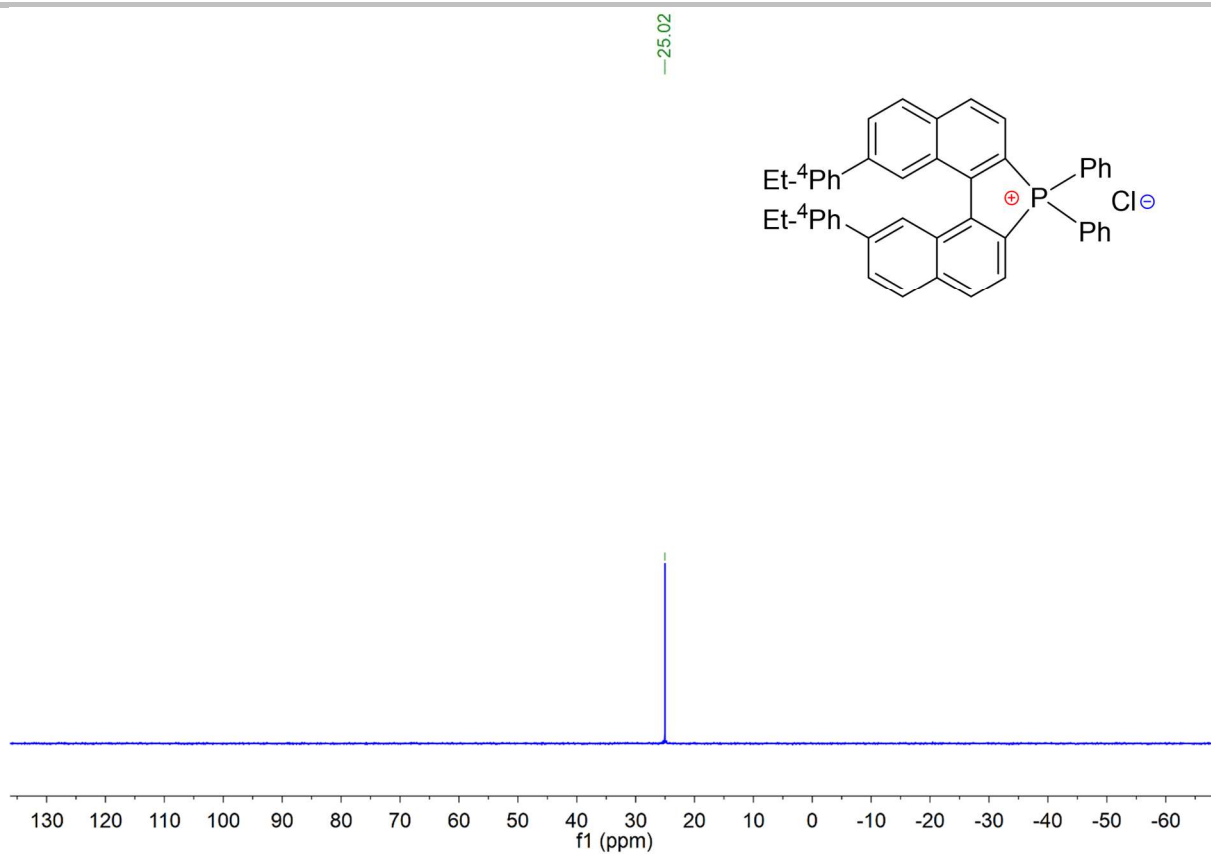
Supporting information



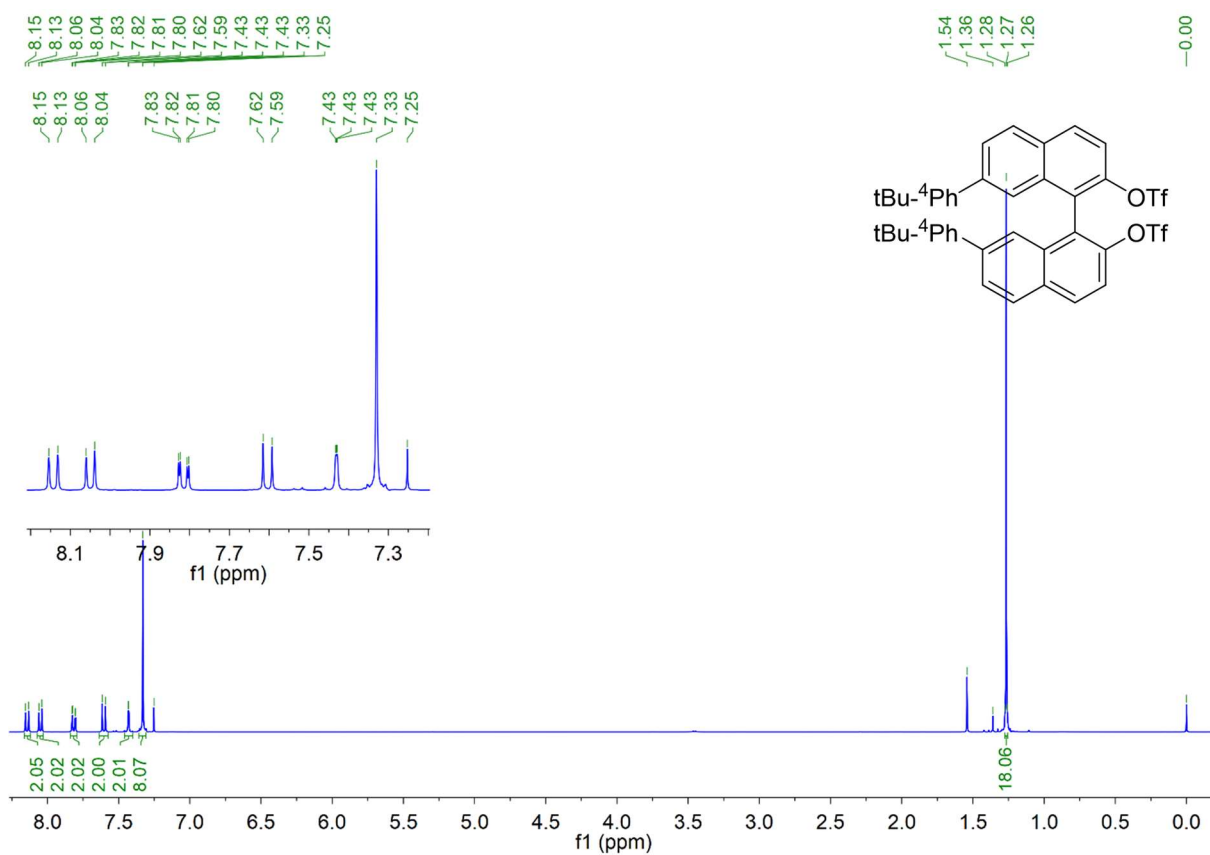
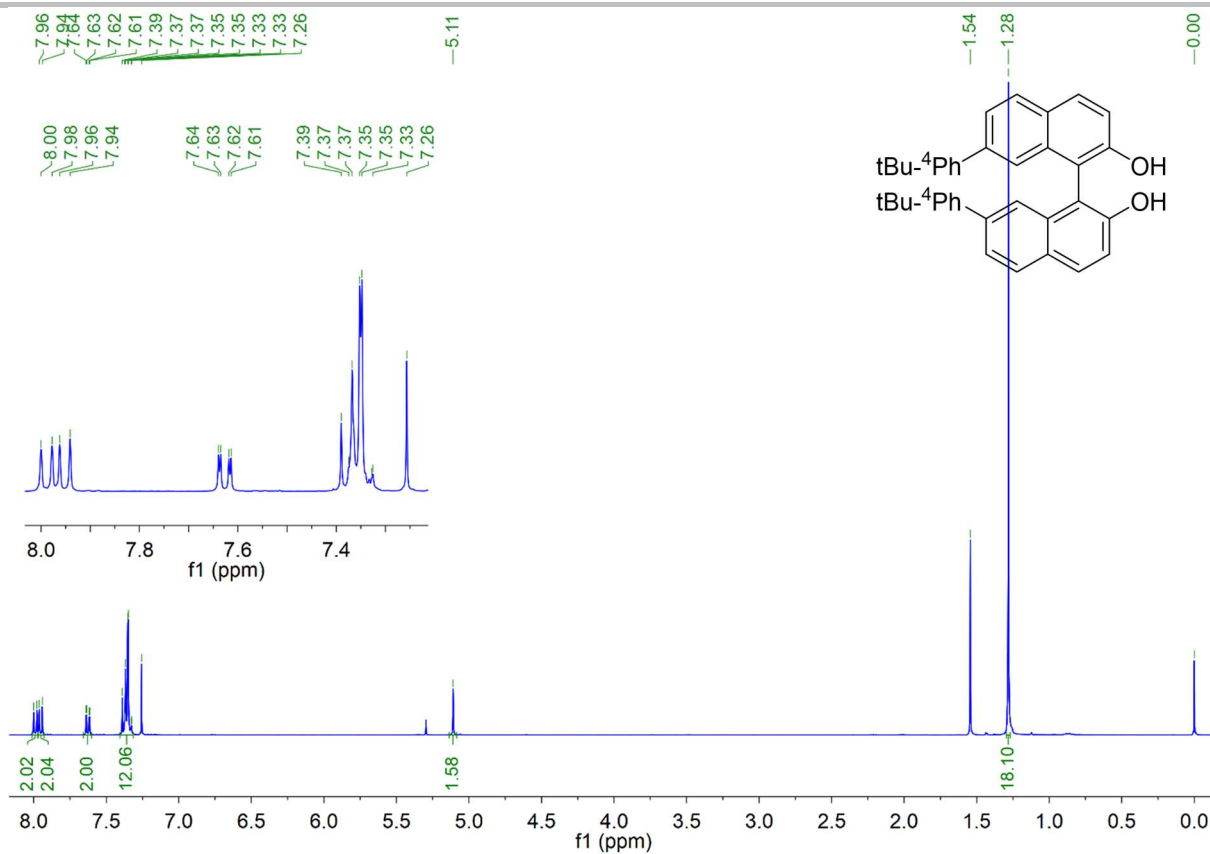
Supporting information



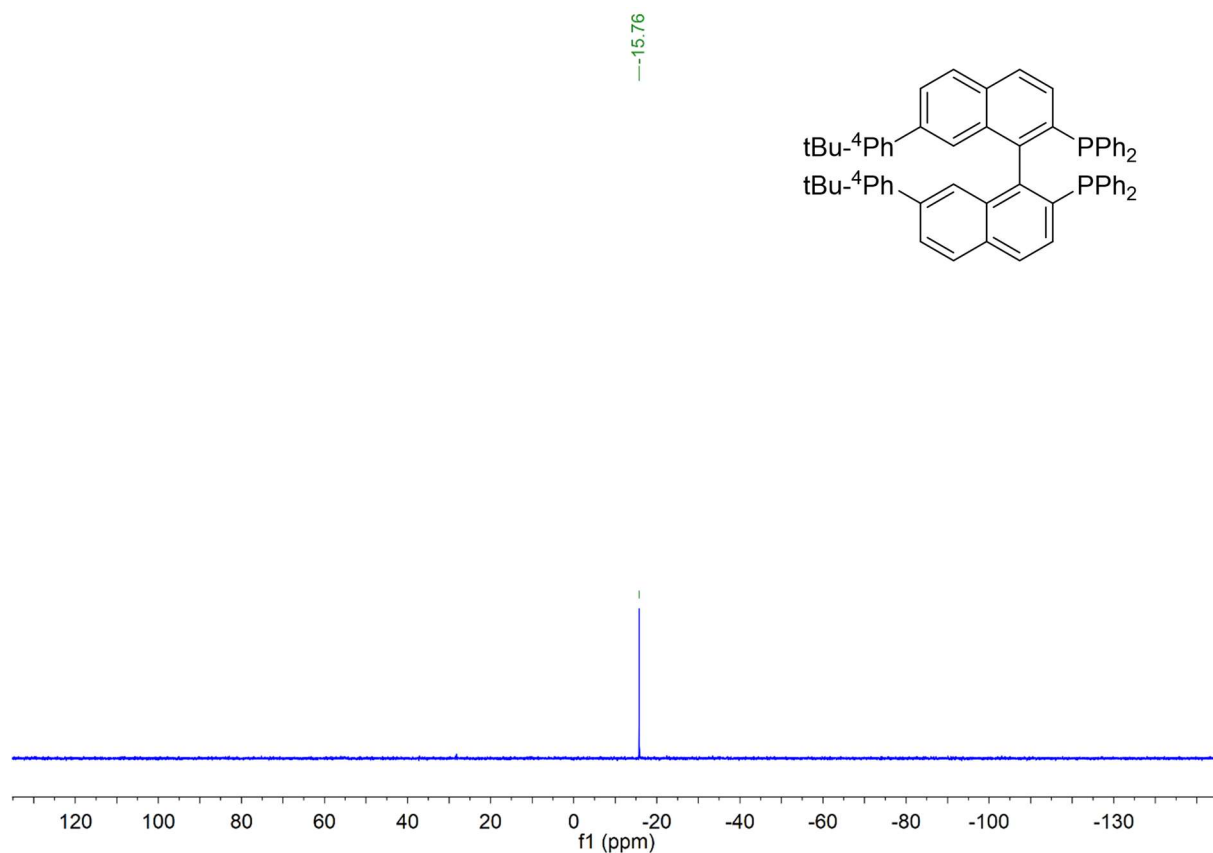
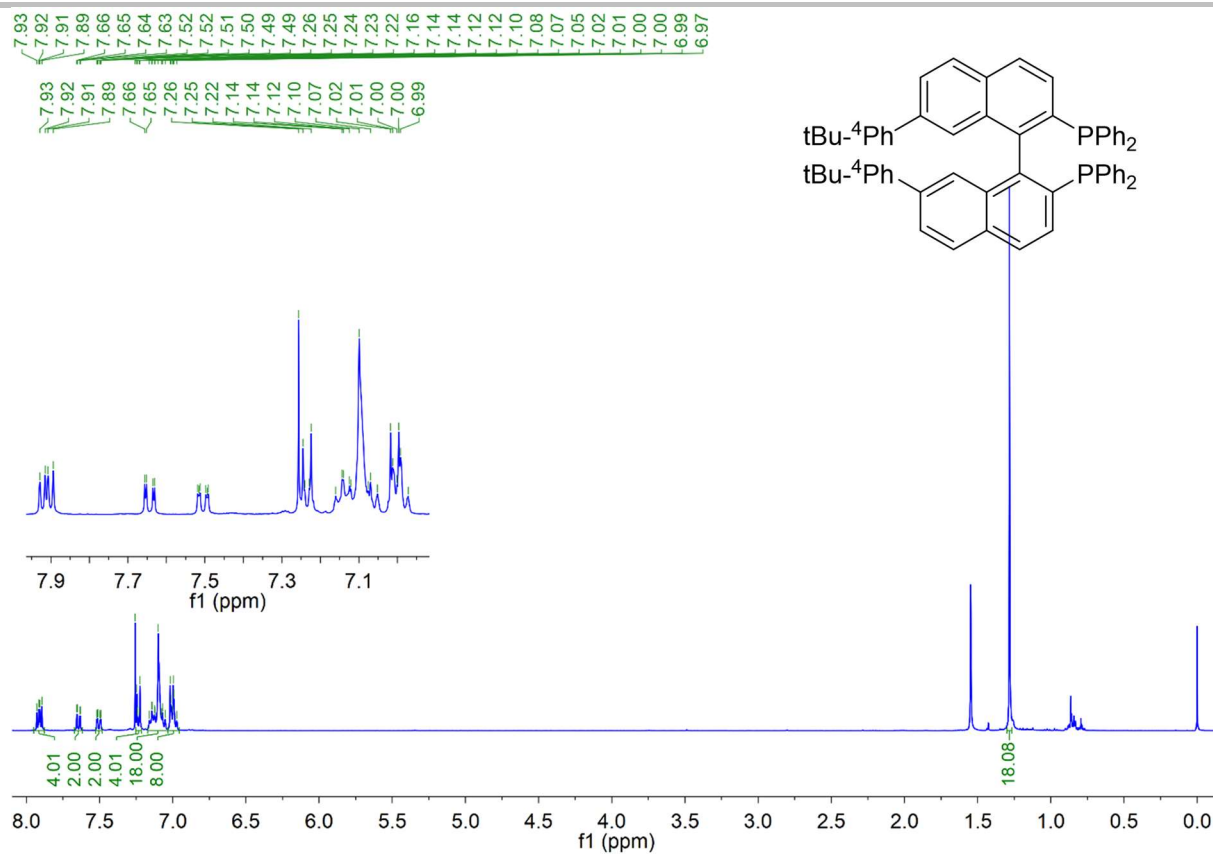
Supporting information



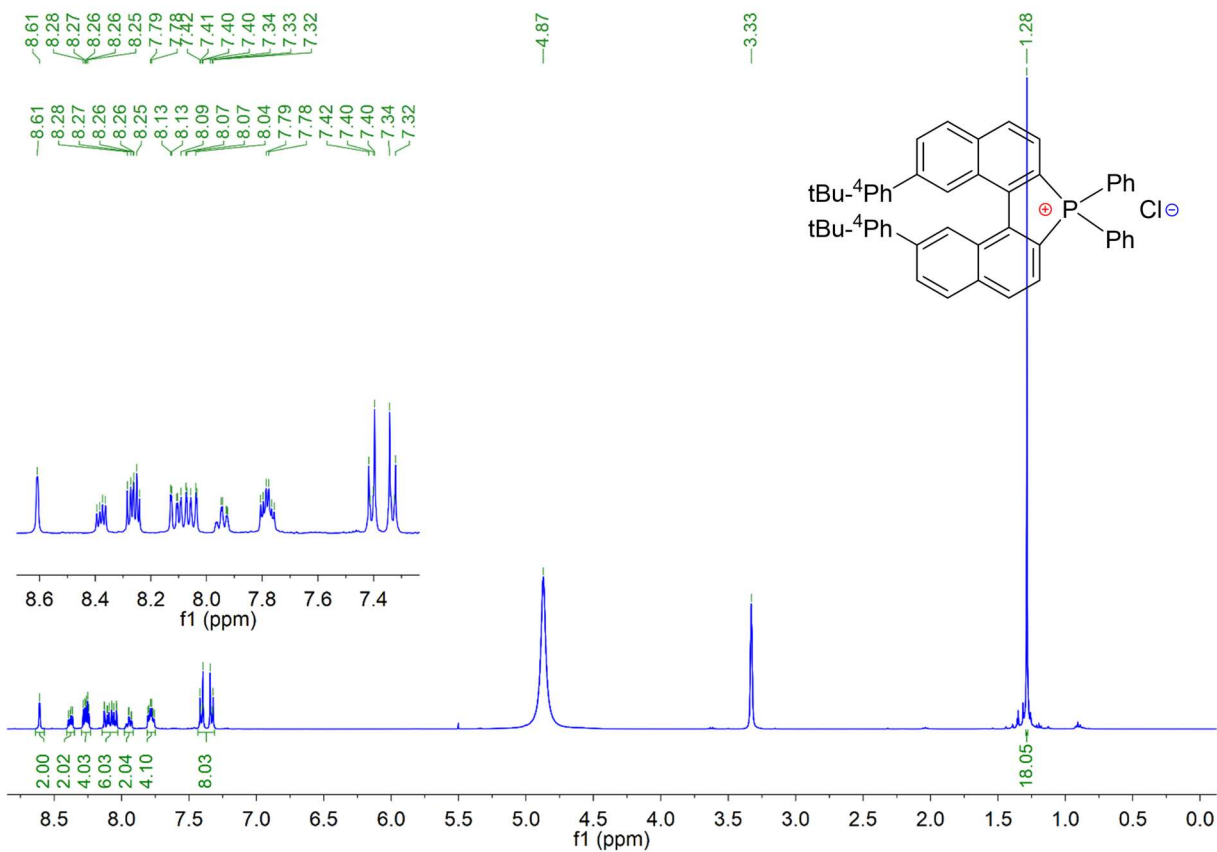
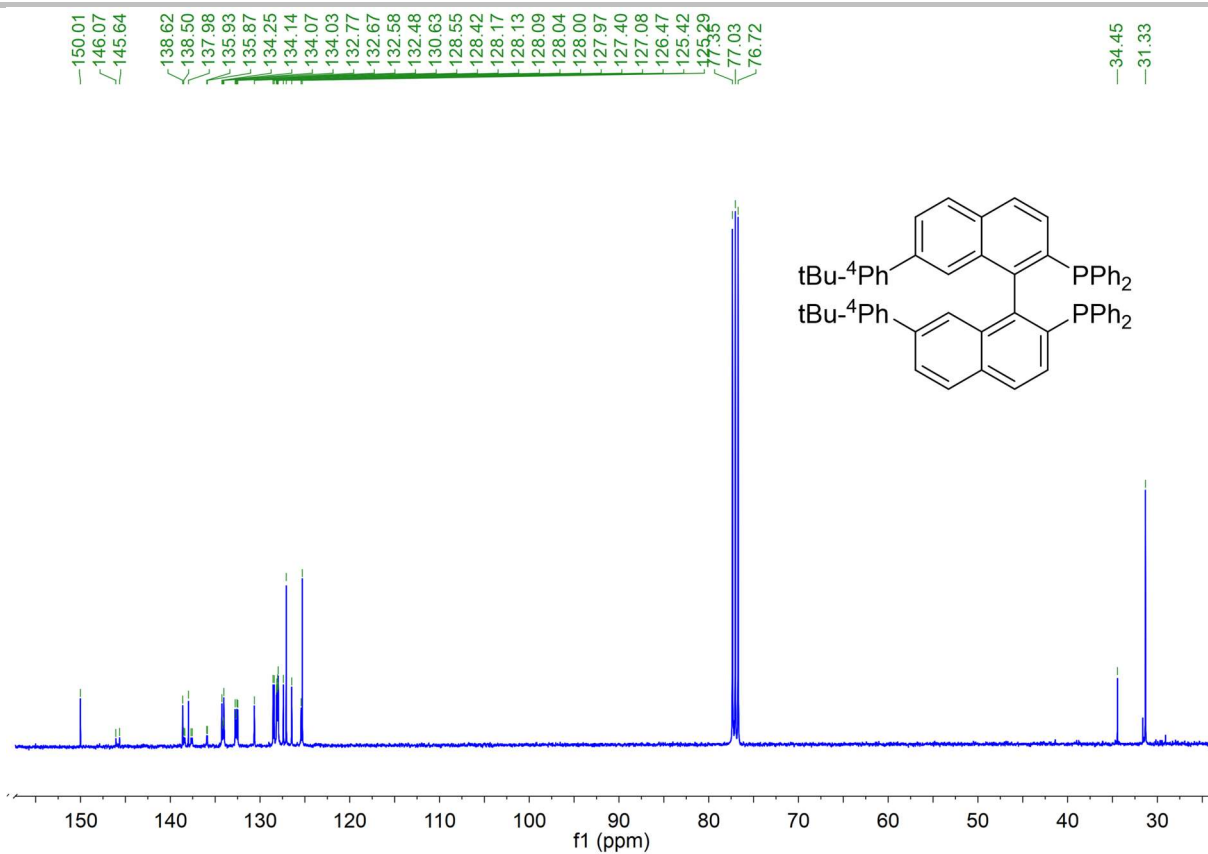
Supporting information



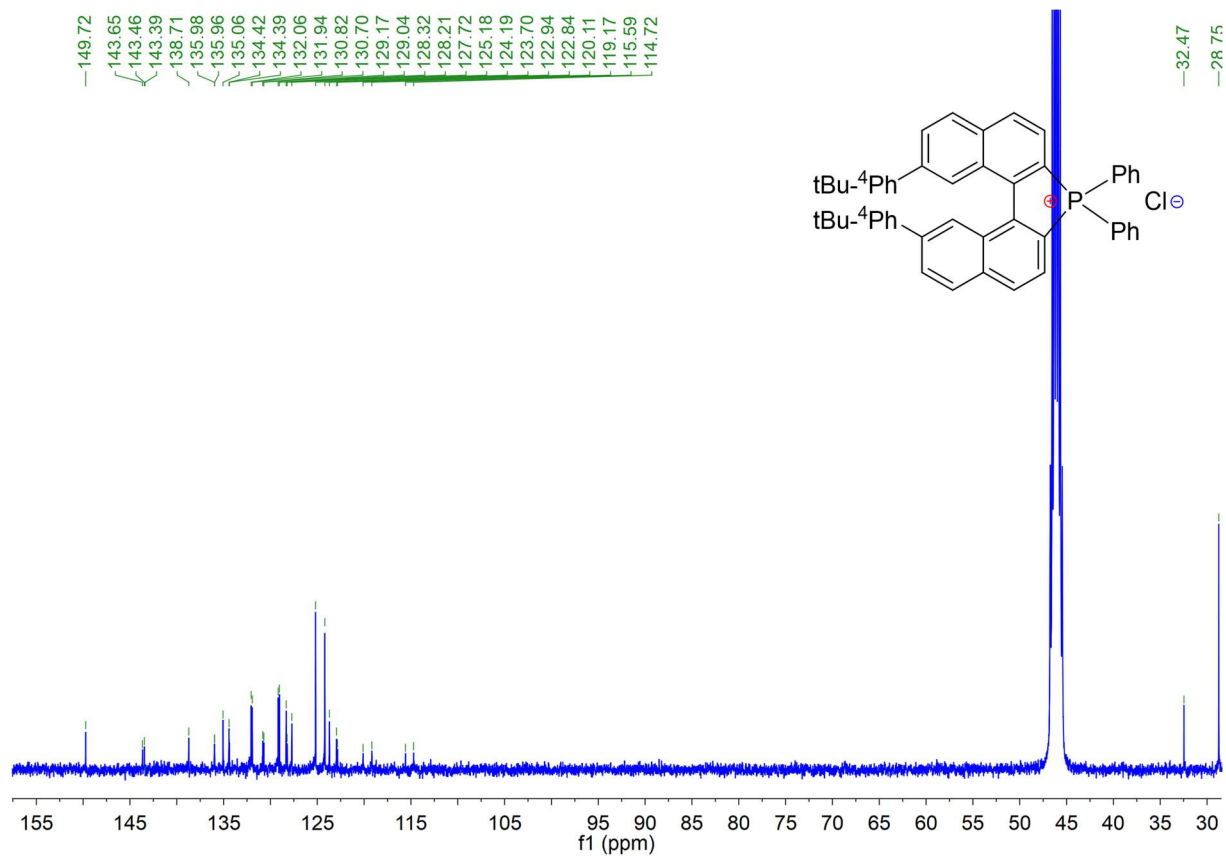
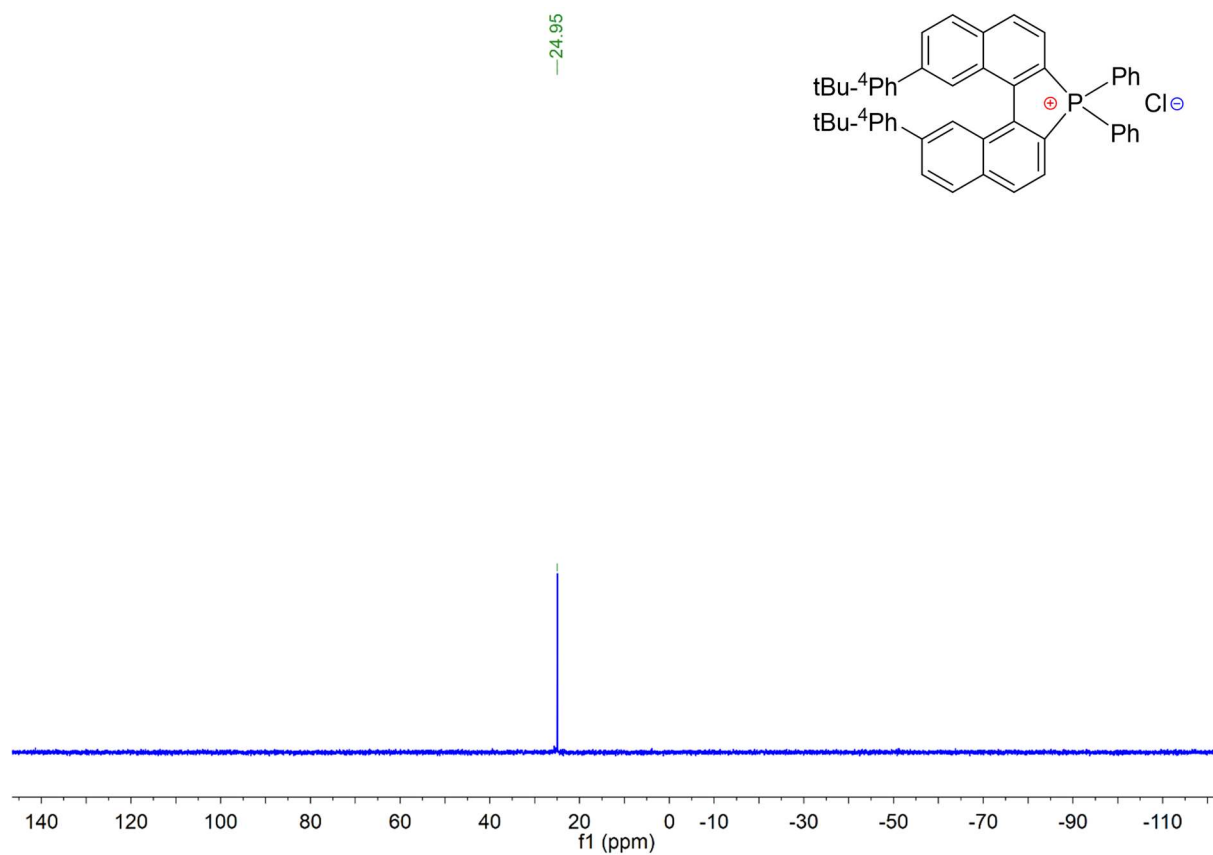
Supporting information



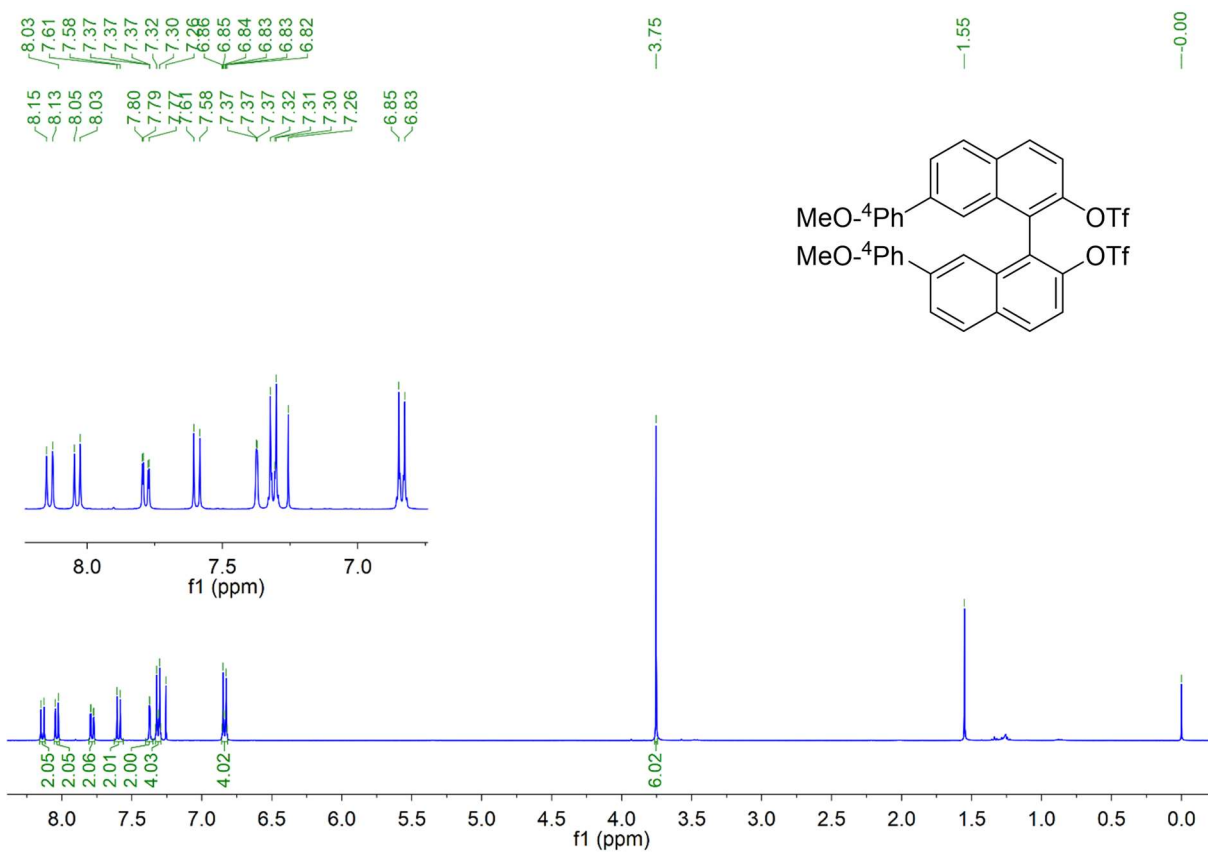
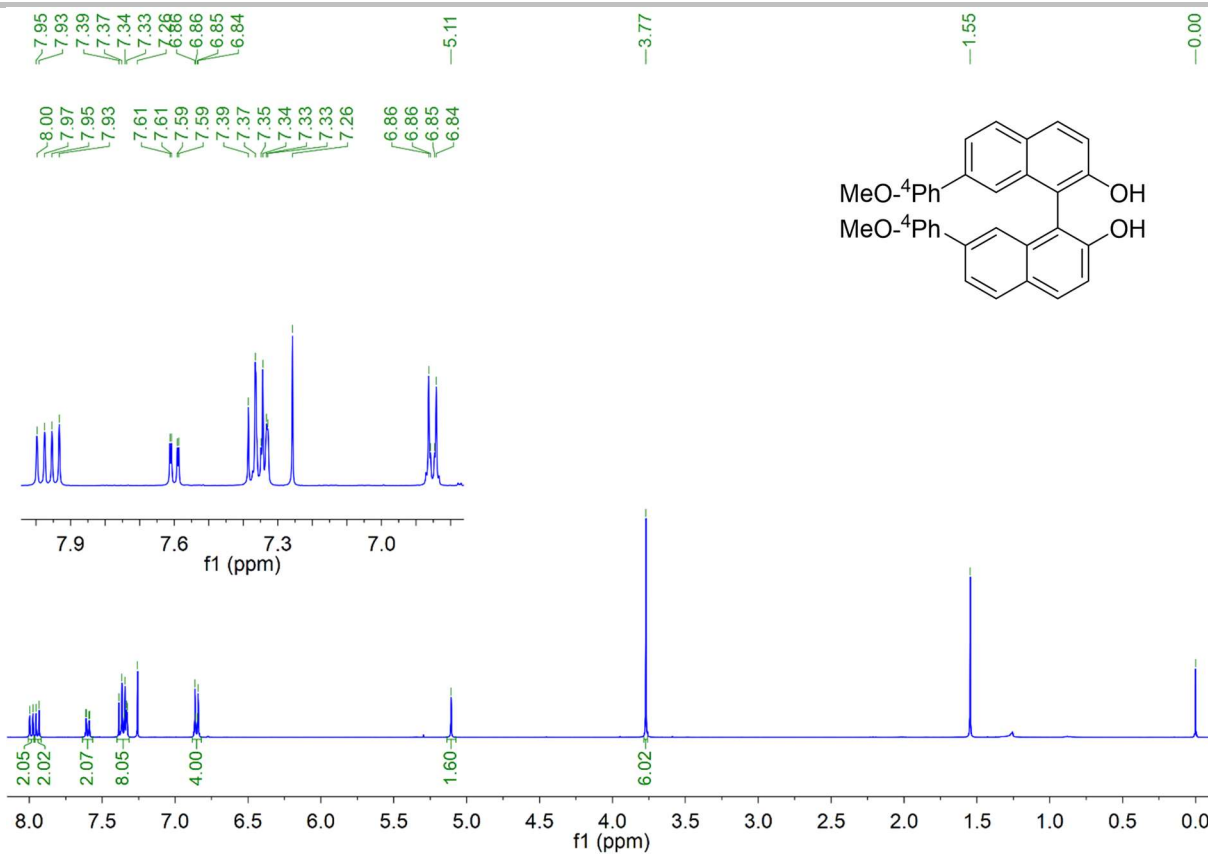
Supporting information



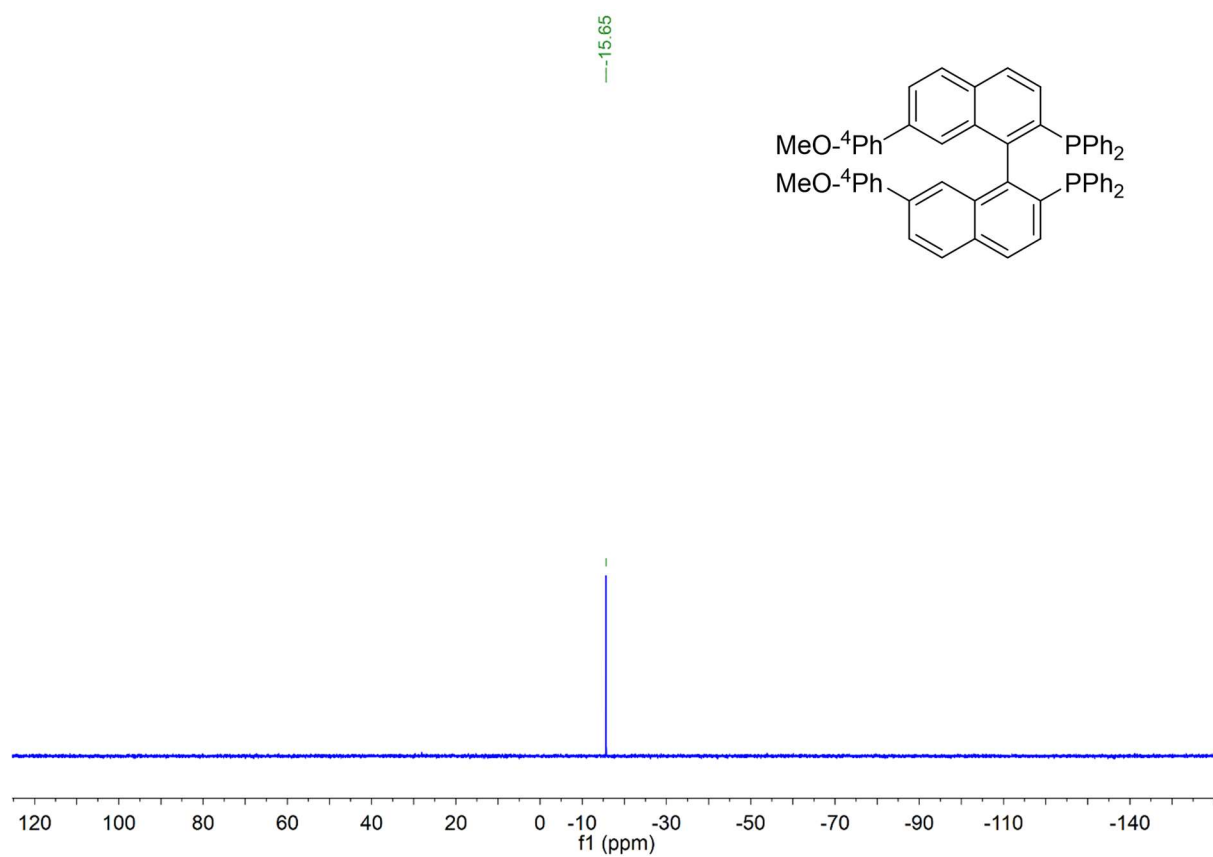
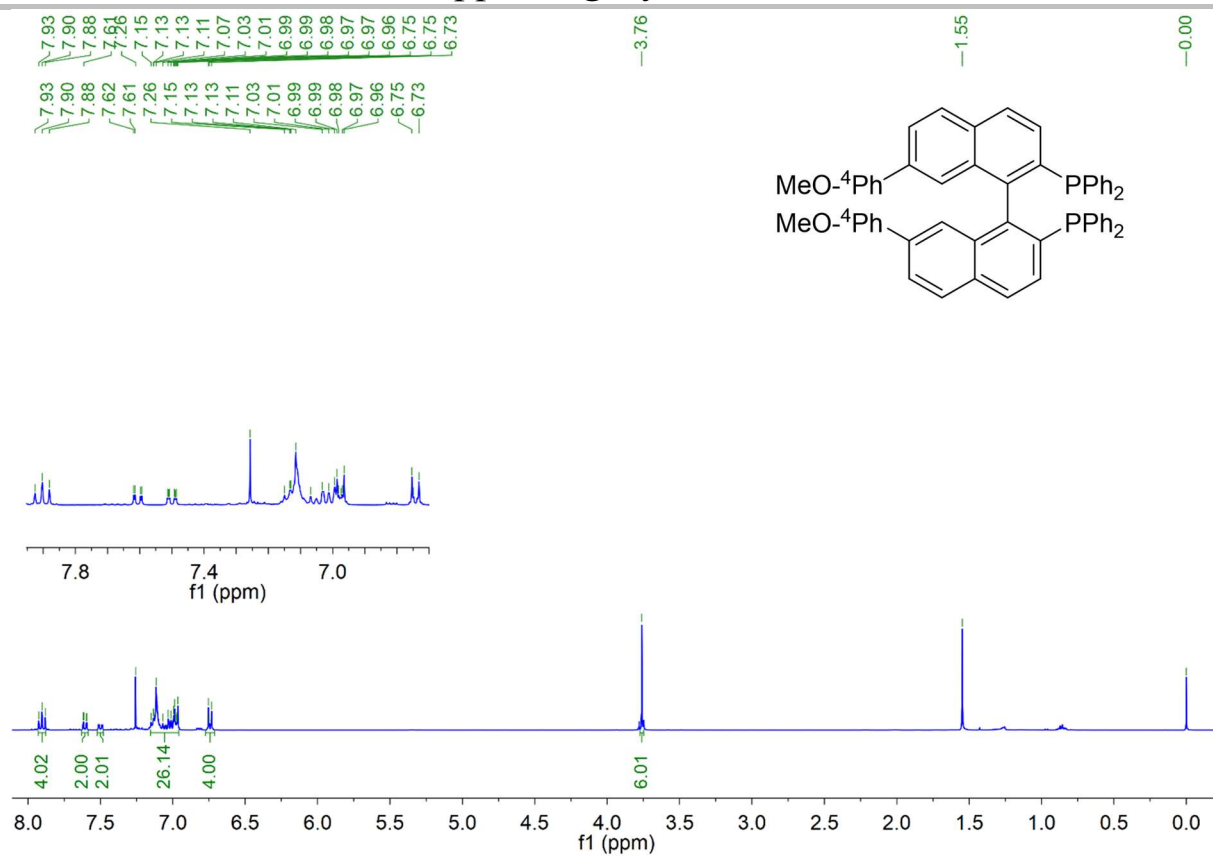
Supporting information



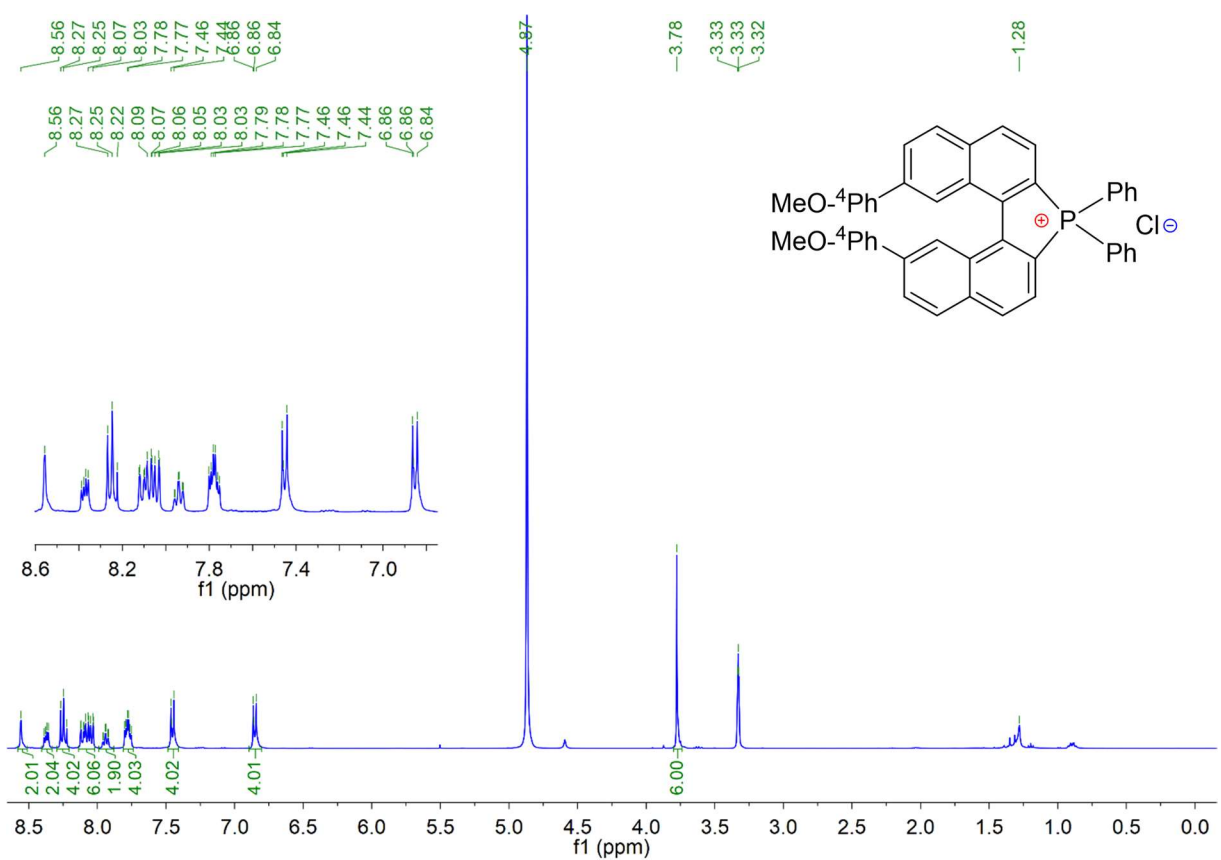
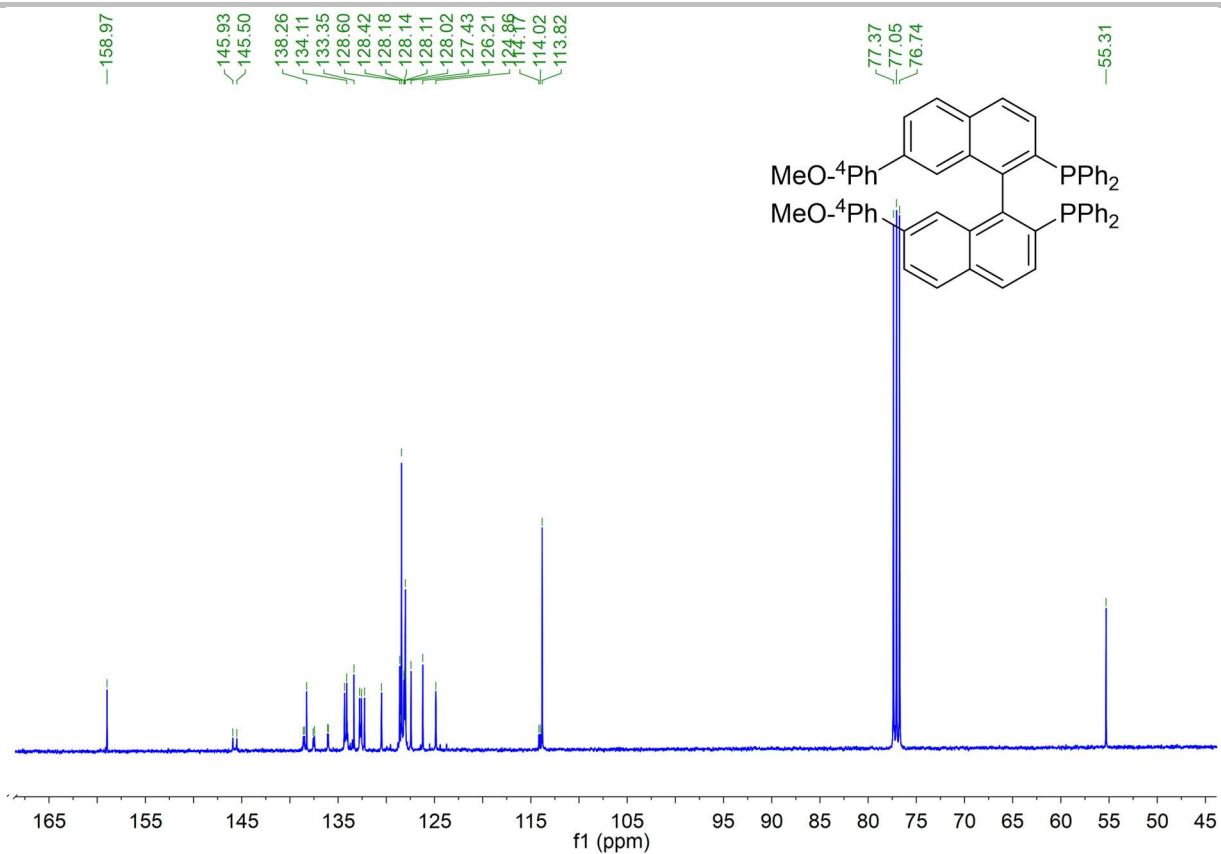
Supporting information



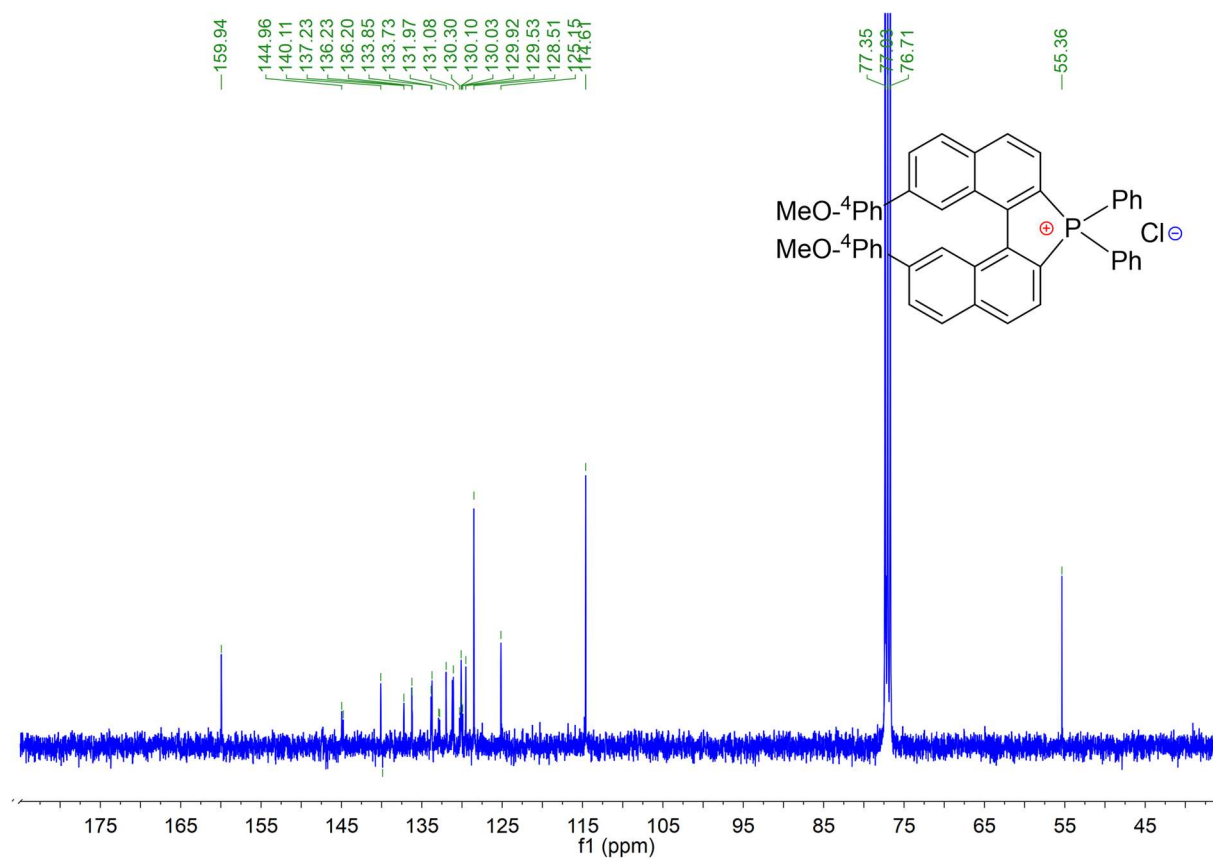
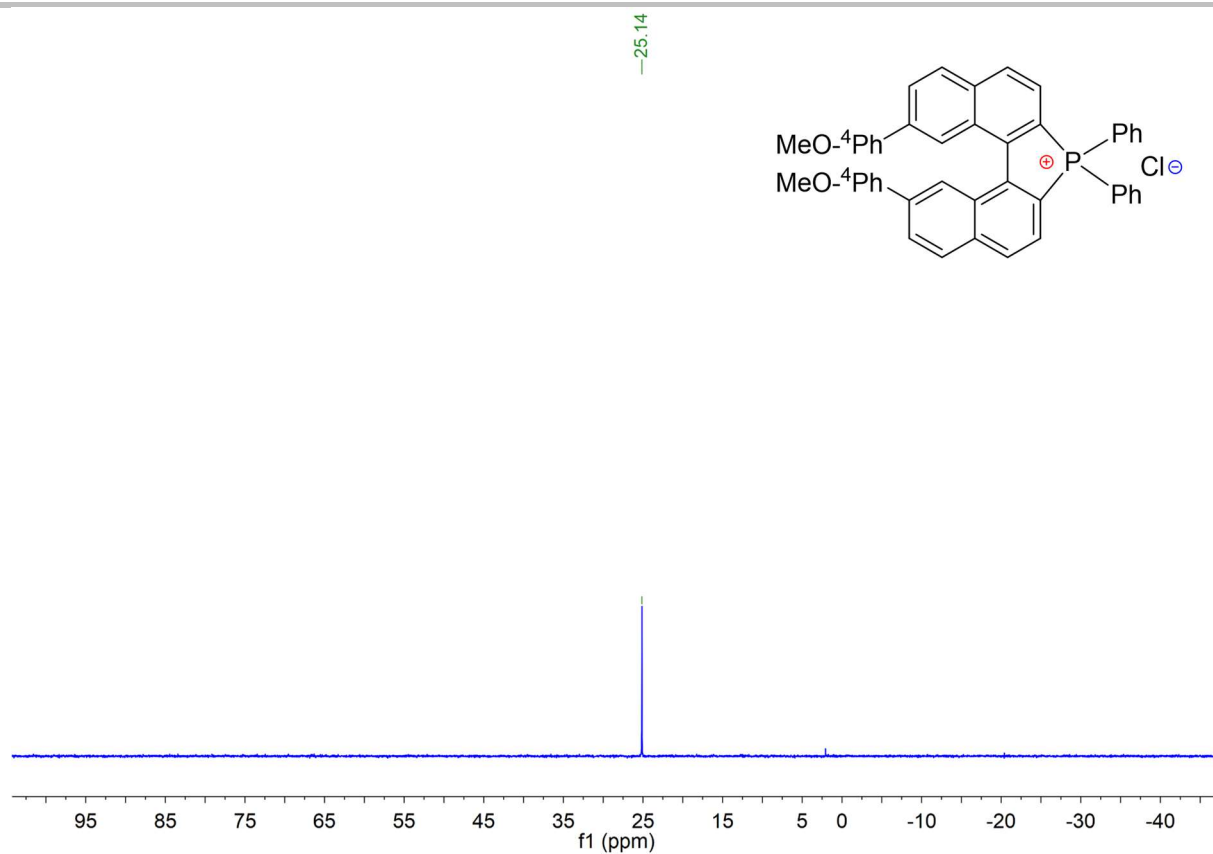
Supporting information



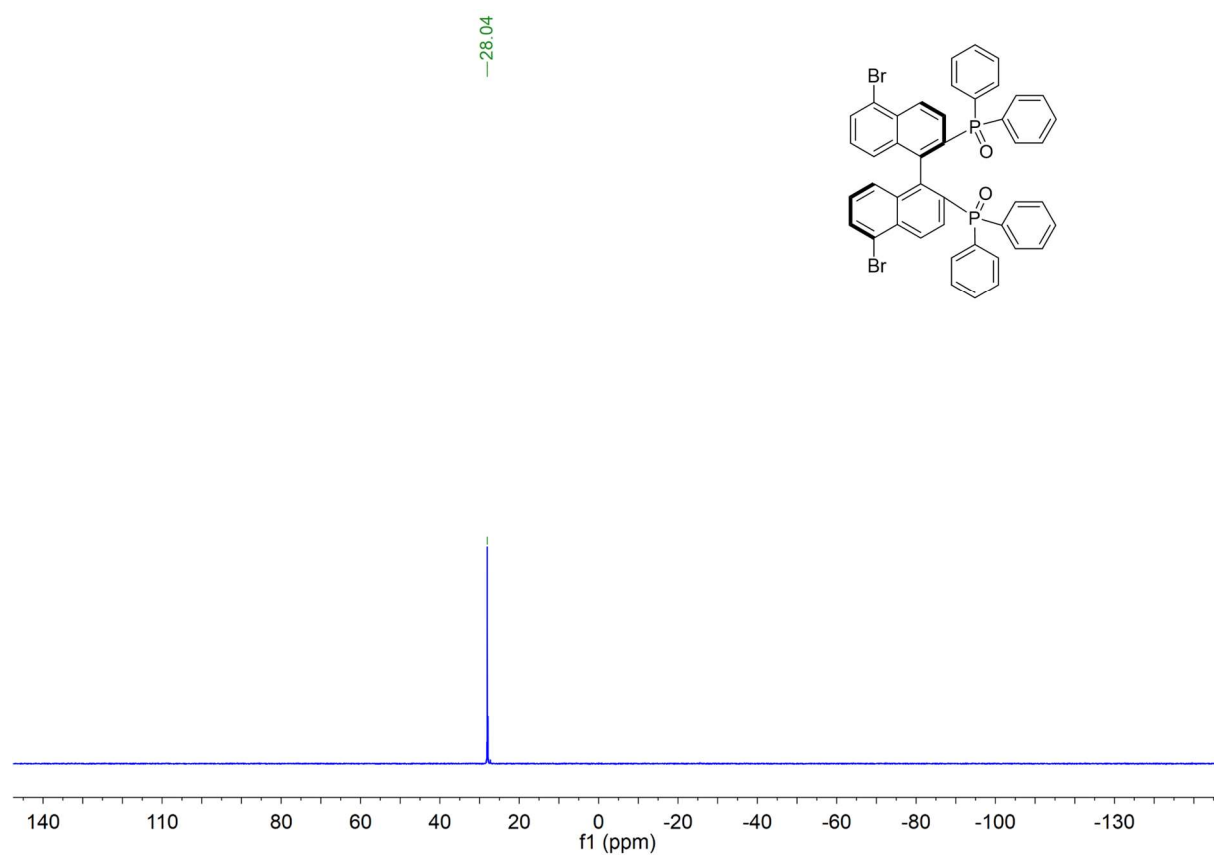
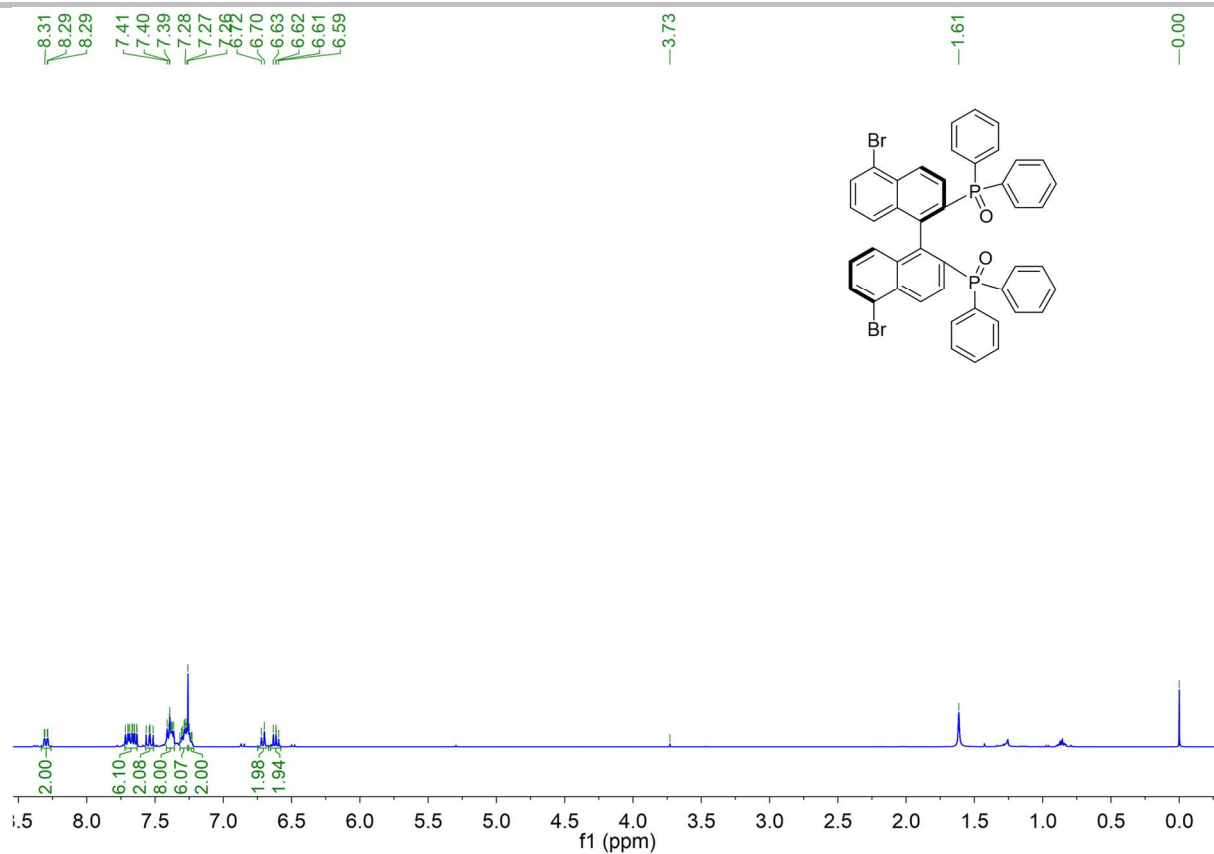
Supporting information



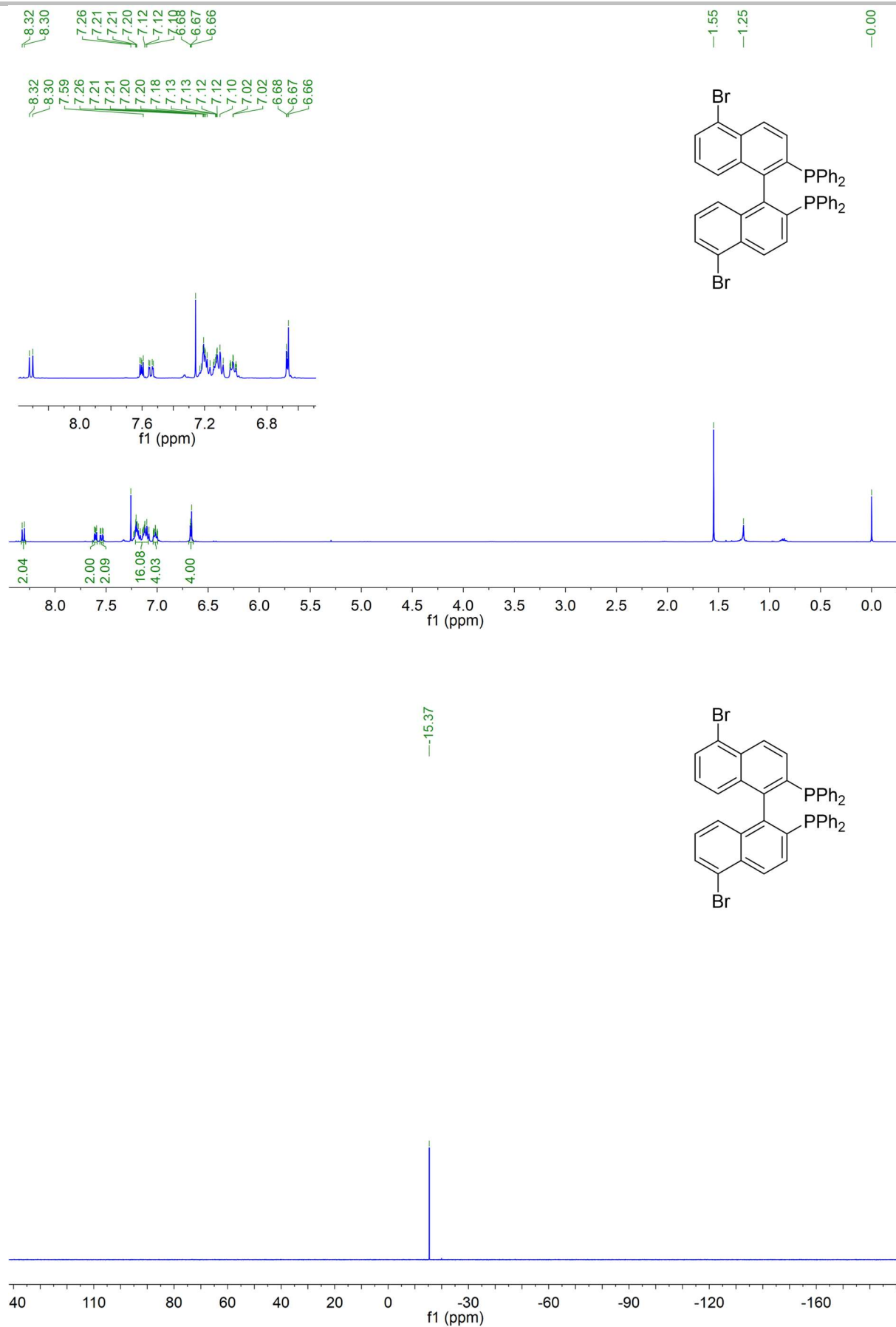
Supporting information



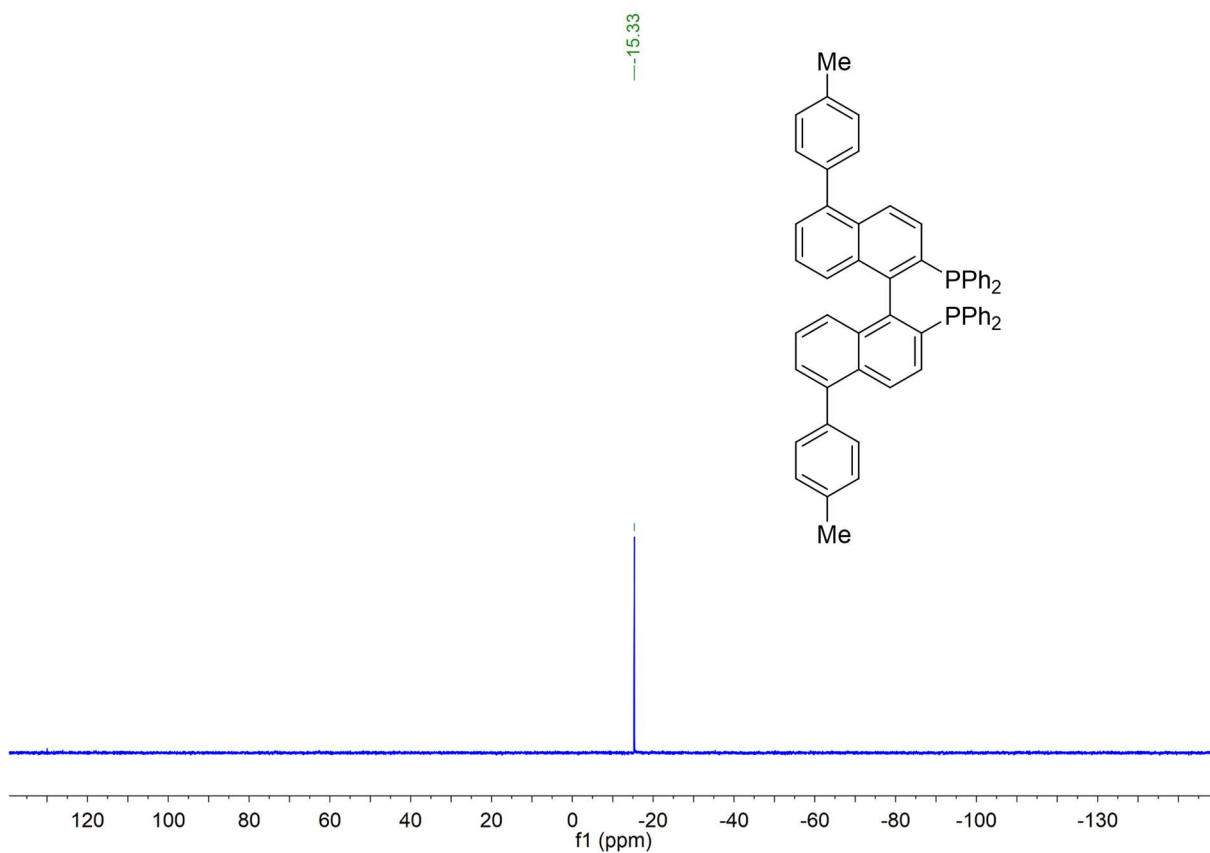
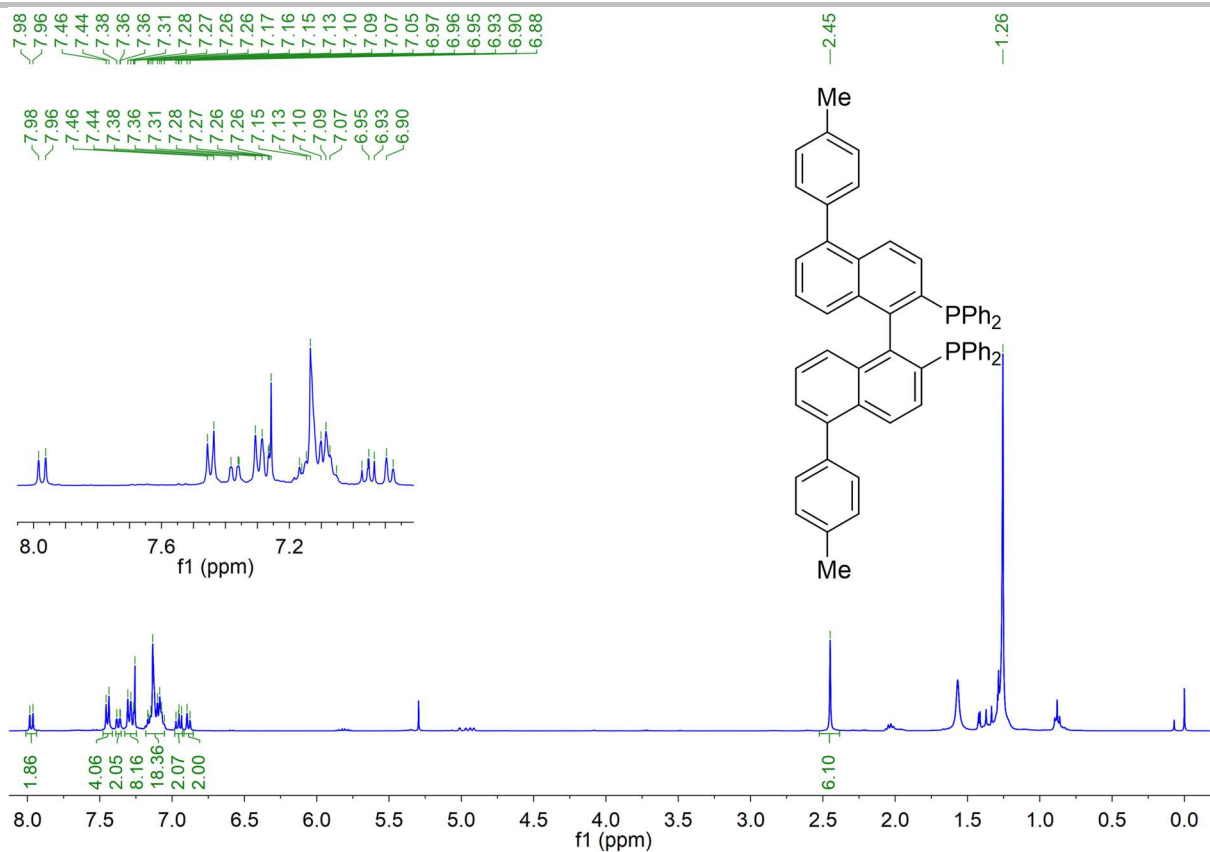
Supporting information



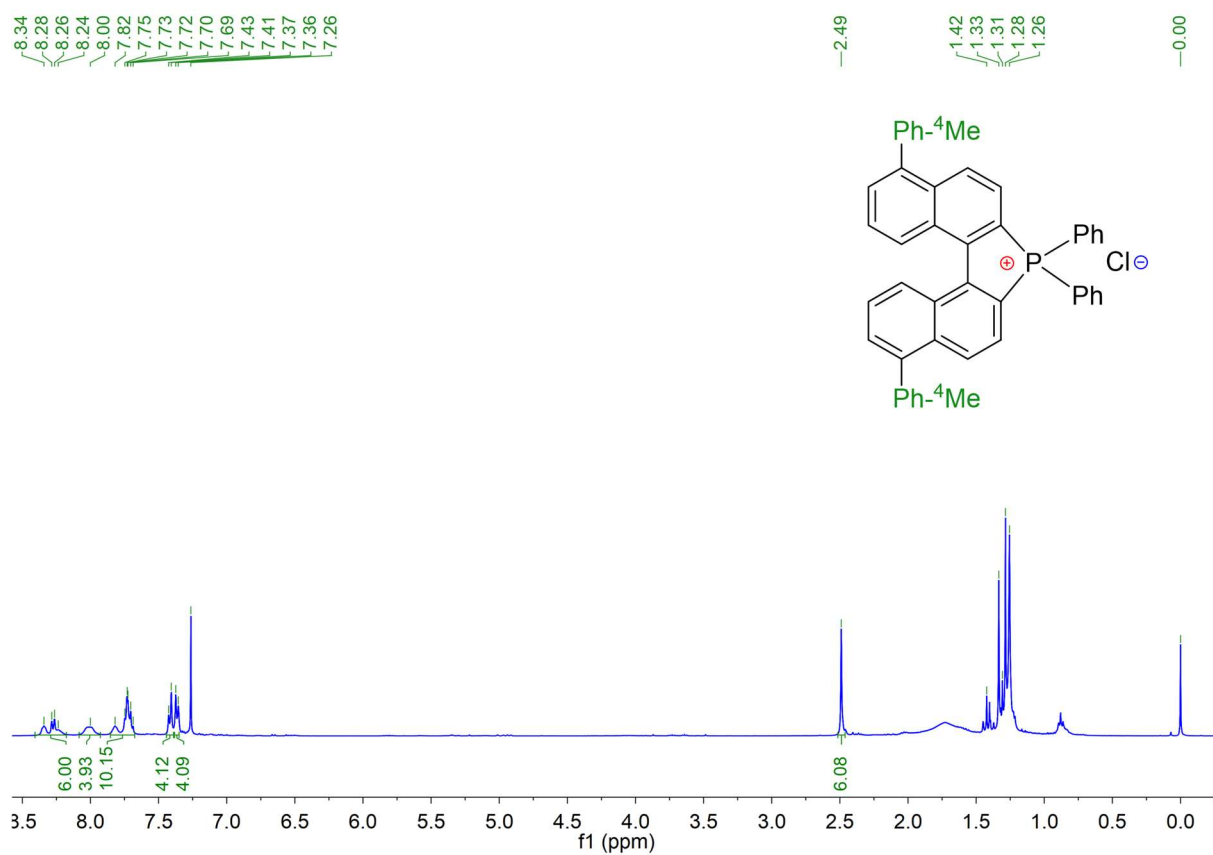
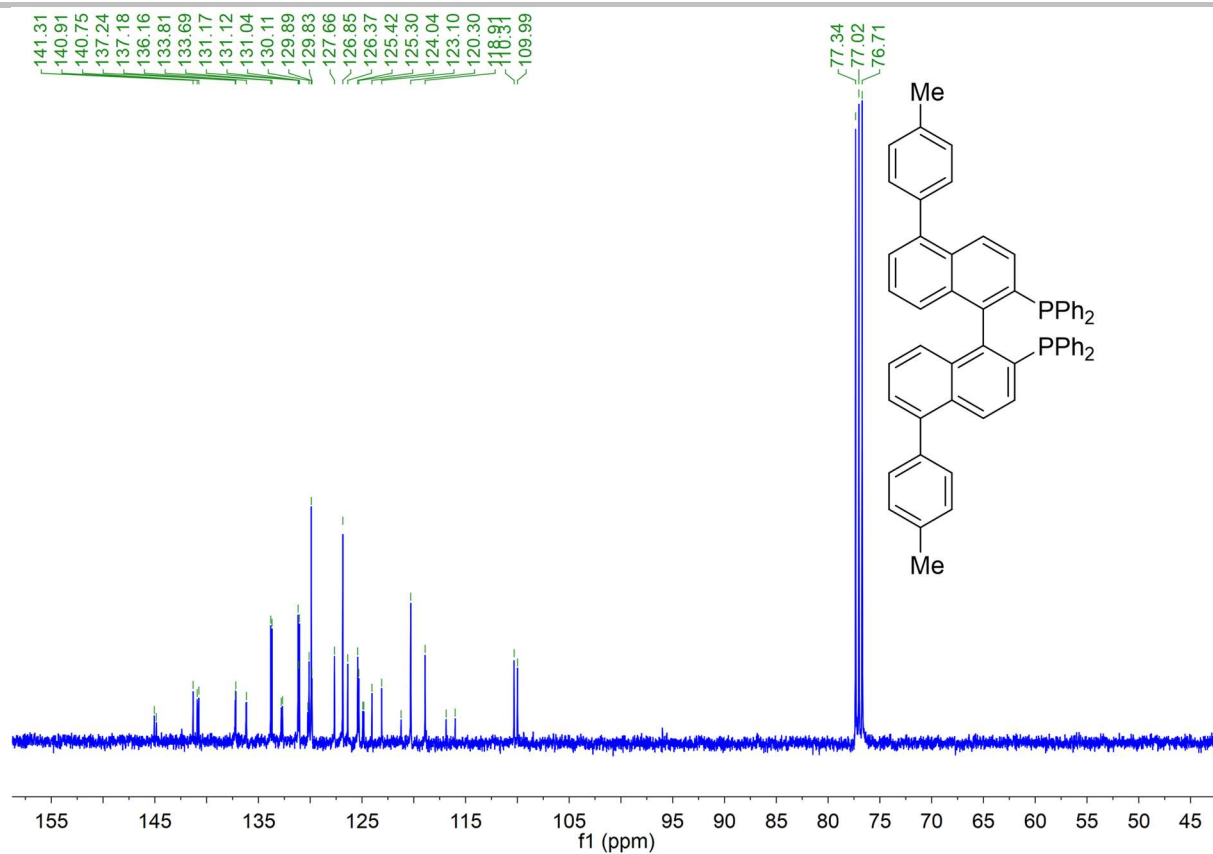
Supporting information



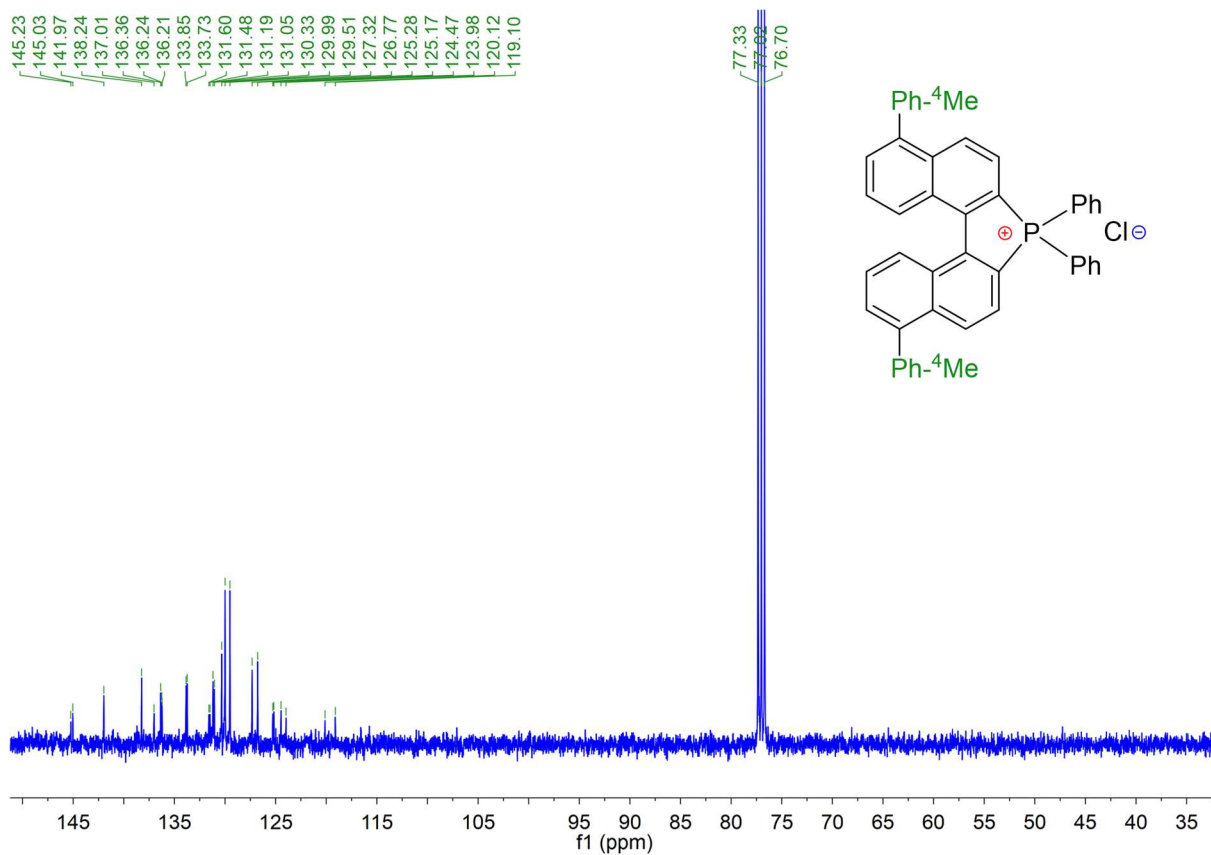
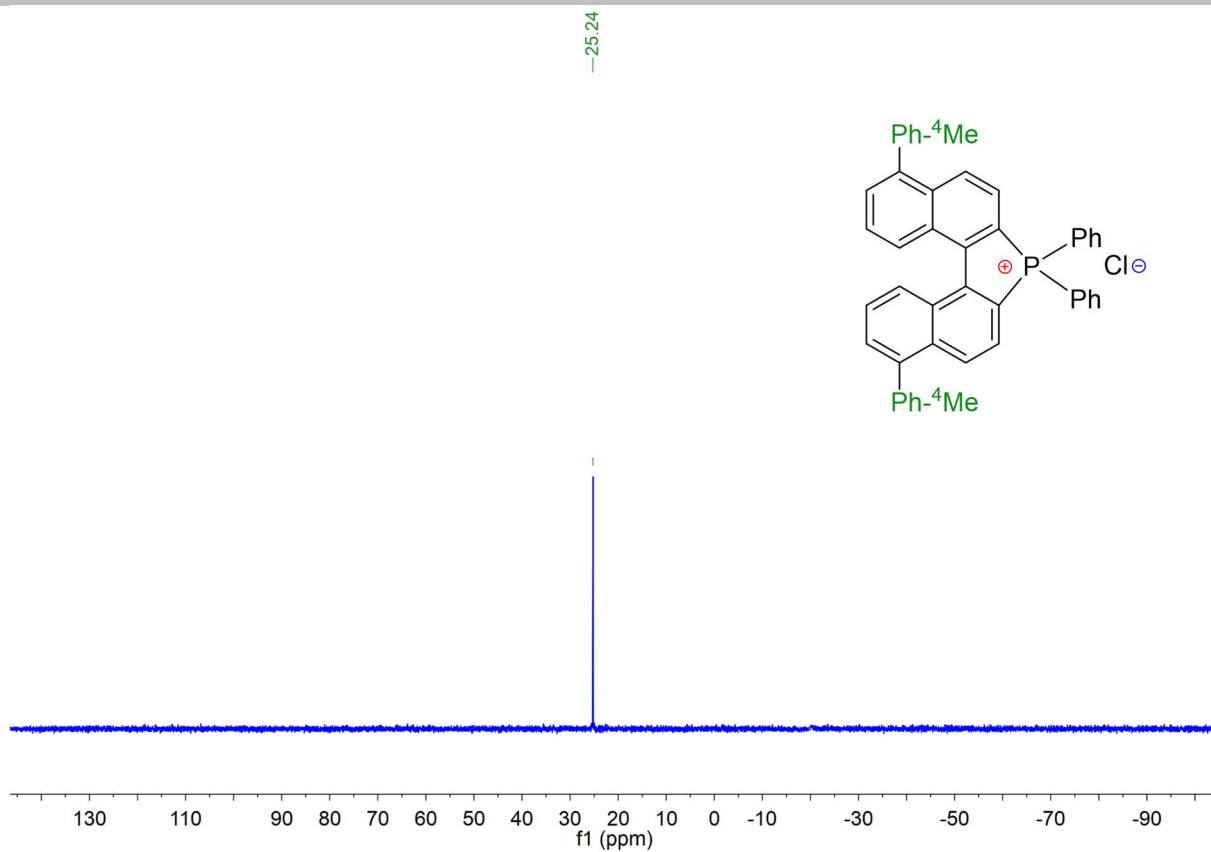
Supporting information



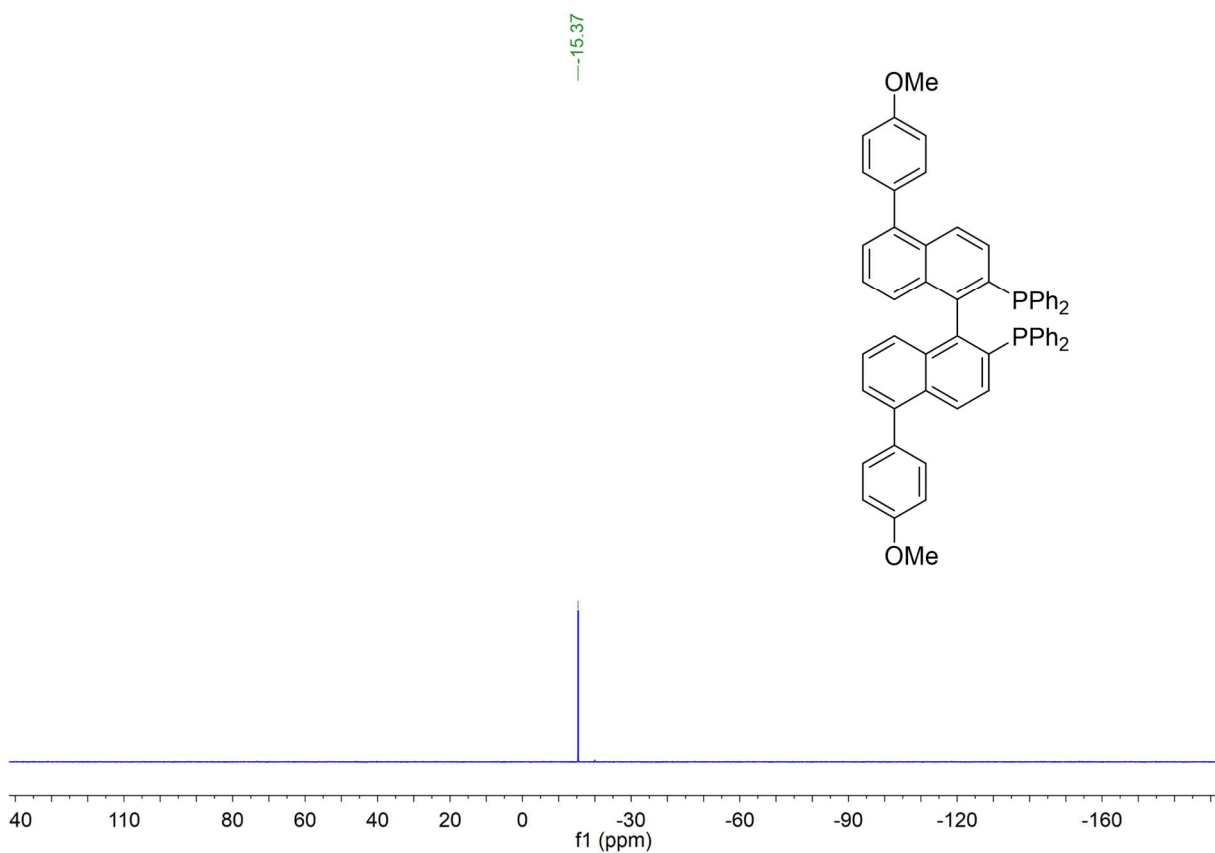
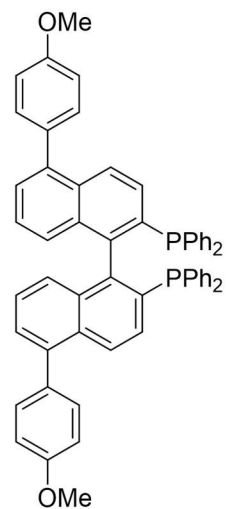
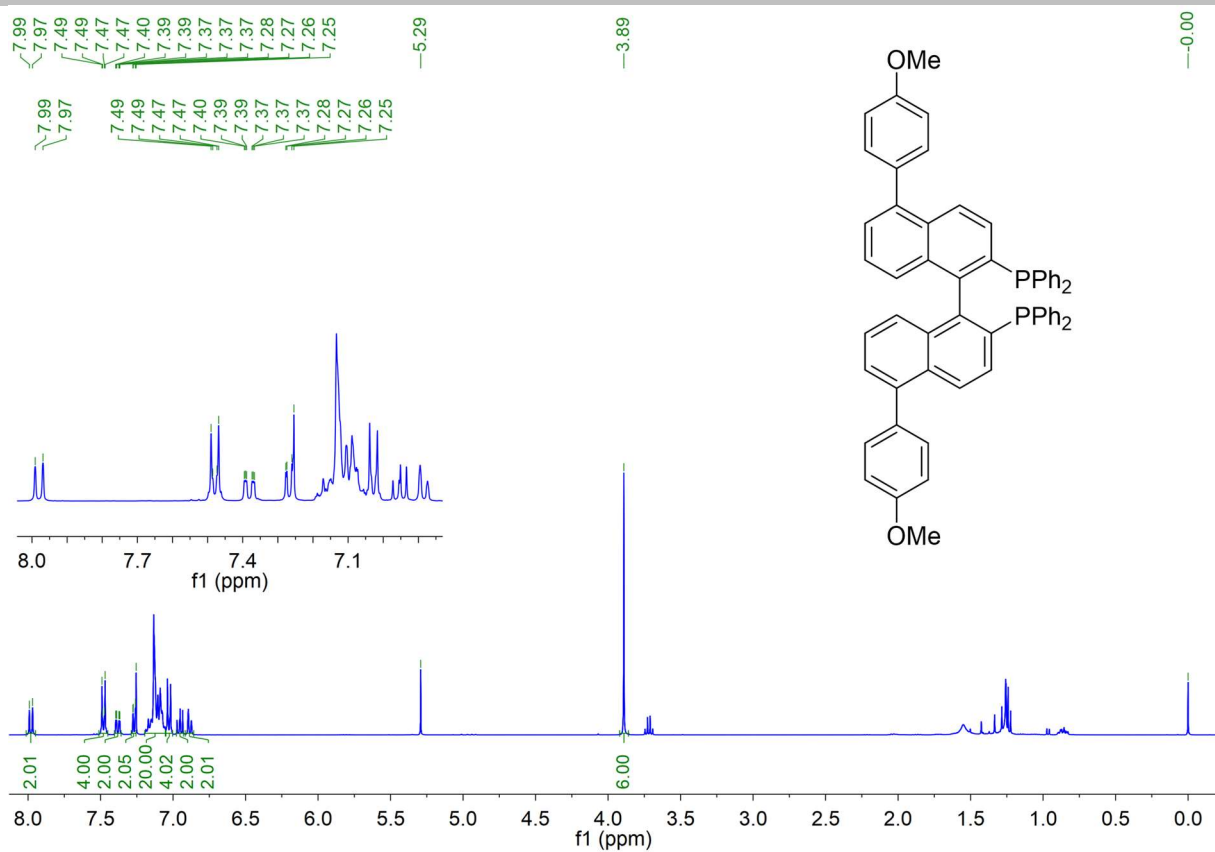
Supporting information



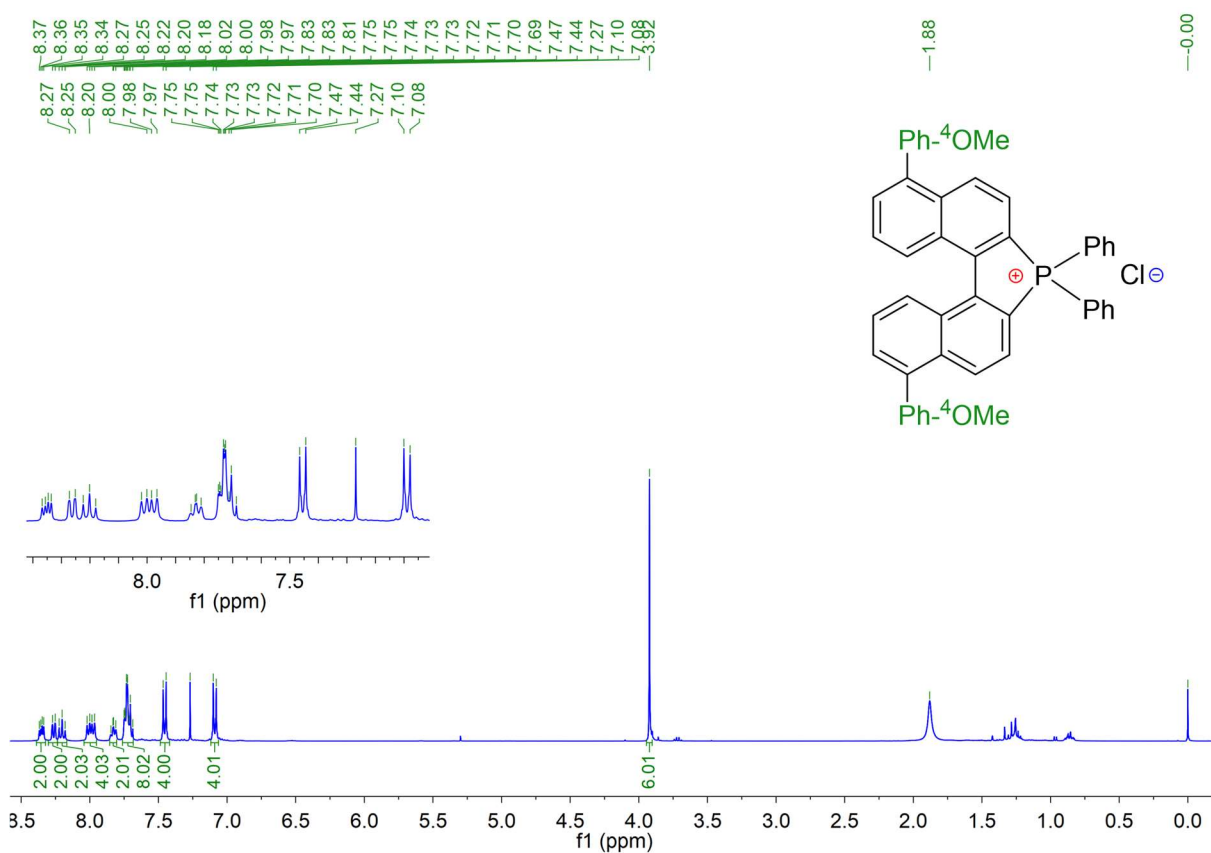
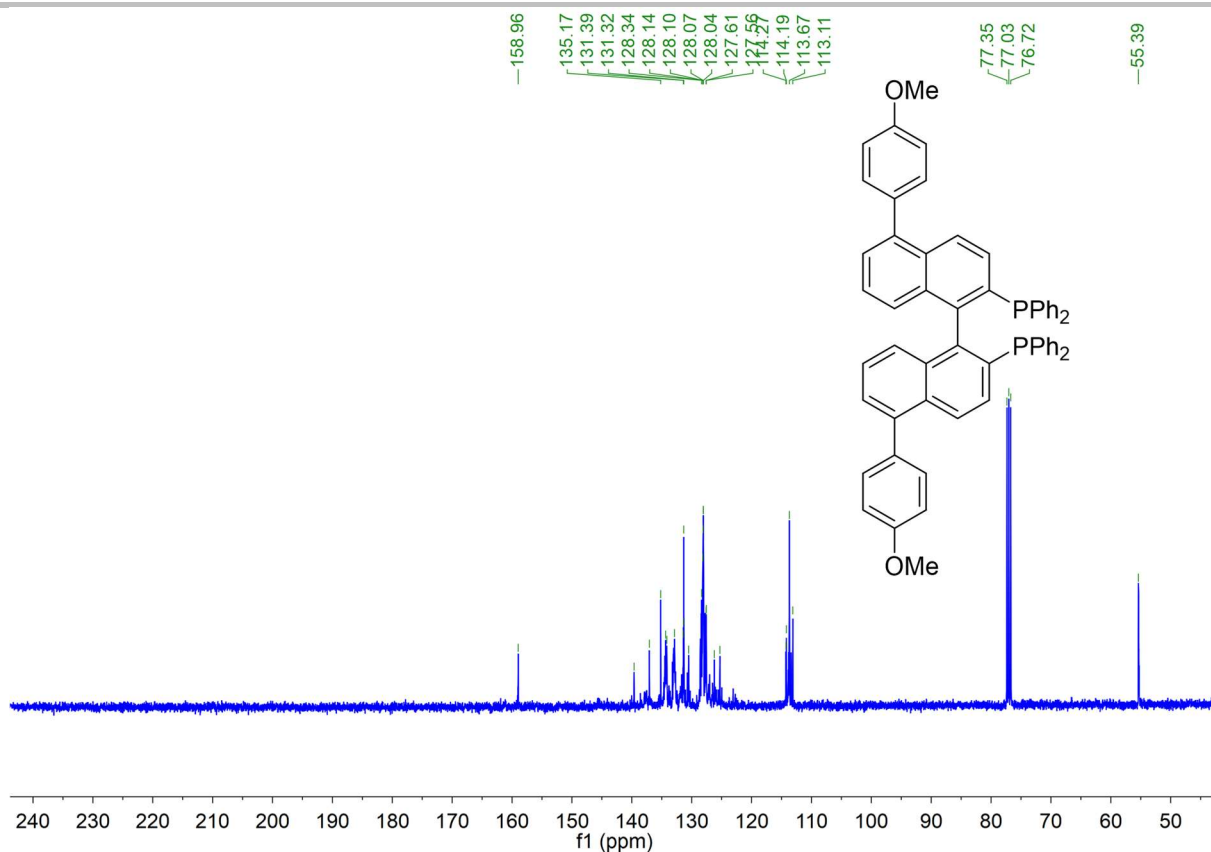
Supporting information



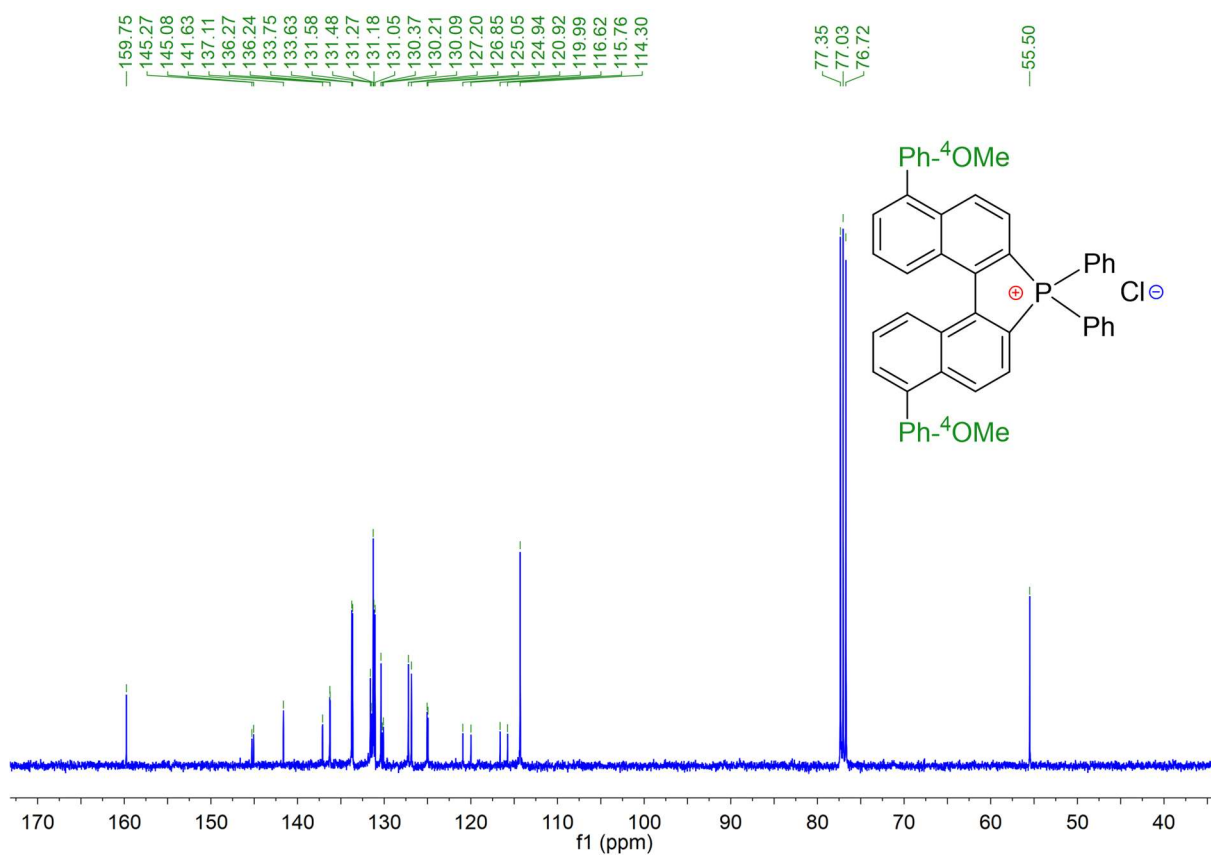
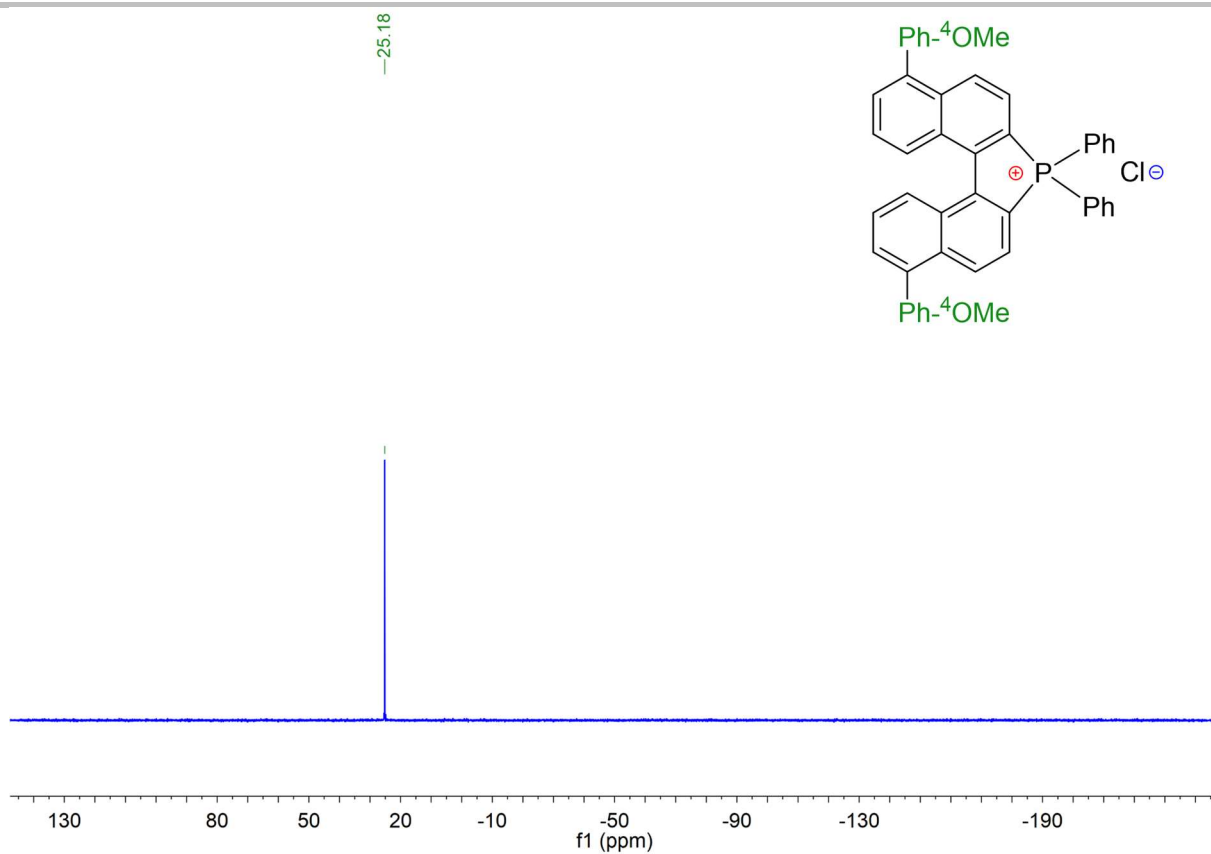
Supporting information



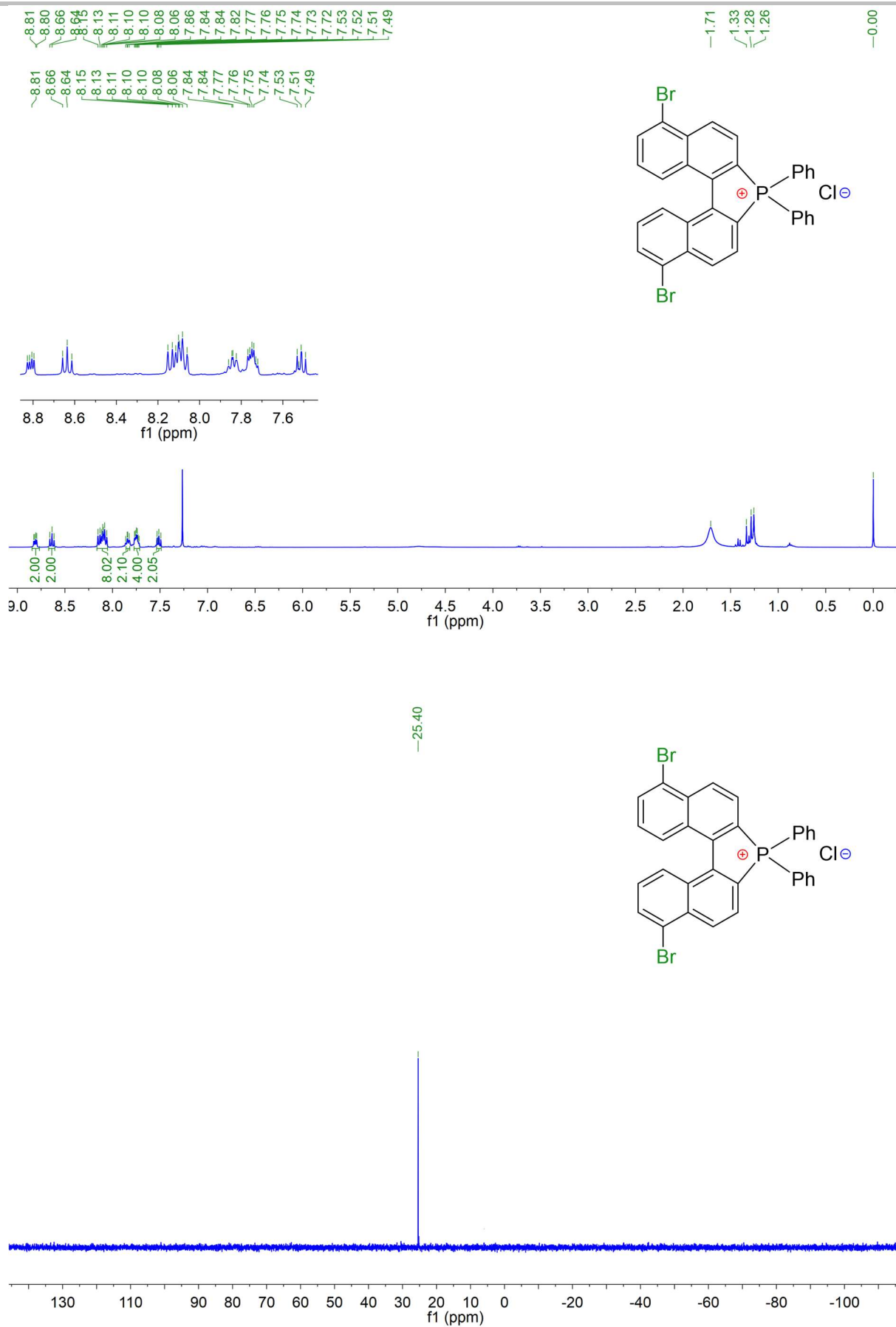
Supporting information



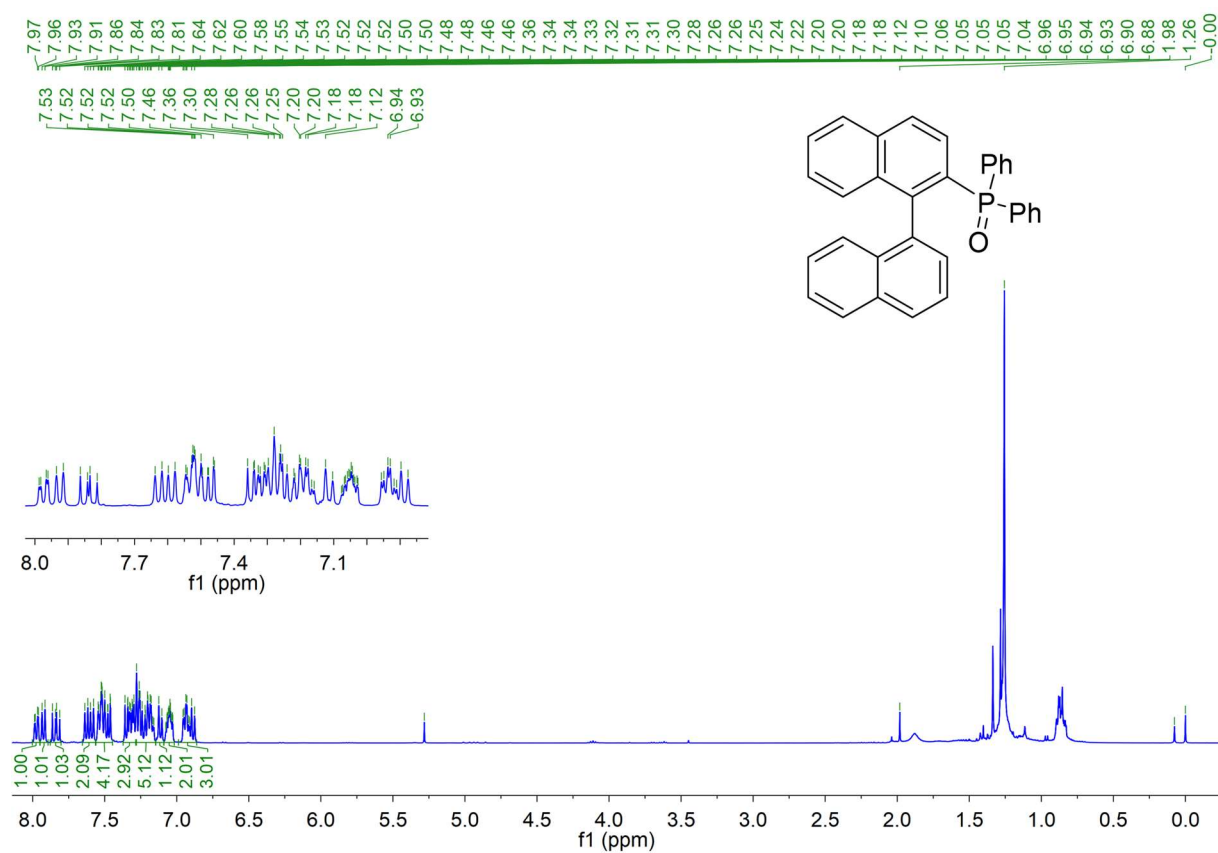
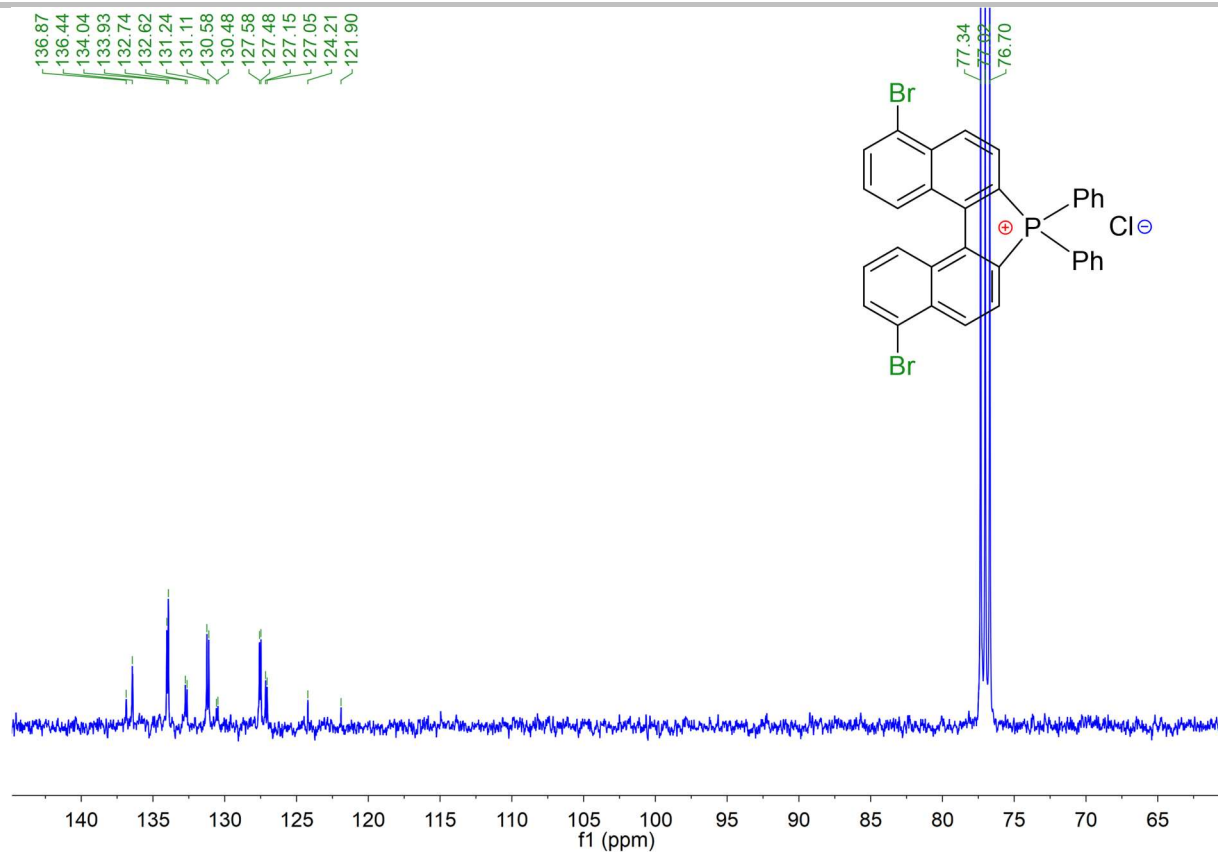
Supporting information



Supporting information



Supporting information



Supporting information

